

Towards the Total Synthesis of Pectenotoxin-4



A thesis submitted to the Board of the Faculty of Physical Sciences
in partial fulfilment of the requirements for the degree of

Doctor of Philosophy

in the

University of Oxford

By

Timothy Kwok

St Peter's College

&

The Chemistry Research Laboratory

Trinity Term 2020

Table of Contents

Declaration	iv
Abstract	v
Acknowledgments	vii
Abbreviations	ix
Chapter 1	1
1.1 Chapter overview	2
1.2 Isolation and structure of the PTXs	2
1.3 Biological activity of the PTXs	8
1.4 Overview of past total syntheses of the PTXs	12
1.5 Evans' total synthesis of PTX-4	13
1.5.1 Retrosynthetic analysis	13
1.5.2 Synthesis of C1–C19 ABC epoxide 4	15
1.5.3 Synthesis of C21–C30 E hydrazone 5	22
1.5.4 Synthesis of C31–C40 F sulfone 2	25
1.5.5 Endgame of Evans' total synthesis of PTX-4.....	28
1.6 Fujiwara's total synthesis of PTX-2	32
1.6.1 Retrosynthetic analysis	32
1.6.2 Synthesis of C8–C20 C fragment 67	34
1.6.3 Synthesis of C21–C30 E fragment 66	38
1.6.4 Synthesis of FG fragment 64	40
1.6.5 Endgame of Fujiwara's total synthesis of PTX-2.....	45
1.7 Donohoe's approach to PTX-4.....	49
Chapter 2	52
2.1 Chapter overview	53
2.2 Retrosynthesis of ABC fragment 139	53
2.3 Synthesis of C11–C16 alkyne 145	54
2.4 Synthesis of C3–C9 aldehyde 146	56
2.5 Carreira alkynylation reaction between 145 and 146	60
2.6 Elaboration of propargylic alcohol 144 to triol 143	63
2.7 Osmium-catalysed oxidative cyclisation of triol 143	65
2.8 Elaboration of <i>bis</i> -THF 142 to 180	70
2.9 Installation of Evans auxiliary	72
2.10 1,2-Hydride shift spiroketalisation cascade.....	75

2.11	Cleavage of the Evans auxiliary	77
2.11.1	Overview and past efforts of auxiliary removal.....	77
2.11.2	Attempted removal of Evans auxiliary from spiroketal 195	79
2.11.3	Attempted removal of Evans auxiliary at an earlier stage of the synthesis.....	80
2.11.4	Evans auxiliary cleavage of 187 and elaboration	84
2.12	Conversion of 221 to chloromesylate 140	89
2.13	Optimisation of 1,2-hydride shift spiroketalisation cascade	90
2.13.1	Pre-optimisation of 1,2-hydride shift reaction	90
2.13.2	Optimisation involving entire cascade.....	93
2.13.3	Formation of <i>tris</i> -THF 228 and instability of chloromestylate 140	95
2.13.4	Optimisation involving HFIP.....	96
2.14	Conclusion.....	99
Chapter 3	101
3.1	Chapter overview	102
3.2	Retrosynthesis of the E fragment.....	102
3.3	Synthesis of C21–C25 alkyne 255	103
3.4	Hydroiodination of alkyne 255 to prepare α -vinyl iodide 252	106
3.4.1	Background of Gao and Hoveyda’s hydroiodination methodology	106
3.4.2	Troubleshooting reproducibility issues of hydroiodination reaction.....	107
3.4.3	Exploring alternate hydroiodination reactions	108
3.5	Alternative forward synthesis to prepare α -vinyl iodide 252	109
3.5.1	Synthesis of ketone 276	109
3.5.2	Synthesis of α -vinyl triflate 277	112
3.5.3	Triflate–iodide exchange and Negishi coupling	114
3.5.4	Summary of α -vinyl iodide 252 synthesis and future work	116
3.6	Osmium-catalysed oxidative cyclisation of alkene 251	117
3.7	Elaboration of silyl ether 250 to 248	119
3.8	Completion of E fragment synthesis	121
3.9	Summary of E fragment synthesis.....	126
3.10	Synthesis of C31–C40 F fragment.....	128
3.10.1	Overview.....	128
3.10.2	Syntheses of C37–C40 alkene 304 and C31–C36 sulfone 307	128
3.10.3	Elaboration of <i>trans</i> -THF 316 into F fragment.....	131
Chapter 4	133
4.1	Chapter overview	134
4.2	Deprotection of ABC fragment 139	135
4.2.1	Optimisation experiments for selective deprotection.....	135

4.2.2	Unexpected instability of ABC alcohol 226	136
4.3	Experiments involving side-product diol 227	137
4.3.1	Attempted derivatisation of diol 227 into crystalline guanidinium sulphate	137
4.3.2	Attempted selective oxidation of diol 227 into hydroxy aldehyde 343	139
4.3.3	Studies examining protecting group manipulations on diol 227	142
4.4	Screening of oxidation conditions to prepare aldehyde 359	146
4.5	Sakurai Allylation of aldehyde 359	150
4.5.1	Background of allylation model systems	150
4.5.2	Sakurai allylation and elaboration	151
4.5.3	Revised route involving different order of key steps	152
4.6	Keck allylation of aldehyde 359	155
4.7	Allylboration of aldehyde 359	160
4.8	Hayashi–Miyaura 1,4-addition reaction	166
4.9	Dihydroxylation–ketalisation reaction	169
4.10	Conclusion	171
4.10.1	Summary of synthesis.....	171
4.10.2	Future work	172
Chapter 5	175
5.1	Experimental	176
5.1.1	Experimental techniques	176
5.1.2	Experimental procedures for ABC fragment	179
5.1.3	Experimental procedures for E and F fragments	286
5.2	Selected NMR spectra	318
References	323

DECLARATION

The work described in this thesis is entirely my own, except where I have either acknowledged help from a named person or given reference to a published source or a thesis.

Timothy Kwok

University of Oxford, Trinity Term 2020

ABSTRACT

Chapter 1: Introduction

This chapter provides the background of the pectenotoxins (PTX), which includes details of their isolation, structure, and biological activity. Subsequently, the total syntheses of PTX-4 by Evans and of PTX-2 by Fujiwara are discussed. Finally, past efforts of the Donohoe group towards the synthesis of PTX-4 are summarised.

Chapter 2: Synthesis of the ABC fragment

This chapter details the retrosynthesis and forward synthesis of the C1–C16 ABC fragment of PTX-4. Moreover, the chapter features extensive discussions on the optimisation efforts for key steps, including the osmium-catalysed double oxidative cyclisation step and the 1,2-hydride shift spiroketalisation cascade. Other major challenges, such as the unexpectedly difficult removal of an Evans oxazolidinone auxiliary, are also discussed.

Chapter 3: Synthesis of the E fragment

This chapter describes the retrosynthesis and forward synthesis of the C19–C30 E fragment of PTX-4. Experiments to troubleshoot and develop workarounds for an irreproducible regioselective hydroiodination step to give a vinyl iodide product early in the synthesis are documented. Finally, the synthesis of the C31–C40 F fragment of PTX-4 is briefly covered.

Chapter 4: Uniting the ABC and E fragments

This chapter discusses the elaboration of the ABC fragment into its vinyl boronic ester analogue for the planned rhodium-catalysed Hayashi–Miyaura 1,4-addition with the E fragment to unite the two major PTX-4 fragments. Optimisation studies for key reactions are

also discussed and include an allylation reaction, the 1,4-addition, and a dihydroxylation–ketalisation cascade to form the D ring.

Chapter 5: Experimental

This chapter lists all experimental procedures for the reactions described in this thesis, as well as the characterisation data for the compounds synthesised.

ACKNOWLEDGMENTS

I thank my PhD supervisor Professor Tim Donohoe for his guidance over the four years of my course. Even as I leave his group, I consider Tim's extensive knowledge of and his enthusiasm towards the science as ideals to work towards in my chemistry career ahead.

I am grateful to all past members of team pectenotoxin, although special mention goes to Dr Melodie Richardson. Thanks for being such a source of fun and unintentional humour. Even in the time since you left, you still hold the title of having F7's cleanest fumehood and dirtiest mouth! I am thankful, also, to my very meticulous proofreaders Chris Hall, Dani Cheang, and Oskar Hoff, who helped me make this thesis as strong as it can be.

Great mentors are hard to find and, for that, I thank Dr James Frost who mentored me during my first year and who continued to be a giver of good advice long after that. I have fond memories of our trips to Chutneys and Byron's, that big conference in Vienna, and the retrosynthesis competition we participated in as a team, which was really my excuse to show off to you all the chemistry I'd learnt since you left the group! On that note, I'd also like to thank Ciaran Lunt, Dana Aynetdinova, and Mihai Popescu for being my team mates in the retrosynthesis competition from the *preceding* year. It was a pleasure to work with and learn from chemists of such diverse talents, and I still count that experience as probably the best "group project" in my entire schooling life! Outside the serious chemistry, I thank Dr Simon Wübbolt, Oskar, and Dana for fun times during cards night (which have somehow endured during lockdown as MS Team meetings). Special thanks also goes to Oskar for being the best fumehood buddy for most of my PhD and the sheriff of F7.

I am also grateful for many other people in the TJD group I've crossed paths with: Max, Chris, Anna, Daniel, CB, Waz, Lydia, Bruno, Dani, Elliot, Lewis, Philip, Roly, Maria, Hamish, and many others. My deepest thanks also goes to the wonderful CRL staff from NMR, mass spectrometry, the electronic and mechanical workshops, and the safety office, who include Tina, Maria, Nader, Tim Claridge, Collin, Ron, John, Martin, and Debbie. It's a little sad having to leave the department where you know everyone, from the person who works at the

adjacent fumehood to the guy who fixes your rotorvap – if the community at the next department I join is even half as welcoming, I would count myself extraordinarily lucky.

Lastly, I thank my family – my sister Kat who's kept me company here in Oxford, and my parents who have always been supportive of both their childrens' choices, even ones as questionable as pursuing a career in chemistry!

ABBREVIATIONS

Ac	acetyl
acac	acetylacetonato
AIBN	2,2'-azobisisobutyronitrile
Ar	aryl
aq.	aqueous
BINAP	(1,1'-binaphthalene-2,2'-diyl)bis(diphenylphosphine)
Boc	<i>tert</i> -butyloxycarbonyl
Bt	benzothiazole
BtSH	mercaptobenzothiazole
cat.	catalytic amount
cod	1,5-cyclooctadiene
cont.	continued
COSY	homonuclear correlation spectroscopy
Cp	cyclopentadienyl
CSA	camphorsulfonic acid
d	doublet
dd	double doublet
ddd	double double doublet
dt	double triplet
DABCO	1,4-diazabicyclo[2.2.2]octane
DCC	<i>N,N'</i> -dicyclohexylcarbodiimide
DDQ	2,3-dichloro-5,6-dicyano- <i>p</i> -benzoquinone
DEIPS	diethylisopropylsilyl
DET	diethyl tartrate
DHQ	dihydroquinine
DHQD	dihydroquinidine
DIBAL-H	diisobutylaluminum hydride
DIAD	diisopropyl azodicarboxylate
DIC	<i>N,N'</i> -diisopropylcarbodiimide
DCM	dichloromethane
DMA	<i>N,N</i> -dimethylacetamide
DMAP	4-(dimethylamino)pyridine
DMF	<i>N,N</i> -dimethylformamide
DMP	Dess–Martin periodinane
DMPU	1,3-dimethyl-3,4,5,6-tetrahydro-2(1 <i>H</i>)-pyrimidinone
DMSO	dimethylsulfoxide
dppb	1,4-bis(diphenylphosphino)butane
dr	diastereomeric ratio
DSP	diarrhetic shellfish poisoning

DTX	dinophysistoxin
ee	enantiomeric excess
equiv.	equivalents
Et	ethyl
HFIP	1,1,1,3,3,3-hexafluoro-2-propanol
HMBC	heteronuclear multiple-bond correlation
HMPA	hexamethylphosphoramide
HRMS	high resolution mass spectrometry
HSQC	heteronuclear single quantum correlation
<i>i</i> -Pr	isopropyl
<i>J</i>	coupling constant
LC ₅₀	median lethal dose
LDA	lithium diisopropylamide
LiDBB	lithium di- <i>tert</i> -butyl diphenylide
LLS	longest linear sequence
LRMS	low resolution mass spectrometry
m	multiplet
Mc	α -chloromesyl
Me	methyl
MLD	minimum lethal dose
m.p.	melting point
MS	molecular sieves
MTPA	Mosher's acid/ α -methoxy- α -trifluoromethylphenylacetic acid
MVK	methyl vinyl ketone
nbd	norbornadiene
NIS	<i>N</i> -iodosuccinimide
NME	<i>N</i> -methylephedrine
NMO	<i>N</i> -methylmorpholine <i>N</i> -oxide
nmp	5,5-dimethyl-1-(4-methylpiperazin-1-yl)hexane-1,2,4-trione
nOe	nuclear Overhauser effect
NOESY	nuclear Overhauser effect spectroscopy
OA	okadaic acid
OTf	triflate
PMB	<i>para</i> -methoxybenzyl
PNO	pyridine <i>N</i> -oxide
Ph	phenyl
PHAL	phthalazine
PhMe	toluene
pin	pinacolato
PPTS	pyridinium <i>para</i> -toluenesulfonate
<i>p</i> -Tol	<i>para</i> -tolyl
q	quartet

quant.	quantitative
RCM	ring-closing metathesis
R _f	retention factor
rt	room temperature
s	singlet
SAD	Sharpless asymmetric dihydroxylation
sat.	saturated
SO ₃ ·py	sulfur trioxide pyridine complex
t	triplet
TAS-F	tris(dimethylamino)sulfonium difluorotrimethylsilicate
TBAI	tetra- <i>n</i> -butylammonium iodide
td	triple doublet
tdd	triple double doublet
TBDPS	<i>tert</i> -butyldiphenylsilyl
TBODPS	<i>tert</i> -butoxydiphenylsilyl
TBS	<i>tert</i> -butylsilyl
<i>t</i> -Bu	<i>tert</i> -butyl
TES	triethylsilyl
TFA	trifluoroacetic acid
TFE	trifluoroethanol
THF	tetrahydrofuran
TIPS	triisopropylsilyl
TLC	thin-layer chromatography
TMEDA	<i>N, N, N', N'</i> -tetramethylethylenediamine
TMS	trimethylsilyl
TPS	triphenylsilyl
Ts	tosyl
YTX	yessotoxin

CHAPTER 1

Introduction

1.1 Chapter overview

This chapter provides the background of the pectenotoxins (PTX), the family of marine natural products to which pectenotoxin-4 (PTX-4) belongs. This description includes details of their isolation, structure, and biological activity. Subsequently, the total syntheses of PTX-4 by Evans and of PTX-2 by Fujiwara are discussed. Finally, past efforts of the Donohoe group towards the synthesis of PTX-4 are summarised.

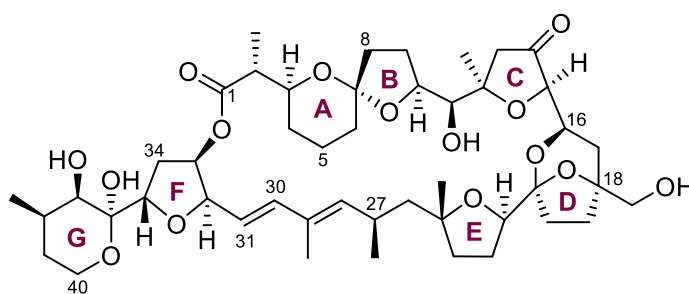


Figure 1.1. Structure of pectenotoxin-4 (PTX-4)

1.2 Isolation and structure of the PTXs

Natural products are a valuable source of chemical inspiration for drug development. Many natural products are biologically active and target enzymes, ion channels, DNA as well as other sites through novel pathways, which in certain cases makes them pharmaceutically useful.¹ Marine natural products in particular are of considerable biological interest, because of their large numbers and diversity – oceans cover more than 70% of the Earth's surface and make up 95% of the biosphere² – and also because of their tendency to display high potency, due to the need to exert a biological effect despite getting rapidly diluted when released into water.²

The PTXs are one such family of marine natural products, whose members are macrocyclic polyethers that display promising biological activity. The first members of the PTX family, PTXs 1–5, were isolated by Yasumoto and co-workers in 1985 off the north-eastern coast of Japan from the digestive glands of the scallop *Patinopecten yessoensis*, after which they were

named.³ Interestingly, however, it is not the scallops themselves that produce the PTXs, but rather a toxigenic strain of marine plankton, *Dinophysis fortii*, which they ingest that does so.⁴

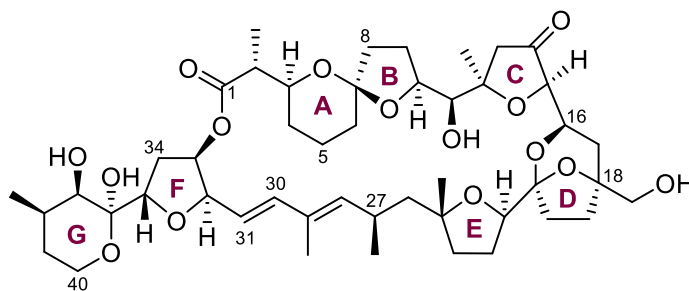
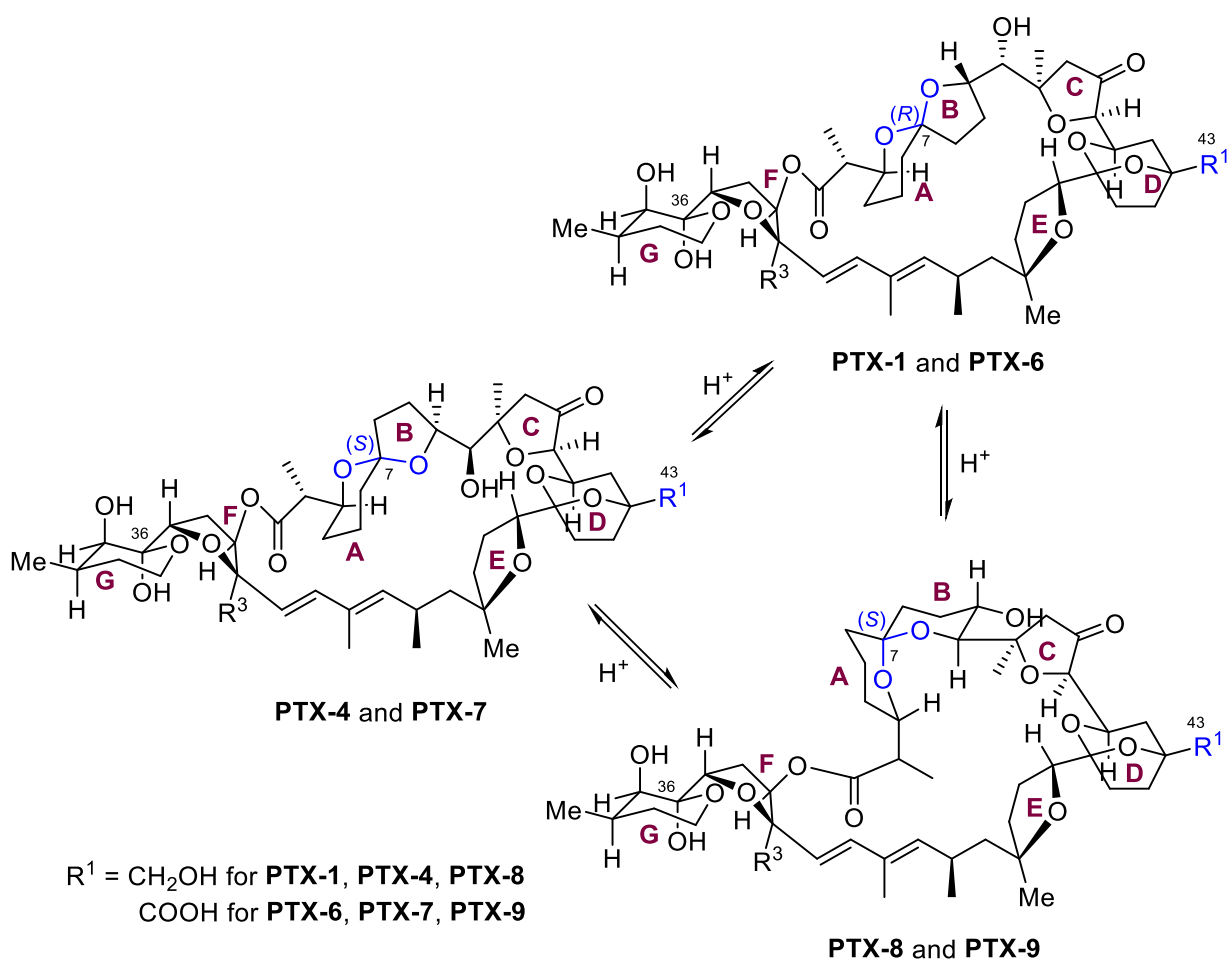


Figure 1.2. Structure of PTX-1

Yasumoto determined the relative configuration of PTX-1 using NMR spectroscopy, IR spectroscopy, mass spectrometry, and X-ray crystallography. However, attempts to assign the absolute configuration through the crystallisation of bromine-containing derivatives were unsuccessful. The absolute stereochemistry of the natural product was only determined later in 1997 by the same group, when they used chiral anisotropic shift reagents to determine the configuration at C18, which was assigned (*S*).⁵ By correlating the various characterisation data, the Yasumoto group also determined the absolute configurations of PTX-2, PTX-3, and PTX-6, in addition to that of PTX-1.

In a separate work, Yasumoto and co-workers reported that equilibrating PTX-1 in TFA gave a 29:14:57 mixture of PTX-1, PTX-4, and PTX-8, while equilibrating PTX-6 in TFA gave a 40:16:44 mixture of PTX-6, PTX-7, and PTX-9 (Scheme 1.1).⁶ PTX-4 and PTX-7 are anomeric (*S*)-[5,6]-spiroketals that are produced from kinetic acidic equilibration of the corresponding non-anomeric (*R*)-[6,5]-spiroketals, PTX-1 and PTX-6. In polyethers such as the PTX family, the occurrence of both epimers of a spiroketal ring system is unusual.⁶ Moreover, the greater thermodynamic distribution of PTX-1 and PTX-6 relative to PTX-4 and PTX-7 was unexpected, because the latter pair enjoy a stabilising anomeric effect. The preference for the non-

anomeric PTX-1 and PTX-6 was suggested to be due to conformational constraints within the macrocycle, which favour the non-anomeric over the anomeric configuration at the [5,6]-spiroketal. PTX-8 and PTX-9, meanwhile, are doubly anomeric [6,6]-spiroketals that are thermodynamically stable products which result from prolonged acidic equilibration, and have not been found in Nature.



Scheme 1.1. Acid-mediated equilibration at C7 of the PTXs

The absence of PTX-8 and PTX-9 in the scallop in contrast to naturally occurring PTX-4 and PTX-7 suggests that epimerisation at C7 of the spiroketal occurs *via* an enzyme-mediated process, as opposed to non-specific acid catalysis. It has been further postulated that this

epimerisation is part of a detoxification process, given that PTX-4 and PTX-7 display lower toxicity than that of their respective epimers, PTX-1 and PTX-6.⁷

All PTXs possess 43 carbons, 19 stereocentres, three THF rings, one spiroketal, one bicyclic ketal, and one pyran ring. By convention, the various rings of the PTXs are referred to as the ABCDEFG rings.⁸ The structures of members of the PTX family bearing (S)-[6,5]-spiroketals and (S)-[6,6]-spiroketals are summarised in Figure 1.3.

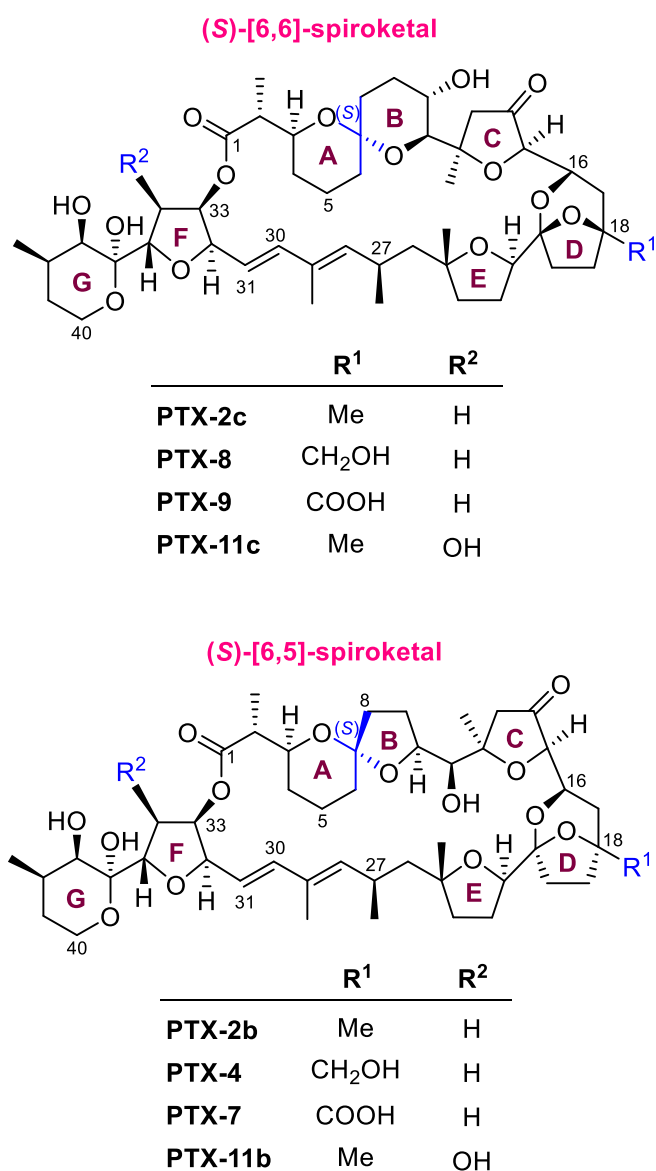


Figure 1.3. Structures of PTXs bearing (S)-[6,5]-spiroketals and (S)-[6,6]-spiroketals

Additionally, the structures of the PTXs bearing (*R*)-[6,5]-spiroketal are shown in Figure 1.4. The individual PTXs can be distinguished from each other by their stereochemical configuration at C7 of the spiroketal, the oxidation levels at C34 and C43, and minor structural variations within the FG ring system.

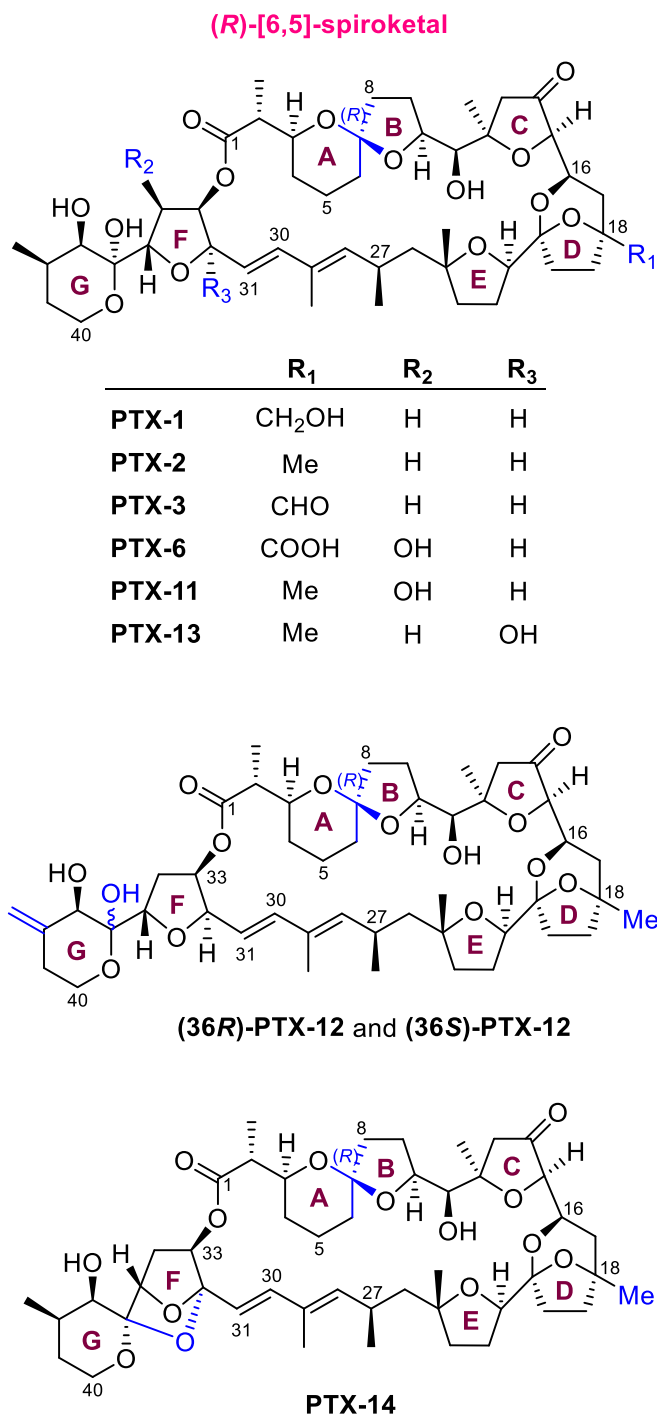


Figure 1.4. Structures of PTXs bearing (*R*)-[6,5]-spiroketal

PTX-2 is thought to be the parent PTX from which the other members of the PTX family arise through metabolism in the scallop gut.^{9,10} This relationship between the PTXs was supported by the presence of PTX-2 in both the extracts of scallop gut and the algae *D. fortii*, in contrast to the other PTXs which were detected only in the scallop gut extracts.⁹

Finally, PTXs can also undergo enzymatic hydrolysis at the ester group during metabolism in the scallop to give a mixture of the corresponding *seco* acids, including epimers at C7 in the spiroketal (Figure 1.5).¹¹

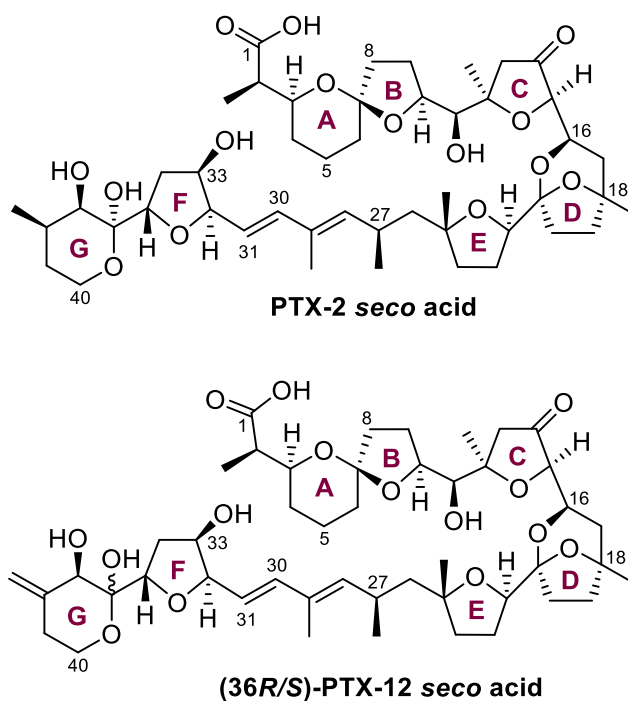


Figure 1.5. Structures of selected PTX seco acids

Suzuki and co-workers demonstrated that these *seco* acids were metabolites and not artefacts from the isolation process by lack of conversion of PTX-2 to its *seco* acid when treated with various phosphate buffers from pH 4.1–9.1.¹² Similar to the epimerisation at C7 at the spiroketal from the non-anomeric to the anomeric configuration as had been previously discussed, enzymatic hydrolysis of PTXs to their *seco* acids is likely part of a detoxication process during metabolism; indeed, the *seco* acids display reduced toxicity compared to the

PTXs from which they are derived.¹³ The following section provides a more detailed discussion about the biological properties of the PTXs.

1.3 Biological activity of the PTXs

The PTXs were originally reported to cause liver damage and diarrhetic shellfish poisoning (DSP) from eating toxic shellfish.¹⁴ The symptoms of DSP include diarrhoea, abdominal cramps, nausea, vomiting, and headache; and it has been suggested that PTX derivatives (e.g., PTX-2 *seco* acid) were responsible for outbreaks of severe diarrhetic illness in Australia.¹⁴

However, the toxicity of the PTXs has since been called into question. Although a 1988 report by the Ishige group demonstrated that oral administration of PTX-2 induced severe diarrhoea in mice,¹⁵ a separate report by the Miles group in 2004 stated that DSP was not observed when PTXs isolated from a different source were administered.¹⁶ The apparent DSP-inducing effects of the PTXs and their derivatives have since been attributed to contamination with other compounds known to cause DSP, such as the dinophysitoxins (DTXs) and okadaic acid (Figure 1.6), which are often co-isolated with the PTXs.⁷ As a result of this conflicting evidence, the PTXs have been re-classified as a group of marine natural products separate from that of DSP toxins.

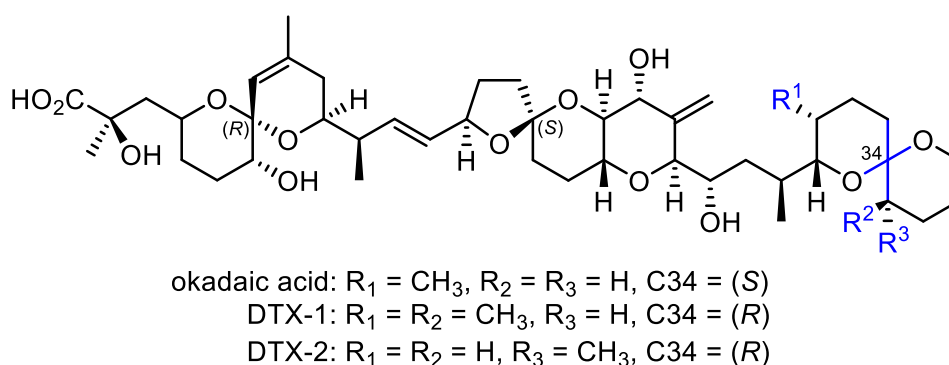


Figure 1.6. Structures of okadaic acid and DTXs

Nevertheless, the PTXs are hepatotoxic and induce apoptosis in rat and salmon hepatocytes.¹⁷ As the parent PTX, PTX-2 is also the most toxic member of the PTX family and has a median lethal dose (LD₅₀) of 219 µg/kg through intraperitoneal injection in mice and a minimum lethal dose (MLD) of 192 µg/kg.¹⁶ In addition, PTX-2 is cytotoxic towards several cell lines of lung, colon, renal, ovarian, breast, and melanoma cancer, giving nanomolar LC₅₀ values.⁴ The cytotoxicity that PTX-2 displays is greater towards cancer cells than normal cells, thus elevating the PTX family's potential pharmaceutical relevance as a drug lead in anticancer research.

PTX-2 exerts its cytotoxic effects by destabilising the actin cytoskeleton, which is weaker in cancer cells than in normal cells.¹⁸ Actin is a family of multi-functional proteins in eukaryotic cells that control vesicle and organelle movement, cell shape, cell motility, cell signalling, and cell division. Under normal conditions, globular actin monomers (G-actin) assemble into long filaments (F-actin) that make up the cytoskeleton. Their importance to cellular function is demonstrated by the fact that these cytoskeletal filaments have been an historic target for cancer chemotherapy.¹⁸ PTX-2 destabilises the actin cytoskeleton by sequestering the G-actin monomer, which inhibits F-actin polymerisation, thus interfering with cancer cell growth and inducing apoptosis. Although other filament-destabilising compounds are known, PTX-2 binds with G-actin at a shallow groove between subdomains 1 and 3, a novel binding site and mode of action that was supported by an X-ray crystal structure of the PTX-2–G-actin complex (Figure 1.7) from a 2007 report by Rayment and co-workers.¹⁹

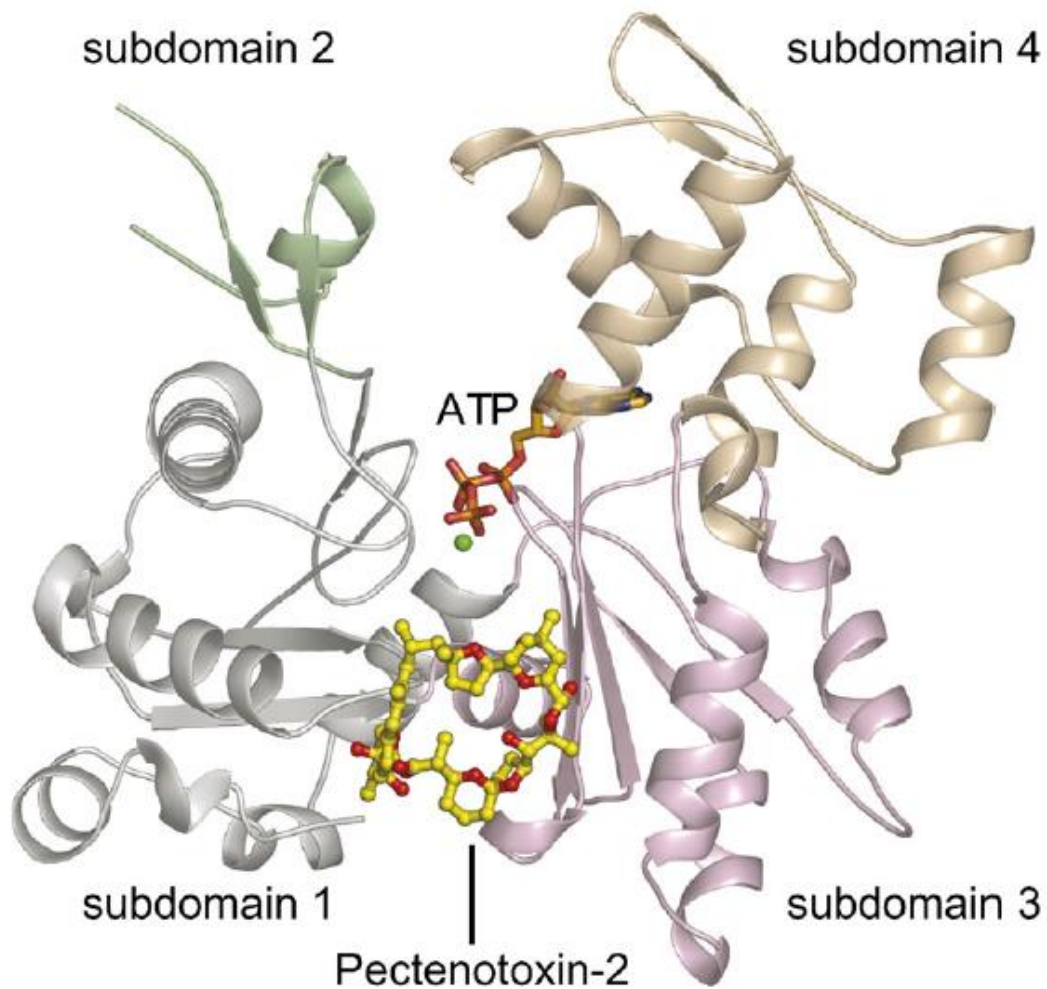


Figure 1.7. The PTX-2–G-actin complex (reprinted from Allingham, J. S.; Miles, C. O.; Rayment, I., 2007)¹⁹

Contrary to earlier stoichiometric studies by Hori and co-workers suggesting that PTX-2 forms a 1:4 complex with G-actin,²⁰ the crystallographic data from the Rayment group indicated that a 1:1 complex was formed instead. The Rayment group also showed that the binding of PTX-2 to actin buries 31% of the former's molecular surface area.

A point-by-point summary of the key PTX-2–G-actin interactions within the complex (Figure 1.8) is provided below:

- a) The PTX-2 macrocycle is centred above the Leu110 side-chain, and situated between Pro112 and His173.

- b) The large macrocyclic portion of PTX-2 lies flat in a shallow groove between subdomain 1 and subdomain 3, where the interactions are mostly hydrophobic.
- c) The “tail” (FG ring system) of PTX-2 interacts primarily with subdomain 1 through the former’s polar atoms, with four hydrogen bonds being present in total.
- d) The G ring sits in a small hydrophobic pocket formed by Ile136, Phe375, and the β -carbon of Asn111.
- e) A key hydrophobic interaction occurs between the C45 methyl group and Ile75.
- f) A hydrogen bonding network is present between the C14 C=O group, a water molecule, and the C=O and amide N–H groups of Arg177.

The roles of certain key moieties of PTX-2 – the C28–C31 conjugated diene, the AB spiroketal, and the macrolactone – are also worth highlighting.

First, the C28–C31 conjugated diene conformationally restricts the ring, allowing the aforementioned crucial PTX-2–G-actin interactions to occur. Second, epimerisation at C7 in the spiroketal to the anomeric configuration (e.g., in PTX-4 and PTX-7–9), is likely to change the morphology of the macrocyclic ring in a way that disrupts the PTX’s crucial hydrophobic interactions with His173 and Leu110, an observation consistent with the reduced potency of the PTXs that are anomeric at C7. Third, based on the crystal structure of the PTX-2–G-actin complex, it is expected that hydrolysis of the macrocycle to the free PTX-2 *seco* acid would also significantly interfere with binding. The stronger binding of the macrocycle relative to the acyclic derivative is a general trend among all cyclic macrolides that bind to actin, and can be

rationalised by the reduced conformational freedom of unbound PTX-2, which in turn reduces the entropic penalty of PTX-2 binding to actin, thus encouraging stronger binding.¹⁹

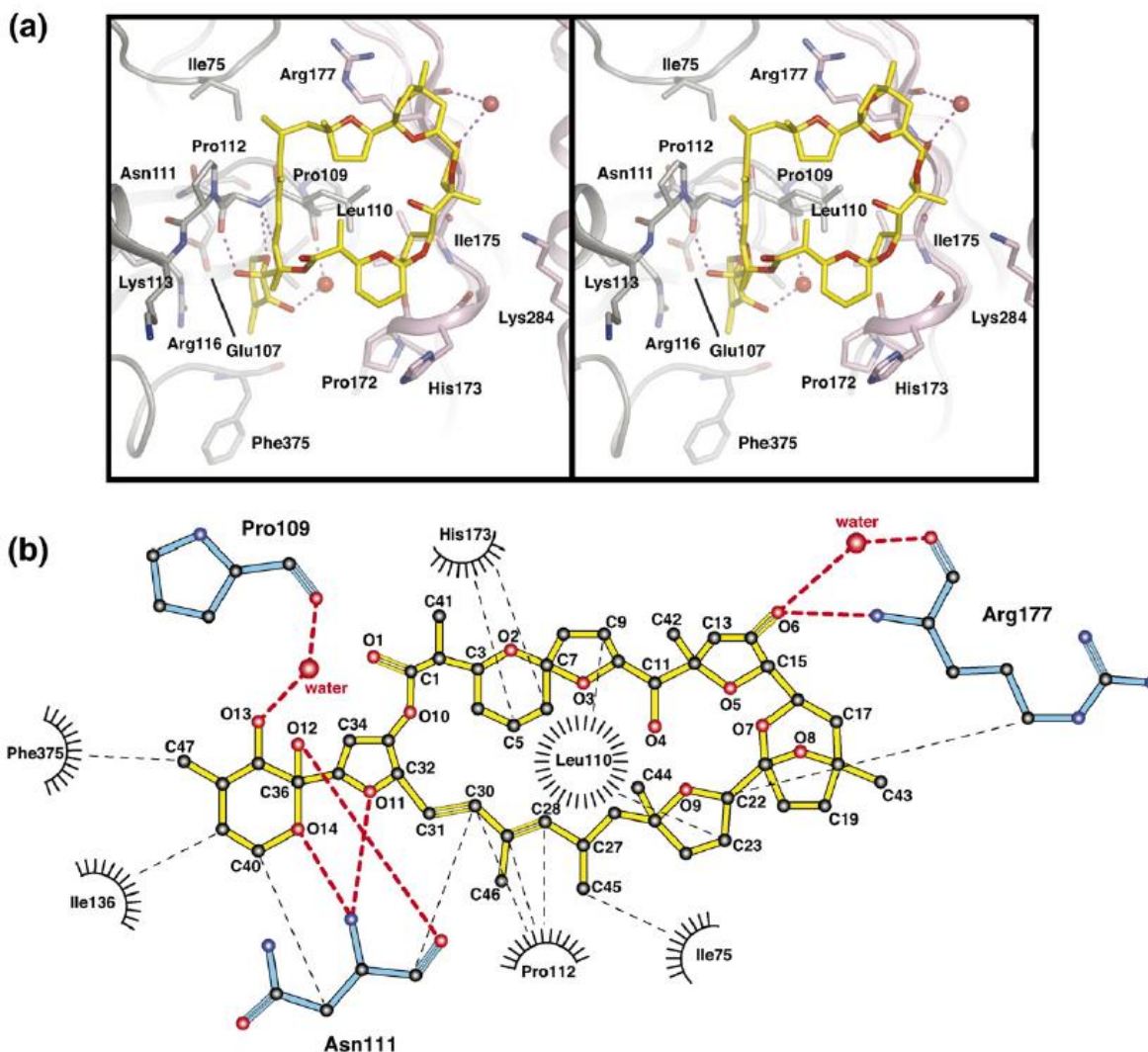


Figure 1.8. Interactions between PTX-2 and G-actin monomer (reprinted from Allingham, J.

*S.; Miles, C. O.; Rayment, I., 2007)*¹⁹

1.4 Overview of past total syntheses of the PTXs

Although numerous natural products have been identified as therapeutic leads, the high costs – both monetary and environmental – of harvesting enough material from Nature have made their total synthesis an attractive alternative to procure these precious compounds for biological screening. The complex molecular architecture and promising biological activity of

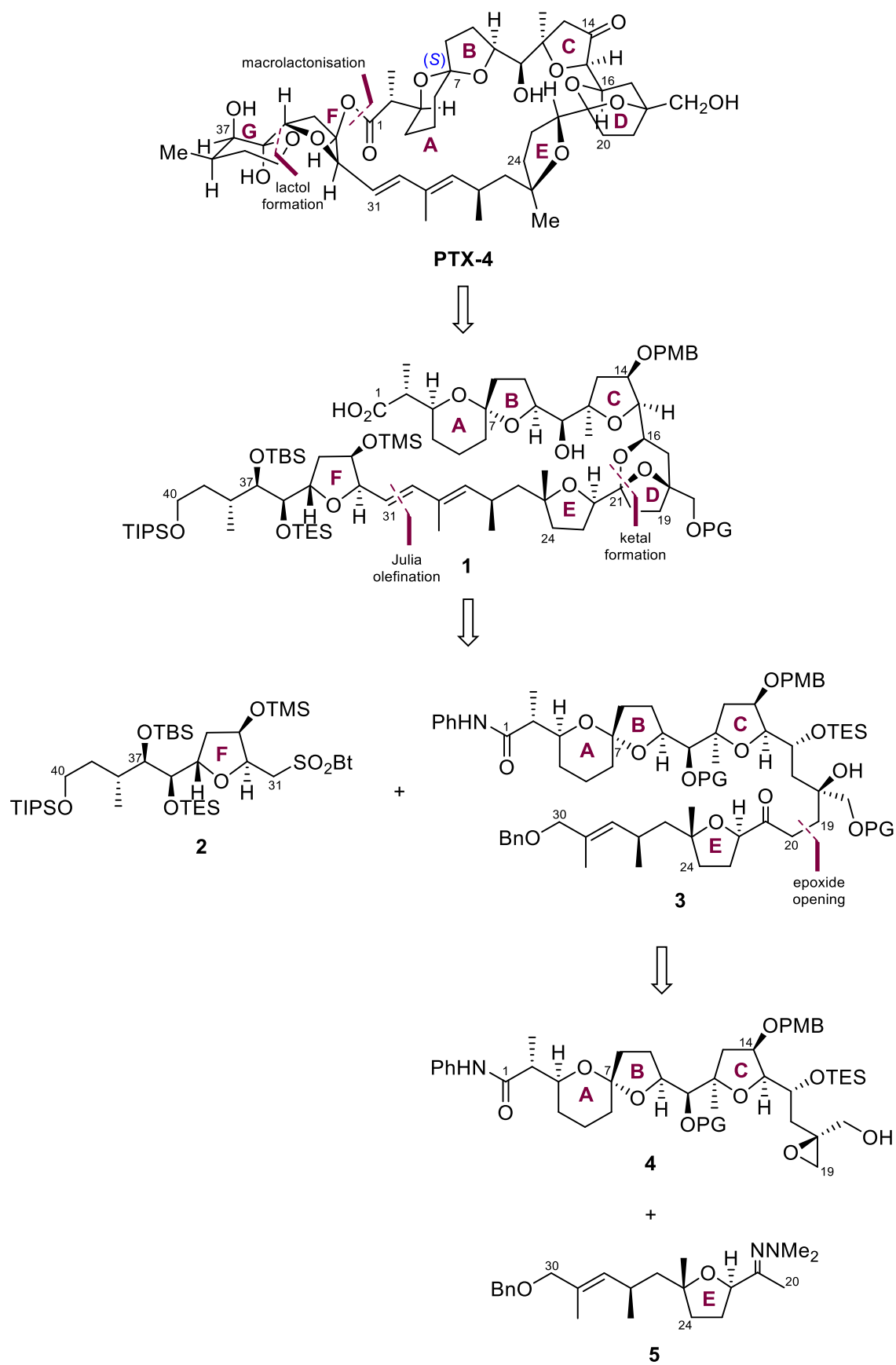
the PTXs have made them attractive synthetic targets in the organic chemistry community. To date, there exist two completed total syntheses of the PTXs: In 2002, the Evans group accomplished the total synthesis of PTX-4, from which they were also able to derive PTX-1 and PTX-8 *via* an acid-mediated equilibration^{21,22} In 2013, the Fujiwara group completed the total synthesis of PTX-2 *via* the analogous acid-mediated equilibration from the C7 spiroketal epimer PTX-2b.^{23–28} These two total syntheses will be discussed in the following sections. The Donohoe group has also been working on the total synthesis of PTX-4;^{29–31} these synthetic efforts will be summarised last.

1.5 Evans' total synthesis of PTX-4

1.5.1 Retrosynthetic analysis

The principal disconnections of Evans' retrosynthetic analysis of PTX-4 are shown in Scheme **1.2**. Evans recognised that although the anomeric spiroketal was the more thermodynamically stable isomer in acyclic precursors of PTX-4, it becomes destabilised relative to the non-anomeric C7 epimer when constrained in a macrocycle after macrolactonisation.^{6,13,22}

As such, macrolactonisation was proposed as one of the first disconnections and hence one of the last forward steps to minimise handling of the unstable AB spiroketal moiety prone to epimerisation. Thus, PTX-4 could be derived from precursor **1** after an appropriate oxidation state manipulation at C14 and C36, macrolactonisation, and global deprotection; spontaneous G ring lactol formation was expected to occur after the global deprotection step.



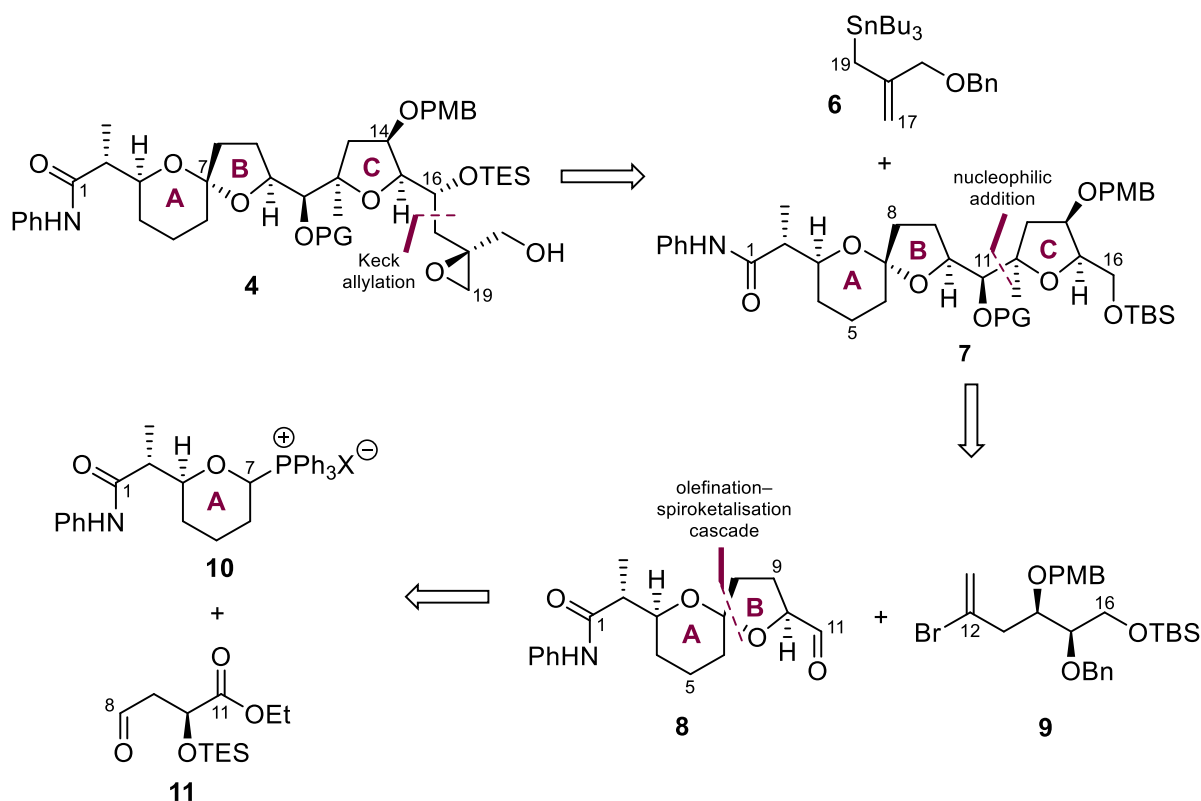
Scheme 1.2. Evans' retrosynthetic strategy for PTX-4

Advanced precursor **1** may then be simplified further by a disconnection at the C30–C31 double-bond and a disconnection of the two oxygens at C21 that would unravel the D ring bicyclic ketal, giving F sulfone **2** and ABCE fragment **3**. ABCE fragment **3** can be simplified further by disconnecting the C19–C20 bond, whose formation can be achieved in the forward sense *via* epoxide opening; this disconnection in turn would give ABC epoxide **4** and E hydrazone **5**.

The rest of this section covering Evans' total synthesis of PTX-4 will discuss the forward syntheses of ABC epoxide **4**, E hydrazone **5**, and F sulfone **2** in that order, before finally describing the endgame of the total synthesis.

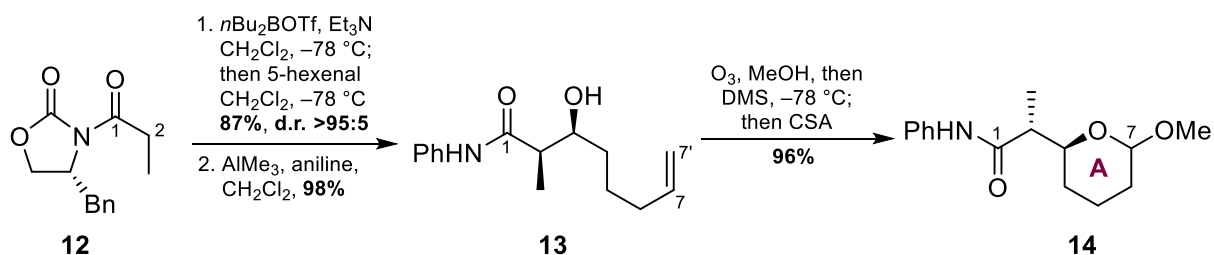
1.5.2 Synthesis of C1–C19 ABC epoxide 4

Evans' retrosynthetic analysis of the C1–C19 ABC epoxide **4** is summarised in Scheme **1.3**. First, ABC epoxide **4** may be further simplified to give allyl stannane **6** and ABC fragment **7** by a disconnection at the C16–C17 bond, which can be formed by a Felkin–Anh-controlled diastereoselective Keck allylation. A disconnection at C11–C12 of ABC fragment **7** simplifies the molecule into the separate AB spiroketal **8** and the C12–C16 sub-fragment **9** which bears the C ring carbon skeleton. Finally, concomitant disconnections at C7–C8 and C7–O of AB spiroketal **8** were proposed to bisect the spiroketal into triphenylphosphonium salt **10** and aldehyde **11**, which can be reacted together in the forward synthesis by a Wittig olefination–spiroketalisation cascade.



Scheme 1.3. Retrosynthetic analysis of C1–C19 ABC epoxide **4**

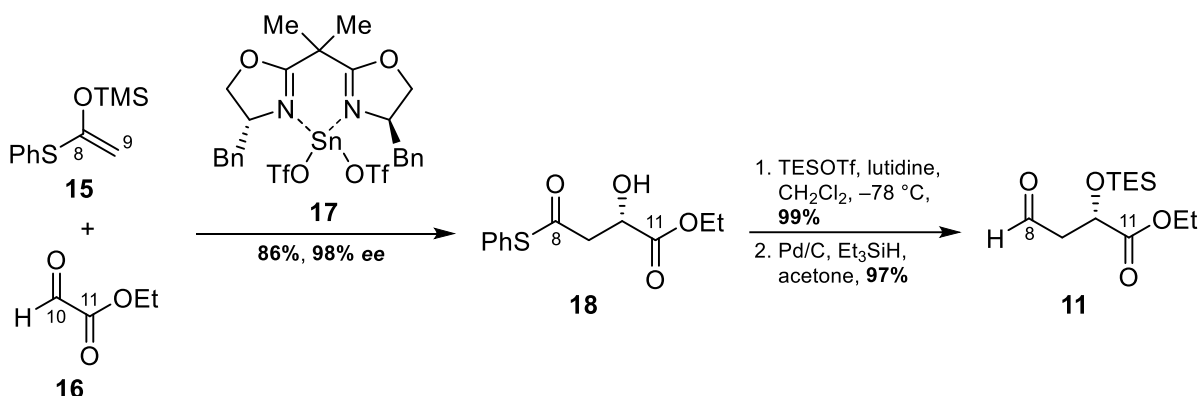
The forward synthesis of ABC epoxide **4** commenced with the three-step sequence to prepare the C1–C7 A pyran ring **14** (Scheme 1.4). First, an Evans aldol addition was conducted between oxazolidinone **12** and 5-hexenal to give the aldol product in 87% yield and >95:5 d.r., which was then transamidated with aniline in the presence of AlMe₃ Lewis acid to give amide **13** in 98% yield. Subsequently, amide **13** was ozonolysed to give a hydroxyaldehyde intermediate that formed a ketal *in situ*, thus affording pyran ring **14** in 96% yield.



Scheme 1.4. Synthesis of C1–C7 A pyran ring **14**

Pyran ring **14** is the direct precursor of the key triphenylphosphonium salt sub-fragment **10** used for the Wittig olefination–spiroketalisation cascade; however, before the

triphenylphosphonium salt could be prepared and the cascade executed, the C8–C11 aldehyde sub-fragment **11** had to be synthesised first (Scheme 1.5).



Scheme 1.5. Synthesis of C8–C11 aldehyde 11

To prepare aldehyde **11**, an aldol reaction was performed between silyl enol ether **15** and ethyl glyoxylate (**16**) to give aldol adduct **18** in 86% yield and in 98% ee. This asymmetric reaction was catalysed by chiral Sn(II) Lewis acid, which induced enantioselectivity by forming a complex with the ethyl glyoxylate *via* bidentate chelation; this bidentate chelation exposes only the *Si* face of the aldehyde to nucleophilic addition (Figure 1.9), thus biasing the reaction towards forming the (*S*)-enantiomer of the aldol adduct.³²

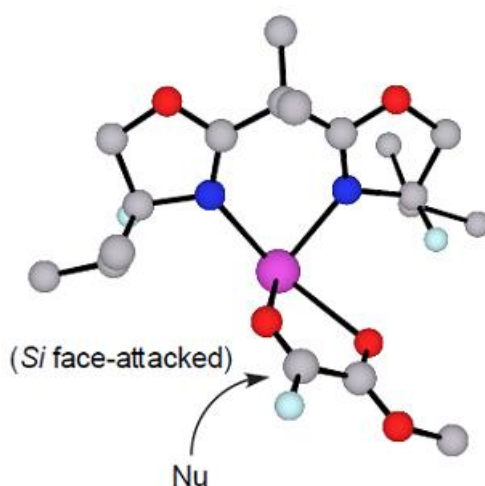
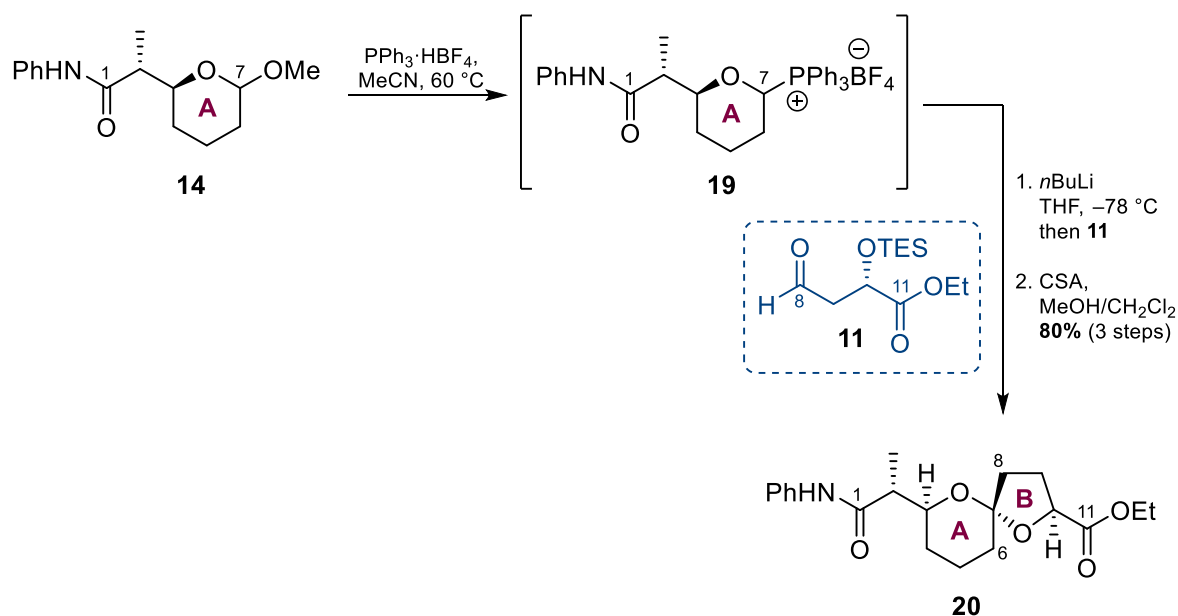


Figure 1.9. 3D stereoselectivity model of chiral Sn(II)-catalysed asymmetric aldol addition

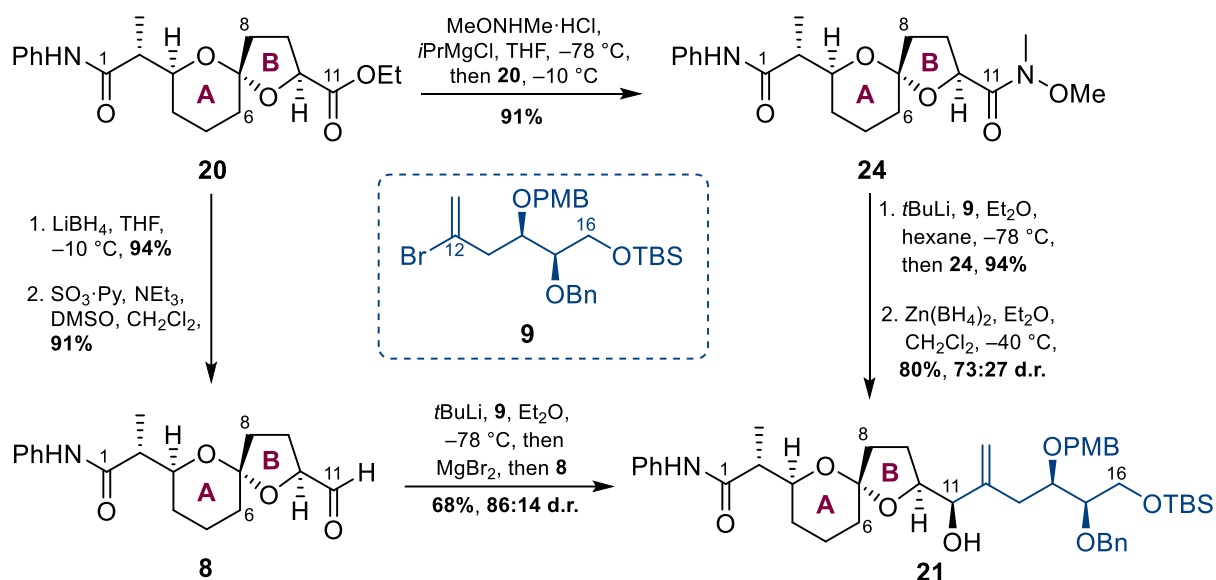
(reprinted from the PhD thesis of Hemaka Anthony Rajapakse)

With A ring **14** and aldehyde **11** having been prepared, the Wittig olefination–spiroketalisation cascade could now be executed (Scheme 1.6). To that end, A ring **14** was treated with $\text{PPh}_3 \cdot \text{HBF}_4$ in MeCN to afford phosphonium salt **19**, which was reacted in the same pot with two equivalents of $n\text{BuLi}$ to deprotonate it to its ylide, with the other equivalent deprotonating the C1 amide. Aldehyde **11** was then added to the mixture to give the Wittig olefination product, an unstable enol ether, which spiroketalised upon addition of CSA in MeOH/ CH_2Cl_2 to at last give AB spiroketal **20** in 80% yield over three steps as a single diastereomer. The spiroketal formed was the desired anomeric and thermodynamically favoured [6,5]-spiroketal, whose structure was confirmed by X-ray crystallography.³³



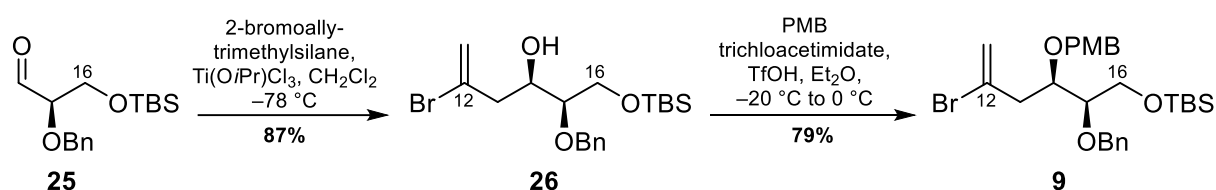
*Scheme 1.6. Synthesis of C1–C11 AB spiroketal **20** via olefination–spiroketalisation cascade*

AB spiroketal **20** was then elaborated into C1–C16 allylic alcohol **21** in two different ways. The first route (Scheme 1.7) involved LiBH_4 reduction of the ester moiety of spiroketal **20** into its primary alcohol in 94% yield, which was then subjected to a Parikh–Doering oxidation reaction to give aldehyde **8** in 91% yield. Aldehyde **8** was then reacted with C12–C16 vinyl bromide **9** pre-treated with $t\text{BuLi}$ to give C1–C16 allylic alcohol **21** in 68% yield and in 86:14 d.r.; the diastereoselectivity was suggested to have arisen from Felkin–Anh control.



*Scheme 1.7. Synthesis of C1–C16 allylic alcohol **21** through two routes*

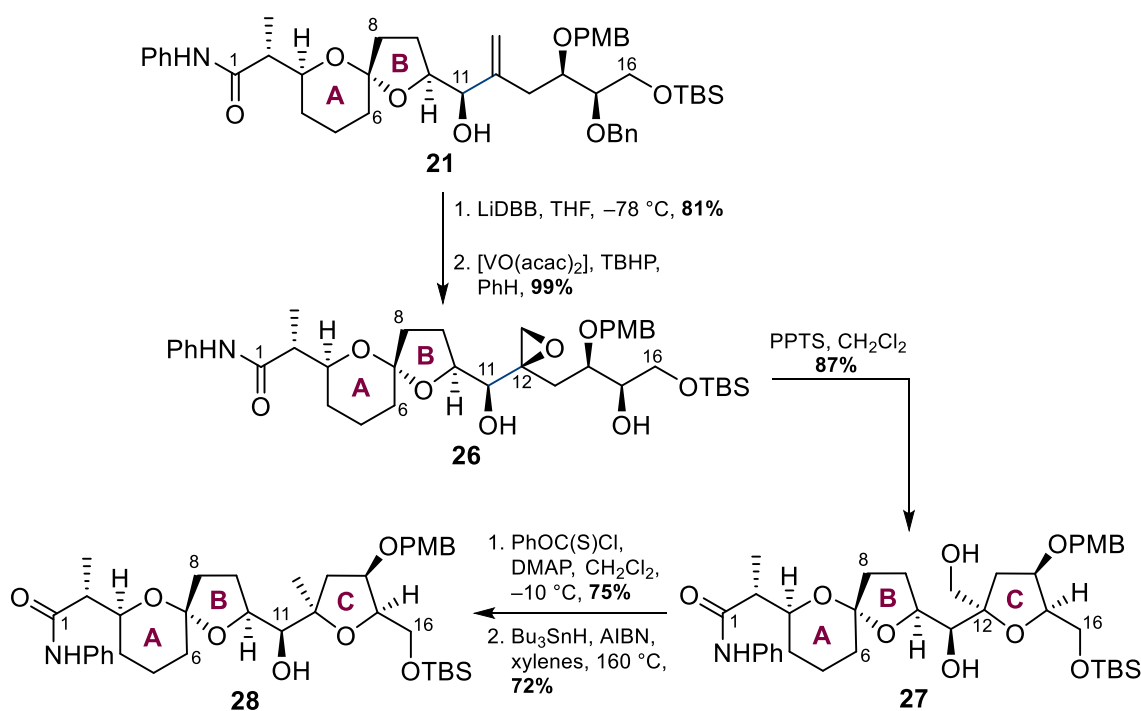
In an alternate synthetic pathway, allylic alcohol **21** was prepared by performing a Weinreb amidation on spiroketal **20** to give Weinreb amide **24** in 91% yield. Weinreb amide **24** was then reacted at $-78\text{ }^{\circ}\text{C}$ with vinyl bromide **9** pre-treated with *t*BuLi to give the enone product in 94% yield, which was then diastereoselectively reduced using $\text{Zn}(\text{BH}_4)_2$ at $-40\text{ }^{\circ}\text{C}$ to give allylic alcohol **21** in 80% yield and in 73:27 d.r. Because of the lower diastereoselectivity (73:27 versus 86:14 d.r.), this route was abandoned in favour of the first route involving LiBH_4 reduction, Parikh–Doering oxidation, and nucleophilic addition.



*Scheme 1.8. Synthesis of C12–C16 vinyl bromide **9***

The C12–C16 vinyl bromide **9**, which was used for both syntheses of allylic alcohol **21**, was in turn prepared by the sequence shown in Scheme **1.8**. The differentially protected aldehyde **25** was subjected to a chelate-controlled Sakurai allylation developed by Reetz³⁴ to give homoallylic alcohol **26** in 87% yield, which was then protected as a PMB ether using PMB trichloroacetimidate to give vinyl bromide **9** in 79% yield.

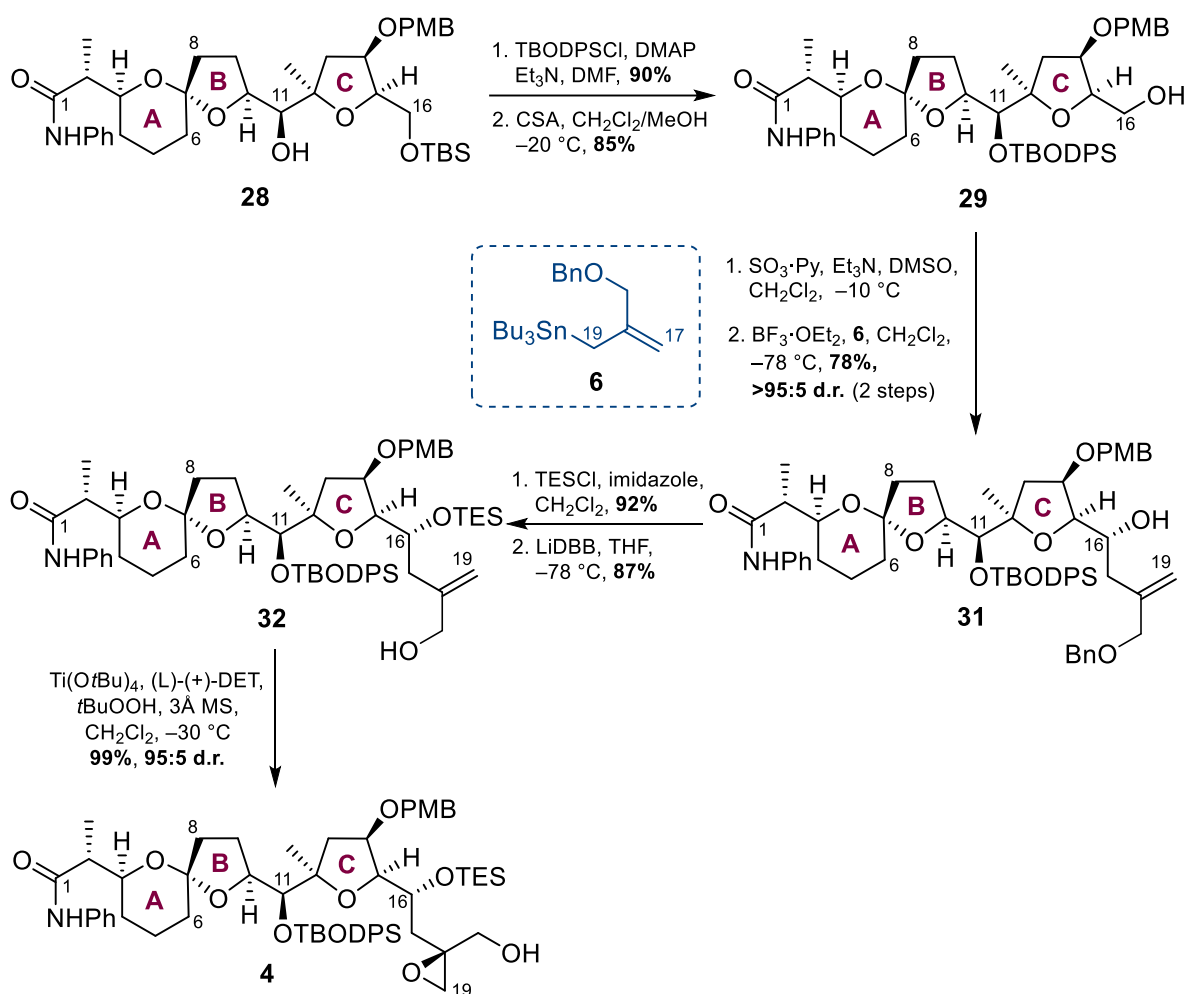
Having prepared allylic alcohol **21** through two routes, this spiroketal system now had to be elaborated into the ABC fragment bearing the additional C THF ring. To that end, allylic alcohol **21** was first debenzylated using LiDBB to give its diol in 81% yield. Subsequent epoxidation using [VO(acac)₂] and TBHP gave epoxide **26** in 99% yield, which was then subjected to an acid-catalysed THF ring formation *via* an intramolecular S_N2-type nucleophilic attack of the C15 hydroxyl group on C12 to give ABC diol **27** in 87% yield. A two-step Barton deoxygenation process was then performed on ABC diol **27**, which first involved its conversion to its carbonothioate in 75% yield *via* acylation with phenylchlorothionoformate at the primary hydroxyl group; this was followed by treatment of the carbonothioate with Bu₃SnH and AIBN at 160 °C for the deoxygenation step to give alcohol **28** in 72% yield.



Scheme 1.9. Elaboration of allylic alcohol **21** to ABC fragment **28**

The secondary hydroxyl group at C11 of alcohol **28** had to be protected with a group that would be stable to all reaction conditions throughout the remainder of the synthesis, yet be sufficiently reactive to be removed during the final global deprotection step to complete the total synthesis. The Evans group planned to use tris(dimethylamino)sulfur-

(trimethylsilyl)difluoride (TAS-F) for the global deprotection reaction because it was a mild and neutral fluoride-based reagent that would be unlikely to epimerise either chiral centres alpha to enolisable ketones in PTX-4 and its precursors, or the acid-sensitive C7 spiroketal moiety.^{33,35} Given these considerations, the *tert*-butoxydiphenylsilyl (TBODPS) ether protecting group was chosen, because it was a stable group yet readily cleaved by TAS-F, as demonstrated by model deprotection studies by Evans.³³

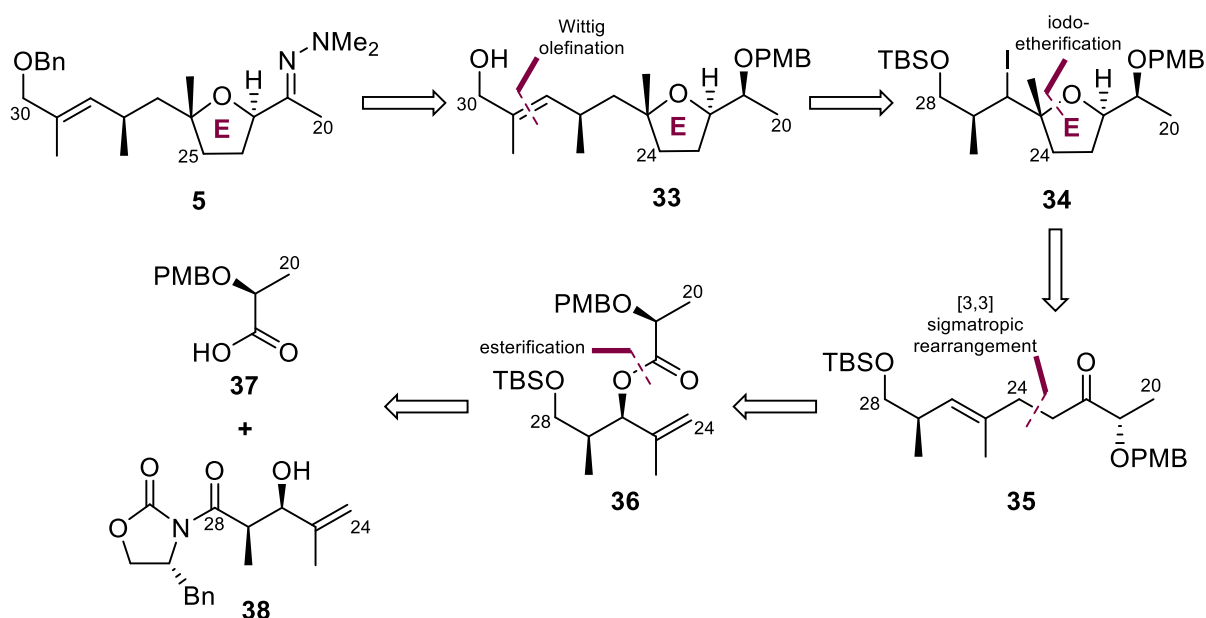


Scheme 1.10. Completion of synthesis of ABC epoxide **4**

Thus, alcohol **28** was treated with TBODPSCI in the presence of DMAP and Et₃N to give the corresponding TBODPS ether in 90% yield (Scheme 1.10). The TBODPS ether was then subjected to CSA in CH₂Cl₂/MeOH to selectively cleave the TBS ether at C16 to give primary alcohol **29** in 85% yield. Subsequently, a Parikh–Doering oxidation reaction was conducted on

primary alcohol **29** to give the corresponding aldehyde, the crude sample of which was directly carried over to the subsequent Keck allylation step involving allyl stannane **6** and $\text{BF}_3 \cdot \text{OEt}_2$ Lewis acid. This two-step sequence gave homoallylic alcohol **31** in 78% yield and in >95:5 d.r. A TES protection of **31**, followed by a LiDBB-mediated debenzoylation gave allylic alcohol **32**. Finally, subjecting alcohol **32** to an asymmetric Sharpless epoxidation reaction afforded ABC epoxide **4** in near quantitative yield and in 95:5 d.r.

1.5.3 Synthesis of C21–C30 E hydrazone **5**

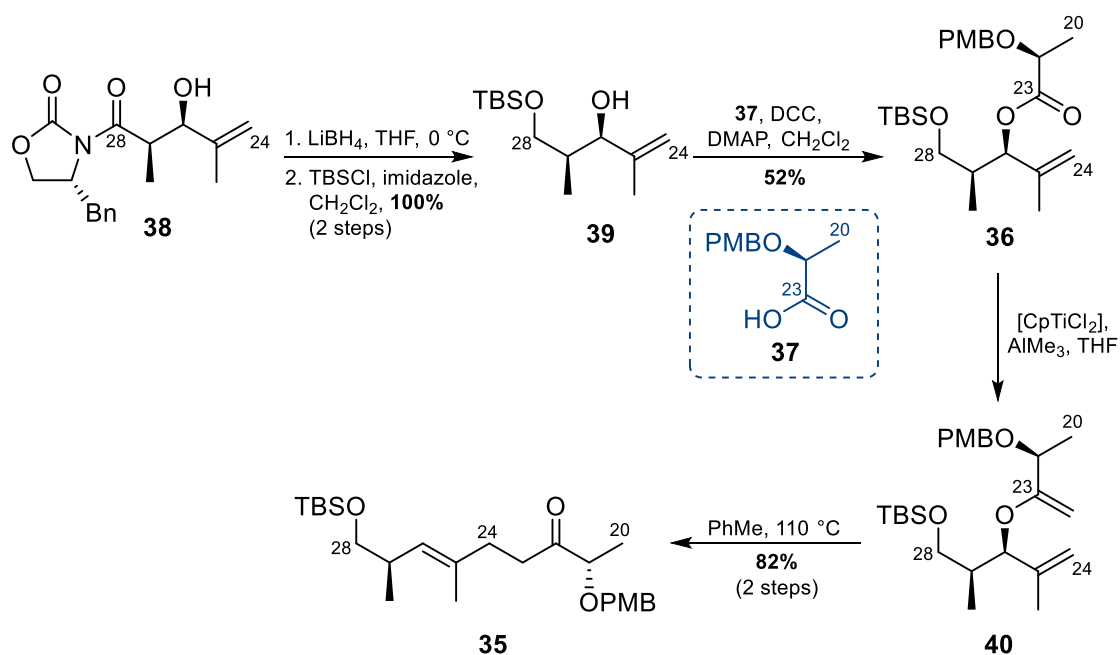


*Scheme 1.11. Retrosynthetic analysis of C20–C30 E hydrazone **5***

Evans' main retrosynthetic disconnections for C21–C30 E hydrazone **5** are summarised in Scheme 1.11. E hydrazone **5** may be derived from precursor **33**. A disconnection can be made at the C28–C29 double bond of precursor **33**, which can be established in the forward synthesis *via* a Wittig olefination reaction. The resulting C20–C28 THF **34** may be in turn derived from linear precursor **35** *via* a key iodoetherification reaction. The C23–C24 bond of linear precursor **35** may be disconnected to give ester **36**, which is a Claisen rearrangement

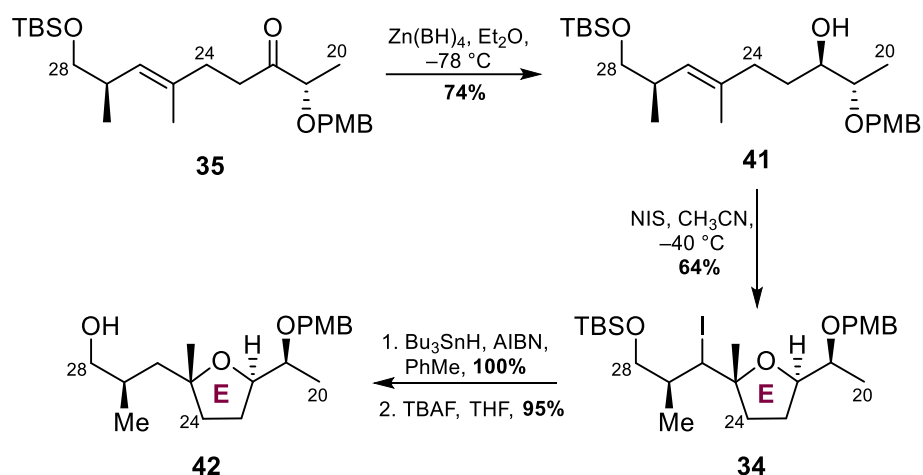
precursor. Finally, a disconnection at the C–O single bond at the ester gives the two building blocks, PMB-protected lactic acid **37** and *syn*-aldol adduct **38**.

The forward synthesis of the C20–C30 E hydrazone **5** commenced with the reduction and selective TBS protection of *syn*-aldol adduct **38** to give alcohol **39** in quantitative yield (Scheme 1.12). Esterification of alcohol **39** with carboxylic acid **37** using DCC and DMAP in CH₂Cl₂ afforded ester **36** in 52% yield, which was then converted to enol ether **40** using Tebbe's reagent; refluxing the species in toluene induced a Claisen [3,3] sigmatropic rearrangement to give C20–C28 ketone **35** in 82% yield over two steps.



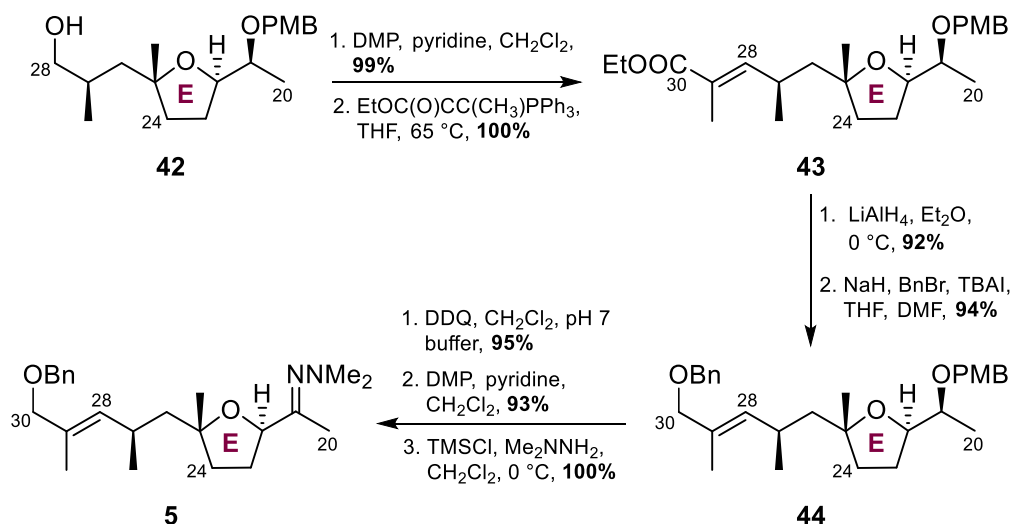
Scheme 1.12. Synthesis of C20–C28 ketone precursor **35**

A chelation-controlled carbonyl reduction of ketone **35** mediated by Zn(BH₄)₂ gave alcohol **41** in 74% yield (Scheme 1.13). The key iodoetherification reaction was then conducted on alcohol **41** using NIS at –40 °C to afford THF **34** in 64% yield. Treatment of THF **34** with AIBN and Bu₃SnH gave the de-iodinated product in quantitative yield and a subsequent TBAF-mediated TBS silyl ether cleavage formed alcohol **42** in 95% yield.



Scheme 1.13. Synthesis of alcohol 42

At this stage of the synthesis, the E THF moiety had been established in C20–C28 THF **42**. However, the additional C29–C30 carbon unit still had to be installed, along with multiple functional group interconversions into the target E hydrazone **5**. THF **42** was thus oxidised to its aldehyde with DMP in 99% yield, which was then subjected to a Wittig olefination with stabilised ylide $\text{EtOC(O)CC(CH}_3\text{)PPh}_3$ to give α,β -unsaturated carbonyl **43** in 100% yield (Scheme 1.14).

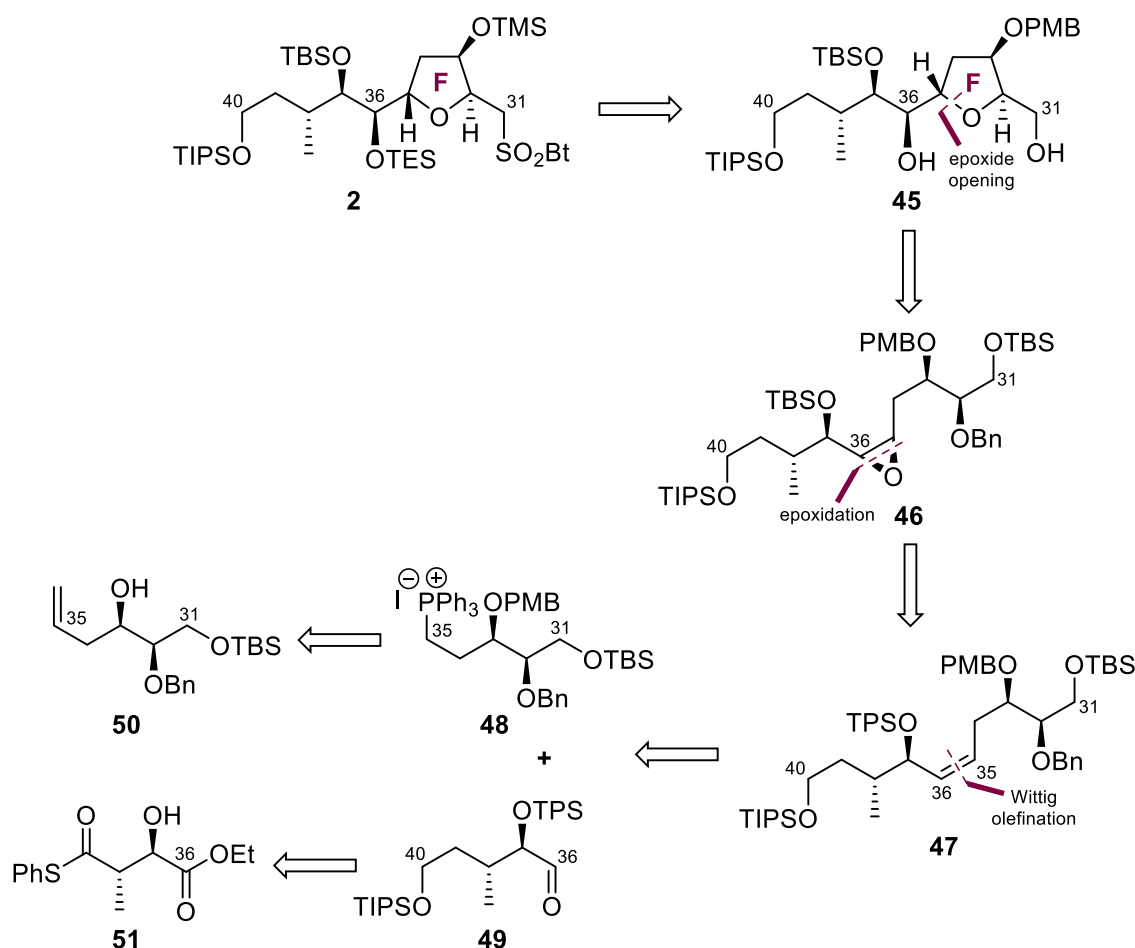


Scheme 1.14. Completion of synthesis of C20–C30 E hydrazone 5

A subsequent LiAlH_4 reduction of α,β -unsaturated carbonyl **43** gave the alcohol in 92% yield, which was benzylated using BnBr , NaH , and TBAI to form advanced precursor **44** in 94% yield. Selective removal of the PMB group at C21 of **44** using DDQ gave the unveiled secondary

alcohol in 95% yield, which was then oxidised to its ketone in 93% yield using DMP. Finally, a condensation reaction between the ketone and Me_2NNH_2 in the presence of TMSCl gave the C20–C30 E hydrazone **5** in quantitative yield.

1.5.4 Synthesis of C31–C40 F sulfone **2**

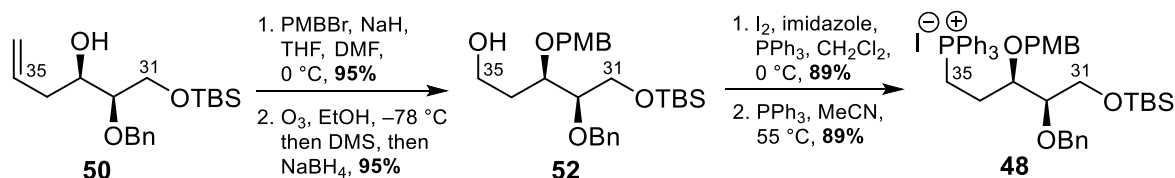


*Scheme 1.15. Retrosynthetic analysis of C31–C40 F sulfone **2***

Evans' main retrosynthetic disconnections for C31–C40 F sulfone **2** are summarised in Scheme **1.15**. F sulfone **2** may be derived from advanced precursor **45** through various protection group manipulations and functional group interconversions. A disconnection at the C35–O bond of precursor **45** can be conducted to unravel the compound into epoxide **46**, which may be derived from alkene **47**. Alkene **47** may be bisected at its C35–C36 double bond

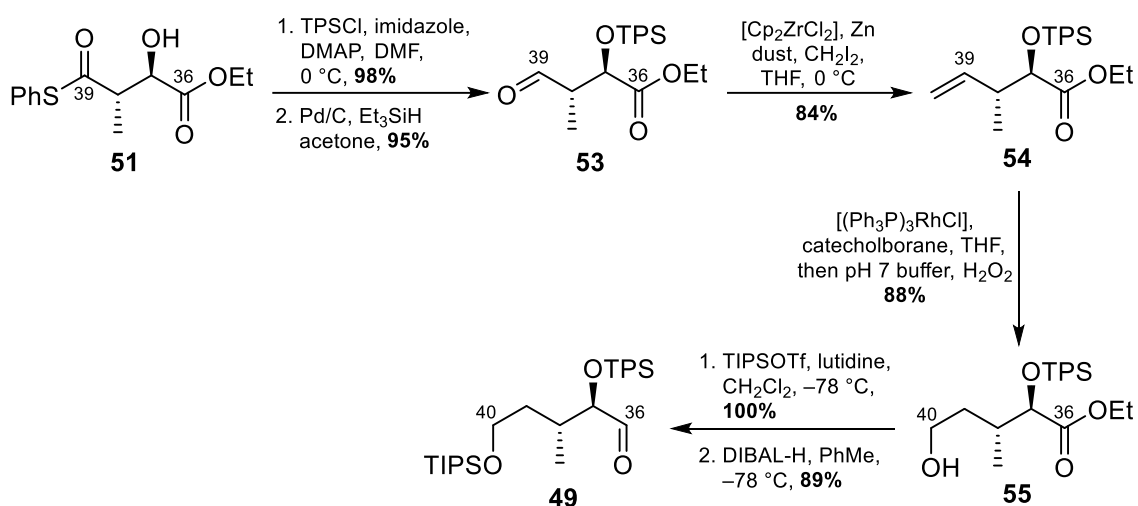
to give the two sub-fragments, triphenylphosphonium salt **48** and aldehyde **49**, which can be derived from building blocks **50** and **51** respectively.

The forward synthesis of C31–C40 F sulfone **2** commenced with the PMB protection of mannitol-derived building block **50**³⁴ to give the corresponding PMB ether in 95% yield (Scheme 1.16). An ozonolysis with a reductive NaBH₄ quench was then conducted on the compound, affording alcohol **52** in 95% yield. Performing an Appel reaction on alcohol **52** converted it to its alkyl iodide in 89% yield, which was then reacted with PPh₃ to give triphenylphosphonium iodide salt **48** – also in 89% yield.



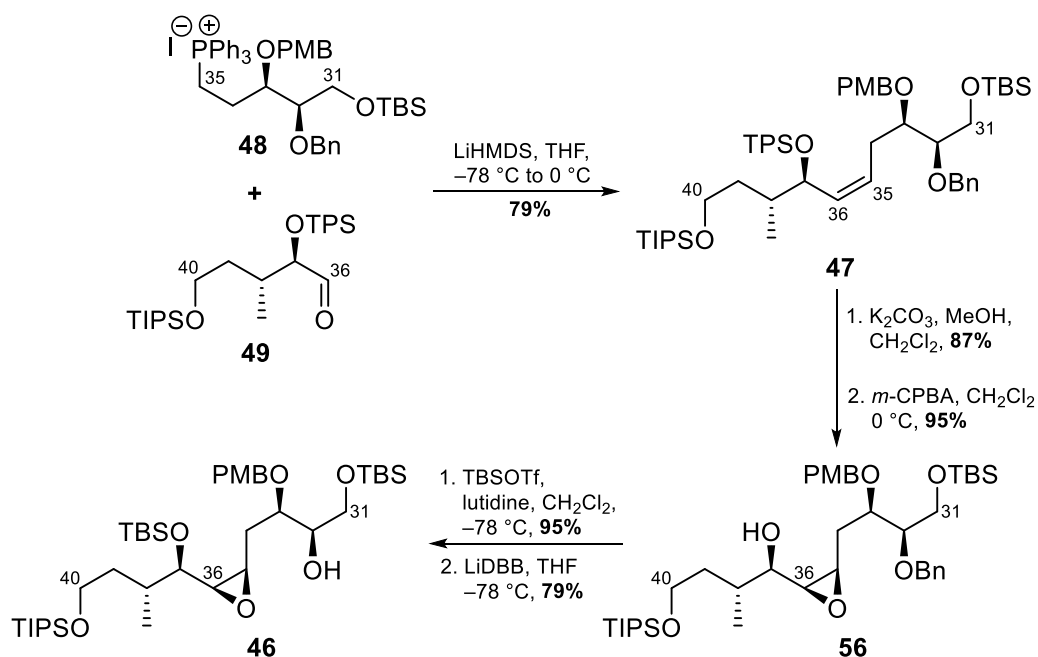
*Scheme 1.16. Synthesis of C31–C35 triphenylphosphonium salt **48***

Aldehyde **49**, the other partner of the planned Wittig olefination reaction, was prepared in a six-step sequence (Scheme 1.17), which began with the protection of the free hydroxyl group of building block **51** as a triphenylsilyl (TPS) ether in 98% yield, followed by Fukuyama reduction of the thioester moiety to give aldehyde **53** in 95% yield. A Lombardo methylenation was then conducted on aldehyde **53** to afford alkene **54** in 84% yield, which was then subjected to a rhodium-catalysed hydroboration reaction with catecholborane followed by a H₂O₂ oxidative work-up to give alcohol **55** in 88% yield. Alcohol **55** was protected as a TIPS ether using TIPSCl in the presence of lutidine in 100% yield. A final DIBAL-H reduction of the resulting ethyl ester afforded C36–C40 aldehyde **49** in 89% yield.



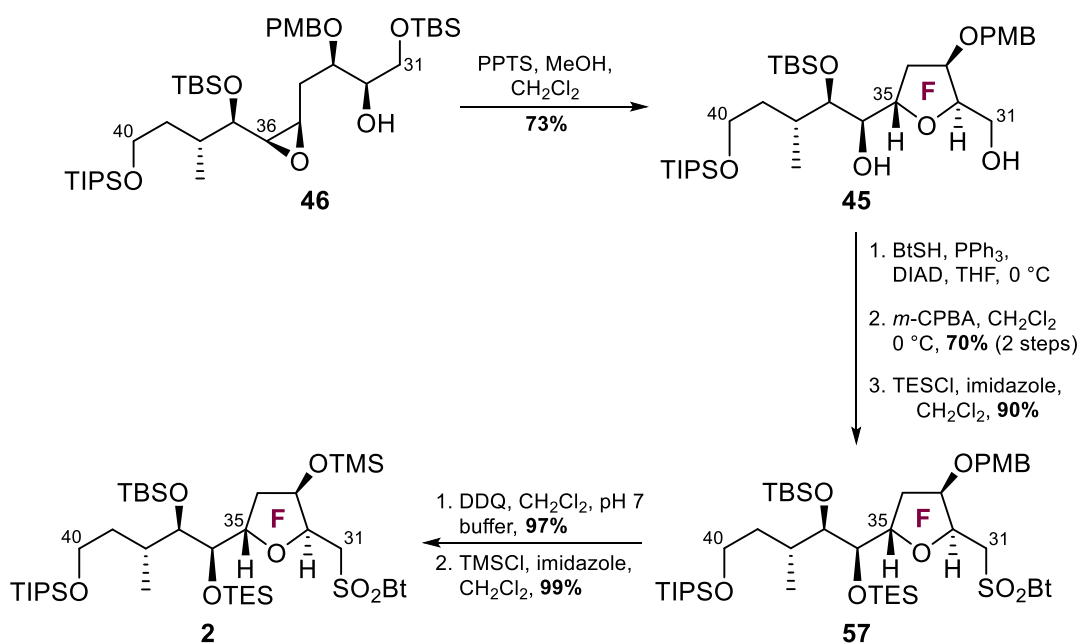
Scheme 1.17. Synthesis of C36–C40 aldehyde **49**

Having prepared both aldehyde **49** and triphenylphosphonium salt **48**, the pair of substrates were coupled *via* a Wittig olefination using LiHMDS to give in 79% yield C31–C40 alkene **47** (Scheme 1.18), which bears the full carbon skeleton of the target F sulfone **2**. Cleavage of the TPS ether of alkene **47** gave the corresponding alcohol in 87% yield, which was then epoxidised with *m*-CPBA to give epoxide **56** in 95% yield. Epoxide **56** was then subjected to two more protecting group manipulations – a TBS protection that gave 95% yield and a LiDBB-mediated debenzylation that gave 79% yield – to afford alcohol **46**.



Scheme 1.18. Synthesis of C31–C40 alcohol **46**

Acid-catalysed etherification and epoxide opening of alcohol **46** was then induced by treatment with PPTS in MeOH/CH₂Cl₂ to give THF **45** in 73% yield (Scheme 1.19); under these acidic conditions, the TBS ether at C31 was also cleaved. A Mitsunobu reaction was then conducted on THF **45** with benzothiazole sulphide (BtSH), PPh₃, and DIAD, followed by an *m*-CPBA oxidation to give the sulfone derivative in 70% yield over two steps. A TES protection of the sulfone gave advanced intermediate **57** in 90% yield. Finally, DDQ-mediated cleavage of the PMB ether of **57** gave the corresponding alcohol in 97% yield, which was then protected as a TMS ether using TMSCl in the presence of imidazole to give C31–C40 F sulfone **2** in 99% yield.

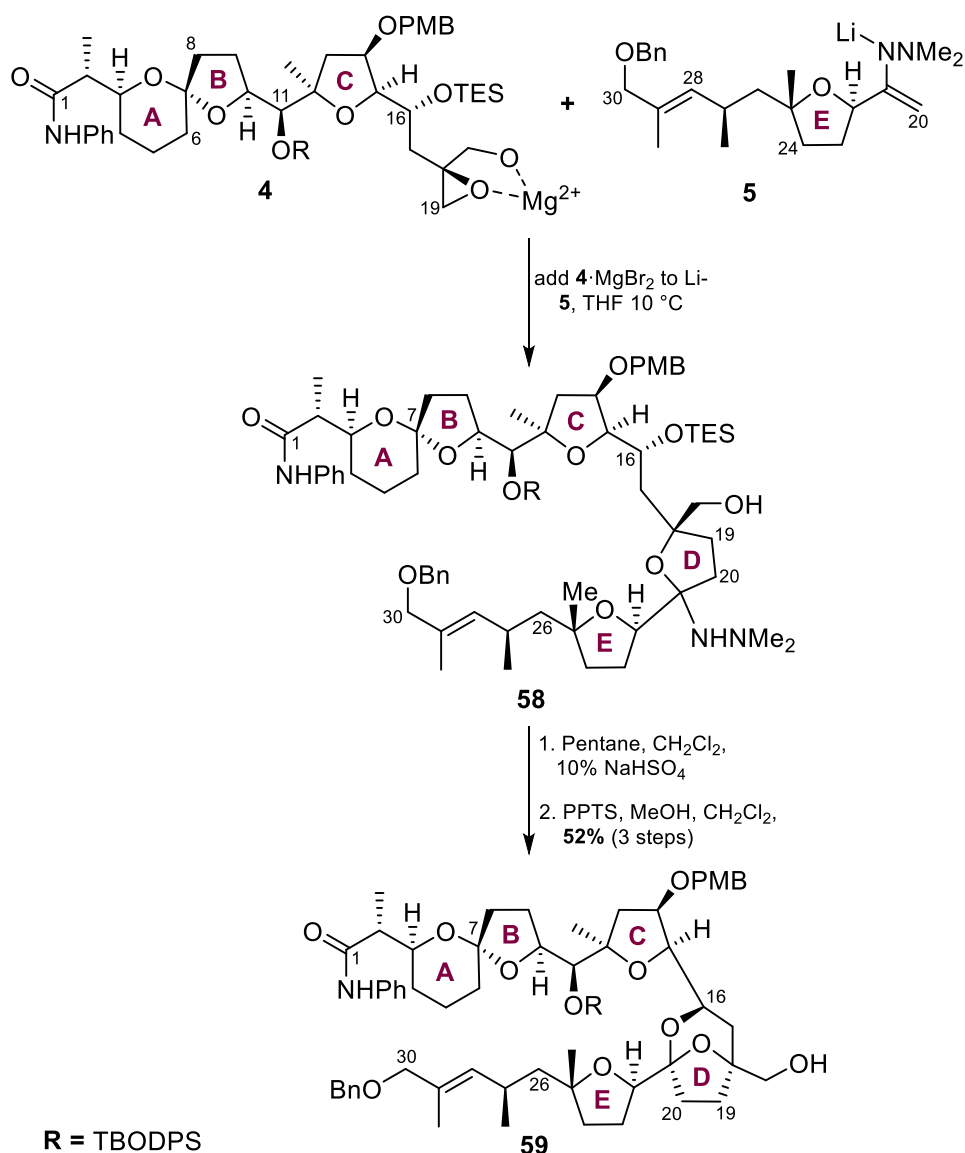


Scheme 1.19. Completion of synthesis of C31–C40 F sulfone **2**

1.5.5 Endgame of Evans' total synthesis of PTX-4

The endgame of Evans' total synthesis of PTX-4 involved sequentially coupling the three main fragments of the molecule, C1–C19 ABC epoxide **4**, C20–C30 E hydrazone **5**, and C31–C40 F sulfone **2**, whose syntheses were described in the previous sections.

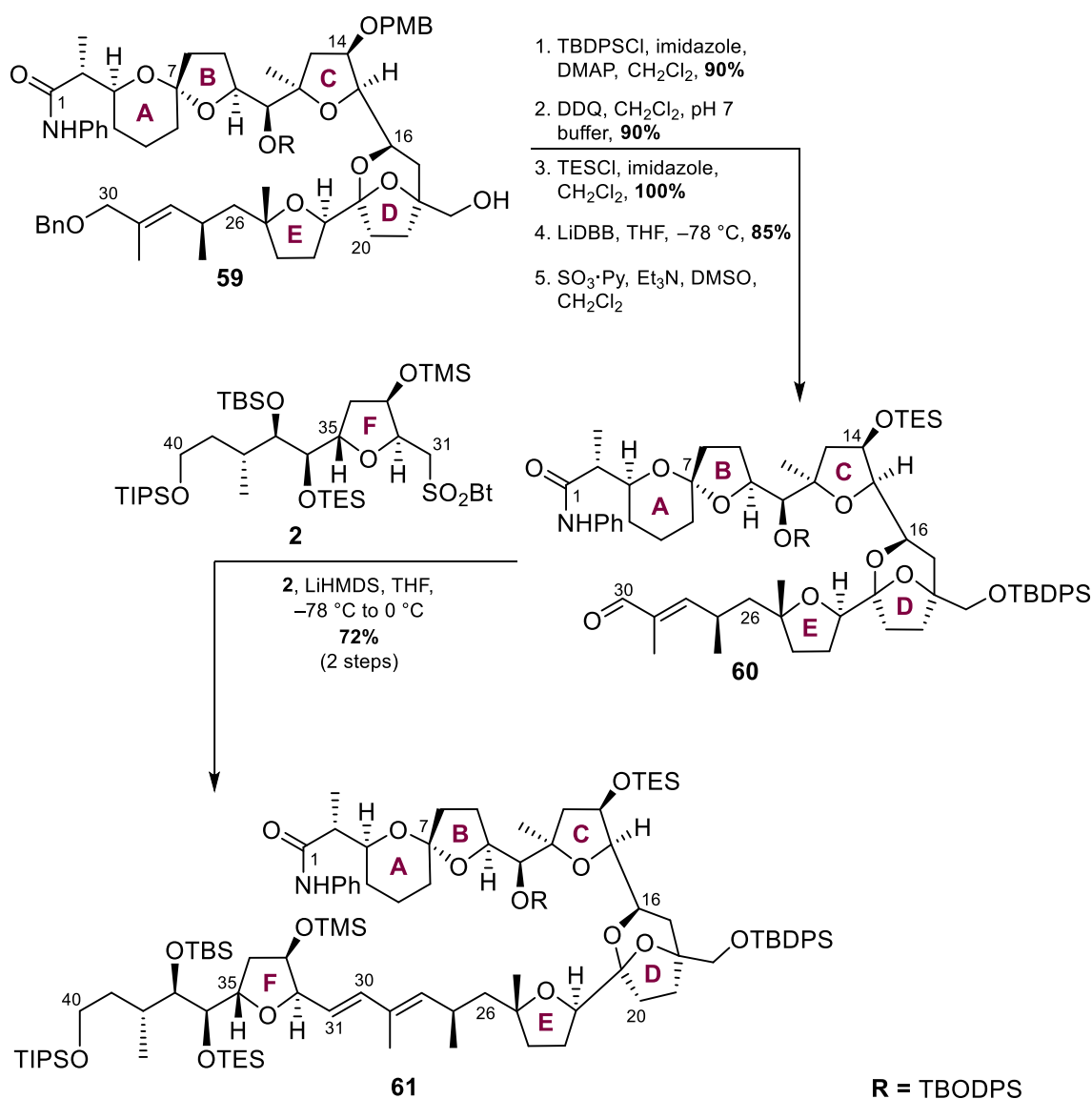
First, ABC epoxide **4** and E hydrazone **5** were coupled together by lithiating E hydrazone **5** with LDA and then reacting it with epoxide **4** pre-activated with MgBr_2 Lewis acid to give ABCE fragment **58** (Scheme 1.20). ABCE fragment **58** was then treated with 10% aq. NaHSO_4 to form the corresponding lactol, which was then exposed to PPTS and MeOH to cleave the TES group at C16 and induce ketalisation to form the bicyclic ketal-bearing ABCDE fragment **59** in 52% yield over three steps.



Scheme 1.20. Synthesis of C1–C30 ABCDE fragment 59

ABCDE fragment **59** was then subjected to a series of protecting group manipulations (Scheme 1.21): TBODPS ether protection of the primary hydroxyl group in 90% yield, removal

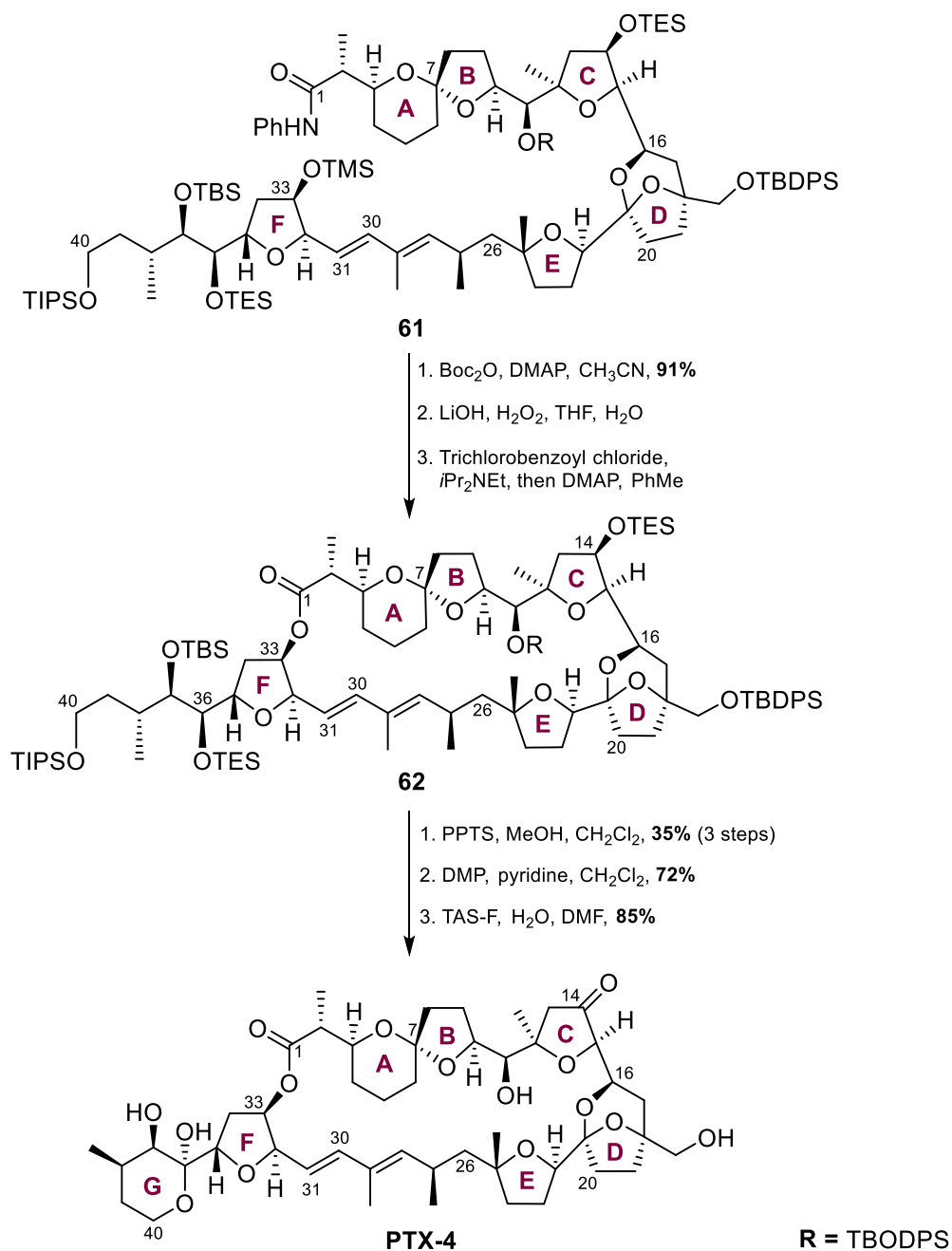
of the C14 PMB ether in 90% yield, TES ether protection of the C14 hydroxyl group in 100% yield, and debenzoylation at C30 in 85% yield. Finally, the unveiled C30 hydroxyl group was oxidised under Parikh–Doering conditions to give aldehyde **60**, which was then subjected to a modified Julia olefination reaction with F sulfone **2** to give ABCDEF fragment **61** in 72% over two steps.



*Scheme 1.21. Synthesis of C1–C40 ABCDEF fragment **61***

ABCDEF fragment **61** bore the full carbon skeleton of PTX-4 and had to be elaborated to establish the key macrolactone moiety in the natural product. First, the aniline amide

protecting group was activated with a Boc group in 91% yield using Boc₂O and DMAP (Scheme 1.22).



Scheme 1.22. Completion of Evans' total synthesis of PTX-4

The activated amide was then treated with LiOH and H₂O₂ to cleave the amide and the TMS ether at C33. A Yamaguchi macrolactonisation reaction was then conducted on the free carboxylic acid product to give macrolactone **62**. Treatment of macrolactone **62** with PPTS in MeOH and CH₂Cl₂ selectively cleaved the TES ethers at C14 and C36 to give the diol in 35%

yield over three steps; the unveiled hydroxyl groups were oxidised with DMP to give the ketone product in 72% yield. Finally, a global deprotection using TAS-F removed the remaining silyl ether protecting groups to give PTX-4 in 85% yield, thus concluding the synthesis. In summary, Evans' total synthesis of PTX-4 was accomplished in 36 linear steps with an overall yield of 0.3%.

The synthetic PTX-4 was subjected to acidic equilibration using 1% TFA in MeCN/H₂O over 12 h, which gave a mixture of PTX-1, PTX-4, and PTX-8 in a ratio of 11:10:79. This distribution of products was inconsistent with the ratio (29:14:57) observed by Yasumoto, who subjected PTX-4 under similar conditions over 48 h.⁶ A possible explanation for this discrepancy is that at least one of the PTX-4 samples had not fully equilibrated.

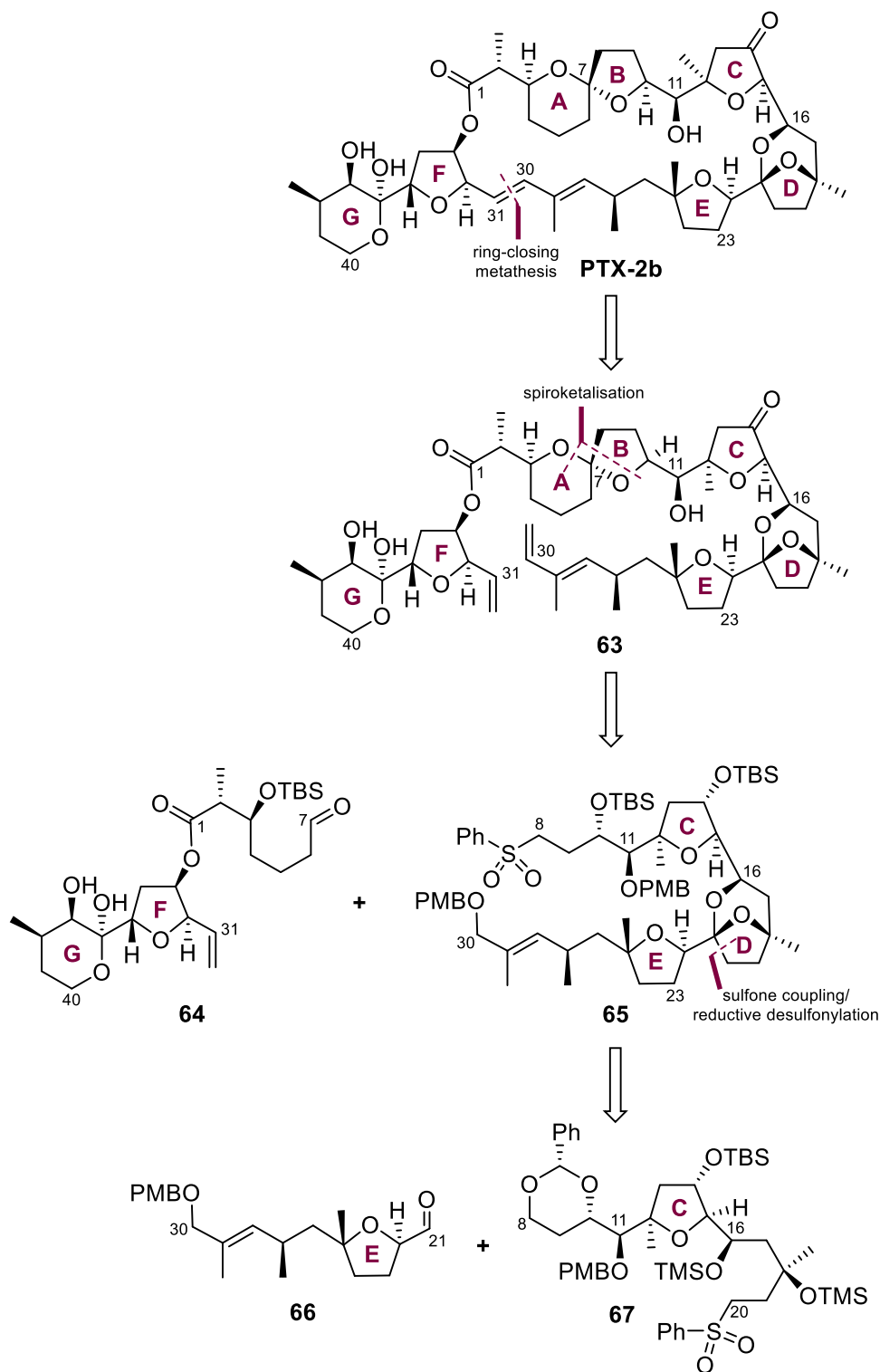
1.6 Fujiwara's total synthesis of PTX-2

1.6.1 Retrosynthetic analysis

Unlike PTX-4 which bears an anomeric [6,5]-spiroketal, PTX-2 has an unstable non-anomeric [6,5]-spiroketal, which increases the synthetic challenge of preparing this natural product and its precursors. Nevertheless, as the parent PTX and the most potent member of the PTX family, PTX-2 is an attractive total synthesis target. Only one total synthesis of PTX-2 has been completed to date, which was achieved by Fujiwara in 2014 after 20 years of work.^{23–28}

To side-step stability issues of handling PTX-2 precursors bearing a thermodynamically unstable non-anomeric spiroketal moiety, Fujiwara's approach was to access PTX-2 from anomeric spiroketal PTX-2b. Although PTX-2b itself is less stable than PTX-2, the former's non-macrocyclic precursors are unlikely to epimerise at the spiroketal centre. Thus, the principal

disconnections of Fujiwara's retrosynthetic analysis are focused on PTX-2b and are summarised in Scheme 1.23.



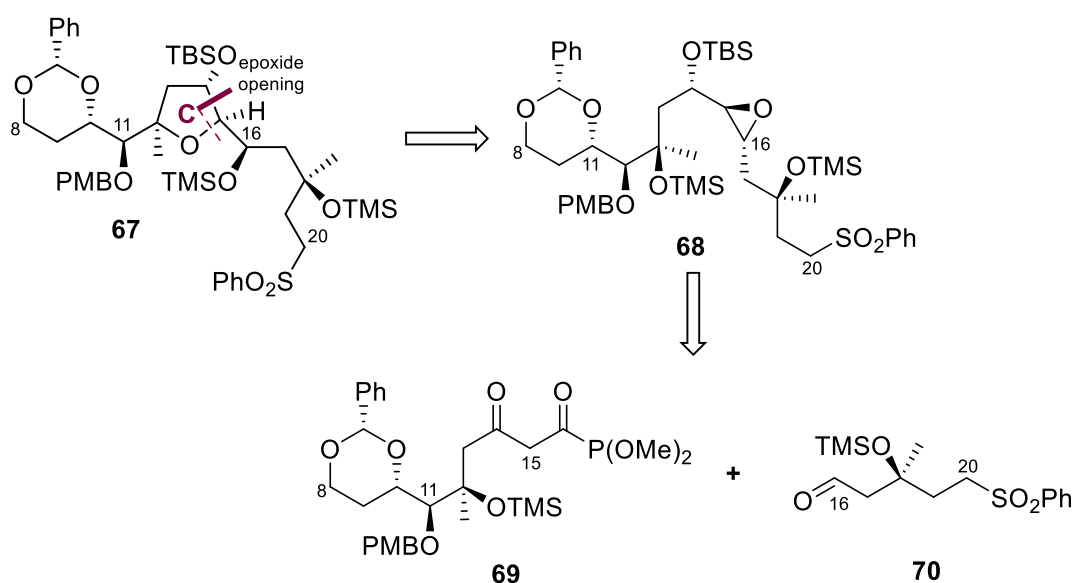
Scheme 1.23. Fujiwara's retrosynthetic strategy for PTX-2 and PTX-2b

A key disconnection at the C30–C31 double bond simplifies PTX-2 into advanced precursor **63**, and it was proposed that this bond will be formed in the forward synthesis *via* a late-stage

ring-closing metathesis reaction, whose mild conditions are suitable for sensitive functionality. A sulfone coupling–desulfonation strategy was intended to establish the AB spiroketal of advanced precursor **63**, and making the corresponding disconnections allows **63** to be simplified to FG fragment **64** and C8–C30 CDE fragment **65**. Using a similar sulfone coupling–desulfonation strategy to form the D bicyclic ketal of CDE fragment **65** allows the fragment to be bisected into C21–C30 E fragment **66** and C8–C20 C fragment **67**. The rest of this section will discuss the forward syntheses of C fragment **67**, E fragment **66**, and FG fragment **64** in that order, before finally describing the endgame of the total synthesis.

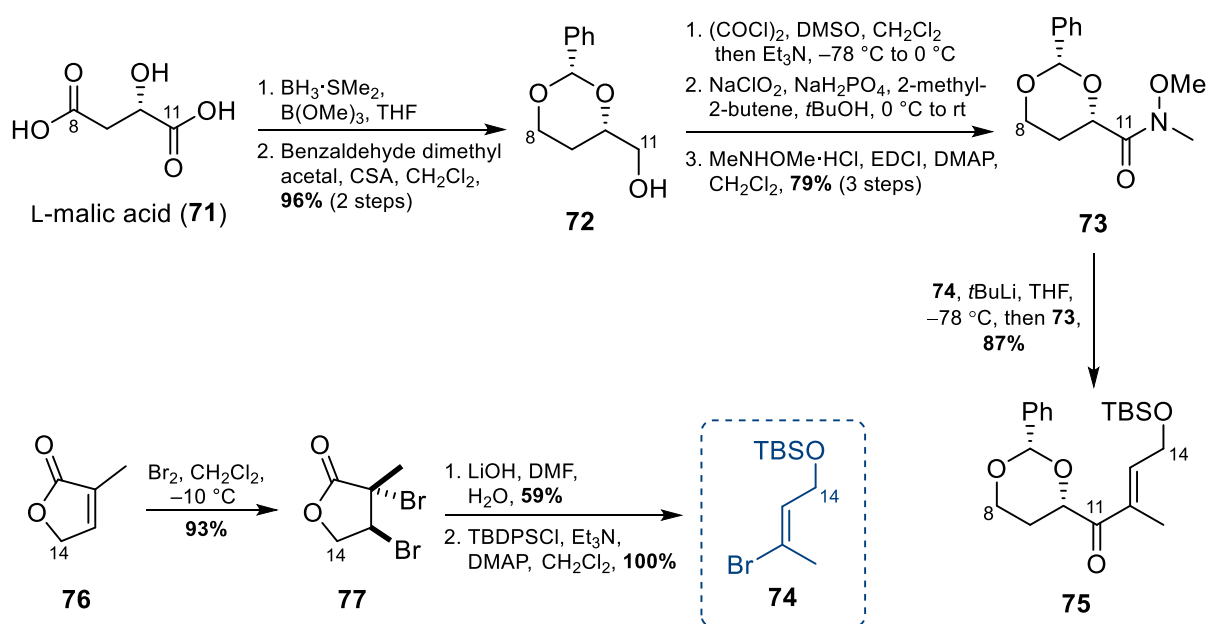
1.6.2 Synthesis of C8–C20 C fragment **67**

Similar to Evans' total synthesis of PTX-4, an intramolecular epoxide-opening strategy was proposed to establish the C THF ring moiety in PTX-2 in the Fujiwara synthesis (Scheme **1.24**). Performing the appropriate C17–O bond disconnection in C fragment **67** simplifies the compound to epoxide **68**, which can in turn be derived from the two sub-fragments, C8–C15 phosphonate **69** and C16–C20 aldehyde **70**, whose forward syntheses will be discussed below.



*Scheme 1.24. Retrosynthetic analysis of C8–C20 C fragment **67***

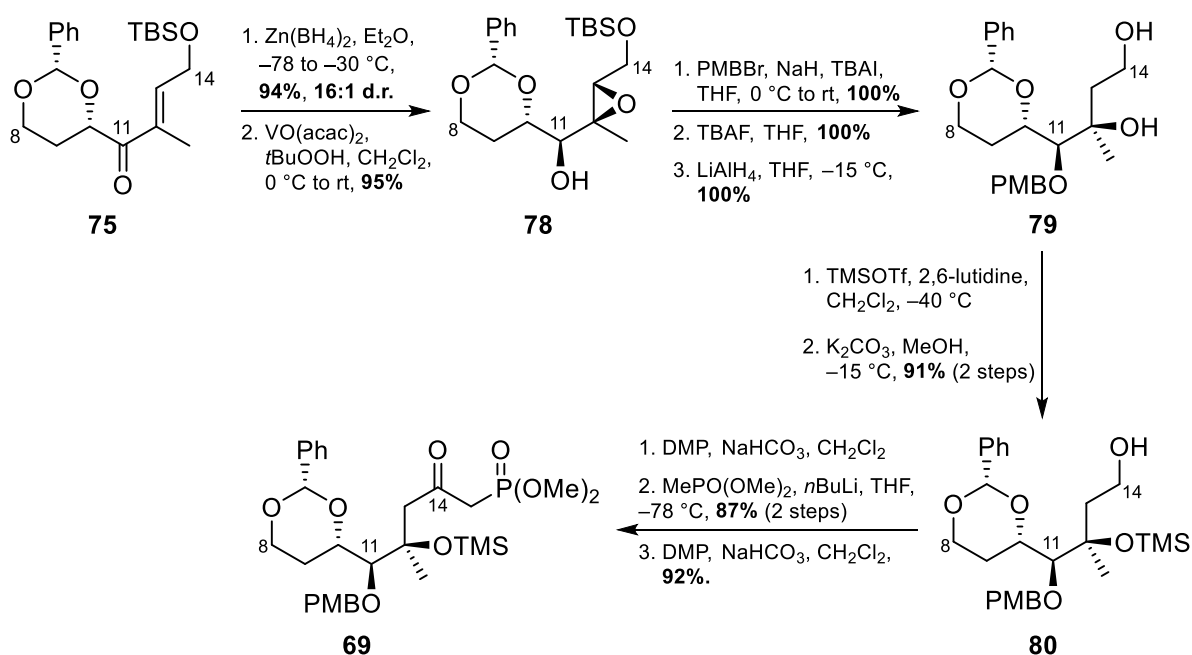
The synthesis of phosphonate **69**, and of PTX-2 as a whole, began with the $\text{BH}_3\cdot\text{SMe}_2$ reduction of L-malic acid (**71**) into its triol, followed by an acetal protection using benzaldehyde dimethyl acetal to give acetal **72** in 96% yield over two steps (Scheme 1.25). A Swern oxidation reaction was performed on acetal **73** to convert it to its aldehyde, which was in turn converted to its carboxylic acid *via* a Pinnick oxidation reaction. Subsequent amidation of the carboxylic acid with MeHOMe-HCl in the presence of EDCI and DMAP gave Weinreb amide **73** in 79% yield over three steps. Weinreb amide **73** was treated with lithiated vinyl bromide **74** to give the acyl substitution product enone **75** in 87% yield. Vinyl bromide **74**, in turn, was accessed from lactone **76** in three steps: First, bromination of lactone **76** gave dibromide **77** in 93% yield; hydrolysis and decarboxylative elimination of bromide **77** under basic conditions gave the allylic alcohol in 59% yield, which was then silylated with TBDPSCI to give vinyl bromide **74** in quantitative yield.



Scheme 1.25. Synthesis of C8–C14 enone **75**

Enone **75** was reduced diastereoselectively with $\text{Zn}(\text{BH}_4)_2$ to an allylic alcohol in 94% yield and in 16:1 d.r., which was then epoxidised with $\text{VO}(\text{acac})_2$ and $t\text{BuOOH}$ to epoxide **78** in 95% yield (Scheme 1.26). Epoxide **78** was then subjected to a PMB protection, TBS cleavage, and a

reductive epoxide opening with LiAlH₄ to give diol **79** in quantitative yield across all three operations. Protection of both hydroxyl groups of diol **79** as TMS ethers, followed by selective TMS cleavage at the C14 primary hydroxyl group using K₂CO₃ and MeOH gave alcohol **80** in 91% yield over two steps. Treatment of alcohol **80** with DMP oxidised it to its aldehyde, which was then reacted with lithiated MePO(OMe)₂ that underwent nucleophilic addition at the aldehyde moiety to produce a secondary alcohol in 87% yield over two steps. Finally, DMP oxidation of the newly generated secondary alcohol gave phosphonate **69** in 92% yield.

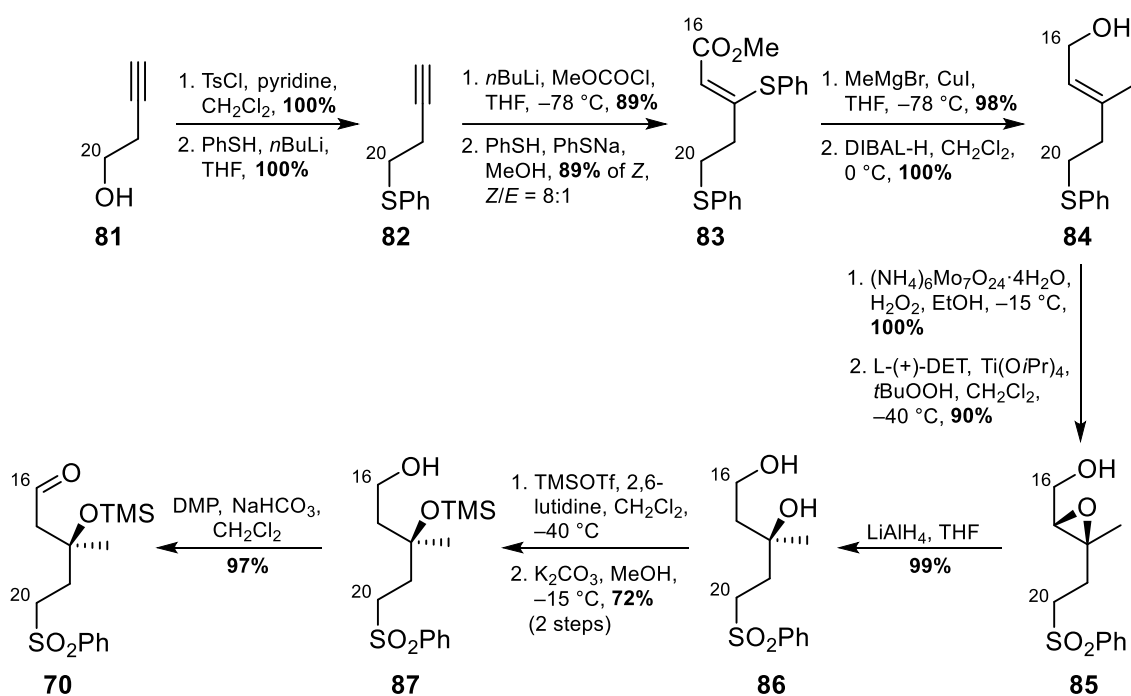


Scheme 1.26. Synthesis of C8–C15 phosphonate **69**

Aldehyde **70**, the other sub-fragment to make C8–C20 C fragment **68**, was prepared in 12 steps from 3-butyn-1-ol (**81**), as summarised in Scheme 1.27. A tosylation of 3-butyn-1-ol, followed by an S_N2 substitution with lithiated PhSH gave sulphide **82** in quantitative yield over both steps. Sulphide **82** was then lithiated with *n*BuLi and subjected to an electrophilic quench with MeOCOCl to give the corresponding ester in 98% yield, which was then reacted with PhSNa to give α,β-unsaturated ester **83** in 89% yield. Conjugate addition of methyl cuprate to α,β-unsaturated ester **83** followed by elimination of the thiophenolate gave the methyl-

substituted analogue in 98% yield, which was then reduced with DIBAL-H to allylic alcohol **84** in 100% yield.

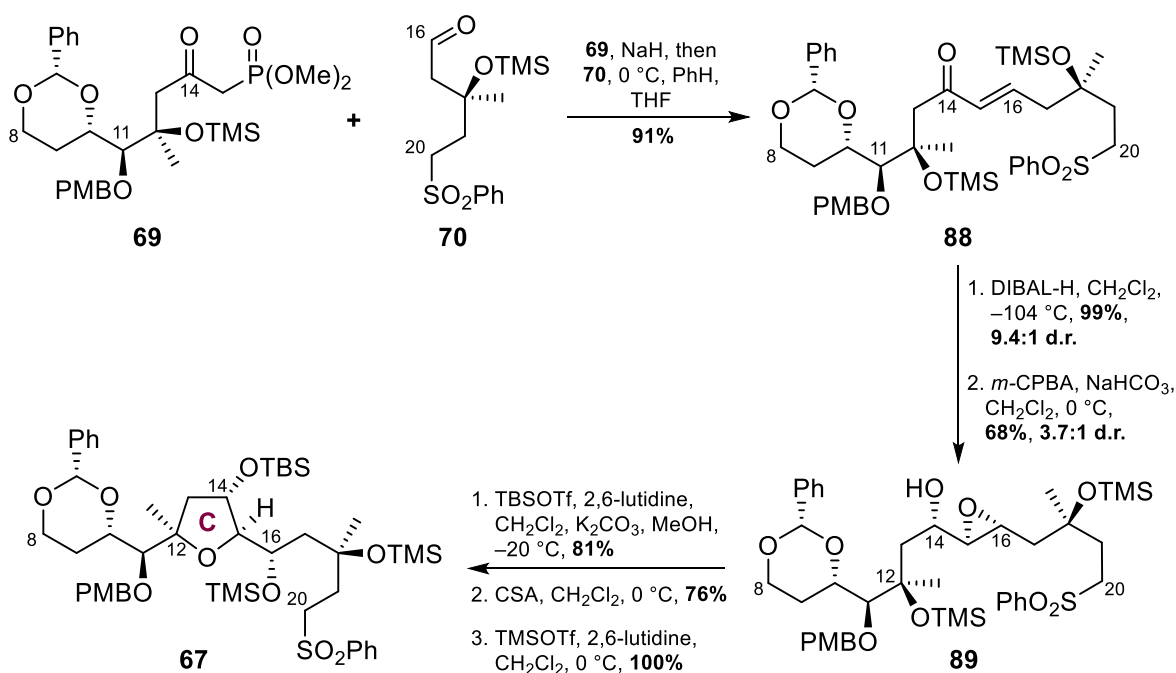
An oxidation of the sulphide moiety in **84** was conducted to give the sulfone in quantitative yield, which was then subjected to a Sharpless asymmetric epoxidation to give **85** in 90% yield. Reductive opening of epoxide **85** at the less hindered carbon was conducted using LiAlH₄ to give diol **86** in 99% yield. A two-step protecting group manipulation sequence that first converted both hydroxyl groups of diol **86** into TMS ethers and then selectively cleaved the TMS ether at the primary position gave alcohol **87** in 72% yield, which was oxidised using DMP to give aldehyde **70** in 97% yield.



Scheme 1.27. Synthesis of C16–C20 aldehyde **70**

Having prepared sub-fragments phosphonate **69** and aldehyde **70**, a Horner–Wadsworth–Emmons olefination reaction was conducted between the pair of substrates to form enone **88** in 91% yield (Scheme 1.28). A DIBAL-H reduction of enone **88** gave the corresponding allylic alcohol in 99% yield and in 9.4:1 d.r.; subsequent hydroxyl-directed epoxidation using *m*-CPBA

gave epoxide **89** in 68% yield and in 3.7:1 d.r. Epoxide **89** was treated with TBSOTf to form the TBS ether at the C14 hydroxyl group in 81% yield. Treatment of the TBS ether with CSA resulted in acid-induced cleavage of the C12 TMS ether and concomitant acid-catalysed epoxide-opening and cyclisation involving the newly unveiled C12 hydroxyl group to give the THF-bearing product in 76% yield. A final TMS protection of the C16 hydroxyl group then gave C fragment **67** in quantitative yield.

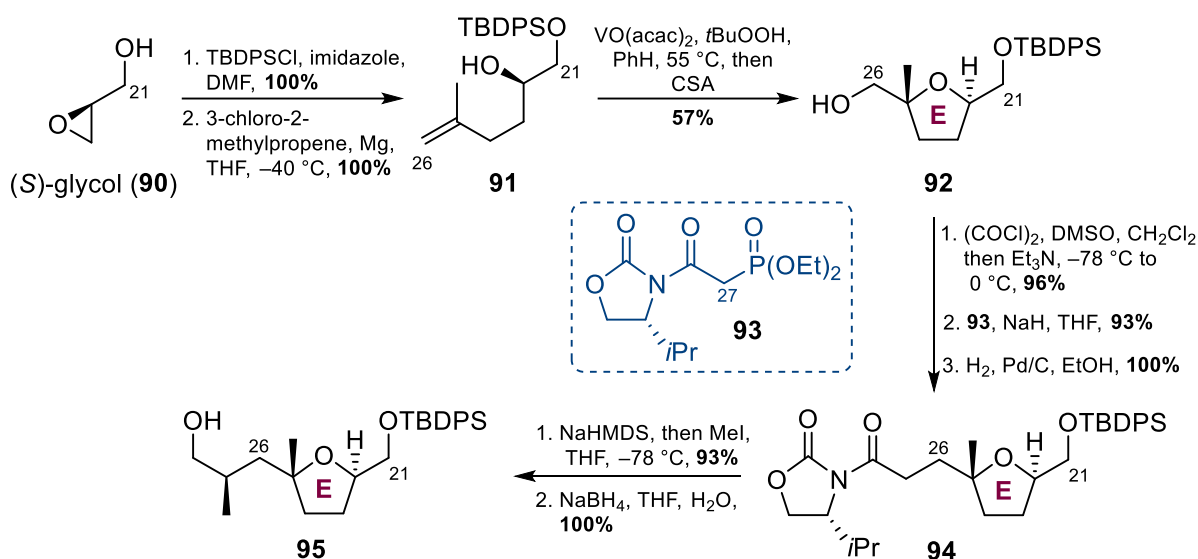


Scheme 1.28. Completion of synthesis of C8–C20 C fragment **67**

1.6.3 Synthesis of C21–C30 E fragment **66**

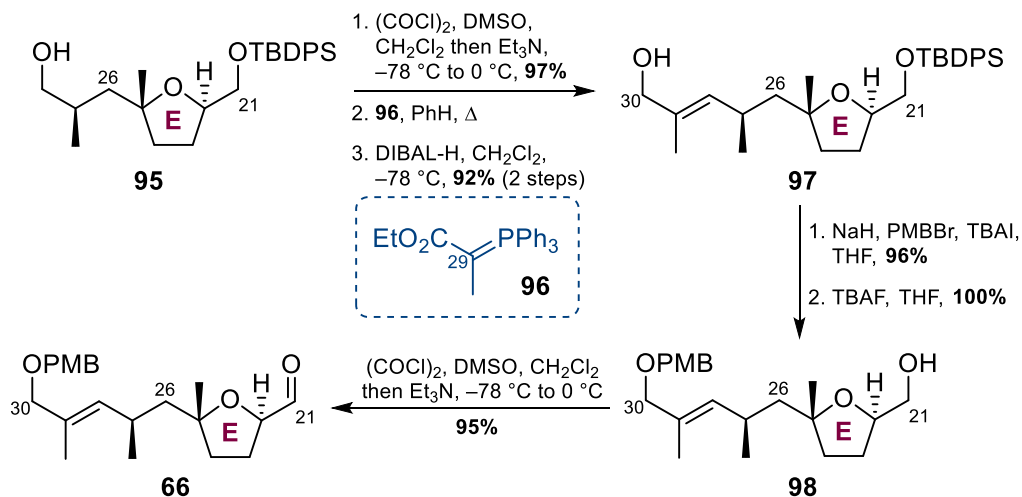
The synthesis of C21–C30 E fragment **66** commenced with the protection of (*S*)-glycidol (**90**) with TBDPSCI and imidazole, which proceeded in 100% yield. The resulting product was then reacted with *in situ* generated Grignard reagent formed from 3-chloro-2-methylpropene and Mg to give alcohol **91** in 100% yield, with the nucleophilic attack and epoxide-opening occurring at the less hindered carbon. Epoxidation of alcohol **91** gave the corresponding epoxide, which underwent epoxide opening from intramolecular nucleophilic attack by the

C20 hydroxyl group, giving THF **92** in 57% yield. A Swern oxidation reaction was then performed on THF **92** to oxidise the primary alcohol to an aldehyde in 96% yield, which was then subjected to a Horner–Wadsworth–Emmons olefination reaction with **93** in the presence of NaH to give the corresponding alkene in 93% yield. Hydrogenation of this alkene afforded THF **94** in quantitative yield. Deprotonation of THF **94**, followed by an electrophilic quench with MeI gave the corresponding methylated product in 93% yield, which was reductively cleaved by NaBH₄ to give alcohol **95** in 100% yield.



Scheme 1.29. Synthesis of alcohol **95**

Alcohol **95** was then subjected to a Swern oxidation reaction to convert it to its aldehyde in 97% yield (Scheme 1.30).

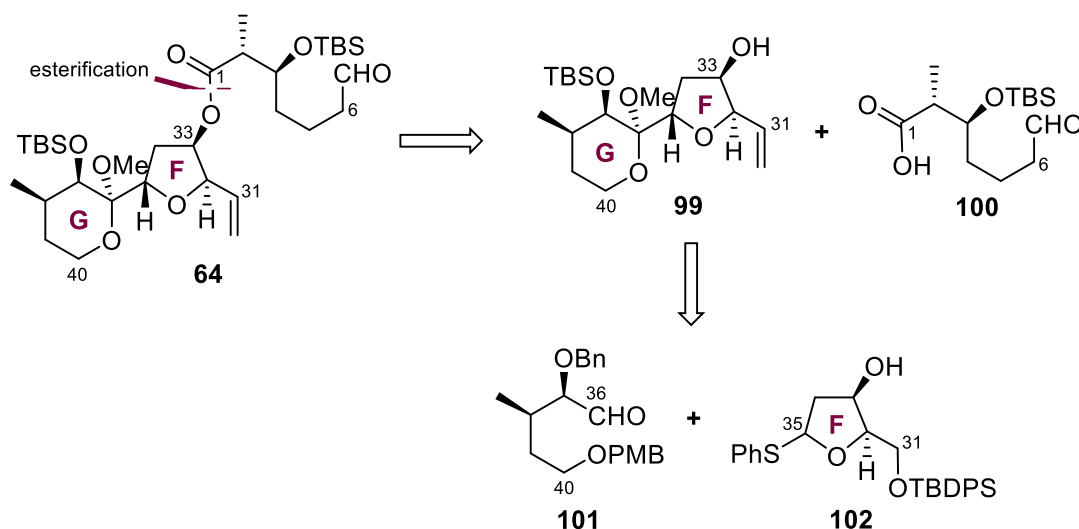


Scheme 1.30. Completion of synthesis of C21–C30 E fragment 66

The aldehyde was treated with ylide **96** in benzene with heating, giving the Wittig olefination α,β -unsaturated ester product, which was then reduced with DIBAL-H at $-78\text{ }^{\circ}\text{C}$ to give allylic alcohol **97** in 92% yield over two steps. PMB protection of allylic alcohol **97** in 96% yield, followed by TBAF-mediated TBDPS ether cleavage gave alcohol **98** in 100% yield. Finally, Swern oxidation of alcohol **98** afforded E fragment **66** in 95% yield.

1.6.4 Synthesis of FG fragment 64

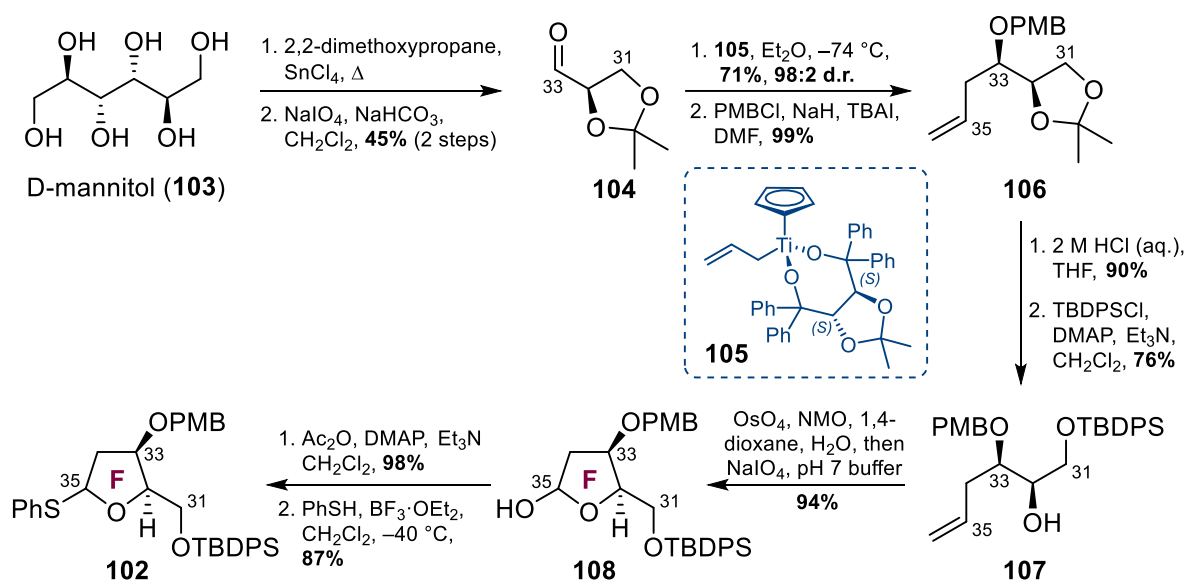
The retrosynthetic analysis of the final major fragment of Fujiwara's synthesis, FG fragment **64**, is shown in Scheme 1.31. A disconnection at the ester C1–O bond is proposed to simplify the compound into the FG alcohol **99** and C1–C6 carboxylic acid **100**. FG alcohol **99** may be further simplified to the two building blocks, aldehyde **101** and F THF **102**, whose forward syntheses will first be described.



Scheme 1.31. Retrosynthetic analysis of FG fragment 64

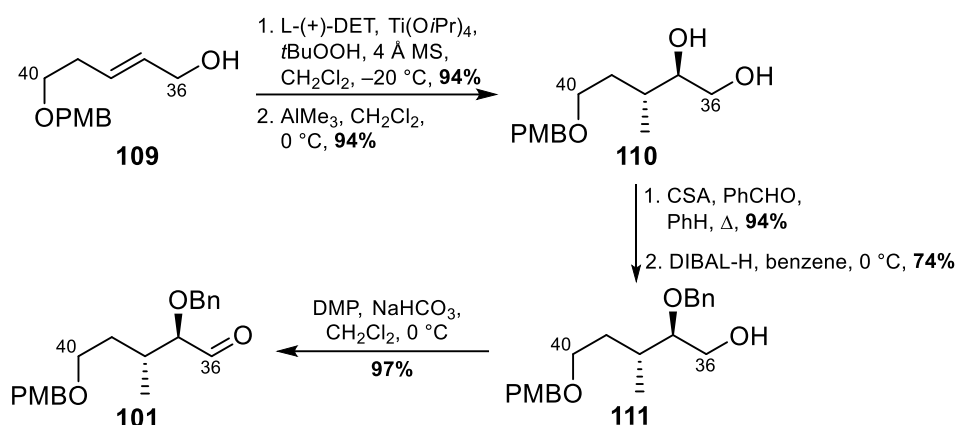
F ring THF **102** was prepared in nine steps from D-mannitol (**103**) as shown in Scheme 1.32. First, D-mannitol was treated with 2,2-dimethoxypropane and SnCl_4 , and the resulting *bis*-acetonide was oxidatively cleaved with NaIO_4 into aldehyde **104** in 45% yield over two steps.

Aldehyde **104** was then allylated with **105** to give the corresponding homoallylic alcohol in 71% yield and in 98:2 d.r., which was then PMB protected to give alkene **106** in 99% yield. Treatment of alkene **106** with aqueous HCl and THF cleaved the acetonide and unveiled the 1,2-diol in 90% yield, which was selectively protected with TBDPSCI at the less hindered primary hydroxyl group to afford alcohol **107** in 76% yield. THF ring cyclisation of alcohol **107** was initiated with oxidative cleavage of the C35 olefin with OsO₄ and NMO to give F THF **108** in 94% yield. Acetylation of the hemiacetal of F THF **108** gave the corresponding acetate in 98% yield, which was converted to thioether **102** in 87% yield *via* acetate displacement with PhSH under Lewis acidic conditions.



Scheme 1.32. Synthesis of THF F **102**

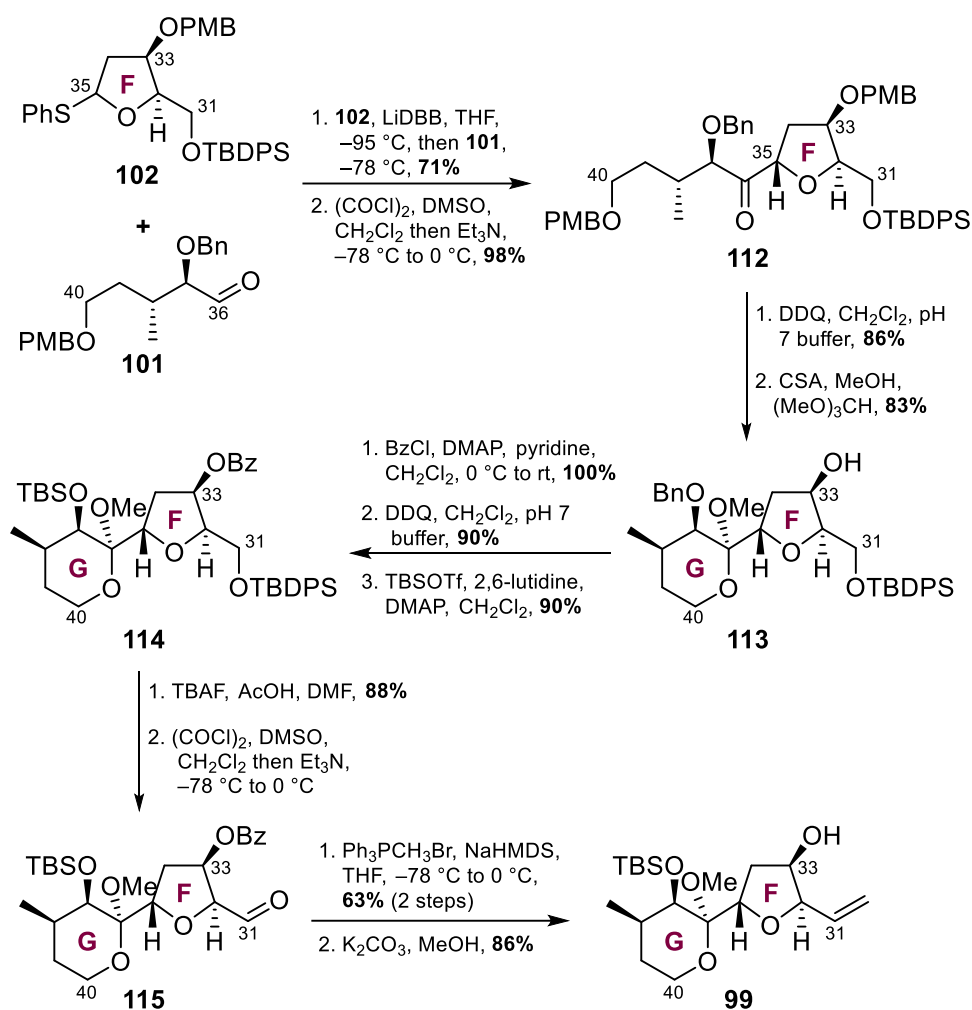
Sub-fragment aldehyde **101** was prepared in a five-step sequence (Scheme 1.33), which began with Sharpless asymmetric epoxidation of allylic alcohol **109** to give the corresponding epoxide in 94% yield.



Scheme 1.33. Synthesis of aldehyde 101

Subsequent epoxide opening at C38 with AlMe₃ gave diol **110** in 94% yield. Treatment of diol **110** with PhCHO in the presence of CSA gave the corresponding cyclic acetal in 94% yield, which was reacted with DIBAL-H to afford alcohol **111** in 74% yield. Finally, a DMP oxidation of alcohol **111** gave aldehyde **101** in 97% yield.

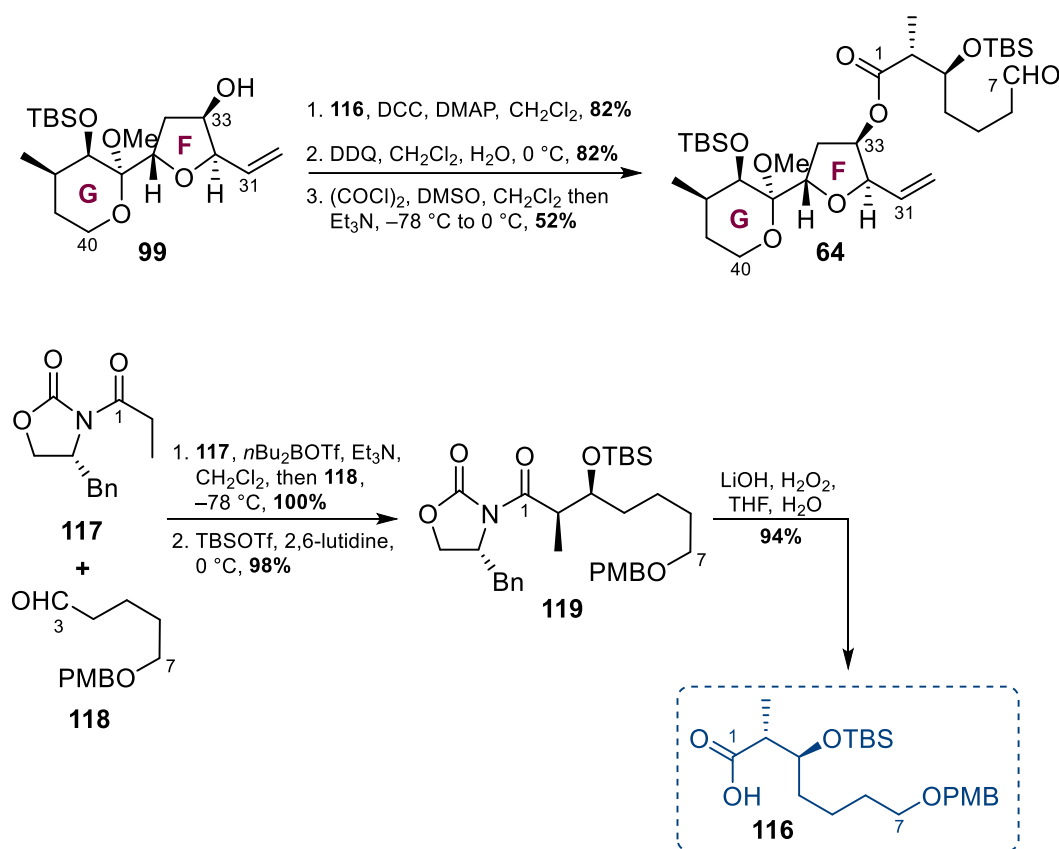
Having prepared sub-fragments aldehyde **101** and F THF **102**, both substrates had to be coupled together and then elaborated into FG alcohol **99**. The coupling of the two substrates was achieved by a Cohen reductive lithiation of F THF **102** with LiDBB, which was then quenched with aldehyde **101** to give the alcohol adduct in 71% yield (Scheme **1.34**).



Scheme 1.34. Synthesis of FG alcohol **99**

Subsequently, the alcohol was subjected to a Swern oxidation reaction to give ketone **112** in 98% yield. DDQ-mediated cleavage of both PMB ethers of ketone **112** gave the corresponding diol in 86% yield. Formation of the G ring cyclic ketal was induced by treatment of the diol with CSA, MeOH, and $(\text{MeO})_3\text{CH}$ to give ketal **113** in 83% yield. Protection of ketal **113** with BzCl in the presence of DMAP and pyridine gave the corresponding ester in quantitative yield. The benzyl ether of the ester product was then replaced with a TBS group in two steps to give silyl ether **114**. TBAF-mediated cleavage of the TBDPS ether of **114** in 88% yield, followed by Swern oxidation of the unveiled primary alcohol gave aldehyde **115**, which was subjected to a Wittig olefination using $\text{Ph}_3\text{PCH}_3\text{Br}$ and NaHMDS to give the corresponding alkene in 63% yield

over two steps. Treatment of the alkene with K_2CO_3 and MeOH hydrolysed the C33 benzoate ester to give FG alcohol **99** in 86% yield.



*Scheme 1.35. Completion of the synthesis of FG fragment **64***

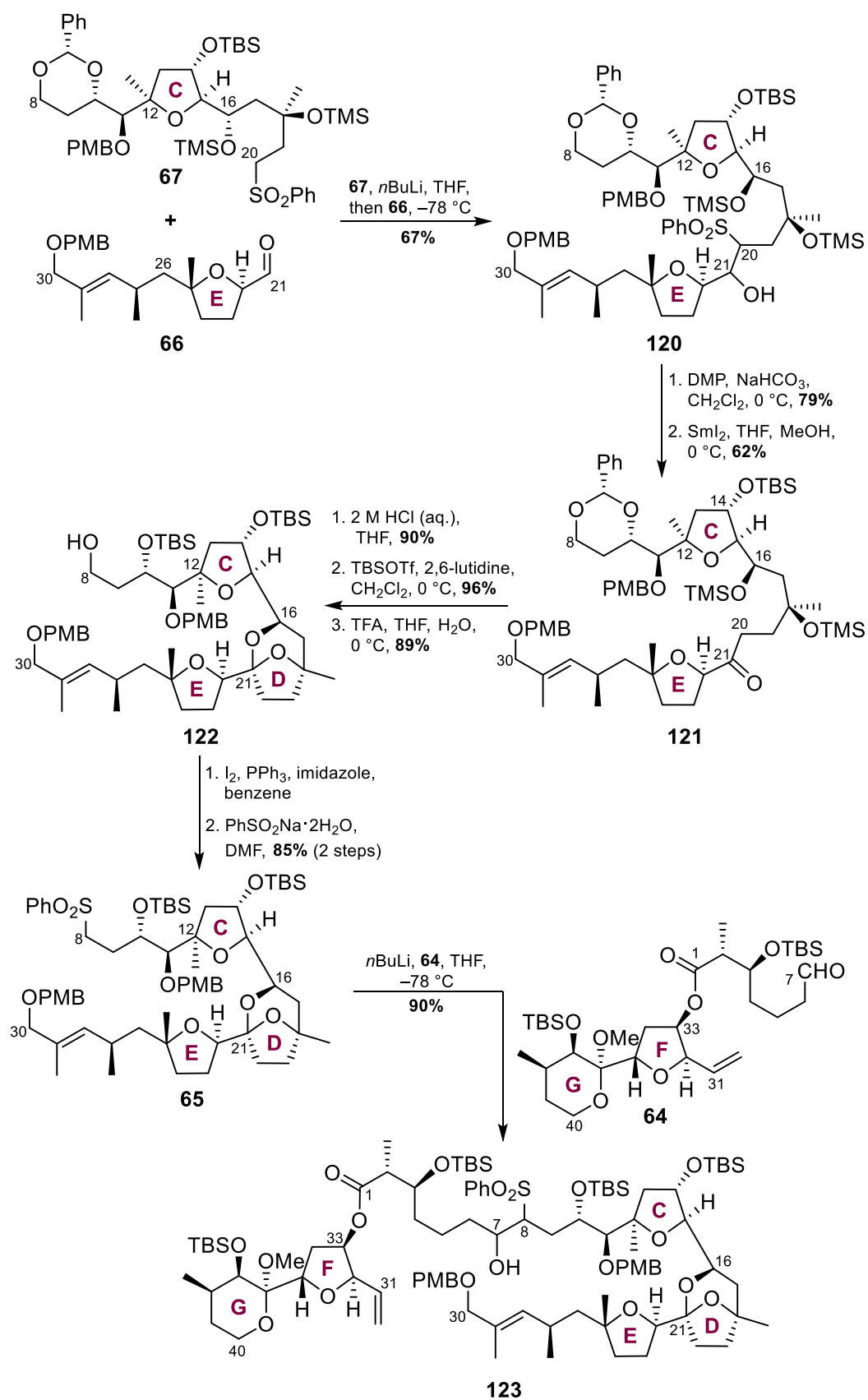
To complete the synthesis of FG fragment **64**, FG alcohol was subjected to an esterification reaction with carboxylic acid **116** to give the corresponding ester in 82% yield (Scheme 1.35). DDQ-mediated PMB ether cleavage in 82% yield, followed by Swern oxidation of the unveiled primary alcohol gave FG fragment **64** in 52% yield.

Carboxylic acid **116** was in turn prepared over three steps (Scheme 1.35). First, an asymmetric Evans aldol addition was conducted between oxazolidinone **117** and aldehyde **118** to give the aldol adduct in quantitative yield, which was TBS protected to give TBS ether **119** in 98% yield. Finally, the oxazolidinone of TSB ether **119** was cleaved using LiOH and H_2O_2 to give carboxylic acid **116** in 94% yield.

1.6.5 Endgame of Fujiwara's total synthesis of PTX-2

The endgame of Fujiwara's total synthesis of PTX-2 involved sequentially coupling the three main fragments of the molecule, C8–C20 C sulfone **67**, C21–C30 E aldehyde **66**, and FG aldehyde **64**, whose syntheses were described in the previous sections.

The sequence began with the lithiation of C sulfone **67** with *n*BuLi, followed by quenching this species with E aldehyde **66** to give CE alcohol **120** in 67% yield (Scheme **1.36**). DMP oxidation of CE alcohol gave the ketone in 79% yield, which was then treated with Sml₂ to remove the sulfone *via* an SET process to afford CE ketone **121** in 62% yield. Treatment of ketone **121** with dilute HCl induced acidic cleavage of both TMS ethers and promoted intramolecular ketalisation between the unveiled hydroxyl groups and the C21 ketone to form the D bicyclic ketal system. These acidic conditions also caused the acidic cleavages of the TBS ether at C14 and of the acetal at C8 and C10, giving the corresponding ketal-bearing triol in an impressive 90% yield despite the complexity of the transformation.

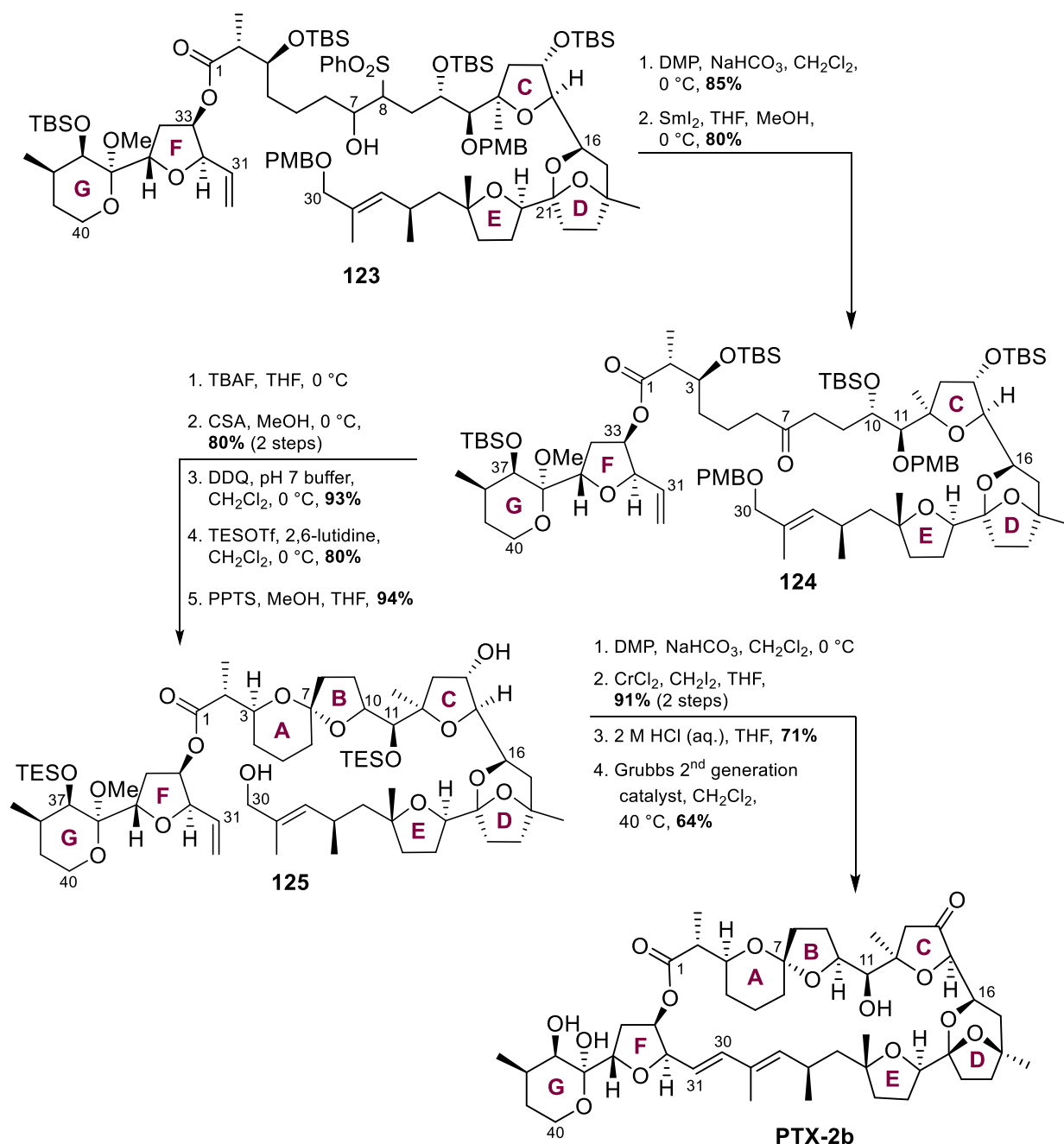


Scheme 1.36. Synthesis of CDEFG advanced precursor **123**

Treatment of this product with excess TBSOTf gave the fully silylated product in 96% yield, which was subjected to a selective TBS cleavage at C8 using TFA to give CDE alcohol **122** in 89% yield. Conversion of CDE alcohol **122** to its alkyl iodide *via* an Appel reaction followed by S_N2 displacement of the iodide with PhSO₂Na gave CDE sulfone **65** in 85% yield over two steps. A second sulfone coupling sequence that involved lithiating sulfone **65** with *n*BuLi and then quenching it with FG aldehyde **64** gave CDEFG fragment **123** in 90% yield.

At this stage of the synthesis, all three major fragments had been coupled together. However, the advanced precursor **123** still had to be further elaborated to form the AB spiroketal moiety and a macrocycle (Scheme **1.37**). Thus, precursor **123** was subjected to DMP oxidation to give the corresponding ketone in 85% yield, which was treated with SmI₂ to reductively cleave the sulfone at C8 to give ketone **124** in 80% yield. Treatment of ketone **124** with excess TBAF cleaved all four TBS ethers in the compound to give the corresponding tetraol. Subjecting the tetraol to a methanolic solution of CSA caused spiroketalisation to occur between the C7 ketone and the two hydroxyl groups at C3 and C10 to form the anomeric AB spiroketal in 80% yield over two steps. Performing a three-step protecting group manipulation sequence afforded diol **125**.

Treatment of diol **125** with DMP oxidised the C14 and C30 hydroxyl groups into a ketone and an aldehyde respectively, and the resulting product was olefinated at the C30 aldehyde *via* a Takai–Utimoto olefination reaction in 91% yield over two steps. Treatment of the product with HCl cleaved the C11 TES ether and converted the G cyclic acetal into a hemiacetal in 71% yield. A final ring-closing metathesis reaction using 2nd generation Grubbs catalyst was performed on the product, giving PTX-2b in 64% yield.

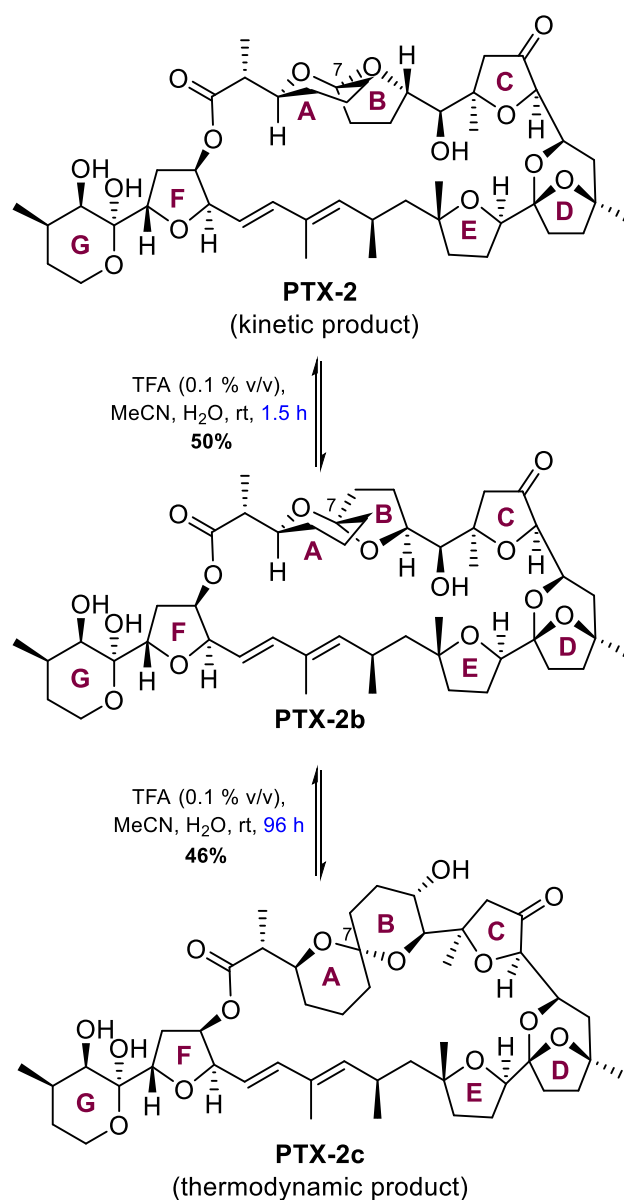


Scheme 1.37. Completion of the synthesis of PTX-2b

Treatment of PTX-2b with TFA over 1.5 h induced isomerisation at C7 of the spiroketal to give a mixture of PTX-2, PTX-2c and PTX-2b in 50%, 11% and 18% yields respectively (Scheme 1.38).

In contrast, subjecting PTX-2b to similar conditions but over a longer period of 96 h gave PTX-2c as the major species (46% yield), together with PTX-2 in 22% yield and PTX-2b in 18% yield.

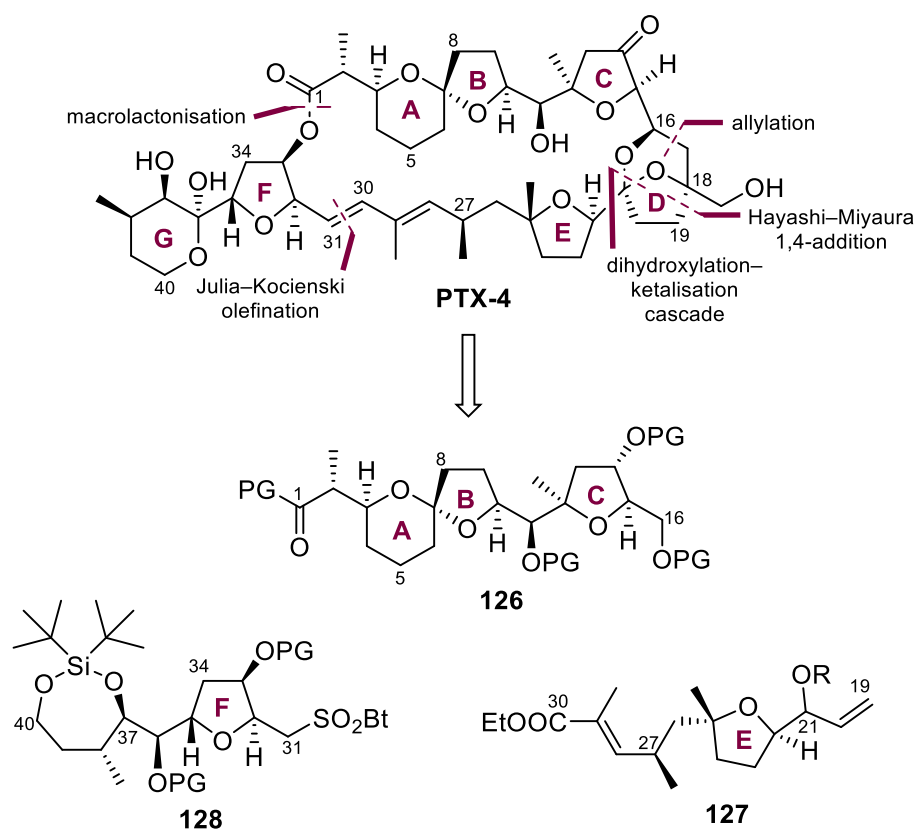
Thus, Fujiwara's total synthesis of PTX-2 was accomplished in 43 linear steps from L-malic acid with an overall yield of 0.2%.



Scheme 1.38. Acid-mediated isomerisations of PTX-2b into PTX-2 and PTX-2c

1.7 Donohoe's approach to PTX-4

The principal disconnections of Donohoe's retrosynthetic analysis of PTX-4 are summarised in Scheme 1.39. These disconnections include: a disconnection at the C1–O ester bond formed *via* macrolactonisation, a disconnection at C16–C17 formed *via* a Felkin–Anh-controlled allylation, a disconnection at C18–C19 formed *via* a Hayashi–Miyaura 1,4-addition reaction, a disconnection at C21 in the D bicyclic ketal system formed *via* a dihydroxylation–ketalisation cascade, and a disconnection at C30–C31 formed *via* a modified Julia olefination reaction.



Scheme 1.39. Donohoe's retrosynthetic strategy for PTX-4

Upon making these disconnections, PTX-4 is simplified into the three major fragments, C1–C16 ABC fragment **126**,³⁰ C19–C30 E fragment **127**,^{29,31} and C31–C40 F fragment **128**.³¹ Derivatives of these three fragments have been previously published by the Donohoe group. However, there remained multiple key challenges that had to be overcome for completion of the total synthesis. These challenges included:

- Preparing gram or multi-gram quantities of complex fragments, whose syntheses may take up to 20 or more linear steps.
- Producing novel derivatives of the fragments where appropriate – these include finetuning the protecting group strategy at C1 of ABC fragment **126**, as well as elaborating the fragment into a suitable coupling partner for the key bond-forming reactions to unite the fragments.

- c) Executing the key bond-forming steps in the real system and optimising them where appropriate. Extensive optimisation studies on simplified models have already been conducted by the Donohoe group for several of the key reactions highlighted in Scheme **1.39**, including the allylation reaction, the Hayashi–Miyaura 1,4-addition reaction, and the dihydroxylation–ketalisation cascade.^{29,36}
- d) Re-optimising certain steps in the fragment syntheses that suffer reproducibility issues.

Detailed discussion and background information of these listed challenges and of the syntheses of the PTX-4 fragments are provided in chapters 2, 3, and 4.

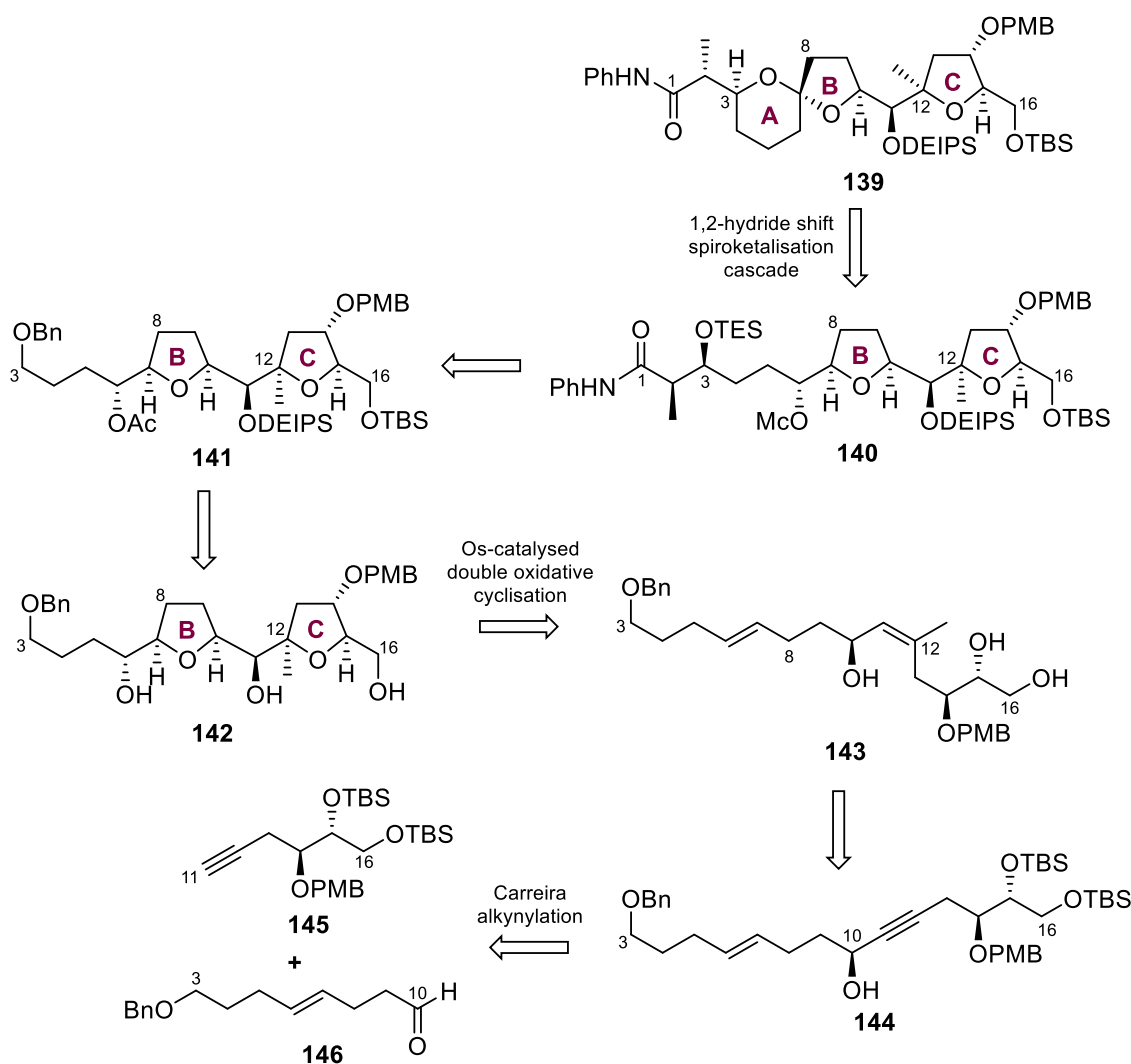
CHAPTER 2

The ABC Fragment

2.1 Chapter overview

This chapter details my work on the C1–C16 ABC fragment of PTX-4. The chapter begins with a retrosynthesis of the fragment and then discusses all the forward steps towards its preparation. Moreover, the chapter features extensive discussions on the optimisation efforts for key steps, including the osmium-catalysed double oxidative cyclisation step and the 1,2-hydride shift spiroketalisation cascade. Other major challenges, such as the unexpectedly difficult removal of an Evans oxazolidinone auxiliary, are also discussed.

2.2 Retrosynthesis of ABC fragment 139

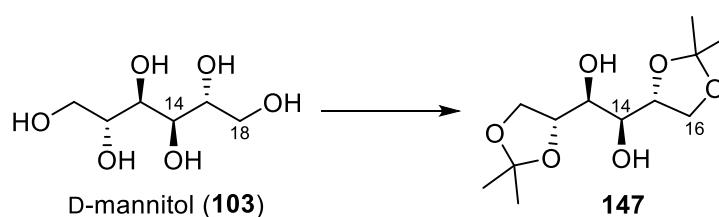


Scheme 2.1. Retrosynthetic analysis of ABC fragment 139

As shown in the retrosynthetic analysis in Scheme 2.1, ABC fragment **139** can be directly accessed from chloromesylate **140** via a 1,2-hydride shift spiroketalisation cascade. Chloromesylate **140** can in turn be derived from **141**, which can be simplified further to *bis*-THF **142**. The THF rings of *bis*-THF **142** can be rapidly established by the osmium-catalysed double oxidative cyclisation of triol **143**. Triol **143** can be obtained in two steps from **144**, which is the Carreira alkynylation product of sub-fragments **145** and **146**, whose forward syntheses the subsequent sections will detail. Close analogues of ABC fragment **139** have been previously prepared by Dr Radoslaw Lipinski³⁷ and Dr Xuezheng Yang,³⁸ former DPhil students in the Donohoe group – my work was based on these past studies.

2.3 Synthesis of C11–C16 alkyne **145**

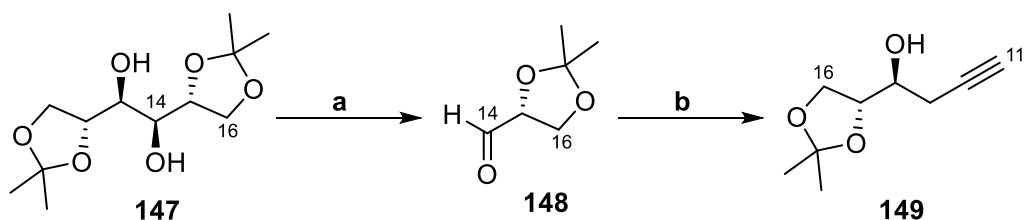
The longest linear sequence of the ABC fragment, and indeed of the proposed overall synthesis of PTX-4, begins with the reaction of D-mannitol (**103**) with 2,2-dimethoxypropane and catalytic *p*TSA to afford *bis*-acetonide **147** in 56% yield (Scheme 2.2). Because the preparation of the ABC fragment was projected to take over 20 linear steps, the reaction was conducted at 100 g scales.



Reagents and conditions: 2,2-dimethoxypropane, *p*TSA, DMSO, rt, 16 h, 56%

*Scheme 2.2. Synthesis of bis-acetonide **147***

bis-Acetonide **147** was then oxidatively cleaved by NaIO₄ at a 30 g scale to give aldehyde **148** (Scheme 2.3), which was directly carried over to the subsequent reaction without purification.



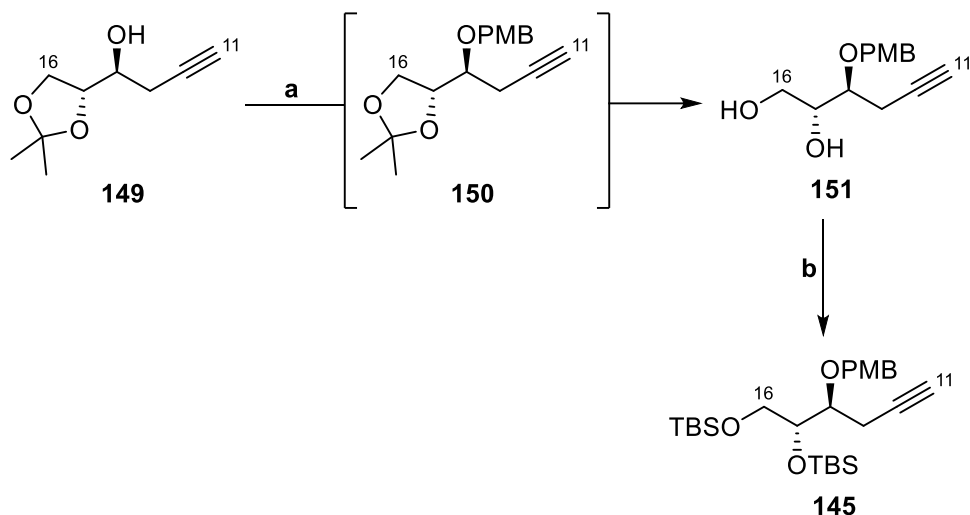
Reagents and conditions: a) NaIO₄, NaHCO₃, CH₂Cl₂, rt, 2 h;
 b) Zn, propargyl bromide, THF, 0 °C to rt, 16 h, 66% over two steps, 4.5:1 d.r.

Scheme 2.3. Synthesis of alcohol **149**

Using a literature-known procedure, crude aldehyde **148** was reacted directly with *in situ* formed propargylic zinc bromide in a Barbier coupling to give **149** in 66% yield over two steps and in 4.5:1 d.r. (Scheme 2.3); the diastereoselectivity was thought to arise from Felkin–Anh control.^{39,40} Care had to be taken to ensure that addition of aldehyde solution to propargylic zinc bromide was slow with good stirring, because the reaction produces a large exotherm that could increase the reaction temperature and erode diastereoselectivity. Nevertheless, even with careful temperature control and monitoring with an internal thermometer, only a maximum d.r. of 5:1 could be achieved in all attempts; the minor undesired diastereomer had to be carried across the next three steps before it could be separated from the product. The major diastereomer of alkyne **149** gave a terminal alkyne proton shift at 2.07 ppm in the ¹H NMR spectrum and a pair of alkyne carbon shifts at 79.8 and 71.2 ppm in the ¹³C NMR spectrum, consistent with previously reported characterisation data.^{37,38}

Alkyne **149** was then treated with NaH and PMBCl in the presence of nucleophilic catalyst TBAI to protect its free hydroxyl group as a PMB ether to give ether **150**. An acidic quench with dilute HCl followed by stirring at 40 °C for 24 h in the same reaction pot deprotected the acetal on **150** to afford diol **151** in 74% yield over the entire sequence (Scheme 2.4). The success of these two protecting group manipulations to obtain **151** was confirmed by the absence of the characteristic 109.4 ppm acetal signal in the ¹³C NMR spectrum, as well as by the presence of

aromatic signals and the prominent 3.80 ppm singlet in the ^1H NMR spectrum caused by the methoxy group of the newly installed PMB ether. Subsequent TBS protection of both hydroxyl groups of **151** gave **145**, which could be partially separated from its minor diastereomer.

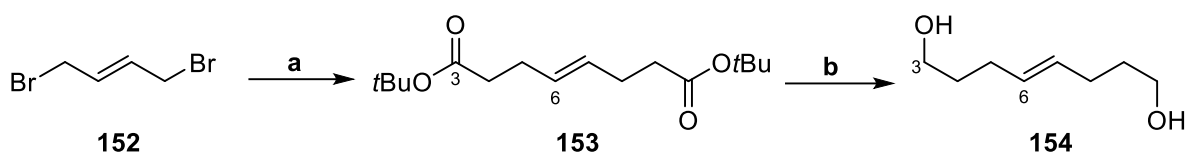


Reagents and conditions: a) NaH, PMBCl, TBAI, THF, 60°C, 16 h; then HCl, MeOH, 60°C, 24 h, 74%
b) TBSCl, imidazole, CH_2Cl_2 , rt, 16 h, 90%

Scheme 2.4. Synthesis of alkyne 145

2.4 Synthesis of C3–C9 aldehyde 146

With alkyne **145** in hand, the other partner of the Carreira alkynylation, aldehyde **146**, had to be prepared. To this end, symmetrical dibromide **152** was converted to ester **153** at 25 g scale and in 60% yield *via* a double enolate alkylation reaction, which involved *in situ* formation of the *t*Butyl enolate from over two equivalents of *t*Butyl acetate and LDA (Scheme 2.5). Successful isolation of ester **153** was confirmed by the presence of the large *t*Butyl singlet at 1.44 ppm in the ^1H NMR spectrum and the signature carbonyl 172.5 ppm signal in the ^{13}C NMR spectrum. Ester **153** was then cleanly reduced to symmetrical diol **154** using excess LiAlH_4 in 83% yield.

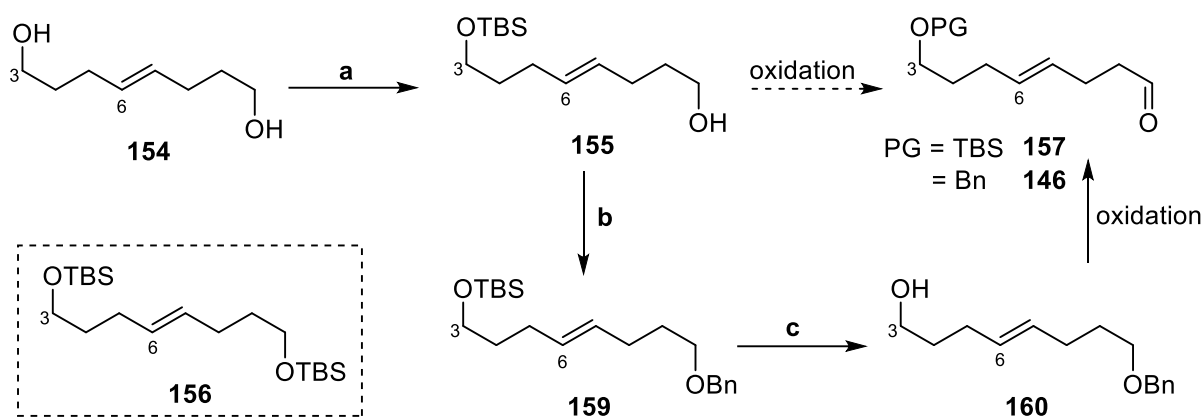


Reagents and conditions: a) *n*BuLi, *i*Pr₂NH, *t*Butyl acetate, THF, -78 °C to rt, 16 h, 60%
 b) LiAlH₄, THF, 0 °C to rt, 4 h, 83%

Scheme 2.5. Synthesis of diol 154

It was subsequently found, however, that there was no need to isolate ester **153**, which could be directly carried as a crude mixture to the LiAlH₄ reduction step. This simplified sequence which saved a column chromatography operation could be conducted at large scales (> 30 g) starting from the symmetrical bromide and gave 62% yield over two steps, which is a higher overall yield than the original sequence that involved isolation of ester **153**.

Diol **154** possesses the full carbon skeleton of sub-fragment aldehyde **146**. However, before the oxidation step could be conducted, diol **154** needed to be *mono*-protected to ensure oxidation of one but not both hydroxyl groups to the aldehyde. The *mono*-protection operation was itself also challenging because the problem of a double-protection occurring would similarly have to be addressed. Dr Xuezheng Yang adopted an elegant phase-transfer strategy which involved reacting diol **154** with one equivalent of TBSCl and NEt₃ in a MeCN/pentane biphasic reaction mixture (Scheme 2.6). Such an approach gave a 77% yield of desired *mono*-silylated product **155**, 12% of unreacted diol **154**, and 10% of the *bis*-silyl ether side-product **156**, which is superior to a purely statistical 50:25:25 mixture of the three species. To rationalise this impressive selectivity, it was suggested that the *mono*-silylated product **155** left the MeCN reaction phase immediately after formation, thus suppressing a second silylation that would form the undesired side-product **156**.



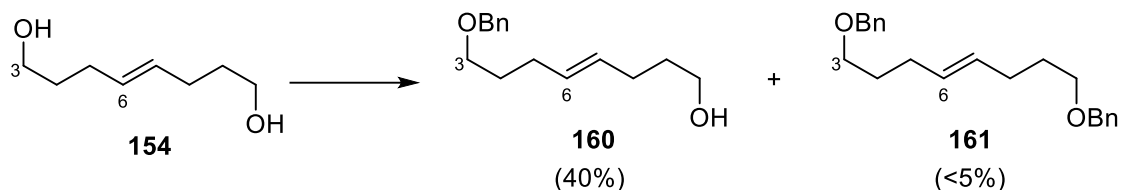
Reagents and conditions: a) TBSCl, NEt₃, MeCN/Pentane (1:7), 0 °C to rt, 24 h, 77%
 b) NaH, BnBr, TBAI, THF, 0 °C to 60 °C, 16 h, 99%
 c) TBAF, THF, TBAI, 0 °C tort, 3 h, 100%

Scheme 2.6. Synthesis of diol 154

Nevertheless, although *mono*-silylated product **155** could in principle be oxidised to its aldehyde and subsequently be used in the Carreira alkynylation, an orthogonal protecting group strategy in the later stages of the synthesis necessitated that aldehyde **146** with a benzyl ether instead of aldehyde **157** with a TBS ether had to be prepared instead. As such, the *mono*-silylated product **155** had to be taken through two more protecting group operations – a benzylation, followed by a TBS deprotection with TBAF – to finally obtain alcohol **160**, a direct precursor of sub-fragment aldehyde **146** (Scheme 2.6).

While high yielding overall, this sequence was too indirect. Moreover, the number of experimental operations required, especially at large scales, would have made the sequence labour intensive. As such, a less elegant but more direct approach was taken to obtain alcohol **160**, which involved reacting diol **154** with 0.8 equivalents of NaH and BnBr in the presence of nucleophilic catalyst TBAI. This reaction was conducted in up to 13 g scale and gave alcohol **160** in 40% yield and 53% of the recovered diol **154** (Scheme 2.7). Although low yielding, this strategy was considered acceptable because recovered diol **154** could be re-subjected to the reaction conditions to obtain more product. Diol **154** was reacted only when a large quantity

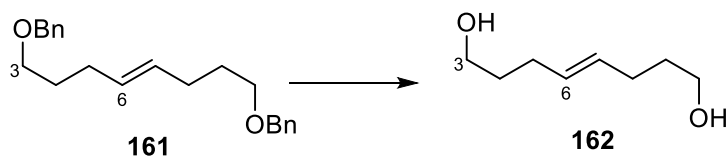
had been accumulated either through recovery or direct synthesis, so as to minimise unnecessary repeats of reaction set-up and product isolation.



Reagents and conditions: NaH, BnBr, TBAI, THF, 0 °C to 70 °C, 16 h

Scheme 2.7. Synthesis of alcohol **160**

bis-Benzylated side-product **161** was also generated in the benzylation reaction, but its exact quantity could not be determined because it could only be obtained as part of a very impure complex mixture; however, based on mass recovery, the quantity of *bis*-benzylated **161** was unlikely to have exceeded 5% yield. During an earlier reaction run involving the benzylation of diol **162**, impure **161** was collected and reacted with BCl₃ in CH₂Cl₂ in an attempt to debenzylate it into diol **162**. However, this overall process of over-benylation and debenylation only resulted in a 2% recovery of diol **162**, when expressed as a fraction of the original starting material. Rather than invest additional efforts to optimise this process, a decision was made to discard *bis*-benzylated **161** in subsequent runs of the benzylation reaction.

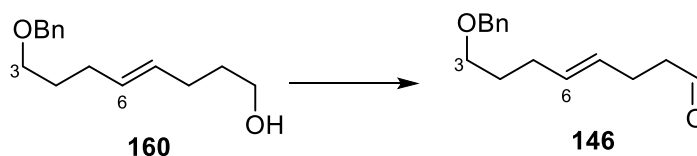


Reagents and conditions: BCl₃, CH₂Cl₂, -78 °C, 1 h, 2% over two steps

Scheme 2.8. Attempted recovery of alcohol **162**

With alcohol **160** in hand, a Parikh–Doering oxidation reaction was conducted to convert it to aldehyde **146**; this reaction has been scaled up to 21 g to give **146** in 88% yield (Scheme 2.7). Formation of aldehyde **146** was confirmed by the appearance of the signature aldehyde triplet

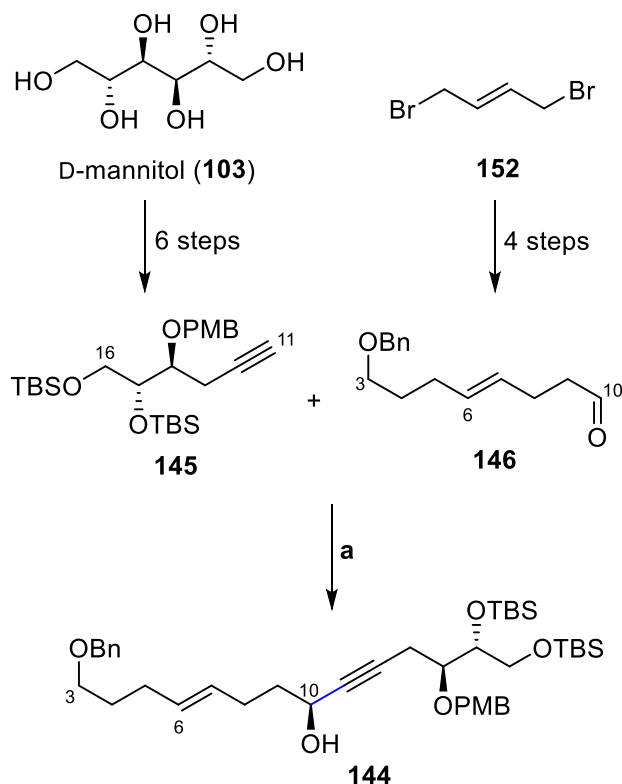
signal at 9.74 ppm in the ^1H NMR spectrum. The quality of the $\text{SO}_3\cdot\text{py}$ reagent was critical to the success of the reaction. On one occasion, only an extremely low 3% yield of aldehyde **146** was obtained on a 10 g scale when a bottle of degraded $\text{SO}_3\cdot\text{py}$ reagent had been mistakenly used. Dr Xuezheng Yang reported similar observations pertaining to $\text{SO}_3\cdot\text{py}$ reagent quality and reaction success.³⁸



Reagents and conditions: $\text{SO}_3\cdot\text{Pyridine}$, $i\text{Pr}_2\text{NH}$, DMSO, CH_2Cl_2 , $0\text{ }^\circ\text{C}$, 45 min, 88%

Scheme 2.9. Synthesis of aldehyde **146**

2.5 Carreira alkylation reaction between **145** and **146**

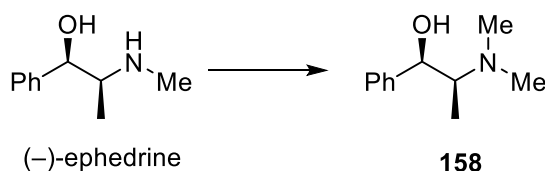


Reagents and conditions: a) (1*R*,2*S*)-*N*-(-)-methylephedrine, NEt_3 , $\text{Zn}(\text{OTf})_2$, PhMe, rt, 36 h, 91%

Scheme 2.10. Carreira alkylation reaction between **145** and **146**

Alkyne **145** and aldehyde **146** have been prepared in deca-gram quantities through 6- and 4-step forward syntheses respectively, which were detailed in the previous two sections (Scheme **2.10**). A Carreira alkylation reaction could thus be performed between the two partners. This methodology relies on chiral additives such as pseudoephedrine or *N*-methylephedrine to induce stereoselectivity at the newly generated chiral secondary alcohol centre, resulting from the coupling between terminal alkyne and aldehyde partners.^{41–43}

For the system described in Scheme **2.10**, (–)-*N*-methylephedrine (**158**) was used as the chiral additive and could be prepared from (–)-ephedrine through an Eschweiler–Clarke reaction, which has been successfully conducted at a 50 g scale in 99% yield (Scheme **2.11**).



Reagents and conditions: Formaldehyde, formic acid, 90 °C , 16 h, 99%

*Scheme 2.11. Preparation of (–)-*N*-methylephedrine (**158**)*

The Carreira alkylation reaction has been adapted to and heavily optimised for this specific system involving alkyne **145** and aldehyde **146** by Dr Xuezheng Yang.³⁸ Through these extensive studies, the following precautions were found to be key for reaction success: a) Prior to use, the Zn(OTf)₂ had to be dried overnight under vacuum at 120 °C to remove residual TfOH from industrial preparation of the reagent; b) The (–)-*N*-methyl ephedrine used as a chiral additive is hygroscopic and had to be rigorously dried overnight under vacuum; c) Aldehyde **146** had to be slowly added to the reaction mixture *via* syringe pump addition over 24 h, due to the aldehyde's instability under reaction conditions and the slowness of the desired alkylation reaction; d) for the reasons described in (c), the alkyne partner had to be

used in large excess (3 eqv) to enhance alkylation reaction rate relative to undesired side-processes.

When all the above precautions were observed, the Carreira alkylation reaction gave up to 92% yield of **144** as a single diastereomer and could be run at scales to give over 15 g of product. Formation and isolation of **144** were confirmed by the disappearance of the aldehyde triplet peak at 9.74 ppm in the ^1H NMR spectrum and the appearance of the aromatic proton peaks with the correct integration ratio from the OPMB and OBn groups present in the Carreira alkylation adduct. Additionally, the stereochemistry at the newly established chiral centre at C11 had been previously confirmed in the Donohoe group by Mosher's ester analysis.⁴⁴

It was possible to recover excess unreacted alkyne **145** for use in subsequent runs. However, it was observed that re-using alkyne **145** across multiple reaction runs resulted in lower yields. A possible explanation for this reduction in yield was the recovered sample becoming increasingly enriched with impurities such as the undesired and less reactive diastereomer of alkyne **145**, *epi-145* (Figure 2.1), whose origin was from the Barbier coupling reaction described in an earlier section (Section 2.3).

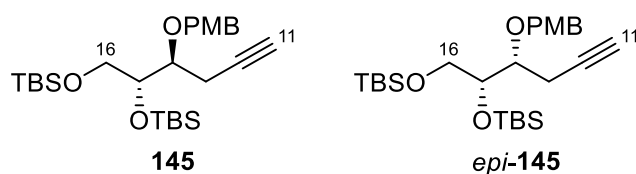


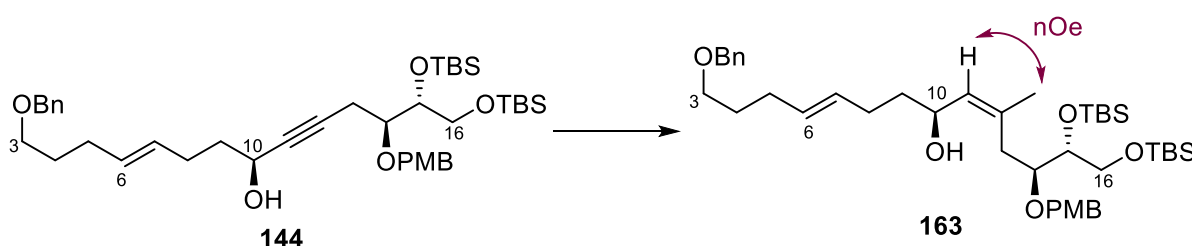
Figure 2.1. Structures of **145** and unreactive *epi-145*

Fortunately, *epi-145* displayed no reactivity towards aldehyde **146**, so the corresponding diastereomeric side-products were not generated. However, the same inertness of diastereomer *epi-145* resulted in its accumulation in the recovered starting material sample

as **145** was consumed, causing a “dilution effect” in the starting material sample and hence a lower alkylation reaction yield due to the reduced equivalence of **145**. This dilution effect could be observed in the ^{13}C NMR spectrum, which showed the carbon peaks corresponding to **145** in recycled samples becoming less intense relative to contaminant peaks that corresponded to diastereomer *epi-145*. Catalyst inhibition by *epi-145* was also possible. Periodically re-subjecting recycled samples of **145** to column chromatography to at least partially remove *epi-145* was thus found to be beneficial to alkylation yields.

2.6 Elaboration of propargylic alcohol **144** to triol **143**

A reliable and heavily optimised protocol had been successfully developed and executed to prepare propargylic alcohol **144** in large quantities and high yields. The compound now had to be converted to triol **143**, which was achieved in two steps. The first step was an iron-catalysed *trans*-carbometallation,⁴⁵ which involved reacting **144** with a large excess of MeMgBr (8 eqv) in the presence of $\text{Fe}(\text{acac})_3$ and 1,2-*bis*(diphenylphosphino)ethane (dppe) to give allylic alcohol **163** in 78% yield (Scheme 2.12). The alkene geometry of **163** was previously confirmed by nOe studies by Dr Xuezheng Yang.³⁸ The Donohoe group was the first to use this methodology in natural product synthesis.³⁰

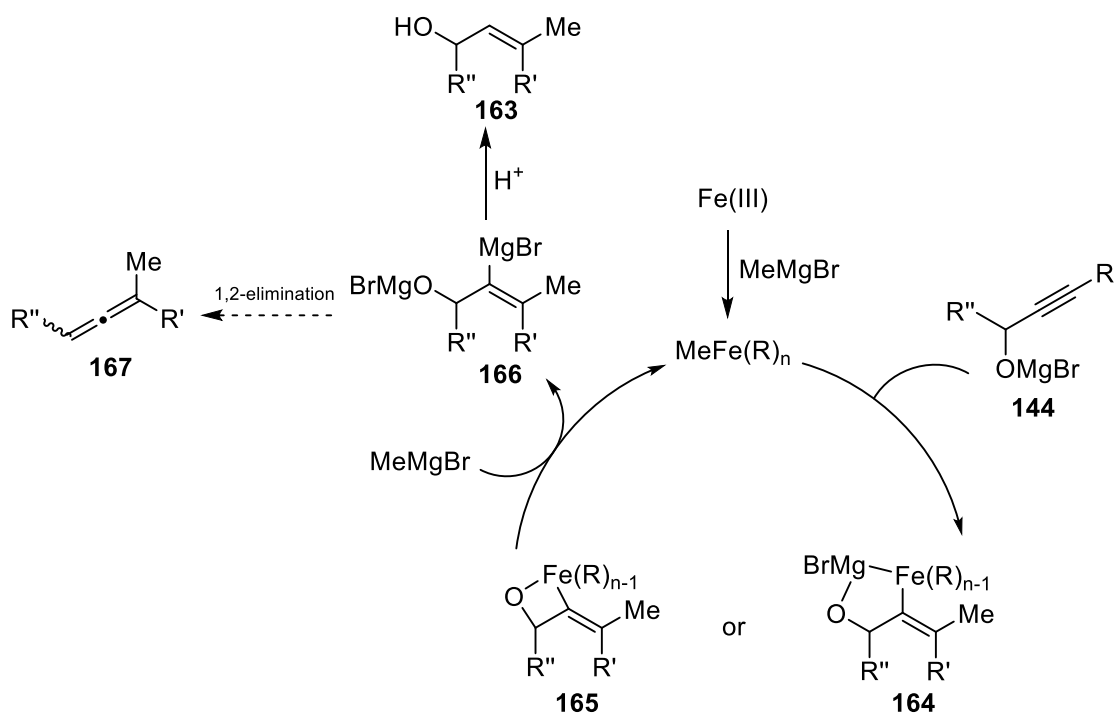


Reagents and conditions: MeMgBr, $\text{Fe}(\text{acac})_3$, dppe, THF, -78 to 0 °C, 18 h, 78%

Scheme 2.12. Ready *trans*-carbometallation of propargyl alcohol **163**

The regioselectivity of the carbometallation can be rationalised by the reaction mechanism (Scheme 2.13). First, the $\text{Fe}(\text{acac})_3$ precatalyst undergoes a ligand exchange and is reduced to

Fe(II) by MeMgBr. Carbometallation to give either intermediate **164** or **165** then occurs which is directed by the alkoxide, accounting for the observed regioselectivity. The species then reacts with another equivalent of MeMgBr to give organomagnesium compound **166** and Fe(II)L_mMe_n, which is free to participate in another catalytic cycle. An acidic NH₄Cl quench upon reaction completion protonates **166** to allylic alcohol **163**.



Scheme 2.13. Catalytic cycle of Ready trans-carbomethylation

Prior to reaction quenching, it was essential that the reaction mixture was cooled to $-78\text{ }^{\circ}\text{C}$ and that the solution of NH₄Cl was added slowly to the mixture. Quenching the reaction too quickly or at an elevated temperature would overheat the reaction mixture, which may induce side-reactions such as 1,2-elimination to generate allene **167** (Figure 2.2); additionally, leaving the reaction to run for too long may lead to over-methylation to give **168**.³⁸

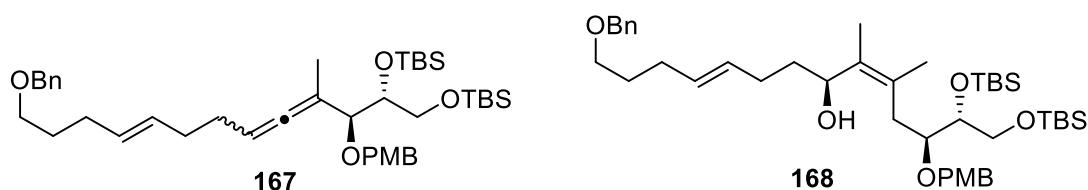
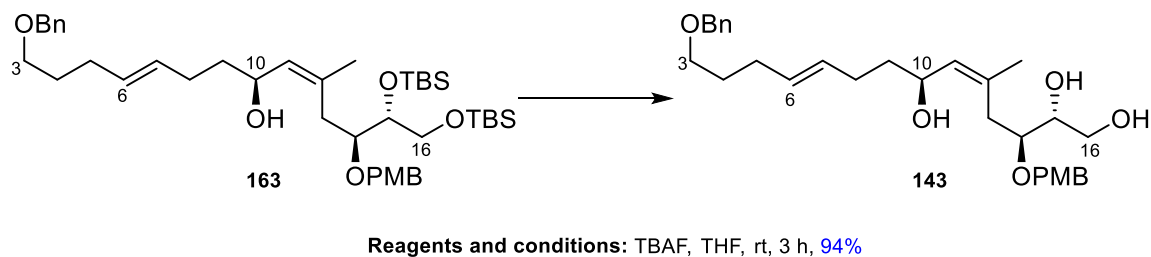


Figure 2.2. Side-products of the Ready trans-carbomethylation

Finally, allylic alcohol **163** was then treated with excess TBAF in THF to give triol **143** in 94% yield (Scheme 2.14), the immediate precursor for the key osmium-catalysed double oxidative cyclisation reaction.

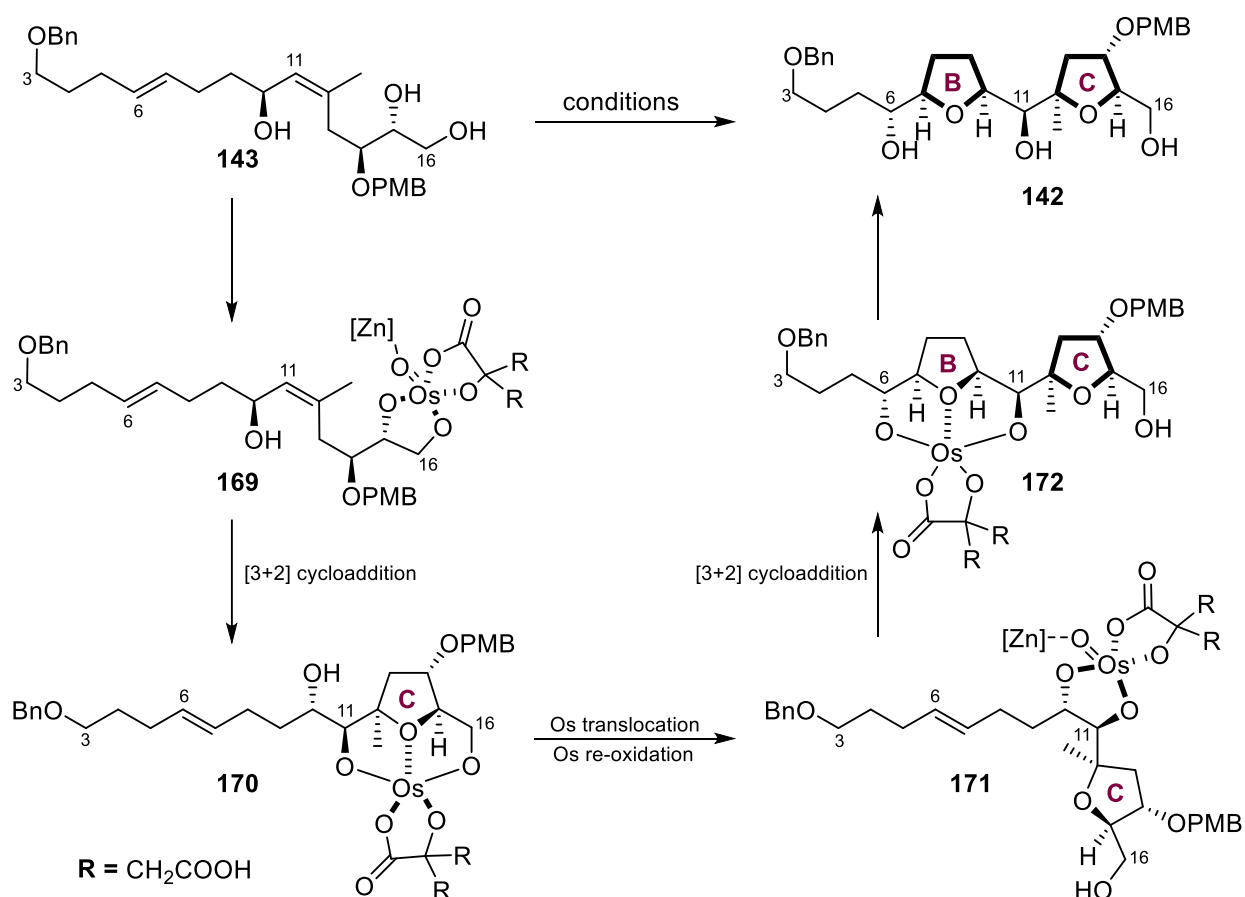


Scheme 2.14. Deprotection of allylic alcohol **163** to triol **143**

2.7 Osmium-catalysed oxidative cyclisation of triol **143**

Although triol **143** possessed the carbon skeleton for much of the ABC fragment, it still lacked the core *bis*-THF framework of the latter. This framework was established using the osmium-catalysed oxidative cyclisation cascade developed by the Donohoe group,⁴⁶ which involved reacting triol **143** with catalytic $K_2OsO_2(OH)_4$, pyridine *N*-oxide, $Zn(OTf)_2$, and citric acid to give *bis*-THF **142** in 82% yield as a single diastereomer.

The mechanism of this key reaction is detailed in Scheme 2.15. First, Os(VI) coordinates to the two hydroxyl groups on C15 and C16, giving species **169**. Citric acid additive was found to be beneficial to the oxidative cyclisation and was hypothesised by Donohoe to serve one or both of the following roles: a) Its coordination to the Os centre stabilises the Os(VI) species against disproportionation; b) The two pendant carboxylate groups increase the hydrophilicity of the Os(VI) species, thus facilitating hydrolytic release of the product from Os and enhancing reaction rate.



Reagents and conditions: K₂OsO₂(OH)₄, pyridine *N*-oxide, citric acid, Zn(OTf)₂, MeCN, pH 6.5 buffer, 60 °C, 12 h, then 80 °C, 24 h, 82%

Scheme 2.15. Mechanism of osmium-catalysed double oxidative addition

The Os=O oxygen coordinates to Zn²⁺, which makes the Os species more electron deficient and promotes a [3+2] oxidative cyclisation to establish the first THF ring and give intermediate **170**. The Os species is then re-oxidised by weakly oxidising pyridine *N*-oxide back to Os(VI), which then translocates to the C10 hydroxyl group to give intermediate **171**. Once in position, the Os(VI) species undergoes a second [3+2] oxidative cyclisation to form the second THF ring, thus producing **172**. Oxidation and hydrolysis of the Os species in **172** releases the final product *bis*-THF **142**.

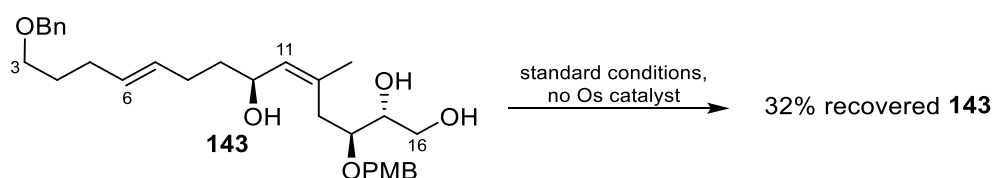
This methodology as applied to triol **143** had been extensively optimised by Dr Xuezheng Yang and Dr Radoslaw Lipinski, who investigated the effects of catalyst loading, pyridine *N*-oxide

equivalents, choice of Lewis acid, reaction duration, temperature and other parameters on yield.^{38,44} Attempting the reaction using these optimised conditions gave the product in high yields on several consecutive occasions. However, the abrupt and unexpected failure of a reaction run performed at a 4.2 g scale and that which gave no desired product prompted a re-investigation into the reaction. After this failed run, subsequent reactions performed at 50 mg test scales consistently gave yields in the range of 10%–20% with poor mass recovery. These low yields persisted despite sequentially and systematically verifying that reagent quality was not responsible for reaction failure – i.e., by using newly purchased bottles of $\text{K}_2\text{OsO}_2(\text{OH})_4$, pyridine *N*-oxide, and $\text{Zn}(\text{OTf})_2$ from multiple commercial suppliers in test reactions.

Eventually, it was discovered that it was substrate purity not reagent quality that was responsible for the repeated reaction failures. Performing a TLC analysis on an impure sample of triol **143** using a 5.5:4.5 pentane:acetone eluent system with a vanillin stain gives a side-product spot ($R_f \approx 0.3$) that appears slightly above that of the product. Subjecting the sample to a second round of flash column chromatography gave both pure and impure fractions, which were concentrated, and stored separately. Performing a 50 mg scale test reaction using triol **143** from the fully purified sample gave *bis*-THF **142** in 58% yield, well above any of the yields from previous control experiments. Reaction scale-ups to 250 mg and 3.1 g of triol **143** afforded product in 84% and 82% yields respectively, validating the hypothesis that substrate impurity was responsible for the initial failures. The identity of the unknown contaminant was briefly investigated; however, ^1H and ^{13}C NMR spectroscopy revealed that the contaminant was not a single species but a complex mixture, which made characterisation impossible. This quality also made mere *detection* of the contaminant in a sample of triol **143** using NMR spectroscopy more challenging; because the contaminant comprised an ensemble of different

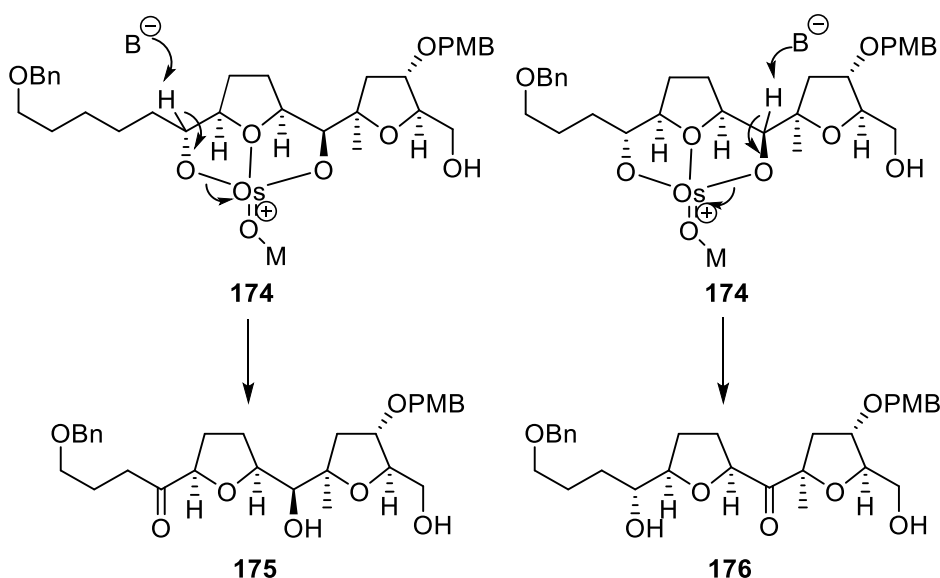
compounds instead of a single species, it possessed no distinct ^1H or ^{13}C NMR signals that clearly stood out from those of triol **143**. Moreover, contaminant present in low quantities was sufficient to drastically reduce yields. To ensure the best compromise between triol **143** purity and isolated yield, it was necessary to perform flash column chromatography between five to seven times on a given batch of triol **143**.

Although these contaminants could not be characterised, it was proposed that some if not all of the species in the mixture are triols, due to their very similar polarity to that of triol **143**, which requires an extremely polar 60:40 pentane:acetone bi-solvent system for elution during column chromatography. Triol contaminants could potentially also sequester the Os catalyst, which would reduce the oxidative cyclisation reaction rate and allow other side-processes to be competitive. The outcome of a control experiment that involved subjecting triol **143** to standard reaction conditions without any Os catalyst was consistent with this – only 32% of starting material was recovered, indicating that triol **143** is unstable under reaction conditions and will steadily degrade if oxidative cyclisation occurs slowly (Scheme **2.16**).



*Scheme 2.16. Control experiment to evaluate stability of **143** under reaction conditions*

Although briefly considered, increasing catalyst loading to counteract potential sequestering of the Os catalyst by triol contaminants is not a tenable strategy, because higher loadings had been previously demonstrated to promote the formation of over-oxidation side-products (Scheme **2.17**).³⁸ Moreover, the optimal catalyst loading is likely to vary with the purity profile of each batch of triol **143**. As such, multiple rounds of column chromatography was the only recourse to ensure reliably high yields.



Scheme 2.17. Formation of over-oxidised side-products from high catalyst loadings

Finally, it was discovered on a separate occasion that the quality of $\text{K}_2\text{OsO}_2(\text{OH})_4$ was also a critical parameter in ensuring high yields. Non-degraded $\text{K}_2\text{OsO}_2(\text{OH})_4$ has the appearance of a free-flowing dark purple crystalline powder, while degraded $\text{K}_2\text{OsO}_2(\text{OH})_4$ often appears as a black clumpy powder. On one occasion, a reaction performed at 1.1 g scale with low-quality $\text{K}_2\text{OsO}_2(\text{OH})_4$ afforded *bis*-THF **142** in only 43% yield despite the high purity of the starting material. On smaller test scales, this low yield was demonstrated to be reproducible. Using a different bottle of $\text{K}_2\text{OsO}_2(\text{OH})_4$ restored the high yields, and subsequent reactions performed using the same batch of triol **143** and this superior bottle of $\text{K}_2\text{OsO}_2(\text{OH})_4$ gave *bis*-THF **142** in 76%, 87%, and 69% yields at 500 mg, 2.4 g, and 5.7 g scales respectively.

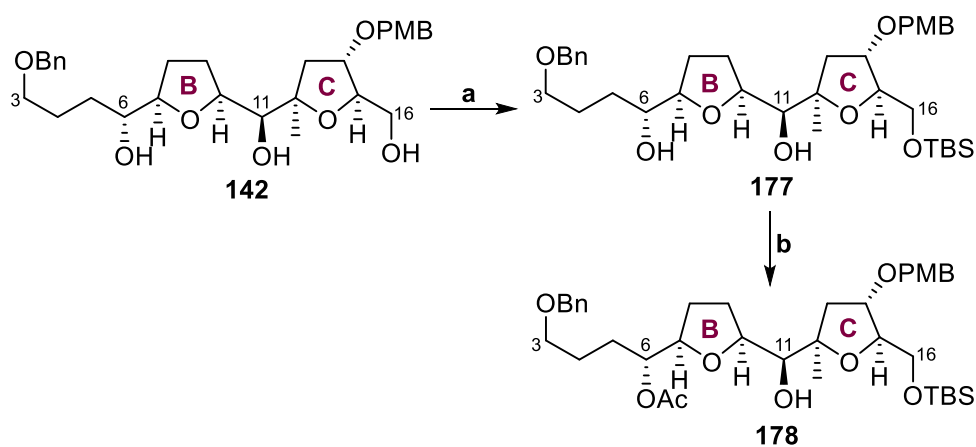
In summary, as a safeguard against unexpected reaction failure at large scales, the following precautions were observed when performing the double oxidative cyclisation on every new batch of triol **143**:

1. Before use, the $\text{K}_2\text{OsO}_2(\text{OH})_4$ catalyst was visually inspected to ensure it was a free-flowing purple crystalline powder.

- Multiple rounds of flash column chromatography were performed on triol **143** and TLC analysis was conducted to check for the contaminant located at a slightly higher R_f value than that of the product.
- Because of the subjective nature of the above two precautions, the reaction was performed at a test scale prior to committing large quantities of valuable starting material to the reaction.

2.8 Elaboration of *bis*-THF **142** to **180**

Performing the heavily optimised osmium-catalysed double oxidative cyclisation with the aforementioned precautions allowed *bis*-THF **142** to be prepared in multi-gram quantities per reaction run in good yields. Each of the three hydroxyl groups of *bis*-THF **142** now had to be sequentially and selectively protected with different protecting groups.



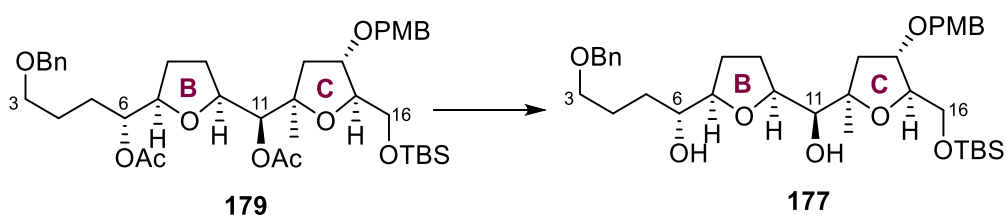
Reagents and conditions: a) TBSCl, imidazole, CH_2Cl_2 , 0 °C to rt, 12 h, 97%
 b) Ac_2O , pyridine, DMAP, CH_2Cl_2 , 0 °C to rt, 18 h, 80%

Scheme 2.18. Installation of protecting groups on **142**

First, a TBS group was installed at the primary hydroxyl group on C16 to give TBS ether **177** in 97% yield (Scheme **2.18**). Subsequent reaction of **177** with Ac_2O with pyridine base and nucleophilic catalyst DMAP gave acetate **178** in 80% yield. Successful formation of acetate **178** was confirmed by the presence of the strong Ac-CH_3 singlet peak at 2.01 ppm in the ^1H NMR

spectrum and by the signature carbonyl peak at 171.1 ppm in the ^{13}C NMR spectrum. Additionally, the proton signal of C(6)H moved downfield from 3.35 to 4.93 ppm, strongly suggesting that the correct hydroxyl group had been protected. Additionally, all characterisation data was consistent with those obtained previously.^{37,38}

Although the secondary hydroxyl group on C6 reacted preferentially with Ac_2O compared to the C11 hydroxyl group, dilute conditions still had to be used to raise this selectivity. The acetylation reaction often did not go to completion even when reaction durations were extended, presumably due to the high-dilution conditions; however, it was possible to recover unreacted TBS ether **177** and re-subject it to the acetylation reaction. Variable quantities (5% to 15%) of *bis*-acetate **179** were also inadvertently generated and surprisingly could not be separated from acetate **178** despite the difference in the number of free hydroxyl groups between the two compounds. *bis*-Acetate **179** could only be isolated as a pure sample in the subsequent step, and could be readily converted back to **177** for re-use by treatment with K_2CO_3 and MeOH (Scheme 2.19).

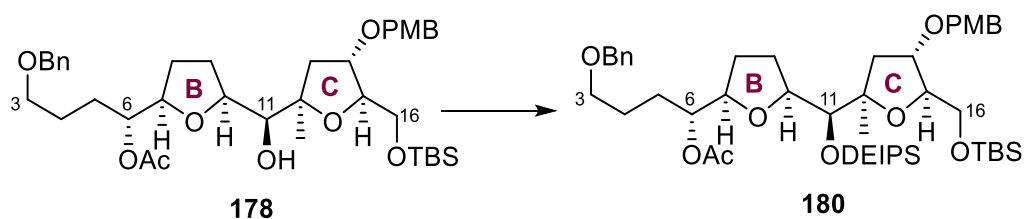


Reagents and conditions: K_2CO_3 , MeOH, rt, 3.5 h, 90%

Scheme 2.19. Conversion of bis-acetate 179 to 177

Finally, the remaining secondary C11 hydroxyl group of acetate **178** was protected with a diethylisopropylsilyl (DEIPS) group (Scheme 2.20). This specific silyl protecting group was chosen because it had to be more stable than the TBS protecting group on the primary C16 hydroxyl group, yet sufficiently reactive to be removed using TAS-F at ambient temperature,

which was the reagent Evans had used in the final global deprotection step of his total synthesis of PTX-4. This protecting group operation initially necessitated treatment of **178** with 8 equivalents of DEIPSCI due to poor conversion and long reaction times (≥ 24 h). However, it was found that DEIPSOTf was a superior and cheaper silylating reagent that was effective at lower equivalences (2 eqv) and that which gave shorter reaction times (7 h), allowing DEIPS ether **180** to be formed in 92% yield. The characterisation data of **180** matched those previous obtained by Dr Xuezheng Yang.³⁸



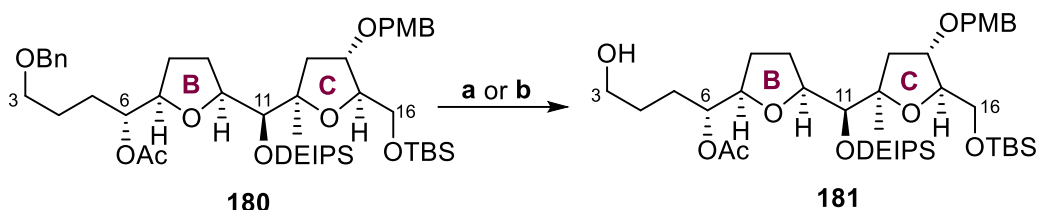
Reagents and conditions: DEIPSOTf, NEt₃, DMAP, DMF, rt, 7 h, 92%

Scheme 2.20. Conversion of acetate 178 to 180

2.9 Installation of Evans auxiliary

With the appropriate protecting groups installed on the C6, C11, and C16 hydroxyl groups, DEIPS ether **180** could now be converted in two steps to its aldehyde for an Evans aldol addition. First, a hydrogenolysis was conducted on benzyl ether **180** to convert it to alcohol **181** (Scheme 2.21). This hydrogenolysis had been previously achieved using Raney[®] nickel under a balloon of hydrogen to give alcohol **181** in 79% yield.³⁸ However, Raney[®] nickel is known to be extremely pyrophoric and there were safety concerns about conducting the reaction at large scales. Thus, Pd(OH)₂/C (Pearlman's catalyst) was used instead as the catalyst. Although performing the hydrogenolysis using Pd(OH)₂/C at room temperature gave alcohol **181** only in 45% yield due to concomitant hydrogenolysis of the PMB ether, performing

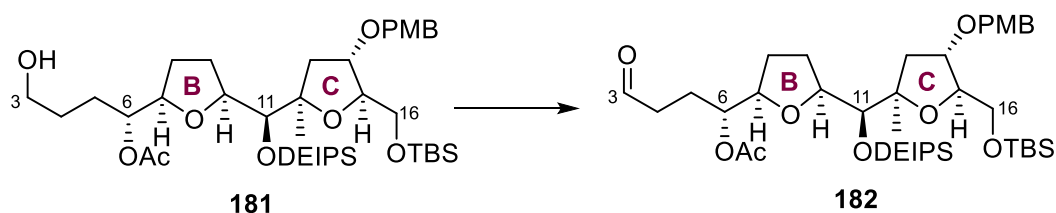
the hydrogenolysis at 0 °C over 30 to 50 min suppressed formation of the over-hydrogenated side-product and gave alcohol **181** in quantitative yield.



Reagents and conditions: a) Raney[®]-Ni 2800 slurry, H₂, EtOAc, 45 °C, 12 h, 78%
 b) Pd(OH)₂/C, H₂, EtOAc, 0 °C, 40 min, 100%

*Scheme 2.21. Conversion of acetate **180** to **181***

A subsequent Parikh–Doering oxidation reaction of alcohol **181** gave aldehyde **182** in 94% yield (Scheme 2.22). The formation of aldehyde **182** was confirmed by the signature aldehyde triplet at 9.74 ppm in the ¹H NMR spectrum and matched the characterisation data previously obtained by Dr Xuezheng Yang.³⁸ To maintain high yields for the oxidation, however, it was necessary to limit the scale of the reaction to 1.5 g at most. However, because >5 g quantities of alcohol **181** needed to be converted at a time, multiple smaller scale reaction pots can be set up simultaneously and then combined after the reaction quench. Such a procedure saved time and effort during the work-up and product isolation, because only a single extraction and column chromatography operation was required when the batches were combined.

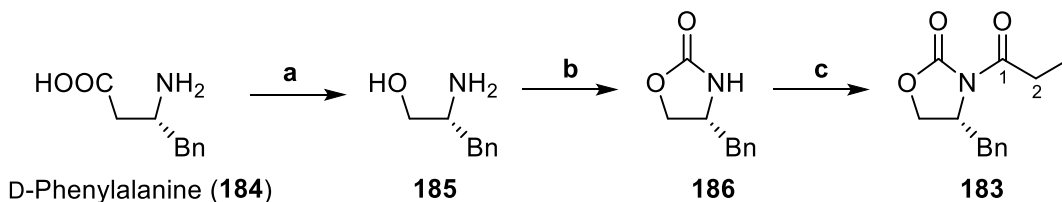


Reagents and conditions: SO₃•Pyridine, *i*Pr₂NEt, DMSO, CH₂Cl₂, –40 to –10 °C, 1 h, 94%

*Scheme 2.22. Parikh–Doering oxidation of **181** to aldehyde **182***

Before the Evans aldol reaction could be performed on aldehyde **182**, the Evans auxiliary oxazolidinone **183** first had to be prepared from D-phenylalanine (**184**) in three steps (Scheme 2.23). D-phenylalanine was first reduced to amino alcohol **185** in 69% yield using

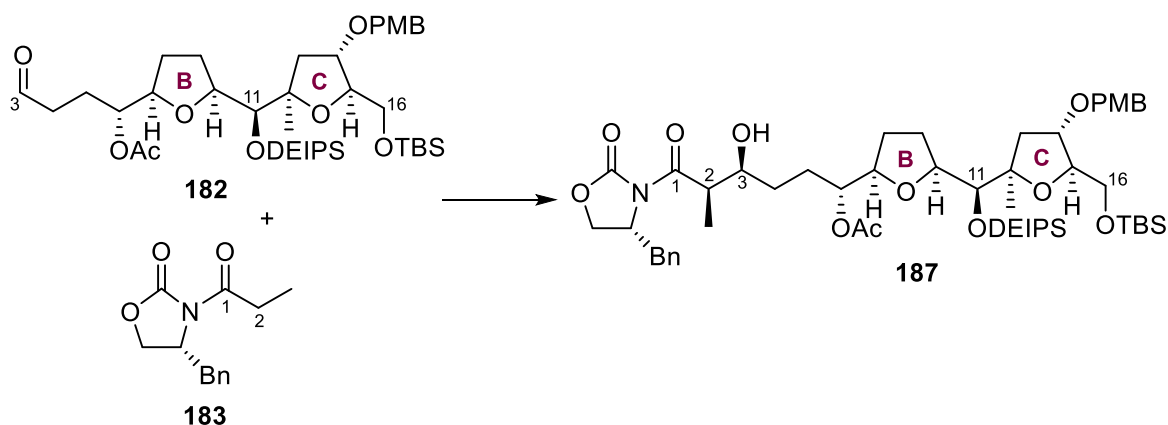
LiAlH₄ in THF at reflux. Treatment of amino alcohol **185** at elevated temperature gave **186** in 84% yield, which was deprotonated at -78 °C with *n*BuLi and then quenched with propionyl chloride to finally give oxazolidinone **183** in 87% yield.



Reagents and conditions: a) LiAlH₄, THF, 0 °C to reflux, 16 h, 69%
 b) Diethylcarbonate, K₂CO₃, 135 °C, 3 h, 84%
 c) *n*BuLi, propionyl chloride, THF, -78 °C, 30 min, 87%

Scheme 2.23. Synthesis of oxazolidinone 183

The Evans aldol addition reaction between aldehyde **182** and oxazolidinone **183** afforded alcohol **187** in an excellent 96% yield as a single diastereomer (Scheme 2.24). This reaction was successfully scaled up to 7 g. Alcohol **187** gave a *J*_{2,3} coupling constant of 2.7 Hz, a value consistent with a *syn* relationship between C(2)*H* and C(3)*H*, which is expected to fall between 2 to 6 Hz. In contrast, an *anti* relationship between the pair of protons would be expected to fall between 7 to 10 Hz.^{47,48} Additionally, the characterisation data of alcohol **187** was consistent with those previously reported.³⁸

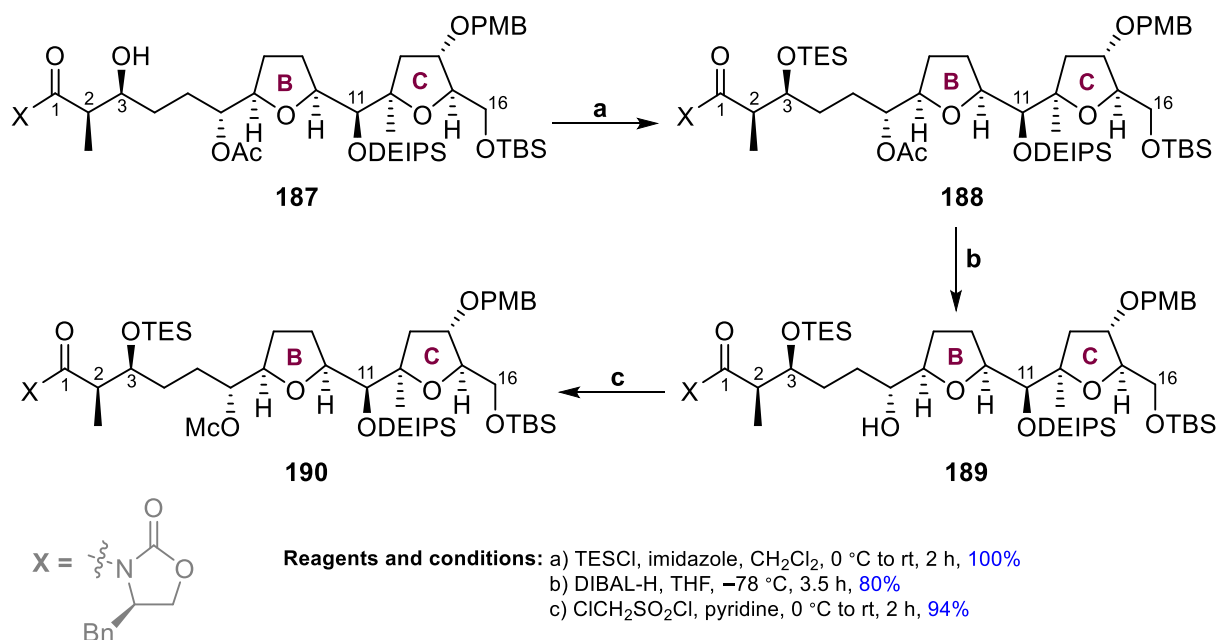


Reagents and conditions: Bu₂BOTf, NEt₃, CH₂Cl₂, -78 °C to 0 °C, 3 h, 96%

Scheme 2.24. Evans aldol addition to synthesis alcohol 187

2.10 1,2-Hydride shift spiroketalisation cascade

Alcohol **187** possesses the full 16-carbon skeleton of the ABC fragment. However, the key 6,5-spiroketal moiety still needed to be installed through the 1,2-hydride shift spiroketalisation cascade. As such, synthesis of the key step precursor commenced with a TES protection of alcohol **187** to give **188** in quantitative yield (Scheme 2.25). Acetate **188** was in turn treated with DIBAL-H in large excess to free the C6 hydroxyl group to give alcohol **189** in 75% yield, with a recovery of 20% of unreacted starting material; the oxazolidinone moiety remained untouched under these conditions.

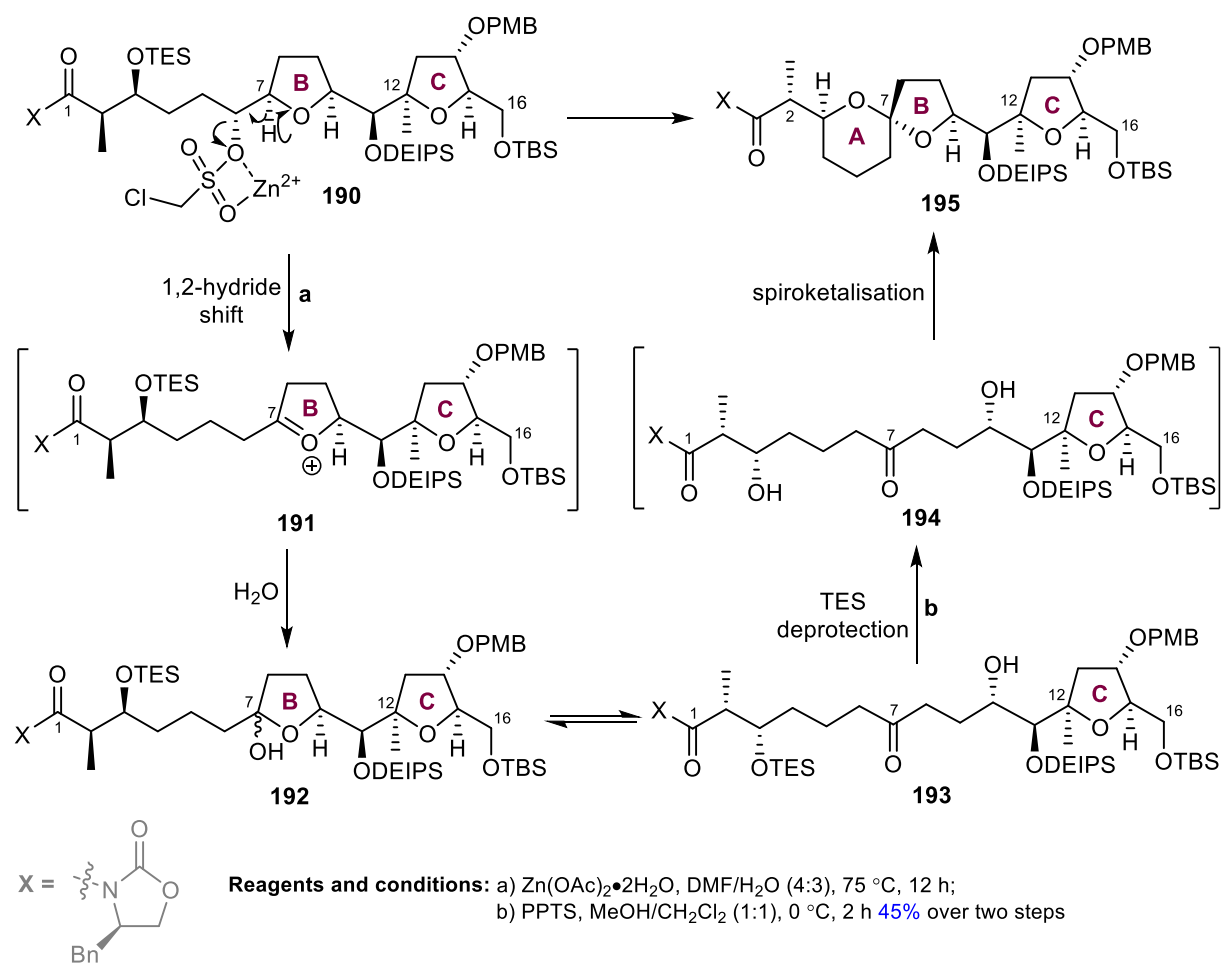


Scheme 2.25. Synthesis of precursor **190**

Finally, treatment of alcohol **189** with chloromethanesulfonyl chloride converted it to precursor **190** in 94% yield. This specific activating group was chosen after extensive model studies by Dr Radoslaw Lipinski, who determined that the chloromesylate moiety was the best compromise between sufficient reactivity for the initial 1,2-hydride shift step in the cascade and sufficient stability such that the activated compound does not rapidly degrade during its isolation and storage.⁴⁴ The formation of precursor **190** was confirmed by the detection of the signature ClCH₂SO₂ AB doublets at 4.73 and 4.86 ppm. Precursor **190** was unstable at room

temperature over long durations and thus had to be stored in a $-30\text{ }^{\circ}\text{C}$ freezer when not in use.

Having obtained precursor **190**, the 1,2-hydride shift spiroketalisation could at last be performed. In this reaction, precursor **190** was treated with Lewis acid $\text{Zn}(\text{OAc})_2$ in large excess (10 eqv) in a polar 4:3 DMF: H_2O solution at $75\text{ }^{\circ}\text{C}$. The reaction mechanism of the cascade is shown in Scheme 2.26.



Scheme 2.26. 1,2-Hydride shift and spiroketalisation of precursor **190**

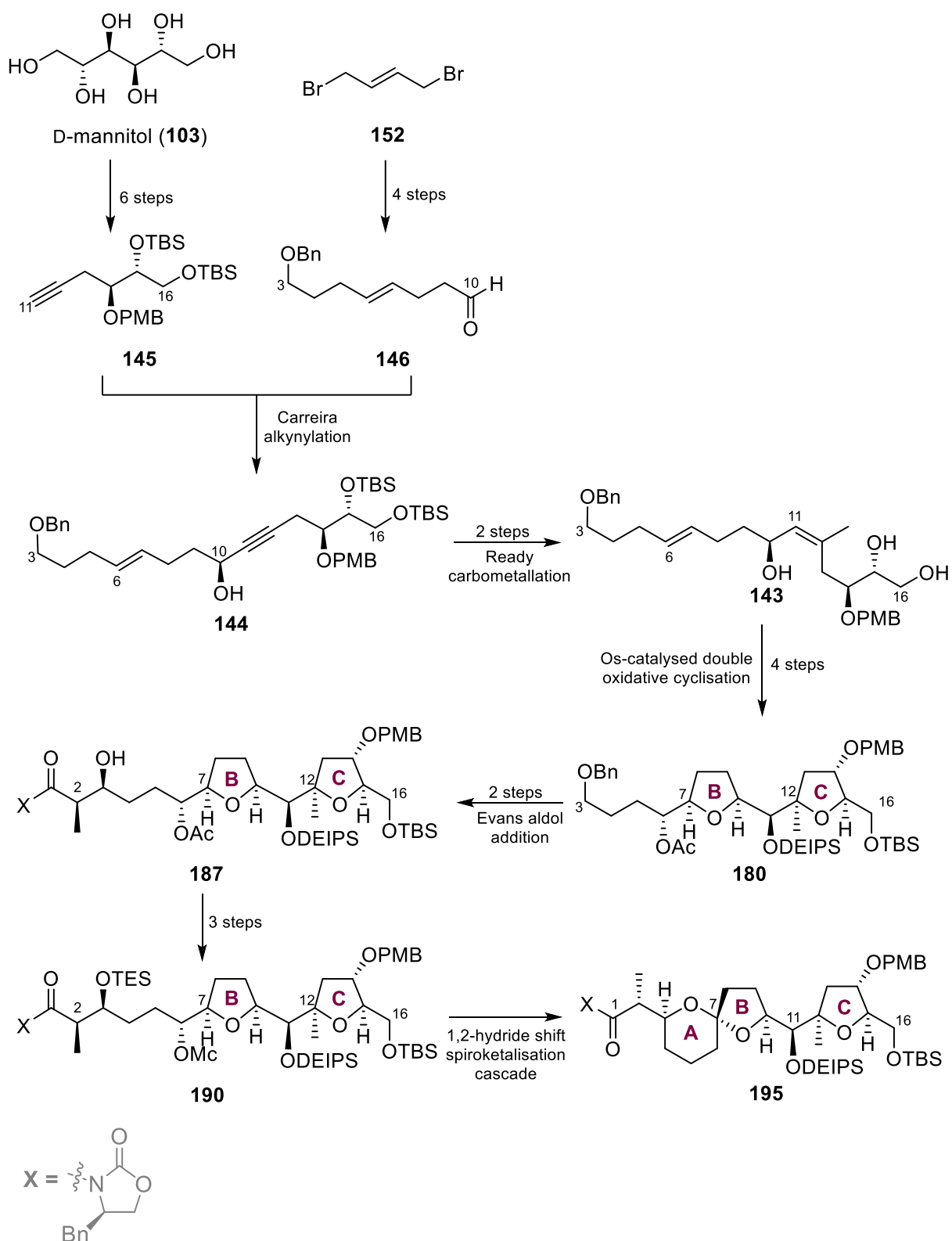
First, Zn^{2+} coordinates to the chloromethyl sulfonate moiety of precursor **190** in the polar solution, activating it further and facilitating the 1,2-hydride shift to give oxonium ion **191**, which is rapidly attacked by a molecule of water to form hemiacetal **192**. Hemiacetal **192** exists in an equilibrium with hydroxy ketone **193**, and thus could not be characterised. Subjecting the

equilibrium mixture to mildly acidic PPTS in a 1:1 MeOH/CH₂Cl₂ solution resulted in the removal of the TES group on C3 to give **194**, allowing subsequent spiroketalisation of the C3 and C10 hydroxyl groups with the ketone at C7, giving spiroketal **195** in 45% over two steps. Formation of spiroketal **195** was confirmed by the signal ketal peak at 105.0 ppm in the ¹³C NMR spectrum. Moreover, this chemical shift value was consistent with the thermodynamic anomeric 6,5-spiroketal found in naturally derived and synthetic pectenotoxins reported by the Fujiwara group. In contrast, the non-anomeric 6,5- and 6,6-spiroketal give ¹³C chemical shift values in the range of 107–111 ppm.²⁵ The characterisation data of spiroketal **195** was fully consistent with those previously reported.³⁸

2.11 Cleavage of the Evans auxiliary

2.11.1 Overview and past efforts of auxiliary removal

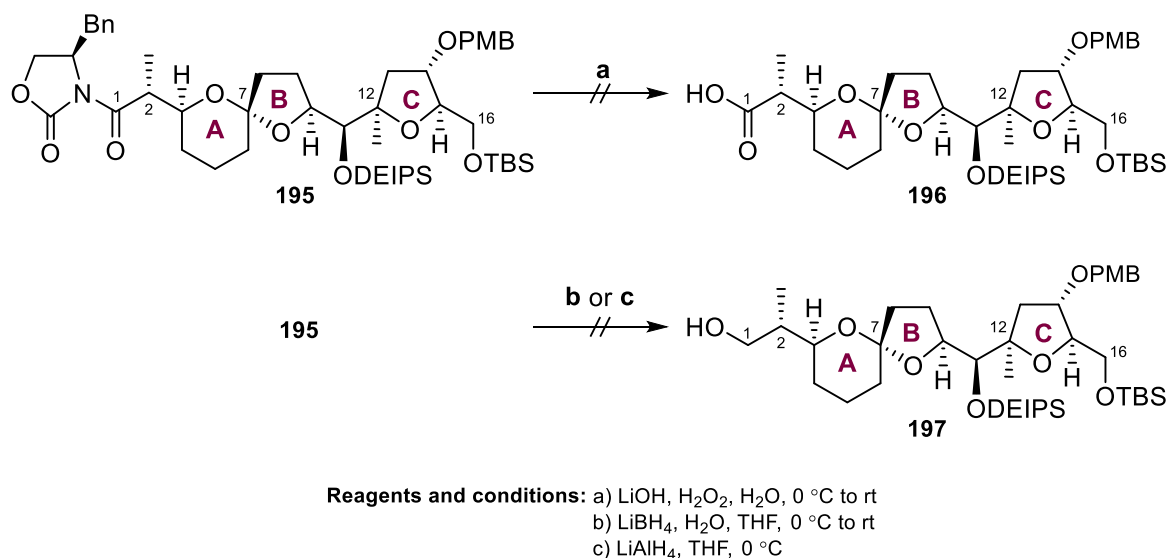
In summary, spiroketal **195** was prepared in 19 linear steps from D-mannitol, as summed up by Scheme **2.27**. However, a significant challenge remained – that is, to remove the chiral oxazolidinone auxiliary that had been installed during the Evans aldol addition step (Section **2.9**) to establish the C2 and C3 stereocentres. The oxazolidinone auxiliary, up until this point, had been used as a pseudo-protecting group for C1 which is at the carboxylic acid oxidation state. However, the auxiliary removal had previously been demonstrated by Dr Xuezheng Yang to be non-trivial.³⁸



Scheme 2.27. Overall synthetic route to spiroketal **195**

Past attempts to do so are summed up in Scheme **2.28** and have included standard Evans auxiliary removal conditions such $\text{LiOH}/\text{H}_2\text{O}_2$, LiBH_4 , and LiAlH_4 . The $\text{LiOH}/\text{H}_2\text{O}_2$ conditions gave minimal product and mostly returned starting material. Spiroketal **195** was similarly inert

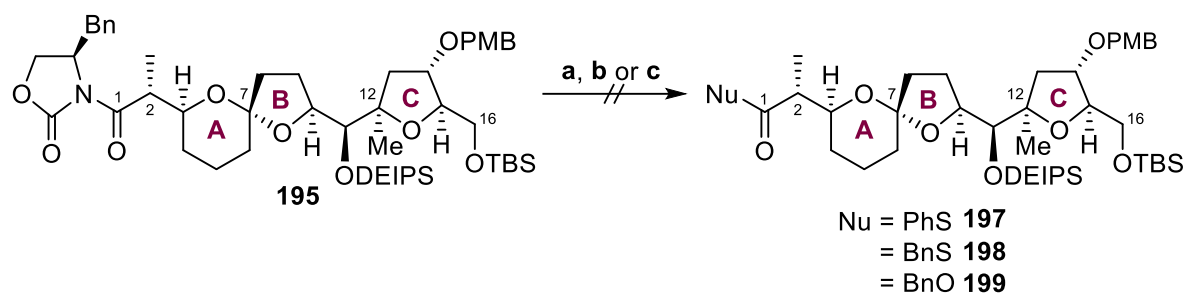
under the reductive LiBH_4 conditions; when more forcing LiAlH_4 conditions were used, starting material decomposition to a complex mixture resulted.



Scheme 2.28. Past attempts to cleave the Evans auxiliary by Dr Xuezheng Yang³⁸

2.11.2 Attempted removal of Evans auxiliary from spiroketal 195

Alternate conditions were sought to cleave the auxiliary. As part of the lactone moiety, C1 in PTX-4 is at the carboxylic acid oxidation state; therefore, using reductive conditions to cleave the auxiliary and reduce C1 to an alcohol would constitute an unproductive redox manipulation, and would necessitate an additional operation to oxidise C1 back up to a carboxylic acid. Thus, the approach to use reductive auxiliary cleavage conditions was abandoned and screening focused on other cleavage methods. A literature search revealed that deprotonated thiols and alcohols have been used as nucleophiles to displace the oxazolidinone moiety *via* an addition–elimination process.⁴⁹ Thus, thiophenol, benzyl thiol, and benzyl alcohol were selected as nucleophiles and were separately deprotonated with $n\text{BuLi}$, before spiroketal **195** was added to the mixture (Scheme 2.29). Unfortunately, these conditions only gave unreacted starting material or complex mixtures.



Reagents and conditions: a) PhSH, *n*BuLi, THF, 0 °C to rt
 b) BnSH, *n*BuLi, THF, 0 °C to rt
 c) BnOH, *n*BuLi, THF, 0 °C to rt

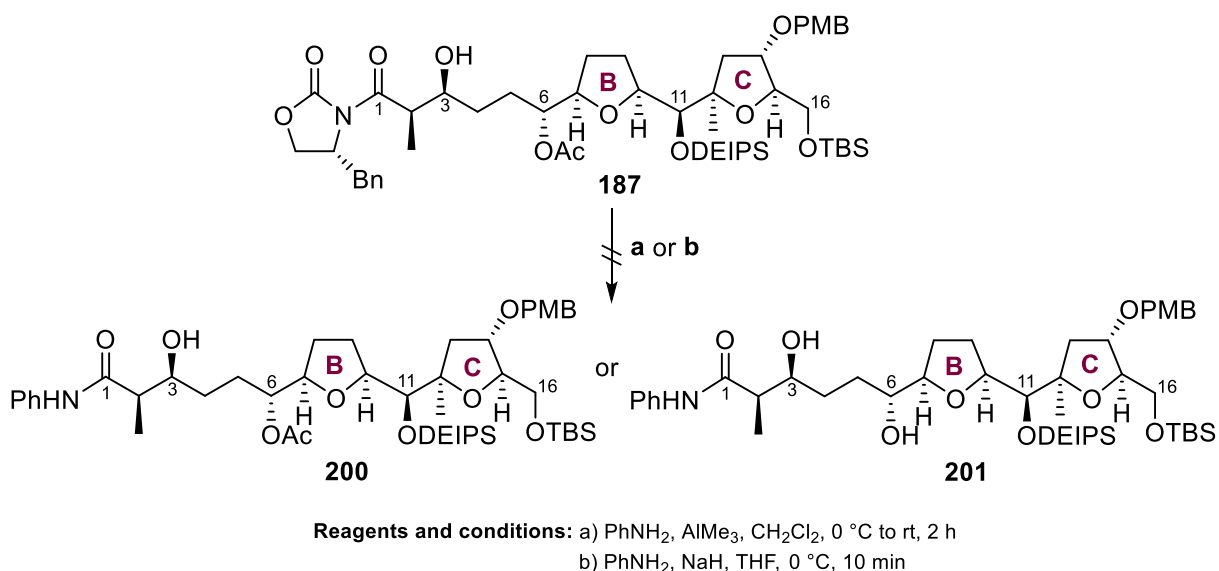
Scheme 2.29. Attempted addition–elimination strategy to cleave Evans auxiliary

2.11.3 Attempted removal of Evans auxiliary at an earlier stage of the synthesis

Because spiroketal **195** was a late-stage intermediate whose preparation was very time and labour intensive, obtaining starting material was a limiting factor in these test reactions to remove the auxiliary, and so another strategy was taken. The following three key points guided this new approach: a) screening focused on removing the auxiliary at an earlier stage of the synthesis, prior to the key 1,2-hydride shift spiroketalisation cascade; b) attempts at auxiliary removal would have the eventual goal of replacing the oxazolidinone moiety with an aniline amide moiety, which was the same tried-and-tested protecting group used at C1 in Evans' total synthesis of PTX-4;^{21,22} c) because of the variety of literature-known auxiliary cleavage methods and the multiple auxiliary-bearing intermediates on which these methods could be performed, the large number of combinations of screening conditions had to be narrowed down to the ones likelier to work to conserve valuable starting material.

To that end, chloromesylate **190** was quickly ruled out as a suitable substrate for oxazolidinone cleavage, because the chloromesylate moiety at C6 would be unlikely to tolerate reaction conditions involving nucleophiles to displace the oxazolidinone. Additionally, reaction screening involving aniline to directly displace the oxazolidinone was prioritised,

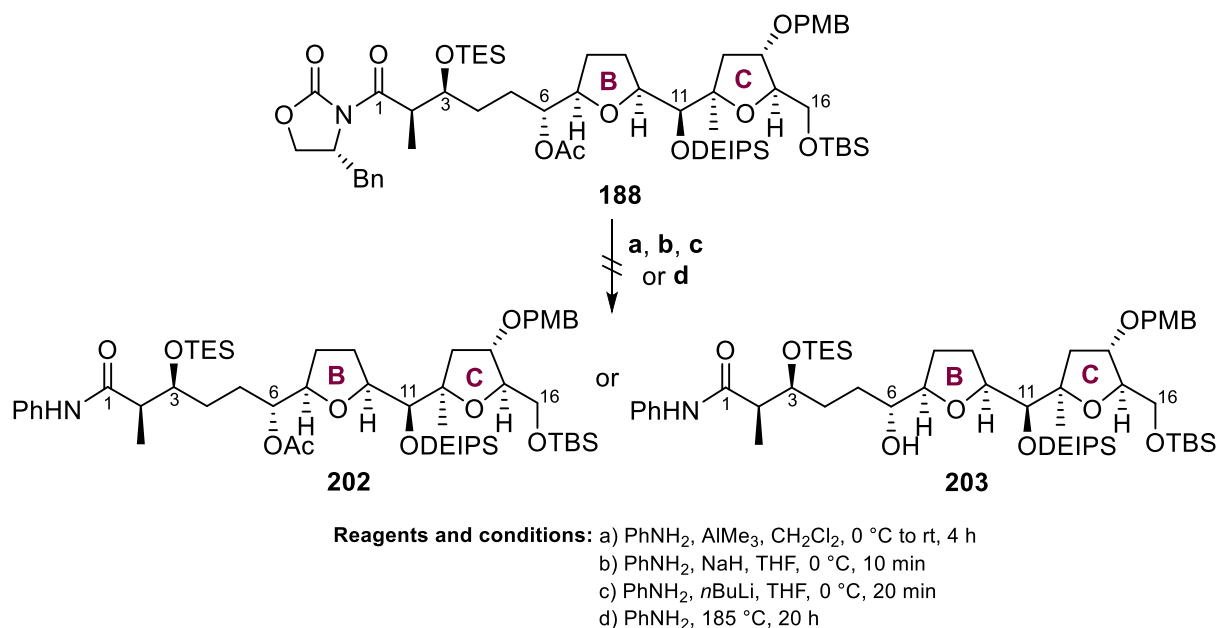
because such a transformation would not involve isolation of an intermediate (e.g., a carboxylic acid, thioester, or ester) that would in turn have to undergo an additional amidation operation. Thus, alcohol **187**, the immediate product of the Evans aldol addition, was reacted with aniline in the presence of superstoichiometric Lewis acid AlMe_3 at 0°C (Scheme **2.30**). This procedure only resulted in decomposition; however, submitting the crude mixture for mass spectrometry gave peaks at 852.4 Da and 894.5 Da which corresponded, respectively, to the $[\text{M} + \text{Na}^+]$ peaks of desired product **200** and the de-acetylated diol **201**, suggesting that traces of these two species had nonetheless formed during the reaction.



*Scheme 2.30. Attempted one-step transamidation of **187***

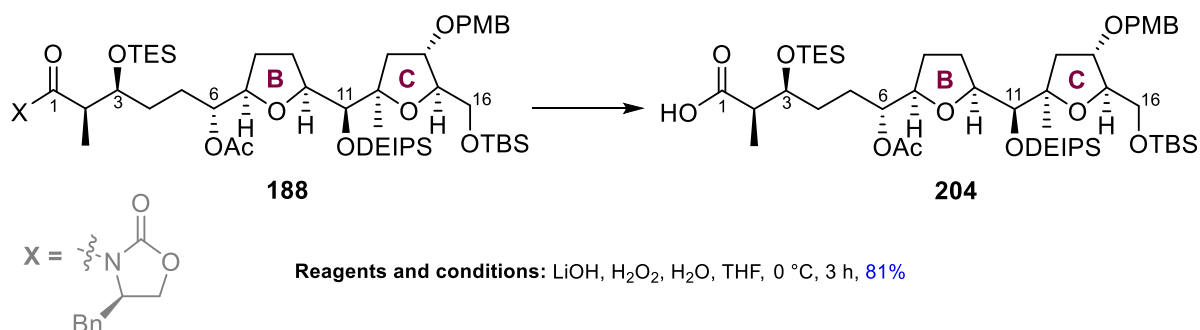
Although neither amides **200** nor **201** could be isolated, the detection of these peaks was taken as a promising sign, because it suggested that optimisation of the $\text{PhNH}_2/\text{AlMe}_3$ conditions could simultaneously perform two transamidations that replace the oxazolidinone and remove the acetate protecting group at C6, which would be desirable if the C3 hydroxyl group was already protected. Thus, silyl ether **188** instead of alcohol **187** was reacted under the same conditions, but once more only a complex mixture resulted (Scheme **2.31**). Alternate transamidation conditions involving PhNH_2 and NaH in THF as well as PhNH_2 and $n\text{BuLi}$ in THF

similarly gave complex mixtures when applied to either substrate. Reacting silyl ether **188** with neat aniline without deprotonation at elevated temperatures (185 °C) was also ineffective.



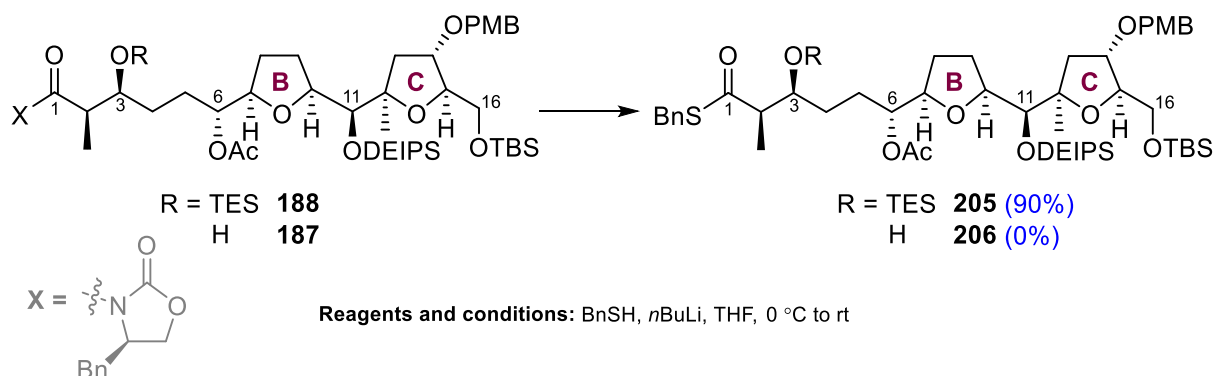
Scheme 2.31. Attempted one-step transamidation of **188**

Given the repeated failure of a direct transamidation, alternate nucleophiles were explored. Dr Xuezheng Yang had previously reported successful auxiliary cleavage of silyl ether **188** using LiOH/H₂O₂ conditions to give 81% yield of carboxylic acid **204** (Scheme 2.32).³⁸ However, attempts to repeat this reaction only gave unreacted starting material. Measures to enhance conversion such as longer reaction times and warming the reaction were similarly met with failure.



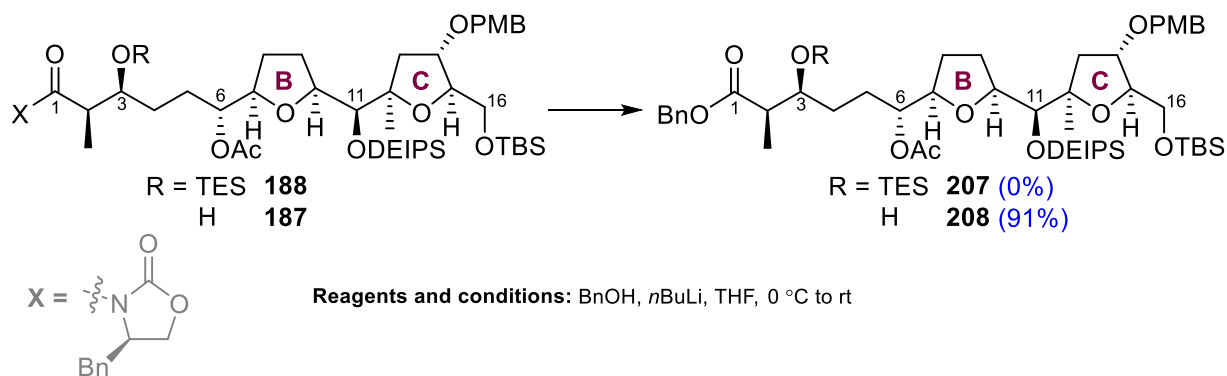
Scheme 2.32. Past successful cleavage of Evans auxiliary by Dr Xuezheng Yang³⁸

The first successful cleavage of the auxiliary was accomplished when deprotonated benzyl thiol was reacted with silyl ether **188** to give thioester **205** in 90% yield (Scheme 2.33); successful formation of thioester **205** was confirmed by the presence of new benzyl aromatic signals in the ^1H NMR spectrum and by the signature thioester carbonyl peak at 201.2 ppm in the ^{13}C NMR spectrum. This thioesterification reaction, however, did not work when alcohol **187** was used as the substrate.



Scheme 2.33. Evans auxiliary cleavage using benzyl thiol

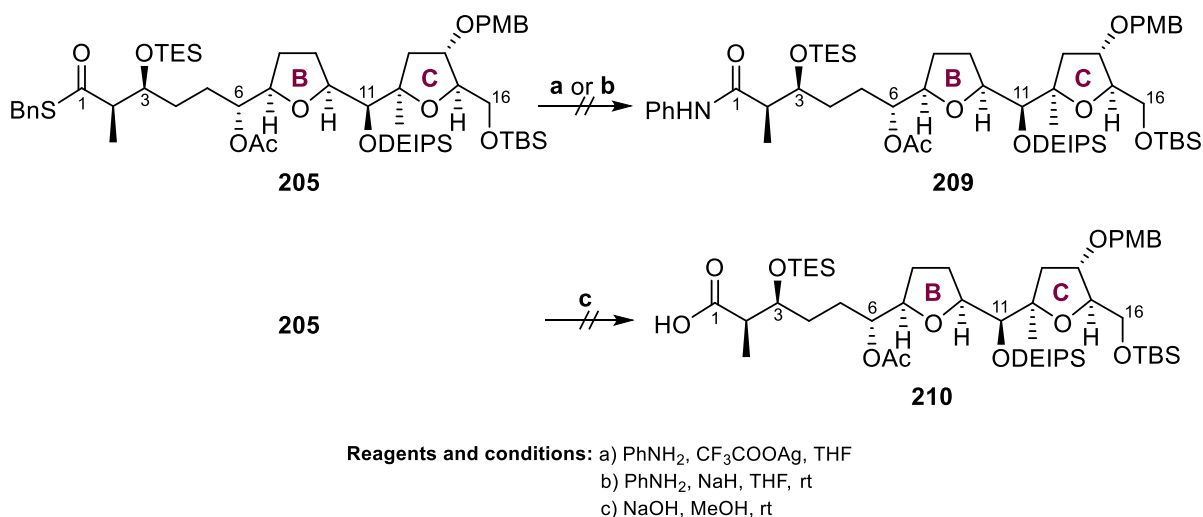
Interestingly, the results when using deprotonated benzyl alcohol were the opposite – alcohol **187** reacted with deprotonated benzyl alcohol to give ester **207** in 91% yield, but no desired product was obtained when silyl ether **188** was used as the substrate (Scheme 2.34).



Scheme 2.34. Evans auxiliary cleavage using benzyl alcohol

It was hoped that the more reactive thioester and ester moieties of **205** and **208** respectively would be more amenable to a transamidation with aniline. As the more reactive of the two functional groups, thioester **205** was made the focus of synthetic efforts at transamidation.

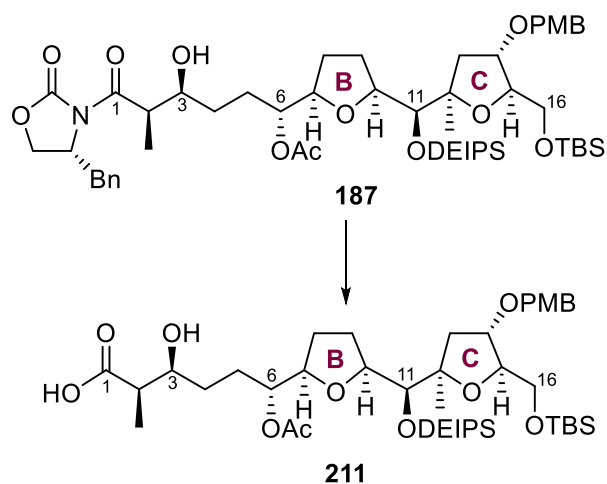
Ley and co-workers had developed a methodology to perform transamidations on thioesters under mild conditions using CF_3COOAg ; the protocol had been demonstrated to work with a variety of amines, including electron-deficient 2-nitroaniline and 2-aminopyridine.⁵⁰ Unfortunately, attempting this reaction using aniline on thioester **205** only returned starting material (Scheme 2.35) and repeating the reaction at higher temperatures only induced degradation. A NaH deprotonation strategy to convert PhNH_2 to a strong nucleophile was also ineffective. Moreover, thioester **205** was also surprisingly recalcitrant to hydrolysis with NaOH.



Scheme 2.35. Attempted transamidation and hydrolysis of thioester 205

2.11.4 Evans auxiliary cleavage of **187** and elaboration

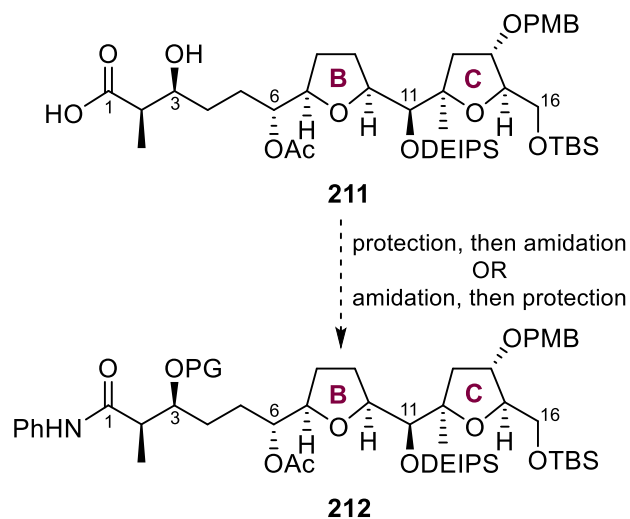
In parallel with these reactions involving thioester **205**, an experiment using $\text{LiOH}/\text{H}_2\text{O}_2$ conditions to cleave the Evans auxiliary in alcohol **187** was conducted, which gave carboxylic acid **211** in 87% yield (Scheme 2.36). This welcome result was surprising, considering that the same reaction with silyl ether **188** had repeatedly failed.



Reagents and conditions: LiOH, H₂O₂, H₂O, THF, 0 °C, 1 h, 87%

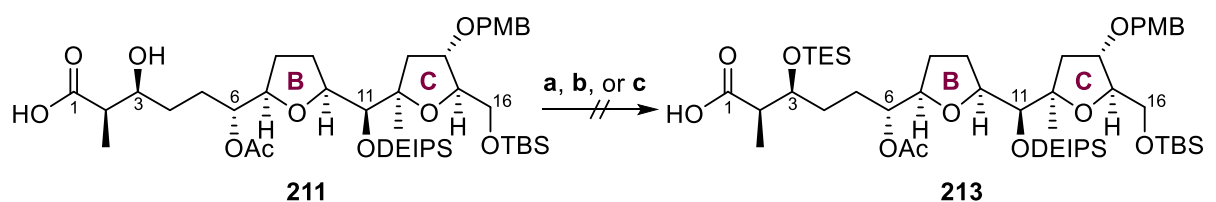
Scheme 2.36. Auxiliary cleavage of 187 to give 211

Synthetic efforts were then focused on converting carboxylic acid **211** to aniline amide **212**, which has a suitable protecting group installed on the C3 hydroxyl group. This could be achieved through two approaches – hydroxyl protection followed by amidation or vice versa (Scheme 2.37). Both approaches were attempted concurrently.

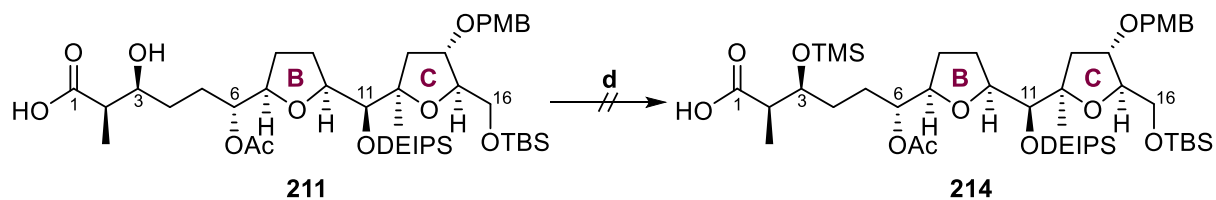


Scheme 2.37. Elaboration of 211 to amide 212

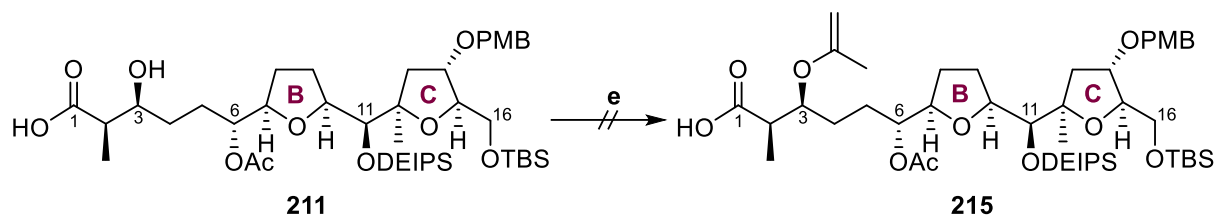
Attempted TES, TMS, and 2-methoxypropene (MOP) protections on carboxylic acid **211** failed and only returned starting material, despite use of excess reagent (Scheme 2.38).



Reagents and conditions: a) TESCl, imidazole, DMAP, CH₂Cl₂, 0 °C to rt
 b) TESCl, 2,6-lutidine, DMAP, CH₂Cl₂, 0 °C to rt
 c) TESOTf, imidazole, DMAP, CH₂Cl₂, 0 °C to rt



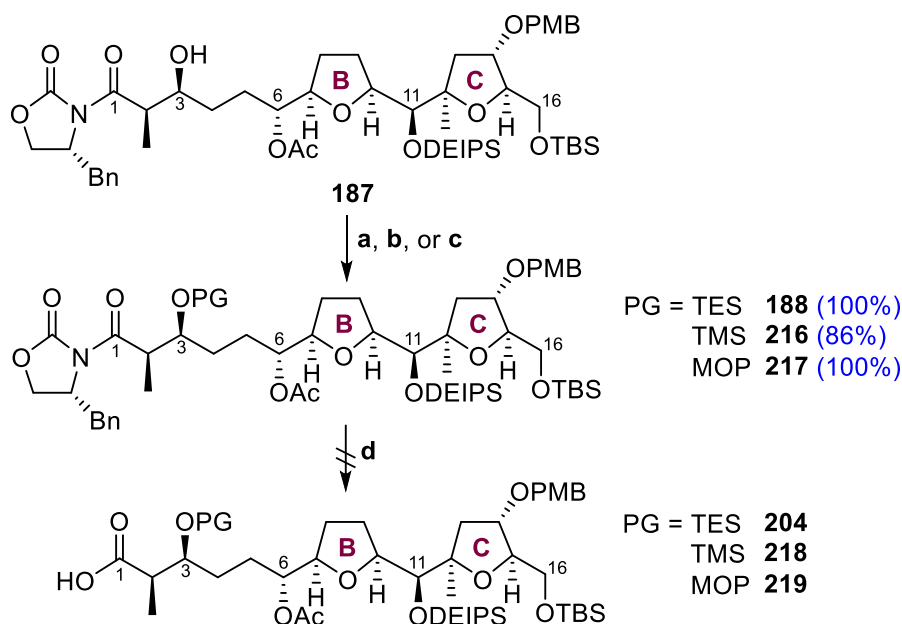
Reagents and conditions: d) TMSOTf, 2,6-lutidine, DMAP, CH₂Cl₂, 0 °C to rt



Reagents and conditions: e) 2-methoxypropene, PPTS, CH₂Cl₂, rt

Scheme 2.38. Attempted protection of carboxylic acid **211**

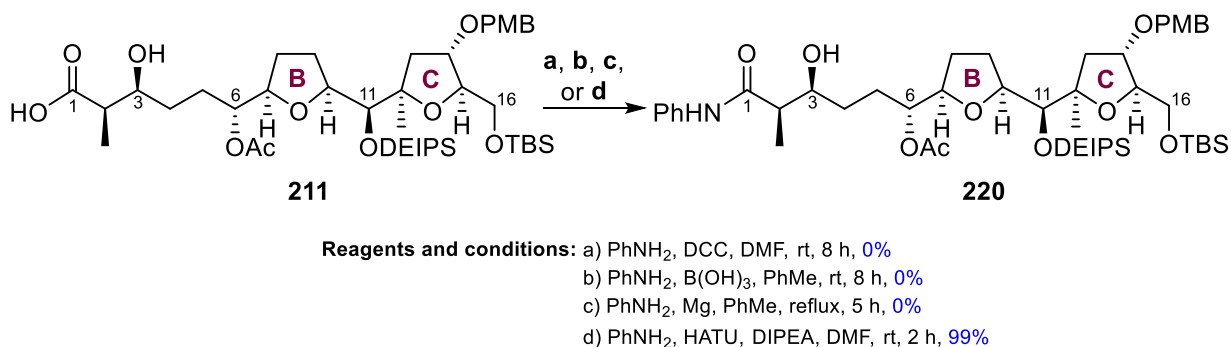
These same protection reactions worked on oxazolidinone-bearing compound **187** in high yields (Scheme **2.39**), suggesting that the nearby carboxylic acid moiety was somehow interfering with the various protecting group installations. These differentially protected oxazolidinone-bearing compounds (**216** and **217**), however, could not be converted to the corresponding carboxylic acids using the LiOH/H₂O₂ cleavage conditions, which implied the importance of a free C3 hydroxyl group for the reaction's success.



Reagents and conditions: a) TESCl, imidazole, DMAP, CH₂Cl₂, 0 °C to rt
 b) TMSCl, imidazole, DMAP, CH₂Cl₂, 0 °C to rt
 c) 2-methoxypropene, PPTS, CH₂Cl₂, rt
 d) LiOH, H₂O₂, THF, H₂O, 0 °C to rt

Scheme 2.39. Protection of 187

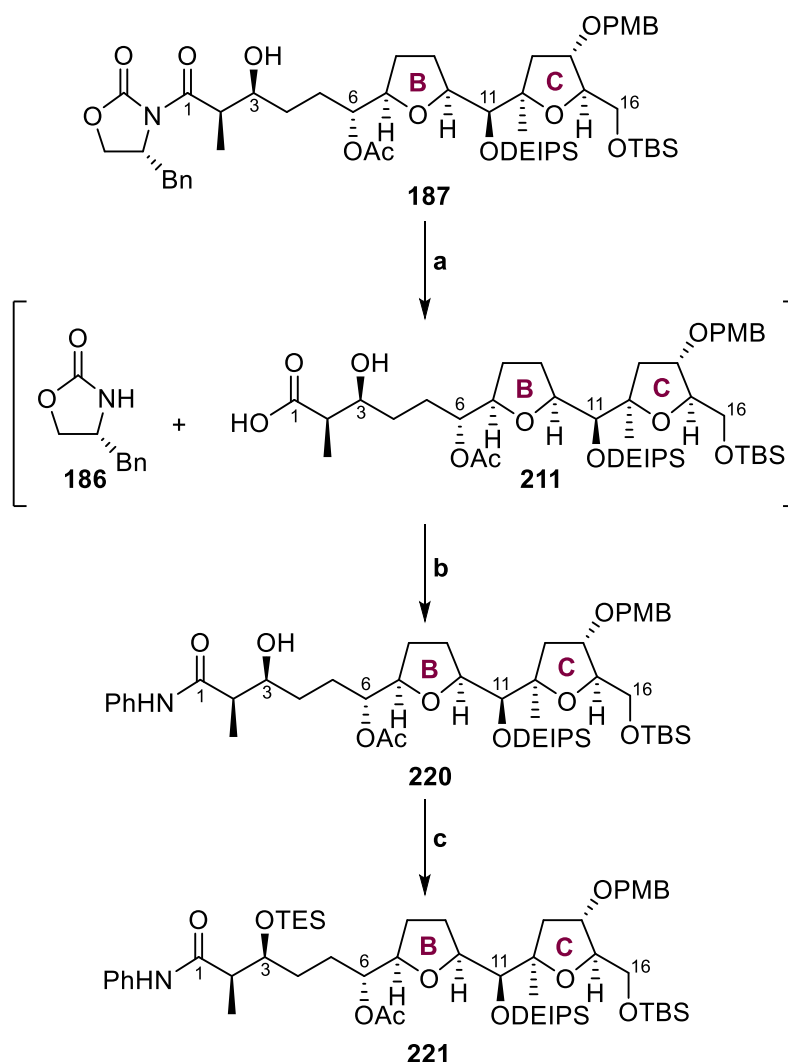
Fortunately, an “amidation, then protection” strategy proved more fruitful for the elaboration of carboxylic acid **211**. Various amidation conditions were attempted with no success, until conditions involving HATU gave amide **220** in 83% yield at a test scale of 11 mg. The reaction was progressively scaled up until it was demonstrated that it could be performed at a 1.46 g scale to give amide **220** in an excellent 99% yield (Scheme **2.40**).



Scheme 2.40. Attempted amidation of carboxylic acid 211

Although the amidation step was reliable and high yielding, the preceding step involving LiOH/H₂O₂-mediated cleavage of oxazolidinone **187** proved to be less so after repeated runs.

For example, an oxazolidinone cleavage attempted much later at a 780 mg scale gave only 44% yield of carboxylic acid **211**. Such low-yielding runs nonetheless gave crude sample NMR spectra that were surprisingly clean, showing the presence of carboxylic acid **211** and the cleaved oxazolidinone by-product **186** as the only dominant species in roughly equal quantity, as determined by ^1H NMR peak integration. Moreover, although by-product **186** could be isolated in quantitative yield during column chromatography, only 40–50% carboxylic acid **211** could be collected despite precautions taken to flush the column of silica with extremely polar eluent. The remaining mass balance could not be accounted for.



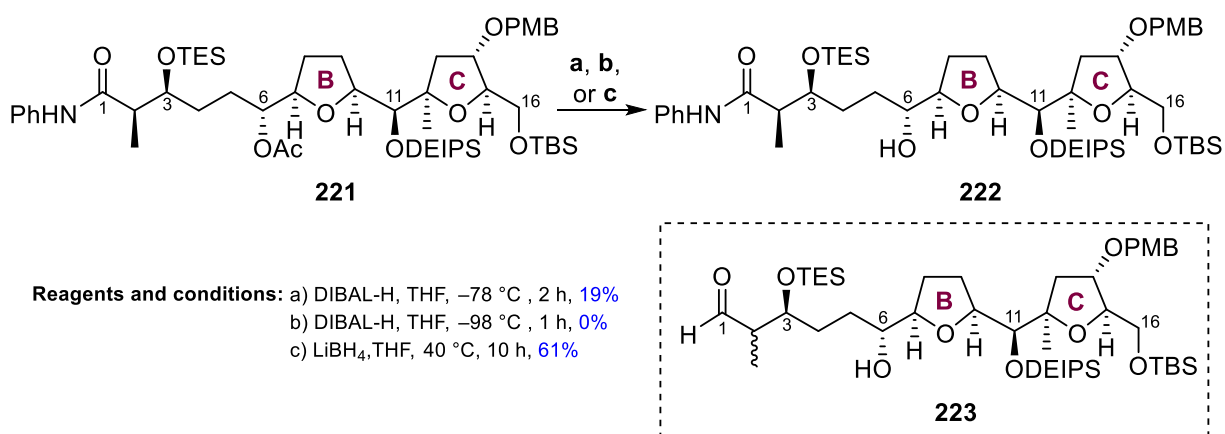
Reagents and conditions: a) LiOH, H_2O_2 , THF, H_2O , 0°C , 1 h
 b) PhNH_2 , HATU, DIPEA, DMF, rt, 2 h, **81%** over two steps
 c) TESCl, imidazole, DMAP, CH_2Cl_2 , rt, 15 min, **97%**

Scheme 2.41. Modified procedure to prepare amide **221**

A re-optimised protocol involving skipping the column chromatography operation and directly carrying crude **211** to the amidation step was eventually developed (Scheme **2.41**), which reliably gave higher overall yields of amide **220** of up to 81% over two steps and could be scaled up to 3.0 g. Thereafter, straightforward TES protection of amide **220** upon treatment with TESCl, imidazole and DMAP gave silyl ether **221** in 97% yield (Scheme **2.41**).

2.12 Conversion of 221 to chloromesylate 140

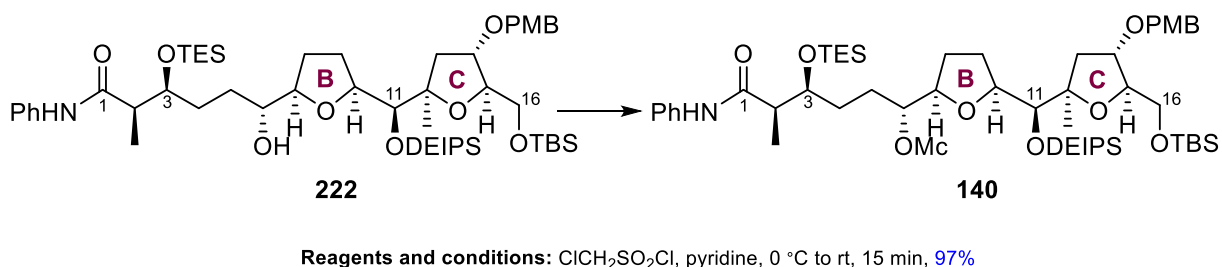
The original DIBAL-H reductive conditions conducted at $-78\text{ }^{\circ}\text{C}$ to deprotect the C6 acetate group of oxazolidinone **188** (Scheme **2.25**) worked poorly for **221**, and gave alcohol **222** in only 19% yield, together with a complex mixture of side-products (Scheme **2.42**). Although these side-products could not be isolated and properly characterised, the ^1H NMR spectrum of the crude sample showed two aldehyde peaks, strongly suggesting that the amide of **221** had been reduced and epimerised at the C2 position to give aldehyde **223**. Performing the reaction at an even lower temperature using a $-98\text{ }^{\circ}\text{C}$ MeOH/liquid N_2 cooling bath was ineffective, and only gave 49% recovered starting material and a mixture of products that could not be identified.



Scheme **2.42**. Removal of acetate group of **221**

However, it was later found that treatment of acetate **221** with LiBH₄ at 40 °C gave alcohol **222** in 61% yield, with 17% recovered starting material (Scheme 2.42). Care had to be taken to monitor the reaction and not to leave it running for excessively long durations due to possible over-reduction of the amide moiety to give the corresponding diol.

Finally, treatment of alcohol **222** with chloromethanesulfonyl chloride in pyridine gave compound **140** in 97% yield (Scheme 2.43), the direct precursor for the 1,2-hydride shift spiroketalisation cascade.



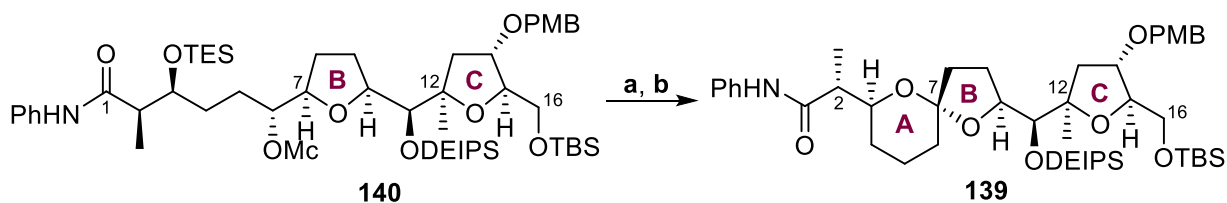
Scheme 2.43. Synthesis of precursor 140

2.13 Optimisation of 1,2-hydride shift spiroketalisation cascade

2.13.1 Pre-optimisation of 1,2-hydride shift reaction

To achieve the 1,2-hydride shift spiroketalisation cascade, precursor **140** was subjected to the same conditions that were optimised for the close analogue oxazolidinone **190**. The reaction sequence, when performed at a 30 mg scale, successfully afforded ABC fragment **139**, albeit in a low yield of 19% over two steps (Scheme 2.44). The sequence produced the anomeric and thermodynamic 6,5-spiroketal, which gave a characteristic ¹³C NMR chemical shift of 105.6 ppm at C7. This value is consistent with the characterisation data of close anomeric spiroketal analogues (oxazolidinone **195** and its C11 TBS-substituted analogue) previously prepared by the Donohoe group and structurally assigned by nOe correlations.^{37,38} Moreover, the C7

chemical shift value was also consistent with natural and synthetic PTXs possessing anomeric 6,5-spiroketal; in contrast, non-anomeric 6,5-spiroketal and 6,6-spiroketal gave chemical shifts from 107.0–111.0 ppm at C7.²⁵

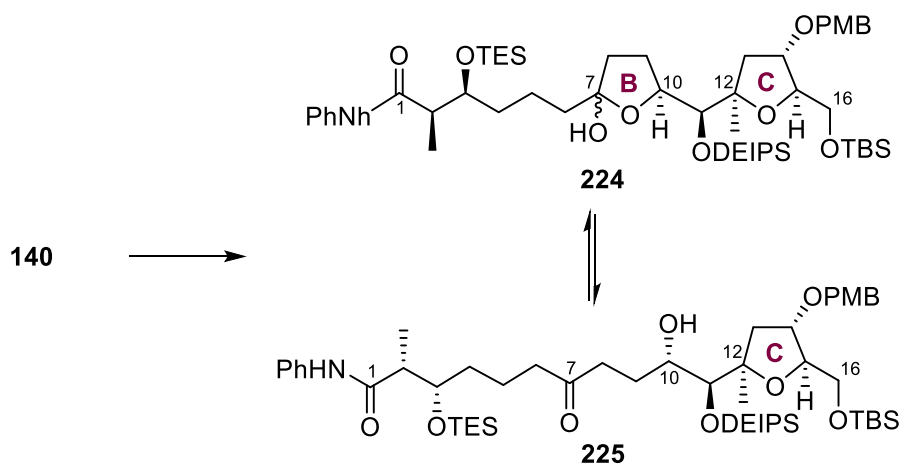


Reagents and conditions: a) $\text{Zn}(\text{OAc})_2 \cdot 2\text{H}_2\text{O}$, DMF/ H_2O (4:3), 75 °C, 12 h;
b) PPTS, MeOH/ CH_2Cl_2 (1:1), 0 °C, 2 h 19% over two steps

Scheme 2.44. 1,2-Hydride shift and spiroketalisation of precursor **140**

The successful formation of spiroketal **139** notwithstanding, the rest of the mass balance could not be accounted for. Nevertheless, it was surmised that the cause of the low yield likely lay with the initial 1,2-hydride shift step involving the unstable chloromesylate **140**, which may participate in undesirable side-processes under the activating conditions of the reaction. Thus, preliminary optimisation efforts focused on the 1,2-hydride shift reaction (Table **2.1**).

First, reaction durations were shortened to minimise potential product degradation under reaction conditions (Table **2.1**, Entries 1–3). However, there was no apparent change in the yields. Next, temperatures were lowered with a concomitant increase in reaction duration to 24 h to ensure full conversion. Only starting material was obtained when the reaction was run at 55 °C (Table **2.1**, Entry 5), while a reaction temperature of 65 °C over 24 h gave the best result at 54% yield (Table **2.1**, Entry 4).



Reagents and conditions: $\text{Zn}(\text{OAc})_2 \cdot 2\text{H}_2\text{O}$, DMF/ H_2O (4:3)

Table 2.1. Preliminary screening of 1,2-hydride shift conditions

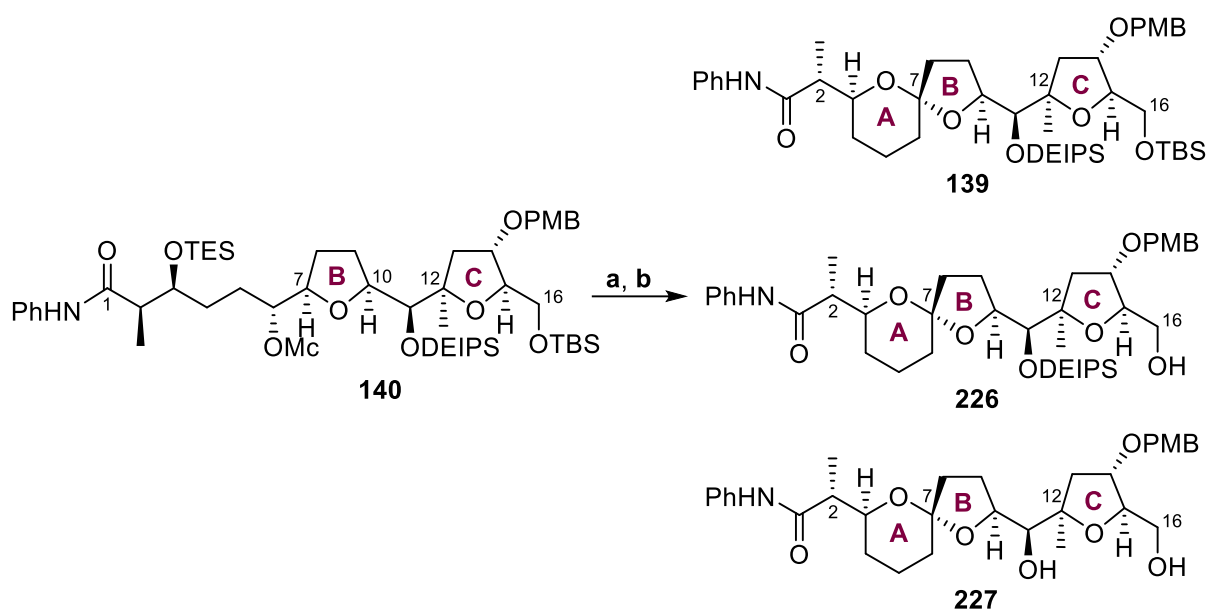
Entry	Temperature ($^{\circ}\text{C}$)	Duration (h)	Yield of 224/225
1	75	12	37%
2	75	7	31%
3	75	2	37%
4	65	24	54%
5	55	24	SM only

This pre-optimisation was helpful in determining pertinent information about the system, such as the minimum temperature required to induce the 1,2-hydride shift and the fact that the immediate 1,2-hydride shift product is stable under reaction conditions, as inferred by the constant yields over longer reaction durations. However, a significant drawback of this pre-optimisation experimental design was the difficulty in ascertaining the purity and hence true yield of the 1,2-hydride shift product, because it existed in an equilibrium mixture of hemiacetal **224** and hydroxy ketone **225**.

2.13.2 Optimisation involving entire cascade

Given the problems with analysis in the pre-optimisation experimental design, subsequent optimisation experiments took into account the yield after two steps to give ABC fragment **139**, which was easier to analyse. The issues with assessing purity and yields of hemiacetal **224** and hydroxyketone **225** notwithstanding, the partially optimised 1,2-hydride shift reaction conditions detailed in Entry 4 of Table **2.1** were assumed to be superior and were thus adapted for the first step in this second round of optimisation experiments (Table **2.2**).

Initially, a one-pot method was attempted in which the PPTS acid catalyst was directly added to the reaction pot at 0 °C after completion of the 1,2-hydride shift (Table **2.2**, Entry 1); however, this resulted in no ABC fragment **139** being formed. In subsequent test reactions, the 1,2-hydride shift reaction was quenched and extracted, but no column chromatography was conducted on the product to minimise transfer losses. Such a procedure was conducted for Entry 2, which gave ABC fragment **139** in 20% yield and alcohol **226** in 12% yield. The co-formation of alcohol **226**, while unexpected, was welcomed because a TBS deprotection at C16 in ABC fragment **139** was in fact the next planned step of the synthesis. It was reasoned that a higher temperature and longer reaction time in the spiroketalisation step would promote greater conversion of silyl ether **139** to alcohol **226**; this was demonstrated by Entry 3, where silyl ether **139** was absent and alcohol **226** was obtained in 45% yield when the reaction was allowed to stir at 30 °C over 24 h. Diol **227** was also formed and isolated in 14% yield, suggesting that the acidic spiroketalisation–deprotection step had room for further optimisation to suppress concomitant deprotection of the DEIPS group at C11 as well.



Reagents and conditions: a) $\text{Zn}(\text{OAc})_2 \cdot 2\text{H}_2\text{O}$, DMF/ H_2O (4:3), 65 °C, 24 h

Table 2.2. Screening of conditions over full sequence

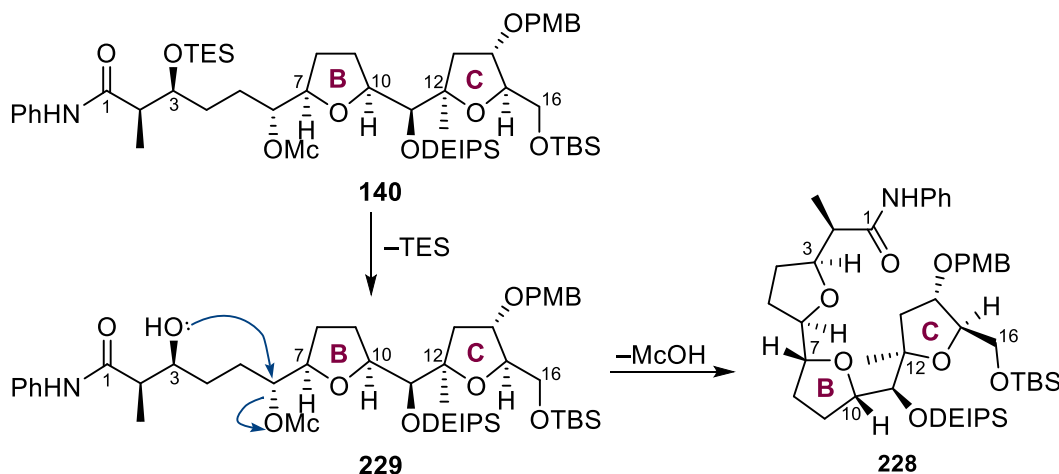
Entry	Step b	Yield of 139	Yield of 226	Yield of 227
1	One pot at 0 °C	0%	0%	0%
2	Extract, then react at 0 °C for 3 h	20%	12%	0%
2R	Extract, then react at 0 °C for 3 h	31%	0%	0%
3	Extract, then react at 0 °C for 3 h, then at 30 °C for 3 h	0%	45%	14%
3R	Extract, then react at 0 °C for 3 h, then at 30 °C for 3 h	11%	28%	0%

Thus, the sequence was repeated (Entry 3R), with more careful reaction monitoring during the spiroketalisation–deprotection step. However, TLC analysis continually indicated a lack of conversion of **139** to alcohol **226**. Eventually, the reaction was stopped at the same time point (after 24 h at 30 °C) as in Entry 3; **139** and **226** were isolated in 11% and 28% yields respectively, with no diol **227** being formed. The discrepancy in the distributions of **139**, **226**, and **227** between Entry 3 and Entry 3R was concerning, because it implied a lack of reaction reproducibility in a key step involving precious starting material. As a precaution, the reaction

conditions for Entry 2 were also repeated, and the resulting product yields were also inconsistent (Entry 2R).

2.13.3 Formation of *tris*-THF **228** and instability of chloromestylate **140**

In addition to reaction reproducibility issues, two other concerns either frustrated and complicated optimisation efforts. First, *tris*-THF **228** was isolated in 0%–10% yields in the reaction runs. This side-product likely formed as a result of premature deprotection of the TES group to give **229**, followed by rapid 5-exo-tet ring-closure from the exposed hydroxyl group attacking the chloromestylate at C6 (Scheme **2.45**). Control experiments using a pH 7.0 phosphate buffer in the 1,2-hydride shift step did not suppress this process; it was instead eventually decided to focus optimisation efforts elsewhere because *tris*-THF **228** only constituted a small percentage of the total mass balance and hence its suppression would give minimal gains to yields of the desired product.



Scheme **2.45**. Formation of *tris*-THF side-product **228**

The second issue concerned the instability of starting material chloromestylate **140**, which had initially been observed to slowly degrade over several weeks even when stored at $-30\text{ }^{\circ}\text{C}$. Hence, as a precaution, only small batches of chloromestylate **140** were prepared at a time from alcohol **222** (Scheme **2.43**). These small batches of substrate were rapidly used for the

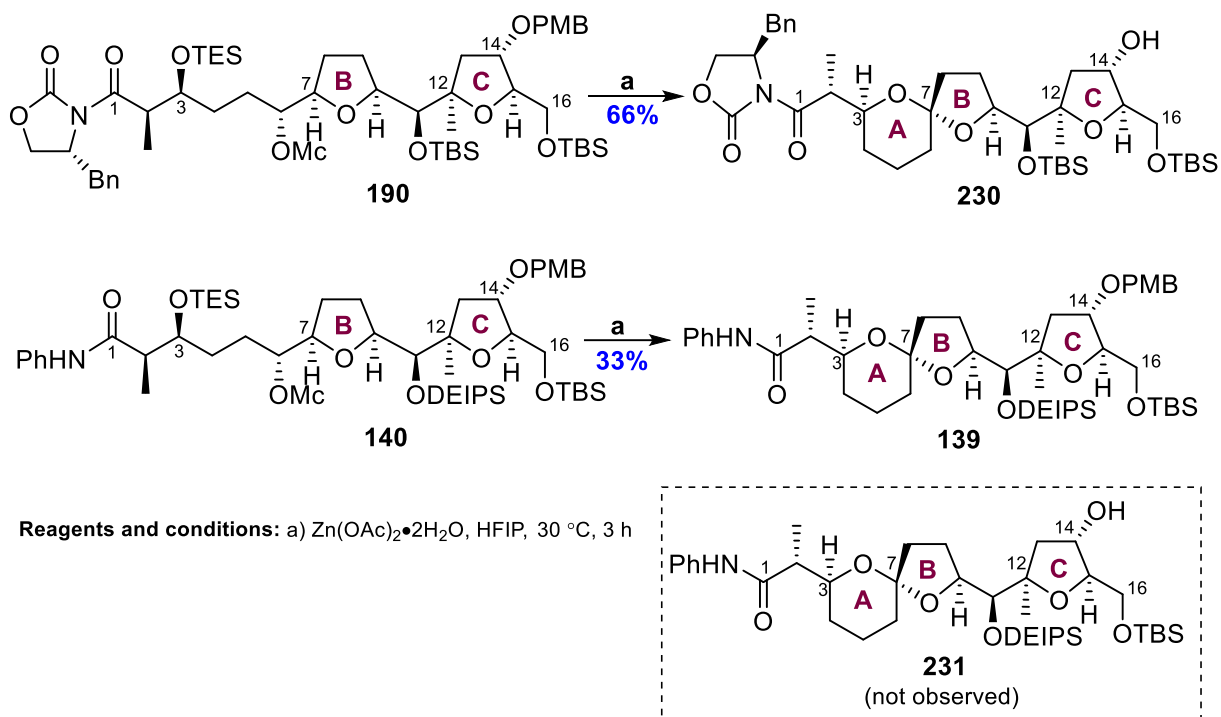
1,2-hydride shift spiroketalisation optimisation experiments, thus preventing inadvertent starting material degradation from prolonged storage. However, the necessity of repeatedly performing the chloromesylation reaction and product isolation contributed to the labour- and time-intensiveness of conducting the optimisation experiments.

Towards the end of the reaction optimisation, when a set of reaction conditions that gave acceptable yields had at last been attained, 1.19 g of alcohol **222** was converted to 1.27 g of chloromesylate **140** in 96% yield; it had been intended to fully consume this batch of **140** in final optimisation and scale-up experiments over a period of two weeks – well within the shelf-life of the chloromesylate as had been observed thus far. However, this large batch of chloromesylate **140** unexpectedly underwent complete degradation to a complex mixture within the first four days of storage, before most of it could be used in the key step. Due to the unpredictability of its decomposition rate and its preciousness, chloromesylate **140** was henceforth reacted in the next step within a day of its preparation.

2.13.4 Optimisation involving HFIP

In parallel with the optimisation studies detailed in section **2.13.2**, an alternate set of 1,2-hydride shift spiroketalisation conditions involving 1,1,1,3,3,3-hexafluoroisopropanol (HFIP) solvent was investigated, on the basis of past success of such a system on oxazolidinone-bearing chloromesylate **190**.³⁰ Treatment of chloromesylate **140** with HFIP and Zn(OAc)₂ at 30 °C gave spiroketal **139** in 66% yield (Scheme **2.46**). Besides the good yield for such a complex transformation, another impressive aspect of the HFIP conditions was that no additional step was required to induce the C3 TES deprotection and spiroketalisation. The major drawback of the conditions as applied to chloromesylate **190** was the undesired HFIP-promoted S_N1 deprotection of the PMB ether at C14 to give alcohol **230**. Nevertheless, this

past result was deemed promising and the HFIP conditions were thus applied to chloromesylate **140** give ABC fragment **139** in 33% yield, with no evidence of PMB ether removal.



Scheme 2.46. 1,2-Hydride shift and spiroketalisation involving HFIP

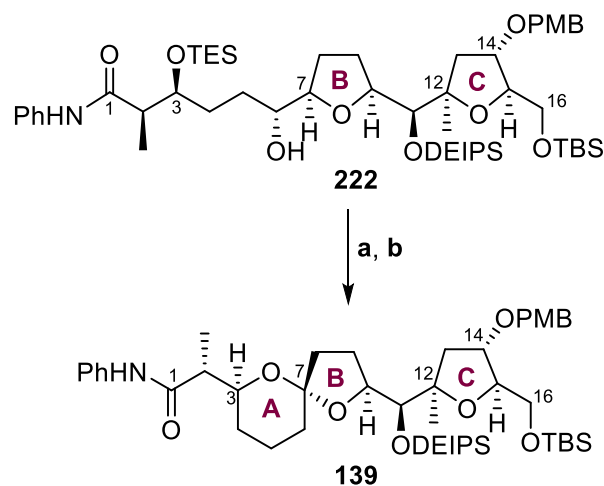
Repeats of the reaction performed on larger scales gave consistent albeit low yields of **139** in the range of 30%–40%. Although the yields were found wanting, these preliminary results were deemed a suitable starting point on which to base optimisation efforts, which are summed up in Table 2.3. Running the reaction at elevated temperatures (60 °C) was counter-productive and only gave PMB-deprotected **231** in 7% yield, with no other isolable species (Table 2.3, Entry 1). A series of test reactions were then run using “hybrid” conditions that were a combination of the HFIP conditions and the higher temperature DMF/H₂O conditions described in section 2.13.2. Eventually, it was found that treating chloromesylate **140** with $\text{Zn}(\text{OAc})_2$ in a 29:21:50 DMF:H₂O:HFIP tri-solvent system at 70 °C gave ABC fragment **139** in 40% yield (Entry 5).

Table 2.3. Screening of conditions involving HFIP

Entry	DMF : H ₂ O : HFIP	Temperature (°C)	Recovered 140	139
1	0 : 0 : 100	60	0%	0%
2	54 : 41 : 5	30	68%*	0%
3	29 : 21 : 50	30	77%*	0%
4	54 : 41 : 5	70	0%	30%
5	29 : 21 : 50	70	0%	49%*/40%
6	95 : 0 : 5	30	41%*	0%
7	50 : 0 : 50	30	52%*	0%

*NMR yields

The conditions in Entry 5 were streamlined to involve reaction of crude chloromesylate **140** without column chromatography from the previous step. Pleasingly, yields using this set of conditions improved significantly upon scale-up. For example, separate 1,2-hydride shift spiroketalisation reactions performed using 570 mg, 990 mg, and 1.45 g of alcohol **222** gave ABC fragment **139** in 77%, 57% and 63% yields over *two* steps (Scheme 2.47).



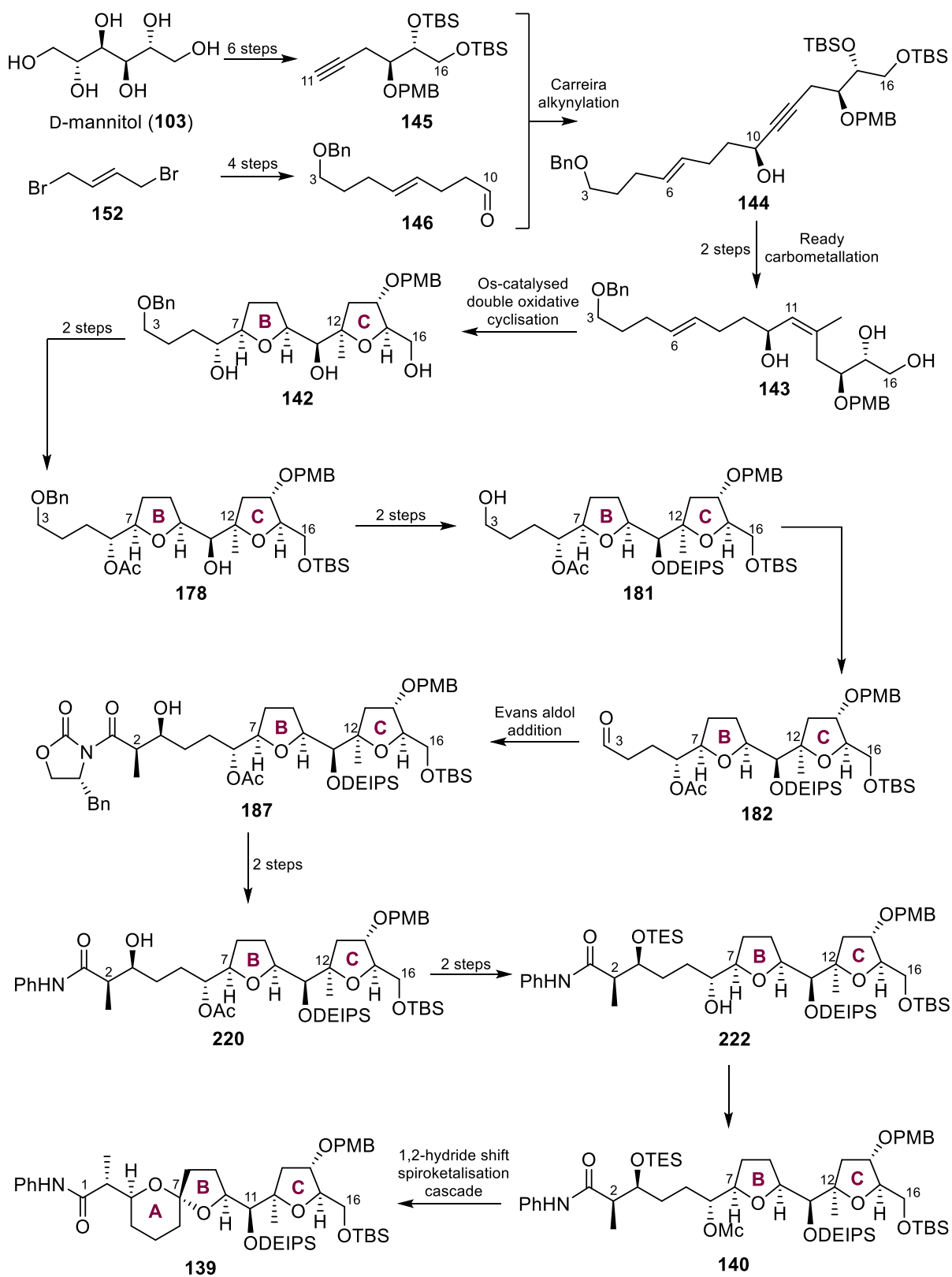
Reagents and conditions: a) ClCH₂SO₂Cl, pyridine, 0 °C to rt, 15 min
b) Zn(OAc)₂•2H₂O, HFIP, DMF, H₂O, 70 °C, 7 h, 57%–77% over two steps

Scheme 2.47. Fully optimised 1,2-hydride shift and spiroketalisation sequence

2.14 Conclusion

In conclusion, ABC fragment **139** was prepared in 21 linear steps from D-mannitol (**103**), which is summarised in Scheme **2.48**. Key steps in the synthesis include a Carreira alkynylation, an osmium-catalysed double oxidative cyclisation, an Evans aldol addition, and a 1,2-hydride shift spiroketalisation cascade. To ensure a robust route to **139**, significant challenges were overcome, such as troubleshooting of the osmium-catalysed double oxidative cyclisation to resolve reproducibility issues, cleavage and replacement of the Evans oxazolidinone auxiliary with an aniline amide protecting group, and optimisation of the low-yielding 1,2-hydride shift spiroketalisation cascade.

Now that a robust synthesis of ABC fragment **139** had been developed, the compound can be elaborated and coupled with the E fragment, the other major fragment of PTX-4. The synthesis of the E fragment is discussed in chapter 3 and the attempts to join the two fragments are discussed in chapter 4.



Scheme 2.48. Overall synthetic route to ABC fragment **139**

CHAPTER 3

The E and F Fragments

3.1 Chapter overview

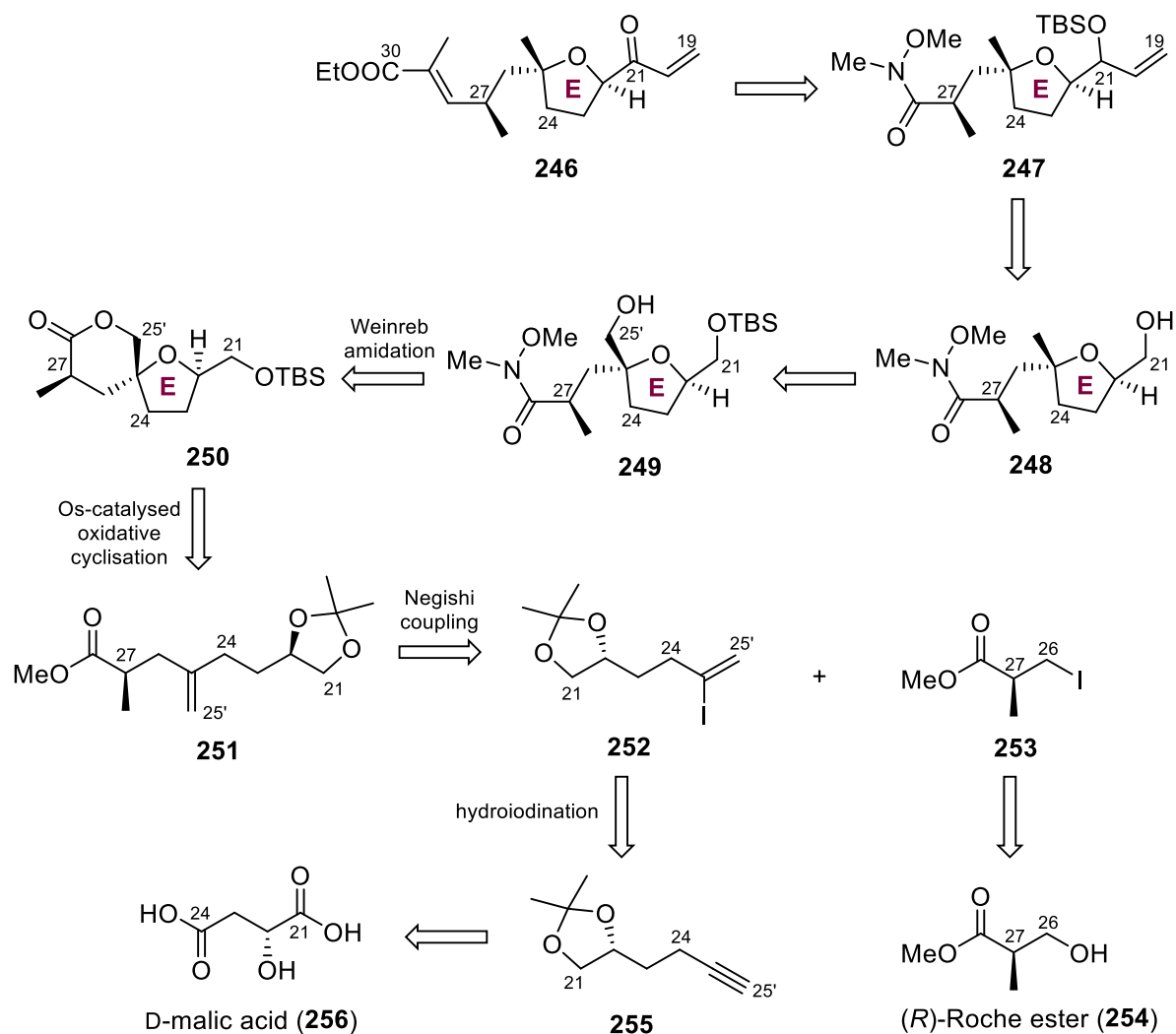
This chapter describes the synthesis of the C19–C30 E fragment of PTX-4, beginning with a brief retrosynthesis of the fragment followed by a discussion of the forward synthesis. Extensive control experiments to troubleshoot an irreproducible regioselective hydroiodination step to give a vinyl iodide product early in the synthesis are documented. Additionally, attempted workarounds for this problematic step including a new forward synthesis towards the vinyl iodide are discussed. Finally, the synthesis of the C31–C40 F fragment of PTX-4 is briefly covered.

3.2 Retrosynthesis of the E fragment

The Donohoe group's synthesis of the E ring was developed by Dr Yifan Liu, Dr Paul Winship, and Dr Melodie Richardson.^{36,51,52} My work involved repeating the synthesis to prepare the E fragment and re-optimising unreliable steps of the route as required. The retrosynthesis of E fragment **246** is outlined in Scheme **3.1**.

E fragment **246** can be derived from protected allyl alcohol **247**, which in turn can be simplified to Weinreb amide **248**. Weinreb amide **248** was derived directly from lactone **250** through a transamidation involving lactone ring opening. Lactone **250**, in turn, can be obtained from alkene **251** through a cascade involving removal of the acetal and an osmium-catalysed oxidative cyclisation. This osmium-catalysed methodology was also used in the preparation of the ABC fragment, which is discussed in chapter 2. Alkene **251** may be derived from the two fragments **252** and **253** through a Negishi cross-coupling. Alkyl iodide **253** may be directly prepared from (*R*)-Roche ester **254** through an Appel reaction, while vinyl iodide **252** may be

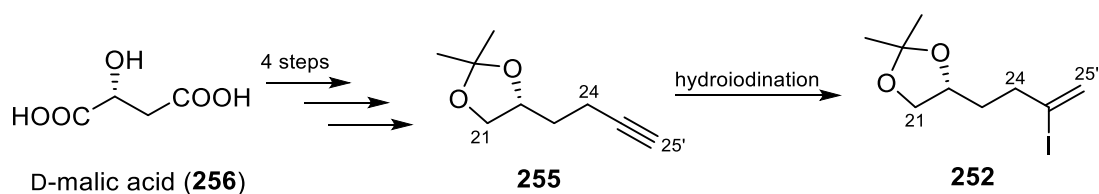
synthesised from alkyne **255** through a hydroiodination reaction. Alkyne **255** was derived from D-malic acid over four steps.



Scheme 3.1. Retrosynthetic analysis of the E fragment 246

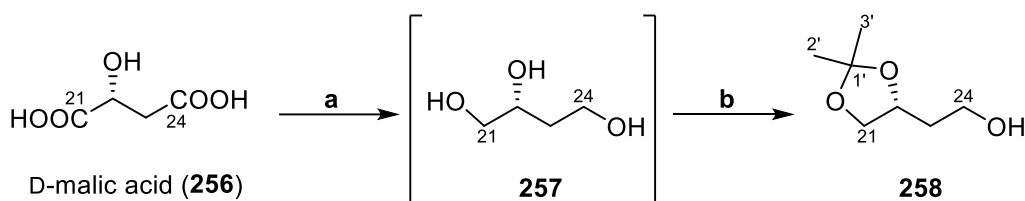
3.3 Synthesis of C21–C25 alkyne **255**

The preparation of E fragment **246** began with the four-step synthesis of alkyne **255**, which is the immediate precursor of the hydroiodination step to make vinyl iodide **252** (Scheme 3.2).



Scheme 3.2. Projected synthesis of alkyne 255

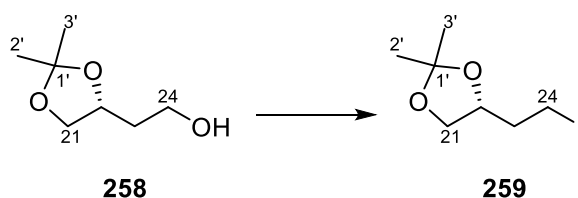
First, D-malic acid (**256**) was reduced to triol **257** using $\text{BH}_3\cdot\text{SMe}_2$. The high polarity of triol **257** made it difficult to handle, and thus it was carried over as a crude mixture for the subsequent acetal protection reaction. Initial attempts of this protection using only acetone and *p*TSA gave poor yields of acetonide **258** (35% over two steps). However, addition of 2,2-dimethoxypropane enhanced conversion and gave acetonide **258** in 54% yield (Scheme 3.3), presumably because acetal formation was more entropically favoured with 2,2-dimethoxypropane which releases two molecules of MeOH by-product when it reacts with triol **257**. The successful formation and isolation of acetonide **258** was confirmed by the appearance of the two strong singlets at 1.45 ppm and 1.38 ppm of the pair of diastereotopic methyl groups in the ^1H NMR spectrum, as well as by the signature acetal carbon signal at 109.1 ppm in the ^{13}C NMR spectrum.



Reagents and conditions: a) $\text{BH}_3\cdot\text{SMe}_2$, $\text{B}(\text{OMe})_3$, THF, 0 °C to rt, 16 h
 b) 2,2-dimethoxypropane, acetone, *p*TSA, THF, rt, 16 h, 54% over two steps

Scheme 3.3. Synthesis of acetonide 258 from D-malic acid (256)

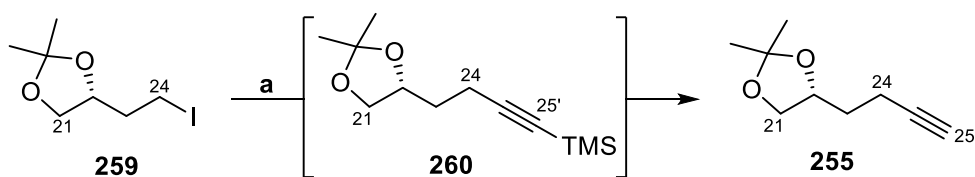
An Appel reaction involving treatment of acetonide **258** with PPh_3 , I_2 , and imidazole afforded alkyl iodide **259** in 87% yield (Scheme 3.4). This reaction was successfully performed on a 10 g scale. Due to its instability to light as a result of the weak C–I bond, upon isolation alkyl iodide **259** had to be stored in the dark in a –30 °C freezer. Alkyl iodide **259**, which was isolated as a colourless oil, slowly turns brown when exposed to light.



Reagents and conditions: PPh₃, I₂, imidazole, Et₂O, MeCN, 0 °C to rt, 1.5 h, 87%

Scheme 3.4. Synthesis of 259 via Appel reaction

Reacting alkyl iodide **259** with lithiated TMS-acetylene in THF and anhydrous DMPU gave alkyne **260** in 59% yield, which in turn could be treated with K₂CO₃ and MeOH to remove the TMS group and give the C21–C25 alkyne **260**. However, this approach was replaced with a more convenient procedure involving one-pot alkynylation, followed by K₂CO₃/MeOH addition to give alkyne **255** directly in 82% yield (Scheme 3.5). Formation and isolation of alkyne **255** was confirmed by appearance of the new ¹³C NMR signals at 83.5 ppm and 69.0 ppm, which respectively correspond to C25 and C25' in the newly installed alkyne.



Reagents and conditions: a) TMS-acetylene, *n*BuLi, DMPU, THF, –78 °C to rt ; then K₂CO₃, MeOH, rt, 82%

Scheme 3.5. One-pot synthesis of alkyne 255

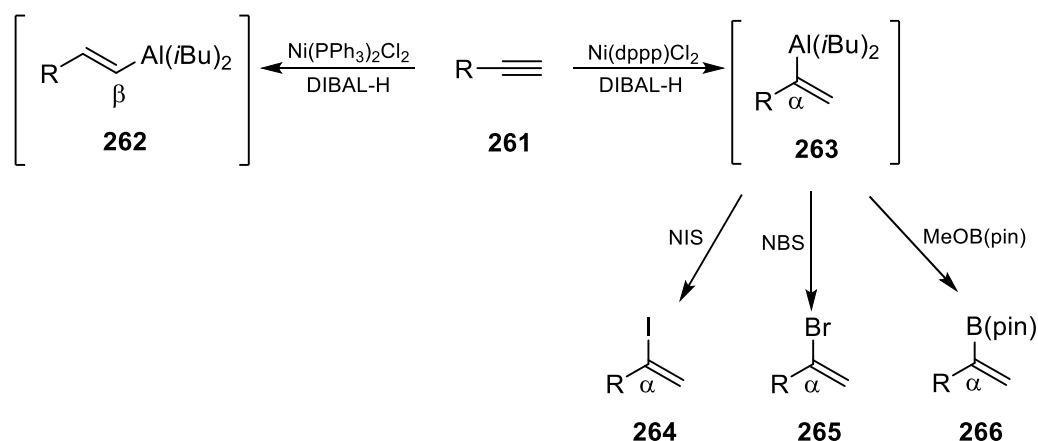
During repeated runs of the reaction, the water content of the DMPU co-solvent was found to be critical for the success of the initial alkynylation step. Even when taken from a freshly opened bottle, DMPU that was used without prior treatment was insufficiently dry and gave only starting material. Performing vacuum distillation of DMPU over CaH₂ was challenging due to the solvent's high boiling point even at reduced pressures and its tendency to polymerise at elevated temperatures. Eventually, a reliable and less labour-intensive means of drying DMPU was used, which involved simple treatment with activated 4Å molecular sieves over

48 h. The reaction has been successfully carried out on large scales, including a successful run using 20 g of iodide **259** that gave **255** in 80% yield.

3.4 Hydroiodination of alkyne **255** to prepare α -vinyl iodide **252**

3.4.1 Background of Gao and Hoveyda's hydroiodination methodology

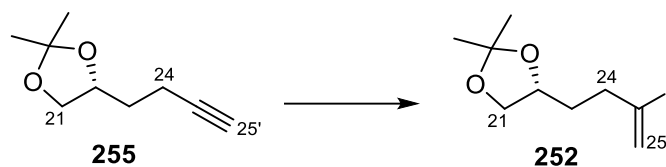
A robust four-step synthetic route allowed alkyne **255** to be rapidly prepared in large quantities, which was then to be used as the substrate to synthesise α -vinyl iodide **252** via a regioselective nickel-catalysed hydroiodination method developed by Gao and Hoveyda.⁵³ This methodology involved treating terminal alkynes with DIBAL-H and Ni(dppp)Cl₂ to regioselectively form an α -vinylaluminium intermediate as opposed to the β -vinylaluminium intermediate (Scheme 3.6). A subsequent quench of the organometallic intermediate with a suitable electrophile gave the final product. In Gao and Hoveyda's original report, electrophiles such as NIS, NBS, and MeOB(pin) had been used successfully to give the corresponding α -vinyl iodides, α -vinyl bromides, and α -vinyl pinacol boronic esters.



Scheme 3.6. Regioselective hydroalumination methodology by Gao and Hoveyda⁵³

Applying this methodology to alkyne **255** on large scale gave over 10 g of α -vinyl iodide **252** in 77% yield, with no β -vinyl iodide detected (Scheme 3.7). Confirmation that the correct vinyl iodide isomer was obtained from ¹H NMR analysis, which indicated a pair of alkene doublets

at 6.07 ppm and 5.71 ppm that both gave J coupling values of $J = 1.4$ Hz, corresponding to geminal coupling. HSQC also verified the presence of an alkene carbon that contained two protons. The characterisation data of α -vinyl iodide **252** matched those previously reported.⁵²



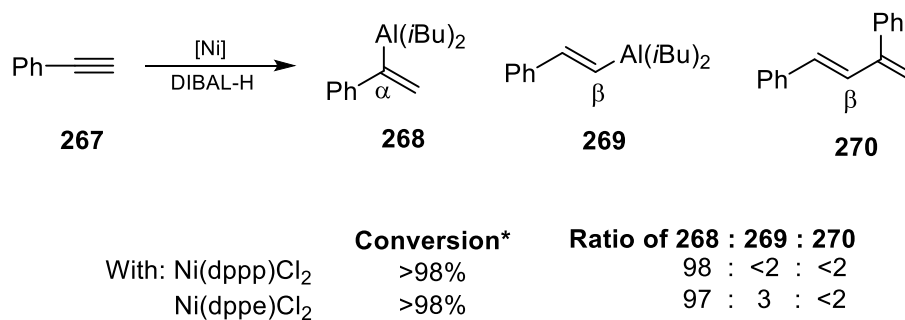
Reagents and conditions: DIBAL-H, Ni(dppp)Cl₂, THF, 0 °C to rt ; then NIS, rt, 77%

Scheme 3.7. Regioselective synthesis of α -vinyl iodide 252

3.4.2 Troubleshooting reproducibility issues of hydroiodination reaction

Unfortunately, after several successful reaction runs, the hydroiodination abruptly stopped working and only gave complex mixtures of unreacted starting material and unidentified side-products. Various control experiments were conducted to systematically determine the cause for repeated reaction failure. These include using newly opened bottles of Ni(dppp)Cl₂ purchased from different suppliers (*Sigma–Aldrich*, *Fluorochem*, and *Strem*), using THF of different dryness (THF deliberately spiked with water, wet THF directly from the solvent bottle, THF collected from a still, and THF collected from a still and then dried with activated 4Å molecular sieves), using newly purchased bottles of DIBAL-H and NIS, using different batches of substrate **255**, azeotropically distilling **255** with benzene, and using an argon atmosphere instead of a nitrogen atmosphere. However, varying these parameters led to no improvement. Additionally, a test reaction using phenylacetylene (**267**) starting material, which had been shown to work well in Gao and Hoveyda's original report, gave none of the expected (1-iodovinyl)benzene product.

A different approach was attempted – instead of using Ni(dppp)Cl₂ as the catalyst, the closely related Ni complex Ni(dppe)Cl₂ was instead added to the reaction mixture. Ni(dppe)Cl₂ was an entry in the optimisation table in Gao and Hoveyda’s original report and the complex displayed comparable conversion and regioselectivity to those of Ni(dppp)Cl₂ (Scheme 3.8).



*By analysis of 400 MHz ¹H NMR spectra of unpurified mixtures after quench with D₂O

Scheme 3.8. Use of Ni(dppp)Cl₂ and Ni(dppe)Cl₂ by Gao and Hoveyda⁵³

A test reaction using 2mol% Ni(dppe)Cl₂ gave α-vinyl iodide **252** in 35% NMR yield. Increasing the catalyst loading to 4mol% gave α-vinyl iodide **252** in 74% isolated yield and the modified conditions were demonstrated to work on a 1 g scale in 75% yield. Disappointingly, however, after this initial set of promising results, the reaction abruptly stopped working once more. Attempts to vary some of the reaction parameters as described earlier, such as THF dryness and starting material batch, were again met with failure. Eventually, it was reasoned that even if the reaction could be made to successfully run once more, its capriciousness meant that it could not be relied upon to consistently prepare α-vinyl iodide **252** on large scale. Thus, a different means to synthesise **252** was sought.

3.4.3 Exploring alternate hydroiodination reactions

Initial efforts were focused on a one-step procedure to prepare α-vinyl iodide **252** directly from alkyne **255**. Conditions **a**, **b**, **c** and **d** listed in Scheme 3.9 were attempted and were similar to each other in that they involved *in situ* generation of HI, which then adds across the alkyne

triple bond to give the vinyl iodide. None of these conditions were successful and instead led to extensive starting material degradation. The *in situ* generated HI was thought to be incompatible with the acid-sensitive acetal moiety in both the starting material and desired product. A more functional group tolerant strategy using $[\text{Cp}^*\text{Ru}(\text{MeCN})_3]\text{PF}_6$ and Et_3SiH to first hydrosilylate the triple bond, followed by *ipso* substitution of the newly installed SiEt_3 group with iodine was also unsuccessful. Only treatment of alkyne **255** with 9-I-BBN, followed by a multi-stage quench with AcOH , followed by NaOH and H_2O_2 gave the desired product, albeit in only 8% NMR yield.



Reagents and conditions: a) TMSI, MeOH, CH_2Cl_2 , rt, 0%
 b) TMSI, NaI, H_2O , MeCN, rt, 0%
 c) PPh_3 , I_2 , H_2O , CDCl_3 , rt, 0%
 d) NaI, CeCl_3 , H_2O , MeCN, reflux, 0%
 e) $[\text{Cp}^*\text{Ru}(\text{MeCN})_3]\text{PF}_6$, Et_3SiH , CH_2Cl_2 , 0 °C to rt;
 then NIS, 2,6-lutidine, HFIP, 0 °C, 0%
 f) 9-I-BBN, hexane, -25 °C; then AcOH , 0 °C;
 then NaOH , H_2O_2 , rt, 8%

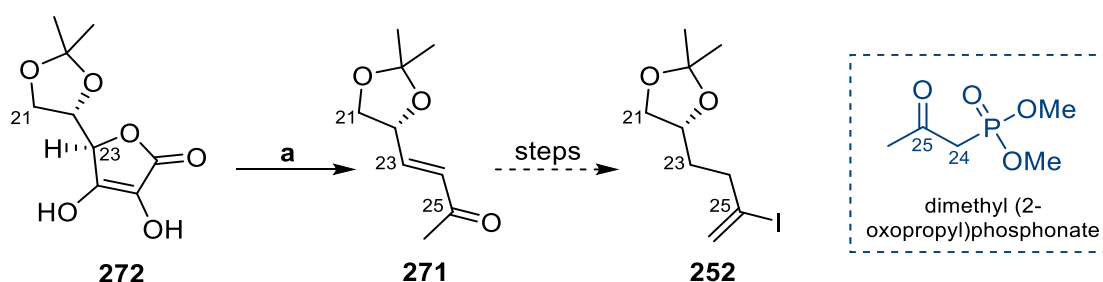
Scheme 3.9. Alternate reactions to prepare α -vinyl iodide 252 from 255

3.5 Alternative forward synthesis to prepare α -vinyl iodide 252

3.5.1 Synthesis of ketone 276

In the previous section, the use of a nickel-catalysed hydroiodination methodology developed by Gao and Hoveyda to prepare α -vinyl iodide **252** from alkyne **255** was described. However, because of the major reaction reproducibility issues that were encountered and the failure of alternative hydroiodination methods, a decision was made to plan a new forward synthesis to access α -vinyl iodide **252**.

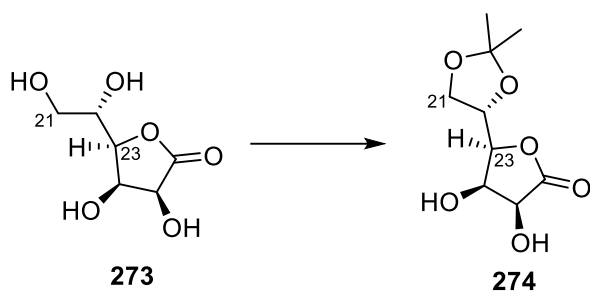
A synthetic plan is outlined in Scheme 3.10. In this new strategy, it was intended to access α -vinyl iodide **252** from enone **271**. Enone **271** would in turn be derived from commercially available **272** through a one-pot procedure that involved LiAlH_4 reduction, followed by a periodate cleavage and then by a Horner–Wadsworth Emmons olefination. This one-pot sequence was executed, which successfully afforded enone **271**, albeit only in 19% yield (Scheme 3.10). Although this one-pot sequence was convenient in that enone **271** could be rapidly accessed in a single step, the disappointing yield raised concerns about its practicality. The number of reagents and reactions involved in the one-pot transformation also indicated that optimisation would not be straightforward. Thus, a slightly modified route was planned and executed.



Reagents and conditions: a) LiAlH_4 , THF, reflux; then H_2O , NaHCO_3 , NaIO_4 , rt; then dimethyl (2-oxopropyl)phosphonate, 0°C , 19%

Scheme 3.10. Planned synthesis of 252 via enone 271

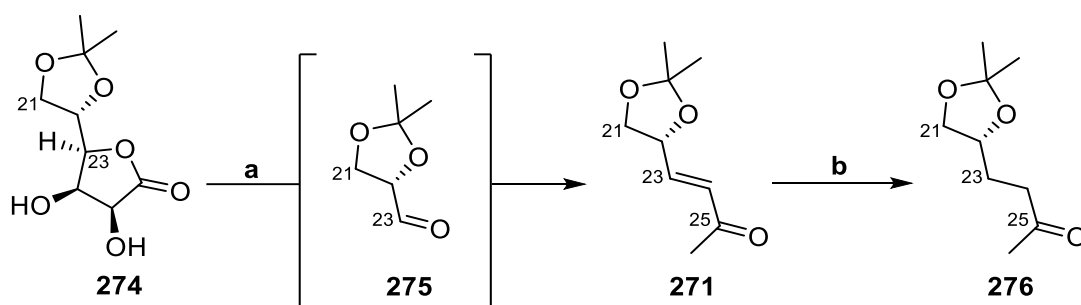
In this revised route, tetraol **273** was treated with anhydrous CuSO_4 in acetone to form acetonide **274** in 85% yield (Scheme 3.11). This step is literature known and the characterisation data of acetonide **274** matched the literature values.⁵⁴ The water content of the CuSO_4 reagent was crucial in achieving high conversions, which could be gauged by the salt's colour – anhydrous CuSO_4 was pale blue, while wet CuSO_4 was a darker blue and gave only low yields between 32% to 40%.



Reagents and conditions: Acetone, CuSO₄, rt, 16 h, 85%

Scheme 3.11. Acetal protection of 273 to form acetonide 274

Subsequently, acetonide **274** was converted to enone **271** in 75% yield through a one-pot procedure that first involved periodate cleavage to aldehyde intermediate **275**, which then underwent a Horner–Wadsworth–Emmons olefination reaction with dimethyl (2-oxopropyl)phosphonate under mildly basic conditions to give the final product as a single geometrical isomer (Scheme 3.12). All NMR spectroscopic data of enone **271** was consistent with literature values



Reagents and conditions: a) NaIO₄, NaHCO₃, H₂O, 0 °C to rt; then dimethyl (2-oxopropyl)phosphonate, K₂CO₃, 0 °C, 75%
b) H₂, Pd/C, EtOAc, rt, 5h, 88%

Scheme 3.12. Synthesis of ketone 276

Although enone **271** was obtained as the pure *E*-isomer, the C=C bond geometry was inconsequential because a subsequent hydrogenation conducted under a balloon of H₂ in the presence of Pd/C catalyst reduced the double bond to give ketone **276** in 88% yield (Scheme 3.12). Alternate conditions using PtO₂ (Adam's catalyst) tended to over-reduce the ketone and give inferior yields, leading to an inseparable mixture of alcohol diastereomers;

thus, only the chemoselective Pd/C hydrogenation conditions were used in all subsequent syntheses.

3.5.2 Synthesis of α -vinyl triflate **277**

Conversion of ketone **276** to α -vinyl triflate **277** was the next step of the synthesis and was anticipated to be challenging. The reaction would involve use of a strong base to convert the ketone to the corresponding enolate, followed by an electrophilic quench with a triflate source. Although the basic transformation was well precedented, regioselectivity issues may arise because of the possibility to form two other undesired vinyl triflates if enolate formation was not selective. Thus, several sets of conditions were screened (Table **3.1**).

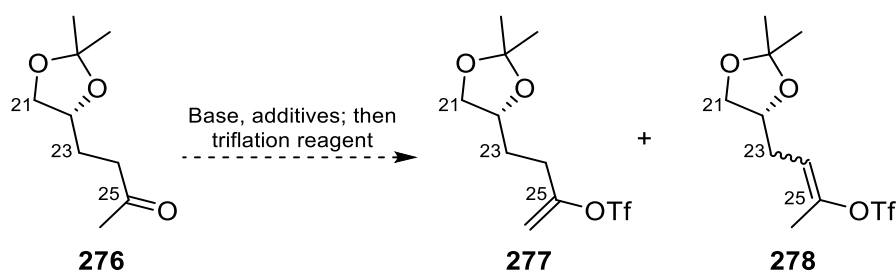


Table 3.1. Screening of conditions for regioselective triflation

Entry	Triflation step	Base	Scale	Yield	Regioselectivity (277 : 278)
1	0 °C for 2 h	LDA	100 mg	61%	100 : 15
2	0 °C for 2 h	LiTMP	100 mg	63%	100 : 14
3	-78 °C for 2 h	LiTMP	100 mg	56%*	100 : 5
4	-78 °C for 2 h	LiTMP	1.00 g	45%	100 : 37
5	-78 °C for 2 h	LiTMP	4.00 g	59%	100 : 17
6	-78 °C for 2 h	LiTMP	5.61g	60%	100 : 16
7	-78 °C for 2 h	LiTMP	9.21 g	61%	100 : 9
8	0 °C for 2 h; Tf ₂ O	LiTMP	100 mg	0%	N/A
9	0 °C for 2 h; McMurry–Hendrickson reagent	LiTMP	100 mg	0%	N/A
10	0 °C for 2 h; 12-crown-4-ether	LiTMP	100 mg	0%	N/A

*NMR yield

To obtain the desired kinetic enolate, a strong bulky base was required and thus, for enolate formation, the reaction was first performed at $-78\text{ }^{\circ}\text{C}$ using LDA, formed *in situ* from diisopropylamine and *n*BuLi, followed by quenching with Comins' reagent (Figure 3.1) at $0\text{ }^{\circ}\text{C}$ (Table 3.1, Entry 1). Gratifyingly, this first experiment successfully furnished α -vinyl triflate **277**, which was obtained in 62% yield and as a 100:15 mixture of inseparable regioisomers as calculated by ^1H NMR integration ratios. It was also observed in this preliminary experiment that the reaction did not proceed to full conversion, with considerable quantities of unreacted ketone **276** remaining (impure, ca. 20%). Thus, subsequent optimisation efforts focused on enhancing both regioselectivity and conversion.

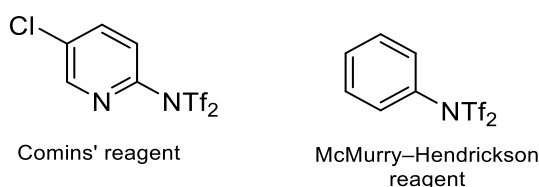


Figure 3.1. Structures of triflating reagents

To enhance the regioselectivity, an even bulkier base, LiTMP, was used (Table 3.1, Entry 2), which gave **277** in similar yield and regioselectivity (63% yield and 100:14 r.r.). The temperature of the triflation step and reaction scale were other potential variables that could affect regioselectivity. Instead of quenching the enolate with triflating reagent at $-78\text{ }^{\circ}\text{C}$ and then immediately warming the mixture to $0\text{ }^{\circ}\text{C}$, the reaction was maintained at $-78\text{ }^{\circ}\text{C}$ for two hours after the quench, before being warmed up (Table 3.1, Entry 3). It was hypothesised that the lower temperature would suppress potential enolate equilibration that would otherwise erode regioselectivity. This modified procedure gave α -vinyl triflate **277** in 56% NMR yield and 100:5 regioselectivity, a promising result. Unfortunately, when conducted on larger scale (Table 3.1, Entries 4–7), the reaction regioselectivity was irreproducible and fluctuated between 100:35 to 100:9 with no clear trend despite precautions taken with temperature control, stirring, and rate of triflation reagent addition.

Efforts to improve conversion by employing alternative triflation sources also failed. Use of either Tf₂O (Table 3.1, Entry 8) or the McMurry–Hendrickson reagent (Table 3.1, Entry 9) gave only unreacted ketone **276**. The success of Comins' reagent as a triflation source was attributed to its greater reactivity; it has been demonstrated, for example, that Comins' reagent shows superior reactivity compared to the McMurry–Hendrickson reagent, which Comins ascribed to the electron-deficient pyridine ring withdrawing electron density from the triflimide group.⁵⁵

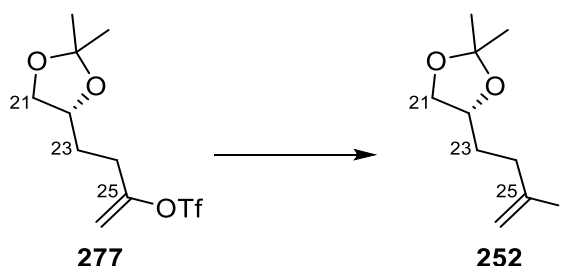
It was hypothesised that incorporation of 12-crown-4-ether additive could enhance enolate reactivity, as it is known to sequester Li⁺ cations; unfortunately, its addition with Comins' reagent only gave starting material (Table 3.1, Entry 10). Reaction failure with 12-crown-4-ether was likely due to its hygroscopicity; this property of the ether, as well as its cost and toxicity, made it untenable to use it as a stoichiometric additive especially on large scale, and therefore this reagent was not used further.

Despite there being no substantial improvement in regioselectivity and yield after these optimisation experiments, it was decided to proceed with the synthesis using the conditions detailed in entries 4–7 (Table 3.1) regardless, with the expectation that the undesired vinyl triflate regioisomers could be gradually separated from the product in subsequent steps.

3.5.3 Triflate–iodide exchange and Negishi coupling

With a four-step synthesis to prepare α -vinyl triflate **277** in multigram quantities having been developed, a triflate–iodide exchange reaction was planned to convert **277** to α -vinyl iodide **252**. To that end, methodology recently published by Reisman and co-workers was used,⁵⁶ which involved treatment of α -vinyl triflate **277** with Ni(OAc)₂·4H₂O, NaI, and 1,5-

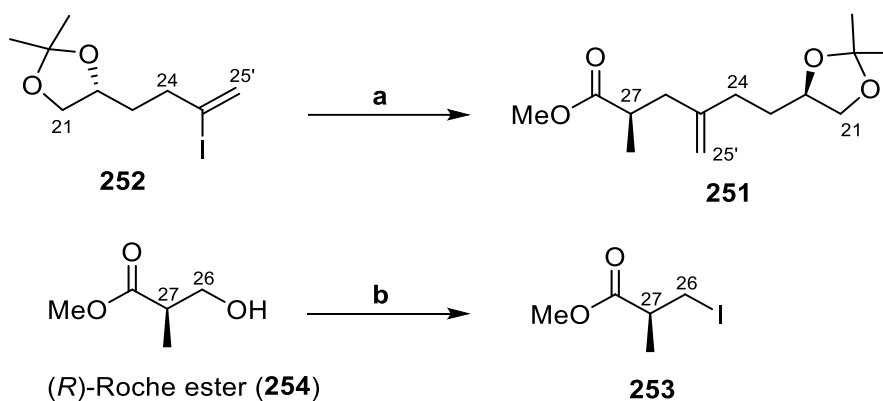
cyclooctadiene to give α -vinyl iodide **252** in 77% yield as a mixture of alkene regioisomers in approximately the same ratio as that of the impure starting material (Scheme 3.13). The characterisation data matched those obtained previously and over 8 g of α -vinyl iodide **252** was prepared using this revised route.



Reagents and conditions: Ni(OAc)₂·4H₂O, NaI, 1,5-cyclooctadiene, DMA, THF, 40 °C, 2 h, 77%

Scheme 3.13. Triflate–iodide exchange reaction

A Negishi coupling reaction was then conducted between α -vinyl iodide **252** and alkyl iodide **253** to give compound **251** as a pure sample in 75% yield (Scheme 3.14); surprisingly, there was no trace of Negishi coupling side-products derived from the regioisomeric impurities from the samples of α -vinyl iodide **252**. Alkyl iodide **253** could be easily prepared in a single step in 96% yield by performing an Appel reaction of (*R*)-Roche ester **254**. Care had to be taken when handling alkyl iodide **253** due to its volatility.

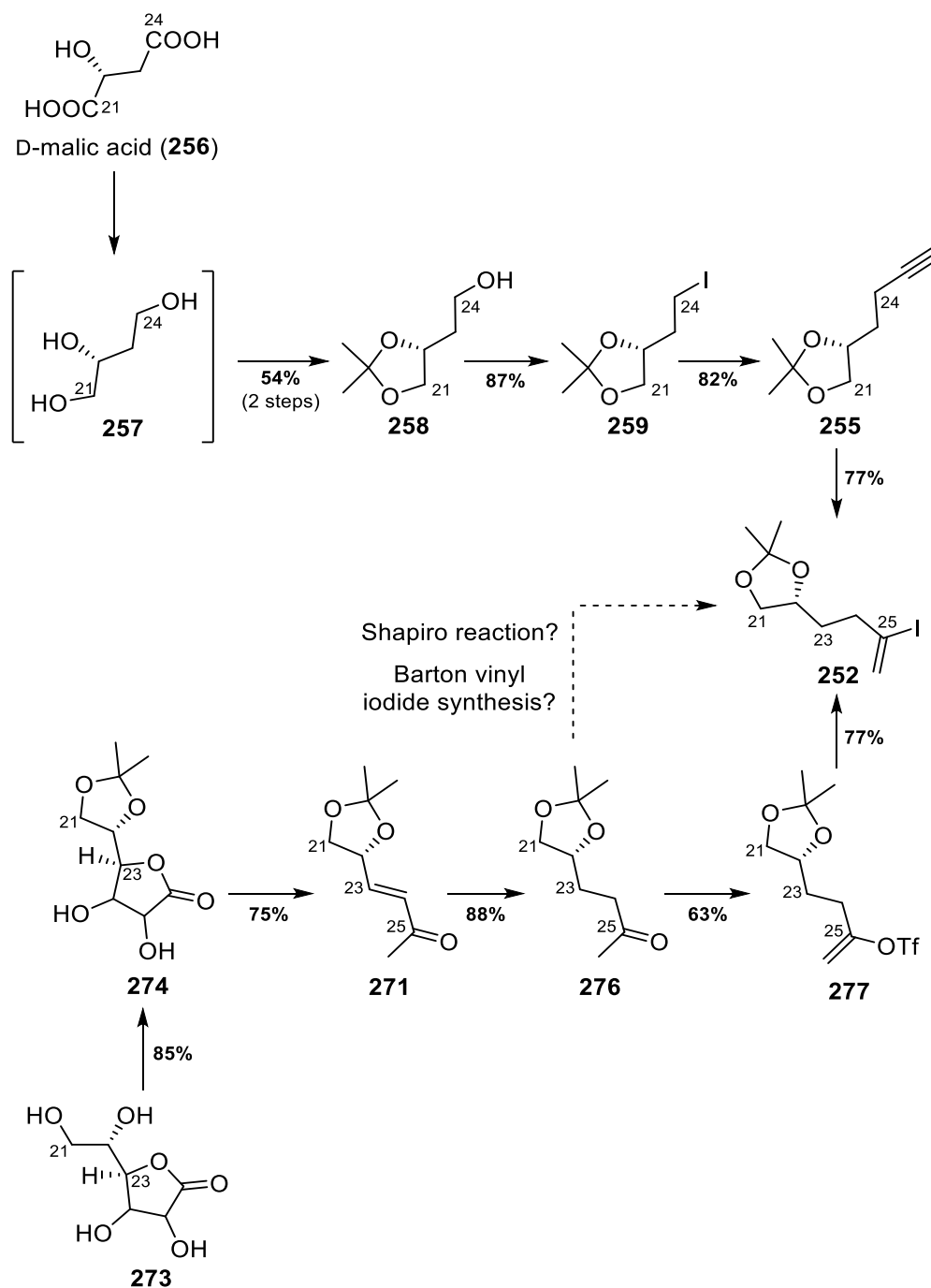


Reagents and conditions: a) Alkyl iodide **253**, Zn/Cu, Pd(PPh₃)₄, HMPA, benzene, DMA, 80 °C, 3 h, 75%
 b) PPh₃, I₂, imidazole, Et₂O, THF, 0 °C to rt, 2 h, 96%

Scheme 3.14. Negishi coupling between 253 and 252

3.5.4 Summary of α -vinyl iodide **252** synthesis and future work

Two synthetic routes to prepare α -vinyl iodide **252** were described (Scheme 3.15).



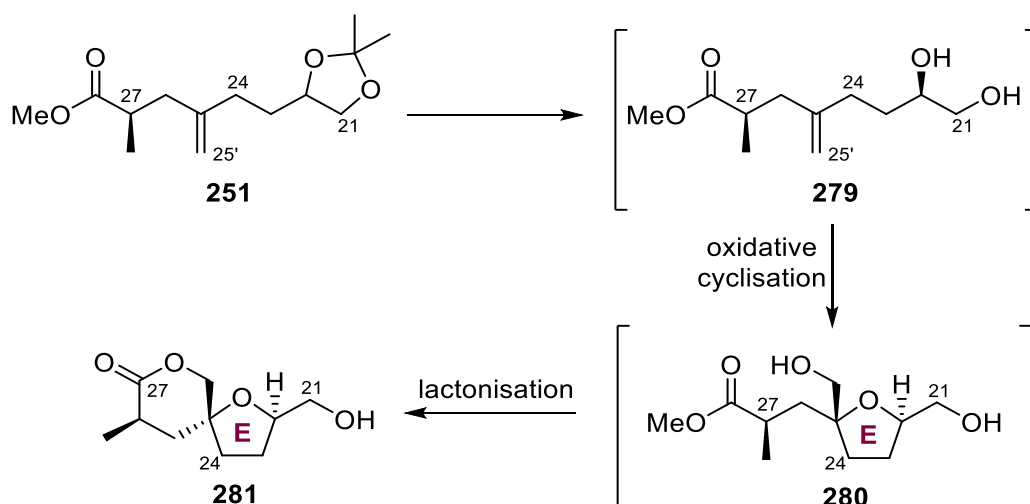
Scheme 3.15. Overview of two routes to α -vinyl iodide **252**

Although the routes are both five steps long and have comparable yields, the new route (Scheme 3.15, bottom) has the distinct advantage of being more robust because it avoids the irreproducible hydroiodination step as discussed in section 3.4. Nevertheless, there remain

opportunities to further streamline the new route. For example, it may be possible to directly convert ketone **276** to α -vinyl iodide **252** through a Barton vinyl iodide synthesis or a Shapiro reaction with an electrophilic iodine quench. Alternatively, Negishi coupling conditions may be optimised for use of α -vinyl triflate **277** as a coupling partner, thus saving a step.

3.6 Osmium-catalysed oxidative cyclisation of alkene **251**

With alkene **251** in hand, the key osmium-catalysed oxidative cyclisation reaction could be performed to give lactone **250**. The overall sequence is shown in Scheme 3.16. First, the acetal of alkene **251** is deprotected under the Lewis acidic conditions to give diol intermediate **279**. The oxidative cyclisation then occurs, giving THF **280**, which rapidly cyclises into the final product lactone **281**. The reaction was performed in the presence of $K_2OsO_2(OH)_4$, pyridine *N*-oxide, $Sc(OTf)_3$, and citric acid at 60 °C to give lactone **281** in 78% yield as a single diastereomer.

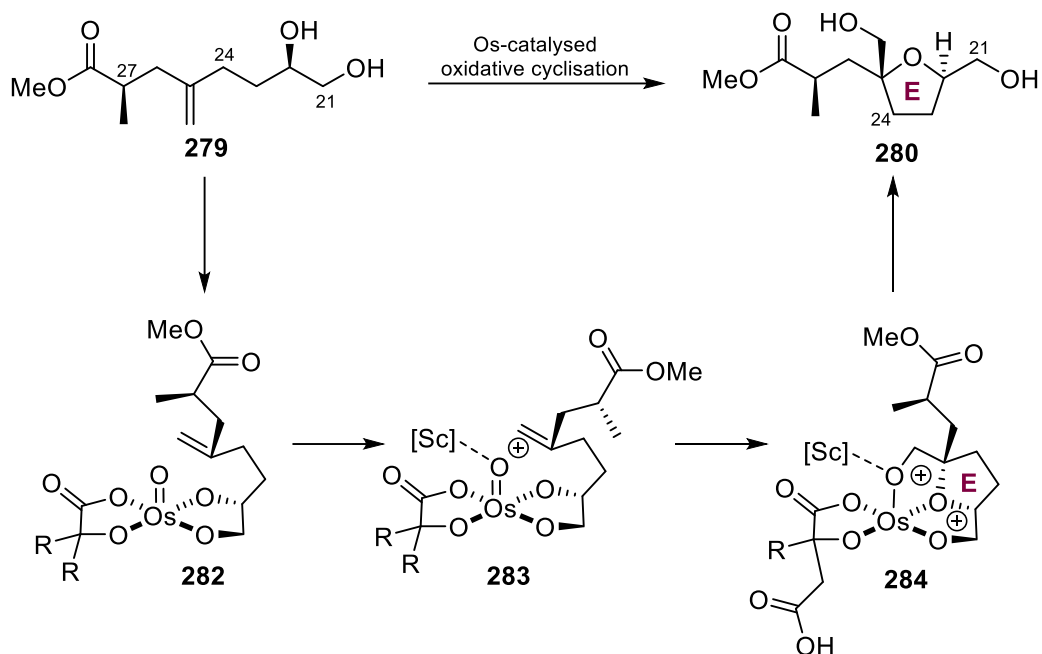


Reagents and conditions: $K_2OsO_2(OH)_4$, pyridine *N*-oxide, $Sc(OTf)_3$, citric acid, H_2O , MeCN, 60 °C, 16 h, 78%

*Scheme 3.16. Oxidative cyclisation lactonisation cascade to synthesise **281***

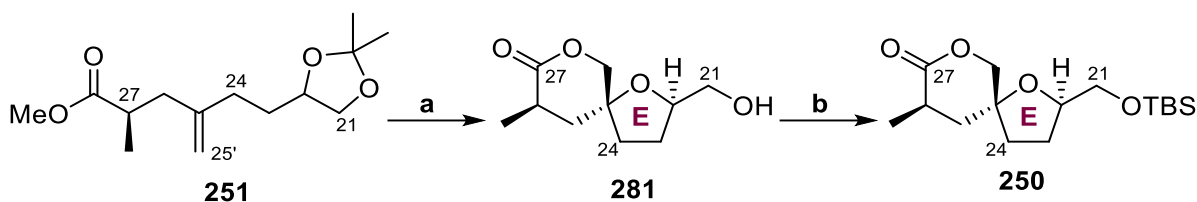
The detailed pathway of the osmium-catalysed oxidative cyclisation is shown in Scheme 3.17. Starting with the de-protected diol intermediate **279**, chelation with potassium osmate occurs

to form complex **282**. The Os=O oxygen then coordinates to the Sc³⁺ Lewis acid, which reduces the electron density at Os and facilitates the subsequent [3+2] cycloaddition with the alkene to give intermediate **283**. The citric acid chelated to the Os promotes the subsequent osmate ester hydrolysis to give THF **284**, which then lactonises to **281** as described earlier.



Scheme 3.17. Oxidative cyclisation pathway

Isolation of lactone **281** as a pure compound during some reaction runs could not be achieved because of contamination with Sc(OTf)₃; Dr Yifan Liu previously reported similar observations, including the recommendation to carry crude lactone **281** directly to the next reaction step which involved TBS protection of the primary hydroxyl group at C21.⁵² This experimental procedure was attempted and gave silyl ether **250** in 65% yield over two steps from alkene **251** (Scheme 3.18).

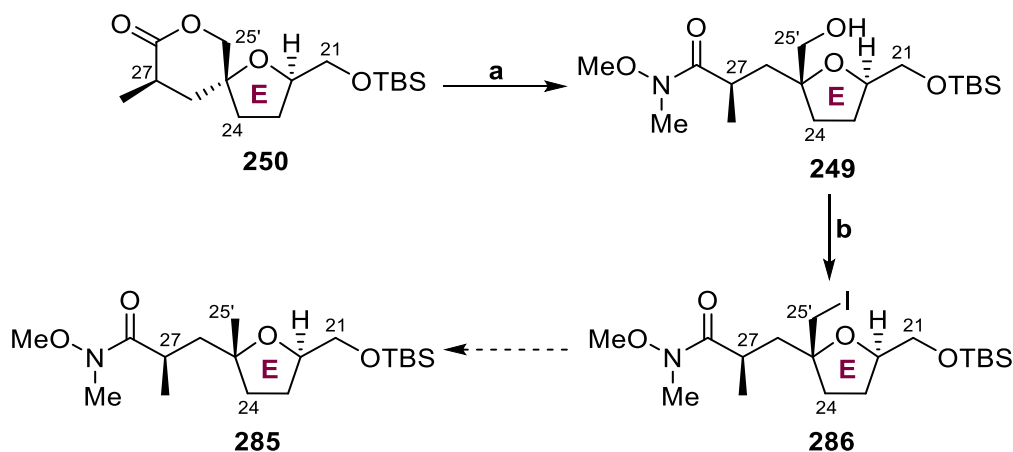


Reagents and conditions: a) $K_2OsO_4 \cdot 2H_2O$, pyridine-*N*-oxide, $Sc(OTf)_3$, citric acid, H_2O , MeCN, 60 °C, 16 h
 b) TBSCl, DMAP, imidazole, CH_2Cl_2 , rt, 2 h, 65% over two steps

Scheme 3.18. TBS protection of 281 to give silyl ether 250

3.7 Elaboration of silyl ether 250 to 248

Silyl ether **250** was then treated with $MeNHOMe \cdot HCl$ and $AlMe_3$, which induced lactone ring opening and amidation to give Weinreb amide **249** in 92% yield (Scheme 3.19).

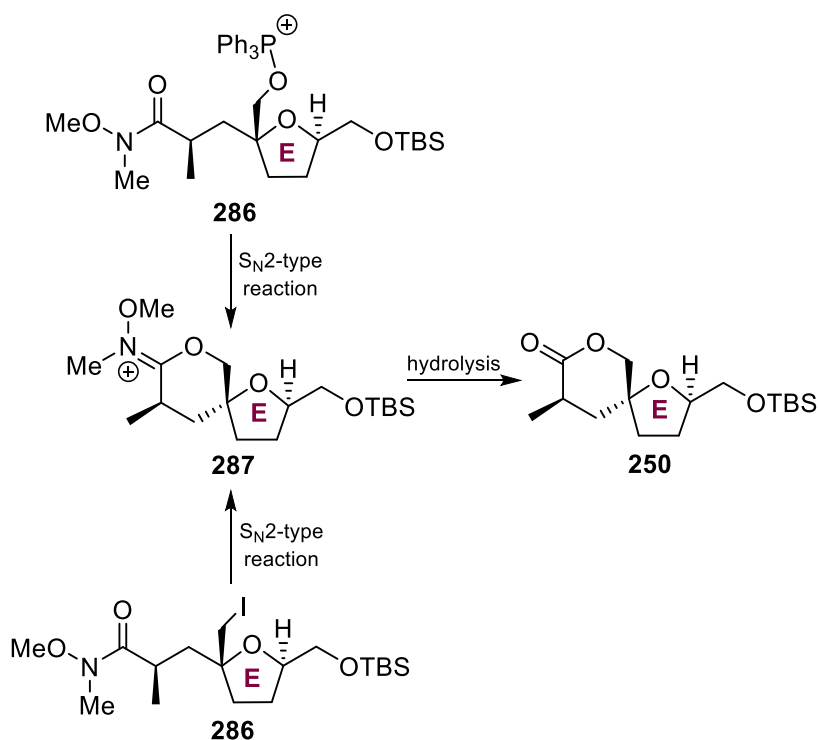


Reagents and conditions: a) $MeNHOMe \cdot HCl$, $AlMe_3$, THF, 0 °C, 5 h, 92%
 b) PPh_3 , I_2 , imidazole, MeCN, Et_2O , 80 °C, 3 h, 78%

Scheme 3.19. Planned synthesis of 285 from lactone 250

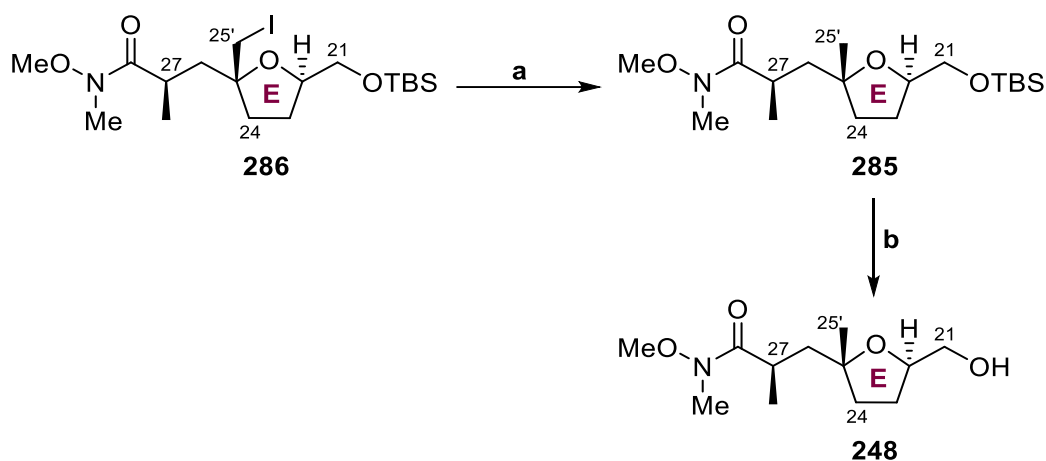
What followed subsequently was a planned removal of the hydroxyl group on C25' in Weinreb amide **249**, which was accomplished in two steps. First, **249** was treated with PPh_3 , I_2 , and imidazole in an Appel reaction to convert the alcohol to iodide **286** in 78% yield (Scheme 3.19). Occasionally, at this relatively high reaction temperature, lactone **250** from the step *before* (Scheme 3.19) was unexpectedly detected as a side-product in the Appel reaction. Lactone **250** was proposed to have formed *via* the pathway outlined in Scheme 3.20. First, the expected Appel reaction pathway occurs with activation of the C25' hydroxyl group by the [I-

$\text{PPh}_3]^+$ salt to give activated species **286**. The carbonyl oxygen from the Weinreb amide then does an intramolecular $\text{S}_{\text{N}}2$ -type reaction at C25', forming the cyclised intermediate **287** which then undergoes hydrolysis during the work-up to give lactone **250**. Alternatively, formation of lactone **250** *via* degradation of the iodide product **286** through a similar process could not be ruled out. Although it was not known why some reaction runs gave lactone side-product and others did not, it was fortunate that it formed only occasionally and that it could be recycled.



Scheme 3.20. Unexpected side-process in Appel reaction

With iodide **286** in hand, a hydrogenation in the presence of Pd/C and NEt_3 under a balloon of hydrogen reduced the alkyl iodide to give compound **285** in quantitative yield (Scheme 3.21). The hydrogenation reaction has been successfully performed on a 6 g scale. Subsequent treatment of **285** with TBAF in THF removed the TBS protecting group to afford alcohol **248** in 99% yield.

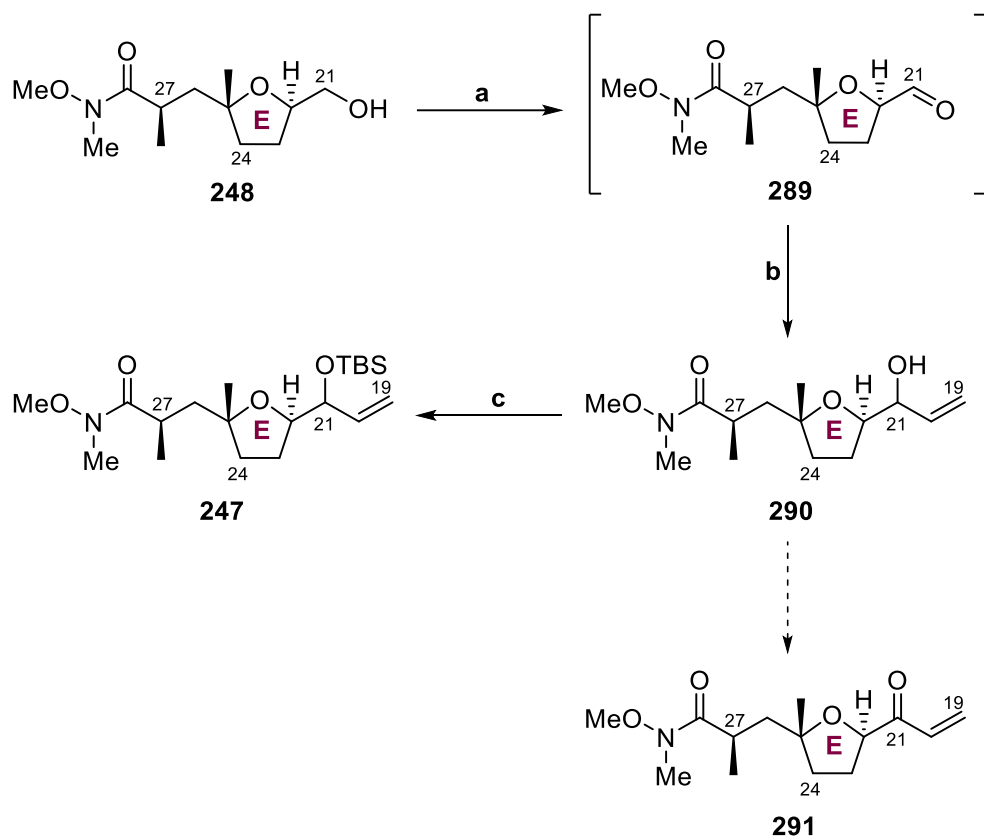


Reagents and conditions: a) Pd/C, H₂, NEt₃, MeOH, rt, 24 h, 100%
 b) TBAF, THF, rt, 3 h, 99%

Scheme 3.21. Synthesis of alcohol 248

3.8 Completion of E fragment synthesis

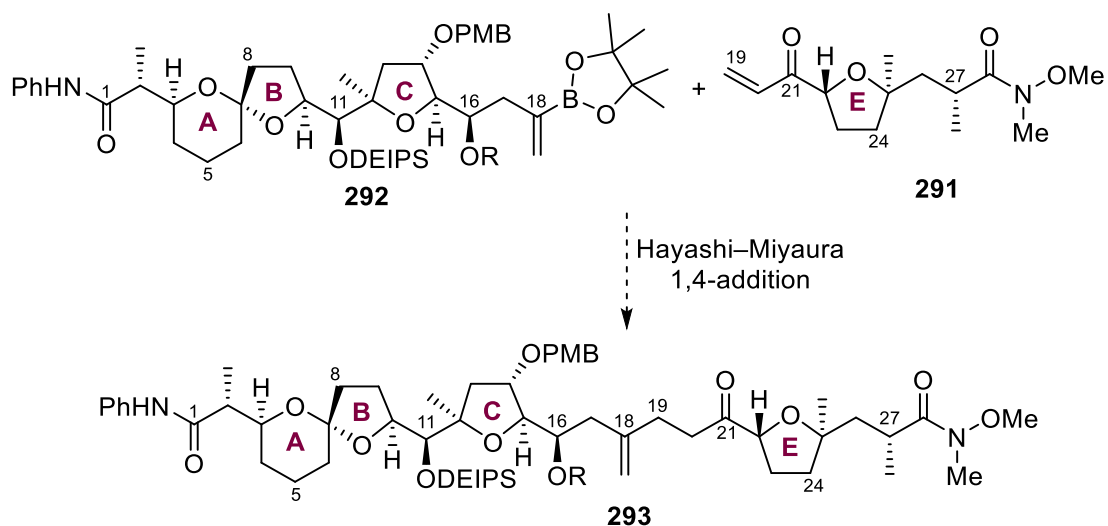
Alcohol **248** was then subjected to a Parikh–Doering oxidation reaction to afford aldehyde **289** (Scheme 3.22). Due to the presence a chiral centre α to the aldehyde and the risk of epimerisation, aldehyde **289** was directly carried over to the next Grignard addition step without purification. Excess vinyl magnesium bromide (> 1.5 eqv) had to be used for full conversion; fortunately, the cryogenic temperatures prevented an unwanted Grignard addition at the less reactive Weinreb amide moiety. Thus, addition of vinyl magnesium bromide to the crude aldehyde successfully gave allylic alcohol **290** in 60% yield over two steps, in a diastereomeric ratio that was undetermined. The stereochemistry at the C21 allylic alcohol centre was, however, inconsequential because it would be eventually oxidised up to the enone in the planned synthesis. The successful isolation of allylic alcohol **290** was confirmed by the presence of the signature alkene signals at 5.74ppm, 5.26 ppm, and 5.12 ppm in the ¹H NMR spectrum.



Reagents and conditions: a) $\text{SO}_3 \cdot \text{pyridine}$, DMSO, NEt_3 , CH_2Cl_2 , 0°C to rt, 2.5 h
 b) Vinyl magnesium bromide, Et_2O , -78°C , 1 h, **60%** over two steps
 c) TBSCl, imidazole, DMAP, CH_2Cl_2 , 0°C to rt, 15 h, **77%**

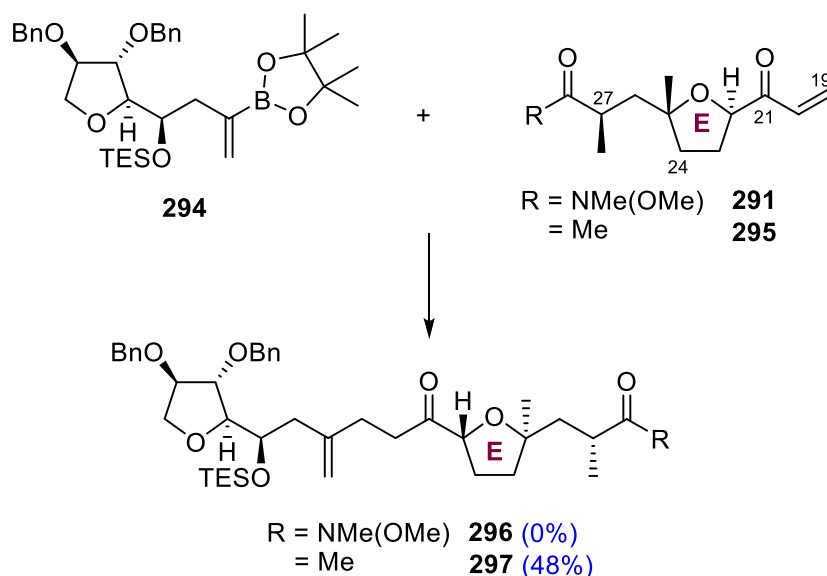
Scheme 3.22. Synthesis of silyl ether 247

Allylic alcohol **290** was then treated with TBSCl, DMAP, and imidazole in CH_2Cl_2 to convert it to silyl ether **247** in 77% yield. Originally, it had been planned to oxidise **290** to enone **291** instead (Scheme 3.22), with the intention of reacting the enone with a vinyl boronic ester derivative of the ABC fragment (**292**) through a rhodium-catalysed Hayashi–Miyaura 1,4-addition reaction, thus uniting the ABC and E fragments (Scheme 3.23).



Scheme 3.23. Initial plan to unite enone **291** with vinyl boronic ester **293**

However, when Dr Melodie Richardson, a former DPhil student in the Donohoe group, prepared enone **291**, and then attempted the 1,4-addition reaction on a model system that incorporated **291** and model boronic ester **294**, no desired product was formed (Scheme 3.24). This negative result prompted a series of further investigations and model studies into the reaction's failure, which eventually pointed to the Weinreb amide moiety as a problematic functional group that shut down the reaction, likely due to chelation and catalyst poisoning.³⁶

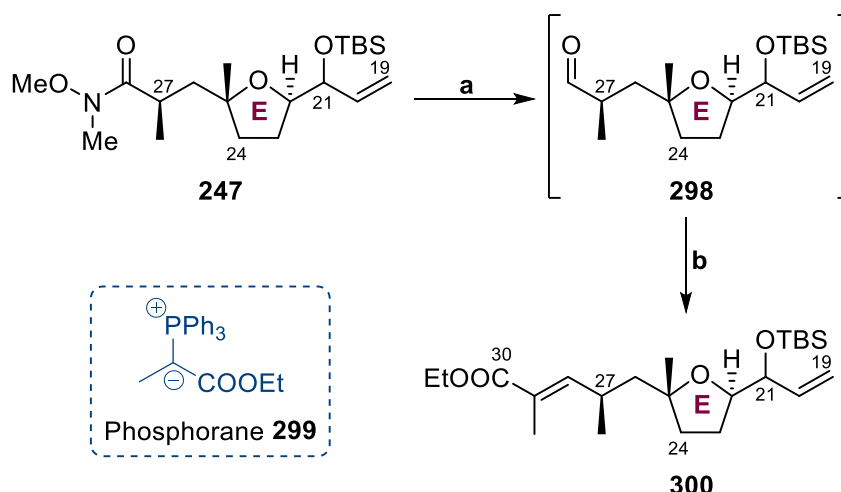


Reagents and conditions: Rh(acac)(CO)₂, dppb, THF, H₂O, 50 °C

Scheme 3.24. 1,4-Addition reaction model studies conducted by Dr Melodie Richardson³⁶

The Weinreb amide's role in the reaction failure was further corroborated by the success of the 1,4-addition reaction between vinyl boronic ester **294** and enone **295** (Scheme 3.24), a close analogue of enone **291** that has the Weinreb amide functionality replaced with a methyl ketone, which gave the expected product **297** in 48% yield.

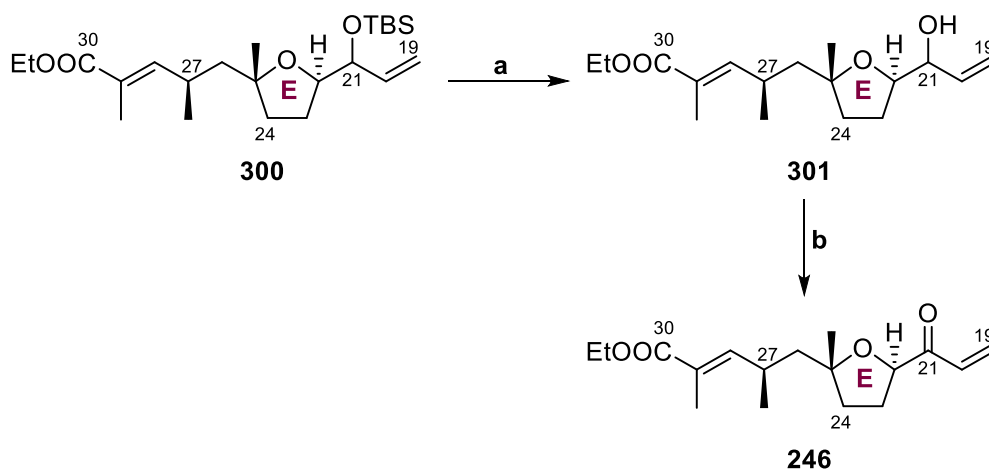
As such, instead of converting allylic alcohol **290** to enone **291** immediately, silyl ether **247** was prepared instead and then further derivatised to α,β -unsaturated ester **300** to remove the Weinreb amide moiety before the Hayashi–Miyaura 1,4-addition. To accomplish this, silyl ether **247** was treated with DIBAL-H in THF at $-78\text{ }^{\circ}\text{C}$ to afford aldehyde **298**, which was carried as a crude sample directly to the next step. Subsequent Wittig olefination, involving stabilised ylide **299**, gave ester **300** in 67% yield over two steps. Care had to be taken when preparing an NMR sample of ester **300** using CDCl_3 solvent, which was sufficiently acidic to epimerise **300** at the C27 stereocentre *via* an extended enol. Using CDCl_3 pre-treated with K_2CO_3 prevented this epimerisation.



Reagents and conditions: a) DIBAL-H, THF, $-78\text{ }^{\circ}\text{C}$, 1.5 h
 b) Phosphorane **299**, benzene, reflux, 17 h, 67% over two steps

Scheme 3.25. Synthesis of ester 300

Finally, the synthesis of the E fragment was concluded in two steps. First, ester **300** was treated with TBAF to remove the TBS group and give alcohol **301** in 68% yield. The free allylic alcohol **301** was then oxidised *via* a DMP oxidation reaction to give E fragment **246** in 100% yield (Scheme 3.26), although conversions varied depending on the dryness of the CH₂Cl₂ solvent and the scale at which the reaction was performed. When the reaction was conducted on medium scale (>40 mg of starting material), CH₂Cl₂ obtained directly from the solvent bottle sufficed to give high conversions; in fact, poor conversions resulted if anhydrous CH₂Cl₂ obtained from a solvent still was used. However, on smaller scale (~10 mg), the outcome was reversed – “wet” CH₂Cl₂ from the solvent bottle shut down the reaction, while use of anhydrous CH₂Cl₂ gave quantitative yields.

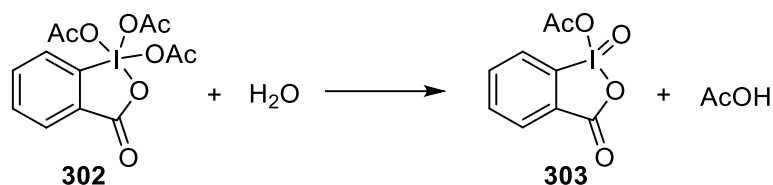


Reagents and conditions: a) TBAF, THF, rt, 8 h, 68%
b) DMP, CH₂Cl₂, rt, 2 h, 100%

Scheme 3.26. Completion of synthesis of E fragment 246

These seemingly contradictory results of the effect of moisture are in fact well documented in the literature,⁵⁷ which contains opposing claims about whether water is beneficial or detrimental to the DMP oxidation reaction. These claims were clarified by Schreiber and Meyer in 1994,⁵⁸ who demonstrated that DMP (**302**) reacts with water to form acetoxyiodinane oxide **303** (Scheme 3.27), a species that oxidises alcohols more quickly and efficiently than DMP itself. However, excess water would cause the destruction of any

oxidising species. At smaller scales, sufficient moisture may be introduced from the atmosphere that would enhance reaction rate; thus, additional water from “wet” CH₂Cl₂ would be unnecessary or even detrimental to the reaction. However, larger scale reactions are less sensitive to the effects of moisture from the atmosphere and thus additional water would have to be supplied in the form of “wet” solvent to achieve enhanced reaction rates.

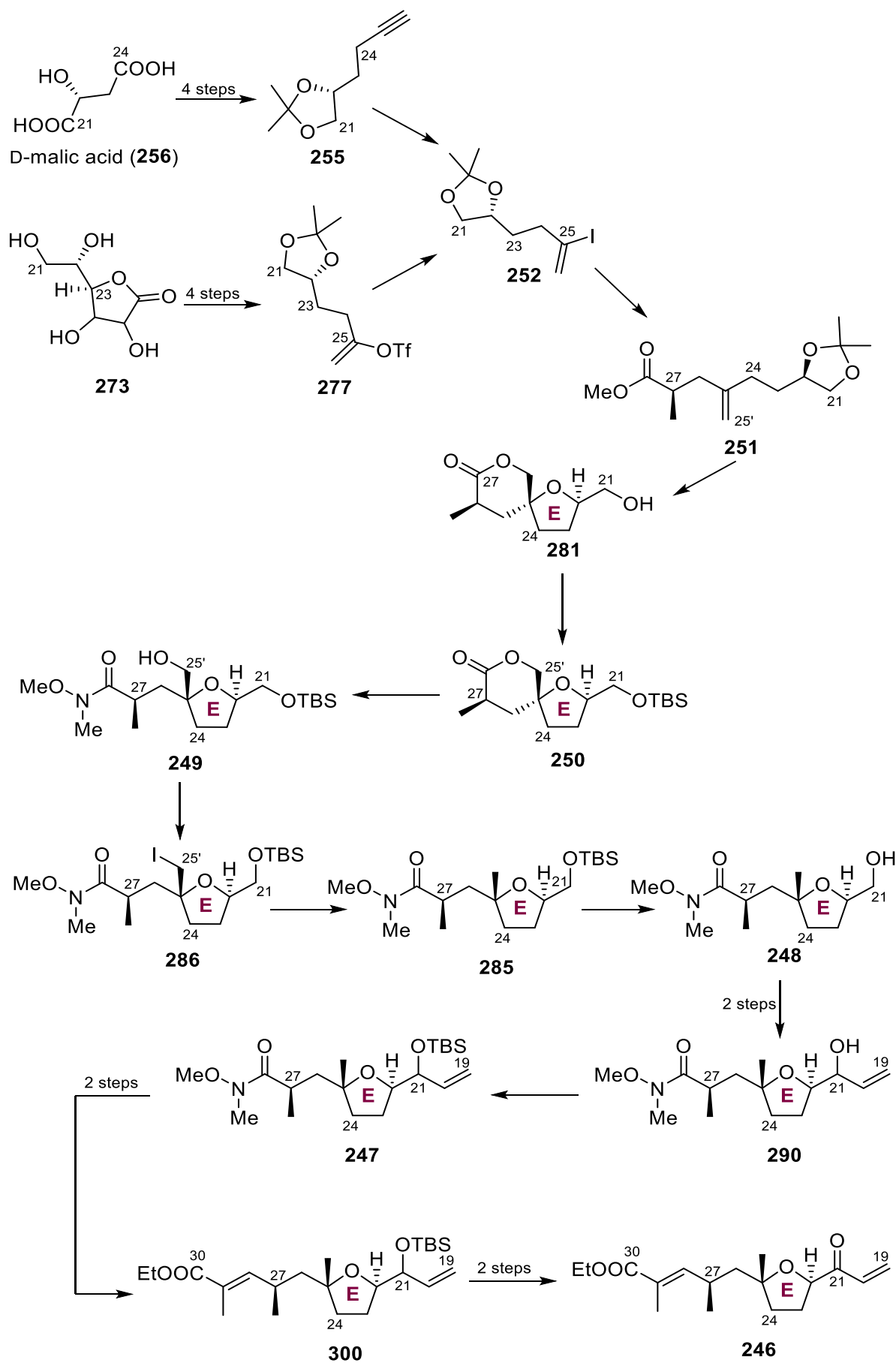


Scheme 3.27. Reaction of DMP (302) with water

The successful isolation of E fragment **246** was confirmed by the downfield shift of the C19 alkene peaks from 5.30 ppm and 5.16 ppm to 6.62 ppm and 6.34 ppm in the ¹H NMR spectrum. Moreover, although allylic alcohol **301** starting material had been used as a mixture of diastereomers at C21, E-fragment **246** was isolated a single pure compound due to loss of the C21 stereocentre from oxidation. Due to the instability of enone **246**, all samples were immediately stored in a –30 °C freezer when not in use.

3.9 Summary of E fragment synthesis

In conclusion, E fragment **246** was prepared in 19 linear steps from either D-malic acid or tetraol **273**, as summarised in Scheme 3.28. Both of these forward routes converge at the common intermediate α -vinyl iodide **252**. However, the route beginning from tetraol **273** was found to be superior because it is more robust and reproducible. Up to 500 mg of the immediate precursor allylic alcohol **301** had been successfully prepared using the syntheses above. Hence, it was now possible to perform the Hayashi–Miyaura 1,4-addition reaction to unite the ABC and E fragments, which is described in chapter 4.

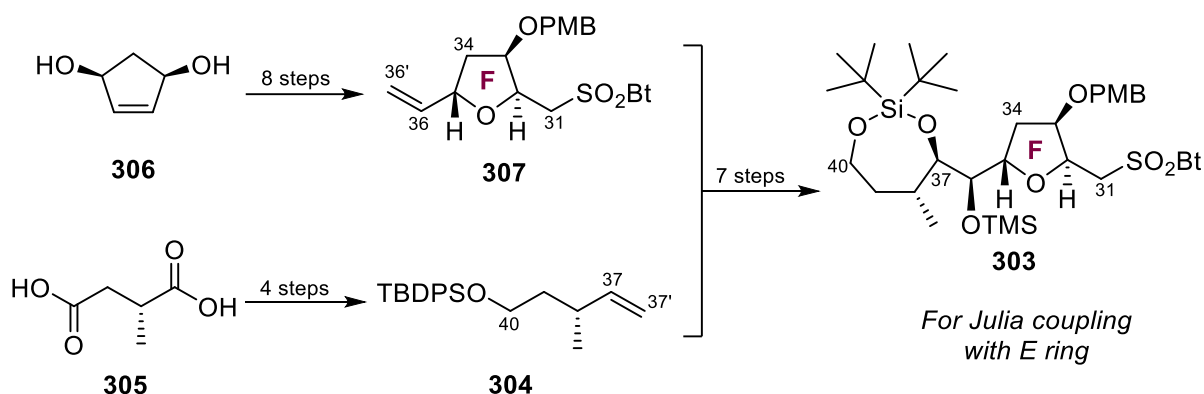


Scheme 3.28. Synthetic route to *E* fragment **246**

3.10 Synthesis of C31–C40 F fragment

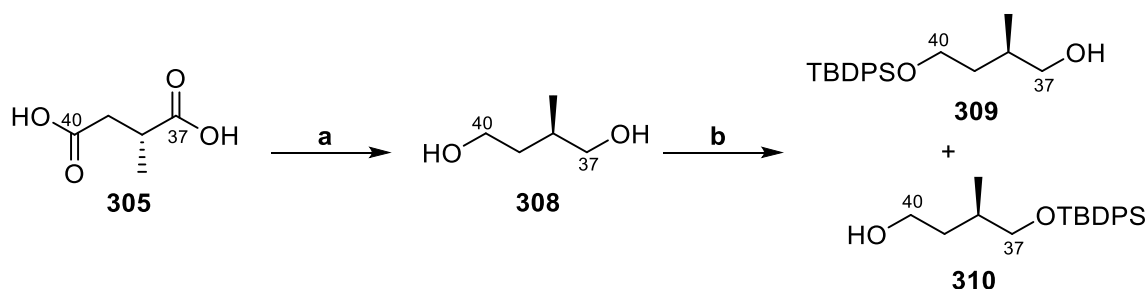
3.10.1 Overview

The third and last fragment of PTX-4, the C31–C40 F fragment **303**, was successfully prepared in 15 linear steps using a route developed by Dr Kirsty Luscombe, Dr Michael Tucker, and Dr Ahria Roushanbakhti (Scheme 3.29).³¹ Only the first four steps of the route had been executed before the step 4 product, alkene **303**, was handed to Dr Melodie Richardson as starting material for the remainder of the synthesis. Therefore, most of the F fragment route will be described only briefly in this chapter.



Scheme 3.29. Overview of synthesis of F fragment **303**

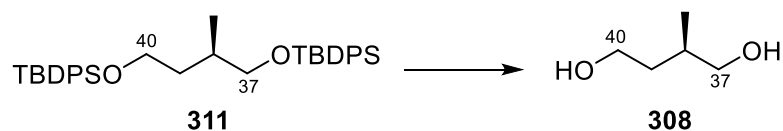
3.10.2 Syntheses of C37–C40 alkene **304** and C31–C36 sulfone **307**



Reagents and conditions: a) $\text{BH}_3 \cdot \text{SMe}_2$, $\text{B}(\text{OMe})_3$, THF, 0 °C to rt, 16 h, 93%
b) TBDPSCI, DMAP, imidazole, CH_2Cl_2 , rt, 16 h, 69%

Scheme 3.30. Synthesis of silyl ether **309**

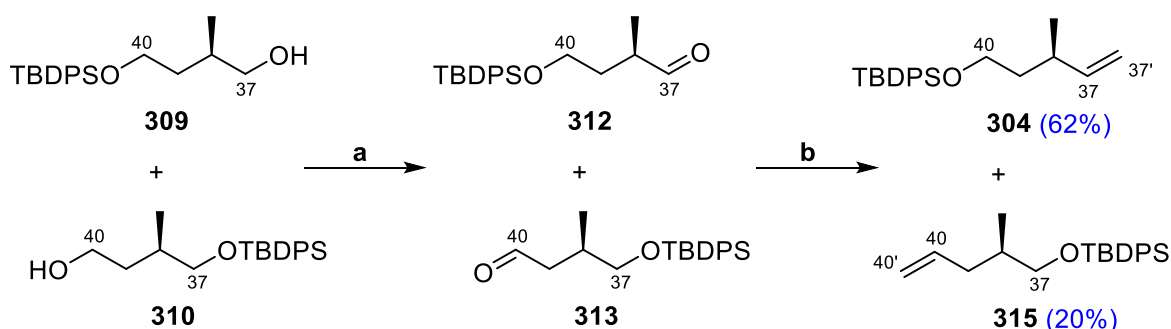
First, (*R*)-methylsuccinic acid (**305**) was reduced using $\text{BH}_3\cdot\text{SMe}_2$ to afford diol **308** in 93% yield on a 10 g scale (Scheme 3.30). Mono-protection of diol **308** using 1.1 eqv TBDPSCI, DMAP, and imidazole gave silyl ethers **309** and **310** as an inseparable mixture in 69% yield. Double-protected side-product **311** was also isolated in 21% yield, but could be readily recycled to diol **308** in 96% yield upon treatment with TBAF at 50 °C (Scheme 3.31).



Reagents and conditions: TBAF, THF, 50 °C, 7 h, 96%

Scheme 3.31. Recycling of **311** into diol **308**

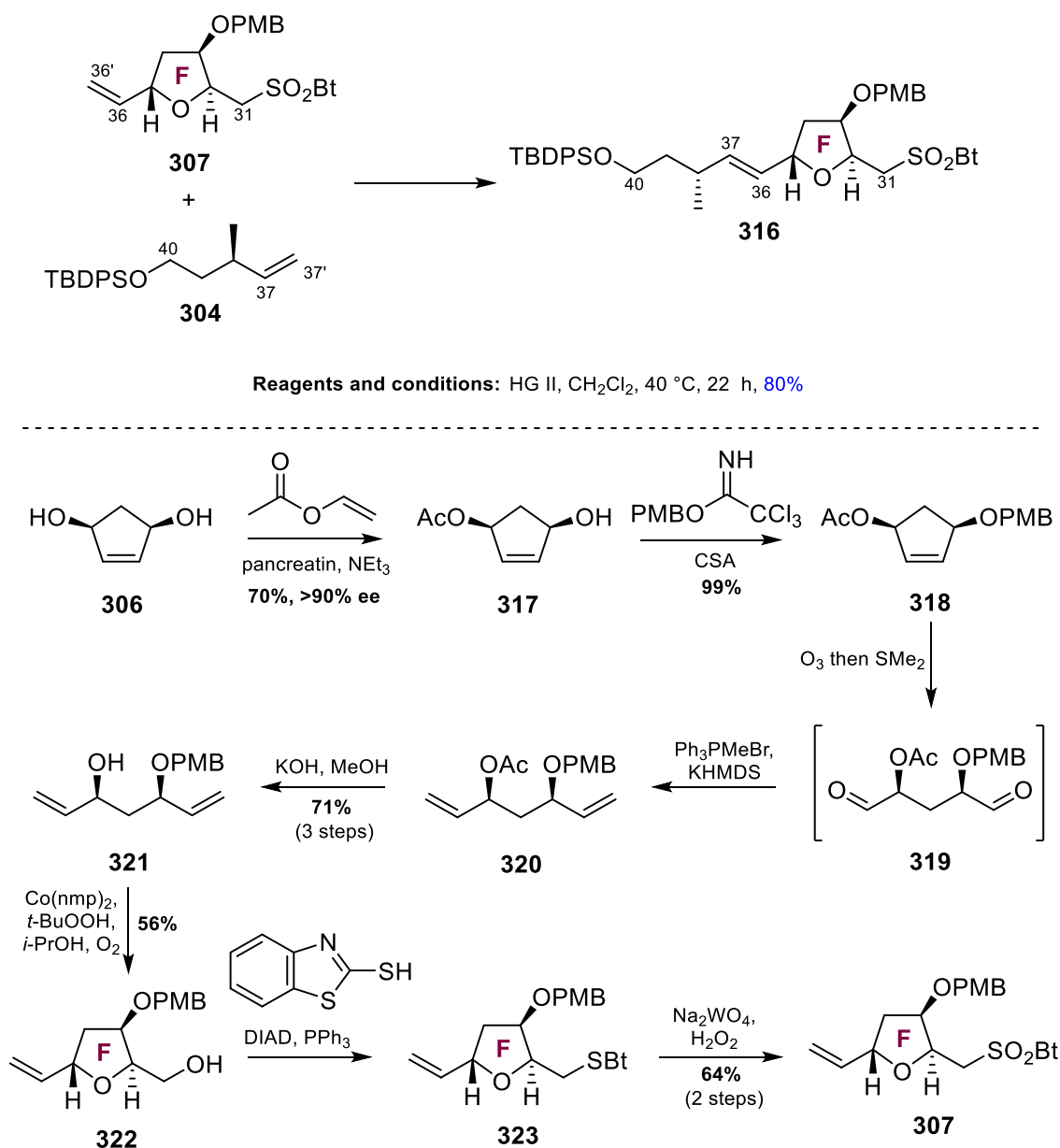
The mixture of silyl ethers **309** and **310** was carried over to the next step, which gave the corresponding aldehydes **312** and **313** via a Swern oxidation reaction (Scheme 3.32). Due to the risk of racemisation at the C38 enolisable stereocentre in aldehyde **312**, the crude mixture was taken directly to the subsequent Wittig olefination step. Treatment of the aldehyde mixture with deprotonated methyltriphenylphosphonium iodide gave alkenes **304** and **315** in 62% and 20% yields over two steps respectively (Scheme 3.32), which were separable. The desired alkene **304** was carried forward and alkene **315** was discarded.



Reagents and conditions: a) $(\text{COCl})_2$, DMSO, NEt_3 , CH_2Cl_2 , -78 to 0 °C, 1.5 h
b) MePPh_3 , $n\text{BuLi}$, THF, 0 °C to rt, 16 h

Scheme 3.32. Synthesis of alkene **304**

Large quantities (> 15 g) of alkene **304** were prepared and handed to Dr Melodie Richardson, who used it as the alkene partner for a cross-metathesis reaction with THF **307** to give compound **316** in 80% yield (Scheme 3.33), before carrying it over four more steps to F fragment **303**.

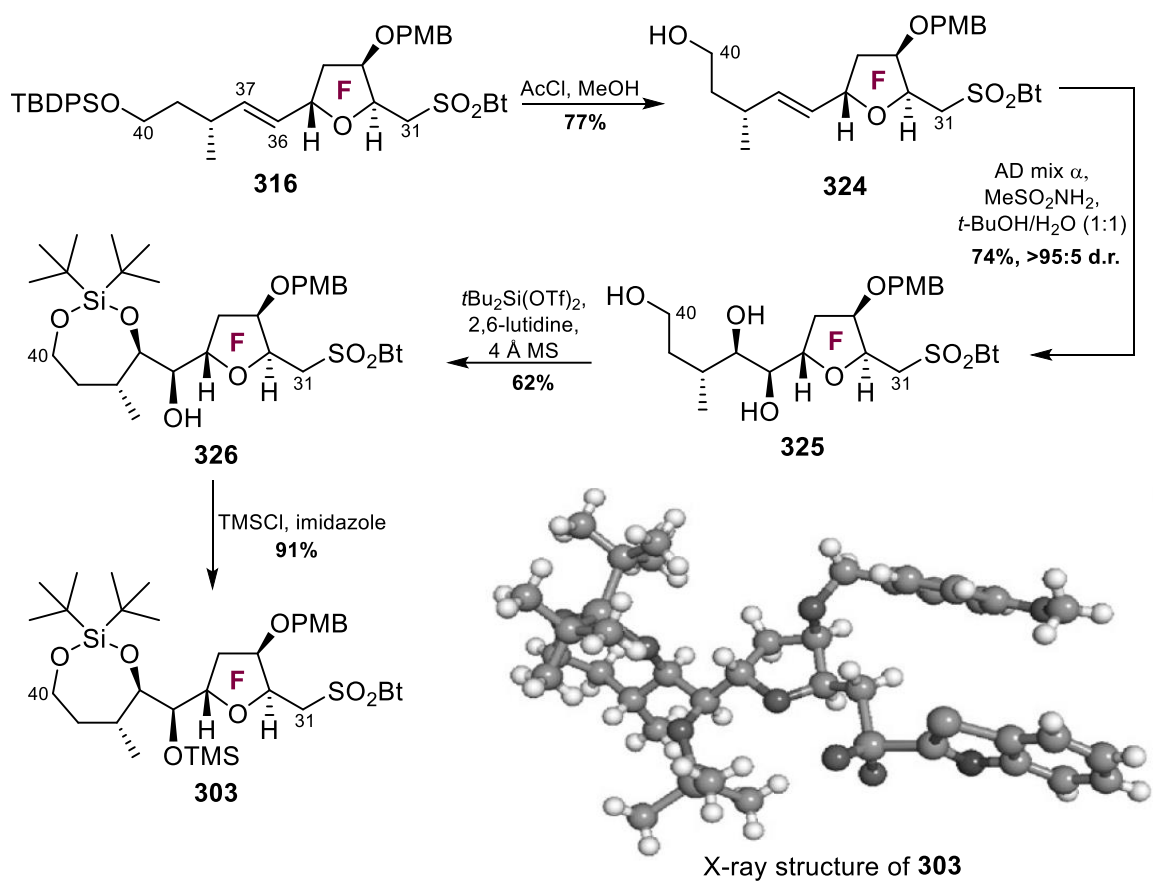


THF **307**, in turn, had been prepared in eight steps from symmetrical diol **306**. First, an enzymatic desymmetrisation was performed on diol **306** using pancreatin from porcine pancreas to give acetate **307** in 70% yield and >90% ee. A PMB protection using PMB

trichloroacetimidate was then conducted on the remaining free hydroxyl group on acetate **307** to afford PMB ether **318** in 99% yield. A three-step sequence first involving ozonolysis of **318** into *bis*-aldehyde **319**, followed by a double Wittig olefination reaction at both aldehyde moieties gave *bis*-alkene **320**, whose acetate group was then hydrolysed under KOH/MeOH conditions to give alcohol **321** in 71% yield over three steps. The key step, a cobalt-catalysed Mukaiyama oxidative cyclisation, was then performed on **321** to give *trans*-THF **322** in 56% yield. A Mitsunobu reaction then replaced the primary hydroxyl group on **322** with mercaptobenzothiazole to give **323**, which was then oxidised using Na₂WO₄ and H₂O₂ to give sulfone **307** in 64% yield over two steps.

3.10.3 Elaboration of *trans*-THF **316** into F fragment

trans-THF **316**, which was obtained from the cross-metathesis between sulfone **307** and alkene **304**, was then carried over four steps by Dr Melodie Richardson to prepare the final F fragment (Scheme **3.34**). First treatment of *trans*-THF **316** with AcCl and MeOH generated HCl *in situ* to deprotect the primary hydroxyl group at C40 to give alcohol **324** in 77% yield. An asymmetric Sharpless dihydroxylation reaction using AD-mix- α was then performed on alcohol **324** to give triol **325** in 74% yield and in >95:5 d.r. The hydroxyl groups at C37 and C40 were then protected using *t*Bu₂Si(OTf)₂ to give silyl ether **326** in 62% yield. A final TMS protection of the remaining hydroxyl group at C36 using TMSCl gave F fragment **303** in 91% yield, whose structure was confirmed by single-crystal X-ray diffraction studies, thus concluding the synthesis. Over 500 mg of F fragment **303** was successfully prepared through this route.



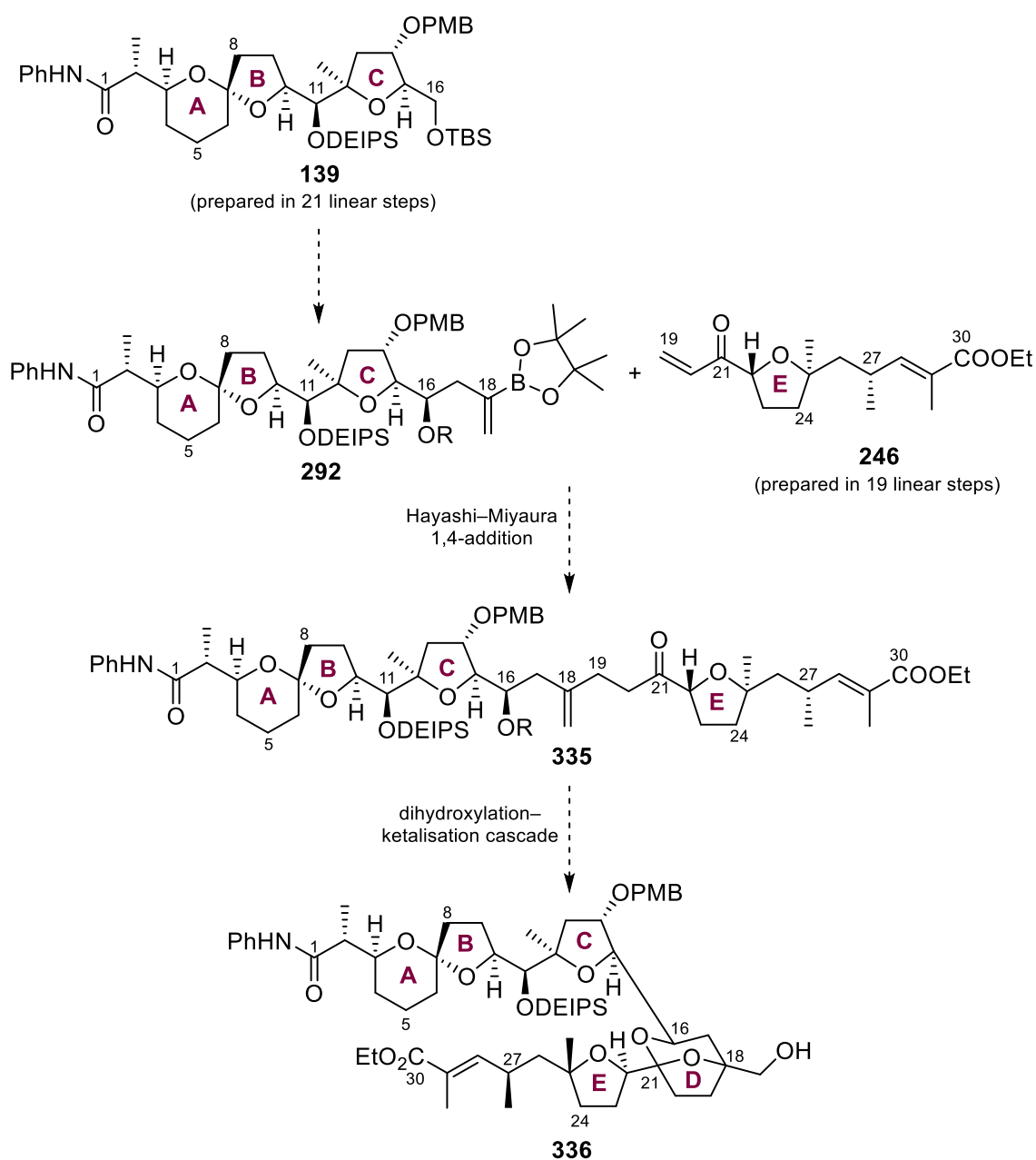
Scheme 3.34. Completion of F fragment **303** by Dr Melodie Richardson

CHAPTER 4

Uniting the ABC and E Fragments

4.1 Chapter overview

This chapter discusses the elaboration of ABC fragment **139** into its vinyl boronic ester analogue **292** for the planned rhodium-catalysed Hayashi–Miyaura 1,4-addition with E fragment **246** to unite the two major PTX-4 fragments to give **335** (Scheme 4.1). Optimisation studies for key reactions are also discussed and include an allylation reaction, the 1,4-addition, and a dihydroxylation–ketalisation cascade to form the D ring.



Scheme 4.1. Planned synthesis of ABCDE ring system **336**

4.2 Deprotection of ABC fragment **139**

4.2.1 Optimisation experiments for selective deprotection

Chapter 2 described the synthesis of the C1–C16 ABC fragment **139**, which was prepared in 21 linear steps from D-mannitol. However, before ABC fragment **139** could be united with the C19–C30 E fragment **246** to form the ABCE ring system **336** (Scheme **4.1**), it first had to be elaborated into the C1–C18 derivative **292**, which possesses the full carbon skeleton of the ABC scaffold as well as a suitable boronic ester molecular handle for the planned Hayashi–Miyaura 1,4-addition. To that end, a selective removal of the TBS ether in ABC fragment **139** to unveil the C16 primary hydroxyl group was first required.

Several deprotection conditions were screened (Table **4.1**). As part of the experimental design, only NMR yields were obtained to mitigate major weighing errors from repeated weighing of products in test reactions using milligram quantities of precious starting material. The two common issues that arose concerned conversion and selectivity – often, unreacted starting material **139** and over-deprotected diol **227** were present in large quantities along with the desired product. For example, treatment of **139** with TBAF in THF at 0 °C gave unreacted starting material, desired alcohol **226**, and undesired diol **227** in 50%, 35% and 42% NMR yields respectively (Entry 1), while performing the reaction at rt gave only diol **227** in 73% isolated yield (Entry 2). Of additional concern was the observation that the NMR yields of the various species, when totalled, exceeded 100%. Despite this limitation in measurement accuracy, it was decided to proceed with this method of yield evaluation, which could still be used as a qualitative measure to determine which deprotection conditions were superior.

Attempted deprotection of **139** using $\text{BF}_3 \cdot \text{OEt}_2$ at $0\text{ }^\circ\text{C}$ gave only a complex mixture (Entry 3). Deprotections that incorporated either CSA (Entry 4) or FeCl_3 (Entry 5–6) gave superior NMR yields and mass recovery. Despite the CSA conditions initially looking more promising, it was decided to proceed with the synthesis using the optimised conditions involving treatment with FeCl_3 at room temperature (Entry 6), because the isolated yields were more reproducible.

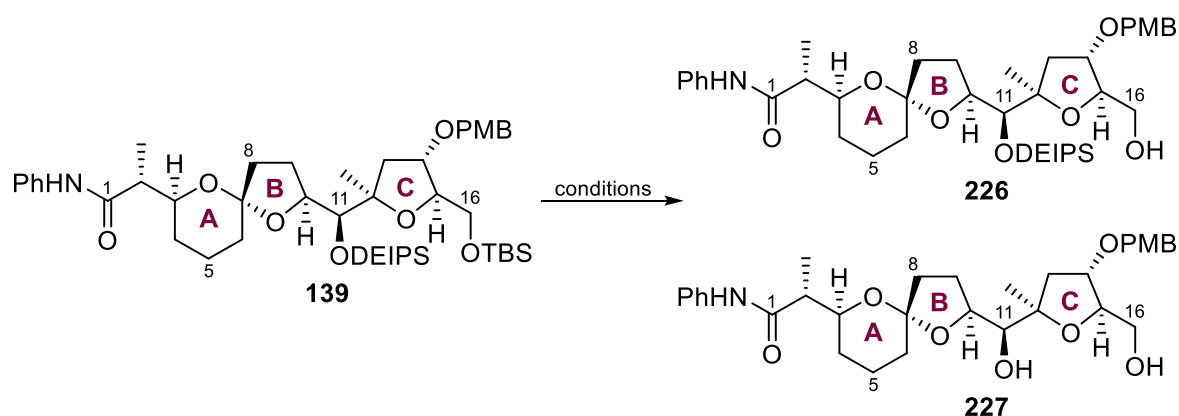


Table 4.1. Selective deprotection of ABC fragment **139**

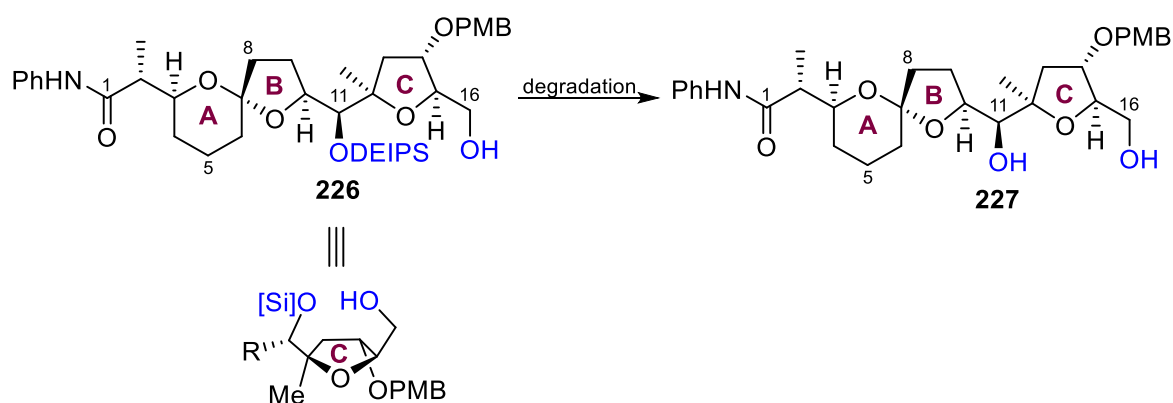
Entry	Conditions	226	227	139
1	TBAF, THF, $0\text{ }^\circ\text{C}$	50%*	35%*	42%*
2	TBAF, THF, rt	0%	73%	0%
3	$\text{BF}_3 \cdot \text{OEt}_2$, CH_2Cl_2 , $0\text{ }^\circ\text{C}$	0%	0%	0%
4	CSA, MeOH, $0\text{ }^\circ\text{C}$	82%*	23%*	25%*
5	FeCl_3 , MeOH, $0\text{ }^\circ\text{C}$	61%*	32%*	12%*
6	FeCl_3 , MeOH, rt	64%	34%	7%

*NMR yield.

4.2.2 Unexpected instability of ABC alcohol **226**

During the deprotection optimisation experiments, it was discovered that alcohol **226** was unstable and degraded over a matter of days even when stored as a pure sample in a $-30\text{ }^\circ\text{C}$ freezer. Analysing the ^1H and ^{13}C NMR spectra of decomposed samples indicated that alcohol **226** had degraded into previously isolated diol **226** *via* deprotection of the $-\text{ODEIPS}$ group at C11. This finding was surprising, given that the $-\text{ODEIPS}$ ether is known to be a stable

protecting group, with an ease of removal between that of the –OTES and –OTBS ethers.⁵⁹ Moreover, close analogues of alcohol **226** which possess the –ODEIPS moiety such as ABC fragment **139** were completely stable and demonstrated no tendency for the silyl group to be removed, outside of deprotection reaction conditions designed for that very purpose. It was suggested that the free hydroxyl at C16 in alcohol **226** may be responsible for the unexpected lability of the –ODEIPS group. O-to-O silyl migrations are well known in the literature as being facile processes, particularly in 1,2- and 1,3-diol systems where the two hydroxyl groups are in close proximity.⁶⁰ Although the C11 –ODEIPS group and the C16 hydroxyl group are five carbons away from each other, certain conformers of alcohol **226** may bring together the two *cis* groups into close proximity (Scheme 4.2). Although a true O-to-O silyl migration does not occur, the close contact of these two groups may induce a similar process in which the silyl group falls off the compound instead of transferring to the other oxygen atom.



Scheme 4.2. Degradation of alcohol **226** to diol **227**

4.3 Experiments involving side-product diol **227**

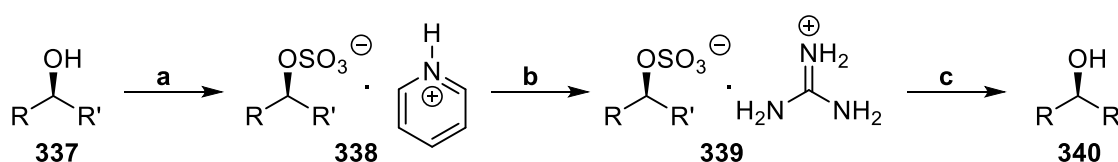
4.3.1 Attempted derivatisation of diol **227** into crystalline guanidinium sulphate

Relatively large quantities of diol **227** were accumulated over time, as a consequence of its generation in unselective deprotections of ABC fragment **139** and alcohol **226** degradation. Although it was not a target compound, diol **227** nevertheless possessed the complex ABC ring

system and substrate scaffold with all stereocentres installed, which prompted a series of experiments to either recycle or re-purpose diol **227**.

For example, it was proposed that diol **227**, a colourless oil, could be derivatised into a solid species that could be recrystallised and then submitted for X-ray crystallography. Although a combination of 2D NMR, ^{13}C NMR chemical shifts of C7 in the anomeric spiroketal, and nOe's of compounds with the ABC ring system had been used to ascertain the structure and stereochemistry of the compounds in the series, an X-ray crystal structure would provide unambiguous compound characterisation.

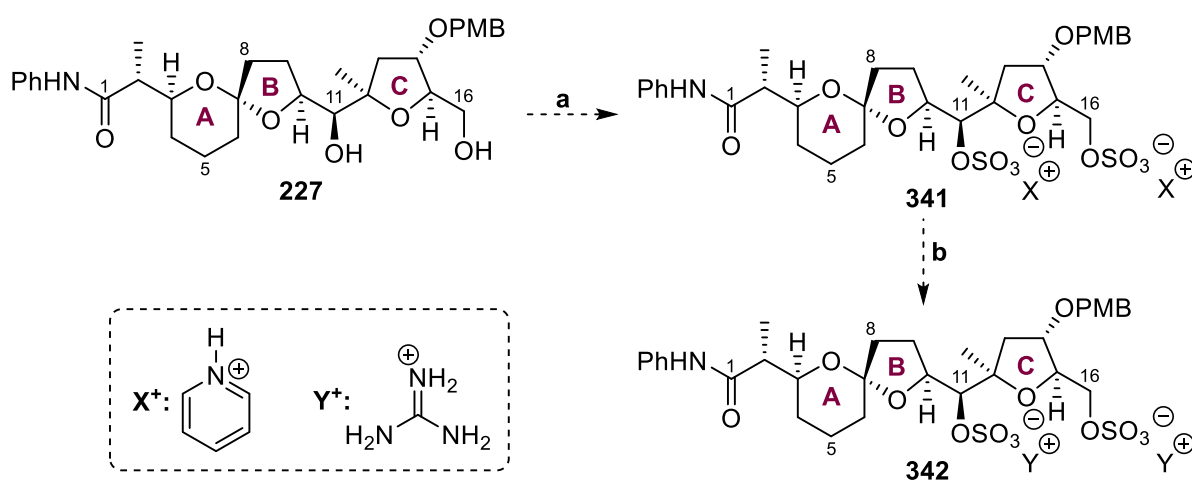
A recent publication by Kolis, Whitehead and co-workers described a method to derivatise chiral enantiopure alcohols into crystalline guanidinium sulphates, which were then submitted for X-ray crystallography and characterisation.⁶¹ These guanidinium sulphate derivatives could then be readily converted back to their parent alcohols through a straightforward hydrolysis (Scheme 4.3). Although only the use of simple alcohols was reported in the methodology, the possibility of appending the charged guanidinium sulphate moiety onto *both* hydroxyl groups of diol **227** seemed like it might be enough to alter its physical properties and make the derivative crystalline despite its greater size and complexity.



Reagents and conditions: a) SO_3^- :pyridine, CH_2Cl_2 , rt
b) Guanidinium chloride, MeOH, rt
c) H_2O , THF, reflux

Scheme 4.3. Derivatization of alcohols into crystalline guanidinium sulphate salts

Thus, diol **227** was subjected to literature reaction conditions, after adjusting the equivalents of $\text{SO}_3 \cdot \text{pyridine}$ and guanidinium chloride accordingly. After the first step, the reaction mixture was filtered to remove unreacted $\text{SO}_3 \cdot \text{pyridine}$ and then concentrated; the resulting crude sample was submitted for ^1H NMR analysis, which indicated that diol **227** had been fully converted. The proton signal integration ratios also indicated that the new species formed possessed two pyridinium rings, suggesting the successful formation of *bis*-sulphate **341**. The crude mixture was directly carried over to the subsequent salt exchange step, which involved treatment with guanidinium chloride in MeOH. Unfortunately, no crystals could be obtained during attempted crystallisation of the product from the crude mixture. As such, no X-ray crystal structure could be obtained.



Reagents and conditions: a) $\text{SO}_3 \cdot \text{pyridine}$, CH_2Cl_2 , rt
b) Guanidinium chloride, MeOH, rt

Scheme 4.4. Attempted derivatisation of diol **227** into its guanidinium sulphate salt

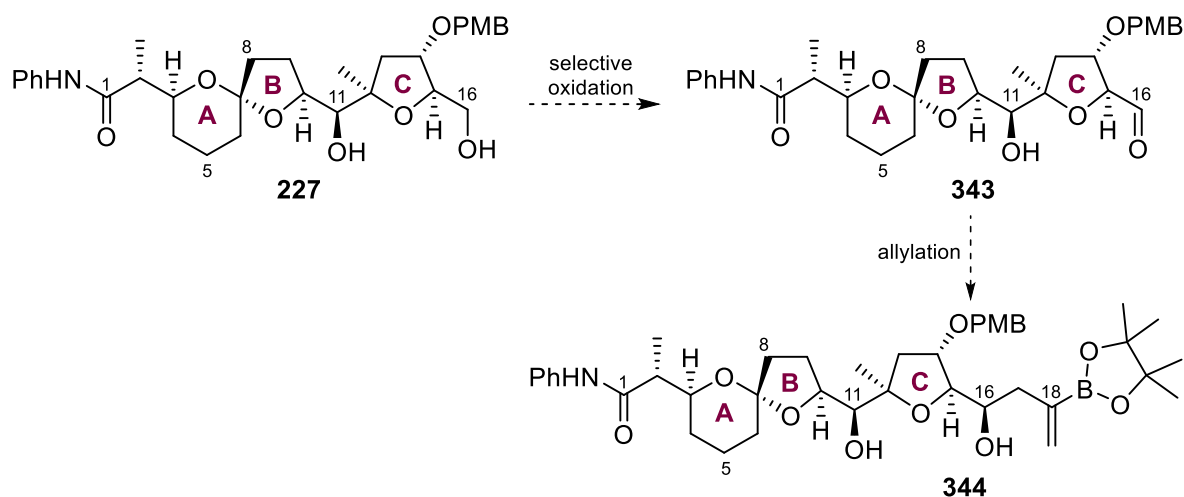
4.3.2 Attempted selective oxidation of diol **227** into hydroxy aldehyde **343**

Besides attempted derivatisation of diol **227** for characterisation purposes, efforts were also made to incorporate diol **227** into the main synthetic route itself to obtain a suitable C1–C18 Hayashi–Miyaura 1,4-addition partner. A selective oxidation of the C16 primary hydroxyl group to give aldehyde **343** was envisaged, followed by an allylation reaction to install the

C17–C18 carbons and the key vinyl boronic ester moiety to give compound **344** (Scheme 4.5).

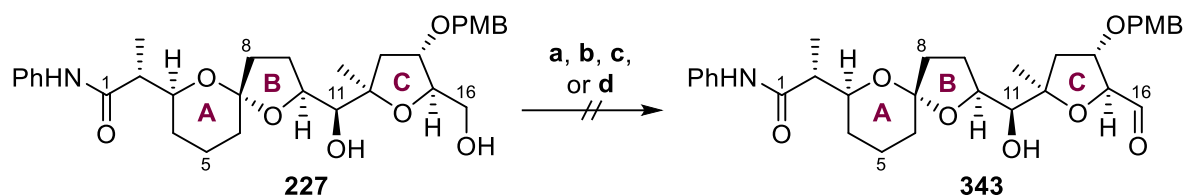
The C11 and C16 hydroxyl groups could then be both converted to suitable silyl ether protecting groups as required.

Accomplishing the first oxidation step would involve the selective oxidation of an unactivated primary alcohol in the presence of a secondary alcohol, which ruled out many robust yet non-selective oxidation methods, including those that had been demonstrated to work in preparing various advanced PTX-4 intermediates, such as the Swern, Parikh–Doering, and DMP oxidations.



*Scheme 4.5. Alternate route to prepare Hayashi–Miyaura coupling partner using diol **227***

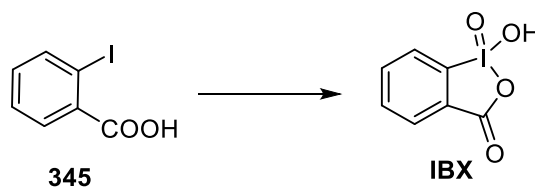
The first of such selective methods attempted involved treatment of diol **227** with stoichiometric $\text{RuCl}_2(\text{PPh}_3)_2$ in benzene, which only returned unreacted starting material (Scheme 4.6). A Cella–Piancatelli-type oxidation was then attempted; in this method, diol **227** was treated with catalytic TEMPO and trichloroisocyanuric acid as the terminal oxidant. However, diol **227** was also inert under these conditions. Modified conditions using NaOCl as the terminal oxidant and KBr additive were similarly ineffective.



Reagents and conditions: a) $\text{RuCl}_2(\text{PPh}_3)_2$, benzene, rt
 b) TEMPO, trichloroisocyanuric acid, CH_2Cl_2 , rt
 c) TEMPO, KBr, NaOCl, NaHCO_3 , CH_2Cl_2 , 0 °C
 d) IBX, DMSO, rt, 1 h

Scheme 4.6. Attempted selective oxidation of diol **227**

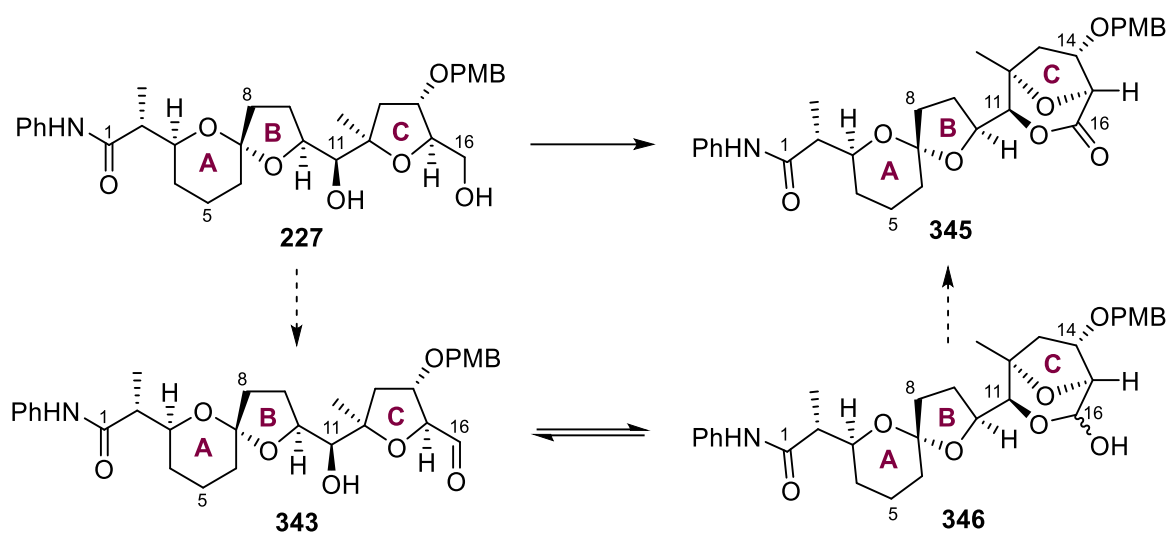
An IBX oxidation was also attempted using freshly made IBX prepared from 2-iodobenzoic acid (**345**) and Oxone in 92% yield (Scheme 4.7); however, no desired product was obtained.



Reagents and conditions: Oxone, H_2O , 70 °C, 5 h, 92%

Scheme 4.7. Preparation of IBX reagent

Surprisingly, changing the terminal oxidant from trichloroisocyanuric acid or NaOCl to BAIB while keeping the TEMPO catalyst was sufficient to promote reactivity, albeit not towards the desired product. Under these conditions, lactone **345** was instead produced in 40% yield, which presumably formed through desired aldehyde **343** as an intermediate, before equilibrating to lactol **346** and then undergoing a second more facile oxidation to the lactone (Scheme 4.8). The formation of lactone **345** cast doubt as to whether achieving a selective oxidation to aldehyde **343** was feasible, because such a reaction system would have to walk a tightrope of oxidising an unactivated primary alcohol in preference to both a secondary alcohol *and* a lactol within a complex molecule.



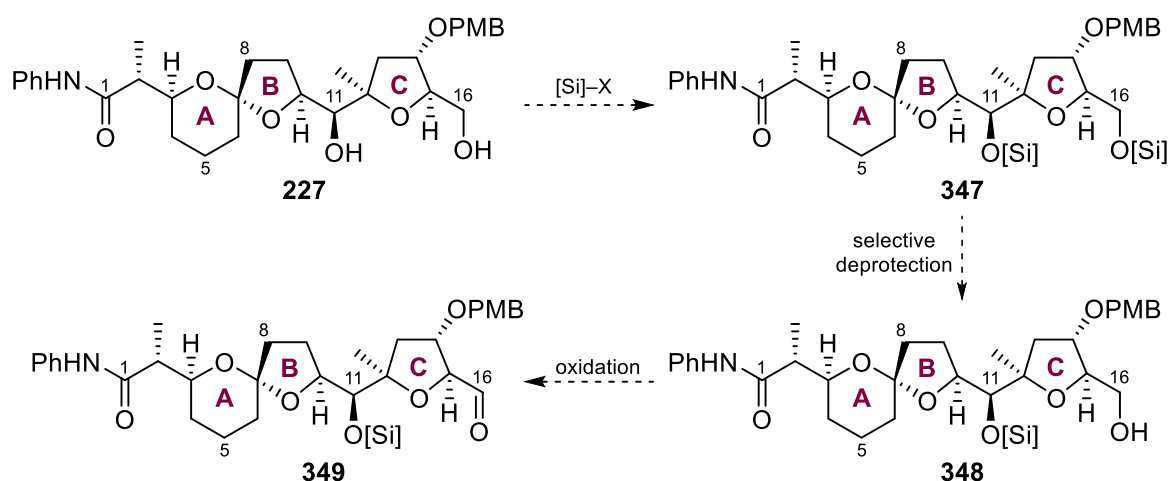
Reagents and conditions: TEMPO, BAIB, CH₂Cl₂, rt, 1 h, 40%

Scheme 4.8. Oxidation of diol 227 into lactone 345

There were also concerns about where the position of the equilibrium between lactol **346** and aldehyde **343** lay, and about whether that would have any effect on the subsequent planned allylation reaction. Despite these discouraging results, the formation of lactone **346** at least provided a deeper understanding of the system. Specifically, lactol and lactone formation constituted circumstantial evidence that the C11 and C16 oxygen atoms are in close spatial proximity to each other, which supported the proposed C16 hydroxyl mediated deprotection of the C11 –ODEIPS group in alcohol **226** that led to its degradation to diol **227**, as described in section **4.2.2**.

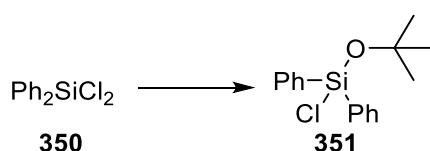
4.3.3 Studies examining protecting group manipulations on diol 227

It was decided to discontinue the selective oxidation strategy outlined in Scheme **4.6** and instead focus on an alternative approach. A proposed strategy involved protecting both hydroxyl groups of diol **227** as suitable silyl ethers in a single operation, followed by a selective deprotection to produce a mono-alcohol which could then be oxidised to its aldehyde in a straightforward fashion (Scheme **4.9**).



Scheme 4.9. Alternate route to recycle diol 227

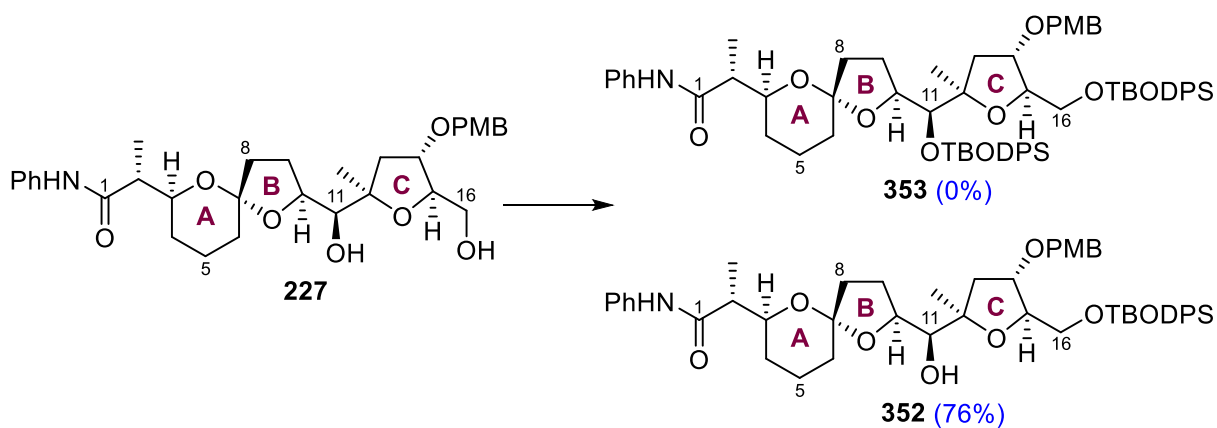
Initially, the silyl group chosen for installation was a *tert*-butoxydiphenylsilyl (TBODPS) group, which was the same silyl ether protecting group at C11 that Evans had used in his total synthesis of PTX-4.^{21,22} The TBODPS group, which had been installed relatively early in the synthesis, withstood various reaction conditions without falling off prematurely, yet could be readily removed during the TAS-F global deprotection in the final step of the total synthesis. A suitable silylating reagent, TBODPSCI (**351**), was prepared in 98% yield by reacting Ph₂SiCl₂ (**350**) with an equivalent of *t*BuOH in the presence of excess NEt₃ (Scheme 4.10).



Reagents and conditions: *t*BuOH, NEt₃, CH₂Cl₂, 40 °C, 40 h, 98%

Scheme 4.10. Preparation of TBODPSCI reagent (351)

However, treatment of diol **227** with a large excess of TBODPSCI (8 eqv.) only afforded the mono-protected alcohol **352** in 76% yield (Scheme 4.11), likely because of the steric bulk of the silylating reagent and of the groups surrounding the hindered secondary alcohol at C11.

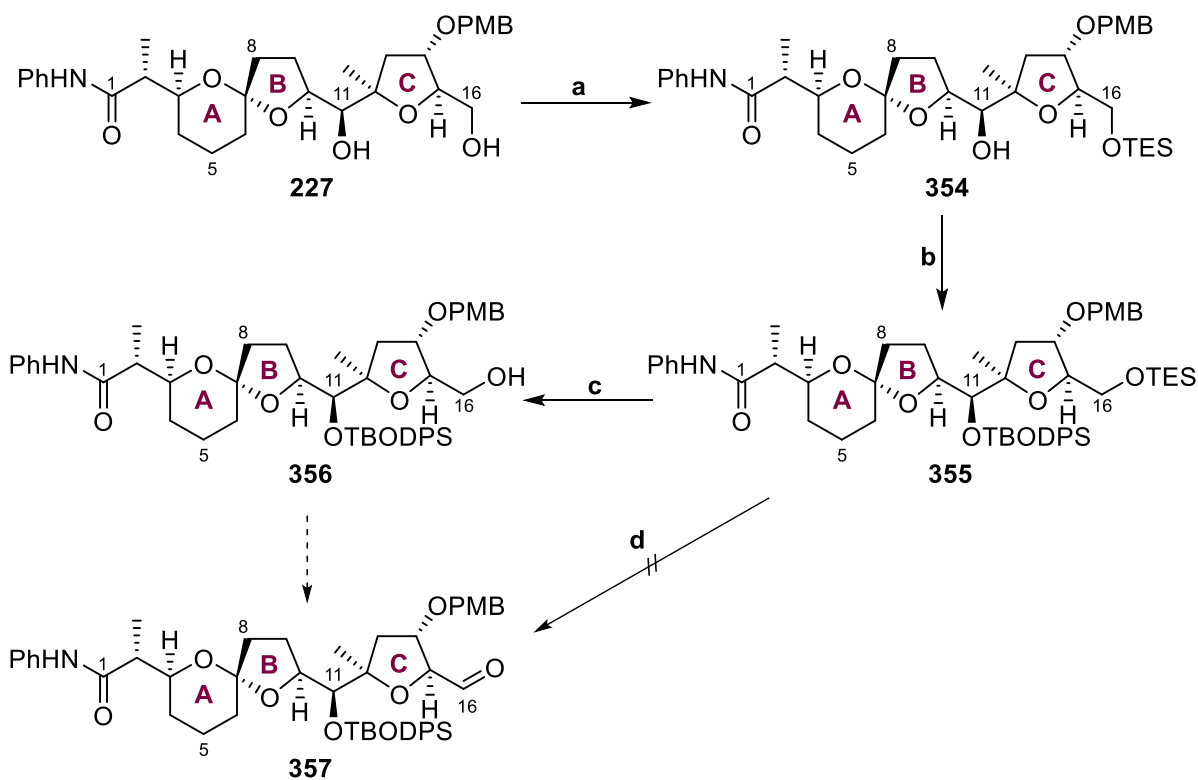


Reagents and conditions: TBODPSCI, DMAP, imidazole, CH₂Cl₂, rt, 22 h

Scheme 4.11. Attempted synthesis of silyl ether 353

An alternate three-step sequence involving a selective mono-TES protection of diol **227**, TBODPS protection of the C11 hydroxyl group, and a selective deprotection of the labile TES ether successfully gave the target compound **356**, which could potentially be oxidised to its aldehyde (**357**) for the subsequent allylation step (Scheme **4.12**). Moreover, alcohol **354** displayed none of the stability issues encountered with the DEIPS-bearing alcohol **226** (Scheme **4.2**).

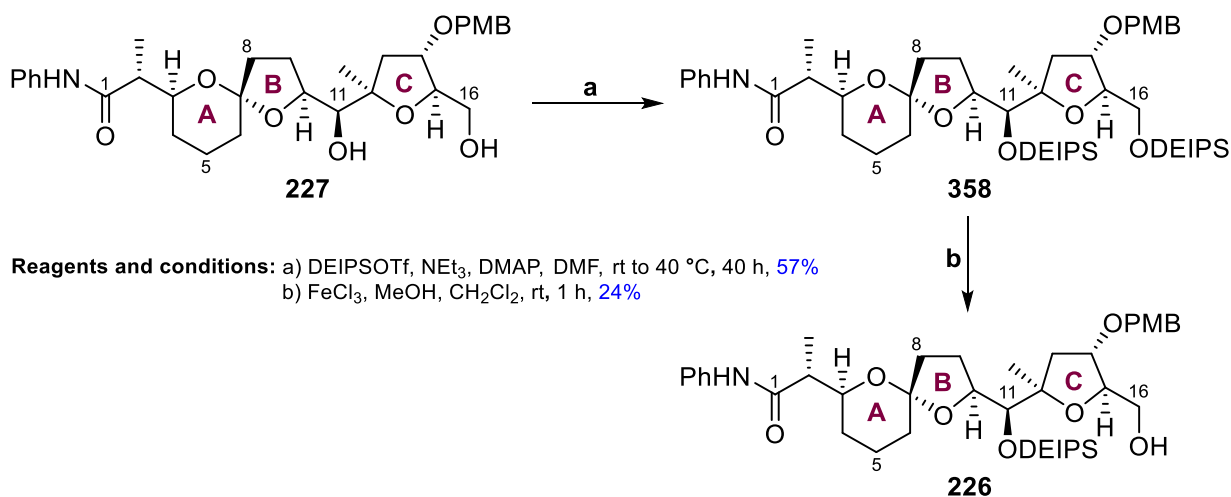
Nevertheless, the overall yield of alcohol **356** from the three-step sequence was a mere 15% because of the low-yielding second step involving installation of the bulky TBODPS ether onto the hindered C11 alcohol. Moreover, an attempt to save a step by directly oxidising TES ether **355** to aldehyde **357** under mildly acidic Cella–Piancatelli conditions involving BAIB, TEMPO, and AcOH gave no desired product. Based on these less than satisfactory results, it was decided to abandon the approach of a protecting group swap at the C11 hydroxyl group, despite concerns of the instability of the original DEIPS group.



Reagents and conditions: a) TESC1, DMAP, 2,6-lutidine, CH₂Cl₂, -78 °C, 2 h, **99%**
 b) TBODPSCI, DMAP, imidazole, CH₂Cl₂, 45 °C, 22 h, **25%**
 c) PPTS, MeOH, CH₂Cl₂, 0 °C, 30 min, **62%**
 d) BAIB, TEMPO, AcOH, CH₂Cl₂, rt, 2 h, **0%**

Scheme 4.12. Alternate strategy to install TBODPS

Instead, a more conservative strategy of *recycling* diol **227** into alcohol **226** was adopted, instead of designing a new route around it. Thus, diol **227** was treated with excess DEIPSOTf in the presence of DMAP and NEt₃ to give silyl ether **358** in 57% yield (Scheme **4.13**). Silyl ether **358** was then selectively deprotected using FeCl₃ to give alcohol **226** in 24% yield. The yield of the deprotection step was surprisingly low and possibly anomalous. Nevertheless, the two-step sequence described in Scheme **4.13** carries the potential for optimisation and provides the means to prepare alcohol **226** from diol **227**, which may otherwise have been discarded.

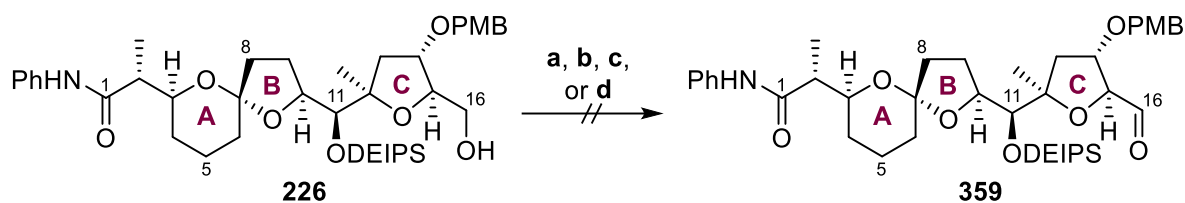


Scheme 4.13. Recycling of diol **227** into alcohol **226**

4.4 Screening of oxidation conditions to prepare aldehyde **359**

As discussed in section 4.2, alcohol **226** could be prepared from ABC fragment **139** in moderate yields *via* a selective deprotection involving treatment with FeCl₃ and MeOH. Moreover, any over-deprotected side-product diol **227** could be recycled into alcohol **226**, as was described in section 4.3.3. Oxidation conditions now had to be screened to convert alcohol **226** into aldehyde **359** in high yields. However, what had appeared in principle to be a trivial operation was complicated by repeated failure of standard oxidation reaction procedures and the instability of alcohol **226**, which had been previously described to degrade into diol **227** if not carried over to the next step immediately after its preparation.

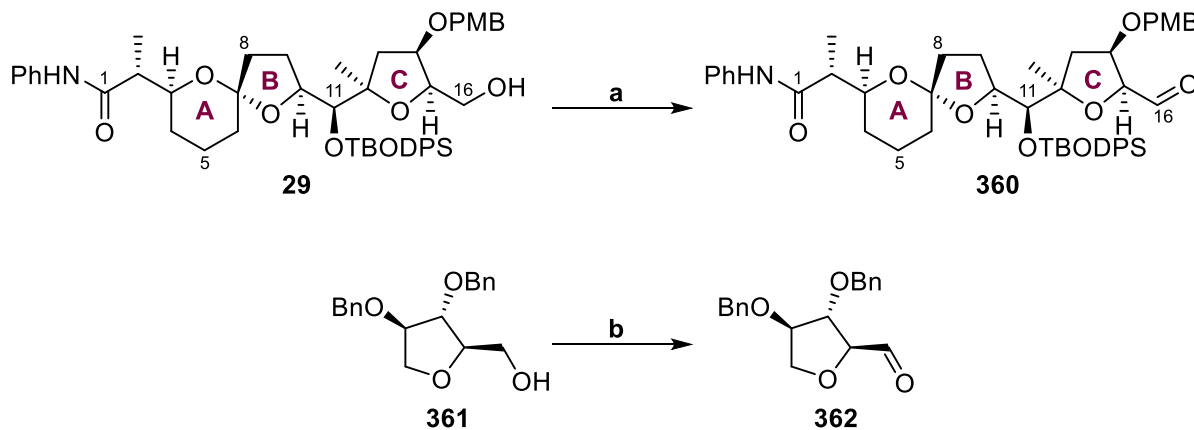
Performing a Swern oxidation reaction of alcohol **226** gave only a complex mixture, while attempting Hendrickson–Swern, DMP and Parikh–Doering oxidation reactions returned only unreacted starting material (Scheme 4.14).



Reagents and conditions: a) (COCl)₂, DMSO, NEt₃, CH₂Cl₂, -78 °C to rt
 b) Tf₂O, DMSO, DIPEA, CH₂Cl₂, -78 °C to 0 °C
 c) DMP, pyridine, CH₂Cl₂, rt
 d) SO₃·pyridine, DMSO, NEt₃, CH₂Cl₂, rt

*Scheme 4.14. Attempted oxidation of alcohol **226** to aldehyde **359***

The failure of the Parikh–Doering reaction was especially surprising, given that Evans had successfully performed that reaction on a very close analogue of alcohol **226** to prepare the corresponding aldehyde **360** (Scheme 4.15).²² A control experiment was conducted using a model system, THF **361**, which had earlier been prepared by Dr Melodie Richardson. The Parikh–Doering test reaction gave model aldehyde **362** in 78% yield (Scheme 4.15), suggesting that experimental error or degraded reagents were unlikely causes for reaction failure when alcohol **226** was used.



Reagents and conditions: a) SO₃·pyridine, DMSO, NEt₃, CH₂Cl₂, -10 °C, >78%
 b) SO₃·pyridine, DMSO, NEt₃, CH₂Cl₂, rt, 78%

*Scheme 4.15. Successful oxidations of Evans' analogue **29**²² and model **361***

Drawing inspiration from earlier oxidation experiments performed on diol **227** (Scheme 4.8), it was decided to attempt Piancatelli–Cella oxidation conditions using TEMPO and BAIB on alcohol **226**. These conditions had previously given the over-oxidised lactone **345** as the sole

product when used on diol **227**. However, because alcohol **226** only possessed one free hydroxyl group, such an over-oxidation would not occur. Thus, oxidation of alcohol **226** was screened under these conditions (Table 4.2). An initial reaction run using 1 eqv TEMPO in CH₂Cl₂ solvent gave a trace amount of aldehyde **359** that was barely detectable by ¹H NMR (Entry 1). AcOH additive was reported by Piancatelli to enhance the rate of oxidation.⁶² Inclusion of AcOH in a subsequent experiment gave aldehyde **359** in 31% NMR yield, which while low was nonetheless an encouraging result (Entry 2). Removing the AcOH additive but increasing the TEMPO loading to 10 eqv gave aldehyde **359** in 22% NMR yield (Entry 3). Maintaining the high 10 eqv TEMPO loading but switching the solvent from CH₂Cl₂ to DMSO gave no product (Entry 4). Finally, combining the desirable conditions of higher TEMPO loading (2 eqv) and AcOH additive gave aldehyde **359** in 69% NMR yield (Entry 5).

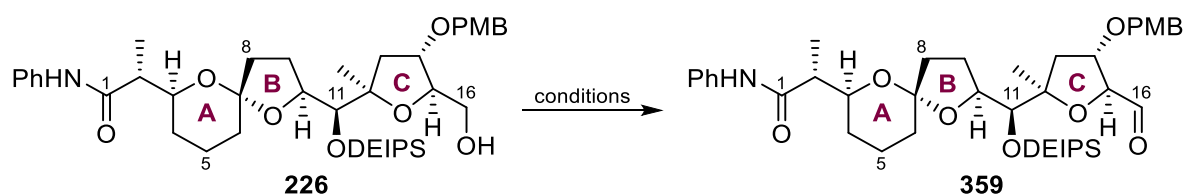
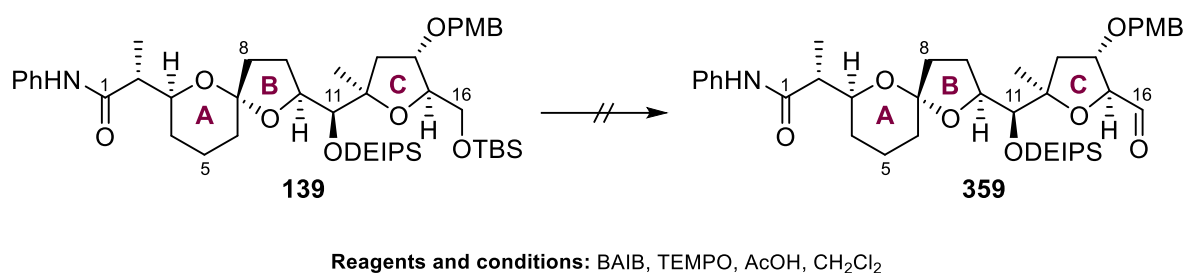


Table 4.2. Oxidation conditions of alcohol **226**

Entry	Conditions	Scale	Yield
1	BAIB, 1 eqv. TEMPO, CH ₂ Cl ₂	3 mg	Trace
2	BAIB, 1 eqv. TEMPO, AcOH, CH ₂ Cl ₂	3 mg	31%*
3	BAIB, 10 eqv. TEMPO, CH ₂ Cl ₂	3 mg	22%*
4	BAIB, 10 eqv. TEMPO, DMSO	3 mg	0%
5	BAIB, 2 eqv. TEMPO, AcOH, CH ₂ Cl ₂	3 mg	69%*
6	BAIB, 2 eqv. TEMPO, AcOH, CH ₂ Cl ₂	34 mg	11%
7	PDC, 3 Å MS, CH ₂ Cl ₂	5 mg	19%*
8	PCC, 3 Å MS, CH ₂ Cl ₂	5 mg	54%*
9	PCC, 3 Å MS, CH ₂ Cl ₂	16 mg	61%*
10	PCC, 3 Å MS, CH ₂ Cl ₂	57 mg	94%
11	PCC, 3 Å MS, CH ₂ Cl ₂	148 mg	91%

*NMR yield.

Up until this point (Entries 1–5), reactions had been performed at test scales using 3 mg of starting material. When the reaction was scaled up to 34 mg using the Entry 5 optimised conditions, the isolated yield sharply decreased to 10% (Entry 6). Repeat experiments confirmed that these oxidative conditions only gave high yields under a very narrow range of low scales. Furthermore, subjecting silyl ether **139** instead of alcohol **226** to the mildly acidic BAIB/TEMPO/AcOH conditions in an attempt to trigger a deprotection–oxidation sequence to save a step only returned starting material (Scheme 4.16).



*Scheme 4.16. Attempt to convert **139** to **359** through deprotection–oxidation sequence*

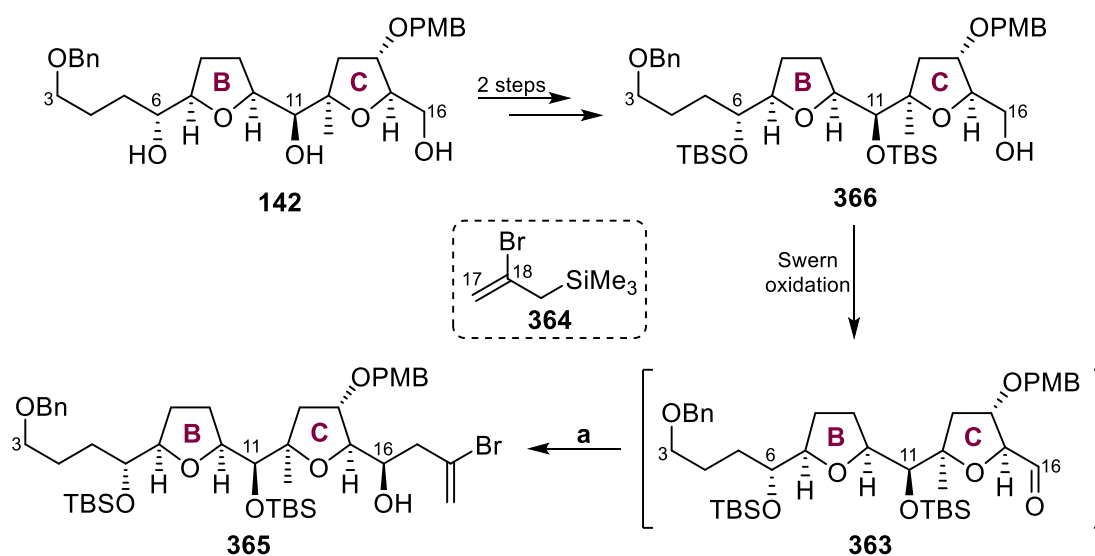
Fortunately, very soon after optimisation efforts for the oxidation were restarted, reliable and high-yielding conditions were found. Using PDC gave aldehyde **359** in only 19% NMR yield (Entry 7), but switching to PCC as an oxidant gave a 54% NMR yield (Entry 8). Unlike with the Cella–Piancatelli conditions, the efficacy of these PCC conditions increased with scale (Entry 9–11); when the reaction was finally scaled up to 148 mg, 91% isolated yield of aldehyde **359** was obtained. Besides giving superior yields, the PCC-mediated oxidation also had the advantages of being rapid and clean, requiring under 30 min of reaction time and a quick filtration through a silica pad to obtain pure product.

Although extended storage of aldehydes with α -chiral centres may result in epimerisation of the compound and other side-reactions, aldehyde **359** was found to be surprisingly stable and displayed no tendency to degrade *via* DEIPS group deprotection, unlike its precursor alcohol **226** (Section 4.2.2).

4.5 Sakurai Allylation of aldehyde 359

4.5.1 Background of allylation model systems

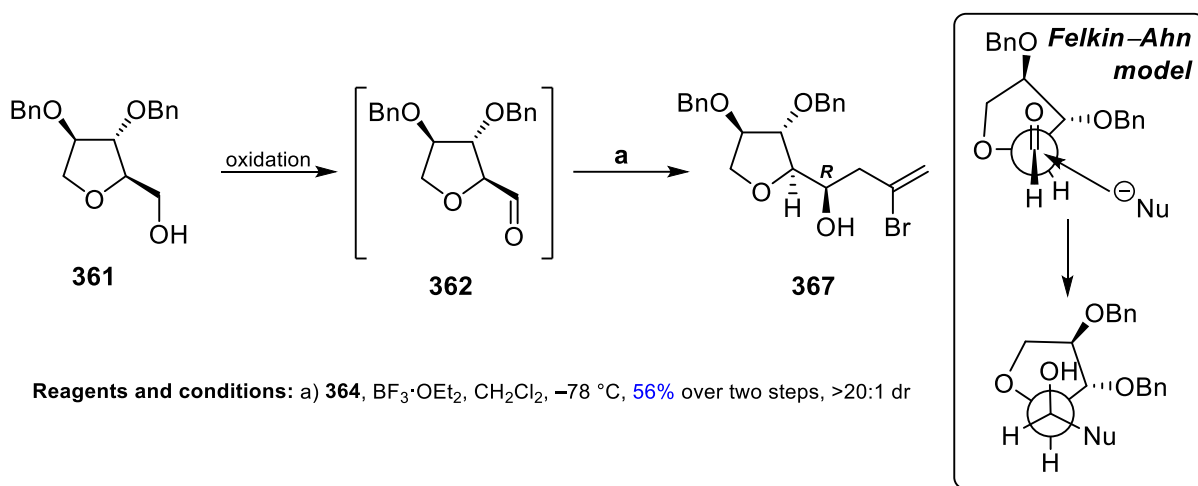
With aldehyde **359** in hand, an allylation reaction could now be conducted. Dr Melodie Richardson had previously performed extensive model studies to develop optimal conditions for this allylation step.³⁶ The most sophisticated model system used was aldehyde **363**, which was derived in three steps from *bis*-THF **142**, whose synthesis is described in chapter 2. Under this system, the optimised conditions involved a Sakurai allylation reaction that used allyl silane **364** as the reaction partner and $\text{BF}_3 \cdot \text{OEt}_2$ as the Lewis acid in CH_2Cl_2 at -78°C , which gave homoallylic alcohol **365** in 22% yield and in >20:1 d.r. over two steps (Scheme 4.17). The low yield was attributed to the unreliability of the oxidation step to make aldehyde **363** from alcohol **366**.



Scheme 4.17. Sakurai allylation reaction on model system by Dr Melodie Richardson³⁶

Indeed, these Sakurai allylation reaction conditions were higher yielding in other (albeit simpler) model systems (Scheme 4.18), in which the preceding oxidation step was more reliable. For homoallylic alcohol **365**, the stereochemistry at the newly generated stereocentre was assigned as the desired (*R*) configuration by Mosher's ester analysis.³⁶ The

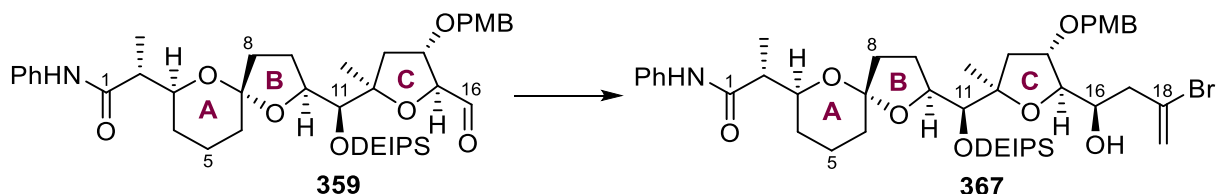
stereochemistry at the newly generated C16 stereocentre can be rationalised by the polar Felkin–Anh model, which places the polar C–O bond perpendicular to the carbonyl group (Scheme 4.18). The nucleophile attacks through the least hindered approach where H is to give the (*R*)-product.



Scheme 4.18. Sakurai allylation reaction on model system **362**

4.5.2 Sakurai allylation and elaboration

Aldehyde **359** was thus subjected to a Sakurai allylation with reagent **364** in the presence of $\text{BF}_3 \cdot \text{OEt}_2$ in CH_2Cl_2 at -78°C , which gave homoallylic alcohol **367** in 53% yield as a single diastereomer; the newly generated stereocentre at C16 was assigned by analogy with compounds **367** (Scheme 4.18) and **31** (Scheme 4.26).

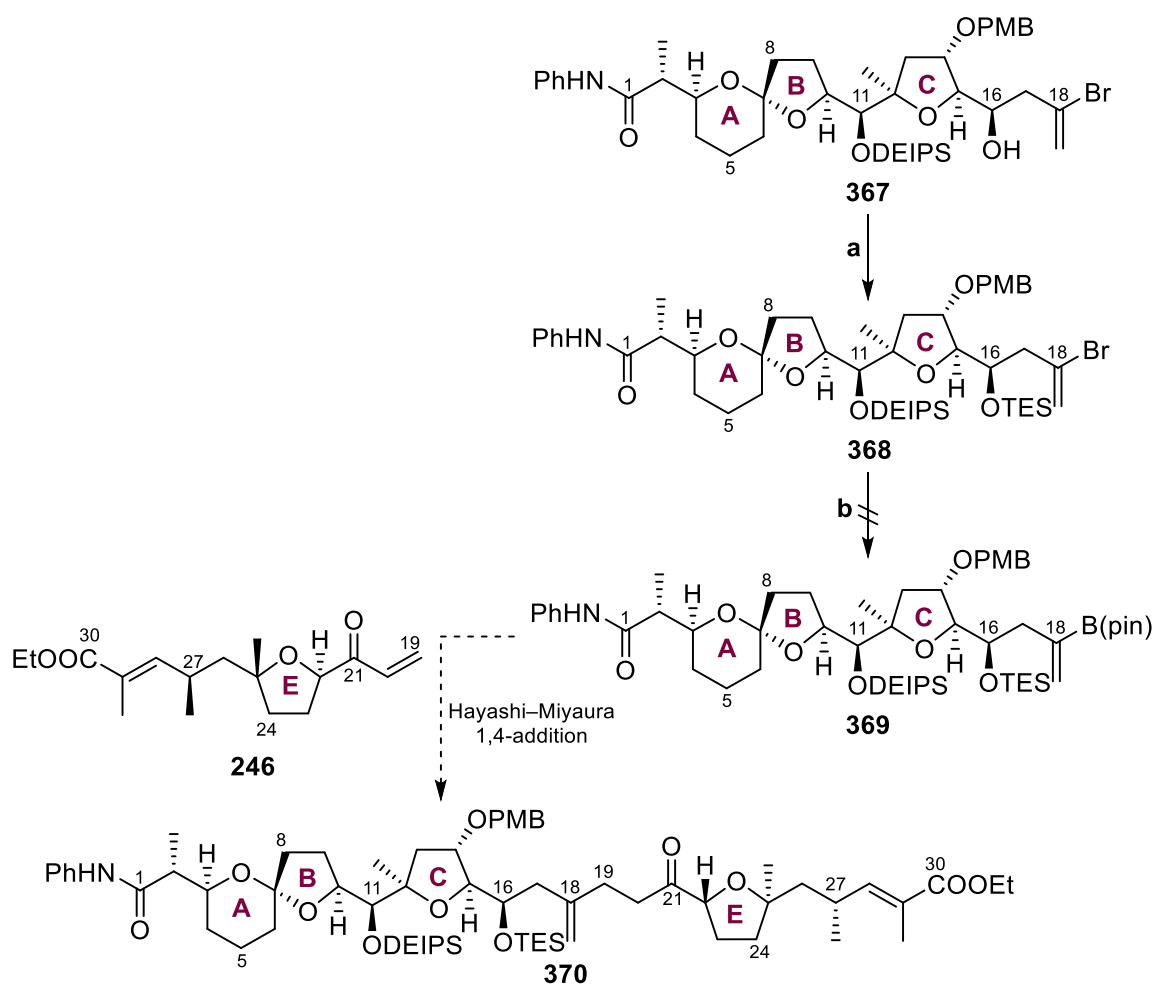


Reagents and conditions: **364**, $\text{BF}_3 \cdot \text{OEt}_2$, CH_2Cl_2 , -78°C , 53%, >20:1 dr

Scheme 4.19. Sakurai allylation reaction on aldehyde **359**

A TES protection was then performed on homoallylic alcohol **367** to give silyl ether **368** in 47% yield (Scheme 4.20). However, the subsequent Miyaura borylation reaction to convert

bromide **368** into boronic ester **369** gave only a complex mixture. Due to the very limited supply of bromide **368**, no repeat reactions could be conducted. It had been intended to use the product boronic ester **369** for the key Hayashi–Miyaura 1,4-addition with E fragment **246** (Scheme 4.20). However, at this stage of the project, a modified synthetic plan was conceived that involved switching the order of the 1,4-addition and the Sakurai allylation steps.



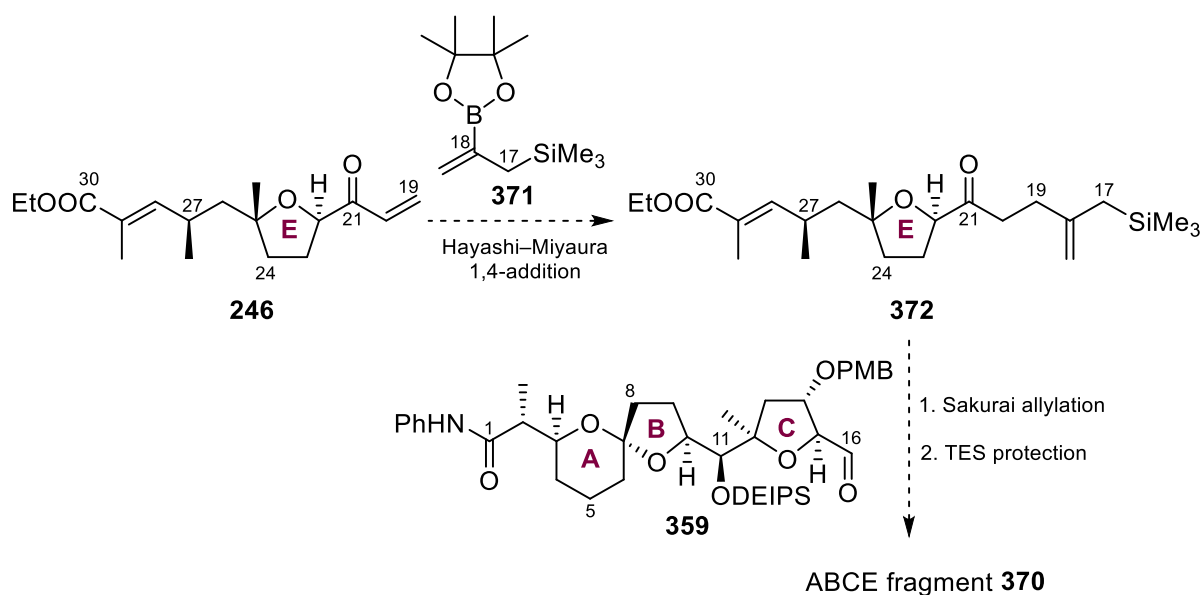
Reagents and conditions: a) TESI, DMAP, imidazole, CH₂Cl₂, 0 °C to rt, 30 min, 47%
 b) PdCl₂(PPh₃)₂, (B(pin))₂, KOPh, PhMe, 50 °C, 3 h, 0%

Scheme 4.20. Planned elaboration of homoallylic alcohol 367

4.5.3 Revised route involving different order of key steps

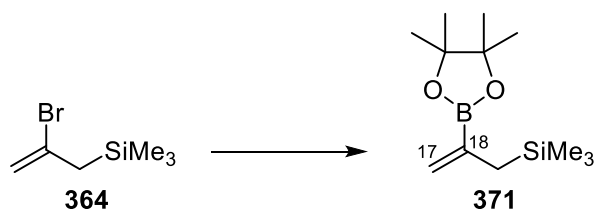
In this modified route, the 1,4-addition was to be performed between E fragment **246** and the much smaller C17–C18 fragment **371** instead to give allyl trimethylsilane **372** (Scheme 4.21).

Allyl trimethyl silane **372** would then be subjected to a Sakurai allylation with aldehyde **369** followed by a TES protection, thus producing the unified ABCE fragment **370** through an alternate sequence. This modified sequence carried two advantages over the original: 1) It bypassed the difficult Miyaura borylation step on bromide **368**; 2) although the total step count remained constant, the modified route was two linear steps shorter.



*Scheme 4.21. Alternate synthetic route to access ABCE fragment **370***

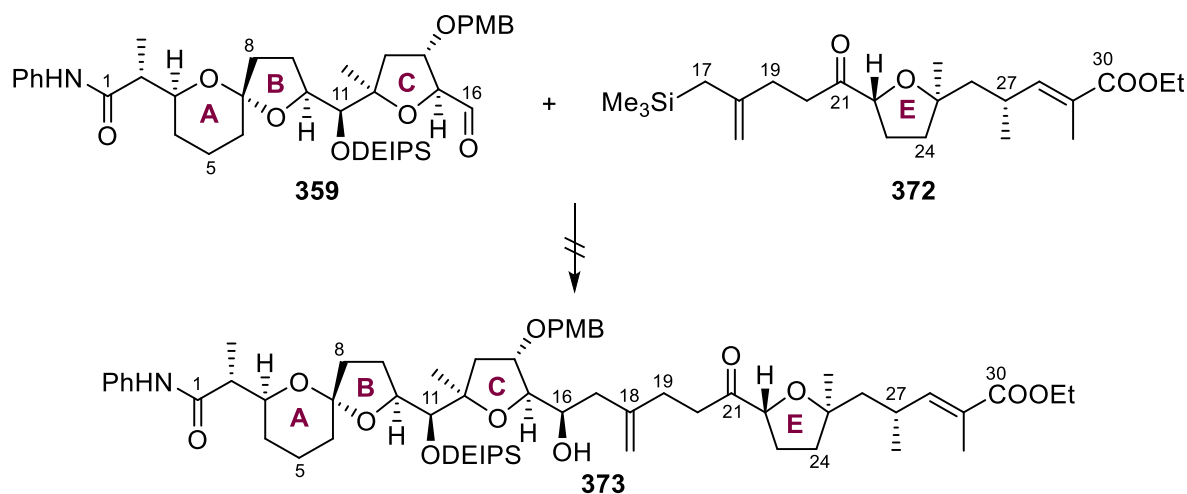
This revised plan was thus attempted. First, the C17–C18 fragment **371** was prepared directly from **364** in 61% yield through a Miyaura borylation reaction (Scheme 4.22). The Hayashi–Miyaura 1,4-addition reaction using C17–C18 fragment **371** and E fragment **246** was then carried out by Dr Melodie Richardson to give allyl trimethylsilane **372** in an unoptimised 18% yield.³⁶ Despite the low yield, this was an encouraging result because it demonstrated that the 1,4-addition step worked even with the fully elaborated E fragment partner and because it was only a single result that could be further optimised.



Reagents and conditions: $\text{PdCl}_2(\text{PPh}_3)_2$, $(\text{B}(\text{pin}))_2$, KOPh , PhMe , $50\text{ }^\circ\text{C}$, 3 h, 61%

Scheme 4.22. Miyaura borylation reaction to prepare C17–C18 fragment **371**

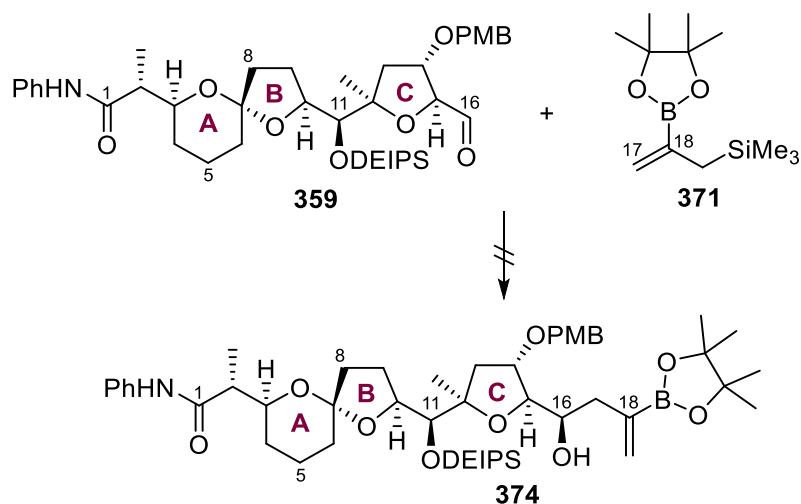
Allyl trimethylsilane **372** and ABC aldehyde **359** were then subjected to the optimised Sakurai allylation conditions as before; unfortunately, the reaction gave no desired product (Scheme 4.23). TLC monitoring throughout the reaction suggested that allyl trimethylsilane **372** was insufficiently reactive to allylate aldehyde **359**, likely due to the enhanced steric bulk of the former compared to allyl trimethylsilane **364**; with no allylation reaction taking place, both substrates gradually degraded under the reaction conditions over time.



Reagents and conditions: $\text{BF}_3 \cdot \text{OEt}_2$, CH_2Cl_2 , $-78\text{ }^\circ\text{C}$

Scheme 4.23. Attempted Sakurai allylation between **359** and **372**

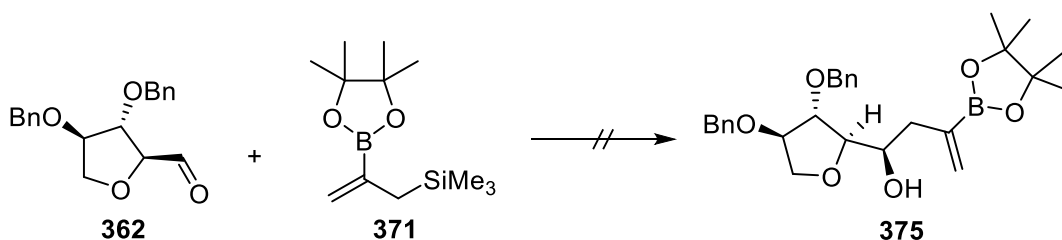
Using allyl trimethylsilane **371** as the allylating partner gave similar disappointing results; only starting material degradation took place and no desired product was obtained (Scheme 4.24).



Reagents and conditions: $\text{BF}_3 \cdot \text{OEt}_2$, CH_2Cl_2 , $-78\text{ }^\circ\text{C}$

*Scheme 4.24. Attempted Sakurai allylation between **359** and **371***

The Sakurai allylation was repeated using the simple ABC fragment model **362** while keeping allyl trimethylsilane **371** as the allylating partner (Scheme 4.25). However, the reaction failed once more.



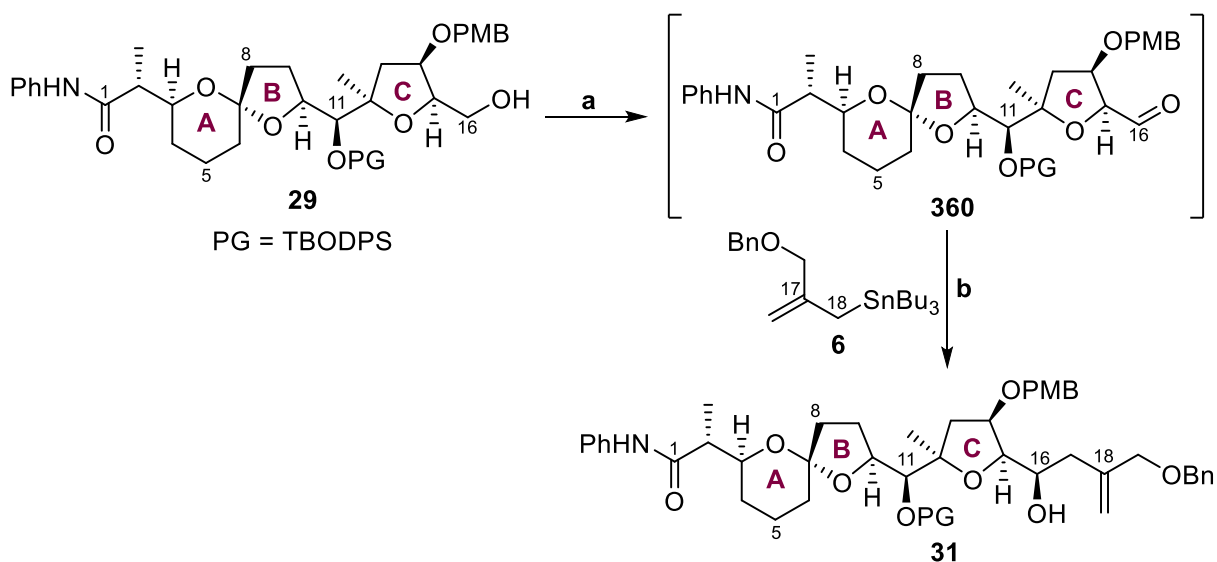
Reagents and conditions: $\text{BF}_3 \cdot \text{OEt}_2$, CH_2Cl_2 , $-78\text{ }^\circ\text{C}$

*Scheme 4.25. Attempted Sakurai allylation between model **362** and **371***

4.6 Keck allylation of aldehyde 359

The outcome of the various Sakurai allylation experiments suggested that, although ABC aldehyde **359** was a suitable electrophile for such a reaction, the sterics of the allylating partner played a critical role in the allylation's success; excessive steric bulk could attenuate reactivity and cause reaction failure. A strategy to counteract the decrease in reactivity from sterics would be to replace the $-\text{SiMe}_3$ group with a group that would have an even stronger

β -heteroatom effect such as $-\text{SnR}_3$, as Evans had done in his synthesis of PTX-4.^{21,22} In Evans' total synthesis, a two-step procedure was conducted on alcohol **29**, which was first oxidised to aldehyde **360** through a Parikh–Doering reaction, which was then reacted with allyl tributylstannane **6** in a Keck reaction to give homoallylic alcohol **31** in an impressive 78% yield over two steps (Scheme 4.26).

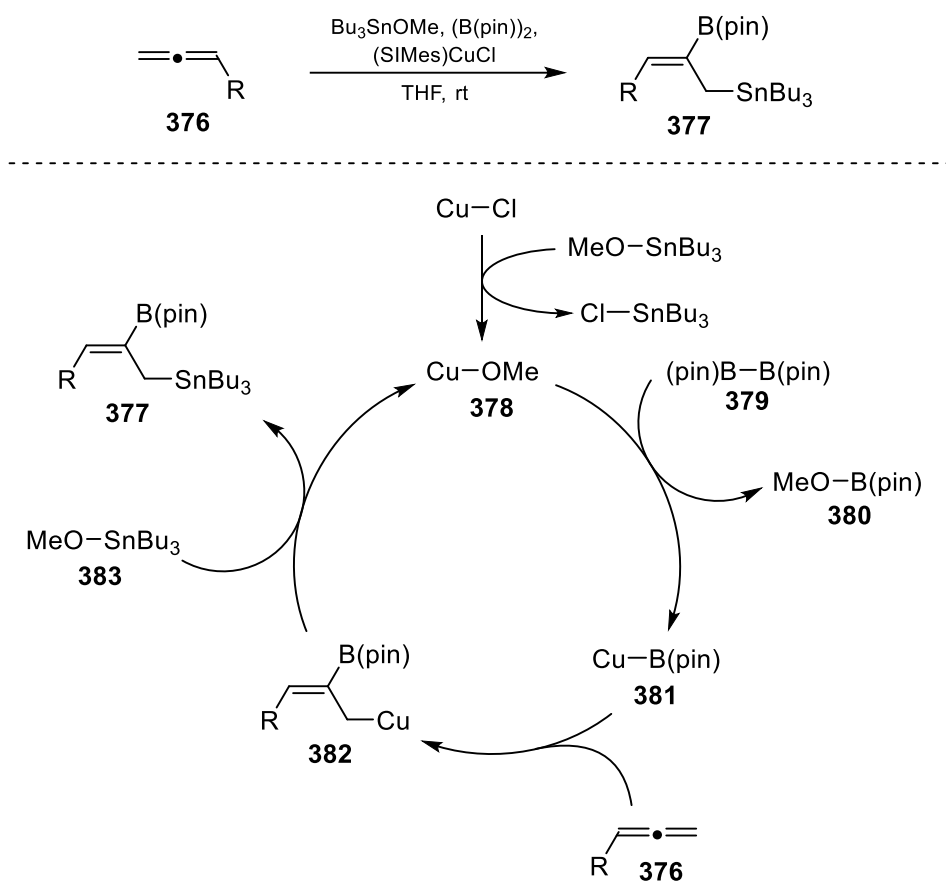


Reagents and conditions: a) $\text{SO}_3 \cdot \text{pyridine}$, DMSO, NEt_3 , CH_2Cl_2 , $-10\text{ }^\circ\text{C}$
 b) $\text{BF}_3 \cdot \text{OEt}_2$, CH_2Cl_2 , $-78\text{ }^\circ\text{C}$, 78% over two steps

Scheme 4.26. Keck allylation performed in Evans' total synthesis of PTX-4

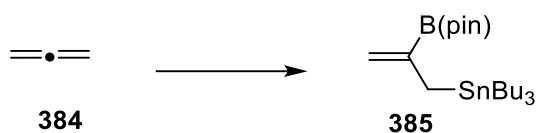
Thus, stannane analogues of the silicon-bearing **364** and **371** were sought. In 2014, Yoshida and co-workers published a report describing a copper-catalysed borylstannylation of alkenes and allenes to access borylstannanes.⁶³ The authors suggested that the reaction proceeded along the following pathway (Scheme 4.27): borylcopper species **376** is first generated from $(\text{B}(\text{pin}))_2$ and $(\text{SIMes})\text{CuCl}$; this species in turn reacts with the allene to selectively generate the (Z) - σ -allylcopper species **382**, which then reacts with Bu_3SnOMe (**383**) to give the final borylstannane product **377**.

Given the regiochemistry of the resulting products, it was thought that this methodology could be performed on propadiene to give borylstannane **385** – the more reactive tributylstannane analogue of the C17–C18 Sakurai allylating partner **371**.



Scheme 4.27. Pathway for borylstannylation of allenenes

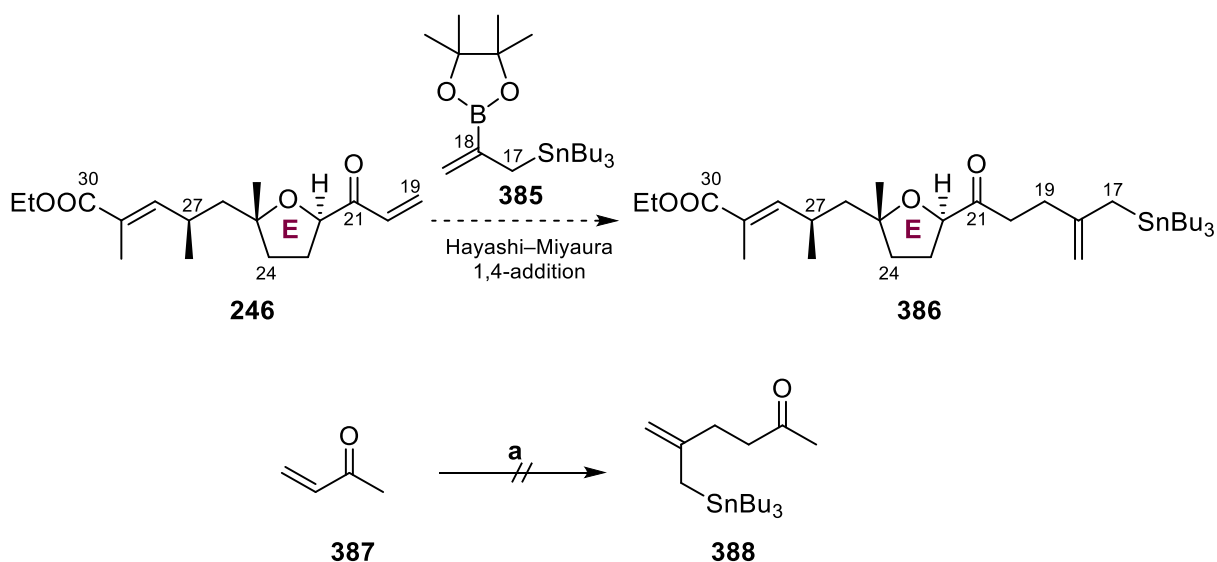
Because propadiene is a gas at room temperature with a boiling point of $-34.4\text{ }^\circ\text{C}$, the borylstannylation had to be performed under modified conditions, which involved slowly bubbling propadiene into the mixture over 20 s using a long needle at $-78\text{ }^\circ\text{C}$, allowing the gas to condense in the solution. The $-78\text{ }^\circ\text{C}$ cooling bath was subsequently removed, allowing the mixture to slowly warm up to and react at room temperature. The use of an empty balloon attached to a needle that was fitted into the rubber septum of the reaction pot prevented over-pressurisation from boiling propadiene, while still maintaining the propadiene atmosphere in the reaction vessel. Pleasingly, these modified conditions were successful on the first attempt, giving borylstannane **385** in 69% yield (Scheme 4.28).



Reagents and conditions: Bu₃SnOMe, (B(pin))₂, (SiMes)CuCl, THF, -78 °C to rt, 2 h, 69%

Scheme 4.28. Borylstannylation of propadiene

Borylstannane **385** could then either be directly reacted with aldehyde **359** through a Keck allylation reaction, or first reacted with the E fragment enone **246** through a Hayashi–Miyaura 1,4-addition reaction, followed by Keck allylation reaction with **359** (Scheme 4.29). Because it led to an overall forward synthesis that would be one linear step shorter, the strategy involving the preliminary 1,4-addition reaction was initially prioritised. It was unknown whether the –SnBu₃ moiety would be compatible with the rhodium-catalysed 1,4-addition reaction conditions, so a test reaction was performed between borylstannane **385** and methyl acrylate (**387**), in order to conserve precious E fragment enone **246** (Scheme 4.29). Unfortunately, the reaction only gave a complex mixture and so this approach was abandoned.

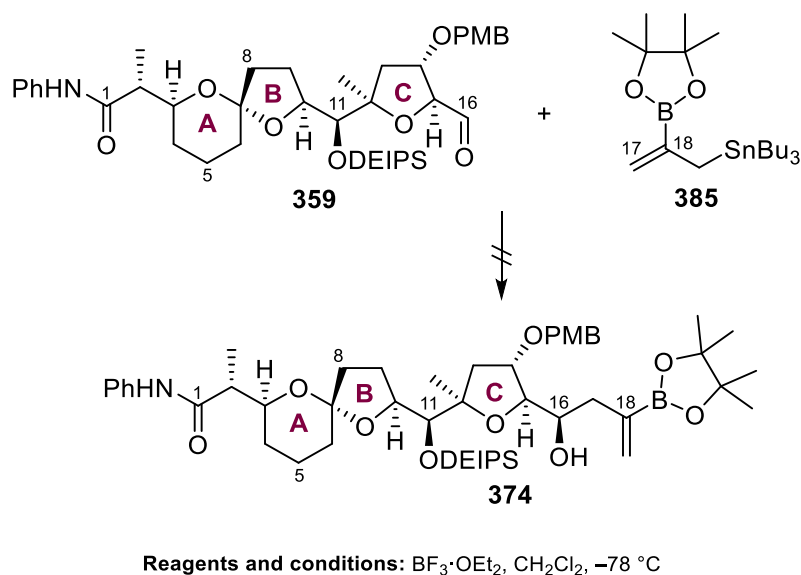


Reagents and conditions: a) XX, [Rh(OH)(1,5-cod)]₂, THF, H₂O, 50 °C

Scheme 4.29. Attempted Hayashi–Miyaura 1,4-addition using borylstannane 385

A Keck allylation was then attempted between aldehyde **359** and borylstannane **385** using similar conditions to those of Evans and of the Sakurai allylations described in earlier sections

(Scheme 4.26). TLC reaction monitoring indicated the formation of a single product spot, while ^1H NMR spectra of the crude reaction mixture suggested the formation of a major new alkene-bearing species. Moreover, when the sample was submitted for mass spectrometry, a peak at 887.6 Da was detected, which corresponded to the $[\text{M} + \text{Na}^+]$ peak of the desired product **374**. However, when flash column chromatography was performed on the crude mixture, this alkene-bearing species could not be recovered. Repeating the reaction, but using preparative TLC for product isolation was also unsuccessful.

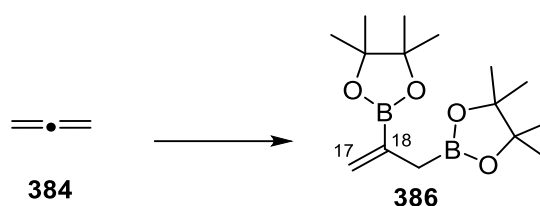


*Scheme 4.30. Attempted Keck allylation between **359** and **385***

Because no product could be recovered, the earlier contradictory results suggesting product formation were initially dismissed as experimental artefacts inherent to the techniques of TLC analysis, mass spectrometry, and interpreting ^1H NMR spectra of crude samples at sub-millimolar quantities. However, subsequent allylation reaction experiments later suggested that the inability to isolate homoallylic alcohol **374** was not due to reaction failure but product instability. These experiments will be discussed more fully in the subsequent section.

4.7 Allylboration of aldehyde 359

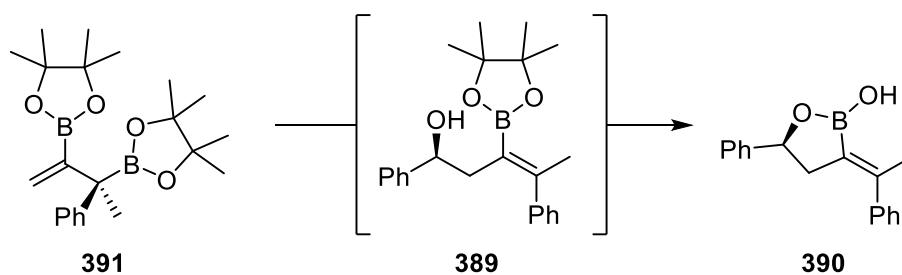
Because of the failures of the allyl stannane and allyl silane reagents, yet another allylating reagent was sought. In 2013, Morken and co-workers disclosed a report describing various enantioselective allyl–allyl cross-couplings using borylated allylboronate **386**, which they prepared directly from propadiene *via* a platinum-catalysed diboration.⁶⁴ This synthesis was repeated successfully to give allylboronate **386** in 78% yield.



Reagents and conditions: Pt(PPh₃)₄, (B(pin))₂, PhMe, -78 °C to 80 °C, 16 h, 78%

Scheme 4.31. Diborylation of propadiene to prepare 386

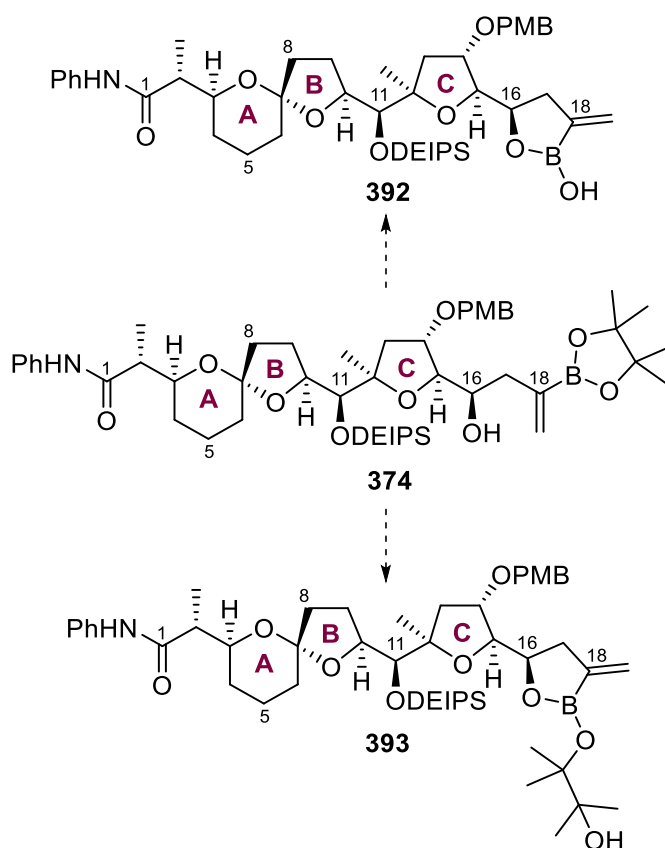
Before reaction with precious ABC aldehyde **359**, the allylation reagent was first tested on simpler aldehydes. Additionally, a literature search was conducted to find out what reaction conditions (e.g., choice of Lewis acid and reaction temperature) were suitable for allylboration. A 2014 report by Aggarwal and co-workers revealed that, unlike the Sakurai and Keck allylations, allylboration reactions could be conducted without aid of a Lewis acid.⁶⁵ An even more surprising discovery from the report was the finding that 1,3-hydroxyborylated compounds such as homoallylic alcohol **389** were not stable, as shown by an example in which boracyclic hemiester **390** was instead isolated after allylboration between 1,2-bisborylated partner **391** and benzaldehyde (Scheme 4.32). Although the Aggarwal conditions involved a strongly basic NaOH quench which could have induced this degradation into the boracyclic hemiester, it was conceivable that such a process could also occur without aid of a strong base, either in the reaction mixture or during the work-up and product isolation.



Reagents and conditions: PhCHO, THF, $-78\text{ }^{\circ}\text{C}$ to rt, 16 h; then NaOH, rt, 1 h, 95%

Scheme 4.32. Allylboration reported by Aggarwal⁶⁵

Boracyclic hemiester **390** was isolated in excellent yield and could be carried through further steps; nevertheless, the degradation from **389** to **390** revealed the possibility that ABC homoallylic alcohol **374** could also either partially or fully degrade into the corresponding boracyclic hemiester **392** or even to pinacol-bearing species **393** (Scheme 4.33).

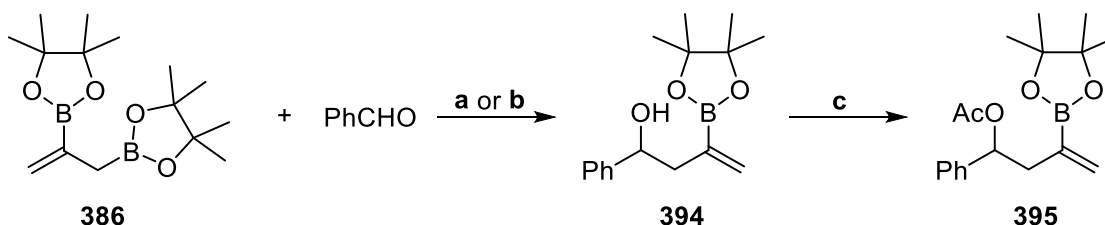


*Scheme 4.33. Possible degradation pathways of homoallylic alcohol **374***

This speciation could complicate analysis, frustrate product isolation efforts especially at small scales, and be detrimental to the subsequent Hayashi–Miyaura 1,4-addition reaction, because

it was not known whether **392** or **393** were competent nucleophilic partners in the coupling reaction.

Fortunately, other workers have addressed this tendency of 1,3-hydroxyborylated compounds to degrade. More recently in 2019, Murakami, Miura, and co-workers reported that this degradation may be prevented by acetylating the free hydroxyl group of the allylboration products.⁶⁶ Although this acetylation had to be performed as a separate step after the allylboration, flash column chromatography was *not* conducted immediately following allylboration as this could induce the degradation. This allylboration–acetylation strategy was tested out on a simple model system involving allylboronate **386** and benzaldehyde, which were first reacted at room temperature without a Lewis acid (condition **a**) to give homoallylic alcohol **394**, which was carried crude over to an acetylation reaction to give desired acetate **395** in 33% yield over two steps (Scheme **4.34**). The yield was increased to 78% when the initial allylboration step was conducted using $\text{BF}_3 \cdot \text{OEt}_2$ at -78°C (condition **b**) instead.

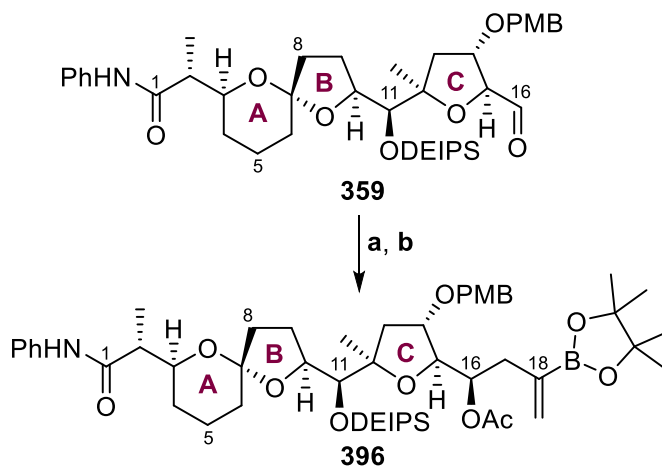


Reagents and conditions: a) CH_2Cl_2 , rt, 22 h
b) $\text{BF}_3 \cdot \text{OEt}_2$, CH_2Cl_2 , -78°C , 2 h
c) Ac_2O , DMAP, pyridine, THF, 50°C , 16 h, 33% (with **a**) or 78% (with **b**) over two steps

Scheme 4.34. Allylboration–acetylation strategy on benzaldehyde

These improved allylboration–acetylation conditions were then applied to ABC aldehyde **359**, which gave acetate **396** in 57% yield over two steps as a single diastereomer; the stereochemistry at C16 was assigned by analogy with compounds **367** (Scheme **4.18**) and **31** (Scheme **4.26**). In contrast, no homoallylic alcohol product could be isolated from a control

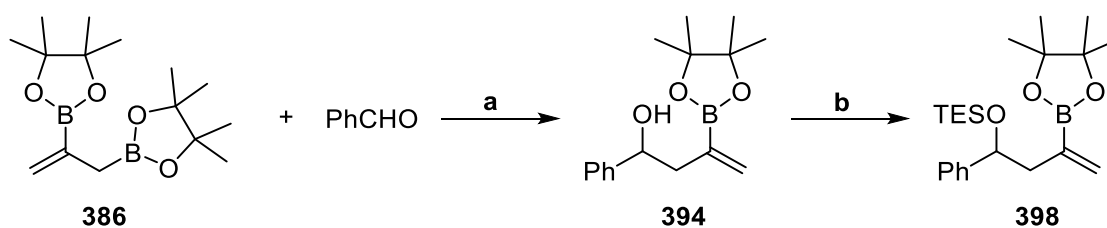
experiment that omitted the second acetylation step, providing additional evidence that the free alcohol intermediate **374** was unstable to column chromatography.



Reagents and conditions: a) **386**, $\text{BF}_3 \cdot \text{OEt}_2$, CH_2Cl_2 , -78°C , 1.5 h
b) Ac_2O , DMAP, pyridine, THF, 50°C , 3 h, 57% over two steps, >95:1 d.r.

Scheme 4.35. Allylboration–acetylation strategy on aldehyde 359

Although the result shown in Scheme 4.35 was encouraging in that it demonstrated that 1,3-hydroxyborylated compound derivatives may be prepared in good yields using the real ABC ring system, the acetate at the newly generated hydroxyl group at C16 was not an appropriate moiety for the PTX-4 synthesis protecting group strategy – a TES group was the preferred protecting group. Thus, the analogous allylboration–silylation was performed on benzaldehyde, giving TES ether **398** in 53% yield over two steps (Scheme 4.36).

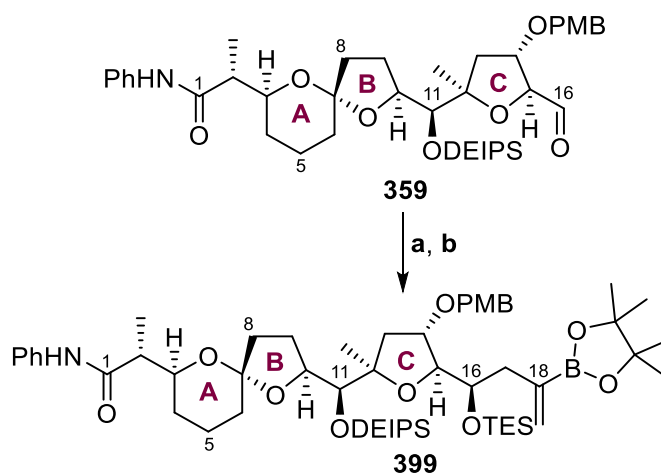


Reagents and conditions: a) $\text{BF}_3 \cdot \text{OEt}_2$, CH_2Cl_2 , -78°C , 2 h
b) TESCl, imidazole, DMAP, CH_2Cl_2 , 0°C to rt, 13 h, 53% over two steps

Scheme 4.36. Allylboration–silylation strategy on benzaldehyde

Performing the reaction using these conditions on ABC aldehyde **359** successfully gave desired product **399**, albeit in only 19% yield over two steps (Scheme 4.37); as with acetate **396**, the

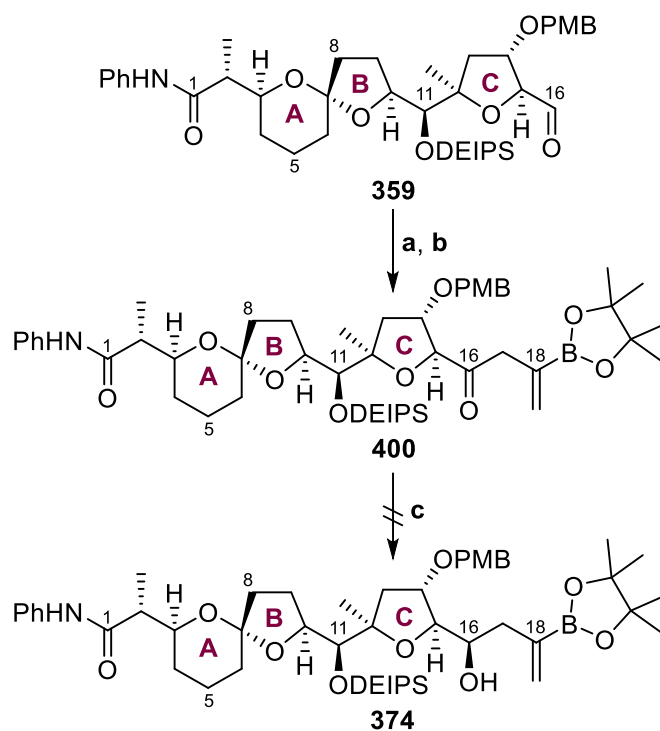
major diastereomer of **399** was tentatively assigned the (*R*) configuration by analogy with compounds **367** (Scheme 4.18) and **31** (Scheme 4.26). Besides the low yield, another concern was the diastereoselectivity, which was variable and often poor across different reaction runs; this was despite the fact that acetate **396** had been isolated as a single diastereomer despite sharing the same diastereoselectivity-determining step (Scheme 4.35). A possible explanation for these discrepancies in diastereoselectivity was that a partial kinetic resolution had occurred during the TES protection, in which the minor homoallylic alcohol diastereomer was preferentially silylated.



Reagents and conditions: a) **386**, $\text{BF}_3 \cdot \text{OEt}_2$, CH_2Cl_2 , -78°C , 1.5 h
 b) TESCl, imidazole, DMAP, CH_2Cl_2 , 0°C to rt, 15 min, 19% over two steps, 2:1 d.r.

Scheme 4.37. Allylboration–acetylation strategy on aldehyde 359

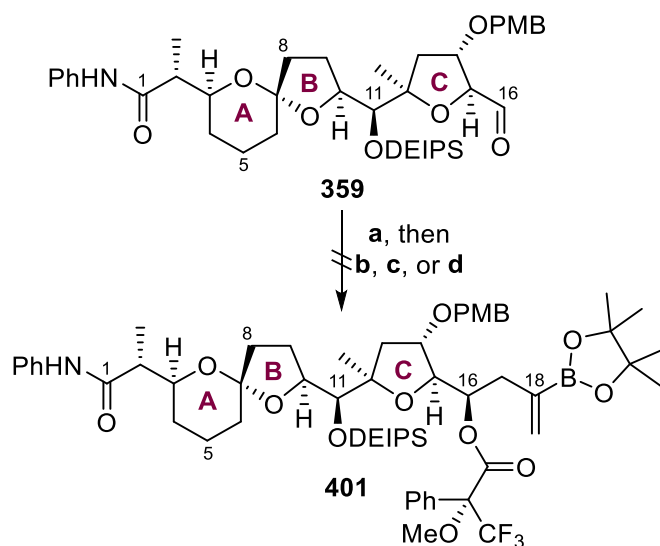
A strategy to improve the diastereoselectivity that involved oxidising the diastereomeric mixture of homoallylic alcohol **374** to ketone **400** and then diastereoselectively reducing it back down was briefly pursued before being abandoned, because of the low-yielding oxidation step and the failed reduction step (Scheme 4.38).



Reagents and conditions: a) **386**, $\text{BF}_3 \cdot \text{OEt}_2$, CH_2Cl_2 , -78°C , 1.5 h
 b) PCC, 3 Å MS, CH_2Cl_2 , rt, 4.5 h, **22%** over two steps
 c) NaBH_4 , MeOH, rt

Scheme 4.38. Oxidation–reduction strategy to obtain diastereopure compound

Moreover, the identity of the major diastereomer could not be conclusively determined. From model studies, it was assumed that polar Felkin–Anh selectivity was operative in the real system, as described in section 4.5.1 (Scheme 4.18). However, efforts to ascertain this through Mosher’s ester analysis failed due to the inability to prepare the ester at the C16 hydroxyl group, despite the screening of various standard esterification conditions (Scheme 4.39). It was suspected that the recalcitrance of the substrate to these otherwise robust conditions was due to the steric bulk around the secondary alcohol at C16.



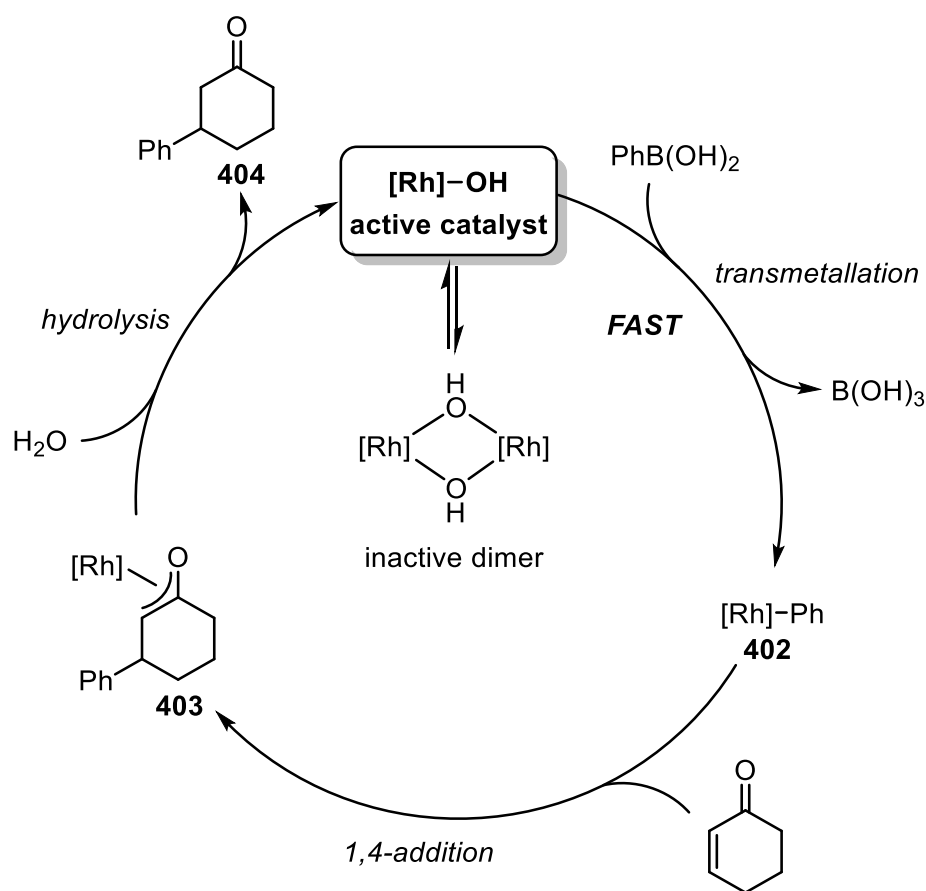
Reagents and conditions: a) **386**, $\text{BF}_3 \cdot \text{OEt}_2$, CH_2Cl_2 , -78°C , 1.5 h
 b) (*R*)-Mosher's acid, DIC, DMAP, CH_2Cl_2 , rt
 c) (*R*)-Mosher's acid, DCC, DMAP, CH_2Cl_2 , rt
 d) (*S*)-Mosher's acid chloride, pyridine, CH_2Cl_2 , rt

Scheme 4.39. Attempted Mosher's ester synthesis

4.8 Hayashi–Miyaura 1,4-addition reaction

Despite the inability to conclusively establish the stereochemical configuration at the C16 stereocentre in allylation product **374** and its derivatives, it was decided to proceed with the Hayashi–Miyaura 1,4-addition reaction. Among other 1,4-additions of organometallic reagents to electron-deficient alkenes, the Hayashi–Miyaura 1,4-addition reaction stands out because of its functional group tolerance, its mild conditions, and its insensitivity to air and water.⁶⁷ Using $\text{PhB}(\text{OH})_2$ and cyclohexanone as example substrates, the mechanism is thought to proceed *via* the pathway shown in Scheme **4.40**.⁶⁸ First, inactive $[\text{Rh}(\text{cod})\text{OH}]_2$ dimer converts to its more reactive monomer, which then transmetalates with $\text{PhB}(\text{OH})_2$ to form the arylrhodium species **402** that undergoes 1,4-addition to cyclohexanone to form Rh enolate **403**. Hydrolysis of Rh enolate **403** gives the product (**404**) and regenerates the active $[\text{Rh}]\text{--OH}$ catalyst.

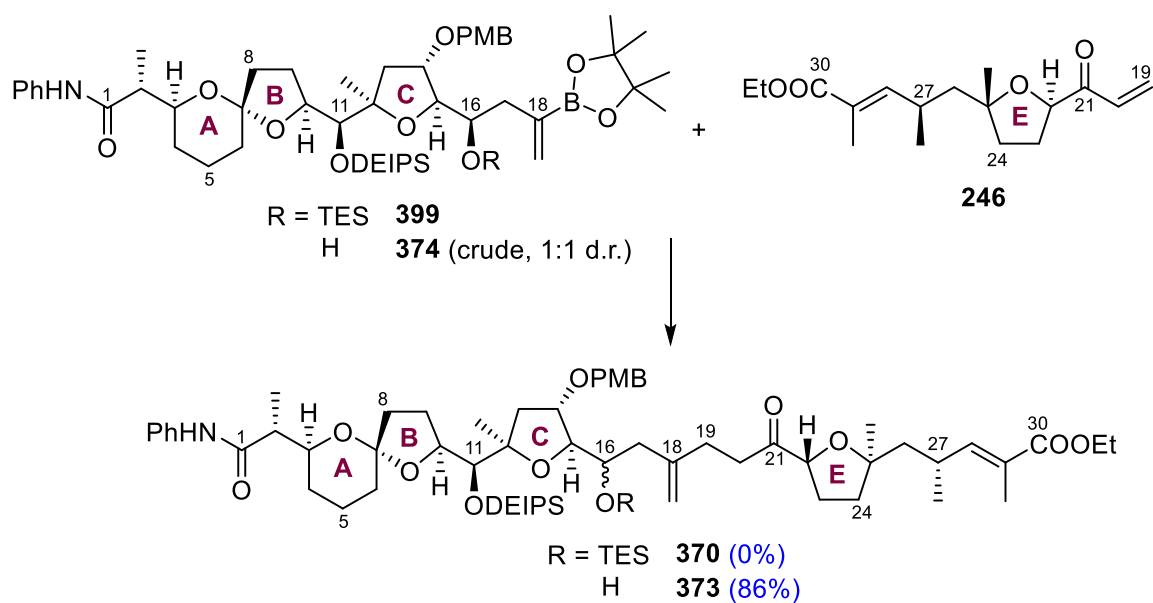
Extensive model and optimisation studies of this key step were conducted by Dr Melodie Richardson, who demonstrated that, among other variables, choice of Rh catalyst was crucial for reaction success. $[\text{Rh}(\text{cod})\text{OH}]_2$ was the superior catalyst because it can be directly converted to the active $[\text{Rh}]\text{-OH}$ monomer to facilitate the difficult transmetallation step. Although other Rh catalysts such as $\text{Rh}(\text{acac})(\text{CO})_2$ could be hydrolysed *in situ* to generate the catalytically active $[\text{Rh}]\text{-OH}$ monomer, the released ligand (i.e., protonated acac) could readily react again with the $[\text{Rh}]\text{-OH}$ monomer to convert it into a less reactive form.⁶⁹



Scheme 4.40. Catalytic cycle of Hayashi-Miyaura 1,4-addition reaction

The optimised Hayashi-Miyaura 1,4-addition reaction conditions were applied to the real system, which involved treatment of vinyl boronic ester **399** and E fragment **246** with $[\text{Rh}(\text{cod})\text{OH}]_2$ in THF/water at 50 °C (Scheme 4.41). No product was obtained. However, when the reaction was repeated using vinyl boronic ester **374** instead (which was obtained as a crude 1:1 diastereomic mixture directly from the allylboration reaction without the TES

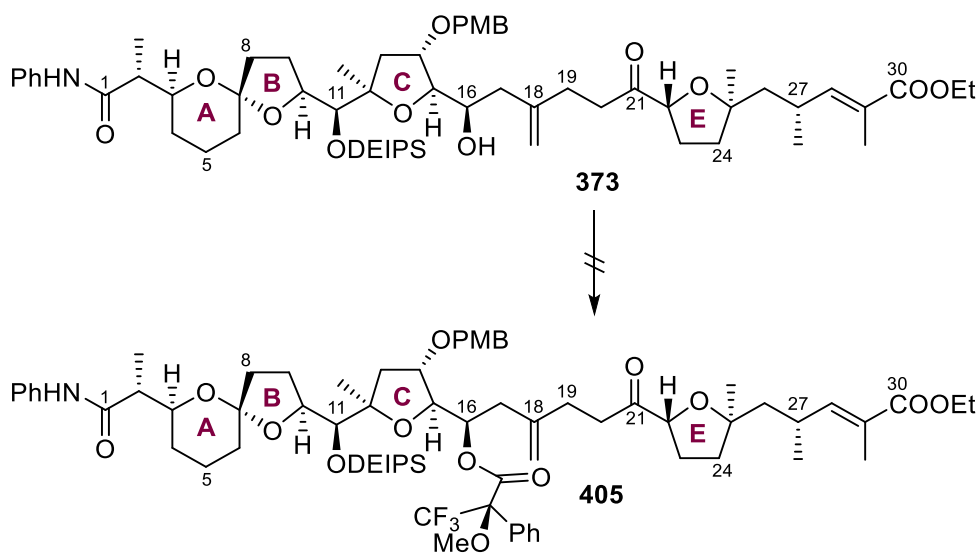
protection step; see Scheme 4.37), the reaction gave ABCE fragment **373** as a 1:1 diastereomic mixture in 86% yield, with respect to the enone partner as the limiting reagent (Scheme 4.41). Besides the difficulty of coupling two large fragments, the high yield was also impressive because crude boronic ester **374** was used for the reaction (because it was unstable to column chromatography and could not be purified). An alternate run that used diastereomically enriched vinyl boronic ester **374** gave ABCE fragment **373** in 35% yield and in 3:1 d.r.



Reagents and conditions: [Rh(cod)OH]₂, THF, H₂O, 50 °C

Scheme 4.41. Hayashi–Miyaura 1,4-addition reaction on real system

Performing a Mosher's ester analysis to ascertain the stereochemical assignment at C16 was once more attempted on ABCE alcohol **373** but, like alcohol **374**, it was inert to these esterification conditions (Scheme 4.42).

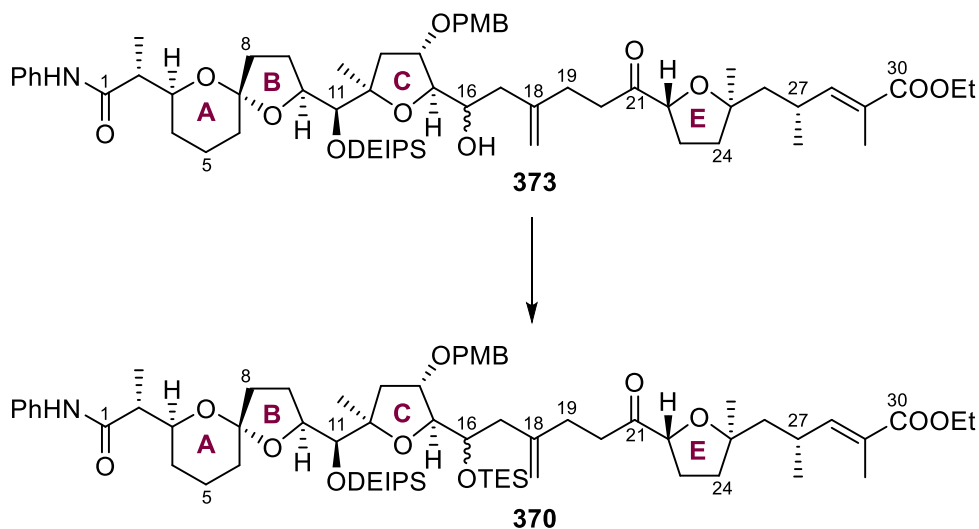


Reagents and conditions: (S)-Moshier's acid chloride, DMAP, pyridine, CH₂Cl₂, rt

Scheme 4.42. Attempted Moshier's ester synthesis

4.9 Dihydroxylation–ketalisation reaction

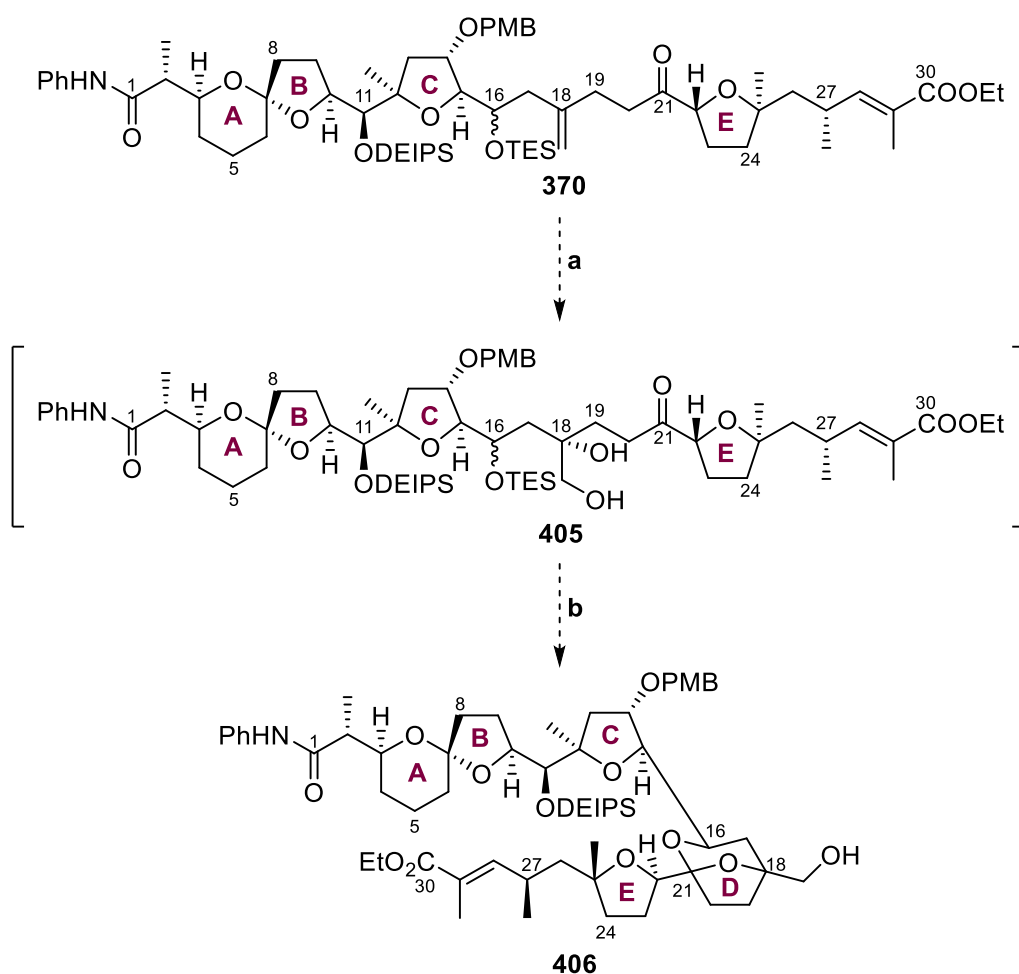
A TES protection was also attempted on ABCE alcohol **373**, which gave silyl ether **370** in 83% yield. Unfortunately, due to the variable diastereoselectivity of the allylboration step, the batch of alcohol **373** used for the silylation step was a 1:1 mixture of diastereomers, which in turn gave silyl ether **370** also as a 1:1 inseparable mixture of diastereomers (Scheme 4.43).



Reagents and conditions: TESOTf, DMAP, imidazole, CH₂Cl₂, rt, 15 min, 83%

Scheme 4.43. TES protection of **373**

That silyl ether **370** could not be obtained as a single diastereomer was especially problematic for characterisation purposes and for issues relating to reactivity, because the subsequent step was the key diastereoselective dihydroxylation–ketalisation reaction which depended on the stereochemistry at C16. Because of time constraints and the limited availability of advanced intermediate, the three-step allylboration–1,4-addition–silylation sequence could not be repeated to obtain a diastereopure sample of **370**.



Reagents and conditions: a) $K_3Fe(CN)_6$, $(DHQD)_2PHAL$, $K_2OsO_2(OH)_4$, K_2CO_3 , $tBuOH$, H_2O , $0\text{ }^\circ C$
 b) PPTS, $MeOH$, rt

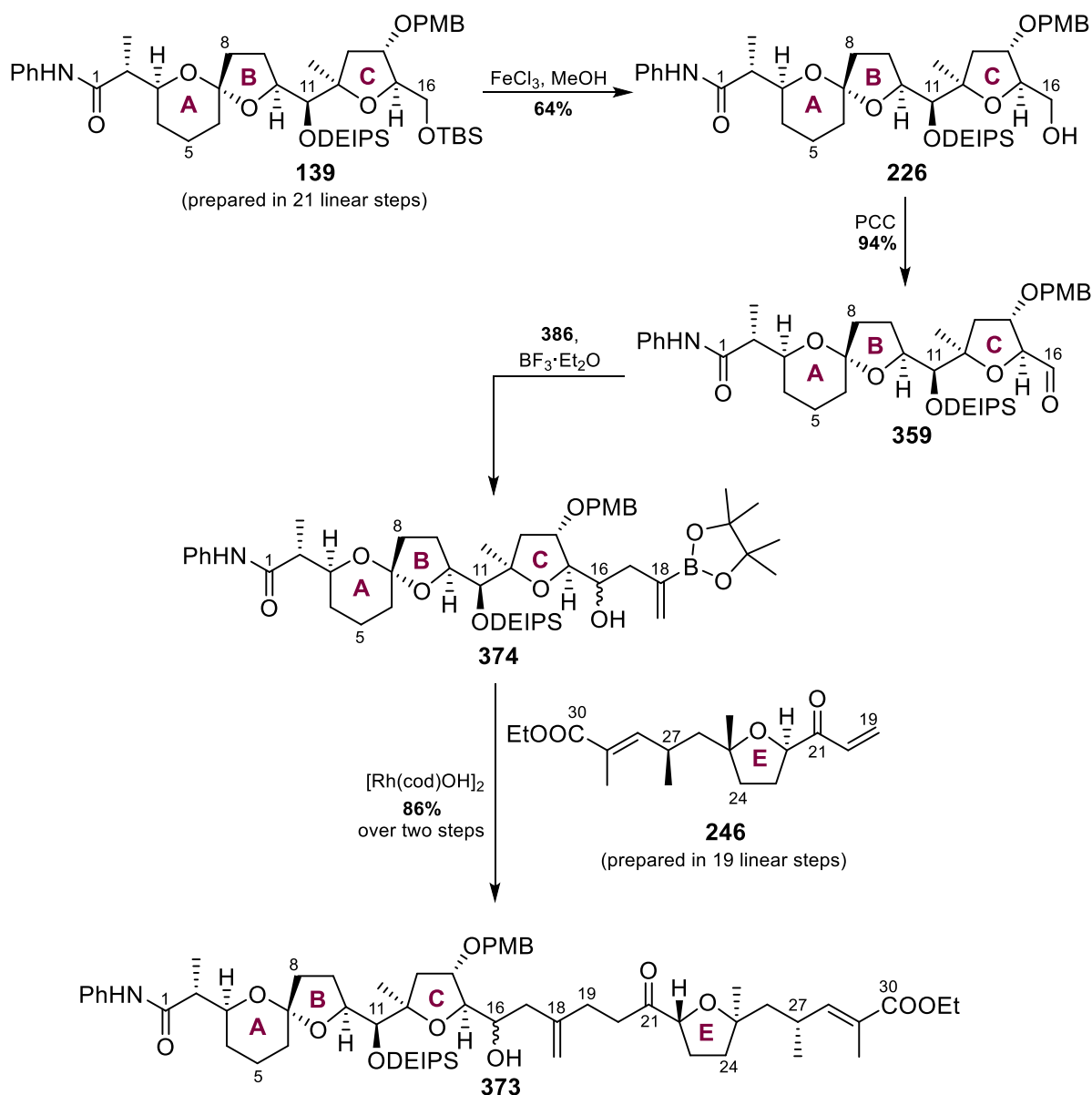
Scheme 4.44. Attempted dihydroxylation–ketalisation sequence

Nevertheless, the mixture of **373** diastereomers were carried over to the dihydroxylation–ketalisation step (Scheme 4.44). When a sample of the crude mixture was submitted for mass spectrometry, two strong peaks at 1048.7 Da and 1170.6 Da were detected, which correspond

to the $[M + H^+]$ and $[M + Na^+]$ peaks of bicyclic ketal **406** respectively. However, no product could be isolated due to the number of species present in the complex mixture and the small scale of the reaction. Moreover, the mass spectrum data could not be taken as evidence of the formation of desired bicyclic ketal **406** even in trace quantities, because the data cannot distinguish between diastereomers of the compound.

4.10 Conclusion

4.10.1 Summary of synthesis

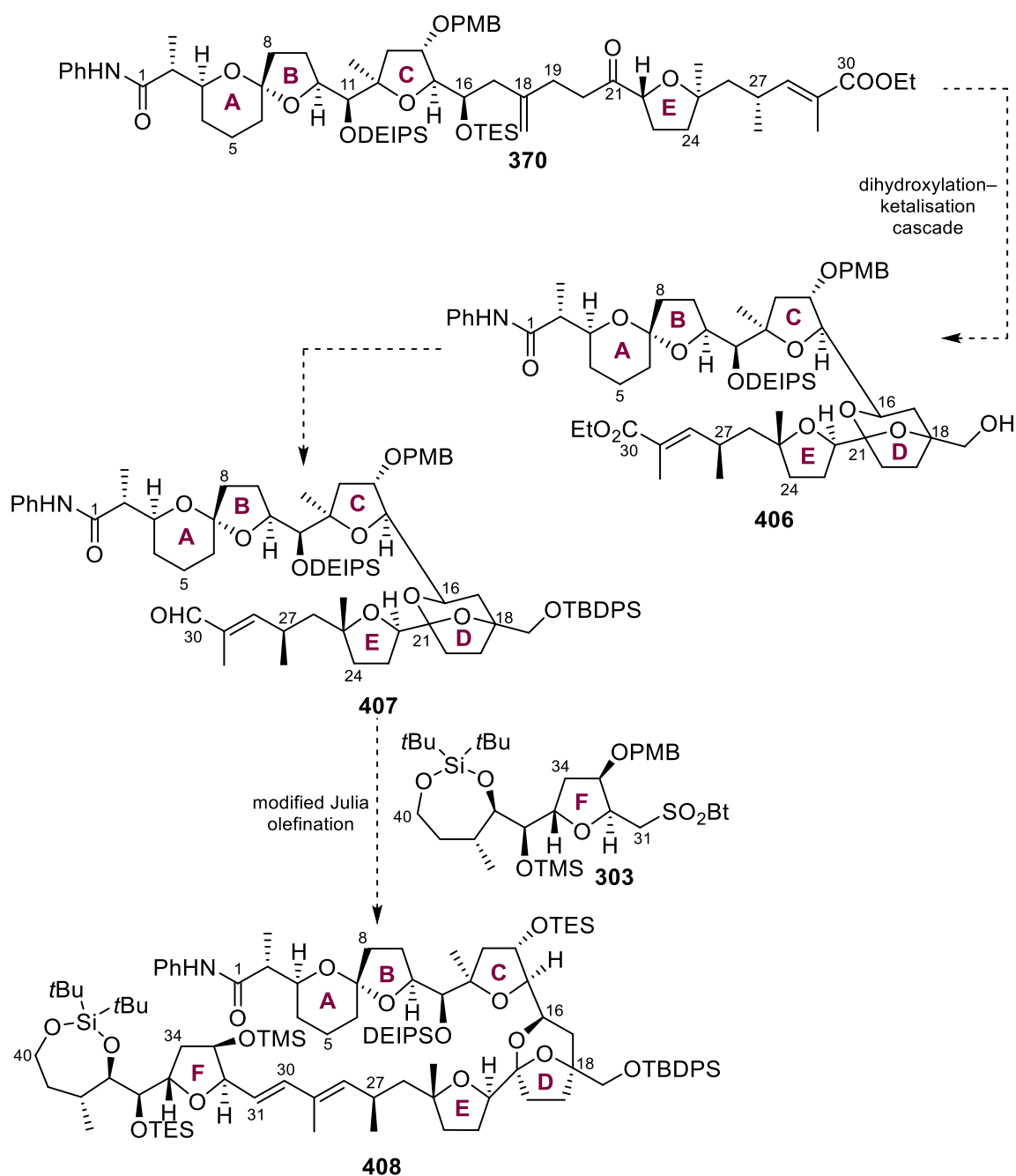


Scheme 4.45. Summary of ABCE ring system synthesis

As shown in Scheme **4.45**, ABC fragment **139** was prepared in 21 linear steps and E fragment **246** was prepared in 19 linear steps. After extensive optimisation studies, ABC fragment **139** was elaborated to vinyl boronic ester **374** over three steps, and then successfully united with E fragment **246** through a rhodium-catalysed Hayashi–Miyaura 1,4-addition reaction. The next key step, the dihydroxylation–ketalisation cascade, was attempted, but no desired product could be isolated.

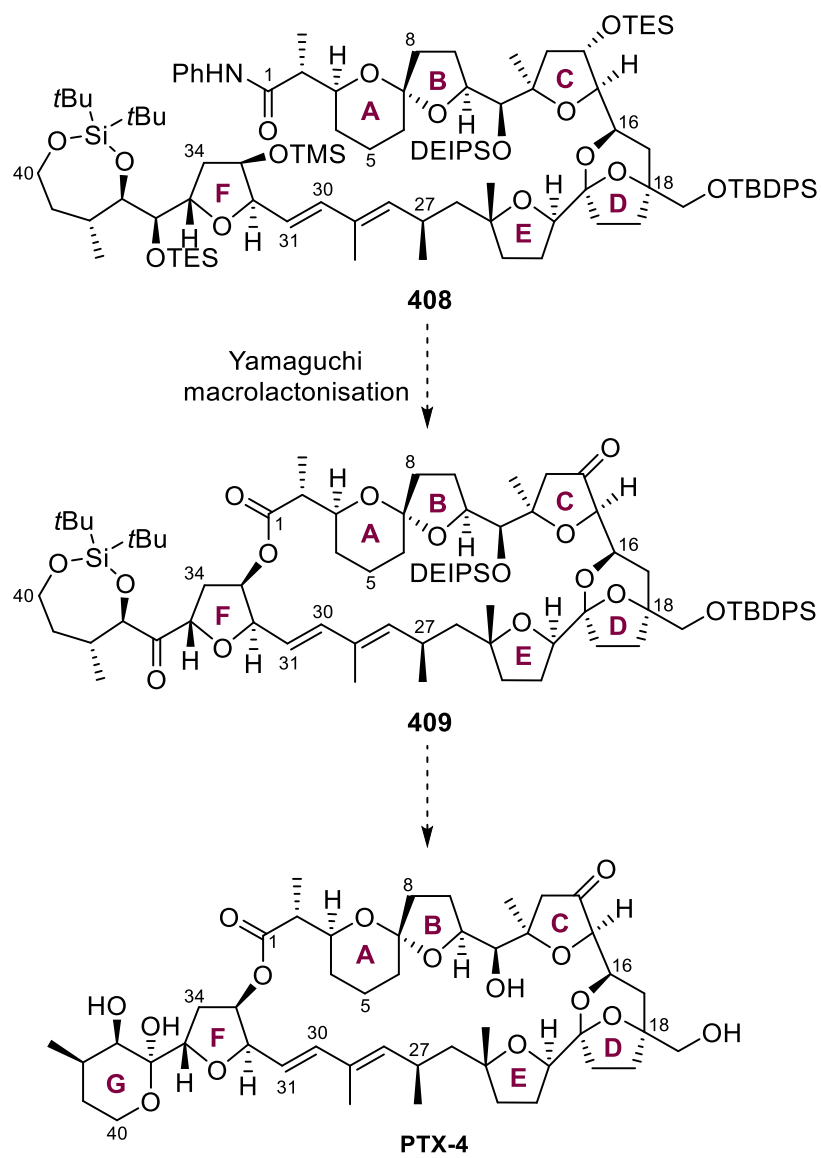
4.10.2 Future work

An overview of the synthetic strategy to finish the total synthesis in PTX-4 is shown in Schemes **4.46** and **4.47**. Performing a dihydroxylation–ketalisation sequence on ABCE alkene **373** is planned, which would give bicyclic ketal **406**. Thereafter, conversion of bicyclic ketal **406** to aldehyde **407** followed by a modified Julia olefination with F fragment **303** would form advanced intermediate **408**, which bears the full carbon skeleton of the natural product.



Scheme 4.46. Planned elaboration of **370** into advanced intermediate **408**

Macrolactonisation of **408** would give macrocycle **409** which, upon global deprotection, would give PTX-4, thus concluding the total synthesis (Scheme **4.47**).



Scheme 4.47. Planned completion of total synthesis of PTX-4

CHAPTER 5

Experimental

5.1 Experimental

5.1.1 Experimental techniques

General: All non-aqueous reactions were carried out under an argon atmosphere in flame-dried glassware unless otherwise stated. All reactions were followed by analytical thin layer chromatography (TLC) and procedure times represent reaction completion as judged accordingly. Reaction temperatures (unless otherwise stated) represent bath temperatures.

Solvents: Anhydrous DMF, benzene, HMPA, DMSO, DMPU, and DMA were used as commercially supplied. CH₂Cl₂, Et₂O, MeCN, MeOH, THF and toluene were purified by filtration through two activated alumina purification columns. In cases where mixtures of solvents were used, the ratios refer to the component volumes. Petrol refers to petroleum ether in the boiling range 30-60 °C.

Reagents: All reagents were used as supplied commercially unless otherwise stated.

Chromatography: Flash column chromatography was carried out using silica gel 40-63 μm unless otherwise stated. Analytical thin layer chromatography (TLC) was performed using aluminium backed pre-coated silica gel 60 F254 plates and visualised under UV radiation at 254 nm and staining with bromocresol green in water, potassium permanganate in water or vanillin in ethanol.

Optical Rotation: Specific rotations (α') were recorded on a Perkin Elmer 341 Polarimeter, with a cell pathlength (l) of 1.0 dm, at the stated temperature (°C) and concentration (c) (measured in units of g/100 mL); specific rotations were converted to optical rotations, $[\alpha]_D$, via the equation: $[\alpha]_D = (100 \cdot \alpha') / (l \cdot c)$.

Melting Points: Melting points were obtained using a Leica Galen III heated-stage microscope and are uncorrected.

Mass Spectrometry: Low resolution mass spectra were recorded on an Agilent 6120 Quadrupole spectrometer equipped with an Agilent 1260 Infinity LC pump, with a flow rate of 0.2 mL/min using H₂O/MeOH/HCO₂H (10:89.9:0.1) as eluent. The mass reported is that containing the most abundant isotopes under electrospray ionisation (ESI). High resolution mass spectra (HRMS) were recorded by the staff of the Chemistry Research Laboratory mass-spec facilities. For the ESI accurate mass service, analyses were performed using a Thermo Exactive mass spectrometer equipped with Waters Acquity liquid chromatography system using the same flow rate and eluent as above. Instrument control and data processing were performed using Thermo Xcalibur Software. The mass spectrometer was operated using the heated electrospray (HESI-II) probe and resolution was set to 50,000 FWHM. Electrospray source conditions were adjusted to maximise sensitivity. For the electron ionisation (EI) and Chemical ionisation (CI) accurate mass service, analyses were performed on an Agilent 7200 quadrupole time of flight (Q-ToF) instrument equipped with a direct insertion probe supplied by Scientific Instrument Manufacturer (SIM) GmbH. Instrument control and data processing were performed using Agilent MassHunter software. Source conditions for both EI and CI were adjusted to maximise sensitivity, the reagent gas used in CI was ammonia. Both systems were calibrated on the day of the analysis and its mass accuracy with external calibration (as used for these experiments) is better than 5 ppm for 24 h following calibration. The mass reported is that containing the most abundant isotopes, with each value to 5 decimal places and within 5 ppm of the calculated mass. Mass to charge ratios (m/z) are reported in Daltons.

NMR Spectroscopy: Proton (¹H) and carbon (¹³C) spectra were recorded on Bruker AVC-500 (AVII 500 with He cryoprobe, 500/126 MHz), Bruker AVF-400 (AVIIIHD 400 nanobay, 400/101/377 MHz) or Bruker DPX-200 (200 MHz) spectrometers in deuterated solvents. ¹³C spectra were recorded with broadband decoupling. Chemical shifts (δ_H and δ_C) are reported in parts per million (ppm) to the nearest 0.01 ppm for ¹H NMR or 0.1 ppm for ¹³C NMR. ¹H and

¹³C NMR spectra were referenced to the solvent residual peak (CDCl₃, δ 7.26 and 77.00 ppm respectively).^{>70,71} Peak assignments were made on the basis of chemical shifts, integrations and coupling constants, using COSY, HSQC, HMBC, DEPT135, DEPTQ, NOESY and TOCSY experiments where appropriate. Multiplets are described as singlet (s), doublet (d), double doublet (dd), triplet (t), quartet (q), double triplet (dt), doublet of doublet of doublets (ddd), doublet of doublet of triplets (ddt), quadruple doublet (qd), multiplet (m), broad (br.) and apparent (app.). Coupling constants (*J*) are rounded to the nearest 0.1 Hz.</sup>

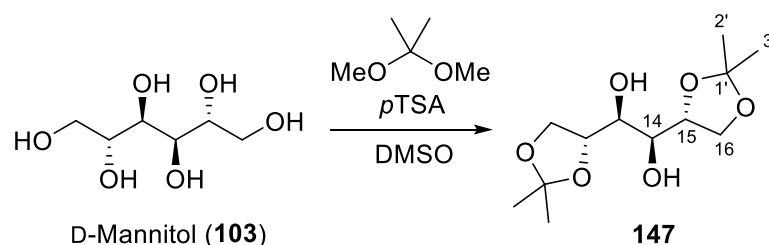
IR Spectroscopy: Infra-red spectra were recorded on a Bruker Tensor 27 FT-IR spectrometer.

Absorption maxima (ν_{\max}) are reported in wavenumbers (cm⁻¹).

5.1.2 Experimental procedures for ABC fragment

*Note: Systematic names of the compounds were generated by ChemDraw according to the guidelines specified by the International Union of Pure and Applied Chemistry (IUPAC). However, the numbering system as represented for **103–400**, en route to the synthesis of the various fragments of PTX-4, is in accordance with the natural product numbering system for PTX-4 and may not reflect that in the IUPAC systematic name.*

(1*S*,2*S*)-1,2-bis((*R*)-2,2-Dimethyl-1,3-dioxolan-4-yl)ethane-1,2-diol (**147**)



2,2-Dimethoxypropane (160 mL, 1.31 mol) was added to a solution of D-mannitol (100 g, 549 mmol), *p*TSA·H₂O (550 mg, 2.89 mmol), and DMSO (164 mL). The reaction mixture was stirred for 16 h at room temperature. After which, it was quenched with a solution of NaHCO₃ (sat., 250 mL), and then extracted with EtOAc (5 × 350 mL). The organic layers were combined and concentrated to ca. 300 mL. The organic layer was then washed with deionised water (4 × 100 mL), dried (MgSO₄), and then filtered. The solution was concentrated to ca. 200 mL and then transferred to a 500-mL conical flask. Hot EtOAc (80 mL) followed by hot pentane (150 mL) was added to the crude product. The resulting solution was slowly cooled to room temperature and placed in a –18 °C freezer overnight. The resulting white crystals were filtered, washed with 75:25 Pentane:Et₂O solution, and then dried under vacuum to give white crystals of acetonide **147** (77.1 g, 54%).

$R_f = 0.4$ (100% EtOAc);

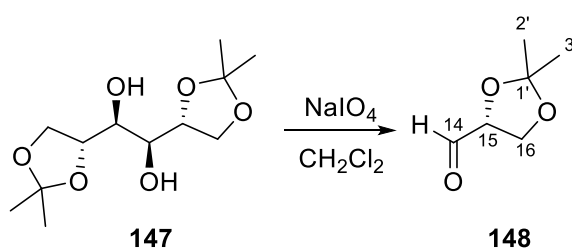
$[\alpha]_D^{20} +8.0$ ($c = 1.35$, CHCl_3);

$^1\text{H NMR}$ (400 MHz, DMSO-d_6) δ_H 4.20 (2H, q, $J = 6.5$ Hz, $\text{C}(15)\text{H} \times 2$), 4.14–4.11 (2H, dd, $J = 8.5$, 6.3 Hz, $\text{C}(16)\text{H}_A\text{H}_B \times 2$), 3.99–3.96 (2H, dd, $J = 8.6$, 5.6 Hz, $\text{C}(16)\text{H}_A\text{H}_B \times 2$), 3.75 (2H, t, $J = 6.2$ Hz, $\text{C}(14)\text{H} \times 2$), 2.56 (2H, s, $\text{OH} \times 2$), 1.42 (6H, s, $\text{CH}_3 \times 2$), 1.36 (6H, s, $\text{CH}_3 \times 2$);

$^{13}\text{C NMR}$ (100 MHz, DMSO-d_6) δ_C 109.4 ($\text{C}1' \times 2$), 76.3 ($\text{C}15 \times 2$), 71.2 ($\text{C}14 \times 2$), 66.7 ($\text{C}16 \times 2$), 26.7 ($\text{CH}_3 \times 2$), 25.2 ($\text{CH}_3 \times 2$);

The spectral data were consistent with those previously reported.³⁸

(*R*)-2,2-Dimethyl-1,3-dioxolane-4-carbaldehyde (**148**)



A solution of NaHCO_3 (sat., 24.0 mL) was added to acetonide **147** (30.0 g, 76.2 mmol) dissolved in CH_2Cl_2 (300 mL). The resulting solution was cooled to 0 °C, and then NaIO_4 (48.9 g, 229 mmol) was added to the stirring solution slowly over 10 min. The solution was stirred at room temperature for 4 h. After which, MgSO_4 (18.0 g) was added to the mixture, with stirring for an additional 20 min. The resulting slurry was filtered through Celite®. The solution was concentrated *in vacuo* to afford aldehyde **148** (29.5 g, 99%) as a colourless oil, which was used directly in the next step without further purification.

$R_f = 0.8$ (80:20 Pentane:EtOAc);

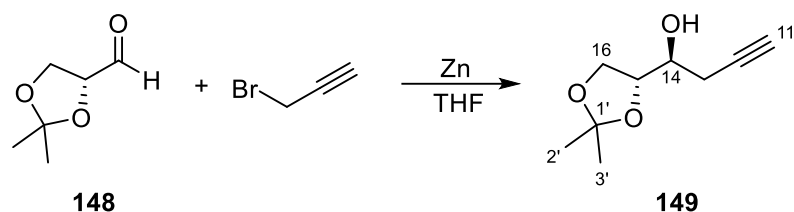
$[\alpha]_D^{25} +63.2$ ($c = 1.27$, CHCl_3 ; lit. +53.8, $c = 2$, CHCl_3);

$^1\text{H NMR}$ (400 MHz, CDCl_3) δ_{H} 9.72 (1H, d, $J = 1.9$ Hz, C(14)H), 4.38 (1H, ddd, $J = 7.4, 4.7, 1.9$ Hz, C(15)H), 4.22–3.98 (2H, m, C(16)H₂), 1.48, (3H, s, CH₃), 1.42 (3H, s, CH₃);

$^{13}\text{C NMR}$ (100 MHz, CDCl_3) δ_{C} 201.9 (C14), 111.2 (C1'), 79.8 (C15), 65.6 (C16), 26.2 (CH₃), 25.1 (CH₃).

The spectral data were consistent with those previously reported.³⁸

(S)-1-((R)-2,2-Dimethyl-1,3-dioxolan-4-yl)but-3-yn-1-ol (148)



Zn¹ (11.5 g, 176 mmol) was ground to a fine powder and added to a two-necked reaction flask with a stirrer and thermometer. THF (37 mL) was added to the two-necked flask, and the suspension was cooled to -10 °C. Propargyl bromide (80% w/v in toluene, 8.09 mL, 107 mmol) was added to the Zn suspension dropwise over 10 min. The reaction mixture was stirred for 30 min at -10 °C and then cooled to -78 °C. Aldehyde **148** (9.92 g, 76.2 mmol) dissolved in THF (12 mL) was added to the reaction mixture *via* cannula. The reaction mixture was stirred for 2 h at -78 °C, warmed to room temperature, and then stirred for 16 h. The reaction mixture was cooled to 0 °C, and then quenched with a solution of NH₄Cl (sat., 60 mL). The mixture was then filtered and the aqueous filtrate was extracted with EtOAc (4 × 125 mL). The organic layers were combined and dried (MgSO₄), filtered, and then concentrated *in vacuo*. Purification by flash column chromatography (SiO₂, 85:15 Pentane:EtOAc, 1% NEt₃) afforded alcohol **149** (7.57 g, 58% over two steps, 4.5:1 d.r.) as a pale yellow oil.

¹ Zn was activated by stirring in 1 M HCl for 1 hour. It was then rinsed five times with water and dried under vacuum at 150 °C for 2 h.

$R_f = 0.6$ (50:50 EtOAc:Pentane);

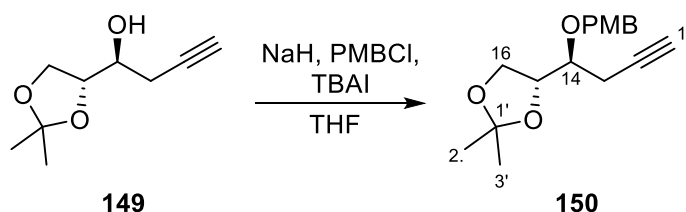
$[\alpha]_D^{20} +3.6$ ($c = 1.17$, CH_2Cl_2);

$^1\text{H NMR}$ (400 MHz, CDCl_3), major diastereomer δ_H 4.11–4.05 (2H, m, C(16) H_AH_B , C(15) H), 4.08–3.94 (1H, m, C(16) H_AH_B), 3.90–3.65 (1H, m, C(14) H), 2.53–2.47 (2H, m, C(13) H_2), 2.22 (1H, br. s, OH), 2.07 (1H, t, $J = 2.7$ Hz, C(11) H), 1.41 (3H, s, C(2') H_3), 1.35 (3H, s, C(3') H_3);

$^{13}\text{C NMR}$ (100 MHz, CDCl_3), major diastereomer δ_C 109.4 (C1'), 79.8 (C12), 77.2 (C15), 71.2 (C11), 70.1 (C14), 65.9 (C16), 26.6 (CH_3), 25.1 (CH_3), 23.6 (C13).

The spectral data were consistent with those previously reported.³⁸

(R)-4-((S)-1-((4-Methoxybenzyl)oxy)but-3-yn-1-yl)-2,2-dimethyl-1,3-dioxolane (150)



Alcohol **149** (17.4 g, 102 mmol) was dissolved in THF (194 mL) and then cooled to 0 °C. NaH (60% suspension in mineral oil, 7.36 g, 307 mmol) was then added to the solution gradually over 5 min, and the solution was stirred at 0 °C for 1 hour. Tetrabutylammonium iodide (1.91 g, 5.16 mmol) was added, followed by 4-methoxybenzyl chloride (14.6 mL, 107 mmol). The reaction mixture was then heated at 60 °C with an air condenser for 16 h. The reaction mixture was cooled and then quenched with a solution of NH_4Cl (sat., 85 mL). The layers were allowed to separate, and the aqueous layer was extracted with Et_2O (4 × 350 mL). The organic layers were combined and dried (MgSO_4), filtered, and then concentrated *in vacuo*. Purification by flash column chromatography (SiO_2 , 95:5 to 80:20 Pentane: Et_2O) afforded PMB ether **150** (30.0 g, 87%) as a pale yellow oil.

$R_f = 0.5$ (60:40 Pentane:Et₂O);

$[\alpha]_D^{25} +37.5$ ($c = 1.16$, CH₂Cl₂; lit. $+37.3$, $c = 1.64$, CH₂Cl₂);

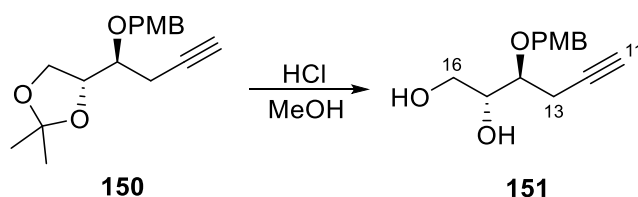
¹H NMR (400 MHz, CDCl₃) δ_H 7.29 (2H, d, $J = 8.6$ Hz, PMB-ArH $\times 2$), 6.88 (2H, d, $J = 8.6$ Hz, PMB-ArH $\times 2$), 4.73 (1H, d, $J = 11.2$ Hz, PMB-CH_AH_B), 4.53 (1H, d, $J = 11.2$ Hz, PMB-CH_AH_B), 4.18 (1H, q, $J = 6.3$ Hz, C(15)H), 4.06 (1H, dd, $J = 8.4, 6.4$ Hz, C(16)H_AH_B), 3.88 (1H, dd, $J = 8.5, 5.4$ Hz, C(16)H_AH_B), 3.81 (3H, s, PMB-OCH₃), 3.55 (1H, dt, $J = 7.1, 4.9$ Hz, C(14)H), 2.66–2.60 (1H, m, C(13)H_AH_B), 2.54–2.48 (1H, m, C(13)H_AH_B), 2.05–2.04 (1H, m, C(11)H), 1.41 (3H, s, CH₃), 1.35 (3H, s, CH₃);

¹³C NMR (100 MHz, CDCl₃) δ_C 159.3 (PMB-C_{Ar}), 130.4 (PMB-C_{Ar}), 129.7 (PMB-C_{Ar} $\times 2$), 113.8 (PMB-C_{Ar} $\times 2$), 109.3 (C1'), 80.6 (C12), 77.2 (C14), 76.5 (C15), 72.0 (PMB-CH₂), 70.4 (C11), 66.7 (C16), 55.2 (PMB-OCH₃), 26.7 (CH₃), 25.3 (CH₃), 21.0 (C13).

The spectral data were consistent with those previously reported.³⁸

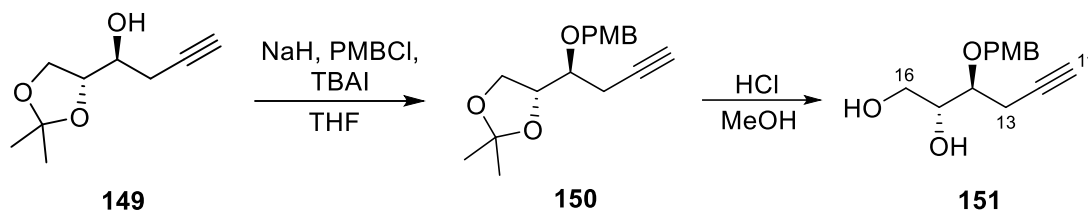
(2R,3S)-3-((4-Methoxybenzyl)oxy)hex-5-yne-1,2-diol (**151**)

Procedure A:



Acetal **150** (29.3 g, 101 mmol) was added to a solution of HCl (1 M, 81.5 mL) and MeOH (907 mL). The reaction mixture was heated to 40 °C and stirred for 20 h. A solution of NaHCO₃ (sat., 140 mL) was gradually added to quench the reaction solution until pH 7 was attained. The solution was then concentrated *in vacuo* to remove the MeOH. An extraction was conducted using EtOAc (4 \times 500 mL). The organic layers were combined, dried (MgSO₄), filtered, and then concentrated *in vacuo*. Purification by flash column chromatography (SiO₂, 95:5 to 80:20 Pentane:Et₂O) afforded diol **151** (20.2 g, 80%) as a pale yellow oil.

Procedure B:



Alcohol **149** (13.9 g, 81.7 mmol, azeotropically distilled thrice with PhMe) was dissolved in dry THF (150 mL) and then cooled to 0 °C. NaH (3.92 g, 57–63% suspension in mineral oil) was then added to the solution gradually over 5 min, and the solution was stirred at 0 °C for 1 hour. Tetrabutylammonium iodide (1.51 g, 4.08 mmol) was added, followed by 4-methoxybenzyl chloride (11.6 mL, 85.8 mmol). The reaction mixture was then heated in an oil bath at 75 °C with an air condenser for 9 h. After reaction completion as judged by TLC analysis, HCl (13.9 mL, 3.0 M) was added to the reaction mixture at room temperature. The reaction mixture was heated to 40 °C and stirred for 24 h.

After which, solid NaHCO₃ was gradually added to quench the reaction solution until pH 7 was attained. An extraction was then conducted using EtOAc (4 × 500 mL); the organic layers were combined, dried (MgSO₄), filtered, and then concentrated. Purification by flash column chromatography (SiO₂, 98:2 to 80:20 Pentane:Acetone) afforded diol **151** (15.1 g, 74% over two steps) as a pale yellow oil.

R_f = 0.5 (60:40 Pentane:Acetone);

[α]_D²⁵ +34.4 (c = 1.10, CH₂Cl₂; lit. +39.5, c = 1.10, CH₂Cl₂);

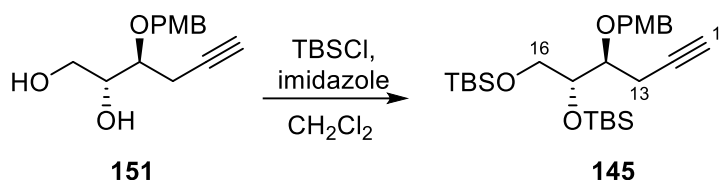
¹H NMR (400 MHz, CDCl₃) δ_H 7.27 (2H, d, J = 8.6 Hz, PMB-ArH × 2), 6.87 (2H, d, J = 8.6 Hz, PMB-ArH × 2), 4.66 (1H, d, J = 11.1 Hz, PMB-CH_AH_B), 4.45 (1H, d, J = 11.1 Hz, PMB-CH_AH_B), 3.78 (3H,

s, PMB-OCH₃), 3.83–3.58 (2H, m, C(16)H₂), 3.62–3.58 (1H, m, C(14)H), 3.57 (1H, dt, *J* = 6.3, 5.2 Hz, C(15)H), 3.42 (1H, br. s, OH), 3.00 (1H, br. s, OH), 2.62–2.45 (2H, m, C(13)H₂), 2.04 (1H, t, *J* = 2.6 Hz, C(11)H);

¹³C NMR (100 MHz, CDCl₃) δ_c 159.4 (PMB-C_{Ar}), 129.8 (PMB-C_{Ar}), 129.7 (PMB-C_{Ar} × 2), 113.9 (PMB-C_{Ar} × 2), 80.9 (C12), 77.5 (C14), 72.2 (C15), 72.0 (PMB-CH₂), 70.5 (C11), 63.4 (C16), 55.3 (PMB-OCH₃), 20.4 (C13).

The spectral data were consistent with those previously reported.³⁸

(*R*)-5-((*S*)-1-((4-Methoxybenzyl)oxy)but-3-yn-1-yl)-2,2,3,3,8,8,9,9-octamethyl-4,7-dioxa-3,8-disiladecane (145)



Diol **151** (21.2 g, 84.7 mmol) was dissolved in CH₂Cl₂ (170 mL) and cooled to 0 °C. Imidazole (28.9 g, 424 mmol) and TBSCl (38.3 g, 254 mmol) were added to the solution with vigorous stirring. The solution was then warmed to room temperature and stirred for 18 h. The reaction mixture was quenched with water (160 mL). After which, the layers were allowed to separate and the aqueous layer was extracted with CH₂Cl₂ (4 × 160 mL). The organic layers were combined, dried (MgSO₄), filtered, and then concentrated *in vacuo*. Purification by flash column chromatography (SiO₂, 99:1 Pentane:Et₂O, then 99:1 Pentane:EtOAc) afforded **145** (36.5 g, 90%) as a colourless oil.

R_f = 0.7 (80:20 Pentane:Et₂O);

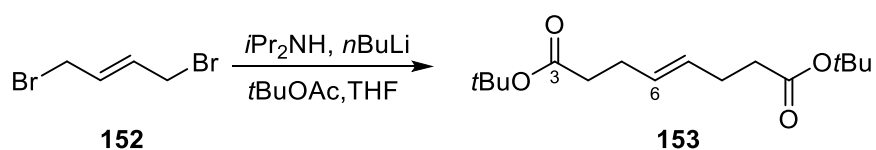
[α]²⁵_D −5.8 (*c* = 1.18, CH₂Cl₂);

¹H NMR (400 MHz, CDCl₃), δ_H 7.29 (2H, d, *J* = 8.6 Hz, PMB-ArH × 2), 6.86 (2H, d, *J* = 8.6 Hz, PMB-ArH × 2), 4.63 (1H, d, *J* = 11.1 Hz, PMB-H_AH_B), 4.55 (1H, d, *J* = 11.2 Hz, PMB-H_AH_B), 3.83 (1H, dd, *J* = 9.6, 4.7 Hz, C15(H)), 3.80 (3H, s, PMB-CH₃), 3.74–3.52 (3H, m, C(16)H₂, C(14)H), 2.61–2.41 (2H, m, C(13)H₂), 1.98 (1H, t, *J* = 2.7 Hz, C(11)H), 0.90 (9H, s, TBS-C(CH₃)₃), 0.88 (9H, s, TBS-C(CH₃)₃), 0.10–0.01 (12H, m, TBS-Si(CH₃)₂ × 2);

¹³C NMR (100 MHz, CDCl₃) δ_C 159.1 (PMB-C_{Ar}), 130.6 (PMB-C_{Ar}), 129.5 (PMB-C_{Ar} × 2), 113.7 (PMB-C_{Ar} × 2), 82.1 (C12), 77.8 (C14), 74.2 (C15), 72.2 (PMB-CH₂), 69.6 (C11), 64.4 (C16), 55.3 (PMB-OCH₃), 26.0 (TBS-C(CH₃)₃), 25.9 (TBS-C(CH₃)₃), 20.4 (C13), 18.3 (TBS-C(CH₃)₃), 18.1 (TBS-C(CH₃)₃), -4.3 (TBS-SiCH₃), -4.5 (TBS-SiCH₃), -5.4 (TBS-SiCH₃ × 2).

The spectral data were consistent with those previously reported.³⁸

(*E*)-Di-*tert*-butyl-oct-4-enedioate (**153**)



*i*Pr₂NH (45.3 mL, 322 mmol) was dissolved in THF (400 mL), and then cooled to -78 °C. *n*BuLi (2.5 M in hexanes, 137 mL, 344 mol) was added dropwise and the solution was stirred for 15 min. After which, *t*BuOAc (39.3 mL, 293 mmol) was added dropwise and the solution was stirred for an additional 30 min. Finally, a solution of bromide **152** (25.0 g, 117 mmol) in THF (100 mL) was added dropwise at -78 °C. The reaction was stirred at -78 °C for 5 h, and then warmed to room temperature and stirred for 16 h. After which, the reaction was cooled to 0 °C and quenched with an aqueous solution of NH₄Cl (sat., 200 mL). The layers were allowed to separate, and the aqueous layer was extracted with EtOAc (4 × 300 mL). The organic layers were combined, dried (MgSO₄), and then concentrated *in vacuo*. Purification by flash column

chromatography (SiO₂, 99:1 to 90:10 Pentane:EtOAc) afforded diester **153** (20.0 g, 60%) as a white solid.

R_f = 0.7 (90:10 Pentane:EtOAc);

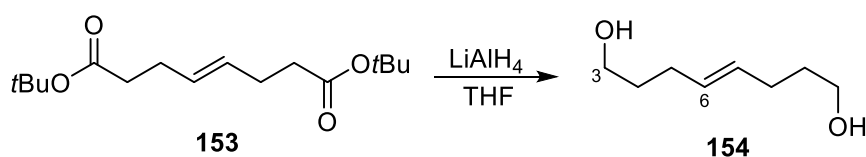
¹H NMR (400 MHz, CDCl₃) δ_H 5.44 (2H, br. s., C(6)H × 2), 2.25 (8H, br. s., C(5)H₂ × 2, C(4)H₂ × 2), 1.44 (18H, s, C(CH₃)₃ × 2);

¹³C NMR (100 MHz, CDCl₃) δ_C 172.5 (C3 × 2), 129.3 (C6 × 2), 80.1 ((CH₃)₃C × 2), 35.4 (C4 × 2), 28.1 (tBu-(CH₃)₃ × 2), 28.0 (C5 × 2);

m.p. 57–58 °C (lit. 59–60 °C).

The spectral data were consistent with those previously reported.³⁸

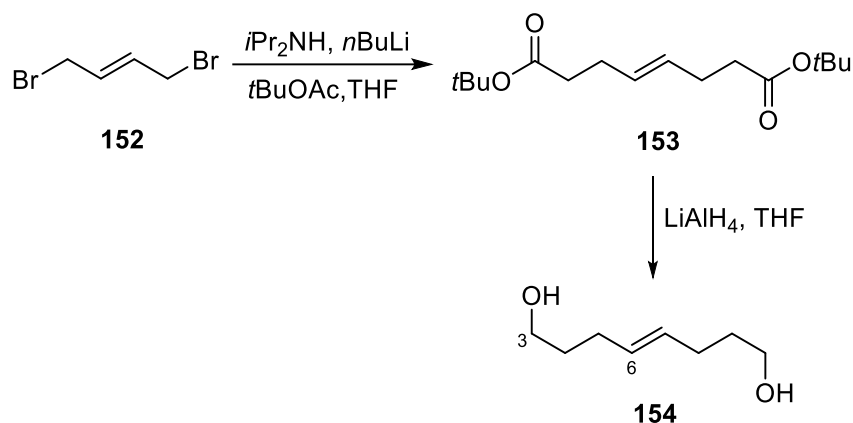
(E)-Oct-4-ene-1,8-diol (**154**)



Procedure A:

Diester **153** was dissolved in THF (74 mL) and cooled to 0 °C. LiAlH₄ (10.7 g, 281 mmol) was added to the solution in small portions over 15 min. The mixture was warmed to room temperature and stirred for 4 h. The reaction was quenched at –78 °C by a dropwise addition of H₂O (10.7 mL), aqueous NaOH (15% w/v, 10.7 mL), and H₂O (32.0 mL). The resulting slurry was filtered through Celite[®], and then concentrated in vacuo. Purification by flash column chromatography (SiO₂, 50:50 to 70:30 EtOAc: Pentane) afforded diol **154** (8.37 g, 83%) as a colourless oil.

Procedure B:



$i\text{Pr}_2\text{NH}$ (63.2 mL, 449 mmol) was dissolved in THF (558 mL), and then cooled to $-78\text{ }^\circ\text{C}$. $n\text{BuLi}$ (2.5 M, 200 mL, 480 mmol) was added dropwise and the solution was stirred for 15 min. $t\text{BuOAc}$ (54.8 mL, 409 mmol) was added dropwise and the solution was stirred for an additional 30 min. Bromide **152** (34.9 g, 163 mmol) was dissolved in THF (140 mL) and added dropwise over 6 h at $-78\text{ }^\circ\text{C}$. The reaction was stirred at $-78\text{ }^\circ\text{C}$ for 5 h, before it was warmed to room temperature and left to stir for 16 h. The reaction was cooled in an ice bath and then quenched with saturated NH_4Cl . The layers were allowed to separate, and the aqueous layer was extracted with EtOAc ($4 \times 350\text{ mL}$). The organic layers were combined, dried (MgSO_4), and then concentrated *in vacuo*.

The crude product **153** (163 mmol, assumed quant.) was dissolved in THF (530 mL) and cooled to $0\text{ }^\circ\text{C}$ in an ice bath. LiAlH_4 (19.5 g, 513 mmol) was added to the solution in small portions over 15 min. The mixture was warmed to room temperature and stirred for 3 h. The reaction was quenched at $-78\text{ }^\circ\text{C}$ by a dropwise addition of H_2O (19.5 mL), aqueous NaOH (15% w/v, 19.5 mL), and H_2O (58.5 mL). Et_2O (200 mL) was then added to the mixture, which was stirred for a further 2 h. The mixture was filtered through cotton wool and the filtrate was concentrated *in vacuo*. Purification by flash column chromatography (SiO_2 , 50:50 EtOAc :Pentane) afforded diol **154** (14.7 g, 62% over two steps) as a colourless oil.

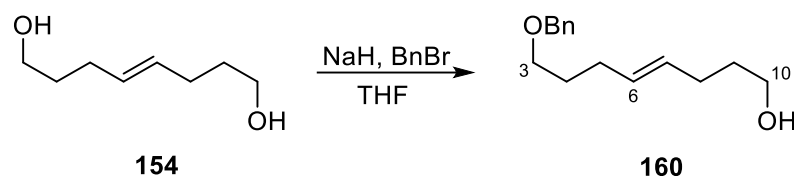
$R_f = 0.5$ (100% EtOAc);

$^1\text{H NMR}$ (400 MHz, CDCl_3) δ_{H} 5.50–5.37 (2H, m, C(6)H \times 2), 3.62 (4H, t, $J = 6.5$ Hz, C(3)H $_2 \times$ 2), 2.13–2.00 (4H, m, C(5)H $_2 \times$ 2), 1.81 (2H, s, OH \times 2), 1.61 (4H, quin, $J = 6.6$ Hz, C(4)H $_2 \times$ 2);

$^{13}\text{C NMR}$ (100 MHz, CDCl_3) δ_{C} 130.2 (C6 \times 2), 62.4 (C3 \times 2), 32.3 (C4 \times 2), 28.8 (C5 \times 2).

The spectral data were consistent with those previously reported.³⁸

(E)-8-(Benzyloxy)oct-4-en-1-ol (160)



Diol **154** (13.5 g, 93.6 mmol) was dissolved in THF (186 mL) and cooled to 0 °C. NaH (60% in mineral oil, 1.80 g, 74.9 mmol) was added, and the mixture was stirred for 1 hour at 0 °C. After which, tetra-butylammonium iodide (1.75 g, 4.73 mmol) was added, followed by a dropwise addition of BnBr (8.88 mL, 74.9 mmol). The mixture was warmed to room temperature and refluxed for 16 h. The reaction was then quenched with a solution of NH_4Cl (sat., 135 mL). The layers were allowed to separate, and the aqueous layer was extracted with EtOAc (4 \times 300 mL). The organic layers were combined, dried (MgSO_4), filtered, and then concentrated *in vacuo*. Purification by flash column chromatography (SiO_2 , 40:60 to 80:20 EtOAc:Pentane) afforded **160** (8.67 g, 37.0 mmol, 40%) as a yellow oil. Diol **154** (7.66 g, 53%) was also recovered as a yellow oil.

$R_f = 0.5$ (50:50 EtOAc:Pentane);

$^1\text{H NMR}$ (400 MHz, CDCl_3) δ_{H} 7.44–7.24 (5H, m, Bn-ArH \times 5), 5.44 (2H, t, $J = 5.6$ Hz, C(6)H, C(7)H), 4.50 (2H, s, Bn-CH $_2$), 3.63 (2H, t, $J = 6.5$ Hz, C(10)H $_2$), 3.47 (2H, t, $J = 6.5$ Hz, C(3)H $_2$),

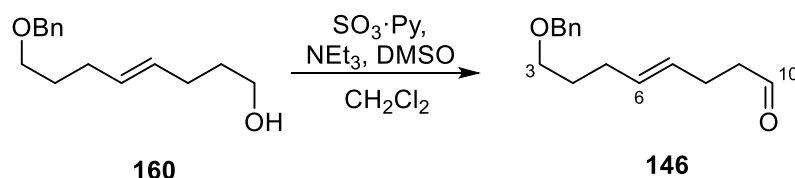
2.14–2.02 (4H, m, C(5)H₂, C(8)H₂), 1.69 (2H, quin, *J* = 6.6 Hz, C(4)H₂), 1.68–1.56 (2H, m, C(9)H₂), 1.41 (1H, s, OH);

¹³C NMR (100 MHz, CDCl₃) δ_c 138.6 (Bn-C_{Ar}CH₂), 130.3 (1 C, C6 or C7), 130.0 (1 C, C6 or C7), 128.3 (Bn-C_{Ar} × 2), 127.6 (Bn-C_{Ar} × 2), 127.5 (Bn-C_{Ar}), 72.8 (Bn-CH₂), 69.7 (C3), 62.5 (C10), 32.4 (C9), 29.5 (C4), 29.1 (C5), 28.9 (C8).

The spectral data were consistent with those previously reported.³⁸

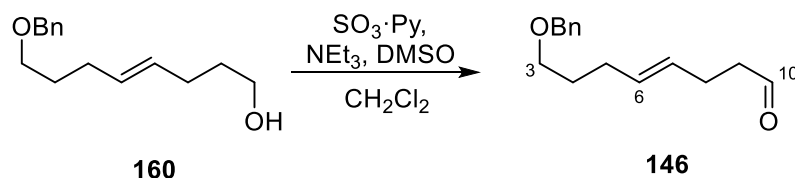
(*E*)-8-(Benzyloxy)oct-4-enal (**146**)

Procedure A:



Alcohol **160** (7.00 g, 29.9 mmol) and DMSO (160 mL) were dissolved in CH₂Cl₂ (190 mL), and then cooled to 0 °C. After which, NEt₃ (53.2 mL, 299 mmol) and SO₃·Py (23.8 g, 149 mmol) were added, and the mixture was stirred at 0 °C for 1 hour. The reaction was quenched with water (170 mL). The layers were allowed to separate and the aqueous layer was extracted once with CH₂Cl₂ (170 mL), followed by EtOAc (3 × 170 mL). The combined organic layers were dried (MgSO₄), filtered, and then concentrated in vacuo at room temperature. Purification by flash column chromatography (SiO₂, 95:5 Pentane:EtOAc) afforded aldehyde **146** (5.38 g, 78%) as a colourless oil.

Procedure B:



Alcohol **160** (10.0 g, 42.7 mmol) and DMSO (9.0 mL) were dissolved in CH₂Cl₂ (175 mL) and cooled to 0 °C. DIPEA (22.3 mL, 128 mmol) and SO₃·Py (20.4 g, 128 mmol) were then added, and the mixture was stirred at 0 °C for 2 h. After which, the reaction was quenched with water (240 mL). The layers were allowed to separate and the aqueous layer was extracted with CH₂Cl₂ (4 × 240 mL). The combined organic layers were dried (MgSO₄), filtered, and then concentrated in vacuo. Purification by flash column chromatography (SiO₂, 95:5 Pentane:EtOAc) afforded aldehyde **146** (6.24 g, 63%) as a colourless oil.

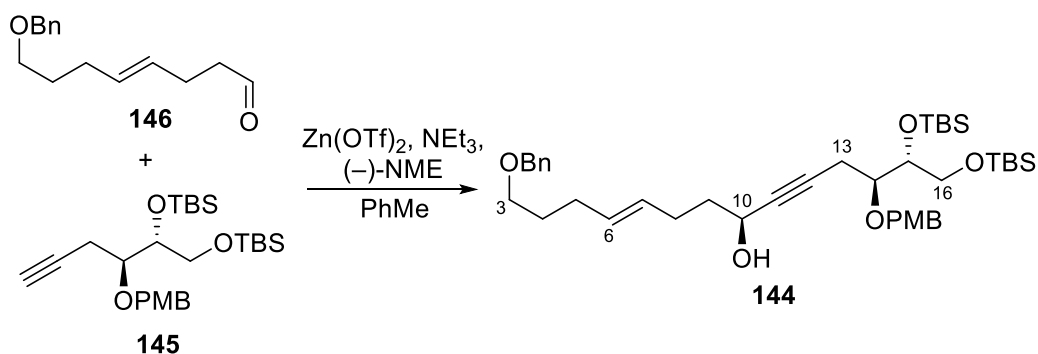
R_f = 0.7 (80:20 Pentane:EtOAc);

¹H NMR (400 MHz, CDCl₃) δ_H 9.74 (1H, t, *J* = 1.7 Hz, C(10)H), 7.37–7.25 (5H, m, Bn-ArH × 5), 5.53–5.34 (2H, m, C(6)H, C(7)H), 4.49 (2H, s, Bn-CH₂), 3.45 (2H, t, *J* = 6.5 Hz, C(3)H₂), 2.47 (2H, dt, *J* = 7.2, 1.7, C(9)H₂), 2.38–2.27 (2H, m, C(8)H₂), 2.15–2.03 (2H, m, C(5)H₂), 1.67 (2H, dt, *J* = 8.3, 6.6 Hz, C(4)H₂);

¹³C NMR (100 MHz, CDCl₃) δ_C 202.3 (C10), 138.5 (Bn-C_{Ar}), 131.1 (C6), 128.3 (C7), 128.2 (Bn-C_{Ar} × 2), 127.6 (Bn-C_{Ar} × 2), 127.5 (Bn-C_{Ar}), 72.8 (Bn-CH₂), 69.6 (C3), 43.4 (C9), 29.3 (C4), 29.0 (C5), 25.1 (C8).

The spectral data were consistent with those previously reported.³⁸

(2*R*,3*S*,7*S*,*E*)-14-(Benzyloxy)-1,2-bis((*tert*-butyldimethylsilyloxy)oxy)-3-((4-methoxybenzyl)oxy)tetradec-10-en-5-yn-7-ol (144**)**



Zn(OTf)₂ (31.0 g, 85.2 mmol) was heated to 125 °C under high vacuum (0.05 mbar) for 12 h with stirring until the solid became a fine powder. The flask was then cooled to room temperature and (–)-*N*-methylephedrine (16.7 g, 93.0 mmol, pre-dried under high vacuum for 12 h) was added. A solution of NEt₃ (13.0 mL, 93.0 mmol) in PhMe (97 mL) was purged with argon for 15 min and then added to the mixture and stirred for 2 h. Alkyne **145** (37.1 g, 77.5 mmol, placed under high vacuum for 12 h) dissolved in PhMe (48 mL) was added dropwise to the reaction mixture, and the resulting slurry was vigorously stirred for 2 h. Aldehyde **146** (6.00 g, 25.8 mmol) was dissolved in PhMe (15 mL) and added dropwise *via* syringe pump over 16 h at room temperature. The reaction mixture was left to stir at room temperature for a further 24 h. After which, the reaction mixture was quenched with NH₄Cl (sat., 110 mL). The layers were allowed to separate and the aqueous layer was extracted with EtOAc (4 × 175 mL). The organic layers were combined, dried (MgSO₄), filtered, and then concentrated *in vacuo*. Purification by flash column chromatography (SiO₂, 95:5 to 80:20 Pentane:EtOAc) afforded alcohol **144** (17.1 g, 91%, 95:5 d.r.) as a colourless oil.

R_f = 0.4 (80:20 Pentane:EtOAc);

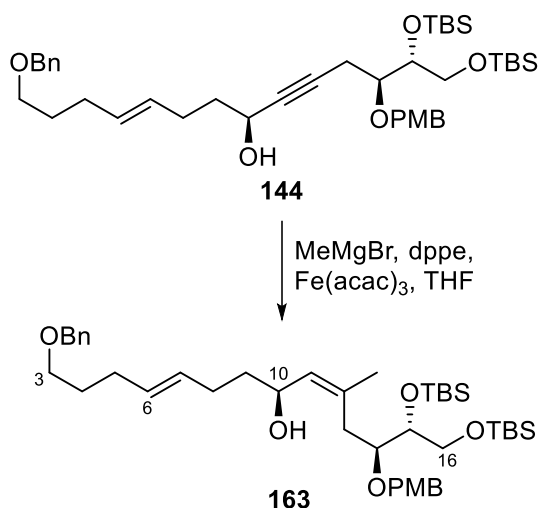
[α]_D²⁵ –2.0 (*c* = 0.53, CH₂Cl₂, lit. –2.4, *c* = 1.08, CH₂Cl₂);

¹H NMR (400 MHz, CDCl₃) δ_H 7.37–7.22 (4H, m, Bn-ArH × 4), 7.27 (2H, d, *J* = 8.1 Hz, PMB-ArH × 2), 7.29 (1H, m, Bn-ArH), 6.84 (2H, d, *J* = 8.1 Hz, PMB-ArH × 2), 5.49–5.34 (2H, m, C(6)H, C(7)H), 4.63–4.51 (2H, m, PMB-CH_AH_B), 4.48 (2H, s, Bn-CH₂), 4.37–4.27 (1H, m, C(10)H), 3.84–3.78 (1H, m, C(15)H), 3.77 (3H, s, PMB-CH₃), 3.68–3.58 (3H, m, C(14)H, C(16)H₂), 3.44 (2H, t, *J* = 6.5 Hz, C(3)H₂), 2.61–2.41 (2H, m, C(13)H₂), 2.17–2.08 (2H, m, C(8)H₂), 2.08–2.00 (2H, m, C(5)H₂), 1.75–1.58 (4H, m, C(9)H₂, C(4)H₂), 0.90–0.85 (18H, m, TBS-C(CH₃)₃ × 2), 0.13–0.02 (12H, m, TBS-Si(CH₃)₂ × 2);

¹³C NMR (100 MHz, CDCl₃) δ_c 159.1 (PMB-C_{Ar}OMe), 138.6 (Bn-C_{Ar}CH₂), 130.7 (PMB-C_{Ar}CH₂), 130.5 (C6), 129.5 (C7), 129.4 (PMB-C_{Ar} × 2), 128.3 (Bn-C_{Ar} × 2), 127.6 (Bn-C_{Ar} × 2), 127.5 (Bn-C_{Ar}), 113.7 (PMB-C_{Ar} × 2), 83.2 (C12), 82.2 (C11), 78.1 (C14), 74.3 (C15), 72.8 (Bn-CH₂), 72.1 (PMB-CH₂), 69.7 (C3), 64.5 (C16), 62.2 (C10), 55.2 (PMB-CH₃), 37.7 (C9), 29.5 (C4), 29.1 (C5), 28.3 (C8), 26.0 (TBS-C(CH₃) × 3), 25.9 (TBS-C(CH₃) × 3), 20.7 (C13), 18.3 (TBS-C(CH₃)₃), 18.1 (TBS-C(CH₃)₃), -4.3 (TBS-SiCH₃), -4.8 (TBS-SiCH₃), -5.4 (TBS-SiCH₃), -5.4 (TBS-SiCH₃);

The spectral data were consistent with those previously reported.³⁸

(2*R*,3*S*,5*Z*,7*S*,10*E*)-14-(Benzyloxy)-1,2-bis((*tert*-butyldimethylsilyl)oxy)-3-((4-methoxybenzyl)oxy)-5-methyltetradeca-5,10-dien-7-ol (163)



Alkyne **144** (7.35 g, 10.3 mmol) was dried under high vacuum with stirring for 12 h and then dissolved in anhydrous THF (74.5 mL) at 0 °C. Iron(III) acetylacetonate (735 mg, 2.09 mmol) and 1,2-bis(diphenylphosphino)ethane (828 mg, 2.08 mmol) were added to the solution. The flask was flushed with argon. After which, the reaction mixture was cooled to -78 °C and stirred for 10 min. MeMgBr (3.0 M in Et₂O, 27.6 mL, 82.8 mmol) was added dropwise *via* syringe pump (1.5 mL per min). The reaction mixture was stirred at -78 °C for an additional 2 h, before being warmed to 0 °C and stirred for 18 h. The reaction mixture was cooled back to -78 °C and then quenched through dropwise addition of a solution of NH₄Cl (sat., 30 mL). The

reaction mixture was diluted with Et₂O (80 mL), warmed, and then extracted with EtOAc (4 × 50 mL). The organic layers were combined, dried (MgSO₄), filtered, and then concentrated *in vacuo*. Purification by flash column chromatography (SiO₂, 90:10 to 70:30 Pentane:Et₂O) afforded **163** (5.83 g, 78%) as a pale yellow oil.

R_f = 0.4 (70:30 Pentane:Et₂O);

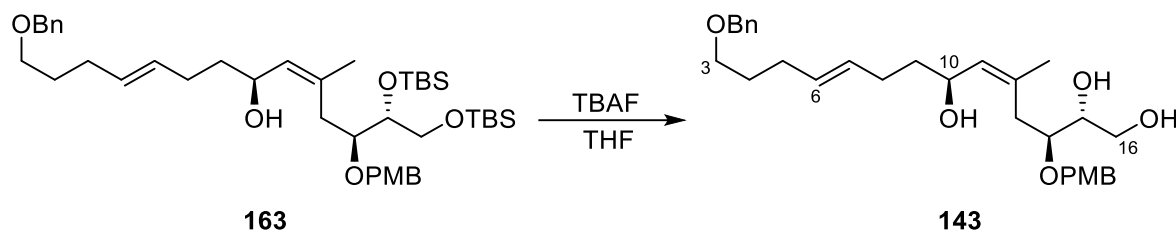
[α]_D²⁰ –4.5 (c = 1.18, CH₂Cl₂; lit. –6.5, c = 0.90, CH₂Cl₂);

¹H NMR (500 MHz, CDCl₃) δ_H 7.39–7.30 (4H, m, Bn-ArH × 4), 7.28–7.18 (2H, m, PMB-ArH × 2), 7.30–7.22 (1H, m, Bn-ArH), 6.84 (2H, d, J = 8.7 Hz, PMB-ArH × 2), 5.43–5.34 (2H, m, C(6)H, C(7)H), 5.27 (1H, d, J = 8.5 Hz, C(11)H), 4.56 (1H, d, J = 11.4 Hz, PMB-CH_AH_B), 4.49 (2H, s, Bn-CH₂), 4.38 (1H, d, J = 11.5 Hz, PMB-CH_AH_B), 4.35–4.29 (1H, m, C(10)H), 3.93–3.84 (1H, m, C(15)H), 3.78 (3H, s, PMB-CH₃), 3.69 (1H, ddd, J = 7.9, 5.0, 2.1 Hz, C(14)H), 3.61–3.53 (2H, m, C(16)H₂), 3.45 (2H, t, J = 6.5 Hz, C(3)H₂), 2.43 (1H, dd, J = 13.8, 8.6 Hz, C(13)H_AH_B), 2.25 (1H, dd, J = 13.8, 5.0 Hz, C(13)H_AH_B), 2.19–2.13 (1H, m, OH), 2.10–2.00 (3H, m, C(5)H₂, C(8)H_AH_B), 2.00–1.92 (1H, m, C(8)H_AH_B), 1.66 (3H, s, C(12)CH₃), 1.64–1.53 (2H, m, C(4)H₂), 1.55–1.41 (2H, m, C(9)H₂), 0.90 (9H, s, TBS-C(CH₃)₃), 0.88 (9H, s, TBS-C(CH₃)₃), 0.13–0.01 (12H, m, TBS-Si(CH₃)₂ × 2);

¹³C NMR (100 MHz, CDCl₃) δ_C 159.0 (PMB-C_{Ar}OMe), 138.6 (Bn-C_{Ar}CH₂), 135.6 (C12), 130.8 (C11), 130.7 (PMB-C_{Ar}CH₂), 130.6 (C6), 129.6 (C7), 129.4 (PMB-C_{Ar} × 2), 128.3 (Bn-C_{Ar} × 2), 127.6 (Bn-C_{Ar} × 2), 127.4 (Bn-C_{Ar}), 113.5 (PMB-C_{Ar} × 2), 77.6 (C14), 74.9 (C15), 72.8 (Bn-CH₂)₂, 71.7 (PMB-CH₂), 69.8 (C3), 67.9 (C10), 64.5 (C16), 55.2 (PMB-CH₃), 37.2 (C9), 32.8 (C13), 29.6 (C4), 29.1 (C5), 28.8 (C8), 25.9 (TBS-C(CH₃)₃), 25.9 (TBS-C(CH₃)₃), 24.1 (C12-CH₃), 18.2 (TBS-C(CH₃)₃), 18.2 (TBS-C(CH₃)₃), –4.6 (TBS-SiCH₃), –4.6 (TBS-SiCH₃), –5.4 (TBS-SiCH₃), –5.5 (TBS-SiCH₃).

The spectral data were consistent with those previously reported.³⁸

(2R,3S,5Z,7S,10E)-14-(Benzyloxy)-3-((4-methoxybenzyl)oxy)-5-methyltetradeca-5,10-diene-1,2,7-triol (143)



Alcohol **163** (13.4 g, 15.6 mmol) was dissolved in THF (190 mL) and then cooled to 0 °C. TBAF (1 M in THF, 64.7 mL, 46.8 mmol) was added dropwise to the reaction mixture. The reaction mixture stirred for 3 h at room temperature, before being quenched with a solution of NH₄Cl (sat., 100 mL). The layers were allowed to separate and the aqueous layer was extracted with EtOAc (5 × 100 mL). The organic layers were combined, dried (MgSO₄), filtered, and then concentrated *in vacuo*. Purification by flash column chromatography (SiO₂, 67:33 Pentane:Acetone) afforded triol **143** (9.22 g, 100%) as a colourless oil.

R_f = 0.4 (60:40 Pentane:Acetone);

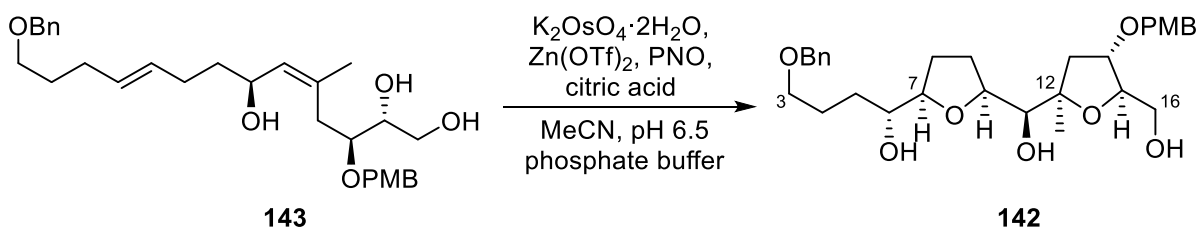
[α]_D²⁵ +11.9 (c = 1.16, CH₂Cl₂; lit. +13.5, c = 1.00, CH₂Cl₂);

¹H NMR (400 MHz, CDCl₃) δ_H 7.29–7.22 (4H, m, Bn-ArH × 4), 7.22–7.17 (1H, m, Bn-ArH), 7.15 (2H, d, J = 8.6 Hz, PMB-ArH × 2), 6.78 (2H, d, J = 8.7 Hz, PMB-ArH × 2), 5.36–5.28 (2H, m, C(6)H, C(7)H), 5.18 (1H, dd, J = 8.5, 1.5 Hz, C(11)H), 4.45 (1H, d, J = 11.1 Hz, PMB-CH_AH_B), 4.40 (2H, s, Bn-CH₂), 4.38 (1H, d, J = 11.1 Hz, PMB-CH_AH_B), 4.30–4.19 (1H, m, C(10)H), 3.70 (3H, s, PMB-CH₃), 3.66–3.49 (4H, m, C(15)H, C(16)H₂, C(14)H), 3.37 (2H, t, J = 6.5 Hz, C(3)H₂), 2.80 (1H, br. s, OH), 2.72 (1H, br. s, OH), 2.40 (1H, dd, J = 13.8, 6.7 Hz, C(13)H_AH_B), 2.26 (1H, dd, J = 13.8, 6.2 Hz, C(13)H_AH_B), 2.08 (1H, br. s, OH), 1.98 (2H, m, C(5)H₂), 1.95–1.88 (2H, m, C(8)H₂), 1.68 (3H, d, J = 1.4 Hz, C(12)CH₃), 1.58 (2H, dq, J = 8.4, 6.7 Hz, C(4)H₂), 1.57–1.44 (1H, m, C(9)H_AH_B), 1.39 (1H, ddt, J = 13.1, 8.5, 6.5 Hz, C(9)H_AH_B);

^{13}C NMR (100 MHz, CDCl_3) δ_{c} 159.3 (PMB- $\text{C}_{\text{Ar}}\text{OMe}$), 138.5 (Bn- $\text{C}_{\text{Ar}}\text{CH}_2$), 136.1 (C12), 130.4 (C11), 130.1 (C7), 130.1 (PMB- $\text{C}_{\text{Ar}}\text{CH}_2$), 130.0 (C6), 129.6 (PMB- $\text{C}_{\text{Ar}} \times 2$), 128.4 (Bn- $\text{C}_{\text{Ar}} \times 2$), 127.7 (Bn- $\text{C}_{\text{Ar}} \times 2$), 127.5 (Bn- C_{Ar}), 113.9 (PMB- $\text{C}_{\text{Ar}} \times 2$), 78.2 (C14), 74.0 (C15), 72.9 (Bn- CH_2), 72.0 (PMB- CH_2), 69.8 (C3), 67.5 (C10), 63.4 (C16), 55.3 (PMB- CH_3), 37.3 (C9), 34.5 (C13), 29.6 (C4), 29.1 (C5), 28.6 (C8), 24.2 (C12- CH_3);

The spectral data were consistent with those previously reported.³⁸

(*R*)-4-(Benzyloxy)-1-((2*R*,5*S*)-5-((*S*)-hydroxy((2*R*,4*S*,5*R*)-5-(hydroxymethyl)-4-((4-methoxybenzyl)oxy)-2-methyltetrahydrofuran-2-yl)methyl)tetrahydrofuran-2-yl)butan-1-ol (142**)**



Triol **143** (7.33 g, 14.7 mmol), pyridine *N*-oxide (4.89 g, 51.5 mmol), and citric acid (2.12 g, 11.0 mmol) were dissolved in CH_3CN (177 mL). Phosphate buffer (pH 6.5, 120 mL), $\text{K}_2\text{OsO}_2(\text{OH})_4$ (110 mg, 0.729 mmol), and $\text{Zn}(\text{OTf})_2$ (2.67 g, 7.35 mmol) were added to the reaction mixture, which was then heated at 60 °C for 13 h. Additional $\text{K}_2\text{OsO}_2(\text{OH})_4$ (107 mg, 0.291 mmol) was added and the reaction mixture was heated to 80 °C and left to stir for 24 h. After which, the mixture was cooled to room temperature and quenched with saturated Na_2SO_3 (200 mL). After 30 min of vigorous stirring, the mixture was diluted with H_2O (200 mL) and EtOAc (200 mL). The layers were allowed to separate and the aqueous layer was extracted with EtOAc (5 \times 200 mL). The organic layers were combined, dried (MgSO_4), filtered, and then concentrated *in vacuo*. Purification by flash column chromatography (SiO_2 , 75:25 to 50:50 Pentane:Acetone) afforded *bis*-THF **142** (6.39 g, 82%, >95:5 d.r.) as a colourless oil.

$R_f = 0.4$ (60:40 Pentane:Acetone);

$[\alpha]_D^{25} +10.2$ ($c = 1.06$, CH_2Cl_2 ; lit. $+13.5$, $c = 1.00$, CH_2Cl_2);

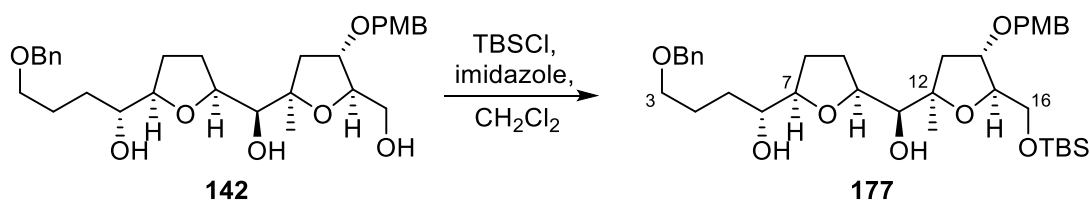
$^1\text{H NMR}$ (400 MHz, CDCl_3) δ_H 7.38–7.29 (4H, m, Bn-ArH \times 4), 7.29–7.25 (1H, m, Bn-ArH), 7.23 (2H, d, $J = 8.4$ Hz, PMB-ArH \times 2), 6.86 (2H, d, $J = 8.6$ Hz, PMB-ArH \times 2), 4.48 (2H, s, Bn-CH₂), 4.48–4.43 (1H, m, PMB-CH_AH_B), 4.37 (1H, d, $J = 11.3$ Hz, PMB-CH_AH_B), 4.15–4.12 (1H, m, C(14)H), 4.10 (1H, d, $J = 7.3$ Hz, C(15)H), 4.07–3.96 (1H, m, C(10)H), 4.02–3.97 (1H, m, C(11)H), 3.87–3.79 (1H, m, C(7)H), 3.78 (3H, s, PMB-CH₃), 3.76–3.66 (1H, m, C(16)H_AH_B), 3.63–3.50 (1H, m, C(16)H_AH_B), 3.48 (2H, t, $J = 5.8$ Hz, C(3)H₂), 3.43 (1H, dt, $J = 7.8, 4.1$ Hz, C(6)H), 2.35 (1H, dd, $J = 13.5, 7.0$ Hz, C(13)H_AH_B), 2.19–2.14 (2H, m, C(9)H_AH_B, C(8)H_AH_B), 2.09–1.90 (2H, m, C(8)H_AH_B, C(4)H_AH_B), 1.97–1.71 (3H, m, C(4)H_AH_B, C(9)H_AH_B, C(13)H_AH_B), 1.71–1.52 (2H, m, C(5)H₂), 1.32 (3H, s, C(12)CH₃);

$^{13}\text{C NMR}$ (100 MHz, CDCl_3) δ_C 159.3 (PMB-C_{Ar}COMe), 138.2 (Bn-C_{Ar}CH₂), 130.2 (PMB-C_{Ar}CH₂), 129.2 (PMB-C_{Ar} \times 2), 128.5 (Bn-C_{Ar} \times 2), 127.9 (Bn-C_{Ar} \times 2), 127.8 (Bn-C_{Ar}), 113.9 (PMB-C_{Ar} \times 2), 86.0 (C12), 83.9 (C14), 81.8 (C15), 81.4 (C7), 80.0 (C10), 76.9 (C11), 73.7 (C6), 73.1 (Bn-CH₂), 71.1 (PMB-CH₂), 70.5 (C3), 63.7 (C16), 55.4 (PMB-CH₃), 37.8 (C13), 31.7 (C5), 28.7 (C8), 26.3 (C4), 24.9 (C9), 24.3 (C12-CH₃);

The spectral data were consistent with those previously reported.³⁸

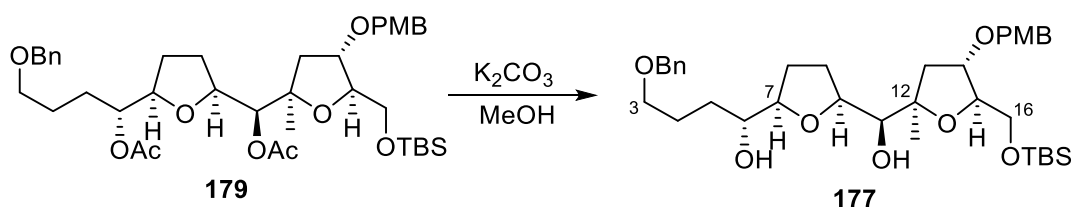
(R)-4-(Benzyloxy)-1-((2R,5S)-5-((S)-((2R,4S,5R)-5-(((tert-butyl)dimethylsilyloxy)methyl)-4-((4-methoxybenzyl)oxy)-2-methyltetrahydrofuran-2-yl)(hydroxy)methyl)tetrahydrofuran-2-yl)butan-1-ol (177**)**

Procedure A:



Triol **142** (2.68 g, 4.00 mmol) and imidazole (849 mg, 12.5 mmol) were dissolved in CH₂Cl₂ (47 mL) and cooled to 0 °C in an ice-water bath. *tert*-Butyldimethylsilyl chloride (799 mg, 5.30 mmol) was dissolved in CH₂Cl₂ (6.7 mL) and added dropwise to the solution at 0 °C. The reaction mixture was warmed to room temperature and stirred for 12 h. The reaction mixture was quenched with a solution of NH₄Cl (sat., 30 mL). The layers were allowed to separate and the aqueous layer was extracted using EtOAc (4 × 30 mL). The organic layers were combined, dried (MgSO₄), filtered, and then concentrated *in vacuo*. Purification by flash column chromatography (SiO₂, 50:50 EtOAc: Pentane) afforded silyl ether **177** (2.57 g, 79%) as a viscous colourless oil.

Procedure B:



K₂CO₃ (1.35 g, 9.75 mmol) was added to a solution of *bis*-acetate **179** (1.42 g, 1.95 mmol) in MeOH (19 mL), and the reaction mixture was stirred vigorously for 3.5 h. MeOH was removed

in vacuo, and purification by flash column chromatography (SiO₂, 50:50 EtOAc: Pentane) afforded silyl ether **177** (1.13 g, 90%) as a colourless oil.

R_f = 0.4 (60:40 Pentane:EtOAc);

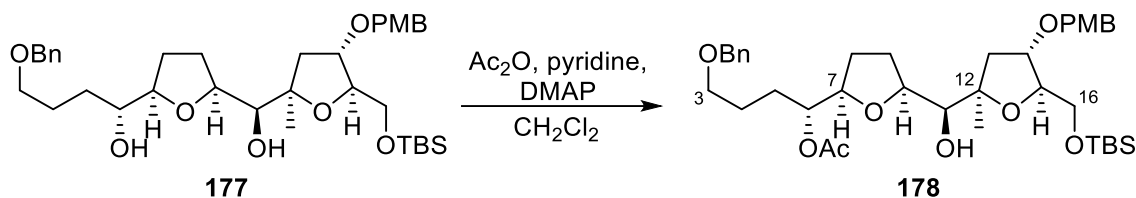
[α]_D²⁵ +16.3 (c = 1.22, CH₂Cl₂; lit. +14.0, c = 1.30, CH₂Cl₂);

¹H NMR (400 MHz, CDCl₃) δ_H 7.35–7.29 (4H, m, Bn-ArH × 4), 7.29–7.25 (1H, m, BnArH), 7.23 (2H, d, J = 8.6 Hz, PMB-ArH × 2), 6.86 (2H, d, J = 8.7 Hz, PMB-ArH × 2), 4.49 (2H, s, Bn-CH₂), 4.45 (1H, d, J = 11.3 Hz, PMB-CH_AH_B), 4.39 (1H, d, J = 11.3 Hz, PMB-CH_AH_B), 4.14 (1H, dt, J = 7.3, 3.6 Hz, 1H, C(14)H), 4.05 (1H, dt, J = 3.5, 1.9 Hz, C(15)H), 3.98 (1H, ddd, J = 8.6, 6.6, 3.8 Hz, C(10)H), 3.87 (2H, m, C(7)H, OH), 3.84 (1H, d, J = 3.8 Hz, C(11)H), 3.78 (3H, s, PMB-CH₃), 3.76 (1H, dd, J = 10.8, 2.6 Hz, C(16)H_AH_B), 3.64 (1H, dd, J = 10.8, 2.0 Hz, C(16)H_AH_B), 3.49 (2H, tdd, J = 9.3, 6.4 Hz, C(3)H₂), 3.42–3.30 (1H, m, C(6)H), 2.32 (1H, dd, J = 13.1, 7.2 Hz, C(13)H_AH_B), 2.18–2.08 (1H, m, C(9)H_AH_B), 2.05–1.77 (3H, m, C(8)H₂, C(4)H_AH_B), 1.77–1.65 (2H, m, C(4)H_AH_B, C(9)H_AH_B), 1.65–1.61 (1H, m, C(13)H_AH_B), 1.61–1.49 (2H, m, C(5)H₂), 1.35 (3H, s, C(12)CH₃), 0.88 (9H, s, TBS-C(CH₃)₃), 0.06–0.03 (6H, m, TBS-Si(CH₃)₂);

¹³C NMR (100 MHz, CDCl₃) δ_C 159.3 (PMB-C_{Ar}COMe), 138.7 (Bn-C_{Ar}CH₂), 130.2 (PMB-C_{Ar}H₂), 129.3 (PMB-C_{Ar} × 2), 128.4 (Bn-C_{Ar} × 2), 127.7 (Bn-C_{Ar} × 2), 127.5 (Bn-C_{Ar}), 113.9 (PMB-C_{Ar} × 2), 86.2 (C12), 83.3 (C15), 81.6 (C7), 81.0 (C14), 79.8 (C10), 78.2 (C11), 74.6 (C6), 72.9 (Bn-CH₂), 71.3 (PMB-CH₂), 70.5 (C3), 63.9 (C16), 55.3 (PMB-CH₃), 37.4 (C13), 31.3 (C5), 29.2 (C8), 26.3 (C4), 25.9 (TBS- C(CH₃)₃), 25.8 (C9), 25.0 (C12-CH₃), 18.5 (TBS-C(CH₃)₃), -5.5 (TBS-SiCH₃), -5.6 (TBS-SiCH₃).

The spectral data were consistent with those previously reported.³⁸

(R)-4-(Benzyloxy)-1-((2R,5S)-5-((S)-((2R,4S,5R)-5-(((tert-butyl)dimethylsilyloxy)methyl)-4-((4-methoxybenzyl)oxy)-2-methyltetrahydrofuran-2-yl)(hydroxy)methyl)tetrahydrofuran-2-yl)butyl acetate (178)



Diol **177** (15.6 g, 24.2 mmol), pyridine (19.5 mL, 242 mmol), and DMAP (296 mg, 2.42 mmol) were dissolved in CH₂Cl₂ (1.47 L) and then cooled to 0 °C. Acetic anhydride (3.16 mL, 33.4 mmol) was added dropwise, and the solution was slowly warmed to room temperature and stirred for 15 h. The reaction was quenched with saturated NaHCO₃ (300 mL). The layers were allowed to separate and the aqueous layer was extracted with EtOAc (4 × 300 mL). The organic layers were combined, dried (MgSO₄), and then concentrated *in vacuo*. Purification by flash column chromatography (SiO₂, 90:10 to 80:20 Pentane:EtOAc, then 70:30 Pentane:Acetone) afforded acetate **178** (13.3 g, 80%) and starting material **177** (986 mg, 6%) as colourless oils.

R_f = 0.7 (60:40 Pentane:EtOAc);

[α]_D²⁵ +19.7 (c = 1.02, CH₂Cl₂; lit. +18.9, c = 1.20, CH₂Cl₂);

¹H NMR (400 MHz, CDCl₃) δ_H 7.38–7.26 (4H, m, Bn-ArH × 4), 7.29–7.24 (1H, m, Bn-ArH), 7.25 (2H, d, J = 8.7 Hz, PMB-ArH × 2), 6.87 (2H, d, J = 8.6 Hz, PMB-ArH × 2), 4.91–4.85 (1H, m, C(6)H), 4.49 (2H, s, Bn-CH₂), 4.47 (1H, d, J = 11.0 Hz, PMB-CH_AH_B), 4.41 (1H, d, J = 11.3 Hz, PMB-CH_AH_B), 4.14 (1H, td, J = 4.2, 2.9 Hz, C(14)H), 4.05 (1H, td, J = 4.2, 2.9 Hz, C(15)H), 3.97–3.87 (1H, m, C(7)H), 3.90–3.80 (1H, m, C(10)H), 3.80 (3H, s, PMB-CH₃), 3.75–3.61 (2H, m, C(16)H₂), 3.50 (1H, d, J = 6.0 Hz, C(11)H), 3.46 (2H, t, J = 5.8 Hz, C(3)H₂), 3.42 (1H, br. s, OH), 2.35 (1H, dd, J = 13.2, 7.4 Hz, C(13)H_AH_B), 2.06 (3H, s, Ac-CH₃), 2.01–1.86 (3H, m, C(9)H₂, C(8)H_AH_B), 1.76

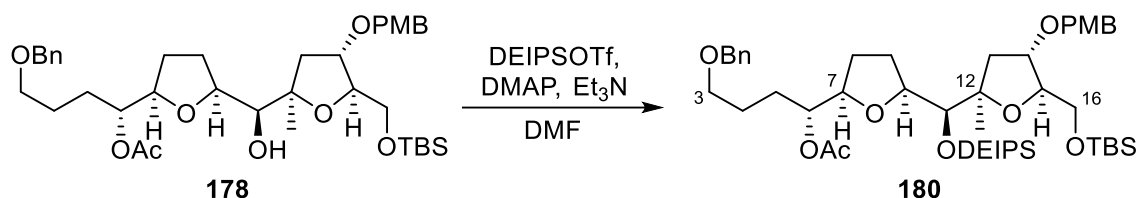
(1H, dd, $J=13.1, 3.8$ Hz, C(13) H_AH_B), 1.72–1.56 (5H, m, C(8) H_AH_B , C(4) H_2 , C(5) H_2), 1.39 (3H, s, C(12) CH_3), 0.88 (9H, s, TBS-C(CH_3) $_3$), 0.05 (6H, s, TBS-Si(CH_3) $_2$);

^{13}C NMR (100 MHz, $CDCl_3$) δ_c 171.1 (Ac-CO), 159.1 (PMB- $C_{Ar}OMe$), 138.4 (Bn- $C_{Ar}CH_2$), 130.3 (PMB- $C_{Ar}CH_2$), 129.1 (PMB- $C_{Ar} \times 2$), 128.3 (Bn- $C_{Ar} \times 2$), 127.6 (Bn- $C_{Ar} \times 2$), 127.5 (Bn- C_{Ar}), 113.8 (PMB- $C_{Ar} \times 2$), 86.0 (C12), 83.3 (C15), 80.4 (C14), 80.1 (C10), 79.8 (C7), 77.7 (C11), 75.4 (C6), 72.8 (Bn- CH_2), 71.2 (PMB- CH_2), 69.7 (C3), 63.3 (C16), 55.2 (PMB- CH_3), 38.0 (C13), 27.8 (C5), 27.7 (C8), 27.6 (C9), 25.9 (TBS-C $CH_3 \times 3$), 25.6 (C4), 24.7 (C12- CH_3), 21.2 (Ac- CH_3), 18.3 (TBS-C(CH_3) $_3$), -5.5 (TBS-Si CH_3), -5.6 (TBS-Si CH_3);

The spectral data were consistent with those previously reported.³⁸

(R)-4-(Benzyloxy)-1-((2R,5S)-5-((S)-((2R,4S,5R)-5-(((tert-butyl)dimethylsilyl)oxy)methyl)-4-((4-methoxybenzyl)oxy)-2-methyltetrahydrofuran-2-yl)((diethyl(isopropyl)silyl)oxy)methyl)tetrahydrofuran-2-yl)butyl acetate (180)

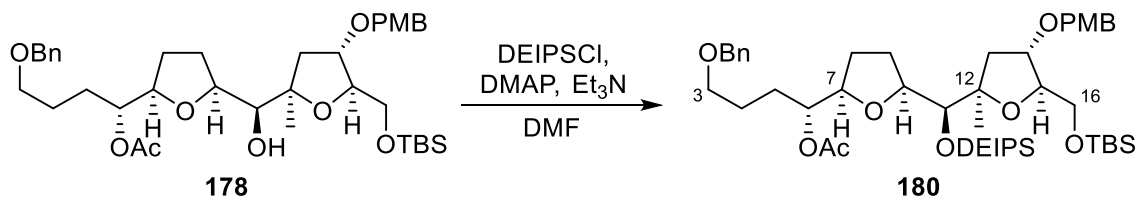
Procedure A:



Acetate **178** (1.40 g, 2.04 mmol), NEt_3 (6.09 mL, 43.7 mmol), and DMAP (711 mg, 5.82 mmol) were dissolved in DMF (30.0 mL) and cooled to 0 °C. DEIPSOTf (0.99 mL, 4.1 mmol) was then added to the reaction mixture dropwise. The reaction mixture was warmed to room temperature and stirred for 7 h. The reaction was quenched by addition of a solution of $NaHCO_3$ (sat., 35 mL). The mixture was diluted with H_2O (35 mL). The layers were allowed to separate and the aqueous layer was extracted using Et_2O (3 \times 70 mL). The combined organic layers were dried ($MgSO_4$), and then concentrated *in vacuo*. Purification by flash column

chromatography (SiO₂, 95:5 to 70:30 Pentane:Et₂O) afforded DEIPS ether **180** (1.53 g, 92%) as a yellow oil.

Procedure B:



Acetate **178** (150 mg, 0.218 mmol), NEt₃ (0.46 mL, 3.3 mmol), and DMAP (53 mg, 0.44 mmol) were dissolved in DMF (2.2 mL) and cooled to 0 °C. DEIPSCI (0.32 mL, 1.7 mmol) was added dropwise to the reaction mixture, which was then warmed to room temperature and stirred for 24 h before being quenched by addition of a solution of NaHCO₃ (sat., 3 mL). The mixture was diluted with H₂O (3 mL). The layers were allowed to separate and the aqueous layer was extracted using Et₂O (3 × 5 mL). The organic layers were combined, dried (MgSO₄), filtered, and then concentrated *in vacuo*. Purification by flash column chromatography (SiO₂, 95:5 to 70:30 Pentane:Et₂O) afforded DEIPS ether **180** (157 mg, 88%) as a yellow oil.

R_f = 0.7 (60:40 Pentane:Et₂O);

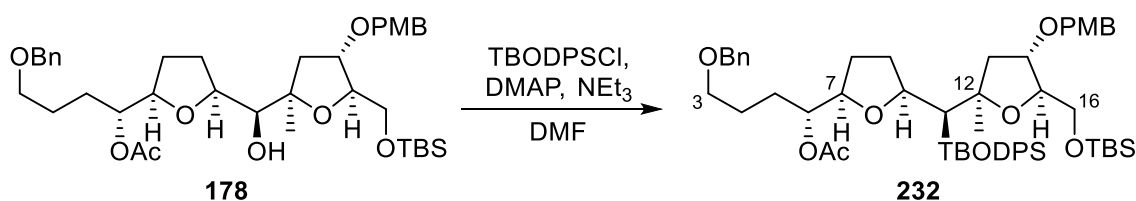
[α]_D²⁵ +4.1 (c = 1.10, CH₂Cl₂);

¹H NMR (500 MHz, CDCl₃) δ_H 7.35–7.27 (4H, m, Bn-ArH × 4), 7.27–7.22 (1H, m, Bn-ArH), 7.21 (2H, d, J = 8.1 Hz, PMB-ArH × 2), 6.83 (2H, d, J = 8.6 Hz, PMB-ArH × 2), 4.93 (1H, dq, J = 7.1, 3.5 Hz, C(6)H), 4.45 (2H, s, Bn-CH₂), 4.43–4.39 (1H, m, PMB-CH_AH_B), 4.36 (1H, d, J = 11.5 Hz, PMB-CH_AH_B), 4.03 (1H, dt, J = 6.3, 3.8 Hz, C(15)H), 3.99 (1H, dt, J = 6.5, 3.0 Hz, C(14)H), 3.92 (1H, ddd, J = 8.7, 6.9, 1.3 Hz, C(10)H), 3.82 (1H, d, J = 1.3 Hz, C(11)H), 3.76 (3H, s, PMB-CH₃), 3.67–3.58 (2H, m, C(16)H_AH_B, C(7)H), 3.49–3.37 (1H, m, C(16)H_AH_B), 3.44–3.38 (2H, m, C(3)H₂), 2.07 (1H, dd, J = 13.3, 7.2 Hz, C(13)H_AH_B), 2.01 (3H, s, Ac-CH₃), 1.97–1.82 (1H, m, C(9)H_AH_B),

1.83–1.72 (2H, m, C(8) H_AH_B , C(13) H_AH_B), 1.72–1.53 (5H, m, C(5) H_2 , C(9) H_AH_B , C(4) H_2), 1.44–1.32 (1H, m, C(8) H_AH_B), 1.21 (3H, s, C(12) CH_3), 0.99–0.89 (13H, m, DEIPS- $CH_3 \times 4$, DEIPS- CH), 0.85 (9H, br. s., TBS- $C(CH_3)_3$), 0.71–0.51 (4H, m, DEIPS- $CH_2 \times 2$), 0.01 (6H, s, TBS- $Si(CH_3)_2$); ^{13}C NMR (100 MHz, $CDCl_3$) δ_c 170.5 (Ac-CO), 159.0 (PMB- $C_{Ar}OMe$), 138.4 (Bn- $C_{Ar}CH_2$), 130.5 (PMB- $C_{Ar}CH_2$), 129.1 (PMB- $C_{Ar} \times 2$), 128.3 (Bn- $C_{Ar} \times 2$), 127.6 (Bn- $C_{Ar} \times 2$), 127.5 (Bn- C_{Ar}), 113.7 (PMB- $C_{Ar} \times 2$), 84.9 (C12), 84.3 (C15), 80.7 (C14), 79.8 (C10), 78.6 (C7), 78.0 (C11), 74.7 (C6), 72.9 (Bn- CH_2), 71.0 (PMB- CH_2), 70.0 (C3), 63.8 (C16), 55.2 (PMB- CH_3), 42.0 (C13), 28.2 (C5), 28.1 (C8), 25.9 (TBS- $C(CH_3)_3$), 25.3 (C4), 23.9 (C9), 22.1 (C12- CH_3), 21.1 (Ac- CH_3), 18.3 (TBS- $C(CH_3)_3$), 17.7 (DEIPS- $iPrCH_3$), 17.5 (DEIPS- $iPrCH_3$), 13.1 (DEIPS- $iPrCH$), 7.3 (DEIPS-Et CH_3), 7.3 (DEIPS-Et CH_3), 4.5 (DEIPS-Et CH_2), 4.1 (DEIPS-Et CH_2), -5.4 (TBS- $SiCH_3$), -5.5 (TBS- $SiCH_3$);

The spectral data were consistent with those previously reported.³⁸

(R)-4-(benzyloxy)-1-((2R,5S)-5-((S)-((tert-butoxydiphenylsilyl)oxy)((2R,4S,5R)-5-(((tert-butyl)dimethylsilyl)oxy)methyl)-4-((4-methoxybenzyl)oxy)-2-methyltetrahydrofuran-2-yl)methyl)tetrahydrofuran-2-yl)butyl acetate (232)



Alcohol **178** (121 mg, 0.177 mmol), NEt_3 (0.37 mL, 2.7 mmol), and DMAP (43.1 mg, 0.353 mmol) were dissolved in DMF (0.80 mL) and cooled to 0 °C. TBODPSCI (411 mg, 1.41 mmol) dissolved in DMF (1.0 mL) was then added to the reaction mixture dropwise. The reaction mixture was warmed to room temperature and stirred for 21 h. The reaction was quenched by addition of a solution of $NaHCO_3$ (sat., 15 mL). The mixture was diluted with H_2O (15 mL). The layers were allowed to separate and an extraction was conducted using Et_2O (3 \times 30 mL).

The combined organic layers were washed with LiCl (5 %, 30 mL), dried (MgSO₄), and then concentrated in vacuo. Purification by flash column chromatography (SiO₂, 95:5 to 91:9 Pentane:EtOAc, then 80:20 Pentane:Acetone) afforded silyl ether **232** (73.5 mg, 44%) as a colourless oil. Additionally, starting material **178** (45.7 mg, 38%) was recovered.

R_f = 0.7 (60:40 Pentane:Et₂O);

[α]_D²⁵ -6.8 (c = 0.75, CH₂Cl₂);

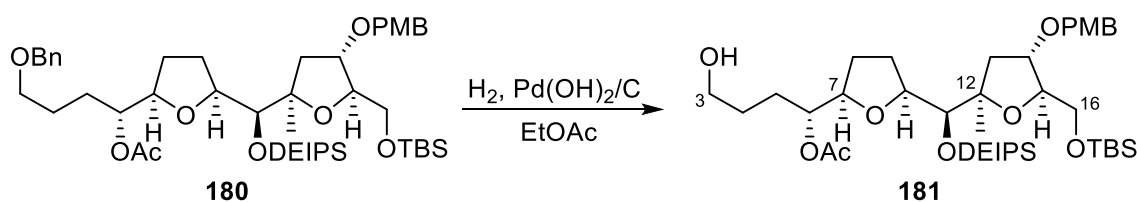
¹H NMR (400 MHz, CDCl₃) δ_H 7.82 (2H, d, J = 6.3 Hz, TBODPS-PhH × 2), 7.71 (2H, d, J = 6.4 Hz, TBODPS-PhH × 2), 7.49–7.32 (11H, m, TBODPS-PhH × 6, Bn-ArH × 5), 7.28 (2H, d, J = 8.6 Hz, PMB-ArH × 2), 6.94 (2H, d, J = 8.6 Hz, PMB-ArH × 2), 4.91–4.83 (1H, m, C(6)H), 4.55 (2H, s, Bn-CH₂), 4.42 (2H, s, PMB-CH₂), 4.21–4.16 (1H, m, C(10)H), 4.05 (1H, dt, J = 6.4, 4.2 Hz, C(15)H), 3.92–3.88 (2H, m, C(11)H, C(14)H), 3.75–3.67 (1H, m, C(7)H), 3.54 (1H, dd, J = 10.6, 4.4 Hz, C(16)H_AH_B), 3.87 (3H, s, PMB-CH₃), 3.50–3.45 (2H, m, C(3)H₂), 3.32 (1H, dd, J = 10.6, 6.3 Hz, C(16)H_AH_B), 2.35–2.27 (2H, m, C(9)H_AH_B, C(13)H_AH_B), 1.83 (3H, s, Ac-CH₃), 1.89 (1H, d, J = 3.5 Hz, C(9)H_AH_B), 1.87–1.84 (2H, m, C(8)H_AH_B, C(13)H_AH_B), 1.71–1.63 (4H, m, C(4)H₂, C(5)H₂), 1.52–1.46 (1H, m, C(8)H_AH_B), 1.41 (3H, s, C(12)CH₃), 1.31 (9H, s, TBODPS-SiOC(CH₃)₃), 0.90 (9H, s, TBS-C(CH₃)₃), 0.04 (3H, s, TBS-SiCH₃), 0.01 (3H, s, TBS-SiCH₃);

¹³C NMR (100 MHz, CDCl₃) δ_C 170.6 (Ac-CO), 159.0 (PMB-C_{Ar}OMe), 138.5 (Bn-C_{Ar}CH₂), 136.1 (Ph-C_{Ar}), 135.9 (Ph-C_{Ar} × 2), 135.3 (Ph-C_{Ar} × 2), 134.0 (Ph-C_{Ar}), 130.6 (PMB-C_{Ar}CH₂), 129.8 (Ph-C_{Ar} × 2), 129.6 (Ph-C_{Ar} × 2), 129.0 (PMB-C_{Ar} × 2), 128.3 (Bn-C_{Ar} × 2), 127.6 (Bn-C_{Ar} × 2), 127.5 (Bn-C_{Ar}), 127.4 (Ph-C_{Ar} × 2), 127.3 (Ph-C_{Ar} × 2), 113.7 (PMB-C_{Ar} × 2), 84.5 (C12), 84.2 (C15), 80.2 (C14), 79.6 (C10), 79.5 (C11), 78.7 (C7), 74.4 (C6), 73.8 (TBODPS-SiOC(CH₃)₃), 72.8 (Bn-CH₂), 70.9 (PMB-CH₂), 70.0 (C3), 63.6 (C16), 55.2 (PMB-CH₃), 42.7 (C13), 32.0 (TBODPS-SiOC(CH₃)₃), 28.0 (C4), 27.8 (C8), 25.9 (TBS-C(CH₃)₃), 25.5 (C5), 25.4 (C9), 22.3 (C12-CH₃), 20.7 (Ac-CH₃), 18.3 (TBS-C(CH₃)₃), -5.4 (TBS-SiCH₃), -5.5 (TBS-SiCH₃);

IR ν_{\max} (film)/ cm^{-1} 2930, 2857, 1737, 1613, 1514, 1429, 1244, 1195, 1115, 1047;

HRMS (ESI⁺, m/z) $\text{C}_{54}\text{H}_{76}\text{O}_{10}\text{NaSi}_2$ calculated 963.48692, found $[\text{M} + \text{Na}^+]$ 963.48615 ($\Delta = -0.81$ ppm).

(R)-1-((2R,5S)-5-((S)-((2R,4S,5R)-5-(((tert-Butyldimethylsilyl)oxy)methyl)-4-((4-methoxybenzyl)oxy)-2-methyltetrahydrofuran-2-yl)((diethyl(isopropyl)silyl)oxy)methyl)tetrahydrofuran-2-yl)-4-hydroxybutyl acetate (181)



Benzyl ether **180** (1.32 g, 1.62 mmol), EtOAc (24 mL), and Pd(OH)₂ on carbon (132 mg) were added to a two-necked flask, and the reaction mixture was cooled to 0 °C. The flask was evacuated and backfilled with hydrogen five times, and then the reaction mixture was stirred vigorously under hydrogen atmosphere (balloon pressure) at 0 °C for 25 min, before being filtered through Celite®. The crude product was then concentrated *in vacuo*, and purification by flash column chromatography (SiO₂, 60:40 Pentane:EtOAc) afforded primary alcohol **181** (1.17 g, 100%) as a colourless oil.

$R_f = 0.4$ (60:40 Pentane:EtOAc);

$[\alpha]_D^{25} +5.4$ ($c = 0.53$, CH₂Cl₂);

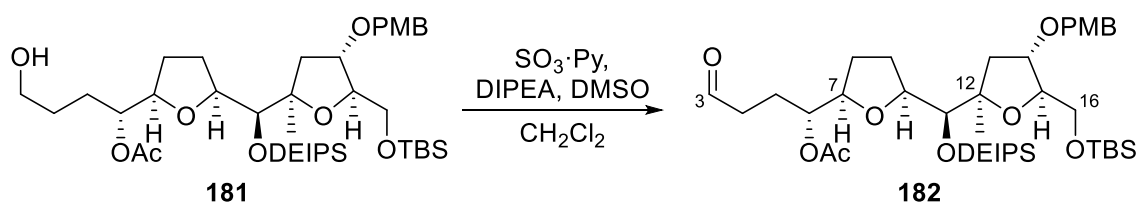
¹H NMR (500 MHz, CDCl₃) δ_H 7.25 (2H, d, $J = 8.6$ Hz, PMB-ArH $\times 2$), 6.87 (2H, d, $J = 8.7$ Hz, PMB-ArH $\times 2$), 4.97 (1H, td, $J = 7.1, 4.2$ Hz, C(6)H), 4.47 (1H, d, $J = 11.5$ Hz, PMB-CH_AH_B), 4.39 (1H, d, $J = 11.5$ Hz, PMB-CH_AH_B), 4.06 (1H, td, $J = 6.3, 3.8$ Hz, C(15)H), 4.01 (1H, dt, $J = 7.1, 3.0$ Hz, C(14)H), 3.95 (1H, ddd, $J = 8.8, 7.1, 1.3$ Hz, C(10)H), 3.85 (1H, d, $J = 1.3$ Hz, C(11)H), 3.80 (3H, s, PMB-CH₃), 3.70–3.59 (4H, m, C(16)H_AH_B, C(3)H₂, C(7)H), 3.48 (1H, dd, $J = 10.5, 6.3$ Hz,

C(16) H_AH_B), 2.11 (1H, dd, $J = 13.3, 7.2$ Hz, C(13) H_AH_B), 2.06 (3H, s, Ac-CH₃), 1.99–1.80 (2H, m, C(9) H_AH_B , C(8) H_AH_B), 1.80–1.67 (2H, m, C(5) H_AH_B , C(13) H_AH_B), 1.67–1.61 (2H, m, C(9) H_AH_B , C(5) H_AH_B), 1.61–1.53 (2H, m, C(4) H_2), 1.49–1.38 (1H, m, C(8) H_AH_B), 1.24 (3H, s, C(12)-CH₃), 1.03–0.91 (13H, m, DEIPS-CH₃ × 4, DEIPS-*i*PrCH), 0.89 (9H, s, TBS-C(CH₃)₃), 0.70–0.55 (4H, DEIPS-CH₂ × 2), 0.03 (6H, s, TBS-Si(CH₃)₂);

¹³C NMR (100 MHz, CDCl₃) δ_c 170.8 (Ac-CO), 159.1 (PMB-C_{Ar}OMe), 130.5 (PMB-C_{Ar}CH₂), 129.1 (PMB-C_{Ar} × 2), 113.8 (PMB-C_{Ar} × 2), 84.9 (C12), 84.3 (C15), 80.7 (C14), 79.9 (C10), 78.6 (C7), 78.1 (C11), 74.8 (C6), 71.1 (PMB-CH₂), 63.8 (C16), 62.7 (C3), 55.3 (PMB-CH₃), 42.1 (C13), 28.2 (C4), 28.0 (C8), 28.0 (C5), 26.0 (TBS-C(CH₃)₃), 24.0 (C9), 22.1 (C12-CH₃), 21.1 (Ac-CH₃), 18.4 (TBS-C(CH₃)₃), 17.7 (DEIPS-*i*PrCH₃), 17.6 (DEIPS-*i*PrCH₃), 13.2 (DEIPS-*i*PrCH), 7.4 (DEIPS-EtCH₃), 7.3 (DEIPS-EtCH₃), 4.5 (DEIPS-EtCH₂), 4.2 (DEIPS-EtCH₂), -5.4 (TBS-SiCH₃), -5.4 (TBS-SiCH₃);

The spectral data were consistent with those previously reported.³⁸

(*R*)-1-((2*R*,5*S*)-5-(((*S*)-((2*R*,4*S*,5*R*)-5-(((*tert*-Butyldimethylsilyl)oxy)methyl)-4-((4-methoxybenzyl)oxy)-2-methyltetrahydrofuran-2-yl)((diethyl(isopropyl)silyl)oxy)methyl)tetrahydrofuran-2-yl)-4-oxobutyl acetate (182**)**



Alcohol **181** (1.19 g, 1.64 mmol) and DMSO (1.16 mL, 16.4 mmol) were dissolved in CH₂Cl₂ (17 mL) and cooled to 0 °C. *i*Pr₂NEt (2.90 mL, 16.4 mmol) was added and the mixture was cooled to -50 °C. SO₃·Py (2.61 g, 16.4 mmol) was added in one portion and the reaction was warmed to -10 °C and stirred for 25 min. The reaction was quenched with a 1:1 mixture of Na₂S₂O₃ and

NaHCO₃ (33 mL). An identical pot using the quantities and procedure previously described was prepared and then combined with the first reaction pot after the quench. The combined mixture was then extracted with Et₂O (4 × 90 mL). The organic layers were combined, dried (MgSO₄), and then concentrated *in vacuo*. Purification by flash column chromatography (SiO₂, 70:30 Pentane:EtOAc) afforded aldehyde **182** (2.19 g, 94%) as a colourless oil.

R_f = 0.7 (60:40 Pentane:EtOAc);

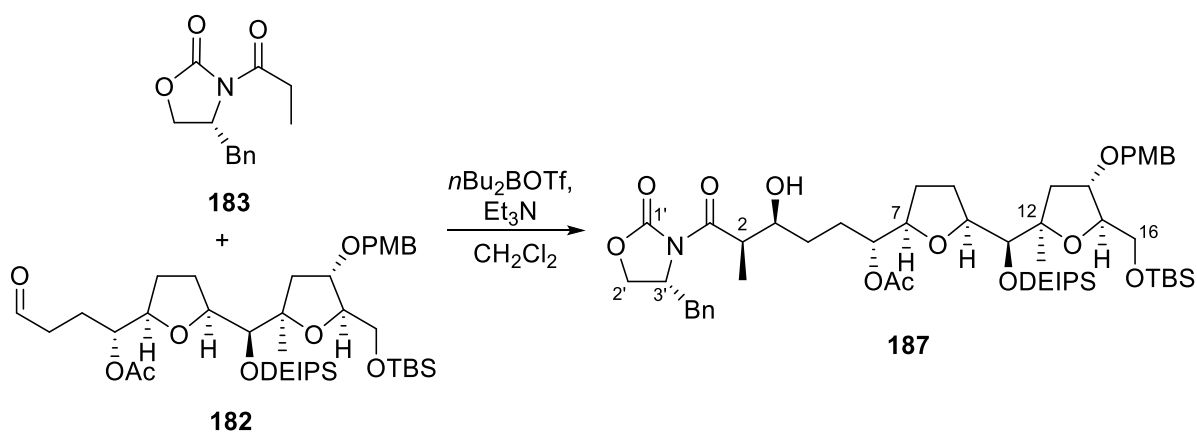
[α]_D²⁵ +6.6 (c = 1.05, CH₂Cl₂);

¹H NMR (400 MHz, CDCl₃) δ_H 9.74 (1H, br. s., C(3)H), 7.24 (2H, d, J = 8.6 Hz, PMB-ArH × 2), 6.86 (2H, d, J = 8.6 Hz, PMB-ArH × 2), 4.95 (1H, ddd, J = 8.6, 6.5, 3.9 Hz, C(6)H), 4.46 (1H, d, J = 11.5 Hz, PMB-CH_AH_B), 4.39 (1H, d, J = 11.5 Hz, PMB-CH_AH_B), 4.06 (1H, dt, J = 6.0, 3.8 Hz, C(15)H), 4.02 (1H, dt, J = 6.6, 3.0 Hz, C(14)H), 4.00–3.91 (1H, m, C(10)H), 3.84 (1H, d, J = 1.3 Hz, C(11)H), 3.79 (3H, s, PMB-CH₃), 3.69–3.59 (2H, m, C(16)H_AH_B, C(7)H), 3.48 (1H, dd, J = 10.5, 6.1 Hz, C(16)H_AH_B), 2.59–2.41 (2H, m, C(4)H₂), 2.10 (1H, dd, J = 13.3, 7.1 Hz, C(13)H_AH_B), 2.04 (3H, s, Ac-CH₃), 2.01–1.90 (2H, m, C(9)H_AH_B, C(5)H_AH_B), 1.90–1.76 (3H, m, C(5)H_AH_B, C(8)H_AH_B, C(13)H_AH_B), 1.75–1.62 (1H, m, C(9)H_AH_B), 1.51–1.38 (1H, m, C(8)H_AH_B), 1.22 (3H, s, C(12)-CH₃), 1.03–0.92 (13H, m, DEIPS-CH₃ × 4, DEIPS-*i*PrCH), 0.88 (9H, s, TBS-C(CH₃)₃), 0.74–0.55 (4H, m, DEIPS-CH₂ × 2), 0.08–0.01 (6H, m, TBS-Si(CH₃)₂);

¹³C NMR (100 MHz, CDCl₃) δ_C 201.2 (C3), 170.6 (Ac-CO), 159.1 (PMB-C_{Ar}OMe), 130.5 (PMB-C_{Ar}CH₂), 129.1 (PMB-C_{Ar} × 2), 113.8 (PMB-C_{Ar} × 2), 84.9 (C12), 84.3 (C15), 80.6 (C14), 80.0 (C10), 78.5 (C7), 78.1 (C11), 73.9 (C6), 71.1 (PMB-CH₂), 63.8 (C16), 55.3 (PMB-CH₃), 42.2 (C13), 39.8 (C4), 28.0 (C8), 26.0 (TBS-C(CH₃)₃), 24.1 (C5), 23.9 (C9), 22.0 (C12-CH₃), 21.0 (Ac-CH₃), 18.4 (TBS-C(CH₃)₃), 17.7 (DEIPS-*i*PrCH₃), 17.6 (DEIPS-*i*PrCH₃), 13.2 (DEIPS-*i*PrCH), 7.3 (DEIPS-EtCH₃), 7.3 (DEIPS-EtCH₃), 4.5 (DEIPS-EtCH₂), 4.2 (DEIPS-EtCH₂), -5.4 (TBS-SiCH₃), -5.4 (TBS-SiCH₃);

The spectral data were consistent with those previously reported.³⁸

(1*R*,4*S*,5*R*)-6-((*R*)-4-Benzyl-2-oxooxazolidin-3-yl)-1-((2*R*,5*S*)-5-((*S*)-((2*R*,4*S*,5*R*)-5-(((*tert*-butyldimethylsilyl)oxy)methyl)-4-((4-methoxybenzyl)oxy)-2-methyltetrahydrofuran-2-yl))((diethyl(isopropyl)silyl)oxy)methyl)tetrahydrofuran-2-yl)-4-hydroxy-5-methyl-6-oxohexyl acetate (**187**)



Oxazolidinone **183** (1.15 g, 3.28 mmol, azeotropically distilled three times in benzene) was dissolved in anhydrous CH_2Cl_2 (3.2 mL) and cooled to 0 °C. Dibutyl(((trifluoromethyl)sulfonyl)oxy)borane (1 M in CH_2Cl_2 , 4.91 mL, 4.91 mmol) and NEt_3 (0.91 mL, 6.6 mmol) were added dropwise. The mixture was stirred for 10 min, cooled to -78 °C and stirred for an additional 10 min. Aldehyde **182** (2.22 g, 3.07 mmol, azeotropically distilled three times in benzene) dissolved in anhydrous CH_2Cl_2 (3.15 mL) was then added dropwise to the reaction mixture. The reaction mixture was stirred for 1 hour at -78 °C, warmed to 0 °C and stirred for 3 h. The reaction was quenched by addition of phosphate buffer (pH 6.5, 4.7 mL) and MeOH (7.1 mL), followed by a 2:1 mixture of MeOH and 30% H_2O_2 solution (7.1 mL). The mixture was stirred for 30 min at 0 °C and extracted with Et_2O (3 × 25 mL). The combined organic layers washed with water (25 mL), and then with NaHCO_3 (25 mL). They were dried (MgSO_4) and concentrated *in vacuo*. Purification by flash column chromatography

(SiO₂, 80:20 to 60:40 Pentane:EtOAc) afforded alcohol **187** (2.64 g, 98%, > 95:5 d.r.) as a colourless oil.

R_f = 0.4 (60:40 Pentane:EtOAc);

[α]_D²⁵ -24.2 (c = 1.57, CH₂Cl₂);

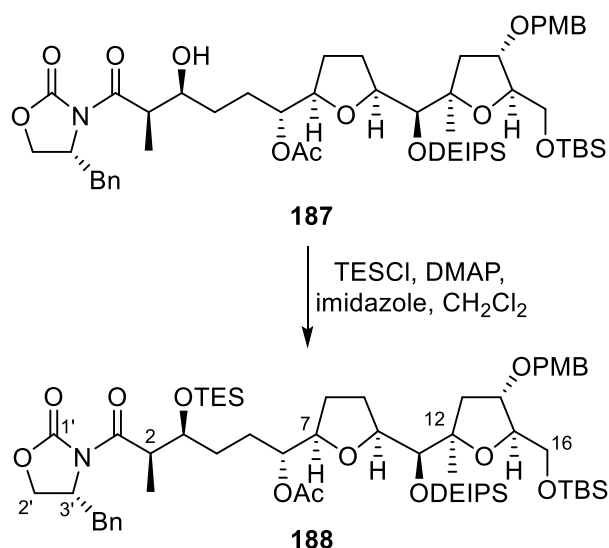
¹H NMR (500 MHz, CDCl₃) δ_H 7.36–7.30 (2H, m, Bn-ArH × 2), 7.30–7.27 (1H, m, Bn-ArH), 7.27–7.22 (2H, m, PMB-ArH × 2), 7.22–7.17 (2H, m, Bn-ArH × 2), 6.86 (2H, d, J = 8.7 Hz, PMB-ArH × 2), 4.96 (1H, td, J = 7.5, 3.6 Hz, C(6)H), 4.69 (1H, ddt, J = 9.4, 7.5, 3.2, Hz C(3')H), 4.46 (1H, d, J = 11.5 Hz, PMB-CH_AH_B), 4.39 (1H, d, J = 11.5 Hz, PMB-CH_AH_B), 4.26–4.16 (2H, m, C(2')H₂), 4.13–4.04 (1H, m, C(15)H), 4.01 (1H, dt, J = 6.6, 3.0 Hz, C(14)H), 3.99–3.92 (1H, m, C(10)H), 3.92–3.87 (1H, m, C(3)H), 3.85 (1H, d, J = 1.1 Hz, C(11)H), 3.79 (3H, s, PMB-CH₃), 3.72 (1H, qd, J = 7.1, 2.7 Hz, C(2)H), 3.70–3.61 (2H, m, C(16)H_AH_B, C(7)H), 3.48 (1H, dd, J = 10.5, 6.3 Hz, C(16)H_AH_B), 3.23 (1H, dd, J = 13.4, 3.4 Hz, Bn-CH_AH_B), 3.14 (1H, br. s., OH), 2.78 (1H, dd, J = 13.4, 9.4 Hz, Bn-CH_AH_B), 2.10 (1H, dd, J = 13.2, 7.1 Hz, C(13)H_AH_B), 2.07 (3H, s, Ac-CH₃), 1.98–1.89 (1H, m, C(9)H_AH_B), 1.90–1.83 (2H, m, C(8)H_AH_B, C(5)H_AH_B), 1.79 (1H, dd, J = 13.3, 2.7 Hz, C(13)H_AH_B), 1.72–1.64 (1H, m, C(9)H_AH_B), 1.63–1.51 (2H, m, C(8)H_AH_B, C(4)H_AH_B), 1.51–1.37 (2H, m, C(4)H_AH_B, C(5)H_AH_B), 1.24 (3H, d, J = 7.0 Hz, C(2)CH₃), 1.24 (3H, s, C(12)CH₃), 1.03–0.91 (13H, m, DEIPS-EtCH₃ × 2, DEIPS-*i*PrCH₃ × 2, DEIPS-*i*PrCH), 0.88 (9H, s, TBS-C(CH₃)₃), 0.72–0.55 (4H, m, DEIPS-EtCH₂ × 2), 0.05 (6H, s, TBS-Si(CH₃)₂);

¹³C NMR (125 MHz, CDCl₃) δ_C 177.3 (C1), 170.9 (Ac-CO), 159.0 (PMB-C_{Ar}OMe), 153.0 (C1'), 134.9 (Bn-C_{Ar}CH₂), 130.4 (PMB-C_{Ar}CH₂), 129.4 (Bn-C_{Ar} × 2), 129.1 (PMB-C_{Ar} × 2), 128.9 (Bn-C_{Ar} × 2), 127.4 (Bn-C_{Ar}), 113.7 (PMB-C_{Ar} × 2), 85.0 (C12), 84.2 (C15), 80.6 (C14), 79.9 (C10), 78.7 (C7), 78.0 (C11), 75.1 (C6), 71.5 (C3), 71.0 (PMB-CH₂), 66.2 (C2'), 63.8 (C16), 55.2 (PMB-CH₃), 55.1 (C3'), 42.2 (C2), 42.0 (C13), 37.7 (Bn-CH₂), 29.3 (C4), 28.5 (C5), 28.1 (C8), 25.9 (TBS-C(CH₃)₃), 23.9 (C9), 22.0 (C12-CH₃), 21.1 (Ac-CH₃), 18.3 (TBS-C(CH₃)₃), 17.6 (DEIPS-*i*PrCH₃),

17.5 (DEIPS-*i*PrCH₃), 13.1 (DEIPS-*i*PrCH), 10.3 (C2-CH₃), 7.3 (DEIPS-EtCH₃), 7.3 (DEIPS-EtCH₃), 4.4 (DEIPS-EtCH₂), 4.1 (DEIPS-EtCH₂), -5.4 (TBS-SiCH₃), -5.5 (TBS-SiCH₃);

The spectral data were consistent with those previously reported.³⁸

(1*R*,4*S*,5*R*)-6-((*R*)-4-Benzyl-2-oxooxazolidin-3-yl)-1-((2*R*,5*S*)-5-((*S*)-((2*R*,4*S*,5*R*)-5-(((*tert*-butyldimethylsilyl)oxy)methyl)-4-((4-methoxybenzyl)oxy)-2-methyltetrahydrofuran-2-yl))((diethyl(isopropyl)silyl)oxy)methyl)tetrahydrofuran-2-yl)-5-methyl-6-oxo-4-((triethylsilyl)oxy)hexyl acetate (188**)**



Alcohol **187** (200 mg, 0.209 mmol) was dissolved in CH₂Cl₂ (2.0 mL) and cooled to 0 °C. Imidazole (72.0 mg, 1.05 mmol) and DMAP (2.3 mg, 19 μmol) were added, followed by the dropwise addition of TESCl (84 μL, 0.49 mmol). The reaction was warmed to room temperature and stirred for 2 h, and then quenched addition of a solution of NaHCO₃ (sat., 15 mL). The layers were allowed to separate, and the aqueous layer was extracted with Et₂O (3 × 15 mL). The organic layers were combined, dried (MgSO₄), filtered, and then concentrated *in vacuo*. Purification by flash column chromatography (SiO₂, 70:30 Pentane:EtOAc) afforded silyl ether **188** (223 mg, 100%) as a colourless oil.

$R_f = 0.75$ (70:30 Pentane:EtOAc);

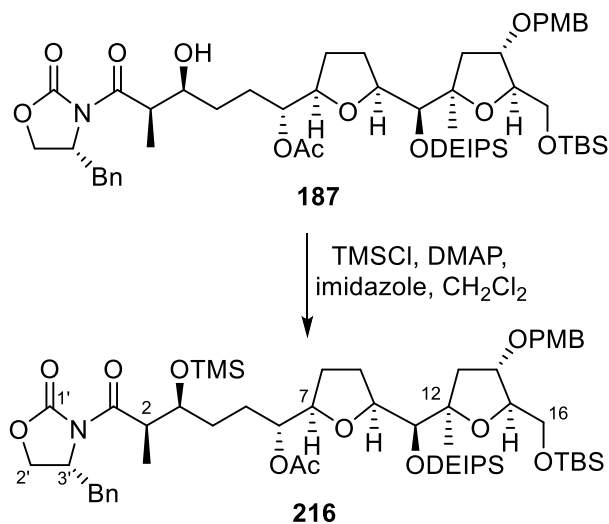
$[\alpha]_D^{25} -12.1$ ($c = 0.28$, CH_2Cl_2);

$^1\text{H NMR}$ (400 MHz, CDCl_3) δ_H 7.37–7.31 (2H, m, Bn-ArH \times 2), 7.30–7.27 (1H, m, Bn-ArH), 7.27–7.23 (2H, m, PMB-ArH \times 2), 7.23–7.18 (2H, m, Bn-ArH \times 2), 6.87 (2H, d, $J = 8.7$ Hz, PMB-ArH \times 2), 4.89 (1H, dt, $J = 7.0, 3.2$ Hz, C(6)H), 4.60 (1H, ddt, $J = 9.6, 6.3, 3.3$ Hz, C(3')H), 4.47 (1H, d, $J = 11.5$ Hz, PMB- CH_AH_B), 4.39 (1H, d, $J = 11.5$ Hz, PMB- CH_AH_B), 4.23–4.13 (2H, m, C(2')H₂), 4.07 (1H, td, $J = 6.9, 3.8$ Hz, C(15)H), 4.02–3.96 (2H, m, C(14)H, C(3)H), 3.98–3.88 (1H, m, C(10)H), 3.88–3.81 (2H, m, C(11)H, C(2)H), 3.80 (3H, s, PMB- CH_3), 3.69–3.59 (2H, m, C(16)H_AH_B, C(7)H), 3.45 (1H, dd, $J = 10.4, 6.7$ Hz, C(16)H_AH_B), 3.30–3.22 (1H, m, Bn- CH_AH_B), 2.76 (1H, dd, $J = 13.3, 9.7$ Hz, Bn- CH_AH_B), 2.10 (1H, dd, $J = 13.4, 7.2$ Hz, C(13)H_AH_B), 2.04 (3H, s, Ac- CH_3), 1.99–1.88 (1H, m, C(9)H_AH_B), 1.88–1.82 (1H, m, C(8)H_AH_B), 1.79 (1H, dd, $J = 13.3, 2.5$ Hz, C(13)H_AH_B), 1.72–1.63 (2H, m, C(5)H_AH_B, C(9)H_AH_B), 1.61–1.49 (3H, m, C(5)H_AH_B, C(4)H₂), 1.46–1.34 (1H, m, C(8)H_AH_B), 1.25 (3H, s, C(12)CH₃), 1.20 (3H, d, $J = 6.8$ Hz, C(2)CH₃), 1.01–0.91 (22H, m, DEIPS- $i\text{PrCH}_3 \times 2$, DEIPS-EtCH₃ \times 2, DEIPS- $i\text{PrCH}$, TES- $\text{CH}_3 \times 3$), 0.88 (9H, s, TBS-C(CH₃)₃), 0.72–0.46 (10H, m, DEIPS-EtCH₂ \times 2, TES-CH₂ \times 3), 0.05 (6H, s, TBS-Si(CH₃)₂);

$^{13}\text{C NMR}$ (100 MHz, CDCl_3) δ_C 175.1 (C1), 170.5 (Ac-CO), 159.1 (PMB-C_{Ar}OMe), 153.1 (C1'), 135.4 (Bn-C_{Ar}CH₂), 130.6 (PMB-C_{Ar}CH₂), 129.5 (Bn-C_{Ar} \times 2), 129.1 (PMB-C_{Ar} \times 2), 129.0 (Bn-C_{Ar} \times 2), 127.4 (Bn-C_{Ar}), 113.8 (PMB-C_{Ar} \times 2), 85.0 (C12), 84.3 (C15), 80.9 (C14), 79.9 (C10), 78.8 (C7), 78.0 (C11), 75.2 (C6), 72.8 (C3), 71.0 (PMB-CH₂), 66.1 (C2'), 63.9 (C16), 55.8 (C3'), 55.3 (PMB-CH₃), 42.6 (C2), 41.9 (C13), 37.7 (Bn-CH₂), 30.8 (C4), 28.2 (C8), 27.0 (C5), 26.0 (TBS-C(CH₃)₃), 23.9 (C9), 22.1 (C12-CH₃), 21.0 (Ac-CH₃), 18.4 (TBS-C(CH₃)₃), 17.7 (DEIPS- $i\text{PrCH}_3$), 17.6 (DEIPS- $i\text{PrCH}_3$), 13.2 (DEIPS- $i\text{PrCH}$), 11.9 (C2-CH₃), 7.4 (DEIPS-EtCH₃), 7.3 (DEIPS-EtCH₃), 7.0 (3 C, TES- $\text{CH}_3 \times 3$), 5.1 (3 C, TES-CH₂ \times 3), 4.5 (DEIPS-EtCH₂), 4.2 (DEIPS-EtCH₂), -5.4 (TBS-SiCH₃), -5.4 (TBS-SiCH₃);

The spectral data were consistent with those previously reported.³⁸

(1*R*,4*S*,5*R*)-6-((*R*)-4-Benzyl-2-oxooxazolidin-3-yl)-1-((2*R*,5*S*)-5-((*S*)-((2*R*,4*S*,5*R*)-5-(((tert-butyl)dimethylsilyl)oxy)methyl)-4-((4-methoxybenzyl)oxy)-2-methyltetrahydrofuran-2-yl)((diethyl(isopropyl)silyl)oxy)methyl)tetrahydrofuran-2-yl)-5-methyl-6-oxo-4-((trimethylsilyl)oxy)hexyl acetate (216**)**



Alcohol **187** (90.0 mg, 94.1 μmol) was dissolved in CH₂Cl₂ (1.8 mL) and cooled to 0 °C. Imidazole (65.0 mg, 0.941 mmol) and DMAP (1.2 mg, 9.4 μmol) were added, followed by the dropwise addition of TMSCl (60 μL , 49 μmol). The reaction was stirred for 5 min, and then quenched with water (1 mL). The layers were allowed to separate and the aqueous layer was extracted with CH₂Cl₂ (3 \times 6 mL). The organic layers were combined, dried (MgSO₄), filtered, and then concentrated *in vacuo*. Purification by flash column chromatography (SiO₂, 100:0 to 90:10 Pentane:EtOAc) afforded silyl ether **216** (83.0 mg, 86%) as a colourless oil .

$R_f = 0.8$ (70:30 Pentane:EtOAc);

$[\alpha]_D^{25} -24.8$ ($c = 0.44$, CH₂Cl₂);

¹H NMR (400 MHz, CDCl₃) δ_H 7.37–7.31 (2H, m, Bn-ArH \times 2), 7.32–7.26 (1H, m, Bn-ArH), 7.25 (2H, d, $J = 10.1$ Hz, PMB-ArH \times 2), 7.23–7.18 (2H, m, Bn-ArH \times 2), 6.87 (2H, d, $J = 8.6$ Hz, PMB-ArH \times 2), 4.94–4.85 (1H, m, C(6)H), 4.61 (1H, ddt, $J = 10.0, 6.4, 2.9$ Hz, C(3')H), 4.47 (1H, d, $J =$

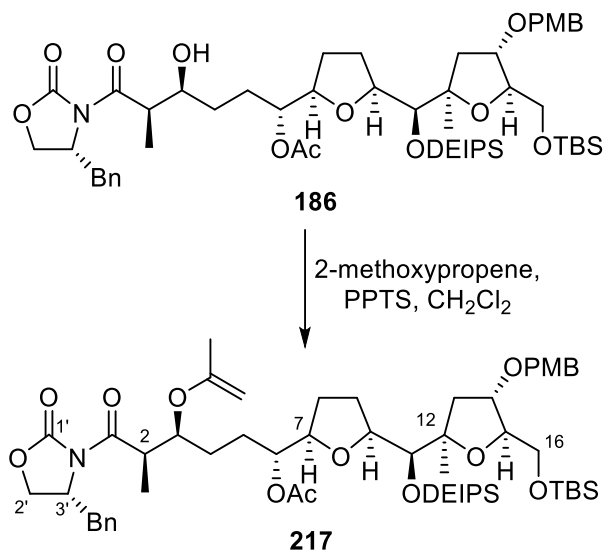
11.5 Hz, PMB-CH_AH_B), 4.39 (1H, d, *J* = 11.5 Hz, PMB-CH_AH_B), 4.24–4.12 (2H, m, C(2')H₂), 4.06 (1H, td, *J* = 6.7, 3.9 Hz, C(15)H), 4.04–3.98 (1H, m, C(14)H), 3.97–3.88 (2H, m, C(3)H, (C10)H), 3.88–3.82 (2H, m, C(11)H, C(2)H), 3.80 (3H, s, PMB-CH₃), 3.69–3.59 (2H, m, C(16)H_AH_B, C(7)H), 3.46 (1H, dd, *J* = 13.3, 3.2 Hz, C(16)H_AH_B), 3.26 (1H, dd, *J* = 13.3, 3.2 Hz, Bn-CH_AH_B), 2.76 (1H, dd, *J* = 13.3, 9.7 Hz, Bn-CH_AH_B), 2.10 (1H, dd, *J* = 13.4, 9.6 Hz, C(13)H_AH_B), 2.04 (3H, s, Ac-CH₃), 1.98–1.87 (1H, m, C(9)H_AH_B), 1.86–1.79 (1H, m, C(8)H_AH_B), 1.79 (1H, dd, *J* = 13.3, 2.8 Hz, C(13)H_AH_B), 1.79–1.64 (2H, m, C(5)H_AH_B, C(9)H_AH_B), 1.60–1.48 (3H, m, C(5)H_AH_B, C(4)H₂), 1.45–1.35 (1H, m, C(8)H_AH_B), 1.24 (3H, s, C(12)CH₃), 1.19 (3H, d, *J* = 6.8 Hz, C(2)CH₃), 1.03–0.93 (13H, m, DEIPS-*i*PrCH₃ × 2, DEIPS-EtCH₃ × 2, DEIPS-*i*PrCH), 0.89 (9H, s, TBS-C(CH₃)₃), 0.70–0.57 (4H, m, DEIPS-EtCH₂ × 2), 0.09 (9H, s, TMS-Si(CH₃)₃), 0.05 (6H, s, TBS-Si(CH₃)₂);

¹³C NMR (100 MHz, CDCl₃) δ_c 175.1 (C1), 170.5 (Ac-CO), 159.1 (PMB-C_{Ar}OMe), 153.1 (C1'), 135.3 (Bn-C_{Ar}CH₂), 130.6 (PMB-C_{Ar}CH₂), 129.4 (Bn-C_{Ar} × 2), 129.1 (PMB-C_{Ar} × 2), 128.9 (Bn-C_{Ar} × 2), 127.3 (Bn-C_{Ar}), 113.8 (PMB-C_{Ar} × 2), 85.0 (C12), 84.3 (C15), 80.9 (C14), 79.9 (C10), 78.8 (C7), 78.1 (C11), 75.1 (C6), 73.2 (C3), 71.0 (PMB-CH₂), 66.0 (C2'), 63.9 (C16), 55.7 (C3'), 55.3 (PMB-CH₃), 43.0 (C2), 42.0 (C13), 37.7 (Bn-CH₂), 30.7 (C4), 28.2 (C8), 27.7 (C5), 25.9 (TBS-C(CH₃)₃), 23.9 (C9), 22.1 (C12-CH₃), 21.0 (Ac-CH₃), 18.3 (TBS-C(CH₃)₃), 17.7 (DEIPS-*i*PrCH₃), 17.6 (DEIPS-*i*PrCH₃), 13.2 (DEIPS-*i*PrCH), 12.1 (C2-CH₃), 7.3 (DEIPS-EtCH₃), 7.3 (DEIPS-EtCH₃), 4.5 (DEIPS-EtCH₂), 4.2 (DEIPS-EtCH₂), 0.3 (3 C, TMS-Si(CH₃)₃), -5.4 (TBS-SiCH₃), -5.4 (TBS-SiCH₃);

IR ν_{max} (film)/cm⁻¹ 2953, 2929, 2860, 2362, 1783, 1736, 1701, 1379, 1248, 1111, 1040, 839;

HRMS (ESI⁺, *m/z*) C₅₄H₈₉O₁₂NNaSi₃⁺ [M + Na⁺] calculated 1050.55848, found 1050.55774 (Δ = -0.7 ppm).

(1*R*,4*S*,5*R*)-6-((*R*)-4-Benzyl-2-oxooxazolidin-3-yl)-1-((2*R*,5*S*)-5-((*S*)-((2*R*,4*S*,5*R*)-5-(((tert-butyl)dimethylsilyl)oxy)methyl)-4-((4-methoxybenzyl)oxy)-2-methyltetrahydrofuran-2-yl))((diethyl(isopropyl)silyl)oxy)methyl)tetrahydrofuran-2-yl)-5-methyl-6-oxo-4-(prop-1-en-2-yloxy)hexyl acetate (217**)**



Alcohol **186** (75.0 mg, 78.0 μ mol) and PPTS (2.0 mg, 7.8 μ mol) were dissolved in CH₂Cl₂ (2.0 mL). After which, 2-methoxypropene (90.0 mg, 1.25 mmol) was added and the resulting mixture was stirred for 1 hour at room temperature. NEt₃ (0.2 mL) was added and the mixture was filtered through a silica plug to afford **217** (78.5 mg, 100%) as a colourless oil.

R_f = 0.8 (60:40 Pentane:EtOAc);

[α]_D²⁵ -25.9 (*c* = 1.65, CH₂Cl₂);

¹H NMR (400 MHz, CDCl₃) δ _H 7.36–7.29 (2H, m, Bn-ArH \times 2), 7.32–7.27 (1H, m, Bn-ArH), 7.27–7.24 (2H, m, PMB-ArH \times 2), 7.24–7.18 (2H, m, Bn-ArH \times 2), 6.87 (2H, d, *J* = 8.6 Hz, PMB-ArH \times 2), 4.89 (1H, td, *J* = 7.2, 3.7 Hz, C(6)H), 4.58 (1H, ddt, *J* = 10.1, 7.0, 2.9, Hz C(3')H), 4.47 (1H, d, *J* = 11.6 Hz, PMB-CH_AH_B), 4.39 (1H, d, *J* = 11.5 Hz, PMB-CH_AH_B), 4.36–4.30 (1H, m, C(3)H), 4.24–4.13 (2H, m, C(2')H₂), 4.09–4.03 (1H, m, C(15)H), 4.03–3.96 (1H, m, C(14)H), 4.03–4.01 (1H, m, C(2)H), 3.94 (1H, ddd, *J* = 8.7, 7.0, 1.3 Hz, C(10)H), 3.89–3.87 (1H, m, C(11)H),

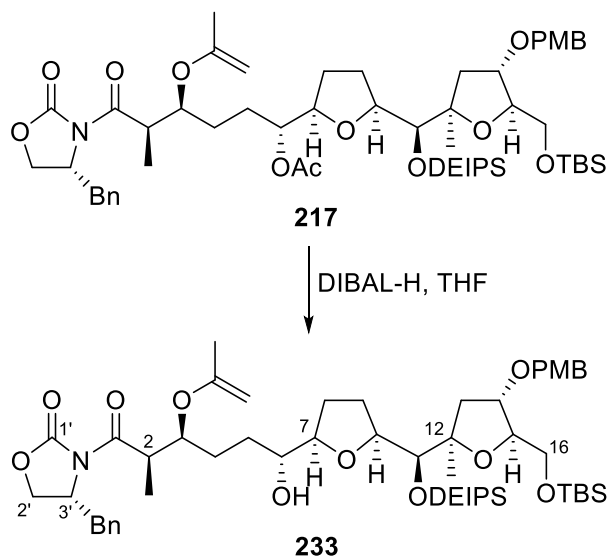
3.87–3.84 (2H, m, $H_2C=COCH_3$), 3.80 (3H, s, PMB- CH_3), 3.71–3.58 (2H, m, C(16) H_AH_B , C(7) H), 3.48 (1H, dd, $J = 10.4, 6.4$ Hz, C(16) H_AH_B), 3.28 (1H, dd, $J = 12.9, 2.9$ Hz, Bn- CH_AH_B), 2.77 (1H, dd, $J = 13.4, 9.6$ Hz, Bn- CH_AH_B), 2.11 (1H, dd, $J = 13.3, 7.2$ Hz, C(13) H_AH_B), 2.05 (3H, s, Ac- CH_3), 1.98–1.88 (1H, m, C(9) H_AH_B), 1.88–1.76 (2H, m, C(8) H_AH_B , C(13) H_AH_B), 1.77 (3H, s, $H_2C=COCH_3$), 1.75–1.59 (5H, m, C(5) H_2 , C(4) H_2 , C(9) H_AH_B), 1.48–1.36 (1H, m, C(8) H_AH_B), 1.25 (3H, d, $J = 7.0$ Hz, C(2) CH_3), 1.24 (3H, s, C(12) CH_3), 1.03–0.91 (13H, m, DEIPS-Et $CH_3 \times 2$, DEIPS- $iPrCH_3 \times 2$, DEIPS- $iPrCH$), 0.89 (9H, s, TBS-C(CH_3) $_3$), 0.72–0.56 (4H, m, DEIPS-Et $CH_2 \times 2$), 0.05 (6H, s, TBS-Si(CH_3) $_2$);

^{13}C NMR (100 MHz, $CDCl_3$) δ_c 174.5 (C1), 170.5 (Ac-CO), 159.2 (PMB- $C_{Ar}OMe$), 159.1 ($H_2C=COCH_3$), 153.1 (C1'), 135.3 (Bn- $C_{Ar}CH_2$), 130.6 (PMB- $C_{Ar}CH_2$), 129.4 (Bn- $C_{Ar} \times 2$), 129.1 (PMB- $C_{Ar} \times 2$), 128.9 (Bn- $C_{Ar} \times 2$), 127.3 (Bn- C_{Ar}), 113.8 (PMB- $C_{Ar} \times 2$), 84.9 (C12), 84.3 (C15), 81.7 ($H_2C=COCH_3$), 80.8 (C14), 79.9 (C10), 78.6 (C7), 78.0 (C11), 75.9 (C3), 75.0 (C6), 71.0 (PMB- CH_2), 66.2 (C2'), 63.8 (C16), 55.3 (PMB- CH_3), 55.3 (C3'), 42.0 (C13), 41.5 (C2), 37.8 (Bn- CH_2), 28.1 (C8), 27.4 (C4), 27.3 (C5), 25.9 (TBS-C(CH_3) $_3$), 23.9 (C9), 22.1 ($H_2C=COCH_3$), 21.3 (C12- CH_3), 21.1 (Ac- CH_3), 18.3 (TBS-C(CH_3) $_3$), 17.7 (DEIPS- $iPrCH_3$), 17.5 (DEIPS- $iPrCH_3$), 13.2 (DEIPS- $iPrCH$), 12.3 (C2- CH_3), 7.3 (DEIPS-Et CH_3), 7.3 (DEIPS-Et CH_3), 4.5 (DEIPS-Et CH_2), 4.2 (DEIPS-Et CH_2), -5.4 (TBS-Si CH_3), -5.4 (TBS-Si CH_3);

IR ν_{max} (film)/ cm^{-1} 2952, 1782, 1736, 1513, 1462, 1375, 1246, 1108, 1040, 837, 779;

HRMS (ESI $^+$, m/z) $C_{54}H_{85}O_{12}NNaSi_2^+$ [$M + Na^+$] calculated 1018.55025, found 1018.54889 ($\Delta = -1.34$ ppm).

(R)-4-benzyl-3-((2R,3S,6R)-6-((2R,5S)-5-((S)-((2R,4S,5R)-5-(((tert-butyl)dimethylsilyl)oxy)methyl)-4-((4-methoxybenzyl)oxy)-2-methyltetrahydrofuran-2-yl))((diethyl(isopropyl)silyl)oxy)methyl)tetrahydrofuran-2-yl)-6-hydroxy-2-methyl-3-(prop-1-en-2-yloxy)hexanoyl)oxazolidin-2-one (233)



Acetate **217** (35.0 mg, 35.1 μmol) was dissolved in THF (1.2 mL), and then cooled to $-78\text{ }^{\circ}\text{C}$. DIBAL-H (1 M in toluene, 0.12 mL, 0.12 mmol) was added dropwise to the solution, which was stirred for 3 h at $-78\text{ }^{\circ}\text{C}$. The reaction was topped up with DIBAL-H (1 M in toluene, 0.80 mL, 0.80 mmol) and stirred for an additional 5.5 h at $-78\text{ }^{\circ}\text{C}$. The reaction mixture was quenched by dropwise addition of EtOAc (3.6 mL) and stirred for 10 min, followed by dropwise addition of Rochelle's Salt (4.0 mL). The mixture was warmed to room temperature and stirred for 20 min. The layers were then allowed to separate, and the aqueous layer was extracted with Et₂O (4 \times 10 mL). The organic layers were combined, dried (MgSO₄), filtered, and concentrated *in vacuo*. Purification by flash column chromatography (SiO₂, 80:20 to 67:33 Pentane:Et₂O, then 85:15 to 75:25 Pentane:EtOAc) afforded **233** (13.6 mg, 41%) as a viscous colourless oil.

$R_f = 0.5$ (80:20 Pentane:EtOAc);

$[\alpha]_D^{25} -31.4$ ($c = 0.98$, CH₂Cl₂);

¹H NMR (400 MHz, CDCl₃) δ_{H} 7.36–7.31 (2H, m, Bn-ArH \times 2), 7.31–7.26 (1H, m, Bn-ArH), 7.25–7.23 (2H, m, PMB-ArH \times 2), 7.23–7.19 (2H, m, Bn-ArH \times 2), 6.87 (2H, d, J = 8.7 Hz, PMB-ArH \times 2), 4.60 (1H, ddt, J = 9.7, 6.4, 3.5 Hz, C(3')H), 4.47 (1H, d, J = 11.5 Hz, PMB-CH_AH_B), 4.42–4.35 (1H, m, C(3)H), 4.39 (1H, d, J = 11.5 Hz, PMB-CH_AH_B), 4.19–4.14 (2H, m, C(2')H₂), 4.10 (1H, dt, J = 6.5, 3.6 Hz, C(15)H), 4.07–3.98 (4H, m, C(2)H, C(14)H, C(10)H, C(15)H), 3.93–3.86 (2H, m, H₂C=COCH₃), 3.80 (3H, s, PMB-CH₃), 3.73 (1H, d, J = 2.6 Hz, C(11)H), 3.67 (1H, dd, J = 10.5, 3.9 Hz, C(16)H_AH_B), 3.56–3.44 (2H, m, C(7)H, C(16)H_AH_B), 3.44–3.37 (1H, m, C(6)H), 3.29 (1H, dd, J = 13.3, 3.2 Hz, Bn-CH_AH_B), 2.80–2.72 (2H, m, Bn-CH_AH_B, OH), 2.09–2.01 (1H, m, C(13)H_AH_B), 1.98–1.86 (2H, m, C(8)H_AH_B, C(9)H_AH_B), 1.86–1.79 (1H, m, C(4)H_AH_B), 1.83 (dd, J = 13.3, 2.6 Hz, C(13)H_AH_B), 1.78 (3H, s, H₂C=COCH₃), 1.78–1.73 (1H, m, C(9)H_AH_B), 1.71–1.62 (2H, m, C(5)H₂), 1.55–1.44 (1H, m, C(8)H_AH_B), 1.44–1.33 (1H, m, C(4)H_AH_B), 1.29 (3H, s, C(12)CH₃), 1.26 (3H, d, J = 6.9 Hz, C(2)CH₃), 1.02–0.94 (13H, m, DEIPS-EtCH₃ \times 2, DEIPS-*i*PrCH₃ \times 2, DEIPS-*i*PrCH), 0.89 (9H, s, TBS-C(CH₃)₃), 0.69–0.57 (4H, m, DEIPS-EtCH₂ \times 2), 0.05 (6H, s, TBS-Si(CH₃)₂);

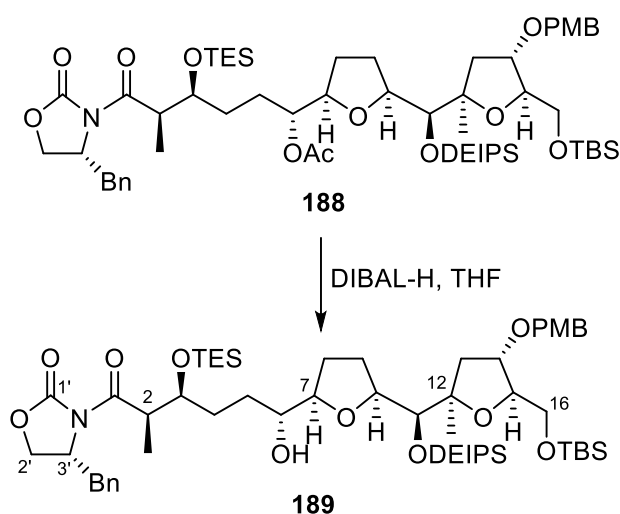
¹³C NMR (125 MHz, CDCl₃) δ_{C} 174.6 (C1), 159.2 (H₂C=COCH₃), 159.1 (PMB-C_{Ar}OMe), 153.1 (C1'), 135.3 (Bn-C_{Ar}CH₂), 130.5 (PMB-C_{Ar}CH₂), 129.5 (Bn-C_{Ar} \times 2), 129.1 (PMB-C_{Ar} \times 2), 128.9 (Bn-C_{Ar} \times 2), 127.3 (Bn-C_{Ar}), 113.8 (PMB-C_{Ar} \times 2), 85.3 (C12), 84.5 (C15), 81.9 (C7), 81.7 (H₂C=COCH₃), 80.5 (C14), 80.1 (C10), 79.0 (C11), 76.4 (C3), 74.2 (C6), 71.1 (PMB-CH₂), 66.1 (C2'), 63.7 (C16), 55.7 (C3'), 55.3 (PMB-CH₃), 42.6 (C13), 41.7 (C2), 37.8 (Bn-CH₂), 29.6 (C4), 28.3 (C5), 27.8 (C8), 25.9 (TBS-C(CH₃)₃), 25.7 (C9), 21.4 (C12-CH₃), 21.3 (H₂C=COCH₃), 18.3 (TBS-C(CH₃)₃), 17.6 (DEIPS-*i*PrCH₃), 17.5 (DEIPS-*i*PrCH₃), 13.4 (DEIPS-*i*PrCH), 12.4 (C2-CH₃), 7.4 (DEIPS-EtCH₃), 7.3 (DEIPS-EtCH₃), 4.8 (DEIPS-EtCH₂), 4.4 (DEIPS-EtCH₂), -5.4 (TBS-SiCH₃), -5.5 (TBS-SiCH₃);

IR ν_{max} (film)/cm⁻¹ 2952, 2935, 2862, 1783, 1696, 1514, 1462, 1382, 1248, 1110, 1099, 1042, 837, 778, 723;

HRMS (ESI⁺, *m/z*) C₅₂H₈₃O₁₁NNaSi₂⁺ [M + Na⁺] calculated 976.53969, found 976.53595

(Δ = -3.83 ppm).

(*R*)-4-Benzyl-3-((2*R*,3*S*,6*R*)-6-((2*R*,5*S*)-5-((*S*)-((2*R*,4*S*,5*R*)-5-(((*tert*-butyldimethylsilyl)oxy)methyl)-4-((4-methoxybenzyl)oxy)-2-methyltetrahydrofuran-2-yl)((diethyl(isopropyl)silyl)oxy)methyl)tetrahydrofuran-2-yl)-6-hydroxy-2-methyl-3-((triethylsilyl)oxy)hexanoyl)oxazolidin-2-one (189)



Acetate **188** (223 mg, 0.208 mmol) was dissolved in THF (6.4 mL), and then cooled to -78 °C. DIBAL-H (1 M in toluene, 0.63 mL, 0.63 mmol) was added dropwise to the solution, which was stirred for 1.5 h at -78 °C. Additional DIBAL-H (1 M in toluene, 0.42 mL, 0.42 mmol) was added before the reaction was stirred for 2 h at -78 °C. The reaction mixture was quenched by dropwise addition of EtOAc (18 mL) and stirred for 10 min, followed by dropwise addition of a solution of Rochelle's Salt (sat., 20 mL). The mixture was warmed to room temperature and stirred for 20 min. The layers were then allowed to separate, and the aqueous layer was extracted with Et₂O (4 × 20 mL). The organic layers were combined, dried (MgSO₄), filtered, and concentrated *in vacuo*. Purification by flash column chromatography (SiO₂, 80:20 to 60:40

Pentane:Et₂O) afforded alcohol **189** (260 mg, 75%) as a viscous colourless oil. Acetate **188** (45.0 mg, 20%) was also recovered.

R_f = 0.3 (60:40 Pentane:Et₂O);

[α]_D²⁵ -25.2 (c = 2.50, CH₂Cl₂);

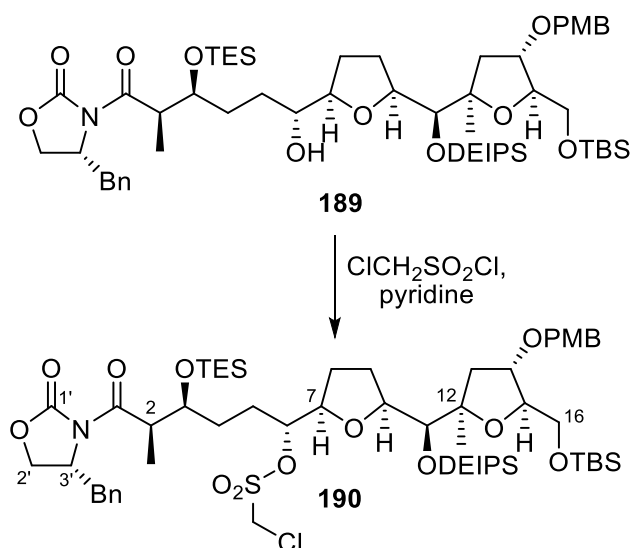
¹H NMR (400 MHz, CDCl₃) δ_H 7.37–7.32 (2H, m, Bn-ArH × 2), 7.32–7.28 (1H, m, Bn-ArH), 7.26 (2H, d, J = 6.0 Hz, PMB-ArH × 2), 7.24–7.20 (2H, m, Bn-ArH × 2), 6.88 (2H, d, J = 8.6 Hz, PMB-ArH × 2), 4.62 (1H, ddt, J = 9.6, 6.8, 3.4 Hz, C(3')H), 4.48 (1H, d, J = 11.5 Hz, PMB-CH_AH_B), 4.40 (1H, d, J = 11.5 Hz, PMB-CH_AH_B), 4.19–4.14 (2H, m, C(2')H₂), 4.10 (1H, dt, J = 6.7, 3.6 Hz, C(15)H), 4.09–3.98 (3H, m, C(14)H, C(10)H, C(3)H), 3.96–3.84 (1H, m, C(2)H), 3.81 (3H, s, PMB-CH₃), 3.75 (1H, d, J = 2.5 Hz, C(11)H), 3.68 (1H, dd, J = 10.5, 3.9 Hz, C(16)H_AH_B), 3.57–3.50 (1H, m, C(7)H), 3.50–3.46 (1H, m, C(16)H_AH_B), 3.46–3.38 (1H, m, C(6)H), 3.30 (1H, dd, J = 13.3, 3.3 Hz, Bn-CH_AH_B), 2.77 (1H, dd, J = 13.4, 9.7 Hz, Bn-CH_AH_B), 2.73 (1H, br. s., OH), 2.07 (1H, dd, J = 13.3, 7.2 Hz, C(13)H_AH_B), 2.02–1.89 (1H, m, C(9)H_AH_B), 1.90–1.73 (4H, m, C(4)H_AH_B, C(13)H_AH_B, C(8)H_AH_B, C(9)H_AH_B), 1.67–1.45 (3H, m, C(4)H_AH_B, C(5)H_AH_B, C(8)H_AH_B), 1.44–1.33 (1H, m, C(5)H_AH_B), 1.30 (3H, s, C(12)CH₃), 1.24 (3H, d, J = 6.9 Hz, C(2)CH₃), 1.04–0.92 (22H, m, TES-CH₃ × 3, DEIPS-EtCH₃ × 2, DEIPS-*i*PrCH₃ × 2, DEIPS-*i*PrCH), 0.90 (9H, s, TBS-C(CH₃)₃), 0.72–0.53 (10H, m, TES-CH₂ × 3, DEIPS-EtCH₂ × 2), 0.06 (6H, s, TBS-Si(CH₃)₂);

¹³C NMR (125 MHz, CDCl₃) δ_C 175.3 (C1), 159.1 (PMB-C_{Ar}OMe), 153.1 (C1'), 135.4 (Bn-C_{Ar}CH₂), 130.5 (PMB-C_{Ar}CH₂), 129.5 (Bn-C_{Ar} × 2), 129.1 (PMB-C_{Ar} × 2), 128.9 (Bn-C_{Ar} × 2), 127.3 (Bn-C_{Ar}), 113.8 (PMB-C_{Ar} × 2), 85.3 (C12), 84.5 (C15), 82.0 (C7), 80.6 (C14), 80.0 (C10), 79.0 (C11), 74.4 (C6), 73.4 (C3), 71.1 (PMB-CH₂), 66.0 (C2'), 63.7 (C16), 55.8 (C3'), 55.3 (PMB-CH₃), 43.0 (C2), 42.6 (C13), 37.7 (Bn-CH₂), 31.4 (C4), 29.3 (C5), 27.8 (C8), 25.9 (3 C, TBS-C(CH₃)₃), 25.6 (C9), 21.5 (C12-CH₃), 18.3 (TBS-C(CH₃)₃), 17.6 (DEIPS-*i*PrCH₃), 17.5 (DEIPS-*i*PrCH₃), 13.4 (DEIPS-*i*PrCH), 12.0 (C2-CH₃), 7.4 (DEIPS-EtCH₃), 7.3 (DEIPS-EtCH₃), 7.0 (3 C, TES-

EtCH₃ × 3), 5.1 (3 C, TES-EtCH₂ × 3), 4.8 (DEIPS-EtCH₂), 4.4 (DEIPS-EtCH₂), -5.4 (TBS-SiCH₃), -5.5 (TBS-SiCH₃);

The spectral data were consistent with those previously reported.³⁸

(1*R*,4*S*,5*R*)-6-((*R*)-4-Benzyl-2-oxooxazolidin-3-yl)-1-((2*R*,5*S*)-5-((*S*)-((2*R*,4*S*,5*R*)-5-(((*tert*-butyldimethylsilyl)oxy)methyl)-4-((4-methoxybenzyl)oxy)-2-methyltetrahydrofuran-2-yl))((diethyl(isopropyl)silyl)oxy)methyl)tetrahydrofuran-2-yl)-5-methyl-6-oxo-4-((triethylsilyl)oxy)hexyl chloromethanesulfonate (190)



Alcohol **189** (100 mg, 97.2 μmol) was dissolved in pyridine (0.77 mL, 9.5 mmol), and then cooled to 0 °C. Chloromethanesulfonyl chloride (22 μL, 0.24 mmol) was added dropwise to the solution, which was stirred for 30 min at 0 °C, warmed to room temperature and stirred for a further 3 h. The reaction mixture was quenched by dropwise addition of water (1.5 mL) and diluted with Et₂O (4.0 mL). The layers were allowed to separate and the aqueous layer was extracted with Et₂O (4 × 4.0 mL). The organic layers were combined, dried (MgSO₄), filtered, and concentrated *in vacuo*. Purification by flash column chromatography (SiO₂, 90:10 to 80:20 Pentane:EtOAc) afforded **190** (104 mg, 94%) as a viscous yellow oil.

$R_f = 0.6$ (80:20 Pentane:EtOAc);

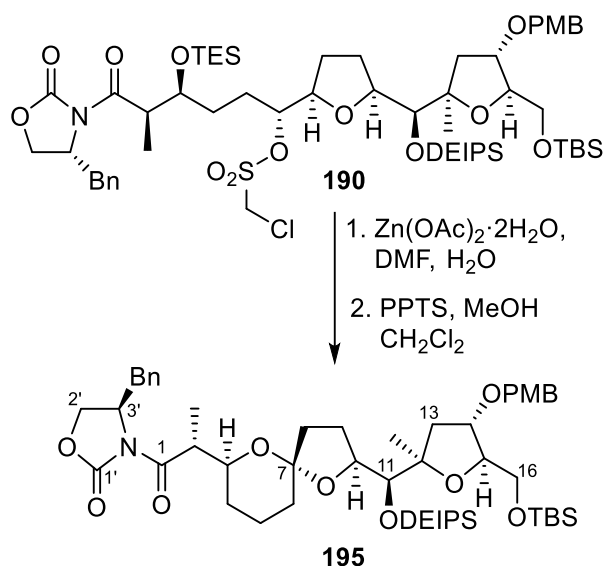
$[\alpha]_D^{25} -38.5$ ($c = 1.63$, CH_2Cl_2);

$^1\text{H NMR}$ (500 MHz, CDCl_3) δ_H 7.36–7.30 (2H, m, Bn-ArH \times 2), 7.31–7.23 (1H, m, Bn-ArH), 7.28–7.23 (2H, m, PMB-ArH \times 2), 7.23–7.18 (2H, m, Bn-ArH \times 2), 6.87 (2H, d, $J = 8.6$ Hz, PMB-ArH \times 2), 4.86 (1H, d, $J = 12.0$ Hz, $\text{SO}_2\text{CH}_A\text{H}_B\text{Cl}$), 4.73 (1H, d, $J = 12.0$ Hz, $\text{SO}_2\text{CH}_A\text{H}_B\text{Cl}$), 4.69–4.62 (2H, m, C(3')H, C(6)H), 4.46 (1H, d, $J = 11.5$ Hz, PMB- CH_AH_B), 4.40 (1H, d, $J = 11.5$ Hz, PMB- CH_AH_B), 4.26 (1H, dd, $J = 8.5, 8.1$ Hz, C(2') H_AH_B), 4.14 (1H, dd, $J = 9.0, 2.1$ Hz, C(2') H_AH_B), 4.13–4.04 (2H, m, C(10)H, C(15)H), 4.05–3.98 (2H, m, C(3)H, C(14)H), 3.95–3.86 (1H, m, C(2)H), 3.80 (3H, s, PMB- CH_3), 3.76–3.71 (1H, m, C(7)H), 3.70 (1H, d, $J = 1.8$ Hz, C(11)H), 3.64 (1H, dd, $J = 10.6, 4.1$ Hz, C(16) H_AH_B), 3.46 (1H, dd, $J = 10.5, 6.3$ Hz, C(16) H_AH_B), 3.25 (1H, dd, $J = 13.4, 3.2$ Hz, Bn- CH_AH_B), 2.78 (1H, dd, $J = 13.4, 9.5$ Hz, Bn- CH_AH_B), 2.11–2.02 (1H, m, C(9) H_AH_B), 2.01–1.94, (1H, m, C(13) H_AH_B), 1.93–1.60 (7H, m, C(13) H_AH_B , C(5) H_AH_B , C(8) H_2 , C(9) H_AH_B , C(4) H_2), 1.46–1.34 (1H, m, C(5) H_AH_B), 1.25 (3H, s, C(12) CH_3), 1.25 (3H, d, $J = 6.6$, C(2) CH_3), 1.03–0.92 (22H, m, DEIPS- $\text{CH}_3 \times 4$, DEIPS-CH, TES- $\text{CH}_3 \times 3$), 0.88 (9H, s, TBS-C(CH_3) $_3$), 0.72–0.53 (10H, m, TES- $\text{CH}_2 \times 3$, DEIPS- $\text{CH}_2 \times 2$), 0.04 (3H, s, TBS-Si CH_3), 0.04 (3H, s, TBS-Si CH_3);

$^{13}\text{C NMR}$ (125 MHz, CDCl_3) δ_C 175.3 (C1), 159.1 (PMB- C_{Ar}OMe), 153.2 (C1'), 135.4 (Bn- C_{Ar}CH_2), 130.5 (PMB- C_{Ar}CH_2), 129.5 (Bn- $\text{C}_{Ar} \times 2$), 129.1 (PMB- $\text{C}_{Ar} \times 2$), 128.9 (Bn- $\text{C}_{Ar} \times 2$), 127.3 (Bn- C_{Ar}), 113.8 (PMB- $\text{C}_{Ar} \times 2$), 88.8 (C6), 85.1 (C12), 84.7 (C15), 80.9 (C14), 80.8 (C10), 79.8 (C7), 79.4 (C11), 73.2 (C3), 71.0 (PMB- CH_2), 66.2 (C2'), 64.0 (C16), 55.6 (C3'), 55.3 (PMB- OCH_3), 54.3 ($\text{SO}_2\text{CH}_2\text{Cl}$), 42.8 (C13, C2), 37.7 (Bn- CH_2), 30.4 (C4), 28.4 (C5), 27.7 (C8), 25.9 (TBS-C(CH_3) $_3$), 24.4 (C9), 21.3 (C12- CH_3), 18.3 (TBS-C(CH_3) $_3$), 17.6 (DEIPS- $i\text{PrCH}_3$), 17.5 (DEIPS- $i\text{PrCH}_3$), 13.3 (C2- CH_3), 13.3 (DEIPS- $i\text{PrCH}$), 7.4 (DEIPS-Et CH_3), 7.3 (DEIPS-Et CH_3), 7.0 (TES- $\text{CH}_3 \times 3$), 5.2 (TES- $\text{CH}_2 \times 3$), 4.8 (DEIPS-Et CH_2), 4.4 (DEIPS-Et CH_2), -5.3 (TBS-Si CH_3), -5.4 (TBS-Si CH_3);

The spectral data were consistent with those previously reported.³⁸

(R)-4-Benzyl-3-((R)-2-((2S,5S,7S)-2-((S)-((2R,4S,5R)-5-(((tert-butyl)dimethylsilyl)oxy)methyl)-4-((4-methoxybenzyl)oxy)-2-methyltetrahydrofuran-2-yl)((diethyl(isopropyl)silyl)oxy)methyl)-1,6-dioxaspiro[4.5]decan-7-yl)propanoyl)oxazolidin-2-one (195)



Chloromethyl sulfonate **190** (19.5 mg, 17.1 μmol) was dissolved in DMF (0.27 mL) and water (0.20 mL). Zn(OAc)₂·2H₂O (38.0 mg, 0.171 mmol) was then added and the resulting mixture was heated to 75 °C and stirred for 12 h. After which, the mixture was cooled to room temperature and diluted with brine (2.5 mL). The layers were allowed to separate and the aqueous layer was extracted with Et₂O (3 \times 2.5 mL). The organic layers were combined, dried (MgSO₄), filtered, and concentrated *in vacuo*. Purification by flash column chromatography (SiO₂, 90:10 to 80:20 Pentane:EtOAc) afforded a mixture of lactol and ketone intermediate (7.1 mg, 40%) as a viscous yellow oil. The mixture was dissolved in CH₂Cl₂ (0.27 mL) and MeOH (0.27 mL), and cooled to 0 °C. Pyridium *p*-toluenesulfonate (PPTS, 1.0 mg, 3.9 μmol) was added to the solution, which was stirred at 0 °C for 2 h. After which, the reaction was quenched with a solution of NaHCO₃ (sat., 0.3 mL). The mixture was diluted with Et₂O (2.5 mL), washed with water (0.5 mL), dried (MgSO₄), filtered, and concentrated *in vacuo*. Purification by flash

column chromatography (SiO₂, 90:10 Pentane:EtOAc) afforded spiroketal **195** (2.8 mg, 45%) as a viscous colourless oil.

R_f = 0.7 (80:20 Pentane:EtOAc);

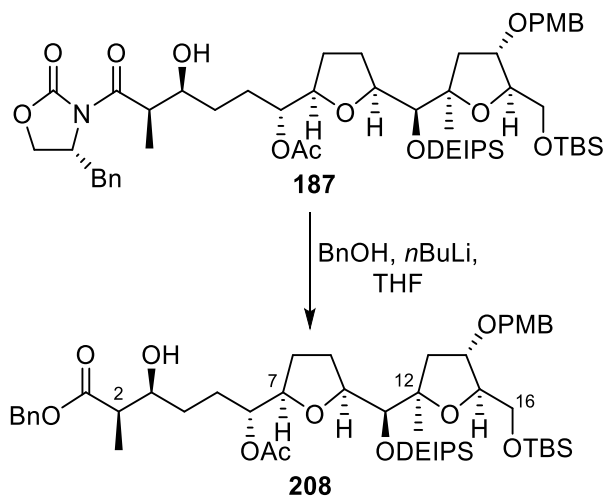
[α]_D²⁵ -6.8 (c = 0.49, CH₂Cl₂);

¹H NMR (400 MHz, CDCl₃) δ_H 7.37–7.23 (5H, m, Bn-ArH × 5), 7.21 (2H, d, J = 8.4 Hz, PMB-ArH × 2), 6.87 (2H, d, J = 8.7 Hz, PMB-ArH × 2), 4.66–4.59 (1H, m, C(3')H), 4.48 (1H, d, J = 11.5 Hz, PMB-CH_AH_B), 4.38 (1H, d, J = 11.5 Hz, PMB-CH_AH_B), 4.22 (1H, t, J = 8.3, C(10)H), 4.20–4.09 (2H, m, C(2')H₂), 4.09–3.93 (3H, m, C(15)H, C(14)H, C(3)H), 3.91–3.82 (2H, m, C(2)H, C(11)H), 3.80 (3H, s, PMB-CH₃), 3.67 (1H, dd, J = 10.3, 4.1 Hz, C(16)H_AH_B), 3.42 (1H, dd, J = 10.4, 7.2 Hz, C(16)H_AH_B), 3.27 (1H, dd, J = 13.3, 3.3 Hz, Bn-CH_AH_B), 2.76 (1H, dd, J = 13.3, 9.6 Hz, Bn-CH_AH_B), 2.09 (1H, dd, J = 13.4, 7.2 Hz, C(13)H_AH_B), 1.97–1.90 (1H, m, C(9)H_AH_B), 1.90–1.69 (4H, m, C(5)H_AH_B, C(8)H_AH_B, C(13)H_AH_B, C(9)H_AH_B), 1.68–1.54 (5H, m, C(5)H_AH_B, C(6)H₂, C(4)H_AH_B, C(8)H_AH_B), 1.31–1.19 (7H, m, C(4)H_AH_B, C(12)CH₃, C(2)CH₃), 1.03–0.93 (13H, m, DEIPS-CH₃ × 4, DEIPS-*i*PrCH), 0.89 (9H, s, TBS-C(CH₃)₃), 0.69–0.51 (4H, m, DEIPS-CH₂ × 2), 0.10–0.02 (6H, m, TBS-Si(CH₃)₂);

¹³C NMR (100 MHz, CDCl₃) δ_C 175.2 (C1), 159.1 (PMB-C_{Ar}OMe), 153.0 (C1'), 135.4 (Bn-C_{Ar}CH₂), 130.7 (PMB-C_{Ar}CH₂), 129.4 (PMB-C_{Ar} × 2), 129.1 (Bn-C_{Ar} × 2), 128.9 (Bn-C_{Ar} × 2), 127.3 (Bn-C_{Ar}), 113.8 (PMB-C_{Ar} × 2), 105.0 (C7), 85.1 (C12), 84.3 (C15), 81.7 (C14), 78.4 (C11), 78.0 (C10), 70.9 (PMB-CH₂), 70.9 (C3), 65.9 (C2'), 64.1 (C16), 55.5 (C3'), 55.3 (PMB-CH₃), 42.5 (C2), 41.3 (C13), 38.0 (C8), 37.9 (Bn-CH₂), 32.3 (C6), 28.0 (C4), 26.0 (TBS-C(CH₃)₃), 22.7 (C9), 22.3 (C12-CH₃), 20.2 (C5), 18.4 (TBS-C(CH₃)₃), 17.7 (DEIPS-*i*PrCH₃), 17.6 (DEIPS-*i*PrCH₃), 13.4 (DEIPS-*i*PrCH), 13.4 (C2-CH₃), 7.3 (DEIPS-EtCH₃), 7.3 (DEIPS-EtCH₃), 4.6 (DEIPS-EtCH₂), 4.3 (DEIPS-EtCH₂), -5.3 (TBS-SiCH₃), -5.4 (TBS-SiCH₃);

The spectral data were consistent with those previously reported.³⁸

Benzyl(2*R*,3*S*,6*R*)-6-acetoxy-6-((2*R*,5*S*)-5-((*S*)-((2*R*,4*S*,5*R*)-5-(((tert-butyl)dimethylsilyl)oxy)methyl)-4-((4-methoxybenzyl)oxy)-2-methyltetrahydrofuran-2-yl)((diethyl(isopropyl)silyl)oxy)methyl)tetrahydrofuran-2-yl)-2-methyl-3-((triethylsilyl)oxy)hexanoate (**208**)



Benzyl alcohol (19.0 mg, 0.173 mmol) was dissolved in THF (0.19 mL), and the solution was cooled to 0 °C. *n*BuLi (1.6 M in hexanes, 0.08 mL, 0.125 mmol) was added dropwise and the solution was stirred for 15 min at 0 °C. Oxazolidinone **187** (15.0 mg, 15.7 μmol) dissolved in THF (0.10 mL) was then added dropwise to the solution. The reaction mixture was stirred at 0 °C for 20 min. An aqueous solution of NaOH (1 M, 0.44 mL) and CH₂Cl₂ (0.44 mL) were added sequentially. The layers were allowed to separate and the aqueous layer was extracted with CH₂Cl₂ (4 × 5.0 mL). The organic layers were combined, dried (MgSO₄), filtered, and concentrated *in vacuo*. Purification by flash column chromatography (SiO₂, 90:10 Pentane:EtOAc, then pure EtOAc) afforded ester **208** as a viscous colourless oil (12.8 mg, 91%).

$R_f = 0.8$ (50:50 EtOAc:Petane);

$[\alpha]_D^{25} +11.3$ ($c = 0.23$, CH₂Cl₂);

¹H NMR (400 MHz, CDCl₃) δ_H 7.40–7.35 (2H, m, Bn-ArH × 2), 7.35–7.34 (2H, m, Bn-ArH), 7.34–7.30 (1H, m, Bn-ArH × 2), 7.28–7.21 (2H, m, PMB-ArH × 2), 6.87 (2H, d, $J = 8.6$ Hz, PMB-

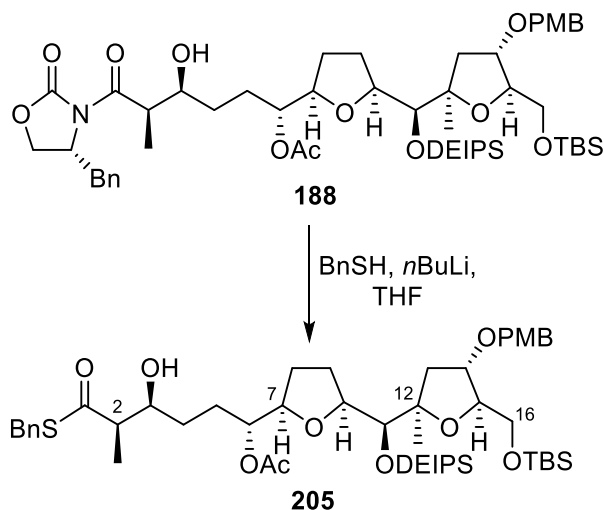
ArH × 2), 5.14 (2H, s, Bn-CH₂), 4.95 (1H, td, *J* = 7.8, 3.9 Hz, C(6)H), 4.47 (1H, d, *J* = 11.6 Hz, PMB-CH_AH_B), 4.39 (1H, d, *J* = 11.6 Hz, PMB-CH_AH_B), 4.06 (1H, dt, *J* = 6.4, 3.8 Hz, C(15)H), 4.02 (1H, dt, *J* = 6.5, 3.0 Hz, C(14)H), 3.98–3.91 (1H, m, C(10)H), 3.91–3.86 (1H, m, C(3)H), 3.85 (1H, d, *J* = 1.3 Hz, C(11)H), 3.80 (3H, s, PMB-CH₃), 3.69–3.59 (2H, m, C(16)H_AH_B, C(7)H), 3.48 (1H, dd, *J* = 10.5, 4.5 Hz, C(16)H_AH_B), 2.64 (1H, br. s., OH), 2.55 (1H, qd, *J* = 7.1, 3.5 Hz, C(2)H), 2.10 (1H, dd, *J* = 13.3, 7.1 Hz, C(13)H_AH_B), 2.04 (3H, s, Ac-CH₃), 1.98–1.86 (1H, m, C(9)H_AH_B), 1.86–1.80 (2H, m, C(8)H_AH_B, C(5)H_AH_B), 1.80–1.75 (1H, m, C(13)H_AH_B), 1.72–1.61 (1H, m, C(9)H_AH_B), 1.61–1.51 (2H, m, C(8)H_AH_B, C(4)H_AH_B), 1.51–1.33 (2H, m, C(4)H_AH_B, C(5)H_AH_B), 1.24 (3H, s, C(12)CH₃), 1.20 (3H, d, *J* = 7.1 Hz, C(2)CH₃), 1.03–0.92 (13H, m, DEIPS-EtCH₃ × 2, DEIPS-*i*PrCH₃ × 2, DEIPS-*i*PrCH), 0.89 (9H, s, TBS-C(CH₃)₃), 0.73–0.56 (4H, m, DEIPS-EtCH₂ × 2), 0.06 (6H, s, TBS-Si(CH₃)₂);

¹³C NMR (100 MHz, CDCl₃) δ_c 175.8 (C1), 170.7 (Ac-CO), 159.1 (PMB-C_{Ar}OMe), 135.7 (Bn-C_{Ar}CH₂), 130.6 (PMB-C_{Ar}CH₂), 129.1 (PMB-C_{Ar} × 2), 128.6 (Bn-C_{Ar} × 2), 128.3 (Bn-C_{Ar}), 128.2 (Bn-C_{Ar} × 2), 113.8 (PMB-C_{Ar} × 2), 84.9 (C12), 84.3 (C15), 80.8 (C14), 79.9 (C10), 78.7 (C7), 78.1 (C11), 75.1 (C6), 71.8 (C3), 71.1 (PMB-CH₂), 66.5 (Bn-CH₂), 63.8 (C16), 55.2 (PMB-CH₃), 44.4 (C2), 42.1 (C13), 29.5 (C4), 28.5 (C5), 28.1 (C8), 26.0 (TBS-C(CH₃)₃), 23.9 (C9), 22.1 (C12-CH₃), 21.1 (Ac-CH₃), 18.4 (TBS-C(CH₃)₃), 17.7 (DEIPS-*i*PrCH₃), 17.6 (DEIPS-*i*PrCH₃), 13.2 (DEIPS-*i*PrCH), 10.6 (C2-CH₃), 7.3 (DEIPS-EtCH₃), 7.3 (DEIPS-EtCH₃), 4.5 (DEIPS-EtCH₂), 4.2 (DEIPS-EtCH₂), -5.4 (TBS-SiCH₃), -5.4 (TBS-SiCH₃);

IR ν_{max} (film)/cm⁻¹ 3484, 2928, 2859, 2360, 1736, 1514, 1462, 1370, 1247, 1094, 940, 807;

HRMS (ESI⁺, *m/z*) C₄₈H₇₈NaO₁₁Si₂⁺ [M + Na⁺] calculated 909.49749, found 909.49683 (Δ = -1.50 ppm).

(1*R*,4*S*,5*R*)-6-(Benzylthio)-1-((2*R*,5*S*)-5-((*S*)-((2*R*,4*S*,5*R*)-5-(((tert-butyl)dimethylsilyl)oxy)methyl)-4-((4-methoxybenzyl)oxy)-2-methyltetrahydrofuran-2-yl)((diethyl(isopropyl)silyl)oxy)methyl)tetrahydrofuran-2-yl)-5-methyl-6-oxo-4-((triethylsilyl)oxy)hexyl acetate (**205**)



Benzyl mercaptan (17 μ L, 0.14 mmol) was dissolved in THF (0.22 mL), and the solution was cooled to 0 °C. *n*BuLi (2.2 M in hexanes, 0.051 mL, 0.11 mmol) was added dropwise and the solution was stirred for 15 min at 0 °C. Oxazolidinone **188** (15.0 mg, 14.0 μ mol) dissolved in THF (0.1 mL) was then added dropwise to the solution. The reaction mixture was stirred at 0 °C for 20 min. An aqueous solution of NaOH (1 M, 0.4 mL) and CH₂Cl₂ (0.4 mL) were added sequentially. The layers were allowed to separate, and the aqueous layer was extracted with CH₂Cl₂ (4 \times 1.0 mL). The organic layers were combined, dried (MgSO₄), filtered, and concentrated *in vacuo*. Purification by flash column chromatography (SiO₂, 98:2 to 90:10 Pentane:EtOAc) afforded thioester **205** (12.7 mg, 90%) as a colourless oil.

R_f = 0.7 (90:10 Pentane:EtOAc);

$[\alpha]_D^{25}$ -6.4 (c = 1.06, CH₂Cl₂);

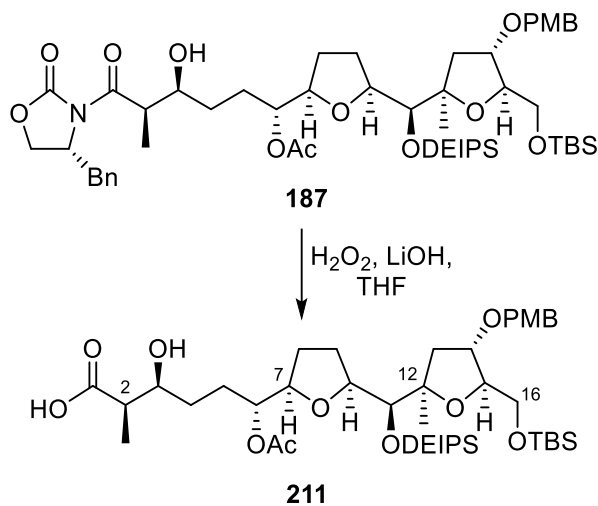
¹H NMR (400 MHz, CDCl₃) δ_{H} 7.33–7.26 (2H, m, Bn-ArH \times 2), 7.30–7.27 (1H, m, Bn-ArH), 7.26–7.23 (2H, m, PMB-ArH \times 2), 7.23–7.17 (2H, m, Bn-ArH \times 2), 6.86 (2H, d, J = 8.6 Hz, PMB-ArH \times 2), 4.87 (1H, dt, J = 7.3, 3.8 Hz, C(6)H), 4.46 (1H, d, J = 11.6 Hz, PMB-CH_AH_B), 4.38 (1H, d, J = 11.6 Hz, PMB-CH_AH_B), 4.09 (2H, s, Bn-CH₂), 4.06 (1H, td, J = 6.7, 3.7 Hz, C(15)H), 4.03–3.96 (2H, m, C(14)H, C(3)H), 3.96–3.89 (1H, m, (C10)H), 3.85–3.83 (1H, m, C(11)H), 3.79 (3H, s, PMB-CH₃), 3.69–3.56 (2H, m, C(16)H_AH_B, C(7)H), 3.46 (1H, dd, J = 10.5, 6.5 Hz, C(16)H_AH_B), 2.72–2.61 (1H, m, C(2)H), 2.10 (1H, dd, J = 13.3, 7.2 Hz, C(13)H_AH_B), 2.01 (3H, s, Ac-CH₃), 1.97–1.89 (1H, m, C(9)H_AH_B), 1.89–1.79 (1H, m, C(8)H_AH_B), 1.79–1.73 (1H, m, C(13)H_AH_B), 1.73–1.58 (2H, m, C(5)H_AH_B, C(9)H_AH_B), 1.59–1.47 (3H, m, C(5)H_AH_B, C(4)H₂), 1.47–1.31 (1H, m, C(8)H_AH_B), 1.23 (3H, s, C(12)CH₃), 1.17 (3H, d, J = 6.9 Hz, C(2)CH₃), 1.02–0.90 (22H, m, DEIPS-*i*PrCH₃ \times 2, DEIPS-EtCH₃ \times 2, DEIPS-*i*PrCH, TES-CH₃ \times 3), 0.88 (9H, s, TBS-C(CH₃)₃), 0.70–0.50 (10H, m, DEIPS-EtCH₂ \times 2, TES-CH₂ \times 3), 0.04 (6H, s, TBS-Si(CH₃)₂);

¹³C NMR (100 MHz, CDCl₃) δ_{C} 201.2 (C1), 170.4 (Ac-CO), 159.1 (PMB-C_{Ar}OMe), 137.5 (Bn-C_{Ar}CH₂), 130.6 (PMB-C_{Ar}CH₂), 129.1 (PMB-C_{Ar} \times 2), 128.8 (Bn-C_{Ar} \times 2), 128.6 (Bn-C_{Ar} \times 2), 127.2 (Bn-C_{Ar}), 113.8 (PMB-C_{Ar} \times 2), 85.0 (C12), 84.3 (C15), 80.8 (C14), 79.9 (C10), 78.7 (C7), 78.1 (C11), 74.9 (C6), 73.3 (C3), 71.1 (PMB-CH₂), 63.8 (C16), 55.3 (PMB-CH₃), 53.2 (C2), 42.0 (C13), 33.1 (Bn-CH₂), 30.9 (C4), 28.1 (C8), 27.0 (C5), 26.0 (TBS-C(CH₃)₃), 23.9 (C9), 22.1 (C12-CH₃), 21.0 (Ac-CH₃), 18.4 (TBS-C(CH₃)₃), 17.7 (DEIPS-*i*PrCH₃), 17.6 (DEIPS-*i*PrCH₃), 13.2 (DEIPS-*i*PrCH), 12.7 (C2-CH₃), 7.3 (DEIPS-EtCH₃), 7.3 (DEIPS-EtCH₃), 6.9 (TES-CH₃ \times 3), 5.1 (TES-CH₂ \times 3), 4.5 (DEIPS-EtCH₂), 4.2 (DEIPS-EtCH₂), -5.4 (TBS-SiCH₃), -5.4 (TBS-SiCH₃);

IR ν_{max} (film)/cm⁻¹ 2953, 2935, 2876, 1739, 1684, 1514, 1496, 1245, 1097, 1039, 836, 724;

HRMS (ESI⁺, m/z) C₅₄H₉₃O₁₀SSi₃⁺ [M + H⁺] calculated 1017.57918, found 1017.57928 (Δ = +0.11 ppm).

(2R,3S,6R)-6-acetoxy-6-((2R,5S)-5-((S)-((2R,4S,5R)-5-(((tert-butyl)dimethylsilyl)oxy)methyl)-4-((4-methoxybenzyl)oxy)-2-methyltetrahydrofuran-2-yl)((diethyl(isopropyl)silyl)oxy)methyl)tetrahydrofuran-2-yl)-3-hydroxy-2-methylhexanoic acid (211**)**



Lithium hydroxide monohydrate (20.1 mg, 0.471 mmol) was dissolved in hydrogen peroxide aqueous solution (30%, 2.4 mL) at 0 °C and stirred for 5 min. Oxazolidinone **187** (150 mg, 0.157 mmol) was dissolved in THF (2.4 mL) and added dropwise to the mixture. The reaction was stirred for 40 min at 0 °C, before being diluted with CH₂Cl₂ (23 mL), quenched by addition of a solution of Na₂SO₃ (sat. 2.4 mL), and acidified with HCl (1 M, 5.0 mL). The layers were separated and the aqueous phase was extracted with CH₂Cl₂ (4 × 45 mL). The organic layers were combined, dried (MgSO₄), filtered and concentrated *in vacuo*. Purification by flash column chromatography (SiO₂, 100:0 to 93:7 CH₂Cl₂:MeOH) afforded carboxylic acid **211** (107 mg, 86%) as a viscous colourless oil.

R_f = 0.4 (90:10 CH₂Cl₂:MeOH);

[α]_D²⁵ -3.8 (c = 1.47, CH₂Cl₂);

¹H NMR (400 MHz, CDCl₃) δ_H 7.25 (2H, d, *J* = 8.5 Hz, PMB-ArH × 2), 6.87 (2H, d, *J* = 8.2 Hz, PMB-ArH × 2), 4.96 (1H, dt, *J* = 11.6, 5.4 Hz, C(6)H), 4.47 (1H, d, *J* = 11.5 Hz, PMB-CH_AH_B), 4.40 (1H,

d, $J = 11.5$ Hz, PMB-CH_AH_B), 4.07 (1H, dt, $J = 6.8, 4.0$ Hz, C(15)H), 4.02 (1H, dt, $J = 6.6, 3.0$ Hz, C(14)H), 3.99–3.88 (2H, m, C(3)H, C(10)H), 3.85 (1 H, d, $J = 1.4$ Hz, C(11)H), 3.80 (3 H, s, PMB-CH₃), 3.71–3.59 (2H, m, C(16)H_AH_B, C(7)H), 3.49 (1H, dd, $J = 10.6, 6.3$ Hz, C(16)H_AH_B), 2.61–2.51 (1H, m, C(2)H), 2.14–2.04 (1H, m, C(13)H_AH_B), 2.07 (3H, s, Ac-CH₃), 1.95–1.86 (1H, m, C(9)H_AH_B), 1.89–1.82 (2H, m, C(5)H_AH_B, C(8)H_AH_B), 1.80 (1H, dd, $J = 13.2, 2.9$ Hz, C(13)H_AH_B), 1.74–1.64 (1H, m, C(9)H_AH_B), 1.64–1.45 (3H, m, C(5)H_AH_B, C(4)H₂), 1.46–1.37 (1H, m, C(8)H_AH_B), 1.24 (3H, s, C(12)CH₃), 1.18 (3H, d, $J = 7.2$ Hz, C(2)CH₃), 1.03–0.92 (13H, m, DEIPS-*i*PrCH₃ × 2, DEIPS-EtCH₃ × 2, DEIPS-*i*PrCH), 0.89 (9H, s, TBS-C(CH₃)₃), 0.71–0.57 (4H, m, DEIPS-EtCH₂ × 2), 0.05 (6H, s, TBS-Si(CH₃)₂);

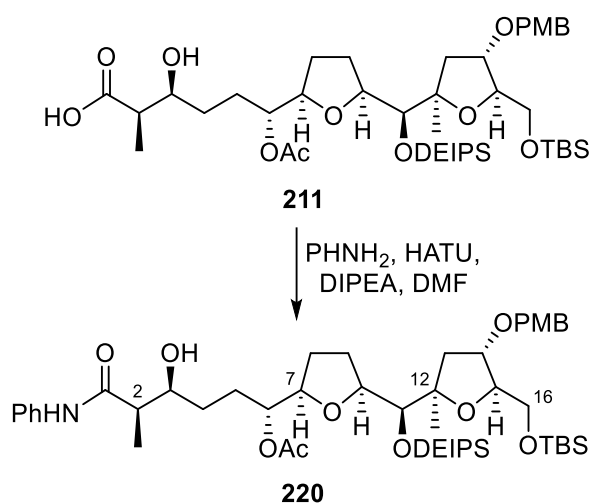
¹³C NMR (100 MHz, CDCl₃) δ_c 180.0 (C1), 171.1 (Ac-CO), 159.1 (PMB-C_{Ar}OMe), 130.5 (PMB-C_{Ar}CH₂), 129.1 (PMB-C_{Ar} × 2), 113.8 (PMB-C_{Ar} × 2), 84.9 (C12), 84.3 (C15), 80.7 (C14), 79.9 (C10), 78.6 (C7), 78.1 (C11), 75.0 (C6), 71.7 (C3), 71.1 (PMB-CH₂), 63.8 (C16), 55.3 (PMB-CH₃), 44.2 (C2), 42.1 (C13), 29.1 (C4), 28.4 (C5), 28.0 (C8), 25.9 (TBS-C(CH₃)₃), 24.0 (C9), 22.0 (C12-CH₃), 21.1 (Ac-CH₃), 18.3 (TBS-C(CH₃)₃), 17.6 (DEIPS-*i*PrCH₃), 17.5 (DEIPS-*i*PrCH₃), 13.2 (DEIPS-*i*PrCH), 10.4 (C2-CH₃), 7.3 (DEIPS-EtCH₃), 7.3 (DEIPS-EtCH₃), 4.5 (DEIPS-EtCH₂), 4.2 (DEIPS-EtCH₂), -5.4 (TBS-SiCH₃), -5.4 (TBS-SiCH₃);

IR ν_{\max} (film)/cm⁻¹ 2951, 1736, 1514, 1463, 1246, 1173, 1129, 1038, 836;

HRMS (ESI⁻, m/z) C₄₁H₇₁O₁₁Si₂⁻ [M⁻] calculated 795.45404, found 795.45349 ($\Delta = -0.89$ ppm).

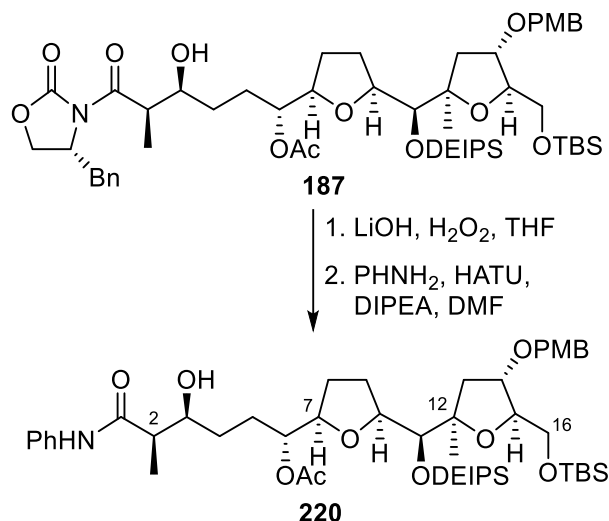
(1*R*,4*S*,5*R*)-1-((2*R*,5*S*)-5-((*S*)-((2*R*,4*S*,5*R*)-5-(((*tert*-Butyldimethylsilyl)oxy)methyl)-4-((4-methoxybenzyl)oxy)-2-methyltetrahydrofuran-2-yl)((diethyl(isopropyl)silyl)oxy)methyl)tetrahydrofuran-2-yl)-4-hydroxy-5-methyl-6-oxo-6-(phenylamino)hexyl acetate (220**)**

Procedure A:



Carboxylic acid **211** (201 mg, 0.252 mmol, azeotropically distilled with benzene three times), DIPEA (0.066 mL, 0.378 mmol), and HATU (105 mg, 0.277 mmol) were dissolved in DMF (2.1 mL) and stirred at room temperature for 30 min. After which, freshly distilled aniline (28.2 mg, 0.303 mmol) was added to the reaction mixture, which was stirred for a further 2 h. The reaction was quenched with a solution of NH₄Cl (sat., 8.0 mL). The layers were allowed to separate and the aqueous layer was extracted with CH₂Cl₂ (4 × 20 mL). The organic layers were combined, washed with brine (10 mL), dried (MgSO₄), and then concentrated *in vacuo*. Purification by flash column chromatography (SiO₂, 80:20 to 65:35 Pentane:EtOAc) afforded amide **220** (215 mg, 98%) as a colourless oil.

Procedure B:



Lithium hydroxide monohydrate (405 mg, 9.66 mmol) was dissolved in 34.5–36.5% hydrogen peroxide aqueous solution (49.4 mL) at 0 °C and stirred for 5 min. Oxazolidinone **187** (3.08 g, 3.22 mmol) was dissolved in THF (49 mL) and added dropwise to the mixture. The reaction was stirred for 1 hour 40 min at 0 °C, before being diluted with EtOAc (160 mL), quenched by addition of aqueous Na₂SO₃ (sat., 500 mL). The resulting mixture was stirred at 0 °C for 1.5 h. After which, HCl (3 M, 4.0 mL) was added to the mixture. The layers were allowed to separate and the aqueous phase was extracted with EtOAc (4 × 260 mL). The organic layers were combined, dried (NaHCO₃), filtered, and concentrated *in vacuo*. Crude carboxylic acid **211** was taken directly to the next step.

Carboxylic acid **211** (3.22 mmol, assumed quant. from previous step, azeotroped with PhMe three times), DIPEA (841 μL, 4.83 mmol), and HATU (1.35 g, 3.54 mmol) were dissolved in DMF (26 mL) and stirred at room temperature for 30 min. After which, aniline (353 μL, 3.86 mmol) was added to the reaction mixture, which was stirred for a further 1 hour 45 min. The reaction was quenched with NH₄Cl (sat., 31 mL) and HCl (3 M, 5.7 mL). The layers were allowed to separate and the aqueous layer was extracted with Et₂O (4 × 40 mL). The organic layers were

combined, washed with a solution made up from brine (95 mL) and NaHCO₃ (sat., 12 mL), dried (MgSO₄), and then concentrated *in vacuo*. Purification by flash column chromatography (SiO₂, 80:20 to 65:35 to 50:50 Pentane:EtOAc) afforded amide **220** (2.29 g, 81% over 2 steps) as a yellow oil.

R_f = 0.8 (50:50 Pentane:EtOAc);

[α]_D²⁵ -8.2 (c = 0.85, CH₂Cl₂);

¹H NMR (400 MHz, CDCl₃) δ_H 8.09 (1H, s, PhNH), 7.54–7.49 (2H, m, PhH × 2), 7.35–7.28 (2H, m, PhH × 2), 7.29–7.21 (2H, m, PMB-ArH × 2), 7.14–7.05 (1H, m, PhH), 6.87 (2H, d, J = 8.6 Hz, PMB-ArH × 2), 4.96 (1H, td, J = 7.6, 4.5 Hz, C(6)H), 4.47 (1H, d, J = 11.6 Hz, PMB-CH_AH_B), 4.39 (1H, d, J = 11.5 Hz, PMB-CH_AH_B), 4.06 (1H, dt, J = 6.3, 3.8 Hz, C(15)H), 4.04–3.99 (1H, m, C(14)H), 3.99–3.91 (2H, m, C(10)H, C(3)H), 3.84 (1H, d, J = 1.3 Hz, C(11)H), 3.80 (3H, s, PMB-CH₃), 3.69–3.62 (2H, m, C(16)H_AH_B, C(7)H), 3.62 (1H, br. s., OH), 3.48 (1H, dd, J = 10.5, 6.2 Hz, C(16)H_AH_B), 2.50 (1H, qd, J = 7.1, 2.8 Hz, C(2)H), 2.10 (1H, dd, J = 13.4, 7.1 Hz, C(13)H_AH_B), 2.04 (3H, s, Ac-CH₃), 2.00–1.89 (1H, m, C(9)H_AH_B), 1.91–1.82 (1H, m, C(8)H_AH_B), 1.80 (1H, dd, J = 13.2, 2.7 Hz, C(13)H_AH_B), 1.74–1.66 (1H, m, C(9)H_AH_B), 1.66–1.60 (4H, m, C(8)H_AH_B, C(4)H_AH_B, C(5)H₂), 1.51–1.40 (1H, m, C(4)H_AH_B), 1.24 (3H, d, J = 7.3 Hz, C(2)CH₃), 1.24 (3H, s, C(12)CH₃), 1.03–0.91 (13H, m, DEIPS-EtCH₃ × 2, DEIPS-*i*PrCH₃ × 2, DEIPS-*i*PrCH), 0.89 (9H, s, TBS-C(CH₃)₃), 0.73–0.57 (4H, m, DEIPS-EtCH₂ × 2), 0.05 (6H, s, TBS-Si(CH₃)₂);

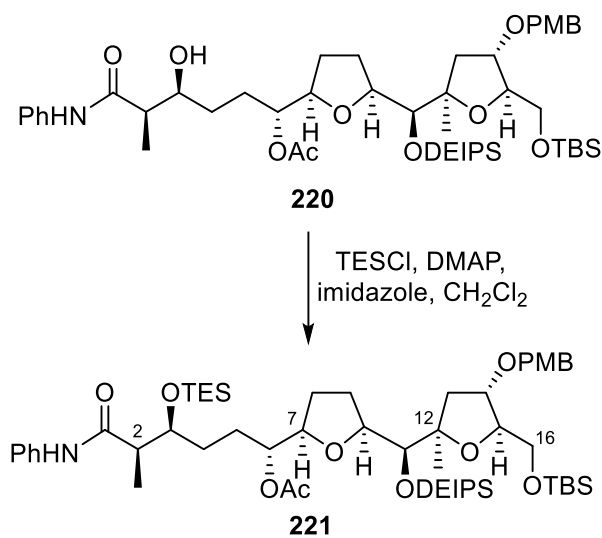
¹³C NMR (100 MHz, CDCl₃) δ_C 173.9 (C1), 171.4 (Ac-CO), 159.1 (PMB-C_{Ar}OMe), 137.8 (Ph-C_{Ar}N), 130.5 (PMB-C_{Ar}CH₂), 129.1 (PMB-C_{Ar} × 2), 129.0 (Ph-C_{Ar} × 2), 124.2 (Ph-C_{Ar}), 119.9 (Ph-C_{Ar} × 2), 113.8 (PMB-C_{Ar} × 2), 84.9 (C12), 84.3 (C15), 80.7 (C14), 79.9 (C10), 78.6 (C7), 78.1 (C11), 75.2 (C6), 72.4 (C3), 71.1 (PMB-CH₂), 63.8 (C16), 55.3 (PMB-CH₃), 46.4 (C2), 42.1 (C13), 28.9 (C4), 28.7 (C5), 28.1 (C8), 25.9 (TBS-C(CH₃)₃), 24.0 (C9), 22.0 (C12-CH₃), 21.1 (Ac-CH₃), 18.3 (TBS-C(CH₃)₃), 17.6 (DEIPS-*i*PrCH₃), 17.5 (DEIPS-*i*PrCH₃), 13.2 (DEIPS-*i*PrCH), 11.5 (C2-CH₃),

7.3 (DEIPS-EtCH₃), 7.3 (DEIPS-EtCH₃), 4.5 (DEIPS-EtCH₂), 4.2 (DEIPS-EtCH₂), -5.4 (TBS-SiCH₃),
-5.4 (TBS-SiCH₃);

IR ν_{\max} (film)/cm⁻¹ 3316, 2953, 2935, 2876, 2861, 1737, 1665, 1601, 1462, 1443, 1248, 1095,
1039, 837, 724;

HRMS (ESI⁺, *m/z*) C₄₇H₇₇O₁₀NNaSi₂⁺ [M + Na⁺] calculated 894.49782, found 894.49719
(Δ = -0.7 ppm).

(1*R*,4*S*,5*R*)-1-((2*R*,5*S*)-5-((*S*)-((2*R*,4*S*,5*R*)-5-(((*tert*-Butyldimethylsilyl)oxy)methyl)-4-((4-methoxybenzyl)oxy)-2-methyltetrahydrofuran-2-yl)((diethyl(isopropyl)silyl)oxy)methyl)tetrahydrofuran-2-yl)-5-methyl-6-oxo-6-(phenylamino)-4-((triethylsilyl)oxy)hexyl acetate (221)



Amide **220** (200 mg, 0.229 mmol) was dissolved in CH₂Cl₂ (3.0 mL) and cooled to 0 °C. Imidazole (156 mg, 2.29 mmol) and DMAP (2.5 mg, 21 μmol) were added, followed by the dropwise addition of TESCI (96 μL, 0.573 mmol). The reaction was warmed to room temperature and stirred for 15 min, and then quenched with water (4.0 mL). The layers were allowed to separate and the aqueous layer was extracted with CH₂Cl₂ (3 × 8.0 mL). The organic layers were combined, dried (MgSO₄), filtered, and then concentrated *in vacuo*. Purification

by flash column chromatography (SiO₂, pure pentane then 85:15 Pentane:EtOAc) afforded silyl ether **221** (218 mg, 97%) as a colourless oil.

R_f = 0.8 (70:30 Pentane:EtOAc);

[α]_D²⁵ -13.8 (c = 0.73, CH₂Cl₂);

¹H NMR (400 MHz, CDCl₃) δ_H 8.50 (1H, s, PhNH), 7.53–7.44 (2H, m, PhH × 2), 7.34–7.27 (2H, m, PhH × 2), 7.27–7.20 (2H, m, PMB-ArH × 2), 7.11–7.03 (1H, m, PhH), 6.86 (2H, d, J = 8.7 Hz, PMB-ArH × 2), 4.87 (1H, dt, J = 6.6, 4.1 Hz, C(6)H), 4.47 (1H, d, J = 11.5 Hz, PMB-CH_AH_B), 4.39 (1H, d, J = 11.5 Hz, PMB-CH_AH_B), 4.06 (1H, td, J = 6.9, 3.9 Hz, C(15)H), 4.03–3.97 (1H, m, C(14)H), 3.91–3.88 (1H, ddd, J = 8.6, 6.9, 1.3 Hz, C(10)H), 3.87–3.84 (1H, m, C(11)H), 3.84–3.82 (1H, m, C(3)H), 3.80 (3H, s, PMB-CH₃), 3.65 (1H, dd, J = 10.4, 4.2 Hz, C(16)H_AH_B), 3.64–3.56 (1H, m, C(7)H), 3.45 (1H, dd, J = 10.4, 6.7 Hz, C(16)H_AH_B), 2.65 (1H, qd, J = 7.2, 3.9 Hz, C(2)H), 2.09 (1H, dd, J = 13.2, 2.7 Hz, C(13)H_AH_B), 1.97 (3H, s, Ac-CH₃), 1.99–1.86 (1H, m, C(9)H_AH_B), 1.84–1.71 (2H, m, C(5)H_AH_B, C(8)H_AH_B), 1.78 (1H, dd, J = 13.4, 2.7 Hz, C(13)H_AH_B), 1.69–1.60 (1H, m, C(9)H_AH_B), 1.58–1.46 (3H, m, C(5)H_AH_B, C(4)H₂), 1.44–1.34 (1H, m, C(8)H_AH_B), 1.23 (3H, s, C(12)CH₃), 1.16 (3H, d, J = 7.2 Hz, C(2)CH₃), 1.06–0.91 (22H, m, DEIPS-*i*PrCH₃ × 2, DEIPS-EtCH₃ × 2, DEIPS-*i*PrCH, TES-CH₃ × 3), 0.88 (9H, s, TBS-C(CH₃)₃), 0.74–0.55 (10H, m, DEIPS-EtCH₂ × 2, TES-CH₂ × 3), 0.00 (6H, s, TBS-Si(CH₃)₂);

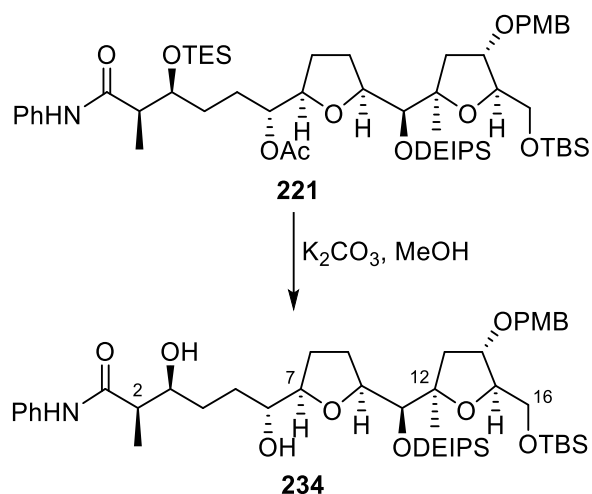
¹³C NMR (100 MHz, CDCl₃) δ_C 171.8 (Ac-CO), 170.4 (C1), 159.1 (PMB-C_{Ar}OMe), 138.3 (Ph-C_{Ar}N), 130.6 (PMB-C_{Ar}CH₂), 129.1 (PMB-C_{Ar} × 2), 129.0 (Ph-C_{Ar} × 2), 123.8 (Ph-C_{Ar}), 119.6 (Ph-C_{Ar} × 2), 113.8 (PMB-C_{Ar} × 2), 85.0 (C12), 84.3 (C15), 81.0 (C14), 79.9 (C10), 78.4 (C7), 78.0 (C11), 75.1 (C6), 74.9 (C3), 71.0 (PMB-CH₂), 63.9 (C16), 55.3 (PMB-CH₃), 46.7 (C2), 41.8 (C13), 28.0 (C4), 28.0 (C5), 28.0 (C8), 25.9 (TBS-C(CH₃)₃), 24.0 (C9), 22.1 (C12-CH₃), 20.9 (Ac-CH₃), 18.3 (TBS-C(CH₃)₃), 17.7 (DEIPS-*i*PrCH₃), 17.6 (DEIPS-*i*PrCH₃), 13.2 (DEIPS-*i*PrCH), 12.8 (C2-

CH₃), 7.3 (DEIPS-EtCH₃), 7.3 (DEIPS-EtCH₃), 6.9 (TES-EtCH₃ × 3), 5.0 (TES-EtCH₂ × 3), 4.5 (DEIPS-EtCH₂), 4.2 (DEIPS-EtCH₂), -5.4 (TBS-SiCH₃), -5.4 (TBS-SiCH₃);

IR ν_{\max} (film)/cm⁻¹ 3318, 2954, 2877, 1740, 1601, 1461, 1442, 1247, 1096, 1040, 837, 725;

HRMS (ESI⁺, *m/z*) C₅₃H₉₂O₁₀NSi₃⁺ [M + H⁺] calculated 986.60235, found 986.60156 (Δ = -0.8 ppm).

(2*R*,3*S*,6*R*)-6-((2*R*,5*S*)-5-((*S*)-((2*R*,4*S*,5*R*)-5-(((*tert*-Butyldimethylsilyl)oxy)methyl)-4-((4-methoxybenzyl)oxy)-2-methyltetrahydrofuran-2-yl)((diethyl(isopropyl)silyl)oxy)methyl)tetrahydrofuran-2-yl)-3,6-dihydroxy-2-methyl-N-phenylhexanamide (**234**)



K₂CO₃ (7.5 mg, 54 μ mol) was added to a solution of **221** (13.3 mg, 13.5 μ mol) in MeOH (1.0 mL). The reaction mixture was stirred at room temperature for 26 h. The reaction was quenched by addition of water (5.0 mL) and CH₂Cl₂ (5.0 mL). The aqueous and organic layers were then allowed to separate, and the aqueous layer was extracted with CH₂Cl₂ (4 × 5 mL). The organic layers were combined, dried (MgSO₄), filtered, and concentrated *in vacuo*. Purification by flash column chromatography (SiO₂, 100:0 to 60:40 Pentane:EtOAc) afforded diol **234** (9.9 mg, 88%) as a viscous colourless oil.

$R_f = 0.2$ (80:20 Pentane:EtOAc);

$[\alpha]_D^{25} -18.1$ ($c = 0.75$, CH_2Cl_2);

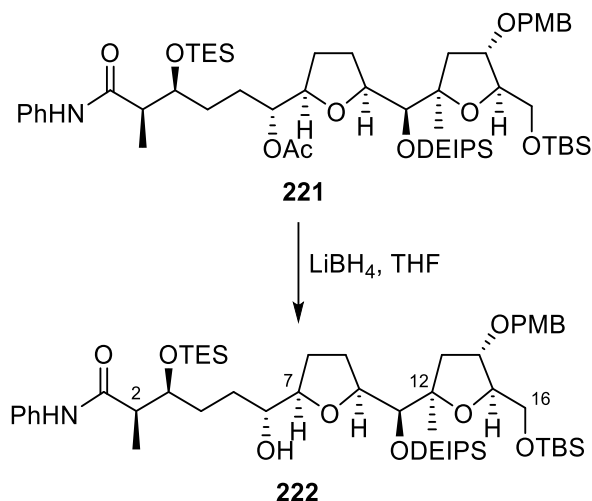
$^1\text{H NMR}$ (400 MHz, CDCl_3) δ_H 8.43 (1H, s, PhNH), 7.57–7.48 (2H, m, PhH \times 2), 7.35–7.28 (2H, m, PhH \times 2), 7.25 (2H, d, $J = 8.7$ Hz, PMB-ArH \times 2), 7.11–7.05 (1H, m, PhH), 6.87 (2H, d, $J = 8.6$ Hz, PMB-ArH \times 2), 4.47 (1H, d, $J = 11.4$ Hz, PMB- CH_AH_B), 4.40 (1H, d, $J = 11.6$ Hz, PMB- CH_AH_B), 4.12 (1H, dt, $J = 6.5, 3.6$ Hz, C(15)H), 4.07–4.02 (2H, m, C(14)H, C(6)H), 4.02–3.94 (2H, m, C(3)H, C(10)H), 3.80 (3H, s, PMB- CH_3), 3.66 (1H, d, $J = 3.4$ Hz, C(11)H), 3.66 (1H, dd, $J = 10.5, 3.7$ Hz, C(16) H_AH_B), 3.64–3.58 (1H, m, C(7)H), 3.49 (1H, dd, $J = 10.4, 6.2$ Hz, C(16) H_AH_B), 3.45 (1H, br. s., OH), 2.60 (1H, qd, $J = 7.1, 2.9$ Hz, C(2)H), 2.03 (1H, dd, $J = 13.3, 7.1$ Hz, C(13) H_AH_B), 1.97–1.79 (4H, m, C(8) H_AH_B , C(9) H_2), 1.86 (1H, dd, $J = 13.3, 2.5$ Hz, C(13) H_AH_B), 1.71–1.59 (4H, m, C(8) H_AH_B , C(4) H_AH_B , C(5) H_2), 1.53–1.44 (1H, m, C(4) H_AH_B), 1.31 (3H, s, C(12) CH_3), 1.25 (3H, d, $J = 7.1$ Hz, C(2) CH_3), 1.03–0.91 (13H, m, DEIPS-Et $\text{CH}_3 \times 2$, DEIPS- $i\text{PrCH}_3 \times 2$, DEIPS- $i\text{PrCH}$), 0.89 (9H, s, TBS-C(CH_3) $_3$), 0.71–0.57 (4H, m, DEIPS-Et $\text{CH}_2 \times 2$), 0.05 (6H, s, TBS-Si(CH_3) $_2$);

$^{13}\text{C NMR}$ (100 MHz, CDCl_3) δ_C 173.8 (C1), 159.1 (PMB- C_{Ar}OMe), 138.2 (Ph- C_{Ar}N), 130.5 (PMB- C_{Ar}CH_2), 129.1 (PMB- $\text{C}_{Ar} \times 2$), 128.9 (Ph- $\text{C}_{Ar} \times 2$), 123.9 (Ph- C_{Ar}), 119.8 (Ph- $\text{C}_{Ar} \times 2$), 113.8 (PMB- $\text{C}_{Ar} \times 2$), 85.7 (C12), 84.7 (C15), 81.4 (C7), 80.4 (C14), 80.2 (C10), 79.6 (C11), 74.1 (C6), 72.4 (C3), 71.1 (PMB- CH_2), 63.6 (C16), 55.3 (PMB- CH_3), 46.4 (C2), 42.8 (C13), 29.7 (C4), 29.2 (C5), 27.8 (C8), 26.4 (C9), 25.9 (TBS-C(CH_3) $_3$), 21.2 (C12- CH_3), 18.3 (TBS-C(CH_3) $_3$), 17.6 (DEIPS- $i\text{PrCH}_3$), 17.5 (DEIPS- $i\text{PrCH}_3$), 13.5 (DEIPS- $i\text{PrCH}$), 11.9 (C2- CH_3), 7.4 (DEIPS-Et CH_3), 7.3 (DEIPS-Et CH_3), 4.8 (DEIPS-Et CH_2), 4.5 (DEIPS-Et CH_2), -5.4 (TBS-Si CH_3), -5.5 (TBS-Si CH_3);

$\text{IR } \nu_{\text{max}}$ (film)/ cm^{-1} 3307, 2952, 2934, 2877, 2862, 1665, 1601, 1543, 1514, 1501, 1249, 1096, 1040, 837, 723;

HRMS (ESI $^+$, m/z) $\text{C}_{45}\text{H}_{75}\text{NO}_9\text{Si}_2\text{Na}^+$ [M + Na $^+$] calculated 852.48726, found 852.48654 ($\Delta = -0.85$ ppm).

(2R,3S,6R)-6-((2R,5S)-5-((S)-((2R,4S,5R)-5-(((tert-Butyldimethylsilyl)oxy)methyl)-4-((4-methoxybenzyl)oxy)-2-methyltetrahydrofuran-2-yl)((diethyl(isopropyl)silyl)oxy)methyl)tetrahydrofuran-2-yl)-6-hydroxy-2-methyl-N-phenyl-3-((triethylsilyl)oxy)hexanamide (222)



Acetate **221** (165 mg, 0.167 mmol, azeotroped three times in benzene) was dissolved in THF (6.9 mL). LiBH₄ (72.9 mg, 3.34 mmol) was added to the solution, which was warmed to 40 °C and stirred for 10 h. The reaction mixture was quenched by dropwise addition of a solution of NH₄Cl (sat., 9.0 mL). The aqueous and organic layers were then allowed to separate, and the aqueous layer was extracted with Et₂O (4 × 30 mL). The organic layers were combined, dried (MgSO₄), filtered, and concentrated *in vacuo*. Purification by flash column chromatography (SiO₂, 85:15 Pentane:EtOAc) afforded alcohol **222** (96.5 mg, 61%) as a pale yellow oil and unreacted diol **221** (28.7 mg, 17%).

R_f = 0.5 (80:20 Pentane:EtOAc);

[α]_D²⁵ -12.5 (c = 0.41, CH₂Cl₂);

¹H NMR (400 MHz, CDCl₃) δ_H 8.72 (1H, s, PhNH), 7.53–7.48 (2H, m, PhH × 2), 7.34–7.27 (2H, m, PhH × 2), 7.27–7.22 (2H, m, PMB-ArH × 2), 7.09–7.04 (1H, m, PhH), 6.87 (2H, d, J = 8.7 Hz, PMB-ArH × 2), 4.47 (1H, d, J = 11.5 Hz, PMB-CH_AH_B), 4.39 (1H, d, J = 11.5 Hz, PMB-CH_AH_B),

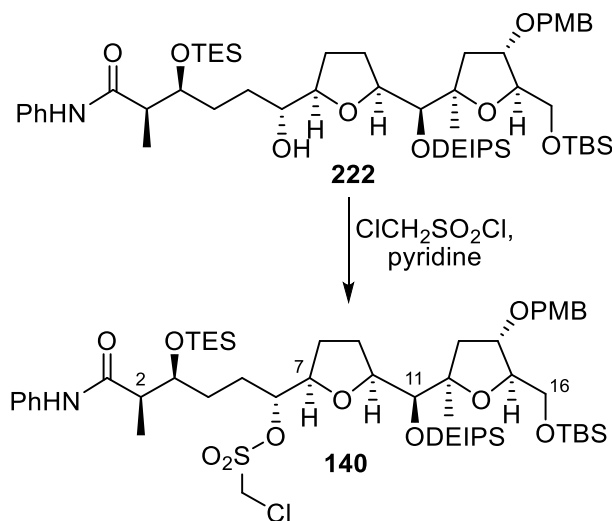
4.14–4.07 (1H, m, C(15)H), 4.05–3.97 (2H, m, C(14)H, C(10)H), 3.88 (1H, dt, $J = 7.9, 3.7$ Hz, C(3)H), 3.80 (3H, s, PMB-CH₃), 3.70 (1H, d, $J = 2.8$ Hz, C(11)H), 3.65 (1H, dd, $J = 10.5, 3.9$ Hz, C(16)H_AH_B), 3.52–3.49 (1H, m, C(7)H), 3.47 (1H, dd, $J = 10.6, 6.3$ Hz, C(16)H_AH_B), 3.38–3.30 (1H, m, C(6)H), 2.85 (1H, d, $J = 3.0$ Hz, OH), 2.69 (1H, qd, $J = 7.2, 3.8$ Hz, C(2)H), 2.08–2.00 (1H, m, C(13)H_AH_B), 1.99–1.86 (1H, m, C(9)H_AH_B), 1.87–1.80 (2H, m, C(4)H_AH_B, C(8)H_AH_B), 1.83 (1H, dd, $J = 13.3, 2.5$ Hz, C(13)H_AH_B), 1.80–1.73 (2H, m, C(9)H_AH_B, C(8)H_AH_B), 1.65–1.59 (1H, m, C(5)H_AH_B), 1.52–1.41 (1H, m, C(4)H_AH_B), 1.28–1.21 (1H, m, C(5)H_AH_B), 1.29 (3H, s, C(12)CH₃), 1.18 (3H, d, $J = 7.2$ Hz, C(2)CH₃), 1.06–0.92 (22H, m, TES-CH₃ × 3, DEIPS-EtCH₃ × 2, DEIPS-*i*PrCH₃ × 2, DEIPS-*i*PrCH), 0.88 (9H, s, TBS-C(CH₃)₃), 0.76–0.55 (10H, m, TES-CH₂ × 3, DEIPS-EtCH₂ × 2), 0.04 (6H, s, TBS-Si(CH₃)₂);

¹³C NMR (125 MHz, CDCl₃) δ_c 172.0 (C1), 159.1 (PMB-C_{Ar}OMe), 138.5 (Ph-C_{Ar}N), 130.5 (PMB-C_{Ar}CH₂), 129.1 (PMB-C_{Ar} × 2), 129.0 (Ph-C_{Ar} × 2), 123.6 (Ph-C_{Ar}), 119.5 (Ph-C_{Ar} × 2), 113.8 (PMB-C_{Ar} × 2), 85.4 (C12), 84.6 (C15), 82.1 (C7), 80.5 (C14), 80.1 (C10), 79.1 (C11), 75.7 (C3), 74.4 (C6), 71.1 (PMB-CH₂), 63.7 (C16), 55.3 (PMB-CH₃), 46.8 (C2), 42.7 (C13), 30.4 (C5), 28.5 (C4), 27.8 (C8), 25.9 (TBS-C(CH₃)₃), 25.9 (C9), 21.4 (C12-CH₃), 18.3 (TBS-C(CH₃)₃), 17.6 (DEIPS-*i*PrCH₃), 17.5 (DEIPS-*i*PrCH₃), 13.4 (DEIPS-*i*PrCH), 12.9 (C2-CH₃), 7.4 (DEIPS-EtCH₃), 7.3 (DEIPS-EtCH₃), 7.0 (TES-EtCH₃ × 3), 5.0 (TES-EtCH₂ × 3), 4.8 (DEIPS-EtCH₂), 4.4 (DEIPS-EtCH₂), -5.4 (TBS-SiCH₃), -5.5 (TBS-SiCH₃);

IR ν_{\max} (film)/cm⁻¹ 3322, 2954, 2877, 1692, 1601, 1540, 1514, 1462, 1442, 1249, 1097, 1041, 837, 751, 724;

HRMS (ESI⁺, m/z) C₅₁H₉₀O₉NSi₃⁺ [M + H⁺] calculated 944.59179, found 944.59064 ($\Delta = -1.2$ ppm).

(1*R*,4*S*,5*R*)-1-((2*R*,5*S*)-5-((*S*)-((2*R*,4*S*,5*R*)-5-(((*tert*-Butyldimethylsilyl)oxy)methyl)-4-((4-methoxybenzyl)oxy)-2-methyltetrahydrofuran-2-yl)((diethyl(isopropyl)silyl)oxy)methyl)tetrahydrofuran-2-yl)-5-methyl-6-oxo-6-(phenylamino)-4-((triethylsilyl)oxy)hexyl chloromethanesulfonate (**140**)



Alcohol **222** (104 mg, 0.110 mmol) was dissolved in pyridine (1.8 mL), and then cooled to 0 °C. Chloromethanesulfonyl chloride (25 μL , 0.28 mmol) was added dropwise to the solution, which was warmed to room temperature and stirred for 15 min. The reaction mixture was quenched by dropwise addition of water (7 mL) and diluted with CH_2Cl_2 . The layers were allowed to separate and the aqueous layer was extracted with CH_2Cl_2 (4 \times 15 mL). The organic layers were combined, dried (MgSO_4), filtered, and concentrated *in vacuo*. Purification by flash column chromatography (SiO_2 , 85:15 Pentane:EtOAc) afforded chloromesylate **140** (96.1 mg, 83%) as a viscous yellow oil.

$R_f = 0.6$ (80:20 Pentane:EtOAc);

$[\alpha]_D^{25} -14.3$ ($c = 0.29$, CH_2Cl_2);

$^1\text{H NMR}$ (500 MHz, CDCl_3) δ_H 8.47 (1H, s, PhNH), 7.54–7.46 (2H, m, PhH \times 2), 7.34–7.27 (2H, m, PhH \times 2), 7.25 (2H, d, $J = 8.7$ Hz, PMB-ArH \times 2), 7.07 (1H, tt, $J = 7.3, 1.2$ Hz, PhH), 6.87 (2H,

d, $J = 8.6$ Hz, PMB-ArH $\times 2$), 4.86 (1H, d, $J = 12.0$ Hz, SO₂CH_AH_BCl), 4.71 (1H, d, $J = 12.0$ Hz, SO₂CH_AH_BCl), 4.68–4.58 (1H, m, C(6)H), 4.46 (1H, d, $J = 11.5$ Hz, PMB-CH_AH_B), 4.39 (1H, d, $J = 11.5$ Hz, PMBCH_AH_B), 4.12–4.02 (3H, m, C(10)H, C(7)H, C(15)H), 4.02–3.94 (2H, m, C(3)H, C(14)H), 3.80 (3H, s, PMB-CH₃), 3.68 (1H, d, $J = 1.9$ Hz, C(11)H), 3.63 (1H, dd, $J = 10.5, 4.1$ Hz, C(16)H_AH_B), 3.45 (1H, dd, $J = 10.5, 6.3$ Hz, C(16)H_AH_B), 2.70–2.62 (1H, m, C(2)H), 2.08–2.00 (1H, m, C(9)H_AH_B), 1.96 (1H, dd, $J = 13.4, 7.1$ Hz C(13)H_AH_B), 1.84–1.60 (6H, m, C(5)H_AH_B, C(8)H₂, C(9)H_AH_B, C(4)H₂), 1.43–1.32 (1H, m, C(5)H_AH_B), 1.86 (1H, dd, $J = 13.3, 1.9$ Hz, C(13)H_AH_B), 1.24 (3H, s, C(12)CH₃), 1.19 (3H, d, $J = 7.1$ Hz, C(2)CH₃), 1.05–0.92 (22H, m, DEIPS-CH₃ $\times 4$, DEIPS-CH, TES-CH₃ $\times 3$), 0.88 (9H, s, TBS-C(CH₃)₃), 0.77–0.56 (10H, m, TES-CH₂ $\times 3$, DEIPS-CH₂ $\times 2$), 0.03 (3H, s, TBS-SiCH₃), 0.02 (3H, s, TBS-SiCH₃);

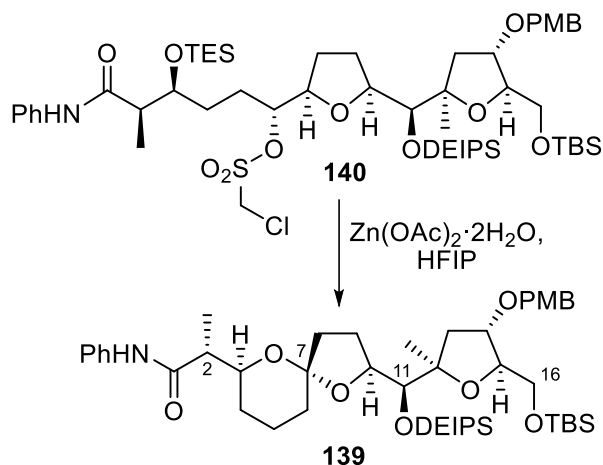
¹³C NMR (125 MHz, CDCl₃) δ_c 171.9 (C1), 159.1 (PMB-C_{Ar}OMe), 138.2 (Ph-C_{Ar}N), 130.5 (PMB-C_{Ar}CH₂), 129.1 (PMB-C_{Ar} $\times 2$), 129.0 (Ph-C_{Ar} $\times 2$), 123.8 (Ph-C_{Ar}), 119.6 (Ph-C_{Ar} $\times 2$), 113.8 (PMB-C_{Ar} $\times 2$), 88.2 (C6), 85.1 (C12), 84.7 (C15), 80.9 (C14), 80.7 (C10), 79.7 (C7), 79.3 (C11), 74.3 (C3), 71.0 (PMB-CH₂), 63.9 (C16), 55.3 (PMB-OCH₃), 54.4 (SO₂CH₂Cl), 46.6 (C2), 42.7 (C13), 28.3 (C5), 28.1 (C4), 28.0 (C8), 25.9 (TBS-C(CH₃)₃), 24.4 (C9), 21.3 (C12-CH₃), 18.3 (TBS-C(CH₃)₃), 17.6 (DEIPS-*i*PrCH₃), 17.5 (DEIPS-*i*PrCH₃), 13.3 (DEIPS-*i*PrCH), 12.8 (C2-CH₃), 7.4 (DEIPS-EtCH₃), 7.3 (DEIPS-EtCH₃), 6.9 (3 C, TES-CH₃ $\times 3$), 5.0 (3 C, TES-CH₂ $\times 3$), 4.8 (DEIPS-EtCH₂), 4.4 (DEIPS-EtCH₂), -5.3 (TBS-SiCH₃), -5.4 (TBS-SiCH₃);

IR ν_{\max} (film)/cm⁻¹ 3321, 2954, 2934, 2877, 2359, 1689, 1601, 1536, 1514, 1462, 1373, 1248, 1096, 1040, 883, 837, 726;

HRMS (ESI⁺, m/z) C₅₂H₉₁O₁₁NCiSSi₃⁺ [M + H⁺] calculated 1056.53037, found 1056.52966 ($\Delta = -0.7$ ppm).

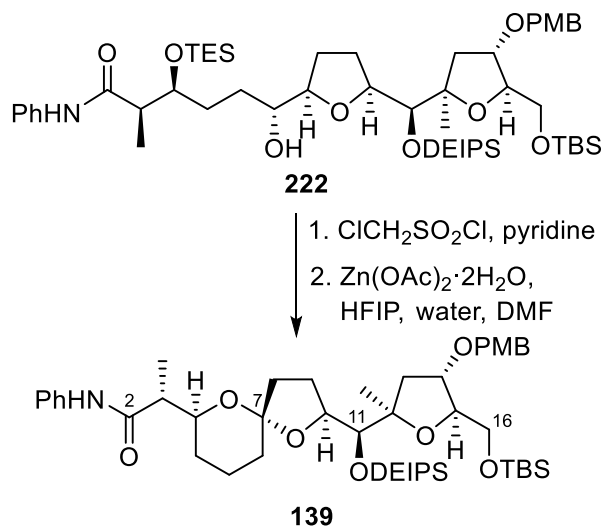
(R)-2-((2S,5S,7S)-2-((S)-((2R,4S,5R)-5-(((tert-Butyldimethylsilyl)oxy)methyl)-4-((4-methoxybenzyl)oxy)-2-methyltetrahydrofuran-2-yl)((diethyl(isopropyl)silyl)oxy)methyl)-1,6-dioxaspiro[4.5]decan-7-yl)-N-phenylpropanamide (139)

Procedure A:



Chloromethyl sulfonate **140** (196 mg, 0.185 mmol) was dissolved in HFIP (1.9 mL). Zn(OAc)₂·2H₂O (204 mg, 0.927 mmol) was added and the reaction was warmed to 30 °C and stirred for 3.5 h, before being diluted with a solution of NaHCO₃ (sat., 5.0 mL). The layers were allowed to separate and the aqueous layer was extracted with EtOAc (4 × 5.0 mL). The organic layers were combined, dried (MgSO₄), filtered and concentrated *in vacuo*. Purification by flash column chromatography (SiO₂, 90:10 to 85:15 to 80:20 Pentane:EtOAc) afforded spiroketal **139** (58.1 mg, 39%) as a colourless oil.

Procedure B:

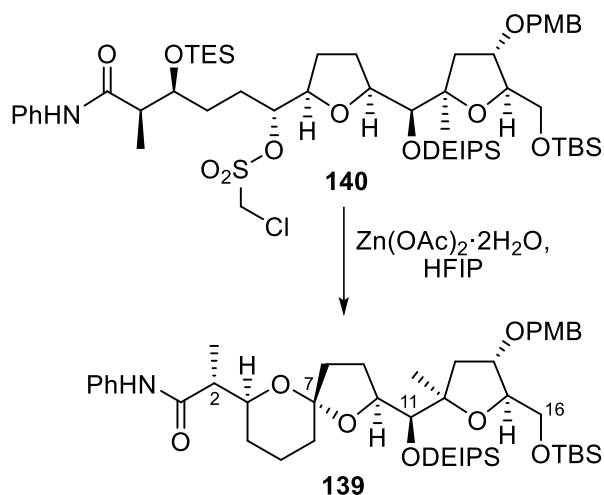


Alcohol **222** (1.45 g, 1.54 mmol) was dissolved in pyridine (24.8 mL), and then cooled to 0 °C. Chloromethanesulfonyl chloride (349 μ L, 3.84 mmol) was added dropwise to the solution, which was warmed to room temperature and stirred for 20 min. The reaction mixture was quenched by dropwise addition of water (19.1 mL) and diluted with CH₂Cl₂. The layers were allowed to separate and the aqueous layer was extracted with CH₂Cl₂ (4 \times 50 mL). The organic layers were combined, dried (MgSO₄), filtered, and concentrated *in vacuo*. The crude sample was filtered through a pad of silica with 80:20 Pentane:EtOAc eluent to afford chloromesylate **140** as a viscous pale yellow oil, which was directly carried over to the next step.

Chloromesylate **140** (1.54 mmol, assumed quant.) was dissolved in a solution of DMF (21 mL), water (15 mL), and HFIP (36 mL). Zn(OAc)₂·2H₂O (1.68 g, 7.68 mmol) was added and the reaction was stirred for 18 h at 70 °C, before being diluted with Et₂O (90 mL) and brine (90 mL). The layers were allowed to separate, and the aqueous layer was extracted with Et₂O (4 \times 90 mL). The organic layers were combined and then concentrated partially to ca. 50 mL, and then washed twice with brine (60 mL). The organic layer was then dried (MgSO₄), filtered and

then concentrated *in vacuo*. Purification by flash column chromatography (SiO₂, 90:10 to 85:15 Pentane:EtOAc) afforded spiroketal **139** (826 mg, 66% over two steps) as a colourless oil.

Procedure C:



Chloromethyl sulfonate **140** (196 mg, 0.185 mmol) was dissolved in HFIP (1.9 mL). Zn(OAc)₂·2H₂O (204 mg, 0.927 mmol) was added and the reaction was warmed to 30 °C and stirred for 3.5 h, before being diluted with a solution of NaHCO₃ (sat., 5.0 mL). The layers were allowed to separate and the aqueous layer was extracted with EtOAc (4 × 5.0 mL). The organic layers were combined, dried (MgSO₄), filtered and concentrated *in vacuo*. Purification by flash column chromatography (SiO₂, 90:10 to 85:15 to 80:20 Pentane:EtOAc) afforded spiroketal **139** (58.1 mg, 39%) as a colourless oil.

$R_f = 0.6$ (80:20 Pentane:EtOAc);

$[\alpha]_D^{25} -24.7$ ($c = 1.00$, CH₂Cl₂);

¹H NMR (500 MHz, CDCl₃) δ_H 8.49 (1H, s, PhNH), 7.52–7.46 (2H, m, PhH × 2), 7.32–7.27 (2H, m, PhH × 2), 7.28–7.22 (2H, m, PMB-ArH × 2), 7.05 (1H, t, $J = 7.3$ Hz, PhH), 6.88 (2H, d, $J = 8.6$ Hz, PMB-ArH × 2), 4.45 (1H, d, $J = 11.5$ Hz, PMB-CH_AH_B), 4.39 (1H, d, $J = 11.4$ Hz, PMB-

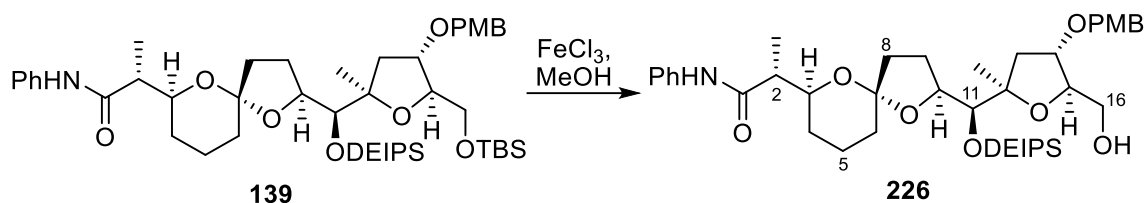
CH_AH_B), 4.30 (1H, t, $J = 7.6$, C(10) H), 4.06–4.00 (1H, m, C(14) H), 4.01–3.97 (2H, m, C(15) H , C(3) H), 3.87–3.84 (1H, m, C(11) H), 3.81 (3H, s, PMB- CH_3), 3.61 (1H, dd, $J = 10.6$, 3.8 Hz, C(16) H_AH_B), 3.44 (1H, dd, $J = 10.6$, 5.7 Hz, C(16) H_AH_B), 2.60 (1H, qd, $J = 7.2$, 3.5 Hz, C(2) H), 2.12–2.03 (1H, m, C(9) H_AH_B), 2.00 (1H, dd, $J = 13.7$, 7.1 Hz, C(13) H_AH_B), 2.00–1.95 (1H, m, C(8) H_AH_B), 1.91–1.74 (4H, m, C(5) H_AH_B , C(8) H_AH_B , C(9) H_AH_B , C(13) H_AH_B), 1.74–1.56 (4H, m, C(6) H_2 , C(5) H_AH_B , C(4) H_AH_B), 1.33–1.23 (1H, m, C(4) H_AH_B), 1.20 (3H, s, C(12) CH_3), 1.19 (3H, d, $J = 7.2$ Hz, C(2) CH_3), 1.06–0.93 (13H, m, DEIPS- $\text{CH}_3 \times 4$, DEIPS- $i\text{PrCH}$), 0.89 (9H, s, TBS-C(CH_3) $_3$), 0.74–0.57 (4H, m, DEIPS- $\text{CH}_2 \times 2$), 0.09–0.01 (6H, m, TBS-Si(CH_3) $_2$);

^{13}C NMR (125 MHz, CDCl_3) δ_{c} 172.5 (C1), 159.1 (PMB- $\text{C}_{\text{Ar}}\text{OMe}$), 138.4 (Ph- $\text{C}_{\text{Ar}}\text{N}$), 130.6 (PMB- $\text{C}_{\text{Ar}}\text{CH}_2$), 129.1 (PMB- $\text{C}_{\text{Ar}} \times 2$), 128.9 (Ph- $\text{C}_{\text{Ar}} \times 2$), 123.6 (Ph- C_{Ar}), 119.5 (Ph- $\text{C}_{\text{Ar}} \times 2$), 113.8 (PMB- $\text{C}_{\text{Ar}} \times 2$), 105.6 (C7), 84.8 (C12), 84.4 (C15), 81.1 (C14), 78.6 (C11), 78.6 (C10), 71.9 (C3), 71.1 (PMB- CH_2), 63.8 (C16), 55.3 (PMB- CH_3), 45.5 (C2), 42.6 (C13), 38.7 (C8), 32.9 (C6), 26.0 (TBS-C(CH_3) $_3$), 25.7 (C4), 22.8 (C9), 21.5 (C12- CH_3), 19.8 (C5), 18.3 (TBS-C(CH_3) $_3$), 17.6 (DEIPS- $i\text{PrCH}_3$), 17.5 (DEIPS- $i\text{PrCH}_3$), 13.3 (DEIPS- $i\text{PrCH}$), 12.3 (C2- CH_3), 7.3 (DEIPS-Et CH_3), 7.3 (DEIPS-Et CH_3), 4.7 (DEIPS-Et CH_2), 4.3 (DEIPS-Et CH_2), -5.2 (TBS-Si CH_3), -5.3 (TBS-Si CH_3);

IR ν_{max} (film)/ cm^{-1} 3455, 3049, 2951, 2876, 1736, 1668, 1638, 1499, 1297, 1248, 1116, 971, 837, 709, 690;

HRMS (ESI $^+$, m/z) $\text{C}_{45}\text{H}_{74}\text{NO}_8\text{Si}_2^+$ [$\text{M} + \text{H}^+$] calculated 812.49475, found 812.49457 ($\Delta = -0.2$ ppm).

(R)-2-((2S,5S,7S)-2-((S)-((diethyl(isopropyl)silyl)oxy)((2R,4S,5R)-5-(hydroxymethyl)-4-((4-methoxybenzyl)oxy)-2-methyltetrahydrofuran-2-yl)methyl)-1,6-dioxaspiro[4.5]decan-7-yl)-N-phenylpropanamide (226)



FeCl₃ (20.0 mg, 0.123 mmol) was added to a solution of spiroketal **139** (59.9 mg, 73.7 μmol) in MeOH (3.0 mL), which was then stirred at room temperature for 2 h. After which, the reaction was quenched with a solution of NaHCO₃ (sat., 6.0 mL), a solution of Rochelle's salt (sat., 6.0 ml), and EtOAc (12.0 mL). The layers were allowed to separate, and the aqueous layer was extracted with EtOAc (4 × 15 mL). The organic layers were combined, dried (MgSO₄), filtered and concentrated *in vacuo*. Purification by flash column chromatography (SiO₂, 95:5 to 80:20 to 50:50 to 0:100 Pentane:EtOAc) afforded alcohol **226** (34.3 mg, 67%), diol **227** (6.1 mg, 12%) and starting material **139** (4.9 mg, 8%) all as colourless oils.

R_f = 0.6 (50:50 Pentane:EtOAc);

[α]_D²⁵ -0.7 (c = 0.33, CH₂Cl₂);

¹H NMR (500 MHz, CDCl₃) δ_H 8.21 (1H, s, PhNH), 7.52–7.46 (2H, m, PhH × 2), 7.33–7.26 (2H, m, PhH × 2), 7.26–7.20 (2H, m, PMB-ArH × 2), 7.05 (1H, t, J = 7.4 Hz, PhH), 6.88 (2H, d, J = 8.6 Hz, PMB-ArH × 2), 4.43 (1H, d, J = 11.4 Hz, PMB-CH_AH_B), 4.40 (1H, d, J = 11.4 Hz, PMB-CH_AH_B), 4.22 (1H, t, J = 6.8 Hz, C(10)H), 4.04 (1H, ddd, J = 11.9, 4.0, 2.3 Hz, C(14)H), 4.01–3.96 (2H, m, C(15)H, C(3)H), 3.85 (1H, d, J = 1.6 Hz, C(11)H), 3.81 (3H, s, PMB-CH₃), 3.70–3.64 (1H, m, C(16)H_AH_B), 3.54–3.48 (1H, m, C(16)H_AH_B), 2.55 (1H, qd, J = 7.2, 3.9 Hz, C(2)H), 2.43 (1H, br. s, OH), 2.19–2.11 (1H, m, C(13)H_AH_B), 2.06–1.93 (2H, m, C(9)H_AH_B, C(8)H_AH_B), 1.89–1.72 (3H,

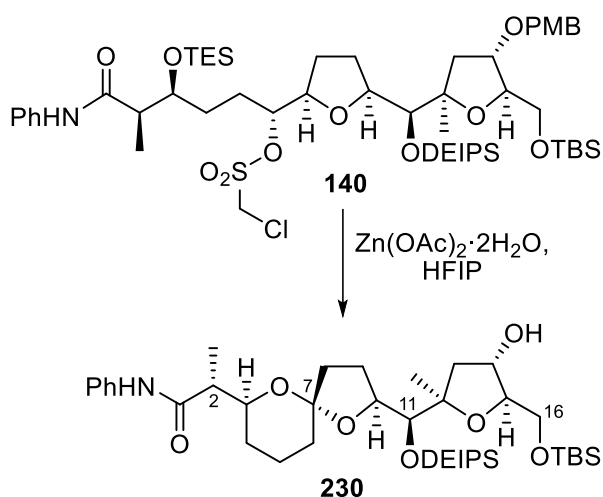
m, C(5)*H_AH_B*, C(8)*H_AH_B*, C(9)*H_AH_B*), 1.72–1.66 (3H, m, C(5)*H_AH_B*, C(6)*H_AH_B*, C(13)*H_AH_B*), 1.66–1.58 (2H, C(4)*H_AH_B*, C(6)*H_AH_B*), 1.39–1.28 (1H, m, C(4)*H_AH_B*), 1.22 (3H, d, *J* = 7.2 Hz, C(2)*CH₃*), 1.16 (3H, s, C(12)*CH₃*), 1.03–0.95 (13H, m, DEIPS-*CH₃* × 4, DEIPS-*iPrCH*), 0.70–0.57 (4H, m, DEIPS-*CH₂* × 2);

¹³C NMR (125 MHz, CDCl₃) δ_c 172.7 (C1), 159.2 (PMB-*C_{Ar}*OMe), 138.2 (Ph-*C_{Ar}*N), 130.2 (PMB-*C_{Ar}*CH₂), 129.2 (PMB-*C_{Ar}* × 2), 129.0 (Ph-*C_{Ar}* × 2), 123.8 (Ph-*C_{Ar}*), 119.6 (Ph-*C_{Ar}* × 2), 113.8 (PMB-*C_{Ar}* × 2), 105.7 (C7), 84.7 (C12), 83.6 (C15), 79.9 (C14), 78.1 (C10), 77.9 (C11), 71.7 (C3), 71.4 (PMB-*CH₂*), 63.4 (C16), 55.3 (PMB-*CH₃*), 46.1 (C2), 41.5 (C13), 38.2 (C8), 32.7 (C6), 26.3 (C4), 23.2 (C9), 22.4 (C12-*CH₃*), 19.9 (C5), 17.6 (DEIPS-*iPrCH₃*), 17.5 (DEIPS-*iPrCH₃*), 13.3 (DEIPS-*iPrCH*), 12.2 (C2-*CH₃*), 7.3 (DEIPS-Et*CH₃*), 7.2 (DEIPS-Et*CH₃*), 4.5 (DEIPS-Et*CH₂*), 4.2 (DEIPS-Et*CH₂*);

IR ν_{\max} (film)/cm⁻¹ 3317, 2918, 2860, 1736, 1667, 1600, 1466, 1378, 1248, 1037, 820, 756, 722;

HRMS (ESI⁺, *m/z*) C₃₉H₆₀NO₈Si⁺ [M + H⁺] calculated 698.40827, found 698.40796 (Δ = -0.45 ppm).

(*R*)-2-((2*S*,5*S*,7*S*)-2-((*S*)-((2*R*,4*S*,5*R*)-5-(((*Tert*-butyldimethylsilyl)oxy)methyl)-4-hydroxy-2-methyltetrahydrofuran-2-yl))((diethyl(isopropyl)silyl)oxy)methyl)-1,6-dioxaspiro[4.5]decan-7-yl)-*N*-phenylpropanamide (230)



Chloromesylate **140** (78.6 mg, 74.4 μmol) was dissolved in HFIP (0.74 mL). $\text{Zn}(\text{OAc})_2 \cdot 2\text{H}_2\text{O}$ (81.6 mg, 0.372 mmol) was added and the reaction was heated to 60 °C and stirred for 3 h, before being diluted with EtOAc (7.0 mL). The resulting mixture was washed with water (3.0 mL), brine (3.0 mL), dried (MgSO_4), filtered and concentrated *in vacuo*. Purification by flash column chromatography (SiO_2 , 90:10 to 60:40 Pentane:EtOAc) afforded spiroketal **230** as a colourless oil (4.3 mg, 8%).

$R_f = 0.2$ (8:2 Pentane:EtOAc);

$[\alpha]_D^{25} -24.6$ ($c = 0.36$, CH_2Cl_2);

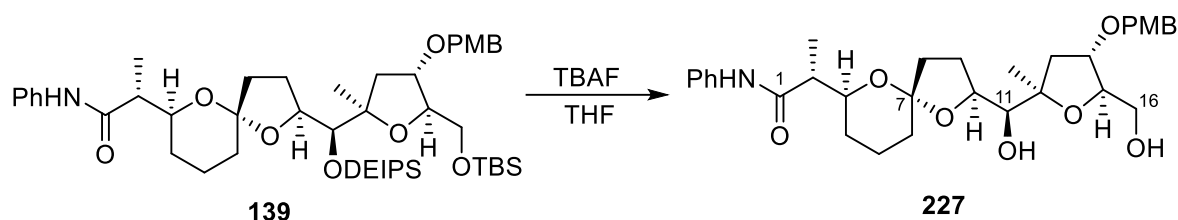
$^1\text{H NMR}$ (500 MHz, CDCl_3) δ_{H} 8.45 (1H, s, PhNH), 7.51–7.47 (2H, m, PhH \times 2), 7.33–7.27 (2H, m, PhH \times 2), 7.06 (1H, t, $J = 7.4$ Hz, PhH), 4.29–4.19 (2H, m, C(14)H, C(10)H), 4.01 (1H, dt, $J = 12.2, 2.8$ Hz, C(3)H), 3.84 (1H, d, $J = 1.2$ Hz, C(11)H), 3.78–3.72 (2H, m, C(15)H, C(16)H_AH_B), 3.50–3.44 (1H, m, C(16)H_AH_B), 2.58 (1H, qd, $J = 7.2, 3.5$ Hz, C(2)H), 2.30 (1H, dd, $J = 13.0, 8.1$ Hz, C(13)H_AH_B), 2.11–1.96 (2H, m, C(9)H_AH_B, C(8)H_AH_B), 1.87–1.77 (3H, m, C(5)H_AH_B, C(8)H_AH_B, C(9)H_AH_B), 1.77–1.72 (1H, m, C(6)H_AH_B), 1.70–1.59 (3H, m, C(5)H_AH_B, C(6)H_AH_B, C(13)H_AH_B), 1.33–1.25 (2H, m, C(4)H₂), 1.20 (3H, d, $J = 7.3$ Hz, C(2)CH₃), 1.20 (3H, s, C(12)CH₃), 1.04–0.95 (13H, m, DEIPS-CH₃ \times 4, DEIPS-*i*PrCH), 0.90 (9H, s, TBS-C(CH₃)₃), 0.70–0.60 (4H, m, DEIPS-CH₂ \times 2), 0.09–0.05 (6H, m, TBS-Si(CH₃)₂);

$^{13}\text{C NMR}$ (125 MHz, CDCl_3) δ_{C} 172.5 (C1), 138.4 (Ph-C_{Ar}N), 128.9 (Ph-C_{Ar} \times 2), 123.6 (Ph-C_{Ar}), 119.4 (Ph-C_{Ar} \times 2), 105.6 (C7), 84.4 (C12), 83.7 (C15), 78.3 (C10), 78.0 (C11), 75.2 (C14), 71.9 (C3), 64.5 (C16), 45.7 (C2), 44.3 (C13), 38.6 (C8), 32.9 (C6), 25.9 (TBS-C(CH₃)₃), 25.8 (C4), 22.8 (C9), 22.5 (C12-CH₃), 19.8 (C5), 18.3 (TBS-C(CH₃)₃), 17.6 (DEIPS-*i*PrCH₃), 17.5 (DEIPS-*i*PrCH₃), 13.3 (DEIPS-*i*PrCH), 12.3 (C2-CH₃), 7.3 (DEIPS-EtCH₃), 7.3 (DEIPS-EtCH₃), 4.6 (DEIPS-EtCH₂), 4.3 (DEIPS-EtCH₂), -5.4 (TBS-SiCH₃), -5.4 (TBS-SiCH₃);

IR ν_{\max} (film)/ cm^{-1} 3317, 2937, 2874, 1667, 1600, 1541, 1514, 1500, 1442, 1248, 1175, 1035, 974, 821, 727;

HRMS (ESI⁺, m/z) C₃₇H₆₅NO₇Si₂Na⁺ [M + Na⁺] calculated 714.41918, found 714.41876 ($\Delta = -0.58$ ppm).

(R)-2-((2S,5S,7S)-2-((S)-Hydroxy((2R,4S,5R)-5-(hydroxymethyl)-4-((4-methoxybenzyl)oxy)-2-methyltetrahydrofuran-2-yl)methyl)-1,6-dioxaspiro[4.5]decan-7-yl)-N-phenylpropanamide (227)



Spiroketal **139** (58.1 mg, 71.5 μmol) was dissolved in THF (2.9 mL) and cooled to 0 °C. The buffered tetrabutylammonium fluoride solution (1.0 M, 29 μL , 29 μmol) was added to the THF solution, which was warmed to room temperature and stirred for 1 hour 15 min, before being quenched with a solution of NaHCO₃ (sat., 1.2 mL). The layers were allowed to separate and the aqueous layer was extracted with EtOAc (3 \times 15 mL). The combined organic layers were dried (MgSO₄), filtered and concentrated *in vacuo*. Purification by flash column chromatography (SiO₂, 50:50 to 0:100 Pentane:EtOAc) afforded diol **227** (32.3 mg, 79%) as a viscous colourless oil.

R_f = 0.4 (Pure EtOAc);

[α]_D²⁵ -4.8 ($c = 0.43$, CH₂Cl₂);

¹H NMR (500 MHz, CDCl₃) δ_{H} 8.27 (1H, s, PhNH), 7.52–7.46 (2H, m, PhH \times 2), 7.33–7.27 (2H, m, PhH \times 2), 7.26–7.21 (2H, m, PMB-ArH \times 2), 7.06 (1H, t, $J = 7.4$ Hz, PhH), 6.88 (2H, d,

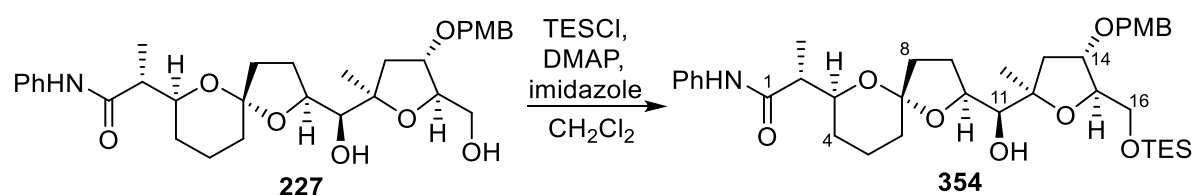
$J = 8.6$ Hz, PMB-ArH $\times 2$), 4.44 (1H, d, $J = 11.3$ Hz, PMB-CH_AH_B), 4.38 (1H, d, $J = 11.3$ Hz, PMB-CH_AH_B), 4.16–4.09 (2H, m, C(10)H, C(15)H), 4.07–4.00 (2H, m, C(3)H, C(14)H), 3.81 (3H, s, PMB-CH₃), 3.80 (1H, d, $J = 2.1$ Hz, C(11)H), 3.79–3.77 (1H, m, C(16)H_AH_B), 3.56 (1H, dd, $J = 11.6$, 2.5 Hz, C(16)H_AH_B), 2.57 (1H, qd, $J = 7.2$, 3.6 Hz, C(2)H), 2.84 (2H, br. s, OH $\times 2$), 2.35 (1H, dd, $J = 13.3$, 6.7 Hz, C(13)H_AH_B), 2.06–2.00 (1H, m, C(8)H_AH_B), 2.00–1.94 (2H, m, C(9)H₂), 1.92–1.85 (1H, m, C(8)H_AH_B), 1.85–1.77 (1H, m, C(5)H_AH_B), 1.76–1.66 (3H, m, C(5)H_AH_B, C(6)H₂), 1.64 (1H, dd, $J = 13.2$, 2.6 Hz, C(13)H_AH_B), 1.68–1.61 (1H, m, C(4)H_AH_B), 1.37–1.33 (1H, m, C(4)H_AH_B), 1.31 (3H, s, C(12)CH₃), 1.23 (3H, d, $J = 7.2$ Hz, C(2)CH₃);

¹³C NMR (125 MHz, CDCl₃) δ_c 172.5 (C1), 159.2 (PMB-C_{Ar}OMe), 138.3 (Ph-C_{Ar}N), 130.1 (PMB-C_{Ar}CH₂), 129.2 (PMB-C_{Ar} $\times 2$), 129.0 (Ph-C_{Ar} $\times 2$), 123.8 (Ph-C_{Ar}), 119.4 (Ph-C_{Ar} $\times 2$), 113.9 (PMB-C_{Ar} $\times 2$), 106.7 (C7), 85.8 (C12), 83.7 (C15), 81.6 (C10), 78.3 (C14), 77.0 (C11), 72.5 (C3), 71.1 (PMB-CH₂), 64.0 (C16), 55.3 (PMB-CH₃), 46.0 (C2), 38.3 (C8), 37.3 (C13), 33.5 (C6), 26.2 (C4), 25.1 (C12-CH₃), 24.8 (C9), 19.8 (C5), 12.3 (C2-CH₃);

IR ν_{\max} (film)/cm⁻¹ 3317, 2937, 1667, 1600, 1514, 1500, 1376, 1248, 1035, 820, 727;

HRMS (ESI⁺, m/z) C₃₂H₄₃NO₈Na⁺ [M + Na⁺] calculated 592.28809, found 592.28778 ($\Delta = -0.52$ ppm).

(R)-2-((2S,5S,7S)-2-((S)-Hydroxy((2R,4S,5R)-4-((4-methoxybenzyl)oxy)-2-methyl-5-(((triethylsilyl)oxy)methyl)tetrahydrofuran-2-yl)methyl)-1,6-dioxaspiro[4.5]decan-7-yl)-N-phenylpropanamide (354)



Diol **227** (8.6 mg, 15 μ mol, azeotropically distilled three times in benzene) was dissolved in CH₂Cl₂ (0.84 mL) and cooled to -78 °C. 2,6-Lutidine (52.5 μ L, 0.453 mmol) and DMAP (0.2 mg,

1.5 μmol) were added, followed by the dropwise addition of TESCl (50.7 μL , 0.302 mmol). The reaction was stirred at $-78\text{ }^\circ\text{C}$ for 2 h, before being quenched with MeOH, and then water. The layers were allowed to separate and the aqueous layer was extracted with EtOAc ($3 \times 4\text{ mL}$). The organic layers were combined, dried (MgSO_4), filtered, and then concentrated *in vacuo*. Purification by flash column chromatography (SiO_2 , 100:0 to 85:15 to 50:50 Pentane:EtOAc) afforded silyl ether **354** (10.2 mg, 99%) as a colourless oil.

$R_f = 0.8$ (50:50 Pentane:EtOAc);

$[\alpha]_D^{25} -1.7$ ($c = 0.21$, CH_2Cl_2);

$^1\text{H NMR}$ (500 MHz, CDCl_3) δ_{H} 8.40 (1H, s, PhNH), 7.55–7.47 (2H, m, PhH $\times 2$), 7.34–7.27 (2H, m, PhH $\times 2$), 7.25–7.21 (2H, m, PMB-ArH $\times 2$), 7.06 (1H, t, $J = 7.4\text{ Hz}$, PhH), 6.88 (2H, d, $J = 8.7\text{ Hz}$, PMB-ArH $\times 2$), 4.42 (1H, d, $J = 11.3\text{ Hz}$, PMB-CH_AH_B), 4.33 (1H, d, $J = 11.3\text{ Hz}$, PMB-CH_AH_B), 4.13–4.07 (1H, m, C(14)H), 3.96–3.88 (1H, m, C(10)H), 4.05–3.98 (2H, m, C(3)H, C(15)H), 3.80 (3H, s, PMB-CH₃), 3.75 (1H, dd, $J = 10.8, 3.4\text{ Hz}$, C(16)H_AH_B), 3.63 (1H, dd, $J = 10.8, 2.2\text{ Hz}$, C(16)H_AH_B), 3.51 (1H, br. s, OH), 3.47 (1H, d, $J = 6.9\text{ Hz}$, C(11)H), 2.56 (1H, qd, $J = 7.2, 3.4\text{ Hz}$, C(2)H), 2.22 (1H, dd, $J = 13.2, 7.4\text{ Hz}$, C(13)H_AH_B), 2.19–2.12 (1H, m, C(9)H_AH_B), 2.08–2.01 (1H, m, C(9)H_AH_B), 1.99–1.81 (2H, m, C(8)H₂), 1.81–1.71 (1H, m, C(5)H_AH_B), 1.70–1.63 (3H, m, C(5)H_AH_B, C(6)H₂), 1.61 (1H, dd, $J = 13.1, 3.9\text{ Hz}$, C(13)H_AH_B), 1.58–1.54 (1H, m, C(4)H_AH_B), 1.35–1.29 (1H, m, C(4)H_AH_B), 1.38 (3H, s, C(12)CH₃), 1.23 (3H, d, $J = 7.3\text{ Hz}$, C(2)CH₃), 0.93 (9H, t, $J = 7.9\text{ Hz}$, TES-CH₃ $\times 3$), 0.59 (6H, q, $J = 8.1\text{ Hz}$, TES-CH₂ $\times 3$);

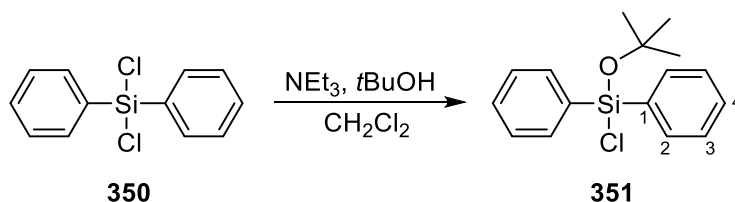
$^{13}\text{C NMR}$ (125 MHz, CDCl_3) δ_{C} 172.8 (C1), 159.2 (PMB-C_{Ar}OMe), 138.4 (Ph-C_{Ar}N), 130.3 (PMB-C_{Ar}CH₂), 129.2 (PMB-C_{Ar} $\times 2$), 129.0 (Ph-C_{Ar} $\times 2$), 123.7 (Ph-C_{Ar}), 119.4 (Ph-C_{Ar} $\times 2$), 113.8 (PMB-C_{Ar} $\times 2$), 107.1 (C7), 86.6 (C12), 83.2 (C15), 80.3 (C14), 78.7 (C10), 78.0 (C11), 72.2 (C3), 71.2 (PMB-CH₂), 62.8 (C16), 55.3 (PMB-CH₃), 46.0 (C2), 37.7 (C8), 37.1 (C13), 33.6 (C6),

27.0 (C9), 26.3 (C4), 25.4 (C12-CH₃), 19.8 (C5), 12.3 (C2-CH₃), 6.7 (TES-EtCH₃ × 3), 4.1 (TES-EtCH₂ × 3);

IR ν_{\max} (film)/cm⁻¹ 3323, 2935, 2875, 2362, 1684, 1600, 1541, 1457, 1442, 1248, 1097, 1036, 819, 751;

HRMS (ESI⁺, *m/z*) C₃₈H₅₇NO₈SiNa⁺ [M + Na⁺] calculated 736.37457, found 736.37402 ($\Delta = -0.77$ ppm).

***tert*-Butoxychlorodiphenylsilane (351)**



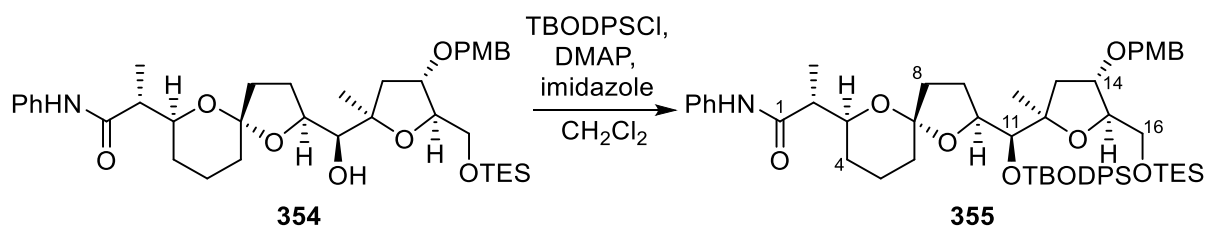
Dichlorodiphenylsilane (3.00 mL, 14.3 mmol) and NEt₃ (2.24 mL, 16.0 mmol) were dissolved in CH₂Cl₂ (22 mL) and the resulting solution was cooled to 0 °C. tBuOH (1.35 mL, 14.3 mmol) was then added dropwise to the stirring solution, which was then heated to 40 °C and stirred for 40 h. The reaction mixture was cooled to room temperature and then concentrated *in vacuo*. The resultant oil was dissolved in a 1:1 mixture of hexane and ether (36 mL), which formed a suspension. The suspension was filtered and concentrated *in vacuo* to afford *tert*-butoxychlorodiphenylsilane **351** (4.06 g, 98%) as a pale yellow oil which was used without further purification.

¹H NMR (400 MHz, CDCl₃) δ_{H} 7.61–7.55 (4H, m, C(2)H × 4), 7.35–7.23 (6H, m, C(3)H × 4, C(4)H × 2), 1.24 (9H, s, C(CH₃)₃);

¹³C NMR (100 MHz, CDCl₃) δ_{C} 134.9 (C1 × 2), 134.3 (C2 × 4), 130.5 (C4 × 2), 127.9 (C3 × 4), 76.4 (C(CH₃)₃), 31.7 (C(CH₃)₃).

The spectral data were consistent with those previously reported.³⁷

(R)-2-((2S,5S,7S)-2-((S)-((Tert-butoxydiphenylsilyl)oxy))((2R,4S,5R)-4-((4-methoxybenzyl)oxy)-2-methyl-5-(((triethylsilyl)oxy)methyl)tetrahydrofuran-2-yl)methyl)-1,6-dioxaspiro[4.5]decan-7-yl)-N-phenylpropanamide (355)



Alcohol **354** (11.0 mg, 16.1 μ mol, azeotropically distilled three times in PhMe), NEt₃ (33.6 μ L, 0.241 mmol), and DMAP (3.9 mg, 32 μ mol) were dissolved in DMF (0.38 mL). TBODPSCI (34.8 μ L, 129 μ mol) was then added to the reaction mixture dropwise, which was then warmed to 45 °C and stirred for 22 h. The reaction was quenched by addition of a solution of NaHCO₃ (sat., 0.5 mL). The mixture was diluted with brine (4 mL). The layers were allowed to separate and the aqueous layer was extracted using Et₂O (3 \times 4 mL); the organic layers were combined, washed with 5% LiCl solution (1 mL), dried (MgSO₄), and then concentrated *in vacuo*. Purification by flash column chromatography (SiO₂, 95:5 to 90:10 to 70:30 to 60:40 Pentane:EtOAc) afforded silyl ether **355** (3.7 mg, 25%) as a colourless oil. Additionally, unreacted **354** (4.3 mg, 39%) was recovered.

R_f = 0.4 (80:20 Pentane:EtOAc);

[α]_D²⁵ -22.5 (*c* = 0.31, CH₂Cl₂);

¹H NMR (500 MHz, CDCl₃) δ _H 8.51 (1H, s, PhNH), 7.73–7.68 (2H, m, TBODPS-ArH \times 2), 7.64–7.58 (3H, m, TBODPS-ArH \times 3), 7.54–7.51 (2H, m, PhH \times 2), 7.49–7.45 (2H, m, TBODPS-ArH \times 2), 7.43–7.32 (3H, m, TBODPS-ArH \times 3), 7.32–7.27 (2H, m, PhH \times 2), 7.23–7.19 (2H, m,

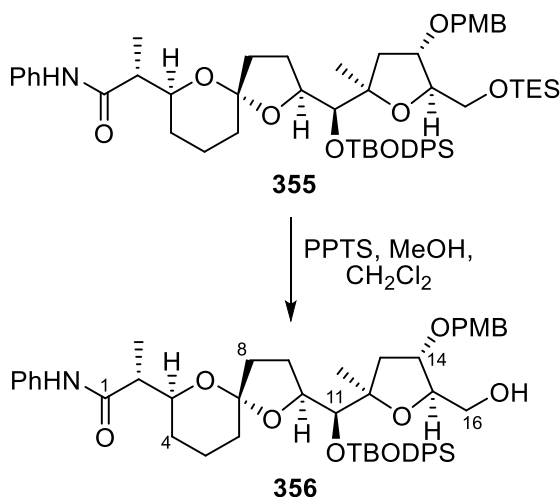
PMB-ArH \times 2), 7.05 (1H, t, $J = 7.4$ Hz, PhH), 6.87 (2H, d, $J = 8.6$ Hz, PMB-ArH \times 2), 4.39–4.34 (1H, m, C(14)H), 4.34 (2H, s, PMB-CH₂), 3.96 (1H, td, $J = 5.9, 3.9$ Hz, C(15)H), 3.92–3.87 (1H, m, C(3)H), 3.87–3.85 (1H, m, C(11)H), 3.86–3.83 (1H, m, C(10)H), 3.81 (3H, s, PMB-CH₃), 3.43 (1H, dd, $J = 10.6, 4.3$ Hz, C(16)H_AH_B), 3.22 (1H, dd, $J = 10.5, 6.0$ Hz, C(16)H_AH_B), 2.57 (1H, qd, $J = 7.2, 3.4$ Hz, C(2)H), 2.37–2.28 (1H, m, C(9)H_AH_B), 2.04 (1H, dd, $J = 13.9, 7.3$ Hz, C(13)H_AH_B), 2.01–1.97 (1H, m, C(9)H_AH_B), 1.95–1.89 (1H, m, C(8)H_AH_B), 1.84 (1H, dd, $J = 13.4, 2.7$ Hz, C(13)H_AH_B), 1.81–1.75 (1H, m, C(8)H_AH_B), 1.75–1.67 (1H, m, C(5)H_AH_B), 1.54–1.51 (2H, m, C(4)H_AH_B, C(5)H_AH_B), 1.49–1.39 (1H, m, C(6)H_AH_B), 1.33 (3H, s, C(12)CH₃), 1.31–1.27 (1H, m, C(6)H_AH_B), 1.25 (9H, s, TBODPS-C(CH₃)₃), 1.24–1.19 (1H, m, C(4)H_AH_B), 1.14 (3H, d, $J = 7.2$ Hz, C(2)CH₃), 0.88 (9H, t, $J = 8.0$ Hz, TES-CH₃ \times 3), 0.49 (6H, q, $J = 8.3$ Hz, TES-CH₂ \times 3);

¹³C NMR (125 MHz, CDCl₃) δ_c 172.5 (C1), 159.1 (PMB-C_{Ar}OMe), 138.4 (Ph-C_{Ar}N), 135.8 (TBODPS-C_{Ar} \times 2), 135.2 (TBODPS-C_{Ar} \times 2), 134.3 (TBODPS-C_{Ar} \times 2), 130.3 (PMB-C_{Ar}CH₂), 129.8 (TBODPS-C_{Ar}), 129.7 (TBODPS-C_{Ar}), 129.1 (PMB-C_{Ar} \times 2), 128.9 (Ph-C_{Ar} \times 2), 127.8 (TBODPS-C_{Ar}), 127.8 (TBODPS-C_{Ar}), 127.4 (TBODPS-C_{Ar} \times 2), 123.6 (Ph-C_{Ar}), 119.5 (Ph-C_{Ar} \times 2), 113.8 (PMB-C_{Ar} \times 2), 105.7 (C7), 84.4 (C12), 84.5 (C15), 80.7 (C10), 79.9 (C11), 78.7 (C14), 73.9 (TBODPS-C(CH₃)₃), 72.0 (C3), 70.9 (PMB-CH₂), 63.4 (C16), 55.3 (PMB-CH₃), 45.3 (C2), 43.3 (C13), 38.5 (C8), 32.5 (C6), 32.0 (TBODPS-C(CH₃)₃), 25.5 (C4), 23.6 (C9), 21.8 (C12-CH₃), 19.7 (C5), 12.3 (C2-CH₃), 6.8 (TES-EtCH₃ \times 3), 4.3 (TES-EtCH₂ \times 3);

IR ν_{\max} (film)/cm⁻¹ 2978, 2875, 1698, 1670, 1515, 1498, 1441, 1248, 1175, 1122, 1051, 1027, 804, 717, 700;

HRMS (ESI⁺, m/z) C₅₄H₇₅NNaO₉Si₂⁺ [M + Na⁺] calculated 960.48726, found 960.48718 ($\Delta = -0.08$ ppm).

(R)-2-((2S,5S,7S)-2-((S)-((Tert-butoxydiphenylsilyl)oxy)((2R,4S,5R)-5-(hydroxymethyl)-4-((4-methoxybenzyl)oxy)-2-methyltetrahydrofuran-2-yl)methyl)-1,6-dioxaspiro[4.5]decan-7-yl)-N-phenylpropanamide (356)



Spiroketal **355** (2.4 mg, 2.6 μmol) was dissolved in CH_2Cl_2 (0.50 mL) and cooled to 0 $^\circ\text{C}$. Pyridium *p*-toluenesulfonate (PPTS, 0.4 mg, 1.5 μmol) dissolved in MeOH (0.50 mL) was added and the mixture was stirred for 30 min at 0 $^\circ\text{C}$. The reaction was quenched by addition of a solution of NaHCO_3 (sat., 5 mL). The mixture was diluted with EtOAc (5 mL) and the layers were allowed to separate. The aqueous layer was then extracted with EtOAc (3 \times 5 mL). The organic layers were combined, dried (MgSO_4), filtered, and then concentrated *in vacuo*. Purification by flash column chromatography (SiO_2 , 90:10 to 80:20 Pentane:EtOAc, then pure acetone) afforded alcohol **356** (1.3 mg, 62%) as a colourless oil.

$R_f = 0.3$ (70:30 Pentane:EtOAc);

$[\alpha]_D^{25} -17.3$ ($c = 0.11$, CH_2Cl_2);

$^1\text{H NMR}$ (500 MHz, CDCl_3) δ_H 8.26 (1H, s, PhNH), 7.75–7.71 (2H, m, TBODPS-ArH \times 2), 7.67–7.63 (2H, m, TBODPS-ArH \times 2), 7.48–7.42 (3H, m, PhH \times 2, TBODPS-ArH), 7.41–7.32 (5H, m, TBODPS-ArH \times 5), 7.31–7.27 (2H, m, PhH \times 2), 7.22–7.18 (2H, m, PMB-ArH \times 2), 7.04 (1H, t, $J = 7.4$ Hz, PhH), 6.87 (2H, d, $J = 8.6$ Hz, PMB-ArH \times 2), 4.36 (1H, d, $J = 11.3$ Hz, PMB-CH_AH_B),

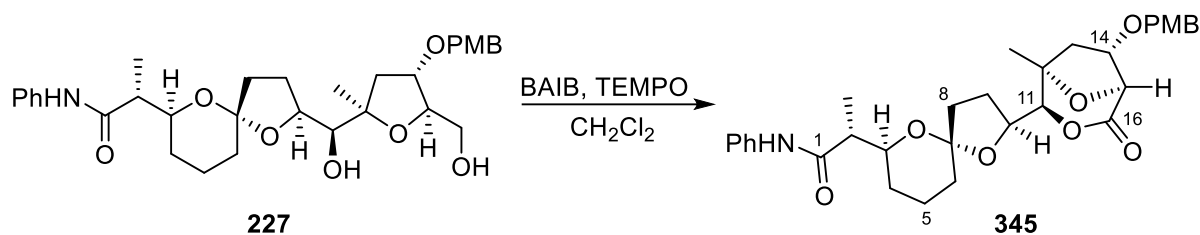
4.28 (1H, d, $J = 11.2$ Hz, PMB-CH_AH_B), 4.22–4.17 (1H, m, C(10)H), 3.99–3.95 (1H, m, C(15)H), 3.95–3.86 (2H, m, C(3)H), C(14)H), 3.82–3.79 (1H, m, C(11)H), 3.81 (3H, s, PMB-CH₃), 3.66–3.61 (1H, m, C(16)H_AH_B), 3.39–3.32 (1H, m, C(16)H_AH_B), 2.94 (1H, br. s, OH), 2.55–2.48 (1H, m, C(2)H), 2.39–2.32 (1H, m, C(13)H_AH_B), 2.20–2.08 (1H, m, C(9)H_AH_B), 1.90–1.83 (2H, m, C(8)H_AH_B, C(9)H_AH_B), 1.63 (1H, dd, $J = 12.9, 4.4$ Hz, C(13)H_AH_B), 1.72–1.66 (2H, m, C(5)H_AH_B, C(8)H_AH_B), 1.60–1.56 (1H, m, C(5)H_AH_B), 1.52–1.49 (1H, m, C(4)H_AH_B), 1.44–1.35 (1H, m, C(6)H_AH_B), 1.25 (9H, s, TBODPS-C(CH₃)₃), 1.26–1.22 (1H, m, C(4)H_AH_B), 1.19 (3H, s, C(12)CH₃), 1.17 (3H, d, $J = 7.3$ Hz, C(2)CH₃), 1.13–1.06 (1H, m, C(6)H_AH_B);

¹³C NMR (125 MHz, CDCl₃) δ_c 172.6 (C1), 159.2 (PMB-C_{Ar}OMe), 138.2 (Ph-C_{Ar}N), 135.9 (TBODPS-C_{Ar} × 2), 135.8 (TBODPS-C_{Ar}Si), 135.2 (TBODPS-C_{Ar} × 2), 133.5 (TBODPS-C_{Ar}Si), 130.3 (PMB-C_{Ar}CH₂), 130.1 (TBODPS-C_{Ar}), 129.9 (TBODPS-C_{Ar}), 129.1 (PMB-C_{Ar} × 2), 128.9 (Ph-C_{Ar} × 2), 127.6 (TBODPS-C_{Ar} × 2), 127.5 (TBODPS-C_{Ar} × 2), 123.8 (Ph-C_{Ar}), 119.5 (Ph-C_{Ar} × 2), 113.8 (PMB-C_{Ar} × 2), 106.1 (C7), 84.6 (C12), 83.8 (C15), 80.0 (C14), 78.3 (C11), 78.2 (C10), 74.2 (TBODPS-C(CH₃)₃), 71.8 (C3), 71.2 (PMB-CH₂), 63.0 (C16), 55.3 (PMB-CH₃), 45.9 (C2), 41.0 (C13), 37.9 (C8), 32.3 (C6), 31.8 (TBODPS-C(CH₃)₃), 26.1 (C4), 24.2 (C9), 22.7 (C12-CH₃), 19.8 (C5), 12.1 (C2-CH₃);

IR ν_{max} (film)/cm⁻¹ 3320, 2918, 2850, 1667, 1599, 1542, 1514, 1442, 1248, 1180, 1122, 1050, 744, 717, 701;

HRMS (ESI⁺, m/z) C₄₈H₆₂NO₉Si⁺ [M + H⁺] calculated 824.41884, found 824.41907 ($\Delta = +0.28$ ppm).

(R)-2-((2S,5S,7S)-2-((1R,2S,5S,6S)-6-((4-Methoxybenzyl)oxy)-1-methyl-4-oxo-3,8-dioxabicyclo[3.2.1]octan-2-yl)-1,6-dioxaspiro[4.5]decan-7-yl)-N-phenylpropanamide (345)



BAIB (3.1 mg, 9.7 μmol) was added to a solution of diol **227** (5.0 mg, 8.8 μmol) and TEMPO (0.1 mg, 0.8 μmol) in CH_2Cl_2 (1.0 mL). The reaction mixture was stirred at room temperature for 6 h. After which, the reaction mixture was diluted with CH_2Cl_2 (3 mL). The organic phase was washed with a solution of $\text{Na}_2\text{S}_2\text{O}_3$ (sat., 1 mL), dried (MgSO_4), filtered and concentrated *in vacuo*. Purification by flash column chromatography (SiO_2 , 80:20 to 60:40 Pentane:EtOAc) afforded lactone **345** (2.0 mg, 40%) as a colourless oil.

$R_f = 0.6$ (50:50 Pentane:EtOAc);

$[\alpha]_D^{25} -11.7$ ($c = 0.17$, CH_2Cl_2);

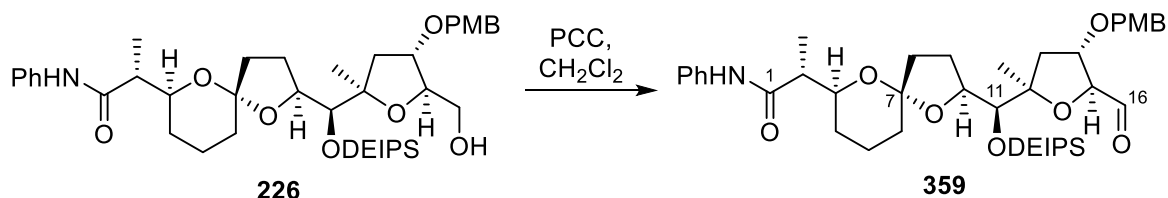
$^1\text{H NMR}$ (500 MHz, CDCl_3) δ_H 8.03 (1H, s, PhNH), 7.51–7.44 (2H, m, PhH \times 2), 7.33–7.21 (4H, m, PhH \times 2, PMB-ArH \times 2), 7.06 (1H, t, $J = 8.0$ Hz, PhH), 6.89 (2H, d, $J = 8.6$ Hz, PMB-ArH \times 2), 4.59 (1H, d, $J = 1.3$ Hz, C(11)H), 4.47 (1H, d, $J = 11.5$ Hz, PMB- CH_AH_B), 4.36 (1H, d, $J = 11.3$ Hz, PMB- CH_AH_B), 4.16 (1H, d, $J = 8.5$ Hz, C(15)H), 3.99–3.93 (2H, m, C(3)H), C(14)H), 3.90–3.84 (1H, m, C(10)H), 3.81 (3H, s, PMB- CH_3), 2.54 (1H, qd, $J = 7.2, 3.6$ Hz, C(2)H), 2.40 (1H, dd, $J = 14.5, 7.4$ Hz, C(13) H_AH_B), 2.01 (1H, ddd, $J = 12.6, 8.6, 3.8$ Hz, C(8) H_AH_B), 2.32–2.24 (1H, m, C(9) H_AH_B), 1.94–1.84 (2H, m, C(8) H_AH_B , C(9) H_AH_B), 1.77–1.70 (3H, m, C(5) H_2 , C(13) H_AH_B), 1.70–1.67 (2H, m, C(6) H_2), 1.63–1.58 (1H, m, C(4) H_AH_B), 1.40–1.32 (1H, m, C(4) H_AH_B), 1.55 (3H, s, C(12) CH_3), 1.23 (3H, d, $J = 7.3$ Hz, C(2) CH_3);

^{13}C NMR (125 MHz, CDCl_3) δ_{c} 172.5 (C1), 166.8 (C16), 159.5 (PMB- $\text{C}_{\text{Ar}}\text{OMe}$), 138.1 (Ph- $\text{C}_{\text{Ar}}\text{N}$), 129.6 (PMB- $\text{C}_{\text{Ar}}\text{CH}_2$), 129.1 (PMB- $\text{C}_{\text{Ar}} \times 2$), 129.0 (Ph- $\text{C}_{\text{Ar}} \times 2$), 124.0 (Ph- C_{Ar}), 119.3 (Ph- $\text{C}_{\text{Ar}} \times 2$), 114.0 (PMB- $\text{C}_{\text{Ar}} \times 2$), 107.7 (C7), 87.1 (C15), 82.0 (C14), 81.2 (C12), 79.7 (C11), 76.3 (C10), 72.6 (C3), 71.5 (PMB- CH_2), 55.3 (PMB- CH_3), 46.4 (C2), 38.1 (C13), 37.0 (C8), 33.1 (C6), 27.7 (C9), 26.5 (C4), 23.5 (C12- CH_3), 19.9 (C5), 12.1 (C2- CH_3);

IR ν_{max} (film)/ cm^{-1} 3324, 2936, 1755, 1667, 1599, 1514, 1500, 1441, 1363, 1247, 1033, 865, 757;

HRMS (ESI $^+$, m/z) $\text{C}_{32}\text{H}_{39}\text{NO}_8\text{Na}^+$ $[\text{M} + \text{Na}^+]$ calculated 588.25679, found 588.25671 ($\Delta = -0.13$ ppm).

(R)-2-((2S,5S,7S)-2-((S)-((Diethyl(isopropyl)silyl)oxy)((2R,4S,5S)-5-formyl-4-((4-methoxybenzyl)oxy)-2-methyltetrahydrofuran-2-yl)methyl)-1,6-dioxaspiro[4.5]decan-7-yl)-N-phenylpropanamide (359)



PCC (69.8 mg, 0.324 mmol) was added to a solution of alcohol **226** (56.5 mg, 80.9 μmol) dissolved in CH_2Cl_2 (5.7 mL) containing powdered 3Å molecular sieves (169 mg) and the mixture was stirred for 25 min at room temperature. After which, the reaction mixture was filtered through a long pad of silica with 70:30 Pentane:EtOAc eluent and then concentrated *in vacuo* to afford pure aldehyde **359** (52.9 mg, 94%) as a colourless oil.

$R_f = 0.6$ (50:50 Pentane:EtOAc);

$[\alpha]_{\text{D}}^{25} -13.4$ ($c = 0.33$, CH_2Cl_2);

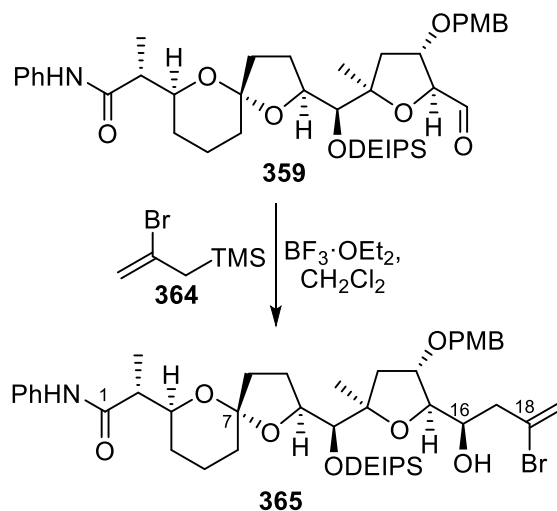
¹H NMR (600 MHz, CDCl₃) δ_{H} 9.59 (1H, d, $J = 1.1$ Hz, C(16)H), 8.36 (1H, s, PhNH), 7.51–7.46 (2H, m, PhH \times 2), 7.32–7.26 (2H, m, PhH \times 2), 7.26–7.22 (2H, m, PMB-ArH \times 2), 7.04 (1H, tt, $J = 7.4$, 1.2 Hz, PhH), 6.89 (2H, d, $J = 8.6$ Hz, PMB-ArH \times 2), 4.49 (1H, d, $J = 11.5$ Hz, PMB-CH_AH_B), 4.42 (1H, d, $J = 11.5$ Hz, PMB-CH_AH_B), 4.30–4.27 (1H, m, C(10)H), 4.27 (1H, dd, $J = 3.8$, 1.2 Hz, C(15)H), 4.12 (1H, ddd, $J = 7.5$, 3.8, 2.6 Hz, C(14)H), 4.05 (1H, ddd, $J = 11.9$, 3.7, 2.3 Hz, C(3)H), 3.90 (1H, d, $J = 1.4$ Hz, C(11)H), 3.81 (3H, s, PMB-CH₃), 2.57 (1H, qd, $J = 7.1$, 3.6 Hz, C(2)H), 2.09 (1H, dd, $J = 13.3$, 7.6 Hz, C(13)H_AH_B), 2.05–1.98 (2H, m, C(8)H_AH_B, C(9)H_AH_B), 1.90–1.78 (3H, m, C(5)H_AH_B, C(8)H_AH_B, C(9)H_AH_B), 1.75 (1H dd, $J = 13.3$, 2.6 Hz, C(13)H_AH_B), 1.73–1.63 (2H, m, C(5)H_AH_B, C(6)H₂), 1.60–1.57 (1H, m, C(4)H_AH_B), 1.36–1.30 (1H, m, C(4)H_AH_B), 1.22 (3H, d, $J = 7.2$ Hz, C(2)CH₃), 1.21 (3H, s, C(12)CH₃), 1.03–0.93 (13H, m, DEIPS-CH₃ \times 4, DEIPS-*i*PrCH), 0.69–0.56 (4H, m, DEIPS-CH₂ \times 2);

¹³C NMR (150 MHz, CDCl₃) δ_{C} 201.7 (C16), 172.7 (C1), 159.3 (PMB-C_{Ar}OMe), 138.4 (Ph-C_{Ar}N), 129.7 (PMB-C_{Ar}CH₂), 129.3 (PMB-C_{Ar} \times 2), 129.0 (Ph-C_{Ar} \times 2), 123.7 (Ph-C_{Ar}), 119.4 (Ph-C_{Ar} \times 2), 113.9 (PMB-C_{Ar} \times 2), 105.7 (C7), 88.3 (C15), 86.5 (C12), 80.6 (C14), 78.2 (C10), 77.4 (C11), 71.7 (C3), 71.4 (PMB-CH₂), 55.3 (PMB-CH₃), 46.1 (C2), 41.6 (C13), 38.4 (C8), 32.8 (C6), 26.2 (C4), 22.9 (C9), 21.8 (C12-CH₃), 19.9 (C5), 17.6 (DEIPS-*i*PrCH₃), 17.5 (DEIPS-*i*PrCH₃), 13.3 (DEIPS-*i*PrCH), 12.3 (C2-CH₃), 7.3 (DEIPS-EtCH₃), 7.2 (DEIPS-EtCH₃), 4.6 (DEIPS-EtCH₂), 4.2 (DEIPS-EtCH₂);

IR ν_{max} (film)/cm⁻¹ 3317, 2935, 1733, 1666, 1600, 1542 1442, 1379, 1248, 1034, 973, 820, 756, 723;

HRMS (ESI⁺, m/z) C₃₉H₅₈NO₈Si⁺ [M + H⁺] calculated 696.39262, found 696.39252 ($\Delta = -0.15$ ppm).

(R)-2-((2S,5S,7S)-2-((S)-((2R,4S,5R)-5-((R)-3-Bromo-1-hydroxybut-3-en-1-yl)-4-((4-methoxybenzyl)oxy)-2-methyltetrahydrofuran-2-yl))((diethyl(isopropyl)silyl)oxy)methyl)-1,6-dioxaspiro[4.5]decan-7-yl)-N-phenylpropanamide (365)



A solution of bromide **364** (6.2 mg, 32 μmol) in CH_2Cl_2 (0.50 mL) was added to a flask charged with aldehyde **359** (3.7 mg, 5.3 μmol , azeotropically distilled three times with PhMe). The resulting solution was cooled to $-78\text{ }^\circ\text{C}$, and then $\text{BF}_3\cdot\text{OEt}_2$ (1.4 μL , 11 μmol) was added dropwise. The reaction was stirred at $-78\text{ }^\circ\text{C}$ for 6 h, before it was quenched with a solution of NaHCO_3 (sat., 2 mL) and a solution of Rochelle's salt (sat., 2 mL). The mixture was diluted with EtOAc (2 mL) and the layers were separated. The aqueous layer was extracted with EtOAc (3×4 mL). The combined organic layers were dried (MgSO_4), filtered and then concentrated *in vacuo*. Purification by column chromatography (SiO_2 , 80:20 to 70:30 to 60:40 to 40:60 Pentane:EtOAc) afforded alcohol **365** (2.3 mg, 53%) as a colourless oil.

$R_f = 0.6$ (70:30 Pentane:EtOAc);

$[\alpha]_D^{25} -21.2$ ($c = 0.12$, CH_2Cl_2);

$^1\text{H NMR}$ (500 MHz, CDCl_3) δ_H 8.31 (1H, s, PhNH), 7.49 (2H, d, $J = 7.9$ Hz, PhH $\times 2$), 7.29 (2H, t, $J = 7.7$ Hz, PhH $\times 2$), 7.26–7.22 (2H, m, PMB-ArH $\times 2$), 7.05 (1H, t, $J = 7.4$ Hz, PhH), 6.88 (2H, d,

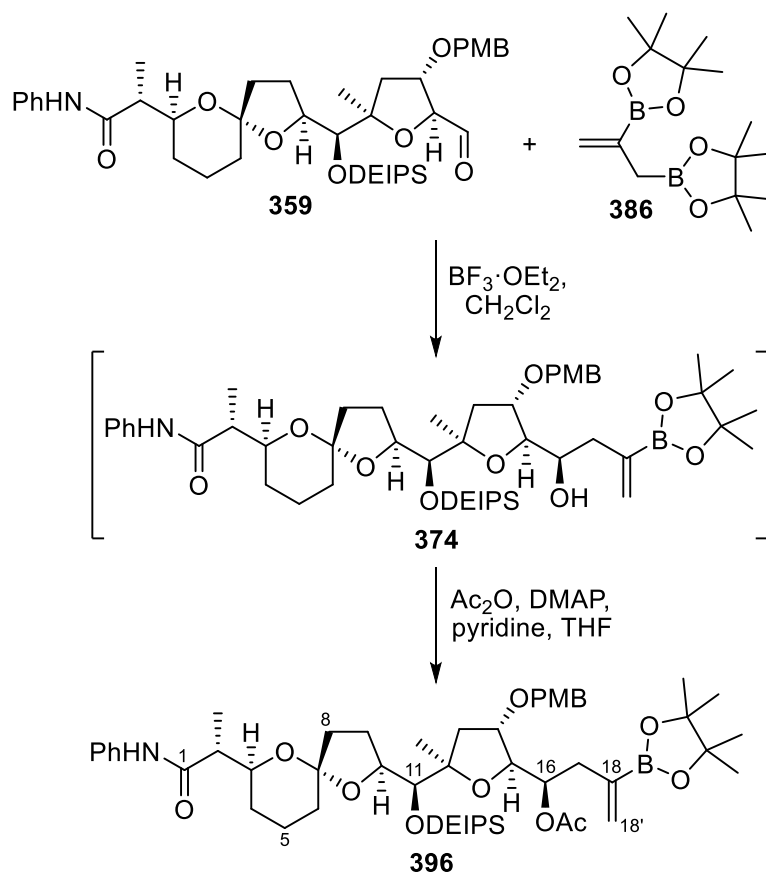
$J = 8.5$ Hz, PMB-ArH $\times 2$), 5.68–5.65 (1H, m, RBrC=CH_AH_B), 5.51 (1H, d, $J = 1.6$ Hz, RBrC=CH_AH_B), 4.45 (1H, d, $J = 11.5$ Hz, PMB-CH_AH_B), 4.39 (1H, d, $J = 11.5$ Hz, PMB-CH_AH_B), 4.24 (1H, t, $J = 7.5$ Hz, C(10)H), 4.14–4.09 (1H, m, C(14)H), 4.06–4.01 (1H, m, C(3)H), 3.95–3.85 (1H, m, C(16)H), 3.87–3.83 (2H, m, C(11)H, C(15)H), 3.81 (3H, s, PMB-CH₃), 2.66 (1H, br. s, OH), 2.64–2.59 (1H, m, C(17)H_AH_B), 2.58–2.55 (1H, m, C(2)H), 2.44–2.36 (1H, m, C(17)H_AH_B), 2.11 (1H, dd, $J = 13.2$, 7.1 Hz, C(13)H_AH_B), 2.04–1.95 (2H, m, C(8)H_AH_B, C(9)H_AH_B), 1.87–1.77 (3H, m, C(5)H_AH_B, C(8)H_AH_B, C(9)H_AH_B), 1.76–1.59 (5H, m, C(4)H_AH_B, C(5)H_AH_B, C(6)H₂, C(13)H_AH_B), 1.33–1.27 (1H, m, C(4)H_AH_B), 1.21 (3H, d, $J = 7.3$ Hz, C(2)CH₃), 1.17 (3H, s, C(12)CH₃), 1.03–0.95 (13H, m, DEIPS-CH₃ $\times 4$, DEIPS-*i*PrCH), 0.71–0.59 (4H, m, DEIPS-CH₂ $\times 2$);

¹³C NMR (125 MHz, CDCl₃) δ_c 172.6 (C1), 159.3 (PMB-C_{Ar}OMe), 138.3 (Ph-C_{Ar}N), 130.4 (C18), 130.0 (PMB-C_{Ar}CH₂), 129.4 (PMB-C_{Ar} $\times 2$), 129.0 (Ph-C_{Ar} $\times 2$), 123.8 (Ph-C_{Ar}), 119.5 (Ph-C_{Ar} $\times 2$), 119.4 (RCBr=CH₂), 113.8 (PMB-C_{Ar} $\times 2$), 105.8 (C7), 85.4 (C15), 84.8 (C12), 79.1 (C14), 78.2 (C11), 78.2 (C10), 71.8 (C3), 71.1 (PMB-CH₂), 69.3 (C16), 55.3 (PMB-CH₃), 45.9 (C2), 44.8 (C17), 41.6 (C13), 38.2 (C8), 32.8 (C6), 26.1 (C4), 23.4 (C9), 22.3 (C12-CH₃), 19.8 (C5), 17.6 (DEIPS-*i*PrCH₃), 17.5 (DEIPS-*i*PrCH₃), 13.3 (DEIPS-*i*PrCH), 12.2 (C2-CH₃), 7.3 (DEIPS-EtCH₃), 7.3 (DEIPS-EtCH₃), 4.5 (DEIPS-EtCH₂), 4.2 (DEIPS-EtCH₂);

IR ν_{\max} (film)/cm⁻¹ 2934, 2873, 1668, 1600, 1540, 1514, 1442, 1362, 1248, 1034, 820, 754, 724;

HRMS (ESI⁺, m/z) C₄₂H₆₂O₈NBrNaSi⁺ [M + Na⁺] calculated 838.33203, found 838.33234 ($\Delta = +0.37$ ppm).

(R)-1-((2S,3S,5R)-5-((S)-((diethyl(isopropyl)silyl)oxy))((2S,5S,7S)-7-((R)-1-oxo-1-(phenylamino)propan-2-yl)-1,6-dioxaspiro[4.5]decan-2-yl)methyl)-3-((4-methoxybenzyl)oxy)-5-methyltetrahydrofuran-2-yl)-3-(4,4,5,5-tetramethyl-1,3,2-dioxaborolan-2-yl)but-3-en-1-yl acetate (396)



To a Schlenk tube was added **359** (5.0 mg, 7.2 μmol) dissolved in CH_2Cl_2 (0.50 mL) and **386** (8.5 mg, 29 μmol) dissolved in CH_2Cl_2 (0.50 mL). The Schlenk tube was evacuated and backfilled with N_2 five times, with care taken to prevent the solution from bumping. The resulting solution was cooled to -78°C . $\text{BF}_3 \cdot \text{Et}_2\text{O}$ (3.6 μL , 28 μmol) dissolved in CH_2Cl_2 (0.50 mL) was then added dropwise to the reaction mixture, which was stirred at -78°C for 1.5 h and then quenched with a solution of NaHCO_3 (sat., 2 mL). The aqueous layer was extracted with Et_2O (3 \times 4 mL). The combined organic layers were dried (MgSO_4), filtered and then concentrated *in vacuo*.

The crude mixture was transferred to a 10-mL RBF. To the RBF were added DMAP (1.8 mg, 14 μ mol), Ac₂O (2.0 μ L, 21 μ mol), pyridine (3.5 μ L, 43 μ mol), and THF (1.00 mL). The reaction mixture was heated to 50 °C and stirred for 3 h. The reaction mixture was quenched with a solution of NaHCO₃ (sat., 2 mL). The aqueous layer was extracted with Et₂O (3 \times 4 mL). The combined organic layers were dried (MgSO₄), filtered and then concentrated *in vacuo*. Purification by column chromatography (SiO₂, 98:2 to 90:10 to 85:15 to 80:20 Pentane:EtOAc) afforded acetate **396** (3.7 mg, 57%) as a colourless oil.

R_f = 0.5 (70:30 Pentane:EtOAc);

[α]_D²⁵ -3.8 (*c* = 0.31, CH₂Cl₂);

¹H NMR (500 MHz, CDCl₃) δ _H 8.61 (1H, s, PhNH), 7.54–7.46 (2H, m, PhH \times 2), 7.33–7.26 (2H, m, PhH \times 2), 7.27–7.22 (2H, m, PMB-ArH \times 2), 7.05 (1H, t, *J* = 7.6 Hz, PhH), 6.91–6.83 (2H, m, PMB-ArH \times 2), 5.81 (1H, d, *J* = 3.5 Hz, C(18')H_AH_B), 5.60 (1H, d, *J* = 3.5 Hz, C(18')H_AH_B), 5.24 (1H, dt, *J* = 9.9, 4.0 Hz, C(16)H), 4.47–4.36 (3H, m, C(10)H, PMB-CH₂), 4.06–4.01 (1H, m, C(15)H), 3.97 (1H, ddd, *J* = 11.9, 4.8, 2.3 Hz, C(14)H), 3.92–3.86 (1H, m, C(3)H), 3.88–3.84 (1H, m, C(11)H), 3.80 (3H, s, PMB-CH₃), 2.59 (1H, qd, *J* = 7.1, 4.4 Hz, C(2)H), 2.50 (1H, dd, *J* = 13.6, 3.7 Hz, C(17)H_AH_B), 2.31 (1H, dd, *J* = 13.6, 9.7 Hz, C(17)H_AH_B), 2.28 (1H, dd, *J* = 12.8, 7.8 Hz, C(13)H_AH_B), 2.11–2.01 (1H, m, C(9)H_AH_B), 2.00 (3H, s, Ac-CH₃), 1.99–1.93 (1H, m, C(8)H_AH_B), 1.93–1.80 (2H, m, C(5)H_AH_B, C(9)H_AH_B), 1.80–1.70 (3H, m, C(6)H_AH_B, C(13)H_AH_B, C(8)H_AH_B), 1.70–1.60 (3H, m, C(4)H_AH_B, C(5)H_AH_B, C(6)H_AH_B), 1.27–1.23 (1H, m, C(4)H_AH_B), 1.27 (6H, s, Bpin-C(CH₃)₂), 1.24 (6H, s, Bpin-C(CH₃)₂), 1.19 (3H, s, C(12)CH₃), 1.17 (3H, d, *J* = 7.2 Hz, C(2)CH₃), 1.03–0.95 (13H, m, DEIPS-CH₃ \times 4, DEIPS-*i*PrCH), 0.70–0.56 (4H, m, DEIPS-CH₂ \times 2);

¹³C NMR (125 MHz, CDCl₃) δ _C 172.3 (C1), 170.6 (AcO-C(O)Me), 159.3 (PMB-C_{Ar}OMe), 138.5 (Ph-C_{Ar}N), 131.8 (C18'), 130.1 (PMB-C_{Ar}CH₂), 129.2 (PMB-C_{Ar} \times 2), 128.9 (Ph-C_{Ar} \times 2), 123.5 (Ph-C_{Ar}), 119.4 (Ph-C_{Ar} \times 2), 113.8 (PMB-C_{Ar} \times 2), 105.4 (C7), 84.5 (C12), 83.9 (C15), 83.5 (Bpin-

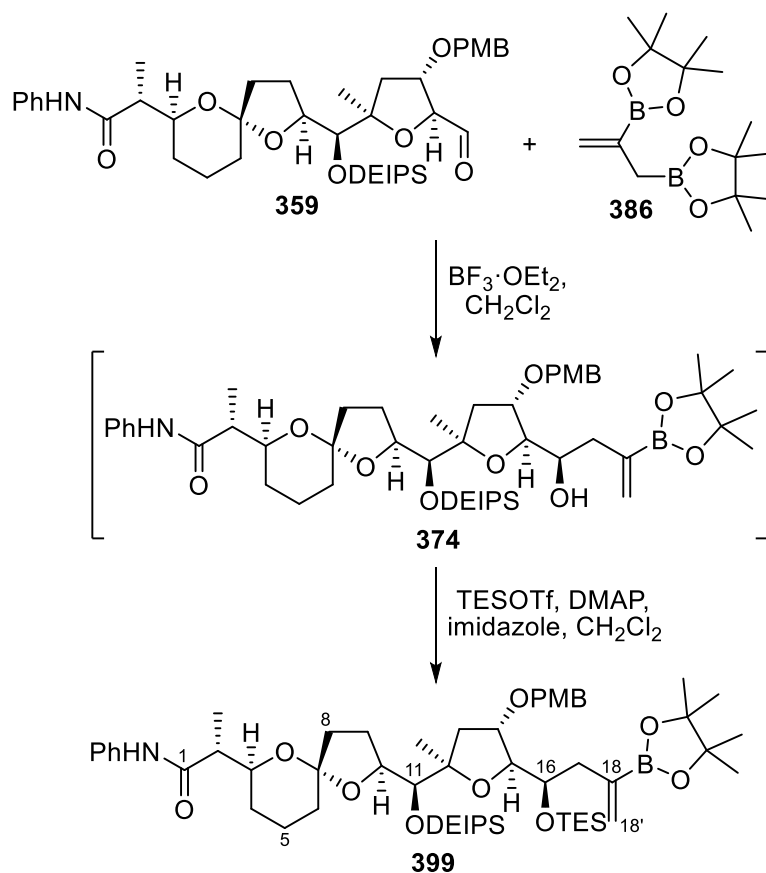
C(CH₃)₂ × 2), 80.1 (C3), 78.1 (C10), 77.7 (C11), 73.4 (C16), 72.0 (C14), 71.6 (PMB-CH₂), 55.3 (PMB-CH₃), 46.2 (C2), 42.6 (C13), 38.5 (C8), 38.1 (C17), 32.7 (C6), 25.9 (C4), 24.9 (Bpin-C(CH₃)₂), 24.5 (Bpin-C(CH₃)₂), 22.7 (C9), 22.1 (C12-CH₃), 19.8 (C5), 17.6 (DEIPS-*i*PrCH₃), 17.5 (DEIPS-*i*PrCH₃), 13.3 (DEIPS-*i*PrCH), 12.7 (C2-CH₃), 7.4 (DEIPS-EtCH₃), 7.3 (DEIPS-EtCH₃), 4.7 (DEIPS-EtCH₂), 4.2 (DEIPS-EtCH₂);

HRMS (ESI⁺, *m/z*) C₅₀H₇₆O₁₁NBNaSi⁺ [M + Na⁺] calculated 928.51812, found 928.51727 (Δ = -0.12 ppm).

IR ν_{max} (film)/cm⁻¹ 2939, 2876, 1739, 1717, 1601, 1541, 1514, 1441, 1247, 1142, 1033, 973, 755, 721.

(The carbon attached to boron (C18) was not observed due to quadrupolar relaxation.)

(R)-2-((2S,5S,7S)-2-((S)-((diethyl(isopropyl)silyl)oxy)((2R,4S,5S)-4-((4-methoxybenzyl)oxy)-2-methyl-5-((R)-3-(4,4,5,5-tetramethyl-1,3,2-dioxaborolan-2-yl)-1-((triethylsilyl)oxy)but-3-en-1-yl)tetrahydrofuran-2-yl)methyl)-1,6-dioxaspiro[4.5]decan-7-yl)-N-phenylpropanamide
(399)



To a Schlenk tube was added **359** (14.4 mg, 20.7 μmol) dissolved in CH_2Cl_2 (0.50 mL) and **386** (24.3 mg, 82.8 μmol) dissolved in CH_2Cl_2 (0.50 mL). The Schlenk tube was evacuated and backfilled with N_2 five times, with care taken to prevent the solution from bumping. The resulting solution was cooled to -78°C . $\text{BF}_3 \cdot \text{Et}_2\text{O}$ (10.5 μL , 82.8 μmol) dissolved in CH_2Cl_2 (0.50 mL) was then added dropwise to the reaction mixture, which was stirred at -78°C for 1.5 h and then quenched with a solution of NaHCO_3 (sat., 2.0 mL). The aqueous layer was extracted with Et_2O (3×4 mL). The combined organic layers were dried (MgSO_4), filtered and then concentrated *in vacuo*.

The crude mixture was dissolved in CH₂Cl₂ (3.0 mL), and a portion of the solution (1.0 mL) was transferred to a 10-mL RBF. Imidazole (10.0 mg, 0.147 mmol) and DMAP (0.9 mg, 7 μmol) were then added, followed by the dropwise addition of TESOTf (16.6 μL, 73.4 μmol). The reaction was stirred for 15 min, and then quenched with MeOH (0.5 mL) and then water (2.0 mL). The layers were allowed to separate and the aqueous layer was extracted with Et₂O (3 × 4 mL). The organic layers were combined, dried (MgSO₄), filtered, and then concentrated *in vacuo*. Purification by flash column chromatography (SiO₂, 90:10 to 80:20 to 70:30 Pentane:EtOAc) afforded silyl ether **399** (1.3 mg, 19%, 2:1 d.r.) as a colourless oil.

R_f = 0.8 (70:30 Pentane:EtOAc);

[α]_D²⁵ -1.7 (c = 0.24, CH₂Cl₂);

¹H NMR (500 MHz, CDCl₃) δ_H 8.40 (1H, s, PhNH), 7.52–7.46 (2H, m, PhH × 2), 7.33–7.21 (2H, m, PhH × 2, PMB-ArH × 2), 7.04 (1H, t, J = 7.5 Hz, PhH), 6.87 (2H, d, J = 8.6 Hz, PMB-ArH × 2), 5.88 (1H, d, J = 3.6 Hz, C(18')H_AH_B), 5.68 (1H, d, J = 3.6 Hz, C(18')H_AH_B), 4.46–4.36 (2H, m, PMB-CH₂), 4.33–4.27 (1H, m, C(10)H), 4.07–4.01 (1H, m, C(14)H), 4.01–3.95 (1H, m, C(16)H), 3.94–3.88 (2H, m, C(11)H, C(15)H), 3.70–3.63 (1H, m, C(3)H), 3.80 (3H, s, PMB-CH₃), 2.60 (1H, qd, J = 7.2, 3.4 Hz, C(2)H), 2.35–2.32 (2H, m, C(8)H₂), 2.12 (1H, dd, J = 13.2, 7.3 Hz C(13)H_AH_B), 2.07–1.94 (2H, m, C(9)H_AH_B, C(17)H_AH_B), 1.91–1.80 (3H, m, C(5)H_AH_B, C(9)H_AH_B, C(17)H_AH_B), 1.80–1.65 (4H, m, C(5)H_AH_B, C(6)H₂, C(13)H_AH_B), 1.65–1.58 (1H, m, C(4)H_AH_B), 1.27–1.23 (1H, m, C(4)H_AH_B), 1.28–1.22 (12H, s, Bpin-C(CH₃)₂ × 2), 1.19 (3H, s, C(12)CH₃), 1.17 (3H, d, J = 7.2 Hz, C(2)CH₃), 1.05–0.91 (22H, m, DEIPS-CH₃ × 4, DEIPS-CH₃ × 3, DEIPS-*i*PrCH), 0.68–0.56 (10H, m, TES-EtCH₂ × 3, DEIPS-CH₂ × 2);

¹³C NMR (125 MHz, CDCl₃) δ_C 172.3 (C1), 159.3 (PMB-C_{Ar}OMe), 138.4 (Ph-C_{Ar}N), 132.1 (C18'), 130.4 (PMB-C_{Ar}CH₂), 129.2 (PMB-C_{Ar} × 2), 129.0 (Ph-C_{Ar} × 2), 123.6 (Ph-C_{Ar}), 119.4 (Ph-C_{Ar} × 2), 113.8 (PMB-C_{Ar} × 2), 105.7 (C7), 85.8 (C15), 85.0 (C12), 83.6 (Bpin-C(CH₃)₂ × 2), 81.3 (C14),

78.4 (C10), 78.3 (C11), 72.1 (C16), 72.0 (C3), 71.2 (PMB-CH₂), 55.3 (PMB-CH₃), 45.6 (C2), 41.9 (C13), 40.7 (C8), 38.4 (C17), 32.7 (C6), 25.7 (C4), 24.8 (Bpin-C(CH₃)₂), 24.7 (Bpin-C(CH₃)₂), 23.1 (C9), 22.0 (C12-CH₃), 19.8 (C5), 17.6 (DEIPS-*i*PrCH₃), 17.5 (DEIPS-*i*PrCH₃), 13.3 (DEIPS-*i*PrCH), 12.4 (C2-CH₃), 7.3 (DEIPS-EtCH₃), 7.3 (DEIPS-EtCH₃), 6.6 (TES-EtCH₃ × 3), 5.8 (TES-EtCH₂ × 3), 4.6 (DEIPS-EtCH₂), 4.3 (DEIPS-EtCH₂);

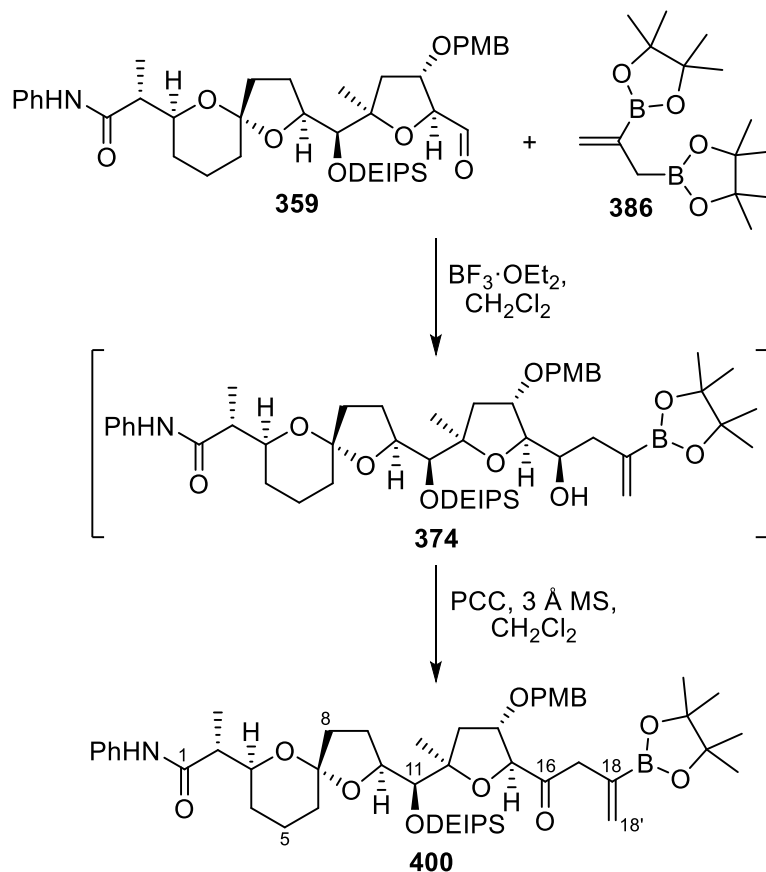
HRMS (ESI⁺, *m/z*) C₅₄H₈₈O₁₀NBNaSi₂⁺ [M + Na⁺] calculated 1000.5941, found 1000.5931

(Δ = +0.21 ppm);

IR ν_{max} (film)/cm⁻¹ 2939, 2876, 1667, 1600, 1514, 1500, 1460, 1442, 1371, 1307, 1249, 1141, 1034, 972, 755.

(The carbon attached to boron (C18) was not observed due to quadrupolar relaxation.)

(R)-2-((2S,5S,7S)-2-((S)-((Diethyl(isopropyl)silyl)oxy)((2R,4S,5S)-4-((4-methoxybenzyl)oxy)-2-methyl-5-(3-(4,4,5,5-tetramethyl-1,3,2-dioxaborolan-2-yl)but-3-enoyl)tetrahydrofuran-2-yl)methyl)-1,6-dioxaspiro[4.5]decan-7-yl)-N-phenylpropanamide (400)



To a Schlenk tube was added aldehyde **359** (10.0 mg, 14.4 μmol) dissolved in CH_2Cl_2 (0.50 mL) and **386** (5.1 mg, 17 μmol) dissolved in CH_2Cl_2 (0.50 mL). The Schlenk tube was evacuated and backfilled with N_2 five times, with care taken to prevent the solution from bumping. The resulting solution was cooled to $-78 \text{ }^\circ\text{C}$. $\text{BF}_3 \cdot \text{Et}_2\text{O}$ (7.3 μL , 58 μmol) in CH_2Cl_2 (0.50 mL) was then added dropwise to the reaction mixture, which was stirred at $-78 \text{ }^\circ\text{C}$ for 1.5 h and then quenched with a solution of NaHCO_3 (sat., 2 mL). The aqueous layer was extracted with Et_2O ($3 \times 6 \text{ mL}$). The combined organic layers were dried (MgSO_4), filtered and then concentrated *in vacuo*. Crude alcohol **374** was directly carried over to the next step as described below.

PCC (12.4 mg, 57.6 μmol) was added to a solution of **374** (assumed quant., 14.4 μmol) dissolved in CH_2Cl_2 (1.00 mL) containing powdered 3 \AA molecular sieves (30.2 mg)

and the mixture was stirred for 4.5 h at room temperature. After which, the reaction mixture was filtered through a short pad of silica with 70:30 Pentane:EtOAc and then concentrated *in vacuo*. Purification by column chromatography (SiO₂, 98:2 to 90:10 to 85:15 to 80:20 Pentane:EtOAc) afforded ketone **400** (2.7 mg, 22%) as a colourless oil.

$R_f = 0.7$ (70:30 Pentane:EtOAc);

$[\alpha]_D^{25} -30.7$ ($c = 0.23$, CH₂Cl₂);

¹H NMR (500 MHz, CDCl₃) δ_H 8.47 (1H, s, PhNH), 7.52–7.46 (2H, m, PhH × 2), 7.33–7.22 (4H, m, PhH × 2, PMB-ArH × 2), 7.05 (1H, t, $J = 7.5$ Hz, PhH), 6.91–6.84 (2H, m, PMB-ArH × 2), 5.93 (1H, d, $J = 3.1$ Hz, C(4)*H_AH_B*), 5.62 (1H, d, $J = 3.1$ Hz, C(4)*H_AH_B*), 4.53 (1H, d, $J = 11.6$ Hz, PMB-CH_AH_B), 4.42 (1H, d, $J = 11.4$ Hz, PMB-CH_AH_B), 4.46–4.40 (2H, m, C(10)*H*, C(15)*H*), 4.22–4.18 (1H, m, C(14)*H*), 4.05–3.97 (1H, m, C(3)*H*), 3.95–3.92 (1H, m, C(11)*H*), 3.80 (3H, s, PMB-CH₃), 3.35 (2H, s, C(17)*H*₂), 2.61 (1H, qd, $J = 7.3, 3.8$ Hz, C(2)*H*), 2.11–1.96 (3H, m, C(8)*H_AH_B*, C(9)*H_AH_B*, C(13)*H_AH_B*), 1.92–1.83 (2H, m, C(9)*H_AH_B*, C(13)*H_AH_B*), 1.83–1.77 (2H, m, C(5)*H_AH_B*, C(8)*H_AH_B*), 1.75–1.63 (1H, m, C(5)*H_AH_B*), 1.63–1.53 (4H, m, C(4)*H*₂, C(6)*H*₂), 1.25 (6H, s, Bpin-C(CH₃)₂), 1.23 (6H, s, Bpin-C(CH₃)₂), 1.22 (3H, s, C(12)CH₃), 1.17 (3H, d, $J = 7.2$ Hz, C(2)CH₃), 1.03–0.94 (13H, m, DEIPS-CH₃ × 4, DEIPS-*i*PrCH), 0.69–0.55 (4H, m, DEIPS-CH₂ × 2);

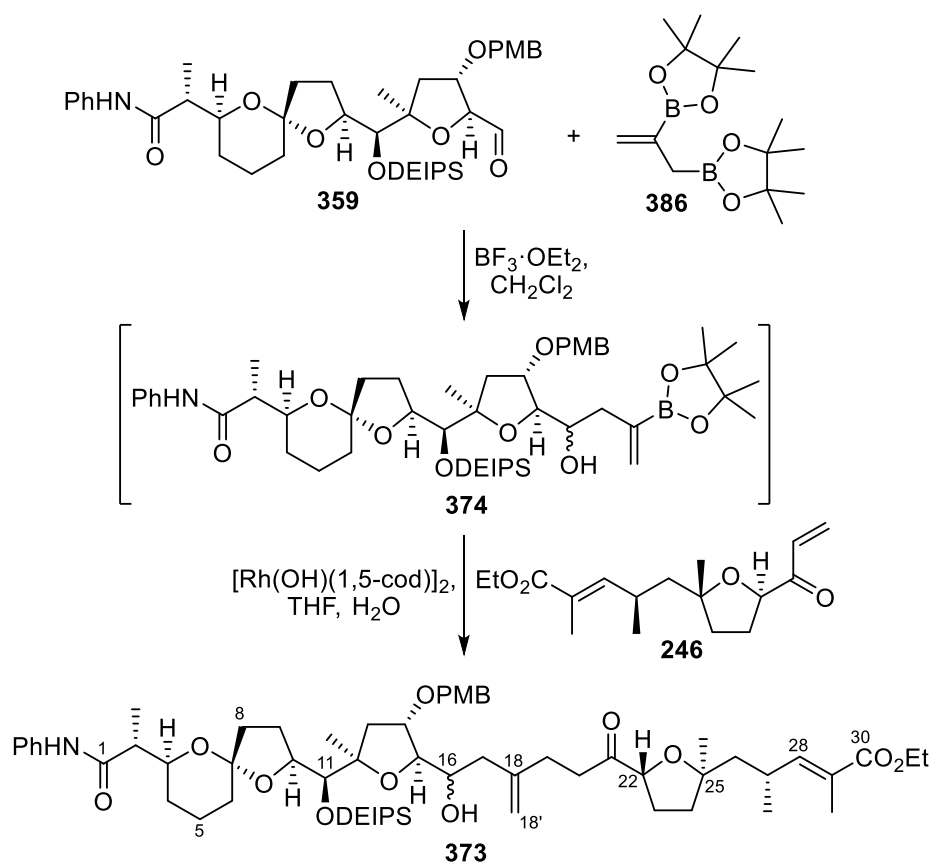
¹³C NMR (125 MHz, CDCl₃) δ_C 208.5 (C16), 172.5 (C1), 159.2 (PMB-C_{Ar}OMe), 138.5 (Ph-C_{Ar}N), 132.4 (RCBpin=CH₂), 130.0 (PMB-C_{Ar}CH₂), 129.4 (PMB-C_{Ar} × 2), 128.9 (Ph-C_{Ar} × 2), 123.6 (Ph-C_{Ar}), 119.4 (Ph-C_{Ar} × 2), 113.8 (PMB-C_{Ar} × 2), 105.5 (C7), 88.6 (C15), 86.4 (C12), 83.6 (Bpin-C(CH₃)₂ × 2), 81.4 (C14), 78.4 (C10), 78.2 (C11), 71.9 (C3), 71.3 (PMB-CH₂), 55.3 (PMB-CH₃), 45.7 (C2), 45.6 (C17), 43.3 (C13), 38.5 (C8), 32.7 (C6), 25.9 (C4), 24.7 (Bpin-C(CH₃)₂ × 2), 22.8 (C9), 21.2 (C12-CH₃), 19.8 (C5), 17.6 (DEIPS-*i*PrCH₃), 17.5 (DEIPS-*i*PrCH₃), 13.2 (DEIPS-*i*PrCH), 12.3 (C2-CH₃), 7.3 (DEIPS-EtCH₃), 7.3 (DEIPS-EtCH₃), 4.7 (DEIPS-EtCH₂), 4.1 (DEIPS-EtCH₂);

IR ν_{\max} (film)/ cm^{-1} 2938, 1690, 1600, 1539, 1514, 1459, 1441, 1256, 1139, 1011, 863, 789, 725, 694;

HRMS (ESI⁺, m/z) $\text{C}_{48}\text{H}_{72}\text{NO}_{10}\text{BSiNa}^+$ [$\text{M} + \text{Na}^+$] calculated 884.4918, found 884.4909 ($\Delta = -0.44$ ppm).

(The carbon attached to boron (C18) was not observed due to quadrupolar relaxation.)

Ethyl (*R,E*)-5-((*2R,5R*)-5-((*R*)-6-((*2R,3S,5R*)-5-((*S*)-((diethyl(isopropyl)silyl)oxy)((*2S,5S,7S*)-7-((*R*)-1-oxo-1-(phenylamino)propan-2-yl)-1,6-dioxaspiro[4.5]decan-2-yl)methyl)-3-((4-methoxybenzyl)oxy)-5-methyltetrahydrofuran-2-yl)-6-hydroxy-4-methylenehexanoyl)-2-methyltetrahydrofuran-2-yl)-2,4-dimethylpent-2-enoate (**373**)



To a Schlenk tube was added aldehyde **359** (21.2 mg, 30.5 μmol) dissolved in CH_2Cl_2 (1.0 mL) and **386** (10.7 mg, 36.6 μmol) dissolved in CH_2Cl_2 (0.50 mL). The Schlenk tube was evacuated and backfilled with N_2 five times, with care taken to prevent the solution from bumping. The

resulting solution was cooled to $-78\text{ }^{\circ}\text{C}$. $\text{BF}_3\cdot\text{Et}_2\text{O}$ ($15.4\text{ }\mu\text{L}$, 0.122 mmol) in CH_2Cl_2 (0.50 mL) was then added dropwise to the reaction mixture, which was stirred at $-78\text{ }^{\circ}\text{C}$ for 1.5 h and then quenched with a solution of NaHCO_3 (sat., 2.0 mL). The aqueous layer was extracted with Et_2O ($3 \times 6\text{ mL}$). The combined organic layers were dried (MgSO_4), filtered and then concentrated *in vacuo*.

A Schlenk tube was charged with the crude alcohol ($30.5\text{ }\mu\text{mol}$, assumed quant.), enone **246** (5.0 mg , $17\text{ }\mu\text{mol}$), and $[\text{Rh}(\text{cod})\text{OH}]_2$ (3.5 mg , $7.6\text{ }\mu\text{mol}$). THF (2.0 mL) and water (0.34 mL) was added and the resulting solution was warmed to $50\text{ }^{\circ}\text{C}$ and stirred for 2 h . The reaction mixture was then diluted with water (5 mL) and then extracted with EtOAc ($4 \times 5\text{ mL}$). The organic layers were combined, dried (MgSO_4), and concentrated *in vacuo*. Purification by flash column chromatography (SiO_2 , 95:5 to 80:20 to 60:40 Pentane:EtOAc) afforded alkene **373** (15.1 mg , 86%, 1:1 d.r.) as a pale yellow oil.

$R_f = 0.4$ (70:30 Pentane:EtOAc);

$[\alpha]_D^{25} -2.5$ ($c = 1.24$, CH_2Cl_2);

$^1\text{H NMR}$ (500 MHz , CDCl_3) δ_{H} 8.35 (1H, s, PhNH), 7.49 (2H, d, $J = 8.0\text{ Hz}$, PhH $\times 2$), 7.29 (2H, t, $J = 7.8\text{ Hz}$, PhH $\times 2$), 7.26–7.21 (2H, m, PMB-ArH $\times 2$), 7.07–7.01 (1H, m, PhH), 6.88 (2H, d, $J = 8.6\text{ Hz}$, PMB-ArH $\times 2$), 6.62 (1H, d, $J = 10.2\text{ Hz}$, C(28)H), 4.84 (1H, d, $J = 9.7\text{ Hz}$, C(18')H_AH_B), 4.86–4.82 (1H, m, C(18')H_AH_B), 4.81–4.77 (1H, m, C(18')H_AH_B), 4.47–4.40 (1H, m, PMB-CH_AH_B), 4.38 (1H, d, $J = 11.4\text{ Hz}$, PMB-CH_AH_B), 4.25 (1H, t, $J = 7.8\text{ Hz}$, C(10)H), 4.28–4.21 (1H, m, C(22)H), 4.21–4.15 (2H, m, COOEt-EtCH₂), 4.04–3.96 (2H, m, C(3)H, C(14)H), 3.70–3.62 (1H, m, C(16)H), 3.92–3.90 (1H, m, C(11)H), 3.87–3.85 (1H, m, C(15)H), 3.80 (3H, s, PMB-CH₃), 2.78–2.67 (3H, m, C(20)H₂, C(27)H), 2.60–2.52 (1H, m, C(2)H), 2.31–2.35 (1H, m, C(17)H_AH_B), 2.22–2.17 (3H, m, C(9)H_AH_B, C(13)H_AH_B, C(17)H_AH_B), 2.17–2.13 (1H, m, C(23)H_AH_B), 2.04–2.00 (2H, m,

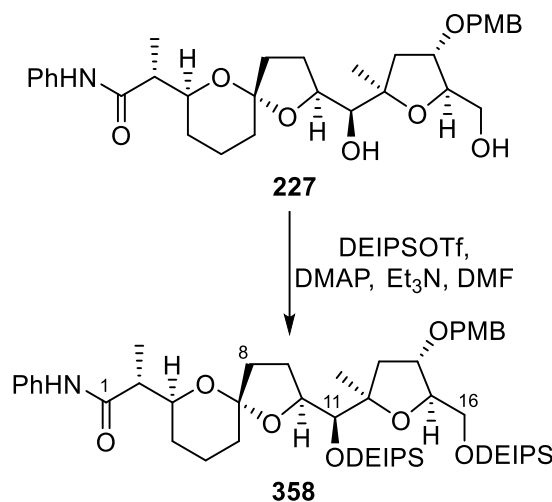
C(4)*H_AH_B*, C(8)*H_AH_B*, 1.99–1.91 (2H, m, C(5)*H_AH_B*, C(23)*H_AH_B*), 1.89–1.84 (6H, m, C(4)*H_AH_B*, C(5)*H_AH_B*, C(9)*H_AH_B*, C(29)*CH₃*), 1.80–1.75 (1H, m, C(8)*H_AH_B*), 1.75–1.58 (6H, m, C(5)*H_AH_B*, C(6)*H₂*, C(13)*H_AH_B*, C(24)*H₂*), 1.29–1.24 (2H, m, C(19)*H₂*), 1.28 (3H, t, *J* = 7.1 Hz, COOEt-Et*CH₃*), 1.21 (3H, s, C(25)*CH₃*), 1.20–1.17 (6H, m, C(2)*CH₃*, C(12)*CH₃*), 1.04 (3H, d, *J* = 6.7 Hz, C(27)*CH₃*), 1.02–0.95 (13H, m, DEIPS-*CH₃* × 4, DEIPS-*iPrCH*), 0.71–0.57 (4H, m, DEIPS-*CH₂* × 2);

¹³C NMR (125 MHz, CDCl₃) δ_c 211.9 (C21), 172.4 (C1), 168.4 (C30), 159.2 (PMB-C_{Ar}OMe), 148.4 (C28), 145.1 (C18), 138.4 (Ph-C_{Ar}N), 130.2 (PMB-C_{Ar}CH₂), 129.2 (PMB-C_{Ar} × 2), 129.0 (Ph-C_{Ar} × 2), 125.2 (C29), 123.7 (Ph-C_{Ar}), 119.4 (Ph-C_{Ar} × 2), 113.8 (PMB-C_{Ar} × 2), 111.8 (C18'), 105.8 (C7), 85.5 (C15), 85.0 (C25), 85.0 (C12), 83.2 (C22), 81.2 (C14), 78.3 (C10), 78.0 (C11), 72.0 (C3), 71.3 (PMB-*CH₂*), 70.2 (C16), 60.5 (OCH₂CH₃), 55.3 (PMB-*CH₃*), 47.8 (C26), 45.8 (C2), 41.6 (C17), 41.5 (C13), 38.3 (C8), 37.4 (C24), 36.2 (C20), 32.7 (C6), 30.0 (C27), 29.7 (C19), 29.2 (C23), 26.3 (C25-*CH₃*) 24.9 (C4), 23.1 (C9), 22.1 (C12-*CH₃*), 21.4 (C27-*CH₃*), 19.8 (C5), 17.6 (DEIPS-*iPrCH₃*), 17.5 (DEIPS-*iPrCH₃*), 14.3 (OCH₂CH₃), 13.3 (DEIPS-*iPrCH*), 12.4 (C29-*CH₃*), 12.3 (C2-*CH₃*), 7.3 (DEIPS-Et*CH₃*), 7.3 (DEIPS-Et*CH₃*), 4.6 (DEIPS-Et*CH₂*), 4.3 (DEIPS-Et*CH₂*);

IR ν_{\max} (film)/cm⁻¹ 3336, 2938, 2361, 1709, 1600, 1541, 1514, 1459, 1442, 1248, 1122, 1034, 973, 754, 722;

HRMS (ESI⁺, *m/z*) C₅₉H₈₉O₁₂NNaSi⁺ [M + Na⁺] calculated 1054.6046, found 1054.6042 (Δ = -0.43 ppm).

**(R)-2-((2S,5S,7S)-2-((S)-((Diethyl(isopropyl)silyl)oxy)((2R,4S,5R)-5-
 (((diethyl(isopropyl)silyl)oxy)methyl)-4-((4-methoxybenzyl)oxy)-2-methyltetrahydrofuran-
 2-yl)methyl)-1,6-dioxaspiro[4.5]decan-7-yl)-N-phenylpropanamide (358)**



Diol **227** (61.3 mg, 0.108 mmol), NEt_3 (0.32 mL, 2.3 mmol), and DMAP (37.5 mg, 0.307 mmol) were dissolved in DMF (1.6 mL). DEIPSOTf (78.1 μL , 323 μmol) was then added to the reaction mixture dropwise. The reaction mixture was stirred for 24 h at room temperature, and then warmed to 40 °C and stirred for an additional 15 h. The reaction was quenched by addition of brine (sat., 4 mL). The layers were allowed to separate and an extraction was conducted using Et_2O (4 \times 5 mL); the organic layers were combined, washed with brine (sat., 5 mL), dried (MgSO_4), and then concentrated *in vacuo*. Purification by flash column chromatography (SiO_2 , 95:5 to 90:10 to 70:30 Pentane: Et_2O , then 80:20 Pentane:Acetone) afforded silyl ether **358** (50.8 mg, 57%) as a yellow oil.

$R_f = 0.8$ (70:30 Pentane: EtOAc);

$[\alpha]_D^{25} -5.6$ ($c = 2.09$, CH_2Cl_2);

$^1\text{H NMR}$ (400 MHz, CDCl_3) δ_H 8.44 (1H, s, PhNH), 7.49–7.42 (2H, m, PhH \times 2), 7.29–7.23 (2H, m, PhH \times 2), 7.23–7.18 (2H, m, PMB-ArH \times 2), 7.00 (1H, t, $J = 7.4$ Hz, PhH), 6.83 (2H, d, $J = 8.7$ Hz, PMB-ArH \times 2), 4.42 (1H, d, $J = 11.5$ Hz, PMB- CH_AH_B), 4.36 (1H, d, $J = 11.5$ Hz, PMB-

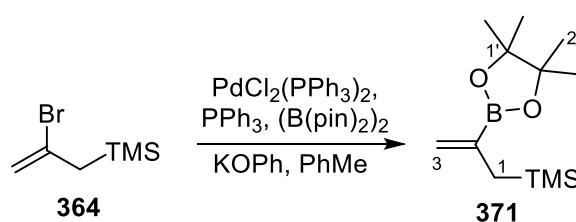
CH_AH_B), 4.25 (1H, t, *J* = 7.3 Hz, C(10)H), 4.07–3.92 (3H, m, C(15)H, C(3)H, C(14)H), 3.85–3.81 (1H, m, C(11)H), 3.76 (3H, s, PMB-CH₃), 3.60 (1H, dd, *J* = 10.3, 3.7 Hz, C(16)H_AH_B), 3.41 (1H, dd, *J* = 10.3, 6.0 Hz, C(16)H_AH_B), 2.56 (1H, qd, *J* = 7.2, 3.5 Hz, C(2)H), 2.09–1.98 (1H, m, C(9)H_AH_B), 1.98–1.89 (1H, m, C(8)H_AH_B, C(13)H_AH_B), 1.87–1.71 (4H, m, C(5)H_AH_B, C(8)H_AH_B, C(9)H_AH_B, C(13)H_AH_B), 1.70–1.52 (4H, m, C(6)H₂, C(5)H_AH_B, C(4)H_AH_B), 1.28–1.21 (1H, m, C(4)H_AH_B), 1.20–1.10 (3H, m, C(2)CH₃, C(12)CH₃), 1.07–0.82 (30H, m, DEIPS-EtCH₃ × 4, DEIPS-*i*PrCH₃ × 4, DEIPS-*i*PrCH × 2), 0.69–0.50 (8H, m, DEIPS-EtCH₂ × 4);

¹³C NMR (100 MHz, CDCl₃) δ_c 172.5 (C1), 159.1 (PMB-C_{Ar}OMe), 138.4 (Ph-C_{Ar}N), 130.6 (PMB-C_{Ar}CH₂), 129.1 (PMB-C_{Ar} × 2), 128.9 (Ph-C_{Ar} × 2), 123.6 (Ph-C_{Ar}), 119.5 (Ph-C_{Ar} × 2), 113.7 (PMB-C_{Ar} × 2), 105.6 (C7), 84.9 (C12), 84.5 (C15), 81.4 (C14), 78.6 (C10), 78.5 (C11), 71.9 (C3), 71.0 (PMB-CH₂), 63.9 (C16), 55.2 (PMB-CH₃), 45.6 (C2), 42.2 (C13), 38.7 (C8), 32.9 (C6), 25.8 (C4), 22.8 (C9), 21.5 (C12-CH₃), 19.7 (C5), 17.6 (DEIPS-*i*PrCH₃), 17.5 (DEIPS-*i*PrCH₃), 17.3 (DEIPS-*i*PrCH₃ × 2), 13.3 (DEIPS-*i*PrCH), 12.7 (DEIPS-*i*PrCH), 12.3 (C2-CH₃), 7.3 (DEIPS-EtCH₃), 7.2 (DEIPS-EtCH₃), 7.0 (DEIPS-EtCH₃ × 2), 4.6 (DEIPS-EtCH₂), 4.3 (DEIPS-EtCH₂), 3.2 (DEIPS-EtCH₂), 3.1 (DEIPS-EtCH₂);

IR ν_{max} (film)/cm⁻¹ 2941, 2875, 1668, 1600, 1539, 1514, 1460, 1441, 1247, 1131, 1095, 1038, 972, 882, 808, 721;

HRMS (ESI⁺, *m/z*) C₄₆H₇₆O₈NSi₂⁺ [M + Na⁺] calculated 826.51040, found 826.51005 (Δ = -0.43 ppm).

Trimethyl(2-(4,4,5,5-tetramethyl-1,3,2-dioxaborolan-2-yl)allyl)silane (371)



To a flask charged with PdCl₂(PPh₃)₂ (16.4 mg, 23.3 μmol), PPh₃ (12.2 mg, 46.6 μmol), bis(pinacolato)diboron (217 mg, 0.854 mmol) and KOPh (154 mg, 1.17 mmol) was added bromide **364** (150 mg, 0.777 mmol) in PhMe (4.8 mL). The reaction was flushed under argon and heated to 50 °C and stirred for 3 h. The reaction was cooled to room temperature and water (5 mL) was added. The layers were separated, and the aqueous layer was extracted with Et₂O (3 × 5 mL). The combined organic layers were dried (MgSO₄), filtered, and then concentrated *in vacuo*. Purification by column chromatography (SiO₂, 100:0 to 99:1 Pentane:Et₂O) afforded allyl trimethylsilane **371** (113 mg, 61%) as a volatile colourless oil.

R_f: 0.6 (95:5 Pentane:Et₂O);

¹H NMR (400 MHz, CDCl₃) δ_H 5.65 (1H, d, *J* = 3.6 Hz, C(3)H_AH_B), 5.40 (1H, d, *J* = 3.6 Hz, C(3)H_AH_B), 1.66 (2H, s, C(1)H₂), 1.26 (12H, s, 4 × C(2')H₃), -0.02 (9H, s, Si(CH₃)₃);

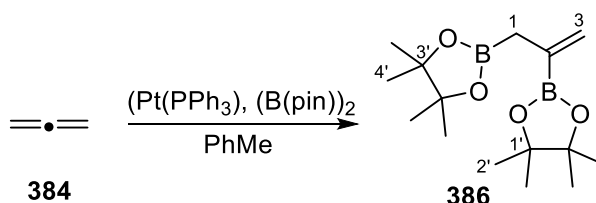
¹³C NMR (101 MHz, CDCl₃) δ_C 126.8 (C3), 83.4 (C1' × 2), 25.4 (C1), 24.8 (C2' × 4), -1.8 (3C, Si(CH₃)₃);

(The carbon attached to boron was not observed due to quadrupolar relaxation.)

A mass spectrum could not be obtained for this compound.

The spectral data were consistent with those previously reported.³⁶

2,2'-(Prop-2-ene-1,2-diyl)bis(4,4,5,5-tetramethyl-1,3,2-dioxaborolane) (**386**)



A Schlenk tube was charged with Pt(PPh₃)₄ (120 mg, 96.0 μmol) and bis(pinacolato)diboron (813 mg, 3.20 mmol). PhMe (6.4 mL) was added and the resulting solution was cooled to

-78 °C. Allene gas was then bubbled into the reaction mixture for ~20 s. The reaction mixture was then heated to 80 °C and stirred for 21 h. The mixture transferred to an RBF and concentrated *in vacuo*. The crude reaction mixture was then purified by Kügelrohr distillation (0.5 torr, 135 °C) to afford **386** (737 mg, 78%) as a colourless oil.

R_f = 0.3 (90:10 Pentane:Et₂O);

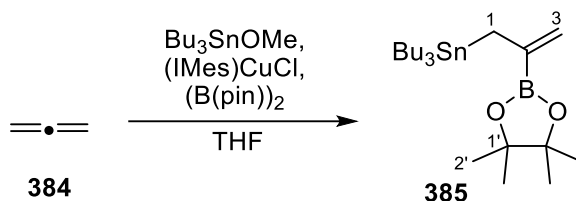
¹H NMR (400 MHz, CDCl₃) δ_H 5.68 (1H, d, J = 3.5 Hz, C=CH_AH_B), 5.59–5.52 (1H, m, C=CH_AH_B), 1.79 (2H, s, C(1)H₂) 1.26–1.20 (24H, m, C(2')H₃ × 4, C(4')H₃ × 4);

¹³C NMR (100 MHz, CDCl₃) δ_C 128.4 (C3), 83.3 (C1'/C3' × 2), 83.0 (C1'/C3' × 2), 24.7 (C2'/C4' × 4), 24.5 (C2'/C4' × 4);

(Both carbons attached to boron were not observed due to quadrupolar relaxation.)

The spectral data were consistent with those previously reported.⁶⁴

Tributyl(2-(4,4,5,5-tetramethyl-1,3,2-dioxaborolan-2-yl)allyl)stannane (**385**)



A Schlenk tube equipped with a magnetic stirring bar was charged with $(\text{IMes})\text{CuCl}$ (4.0 mg, 10 μmol) and bis(pinacolato)diboron (305 mg, 1.20 mmol). THF (4.0 mL) was added and the resulting solution was cooled to -78 °C. Allene gas was then bubbled into the reaction mixture for approximately 20 s. The reaction mixture was then warmed to room temperature and Bu_3SnOMe (0.35 mL, 1.2 mmol) was added. The resulting mixture was stirred at room temperature for 2 h. The mixture was diluted with EtOAc (10 mL) and filtered through a Celite[®] plug in a 10-mL syringe. The organic solution was washed with brine (10 mL), dried (MgSO_4),

and concentrated *in vacuo*. Purification by flash column chromatography (SiO₂, 100:0 to 96:4 Pentane:Et₂O) afford **385** (376 mg, 69%) as a colourless oil.

R_f = 0.4 (95:5 Pentane:Et₂O);

¹H NMR (400 MHz, CDCl₃) δ_H 5.45 (1H, d, *J* = 3.6 Hz, C=CH_AH_B), 5.37 (1H, d, *J* = 3.6 Hz, C=CH_AH_B), 1.90 ppm (2H, s, CH₂SnBu₃), 1.55–1.40 (6H, m, Sn(CH₂CH₂CH₂CH₃)₃), 1.34–1.23 (6H, m, Sn(CH₂CH₂CH₂CH₃)₃), 1.25 (12H, s, Bpin-C(CH₃)₂ × 2), 0.88 (9H, t, *J* = 7.3 Hz, Sn(CH₂CH₂CH₂CH₃)₃), 0.86–0.80 (6H, m, Sn(CH₂CH₂CH₂CH₃)₃);

¹³C NMR (100 MHz, CDCl₃) δ_C 123.4 (C3), 83.3 (Bpin-C(CH₃)₂ × 2), 29.1 (Sn(CH₂CH₂CH₂CH₃)₃), 27.4 (Sn(CH₂CH₂CH₂CH₃)₃), 24.9 (Bpin-C(CH₃)₂ × 2), 17.1 (CH₂SnBu₃), 13.8 (Sn(CH₂CH₂CH₂CH₃)₃), 9.4 (Sn(CH₂CH₂CH₂CH₃)₃);

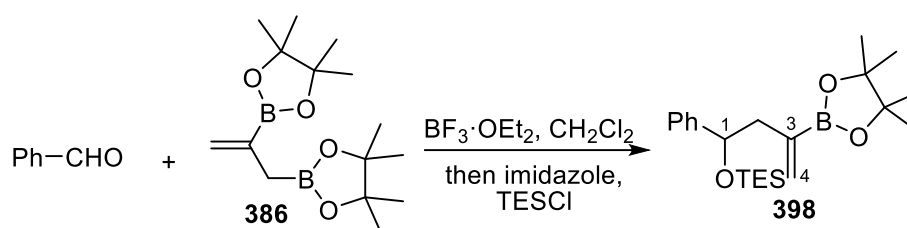
IR ν_{max} (film)/cm⁻¹ 2956, 2925, 1464, 1360, 1307, 1213, 1143, 864, 695.

A mass spectrum could not be obtained for this compound.

(The carbon attached to boron was not observed due to quadrupolar relaxation.)

Triethyl((1-phenyl-3-(4,4,5,5-tetramethyl-1,3,2-dioxaborolan-2-yl)but-3-en-1-yl)oxy)silane

(**398**)



To a Schlenk tube was added freshly distilled benzaldehyde (24.0 μL, 0.236 mmol), and **386** (104 mg, 0.353 mmol). The Schlenk tube was evacuated and backfilled with N₂ five times, and then CH₂Cl₂ (1.20 mL) was added to the mixture. The resulting solution was cooled to -78 °C. BF₃·Et₂O (59.7 μL, 0.471 mmol) was then added dropwise to the reaction mixture, which was

stirred at $-78\text{ }^{\circ}\text{C}$ for 1.5 h and then quenched with a solution of NaHCO_3 (sat., 1.0 mL). The aqueous layer was extracted with Et_2O (3×4 mL). The combined organic layers were dried (MgSO_4), filtered and then concentrated *in vacuo*.

The crude mixture was transferred to a 10-mL RBF. To the RBF were added CH_2Cl_2 (1.20 mL) and imidazole (40.1 mg, 0.589 mmol). The reaction mixture was then cooled to $0\text{ }^{\circ}\text{C}$. After which, TESCl (59.3 μL , 0.353 mmol) was added to the reaction mixture, which was allowed to warm to room temperature and stirred for 13 h. The reaction mixture was quenched with water (2.0 mL) and the layers were allowed to separate. The aqueous layer was extracted with Et_2O (3×4 mL). The combined organic layers were dried (MgSO_4), filtered and then concentrated *in vacuo*. Purification by column chromatography (SiO_2 , 100:0 to 98:2 to 95:5 Pentane: Et_2O) afforded silyl ether **398** (48.9 mg, 53%) as a colourless oil.

$R_f = 0.8$ (90:10 Pentane: EtOAc);

$^1\text{H NMR}$ (400 MHz, CDCl_3) δ_{H} 7.24–7.16 (4H, m, PhH), 7.14–7.09 (1H, m, PhH), 5.71 (1H, d, $J = 3.7$ Hz, C(4) $H_{\text{A}}H_{\text{B}}$), 5.42 (1H, d, $J = 3.6$ Hz, C(4) $H_{\text{A}}H_{\text{B}}$), 4.73 (1H, t, $J = 6.6$ Hz, C(1)H), 2.50 (1H, dd, $J = 12.6, 6.8$ Hz, C(2) $H_{\text{A}}H_{\text{B}}$), 2.39 (1H, d, $J = 12.8, 6.3$ Hz, C(2) $H_{\text{A}}H_{\text{B}}$), 1.18 (12H, s, Bpin- $\text{C}(\text{CH}_3)_2 \times 2$) 0.79 (9H, t, TES- $\text{CH}_3 \times 3$), 0.48–0.39 (6H, m, TES- $\text{CH}_2 \times 3$);

$^{13}\text{C NMR}$ (100 MHz, CDCl_3) δ_{C} 145.5 (Ph- $\text{C}_{\text{Ar}}\text{C}$), 132.6 (C4), 127.7 (Ph- $\text{C}_{\text{Ar}} \times 2$), 126.7 (Ph- C_{Ar}), 126.2 (Ph- $\text{C}_{\text{Ar}} \times 2$), 83.3 (Bpin- $\text{C}(\text{CH}_3)_2 \times 2$), 74.5 (C1), 47.3 (C2), 24.9 (Bpin- $\text{C}(\text{CH}_3)_2$), 24.8 (Bpin- $\text{C}(\text{CH}_3)_2$), 6.8 (TES- $\text{EtCH}_3 \times 3$), 4.9 (TES- $\text{EtCH}_2 \times 3$);

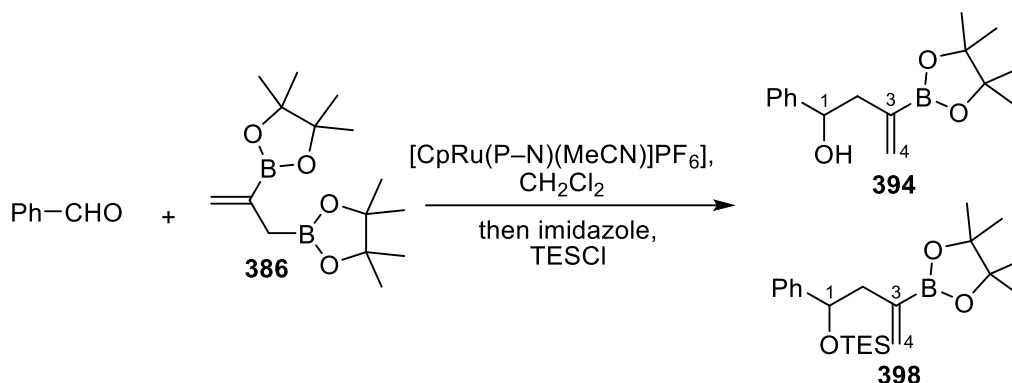
$^{11}\text{B NMR}$ (128 MHz, CDCl_3) δ_{B} 30.2;

(The carbon attached to boron was not observed due to quadrupolar relaxation.)

$\text{IR } \nu_{\text{max}}$ (film)/ cm^{-1} 2978, 2955, 2877, 1370, 1308, 1142, 1087, 1067, 1006, 975, 942, 868, 850, 742, 700;

HRMS (ESI⁺, *m/z*) C₂₂H₃₇O₃NaBSi⁺ [M + Na⁺] calculated 411.2503, found 411.2532
(Δ = -0.32 ppm).

1-Phenyl-3-(4,4,5,5-tetramethyl-1,3,2-dioxaborolan-2-yl)but-3-en-1-ol (394)



To a Schlenk flask was added [CpRu(P-N)(MeCN)]PF₆ (9.7 mg, 4.7 μmol), freshly distilled benzaldehyde (24.0 μL, 0.236 mmol), and **386** (104 mg, 0.353 mmol). The Schlenk flask was evacuated and backfilled with N₂ five times, and then CH₂Cl₂ (1.20 mL) was added to the mixture. The resulting solution was stirred at room temperature was 22 h. After which, imidazole (40.1 mg, 0.589 mmol) and TESCl (59.3 μL, 0.353 mmol) were added. The reaction mixture was stirred for 3 h at room temperature and then quenched with water (2.0 mL). The aqueous layer was extracted with EtOAc (3 × 4 mL). The combined organic layers were dried (MgSO₄), filtered and then concentrated *in vacuo*. Purification by column chromatography (SiO₂, 100:0 to 98:2 to 95:5 Pentane:Et₂O, then 80:20 to 75:25 to 70:30 Pentane:EtOAc) afforded silyl ether **398** (2.1 mg, 2%) and alcohol **394** (17.4 mg, 27%) as colourless oils.

Characterisation data for compound **394**:

R_f = 0.4 (70:30 Pentane:EtOAc);

¹H NMR (400 MHz, CDCl₃) δ_{H} 7.28–7.18 (4H, m, PhH), 7.15–7.10 (1H, m, PhH), 5.82 (1H, d, J = 3.4 Hz, C(4)*H_AH_B*), 5.57 (1H, d, J = 2.9 Hz, C(4)*H_AH_B*), 4.69 (1H, dt, J = 8.6, 3.4 Hz, C(1)*H*), 2.74 (1H, d, J = 2.5 Hz, OH), 2.56 (1H, dd, J = 13.7, 3.1 Hz, C(2)*H_AH_B*), 2.43 (1H, d, J = 13.2, 8.9 Hz, C(2)*H_AH_B*), 1.17 (12H, s, Bpin-C(CH₃)₂ × 2);

¹³C NMR (100 MHz, CDCl₃) δ_{C} 144.4 (Ph-C_{Ar}C), 133.2 (C4), 128.2 (Ph-C_{Ar} × 2), 127.1 (Ph-C_{Ar}), 125.8 (Ph-C_{Ar} × 2), 83.9 (Bpin-C(CH₃)₂ × 2), 73.8 (C1), 46.3 (C2), 24.8 (Bpin-C(CH₃)₂), 24.7 (Bpin-C(CH₃)₂);

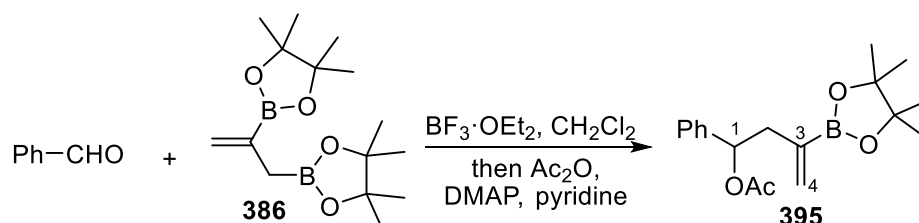
¹¹B NMR (128 MHz, CDCl₃) δ_{B} 30.0;

(The carbon attached to boron was not observed due to quadrupolar relaxation.)

IR ν_{max} (film)/cm⁻¹ 3471, 2978, 1370, 1308, 1138, 1049, 954, 863, 758, 700;

HRMS (ESI⁺, m/z) C₁₆H₂₃O₃NaB⁺ [M + Na⁺] calculated 297.1638, found 296.1671 (Δ = +0.80 ppm).

1-Phenyl-3-(4,4,5,5-tetramethyl-1,3,2-dioxaborolan-2-yl)but-3-en-1-yl acetate (**395**)



To a Schlenk flask was added freshly distilled benzaldehyde (24.0 μL , 0.236 mmol), and **386** (104 mg, 0.353 mmol). The Schlenk tube was evacuated and backfilled with N₂ five times, and then CH₂Cl₂ (1.20 mL) was added to the mixture. The resulting solution was cooled to -78 °C. BF₃·Et₂O (59.7 μL , 0.471 mmol) was then added dropwise to the reaction mixture, which was stirred at -78 °C for 2.5 h and then quenched with a solution of NaHCO₃ (sat., 2.0 mL). The aqueous layer was extracted with Et₂O (3 × 4 mL). The combined organic layers were dried (MgSO₄), filtered and then concentrated *in vacuo*.

The crude mixture was transferred to a 10-mL RBF. To the RBF were added DMAP (5.8 mg, 47 μmol), Ac_2O (57.9 μL , 0.613 mmol), pyridine (59 μL , 0.73 mmol), and THF (200 μL). The reaction mixture was heated to 50 $^\circ\text{C}$ and stirred for 16 h. The reaction mixture was then quenched with 10% aqueous solution of KF (5 mL). The aqueous layer was extracted with Et_2O (3×4 mL). The combined organic layers were dried (MgSO_4), filtered and then concentrated *in vacuo*. Purification by column chromatography (SiO_2 , 98:2 to 95:5 Pentane: Et_2O , then 80:20 to 75:25 to 70:30 Pentane: EtOAc) afforded acetate **395** (57.8 mg, 78%) as a colourless oil.

$R_f = 0.7$ (70:30 Pentane: EtOAc);

$^1\text{H NMR}$ (400 MHz, CDCl_3) δ_H 7.31–7.23 (4H, m, $\text{PhH} \times 4$), 7.23–7.17 (1H, m, PhH), 5.91 (1H, t, $J = 7.0$ Hz, $\text{C}(1)\text{H}$), 5.79 (1H, d, $J = 3.4$ Hz, $\text{C}(4)\text{H}_A\text{H}_B$), 5.57 (1H, d, $J = 3.2$ Hz, $\text{C}(4)\text{H}_A\text{H}_B$), 2.61 (2H, d, $J = 7.0$ Hz, $\text{C}(2)\text{H}_2$), 1.97 (3H, s, Ac-CH_3), 1.20 (12H, s, $\text{Bpin-C}(\text{CH}_3)_2 \times 2$);

$^{13}\text{C NMR}$ (100 MHz, CDCl_3) δ_C 170.1 (Ac-CO), 140.7 ($\text{Ph-C}_{Ar}\text{C}$), 132.4 (C_4), 128.2 ($\text{Ph-C}_{Ar} \times 2$), 127.6 (Ph-C_{Ar}), 126.6 ($\text{Ph-C}_{Ar} \times 2$), 83.5 ($\text{Bpin-C}(\text{CH}_3)_2 \times 2$), 75.1 (C_1), 42.5 (C_2), 24.8 ($\text{Bpin-C}(\text{CH}_3)_2 \times 2$), 24.7 ($\text{Bpin-C}(\text{CH}_3)_2 \times 2$), 21.2 (Ac-CH_3);

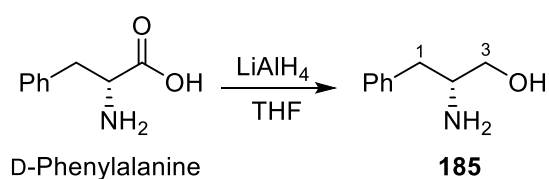
$^{11}\text{B NMR}$ (128 MHz, CDCl_3) δ_B 29.8;

(The carbon attached to boron was not observed due to quadrupolar relaxation.)

$\text{IR } \nu_{\text{max}}$ (film)/ cm^{-1} 2978, 1738, 1369 1311, 1234, 1139, 1022, 857, 760, 699;

HRMS (ESI^+ , m/z) $\text{C}_{18}\text{H}_{25}\text{O}_4\text{NaB}^+$ [$\text{M} + \text{Na}^+$] calculated 339.1738, found 339.1741 ($\Delta = +0.59$ ppm).

(*R*)-2-Amino-3-phenylpropan-1-ol (**185**)



D-Phenylalanine (2.00 g, 12.1 mmol) was dissolved in THF (18.0 mL) and cooled to 0 °C. LiAlH₄ (919 mg, 24.2 mmol) was added portion-wise over 15 min. The reaction mixture was gradually warmed to room temperature and then heated to reflux for 16 h. The reaction was cooled to 0 °C and diluted with Et₂O (18 mL), and then quenched with water (0.92 mL), NaOH solution (15% w/v, 0.92 mL), and additional water (2.8 mL). After stirring for 1 hour, the reaction mixture was filtered through cotton wool and washed with Et₂O (3 × 10 mL). The organic layers were combined and concentrated *in vacuo*. Recrystallisation from EtOAc afforded amino alcohol **185** (1.25 g, 69%) as white crystals.

$[\alpha]_D^{25} +18.3$ ($c = 1.16$, CH₂Cl₂; lit. +25.9, $c = 1.10$, CHCl₃);

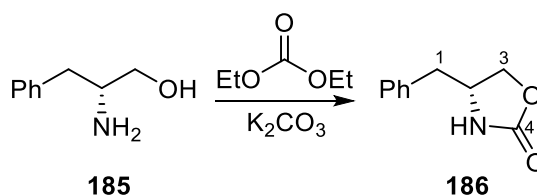
¹H NMR (400 MHz, CDCl₃) δ_H 7.34–7.26 (2H, m, PhH × 2), 7.26–7.21 (1H, m, PhH), 7.21–7.15 (2H, m, PhH × 2), 3.63 (1H, dd, $J = 10.7, 3.8$ Hz, C(3)H_AH_B), 3.39 (1H, dd, $J = 10.6, 7.2$ Hz, C(3)H_AH_B), 3.17–3.07 (1H, m, C(2)H), 2.79 (1H, dd, $J = 13.4, 5.1$ Hz, C(1)H_AH_B), 2.52 (1H, dd, $J = 13.4, 8.7$ Hz, C(1)H_AH_B);

¹³C NMR (100 MHz, CDCl₃) δ_C 138.7 (Ph-C_{Ar}CH₂), 129.0 (Ph-C_{Ar} × 2), 128.6 (Ph-C_{Ar} × 2), 126.4 (Ph-C_{Ar}), 66.3 (C3), 54.2 (C2), 40.9 (C1);

m.p. 90–92 °C (EtOAc).

The spectral data were consistent with those previously reported.³⁸

(R)-4-Benzyloxazolidin-2-one (**186**)



Amino alcohol **185** (1.23 g, 8.13 mmol), K₂CO₃ (112 mg, 0.813 mmol) and diethylcarbonate (1.97 mL, 16.3 mmol) were added to a reaction flask, which was fitted with a distillation kit

with a receiver flask that was cooled in an ice bath. The reaction flask was heated to 135 °C for 2.5 h, and then cooled to room temperature. The reaction mixture was diluted with CH₂Cl₂ (7 mL) and the organic layer was washed with water (3 × 4 mL), dried (MgSO₄), filtered, and then concentrated *in vacuo*. Recrystallisation using 2:1 EtOAc:Pentane (5.0 mL) afforded oxazolidinone **186** (1.21 g, 84%) as white crystals.

[α]_D²⁵ +59.1 (*c* = 1.14, CHCl₃; lit. +64.1, *c* = 1.00, CHCl₃);

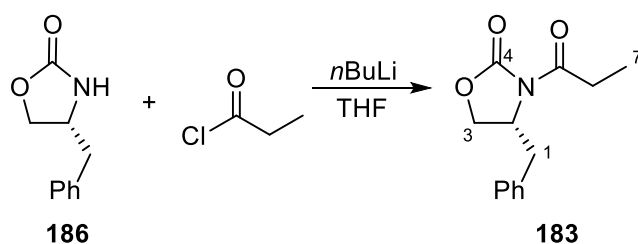
¹H NMR (400 MHz, CDCl₃) δ _H 7.39–7.31 (2H, m, PhH × 2), 7.31–7.21 (1H, m, PhH), 7.21–7.13 (2H, m, PhH × 2), 5.62–5.53 (1H, br. s., NH), 4.50–4.43 (1H, m, C(3)H_AH_B), 4.22–3.97 (2H, m, C(3)H_AH_B, C(2)H), 2.88 (2H, d, *J* = 6.9 Hz, C(1)H₂);

¹³C NMR (100 MHz, CDCl₃) δ _C 159.3 (C₄), 135.9 (Ph-C_{Ar}CH₂), 129.1 (Ph-C_{Ar} × 2), 129.0 (Ph-C_{Ar} × 2), 127.3 (Ph-C_{Ar}), 69.7 (C₃), 53.8 (C₂), 41.5 (C₁);

m.p. 90–92 °C (CH₂Cl₂).

The spectral data were consistent with those previously reported.³⁸

(*R*)-4-Benzyl-3-propionyloxazolidin-2-one (**183**)



Oxazolidinone **186** (972 mg, 5.49 mmol) was dissolved in THF (16 mL) and cooled to –78 °C. *n*BuLi solution (2.18 M, 2.76 mL, 6.02 mmol) was added dropwise and the reaction was stirred for 30 min at –78 °C. Propionyl chloride (0.57 mL, 6.6 mmol) was added dropwise and the reaction was stirred for a further 30 min at –78 °C, and then quenched with a solution of NH₄Cl (sat., 15 mL). The mixture was extracted with EtOAc (4 × 15 mL). The organic layers

were combined, dried (MgSO₄), filtered, and then concentrated *in vacuo*. Purification by flash column chromatography (SiO₂, 85:15 to 75:25 Pentane:EtOAc) afforded **183** (1.12 g, 87%) as white crystals.

R_f = 0.3 (80:20 Pentane:EtOAc);

[α]_D²⁵ –60.6 (*c* = 0.83, CHCl₃; lit. –57.4, *c* = 1.00, CHCl₃);

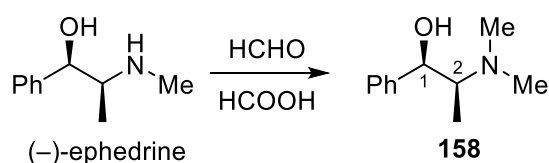
¹H NMR (400 MHz, CDCl₃) δ_H 7.38–7.23 (3H, m, PhH × 3), 7.27–7.17 (2H, m, PhH × 2), 4.67 (1H, ddt, *J* = 9.6, 7.3, 3.3 Hz C(2)H), 4.25–4.13 (2H, m, C(3)H₂), 3.31 (1H, dd, *J* = 13.3, 3.3 Hz, C(1)H_AH_B), 3.07–2.85 (2H, m, C(6)H₂), 2.76 (1H, dd, *J* = 13.4, 9.6 Hz, C(1)H_AH_B), 1.20 (3H, t, *J* = 7.3 Hz, C(7)H₃);

¹³C NMR (100 MHz, CDCl₃) δ_C 174.1 (C5), 153.3 (C4), 135.3 (Ph-C_{Ar}CH₂), 129.4 (Ph-C_{Ar} × 2), 129.0 (Ph-C_{Ar} × 2), 127.4 (Ph-C_{Ar}), 66.2 (C3), 55.2 (C2), 37.9 (C1), 29.2 (C6), 8.3 (C7);

m.p. 44–46 °C (EtOAc).

The spectral data were consistent with those previously reported.³⁸

(1*R*,2*S*)-2-(Dimethylamino)-1-phenylpropan-1-ol (**158**)



(1*R*, 2*S*)-(-)-Ephedrine (42.8 g, 259 mmol) was dissolved in formaldehyde (37% w/v in H₂O, 42.8 mL, 1.55 mol) and cooled to 0 °C. Formic acid (99.0 mL, 2.59 mol) was added and the reaction mixture was warmed to room temperature, and then stirred at 90 °C for 16 h. The reaction mixture was cooled to 0 °C and then quenched with aqueous NaOH (1 M, 204 mL). NaOH pellets were slowly added to the solution at 0 °C until the product precipitated out as a white solid after 3 h. After which, an extraction was conducted using Et₂O (5 × 330 mL). The

organic layers were combined and dried with K_2CO_3 , and then concentrated *in vacuo* to afford **158** (45.0 g, 97%) as white crystals.

$[\alpha]_D^{25}$ -28.1 ($c = 1.2$, CH_2Cl_2 ; lit. -29.2 , $c = 5.0$, MeOH);

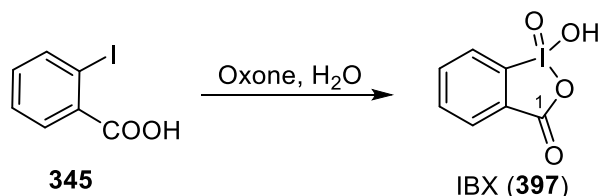
1H NMR (400 MHz, $CDCl_3$) δ_H 7.39–7.33 (4H, m, $PhH \times 4$), 7.30–7.23 (1H, m, PhH), 4.98 (1H, d, $J = 3.7$ Hz, $C(1)H$), 2.56 (1H, qd, $J = 6.8, 3.7$ Hz, $C(2)H$), 2.38 (6H, br.s, $N(CH_3)_2$), 0.84 (3H, d, $J = 6.8$ Hz, $C(2)CH_3$);

^{13}C NMR (100 MHz, $CDCl_3$) δ_C 142.1 ($Ph-C_{Ar}$), 128.0 ($Ph-C_{Ar} \times 2$), 126.8 ($Ph-C_{Ar} \times 2$), 125.9 ($Ph-C_{Ar}$), 72.1 (C1), 65.4 (C2), 43.1 ($NCH_3 \times 2$), 10.2 ($C2-CH_3$);

m.p. 83–86 °C (lit. 86–88 °C).

The spectral data were consistent with those previously reported.³⁸

1-Hydroxy-1-oxo-1*H*-benzo[d][1,2]iodaoxol-3(1*H*)-one (**397**)



2-Iodobenzoic acid (5.00 g, 20.2 mmol) was added to an Oxone solution in deionised water (37.2 g, 60.5 mmol, in 65.0 mL) in a round-bottom flask. The suspension was heated to 70 °C and left to stir for 5 h. The solution remained a murky white colour. Heating was stopped and the reaction mixture was allowed to cool to room temperature. The reaction mixture was then submerged in a dry ice–cyclohexane bath overnight. The resulting mixture was filtered. The residue was rinsed with generous quantities of water, followed by moderate quantities of acetone to afford IBX (5.17 g, 92%) as a white powder.

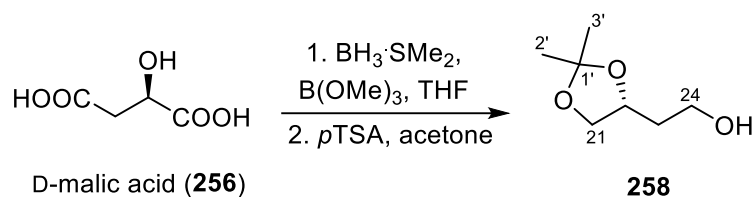
¹H NMR (400 MHz, d₆-DMSO) δ_{H} 8.15 (1H, d, $J = 8.1$ Hz, PhH), 8.07–7.97 (2H, m, PhH \times 2), 7.85 (1H, t, $J = 7.4$ Hz, PhH);

¹³C NMR (100 MHz, d₆-DMSO) δ_{C} 168.1 (C1), 147.1 (Ph-C_{Ar}), 134.0 (Ph-C_{Ar}), 133.5 (Ph-C_{Ar}), 132.0 (Ph-C_{Ar}), 130.6 (Ph-C_{Ar}), 125.5 (Ph-C_{Ar});

The spectral data were consistent with those previously reported.⁷²

5.1.3 Experimental procedures for E and F fragments

(R)-2-(2,2-Dimethyl-1,3-dioxolan-4-yl)ethan-1-ol (258)



Borane dimethyl sulphide (42.5 mL, 447 mmol) was dissolved in THF (100 mL), and then cooled to 0 °C and stirred for 5 min. D-Malic acid (20.0 g, 149 mmol) dissolved in THF (50 mL) was added to the solution dropwise, followed by trimethyl borate (48.3 mL, 433 mmol) in one portion. The reaction mixture was warmed to room temperature and stirred for 16 h. Methanol (40 mL) was added dropwise. The solvent was removed *in vacuo* and the resulting residue purified by filtration through silica (SiO₂, 80:20 EtOAc:MeOH). The resulting triol was dissolved in acetone (600 mL), and 2,2-dimethoxypropane (146 mL, 1.19 mol) and *p*TSA (2.84 g, 14.9 mmol) were added to the solution. The reaction mixture was stirred for 16 h at room temperature. Subsequently, the solvent was removed *in vacuo* and purification by flash column chromatography (SiO₂, 80:20 to 20:80 Pentane:EtOAc) afforded acetonide **258** (11.7 g, 54%) as a colourless oil.

R_f = 0.4 (90:10 CH₂Cl₂:MeOH);

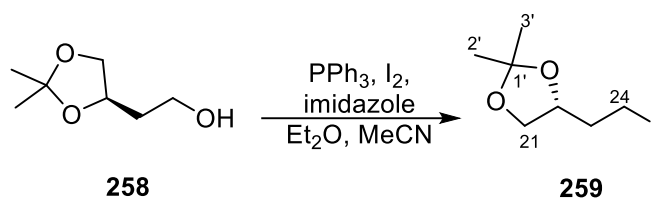
[α]_D²⁵ +2.8 (c = 1.0, CH₂Cl₂);

¹H NMR (400 MHz, CDCl₃) δ_H 4.29 (1H, quin, *J* = 6.0 Hz, C(22)*H*), 4.11 (1H, dd, *J* = 8.1, 6.0 Hz, C(21)*H*_A*H*_B), 3.87–3.76 (2H, m, C(24)*H*₂), 3.62 (1H, d, *J* = 7.7 Hz, C(21)*H*_A*H*_B), 2.25 (1H, t, *J* = 5.3 Hz, *OH*), 1.84 (2H, q, *J* = 5.6 Hz, C(23)*H*₂), 1.45 (3H, s, C(2')*H*₃), 1.38 (3H, s, C(3')*H*₃);

¹³C NMR (100 MHz, CDCl₃) δ_C 109.1 (C1'), 75.1 (C22), 69.5 (C21), 60.6 (C24), 35.6 (C23), 26.9(CH₃), 25.7 (CH₃).

The spectral data were consistent with those previously reported.⁵²

(R)-4-(2-Iodoethyl)-2,2-dimethyl-1,3-dioxolane (259)



Triphenylphosphine (25.1 g, 95.6 mmol) and imidazole (9.29 g, 137 mmol) were dissolved in Et₂O (258 mL) and CH₃CN (83 mL), and then cooled to 0 °C. Iodine (24.3 g, 95.6 mmol) was added portionwise to the solution over 30 min. After which, acetone **258** (9.98 g, 68.3 mmol) was added dropwise. The reaction mixture was stirred at 0 °C for 1 hour, warmed to room temperature, and then stirred for an additional 1 hour. The reaction was quenched by the addition of methanol (45 mL) and the mixture was concentrated *in vacuo*. Purification by flash column chromatography (SiO₂, 98:2 Pentane:Et₂O) afforded iodide **259** (15.1 g, 87%) as a colourless oil.

R_f = 0.4 (90:10 Pentane:Et₂O);

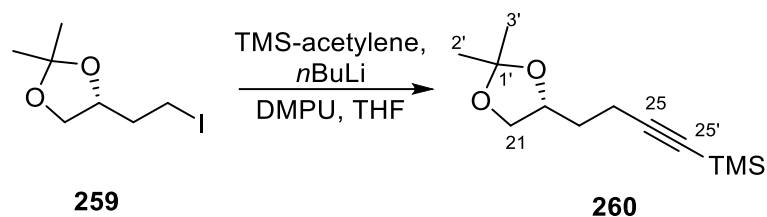
[α]_D²⁵ +23.5 (c = 1.37, CH₂Cl₂);

¹H NMR (400 MHz, CDCl₃) δ_H 4.17 (1H, dtd, *J* = 7.8, 6.2, 4.3 Hz, C(22)H), 4.08 (1H, dd, *J* = 8.0, 6.1, C(21)H_AH_B), 3.57 (1H, dd, *J* = 8.0, 6.4 Hz, C(21)H_AH_B), 3.31–3.17 (2H, m, C(24)H₂), 2.16–1.98 (2H, m, C(23)H₂), 1.40 (3H, s, C(2')H₃), 1.35 (3H, s, C(3')H₃);

¹³C NMR (101 MHz, CDCl₃) δ_C 109.2 (C1'), 75.7 (C22), 68.6 (C21), 37.9 (C23), 27.0 (CH₃), 25.5 (CH₃), 1.2 (C24).

The spectral data were consistent with those previously reported.⁵²

(R)-4-(2,2-Dimethyl-1,3-dioxolan-4-yl)but-1-yn-1-yl)trimethylsilane (260)



TMS-Acetylene (0.41 mL, 2.9 mmol) was dissolved in THF (12 mL) and cooled to $-78\text{ }^{\circ}\text{C}$. 1,3-Dimethyl-3,4,5,6-tetrahydro-2(1H)-pyrimidinone (1.06 mL, 8.81 mmol) was added, followed by *n*BuLi (1.6 M in hexanes, 1.95 mL, 3.12 mmol). The resulting solution was stirred for 30 min before iodide **259** (500 mg, 1.95 mmol) in THF (3 mL) was added. The solution was stirred at $-78\text{ }^{\circ}\text{C}$ for 10 min, warmed to room temperature, and stirred for 1 hour. The reaction was quenched with a solution of NH_4Cl (sat., 6 mL). The layers were allowed to separate and the aqueous layer was extracted with Et_2O ($3 \times 15\text{ mL}$). The combined layers were dried (MgSO_4), filtered, and then concentrated *in vacuo*. Purification by flash column chromatography (SiO_2 , 98:2 Pentane: Et_2O) afforded alkyne **260** (260 mg, 59%) as a colourless oil.

$R_f = 0.4$ (90:10 Pentane: Et_2O);

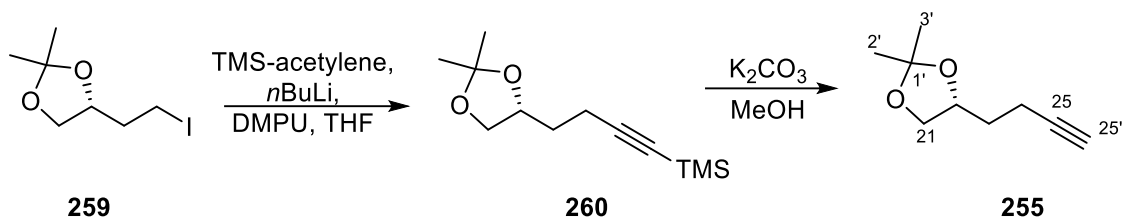
$[\alpha]_D^{25} +13.8$ ($c = 1.78$, CH_2Cl_2);

$^1\text{H NMR}$ (400 MHz, CDCl_3) δ_H 4.16 (1H, quin, $J = 6.4\text{ Hz}$, C(22)*H*), 4.10–4.04 (1H, m, C(21)*H*_A*H*_B), 3.60–3.53 (1H, m, C(21)*H*_A*H*_B), 2.41–2.24 (2H, m, C(24)*H*₂), 1.88–1.76 (1H, m, C(23)*H*_A*H*_B), 1.76–1.65 (1H, m, C(23)*H*_A*H*_B $\text{CH}_2\text{C}\equiv\text{C}$), 1.39 (3H, s, C(2')*H*₃), 1.34 (3H, s, C(3')*H*₃), 0.16–0.10 (9H, m, $\text{Si}(\text{CH}_3)_3$);

$^{13}\text{C NMR}$ (101 MHz, CDCl_3) δ_C 108.7 (C1'), 106.2 (C25'), 85.0 (C25), 74.9 (C22), 69.1 (C21), 32.7 (C23), 26.9 (C2'), 25.6 (C3'), 16.4 (C24), 0.0 (TMS- $\text{CH}_3 \times 3$).

The spectral data were consistent with those previously reported.⁵²

(R)-4-(But-3-yn-1-yl)-2,2-dimethyl-1,3-dioxolane (255)



TMS-acetylene (12.3 mL, 88.7 mmol) was dissolved in THF (150 mL) and cooled to $-78\text{ }^{\circ}\text{C}$. 1,3-dimethyl-3,4,5,6-tetrahydro-2(1H)-pyrimidinone (15.0 mL) was added, followed by *n*BuLi (1.6 M in hexanes, 59.0 mL, 94.4 mmol). The resulting solution was stirred for 30 min before iodide **259** (15.1 g, 59.0 mmol) in THF (150 mL) was added. The solution was stirred at $-78\text{ }^{\circ}\text{C}$ for 10 min, warmed to room temperature with continuous stirring for 2 h. After which, MeOH (78 mL) and K₂CO₃ (14.8 g, 107 mmol) were added. The reaction mixture was stirred for 16 h at room temperature, then partially concentrated *in vacuo*. The crude product was filtered through a silica plug, concentrated *in vacuo* once more, and then purified by flash column chromatography (SiO₂, 98:2 Pentane:Et₂O) to afford alkyne **255** (7.46 g, 82%) as a colourless oil.

R_f = 0.4 (90:10 Pentane:Et₂O);

[α]_D²⁵ +5.6 (*c* = 1.19, CH₂Cl₂);

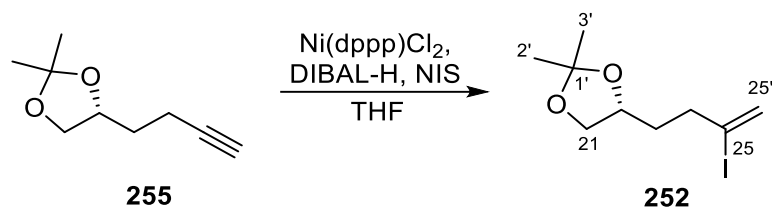
¹H NMR (400 MHz, CDCl₃) δ_{H} 4.25–4.15 (1H, m, C(22)H), 4.07 (1H, dd, *J* = 8.0, 6.0 Hz, C(21)H_AH_B), 3.57 (1H, dd, *J* = 8.1, 6.9 Hz, C(21)H_AH_B), 2.38–2.23 (2H, m, C(24)H₂), 1.96 (1H, t, *J* = 2.7 Hz, C(25)H), 1.87–1.67 (2H, m, C(23)H₂), 1.40 (3H, s, C(2')H₃), 1.35 (3H, s, C(3')H₃);

¹³C NMR (125 MHz, CDCl₃) δ_{C} 108.8 (C1'), 83.5 (C25), 74.7 (C22), 69.0 (C25'), 68.7 (C21), 32.6 (C23), 26.9 (C2'), 25.6 (C3'), 15.0 (C24).

The spectral data were consistent with those previously reported.⁵²

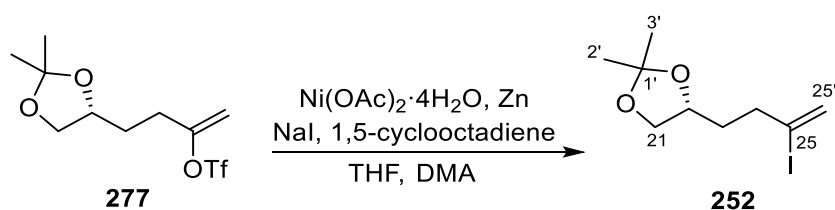
(R)-4-(3-iodobut-3-en-1-yl)-2,2-dimethyl-1,3-dioxolane (252)

Procedure A:



A flame-dried two-necked flask was charged with [1,3]-bis(diphenylphosphino)propane]dichloronickel(II) (759 mg, 1.40 mmol) and purged with argon for 10 min, before THF (52 mL) and DIBAL-H (1.0 M in THF, 60.7 mL, 60.7 mmol) were added in one portion sequentially. The resultant black mixture was cooled to 0 °C before alkyne **255** (7.20 g, 46.7 mmol) in anhydrous THF (20 mL) was added dropwise. The resulting mixture was warmed to room temperature and stirred for 2 h before being cooled to 0 °C. A solution of *N*-iodosuccinimide (21.0 g, 93.4 mmol) in anhydrous THF (125 mL) was added dropwise. The reaction mixture was then warmed to room temperature and stirred for 1 hour before Rochelle's salt solution (sat., 160 mL) was added. The layers were separated and the aqueous layer was extracted with Et₂O (3 × 350 mL). The combined organic layers were dried (MgSO₄), filtered, and concentrated *in vacuo*. Purification by flash column chromatography (SiO₂, 98:2 Pentane: Et₂O) afforded α-vinyl iodide **252** (10.1 g, 77%) as a colourless oil.

Procedure B:



An RBF was charged with Ni(OAc)₂·4H₂O (317 mg, 1.27 mmol), Zn (166 mg, 2.54 mmol), cod (312 μL, 2.54 mmol), and NaI (3.62 g, 24.2 mmol). After which, DMA (13 mL) and α-vinyl triflate

277 (3.87 g, 12.7 mmol) dissolved in THF (38 mL) were added to the RBF and the reaction mixture was warmed to 40 °C and stirred for 2 h. The reaction was quenched by brine (25 mL) and extracted with Et₂O (4 × 25 mL). The organic layers were combined, dried (MgSO₄), filtered, and then concentrated *in vacuo*. Purification by flash column chromatography (SiO₂, 95:5 Pentane:EtOAc) afforded α-vinyl iodide **252** (2.77 g, 77%) as a colourless oil.

R_f = 0.4 (90:10 Pentane:Et₂O);

[α]_D²⁵ -24.3 (*c* = 1.0, CH₂Cl₂);

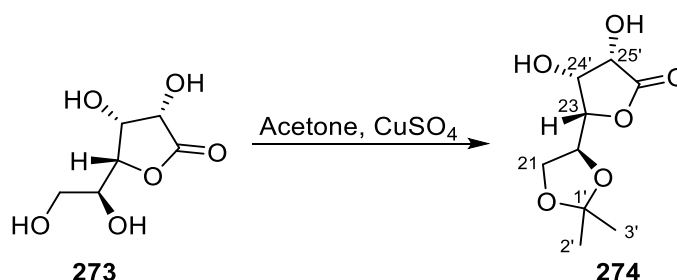
¹H NMR (400 MHz, CDCl₃) δ_H 6.07 (1H, d, *J* = 1.4 Hz, C(25')H_AH_B), 5.71 (1H, d, *J* = 1.4 Hz, C(25')H_AH_B), 4.12–4.00 (2H, m, C(22)H, C(21)H_AH_B), 3.60–3.50 (1H, m, C(21)H_AH_B), 2.60–2.40 (2H, m, C(24)H₂), 1.82–1.73 (2H, m, C(23)H₂), 1.41 (3H, s, C(2')H₃), 1.34 (3H, s, C(3')H₃);

¹³C NMR (101 MHz, CDCl₃) δ_C 126.0 (C25'), 111.0 (C25), 108.9 (C1'), 74.5 (C22), 69.2 (C21), 41.7 (C24), 33.3 (C23), 27.0 (C2'), 25.7 (C3');

The spectral data were consistent with those previously reported.⁵²

(3*S*,4*R*,5*S*)-5-((*S*)-2,2-dimethyl-1,3-dioxolan-4-yl)-3,4-dihydroxydihydrofuran-2(3*H*)-one

(274)



A 1-L RBF was charged with tetraol **273** (12.3 g, 68.8 mmol). Acetone (620 mL) and copper (II) sulphate (24.5 g, 154 mmol) were added, and the resulting solution was stirred at room temperature for 16 h at room temperature. The mixture was filtered through Celite® and the

filtrate was stirred for 1 hour with NaHCO₃ (613 mg). The resulting mixture was then filtered through a plug of Celite® using pure acetone eluent. The filtrate was concentrated to give acetonide **274** (12.7 g, 85%) as a white solid.

R_f = 0.2 (pure EtOAc);

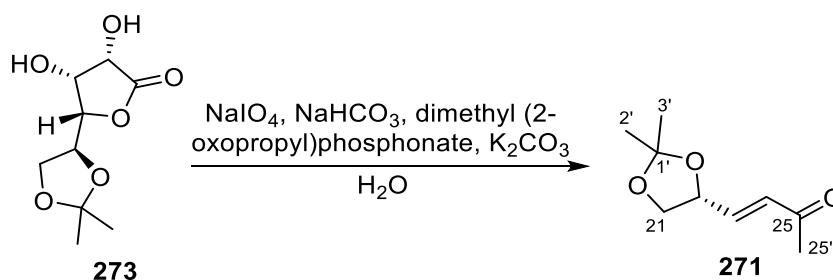
[α]_D²⁵ +9.1 (c = 0.8, MeOH; lit. +38.3, c = 0.7, MeOH);

¹H NMR (400 MHz, DMSO-*d*₆) δ_H 5.89 (1H, br. s, OH), 5.45 (1H, br. s, OH), 4.42 (1H, m, C(25')H), 4.33–4.18 (3H, m, C(22)H, C(23)H, C(24')H), 4.07 (1H, dd, *J* = 8.6, 6.2 Hz, C(21)H_AH_B), 3.76 (1H, dd, *J* = 8.6, 6.0 Hz, C(21)H_AH_B), 1.35 (3H, s, C(2')CH₃), 1.29 (3H, s, C(3')CH₃);

¹³C NMR (101 MHz, DMSO-*d*₆) δ_C 176.0 (C26'), 109.0 (C1'), 81.3 (C25'), 75.0 (C23), 70.2 (C24'), 69.5 (C22), 64.4 (C21), 26.6 (C3'), 25.3 (C2').

The spectral data were consistent with those previously reported.⁵⁴

(*R,E*)-4-(2,2-Dimethyl-1,3-dioxolan-4-yl)but-3-en-2-one (**271**)



To a suspension of acetonide **273** (9.74 g, 44.6 mmol) in 5% NaHCO₃ (207 mL) was added a solution of NaIO₄ (20.0 g, 93.7 mmol) in distilled water (58 mL) at 0 °C. After which, the reaction mixture was warmed to room temperature and stirred for 3 h, before being cooled back to 0 °C. Dimethyl (2-oxopropyl)phosphonate (13.0 mL, 93.7 mmol) and 6 M aq. K₂CO₃ (250 mL) were then added to the reaction mixture, and stirred for 3.5 h at 0 °C. After which, the reaction mixture was extracted with Et₂O (4 × 250 mL). The organic layers were

combined, dried (MgSO₄), filtered, and then concentrated *in vacuo*. Purification by flash column chromatography (SiO₂, 80:20 Pentane:EtOAc) afforded enone **271** (5.71 g, 75%) as a colourless oil.

R_f = 0.4 (60:40 Pentane:EtOAc);

[α]_D²⁵ –37.1 (c = 1.2, CH₂Cl₂);

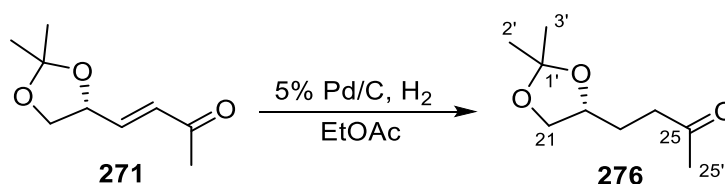
¹H NMR (400 MHz, CDCl₃) δ_H 6.65 (1H, dd, *J* = 16.0, 1.4 Hz, C(23)*H*), 6.27 (1H, dd, *J* = 16.0, 1.4 Hz, C(24)*H*), 4.64 (1H, tdd, *J* = 7.0, 5.7, 1.4 Hz, C(22)*H*), 4.16 (1H, dd, *J* = 8.3, 6.6 Hz, C(21)*H*_A*H*_B), 3.65 (1H, dd, *J* = 8.3, 7.1 Hz, C(21)*H*_A*H*_B), 2.24 (3H, s, C(25')*H*₃), 1.41 (3H, s, C(2')*H*₃), 1.37 (3H, s, C(3')*H*₃);

¹³C NMR (101 MHz, CDCl₃) δ_C 197.8 (C25), 143.1 (C23), 131.0 (C24), 110.2 (C1'), 75.0 (C22), 68.8 (C21), 27.3 (25'), 26.4 (C2'), 25.6 (C3');

IR ν_{max} (thin film)/cm⁻¹ 2988, 1679, 1371, 1252, 1215, 1154, 1058, 978, 856.

A mass spectrum could not be obtained for this compound.

(R)-4-(2,2-dimethyl-1,3-dioxolan-4-yl)butan-2-one (**276**)



A 250-mL two-necked RBF was charged with enone **271** (7.36 g, 32.2 mmol), EtOAc (76 mL), and 5% palladium on carbon (840 mg), which was then evacuated and backfilled with hydrogen five times. The reaction mixture was stirred vigorously under hydrogen atmosphere (balloon pressure) at room temperature for 4.5 h. The catalyst was removed by filtration through a short plug of silica using pure Et₂O eluent. The resulting solution was concentrated

in vacuo. Purification by flash column chromatography (SiO₂, 75:25 Pentane:EtOAc) was conducted to afford ketone **276** (6.53 g, 88%) as a colourless oil.

R_f = 0.4 (60:40 Pentane:EtOAc);

[α]_D²⁵ +3.7 (c = 1.2, CH₂Cl₂);

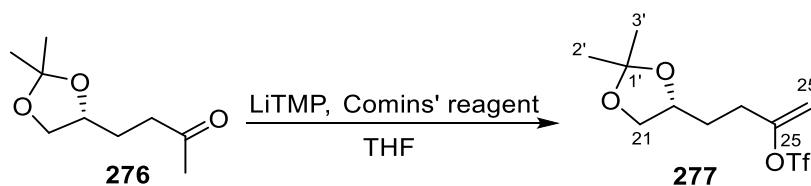
¹H NMR (400 MHz, CDCl₃) δ_H 4.09–4.02 (1H, m, C(22)H), 3.99 (1H, m, C(21)H_AH_B), 3.48 (1H, dd, J = 7.7, 6.6 Hz, C(21)H_AH_B), 2.64–2.44 (2H, m, C(24)H₂), 2.12 (3H, s, C(25')H₃), 1.83 (1H, dtd, J = 14.0, 8.1, 6.0 Hz, C(23)H_AH_B), 1.71 (1H, dtd, J = 14.0, 8.1, 6.0 Hz, C(23)H_AH_B), 1.35 (3H, s, C(2')H₃), 1.29 (3H, s, C(3')H₃);

¹³C NMR (101 MHz, CDCl₃) δ_C 207.9 (C25), 108.8 (C1'), 74.9 (C22), 69.1 (C21), 39.5 (C24), 29.9 (25'), 27.3 (C23), 26.8 (C2'), 25.5 (C3');

IR ν_{max} (thin film)/cm⁻¹ 2986, 1715, 1369, 1214, 1155, 1056, 843;

HRMS (ESI⁺, *m/z*) C₉H₁₆O₃Na [M+Na⁺] calculated 195.0992, found 195.0993 (Δ = +0.48 ppm).

(*R*)-4-(2,2-Dimethyl-1,3-dioxolan-4-yl)but-1-en-2-yl trifluoromethanesulfonate (**277**)



To an oven-dried Schlenk tube was added TMP (11.9 mL 70.1 mmol). After which, THF (190 mL) was added and the resulting solution was cooled to 0 °C. A solution of *n*BuLi (2.40 M in hexanes, 29.2 mL, 70.1 mmol) was then added dropwise to the Schlenk tube and the mixture was warmed to room temperature and stirred for 45 min. After which, the solution was cooled to –78 °C and a solution of ketone **276** (9.21 g, 53.5 mmol) in THF (190 mL) was added dropwise to the LiTMP solution and then left to stir at –78 °C for 1 hour. A solution of Comins' reagent (27.2 g, 70.1 mmol) in THF (190 mL) was then added dropwise to the reaction mixture, which

was then warmed to 0 °C and stirred for 1.5 h. The reaction mixture was quenched with a solution of NH₄Cl (sat., 190 mL). The layers were allowed to separate and the aqueous layer was extracted with Et₂O (4 × 125 mL). The organic layers were combined, dried (MgSO₄), filtered, and then concentrated *in vacuo*. Purification by flash column chromatography (SiO₂, 98:2 to 97:3 to 85:15 Pentane:EtOAc) was conducted to afford α-vinyl iodide **277** (9.87 g, 61%) as a pale yellow oil and impure starting material **276** (3.93 g) as a colourless oil.

R_f = 0.8 (70:30 Pentane:EtOAc);

[α]_D²⁵ +1.9 (c = 1.2, CH₂Cl₂);

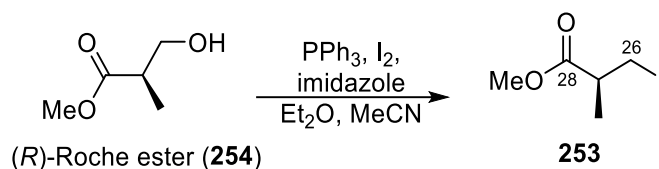
¹H NMR (400 MHz, CDCl₃) δ_H 5.11 (1H, d, *J* = 3.7 Hz, C(25')H_AH_B), 4.97 (1H, d, *J* = 3.6 Hz, C(25')H_AH_B), 4.19–3.98 (2H, m, C(22)H, C(21)H_AH_B), 3.58–3.50 (1H, m, C(21)H_AH_B), 2.57–2.35 (2H, m, C(24)H₂), 1.76 (2H, td, *J* = 7.8, 5.9 Hz, C(23)H₂), 1.39 (3H, s, C(2')H₃), 1.32 (3H, s, C(3')H₃);

¹³C NMR (101 MHz, CDCl₃) δ_C 156.1 (C25), 118.5 (q, *J* = 319.9 Hz, CF₃), 109.1 (C1'), 104.6 (C25'), 74.4 (C22), 68.9 (C21), 30.3 (C23/C24), 30.2 (C23/C24), 26.8 (C2'), 25.5 (C3');

IR ν_{max} (thin film)/cm⁻¹ 2988, 1671, 1416, 1205, 1139, 1069, 945, 902, 855, 706;

HRMS (ESI⁺, *m/z*) C₁₀H₁₆O₅F₃S [M+H⁺] calculated 305.0665, found 305.0666, (Δ = +0.33 ppm).

Methyl (S)-3-iodo-2-methylpropanoate (**253**)



Triphenylphosphine (26.4 g, 101 mmol) and imidazole (7.12 g, 105 mmol) were dissolved in Et₂O (230 mL) and acetonitrile (75 mL), and then cooled to 0 °C. Iodine (26.5 g, 105 mmol) was added portion wise to the solution over 30 min. After which, (R)-roche ester (8.91 mL, 80 mmol) was added dropwise. The reaction mixture was stirred at 0 °C for 1 hour and then at

room temperature for 1 hour. The reaction was quenched by the addition of methanol (39 mL) and the mixture was concentrated *in vacuo*. Purification by flash column chromatography (SiO₂, 93:7 Pentane:Et₂O) afforded iodide **253** (17.6 g, 96%) as a colourless oil.

R_f = 0.4 (90:10 Pentane:Et₂O);

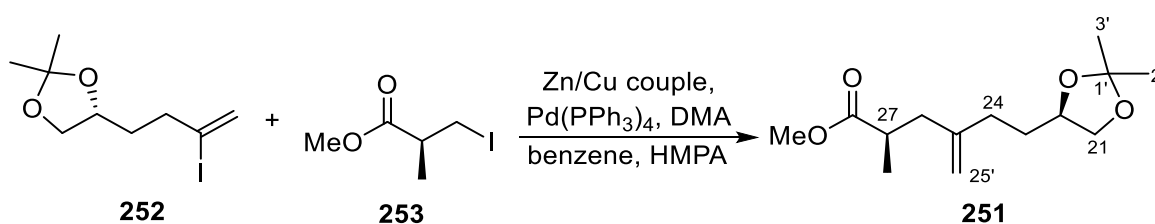
[α]_D²⁵ –20.7 (c = 1.28, CH₂Cl₂);

¹H NMR (400 MHz, CDCl₃) δ_H 3.72 (3H, s, OCH₃), 3.37 (1H, ddd, J = 9.9, 6.6, C(26)H_AH_B), 3.25 (1H, dd, J = 9.8, 6.2 Hz, C(26)H_AH_B), 2.84–2.74 (1H, m, C(27)H), 1.27 (3H, d, J = 7.0 Hz, C(27)CH₃);

¹³C NMR (125 MHz, CDCl₃) δ_C 173.8 (C28), 52.1 (OCH₃), 42.2 (C27), 18.2 (C27-CH₃), 6.9 (C26);

The spectral data were consistent with those previously reported.⁵²

Methyl (*R*)-6-((*R*)-2,2-dimethyl-1,3-dioxolan-4-yl)-2-methyl-4-methylenehexanoate (**251**)



Iodide **253** (14.6 g, 63.8 mmol) was dissolved in benzene (258 mL). Zn/Cu couple powder (14.1 g) and DMA (25.7 mL) were added to the solution. The mixture was degassed with argon and then sonicated at 45 °C for 2 h. Tetrakis(triphenylphosphine)palladium(0) (1.11 g, 0.957 mmol) was added to a separate two-neck flask containing a solution of α-vinyl iodide **252** (9.00 g, 31.9 mmol) in benzene (257 mL). The solution was degassed with argon and then HMPA (25.7 mL) was added. The solution of organozinc was then added to it, and the combined mixture was heated at 80 °C for 3 h before being diluted with EtOAc (520 mL) and filtered through Celite[®]. The filtrate was washed with a solution of NaHCO₃ (sat., 260 mL), brine (260 mL), dried

(MgSO₄), filtered, and concentrated *in vacuo*. Purification by flash column chromatography (SiO₂, 95:5 to 93:7 Pentane:EtOAc) afforded alkene **251** (5.37 g, 66%) as a colourless oil.

R_f = 0.3 (80:20 Pentane:Et₂O);

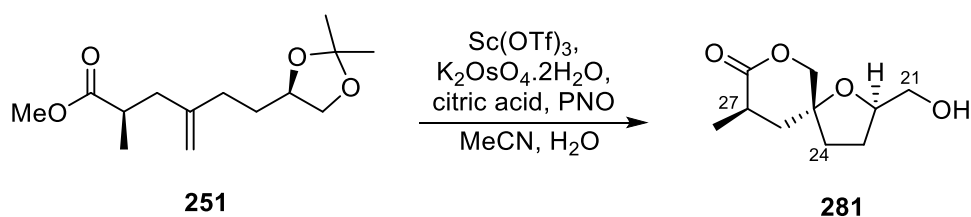
[α]_D²⁵ –20.2 (c = 0.87, CH₂Cl₂);

¹H NMR (400 MHz, CDCl₃) δ_H 4.80 (1H, s, C(25')H_AH_B), 4.76 (1H, s, C(25')H_AH_B), 4.12–4.00 (2H, m, C(22)H, C(21)H_AH_B), 3.66 (3H, s, OCH₃), 3.53 (1H, t, J = 7.0 Hz, C(21)H_AH_B), 2.65 (1H, sxt, J = 7.1 Hz, C(27)H), 2.44 (1H, dd, J = 14.4, 7.5 Hz, C(26)H_AH_B), 2.18–1.94 (3H, m, C(26)H_AH_B, C(24)H₂), 1.83–1.73 (1H, m, C(23)H_AH_B), 1.69–1.57 (1H, m, C(23)H_AH_B), 1.41 (3H, s, C(2')H₃), 1.35 (3H, s, C(3')H₃), 1.14 (3H, d, J = 7.1 Hz, C(27)CH₃);

¹³C NMR (101 MHz, CDCl₃) δ_C 176.8 (C28), 145.9 (C25), 111.3 (C25'), 108.7 (C1'), 75.6 (C22), 69.3 (C21), 51.6 (OCH₃), 40.2 (C26), 37.8 (C27), 31.7 (C23), 31.7 (C24), 27.0 (C2'), 25.7 (C3'), 17.0 (C27-CH₃);

The spectral data were consistent with those previously reported.⁵²

(2*R*,5*R*,9*R*)-2-(Hydroxymethyl)-9-methyl-1,7-dioxaspiro[4.5]decan-8-one (**281**)



Alkene **251** (200 mg, 0.780 mmol) was dissolved in MeCN (8.1 mL). Pyridine *N*-oxide (145 mg, 1.56 mmol), citric acid (110 mg, 0.570 mmol) in water (2.7 mL), and potassium osmate dihydrate (7.2 mg, 20 μmol) in water (2.7 mL) were added sequentially. The resulting green solution was stirred for 5 min, before Sc(OTf)₃ (384 mg, 0.780 mmol) was added. The mixture was heated to 60 °C for 16 h. The reaction was then cooled to room temperature, before being

quenched with Na₂SO₃ (50 mg) and stirred for 30 min. EtOAc (5.0 mL) and water (2.5 mL) were added. The layers were allowed to separate and the aqueous layer was extracted with EtOAc (3 × 10 mL). The combined organic layers were dried (MgSO₄), filtered, and concentrated *in vacuo*. Purification by flash column chromatography (SiO₂, 67:33 to 33:67 Pentane:EtOAc) afforded THF **281** (121 mg, 78%) as a colourless oil.

R_f = 0.3 (100% EtOAc);

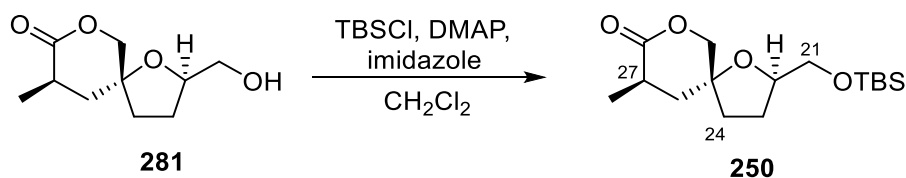
[α]_D²⁵ −8.3 (c = 0.53, CH₂Cl₂);

¹H NMR (400 MHz, CDCl₃) δ_H 4.22–4.10 (3H, m, C(22)H, C(25)CH₂O), 3.70 (1H, dd, J = 11.3, 4.3 Hz, C(21)H_AH_B), 3.50 (1H, dd, J = 11.7, 5.4 Hz, C(21)H_AH_BOH), 2.87 (1H, dq, J = 13.5, 6.9 Hz, C(27)H), 2.16 (1H, dd, J = 13.9, 6.4 Hz, C(26)H_AH_B), 2.06–1.74 (5H, m, C(23)H₂, C(24)H₂, OH), 1.65 (1H, t, J = 13.3 Hz, C(26)H_AH_B), 1.24 (3H, d, J = 6.8 Hz, C(27)CH₃);

¹³C NMR (101 MHz, CDCl₃) δ_C 174.6 (C28), 79.8 (C22), 79.4 (C25), 75.3 (C25-CH₂O), 64.7 (C21), 39.8 (C26), 35.4 (C23), 32.3 (C27), 26.5 (C24), 16.2 (C27-CH₃);

The spectral data were consistent with those previously reported.⁵²

(2R,5R,9R)-2-(((tert-Butyldimethylsilyl)oxy)methyl)-9-methyl-1,7-dioxaspiro[4.5]decan-8-one (250)



DMAP (57.0 mg, 0.468 mmol) and imidazole (637 mg, 9.36 mmol) were added to a solution of alcohol **281** (0.937 g, 4.68 mmol) in CH₂Cl₂ (47 mL). The resultant solution was stirred until all the reagents had dissolved, before TBS-Cl (776 mg, 5.15 mmol) was added in one portion. The solution was stirred for 2 h at room temperature. EtOAc (70 mL) and water (35 mL) were then

added. The layers were separated and the aqueous layer was extracted with EtOAc (3 × 45 mL). The combined organic layers were dried (MgSO₄), filtered, and concentrated *in vacuo*. Purification by flash column chromatography (SiO₂, 93:7 to 90:10 Pentane:EtOAc) afforded silyl ether **250** as a colourless oil (807 mg, 55% over 2 steps).

$R_f = 0.3$ (80:20 Pentane:Et₂O);

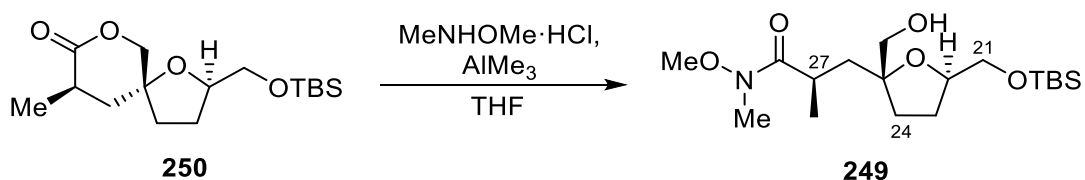
$[\alpha]_D^{25} +2.3$ ($c = 0.86$, CH₂Cl₂);

¹H NMR (400 MHz, CDCl₃) δ_H 4.19–4.08 (3H, m, C(22)H, C(25)CH₂O), 3.63 (1H, dd, $J = 10.8, 4.3$ Hz, C(21)H_AH_B), 3.57 (1H, dd, $J = 10.8, 3.8$ Hz, C(21)H_AH_B), 2.85 (1H, dquin, $J = 13.1, 6.7, 6.7, 6.7, 6.7$ Hz, C(27)H), 2.14 (1H, dd, $J = 13.9, 6.4$ Hz, C(26)H_AH_B), 2.04–1.85 (3H, m, C(24)H₂, C(23)H_AH_B), 1.78–1.70 (1H, m, C(23)H_AH_B), 1.63 (1H, t, $J = 13.0$ Hz, C(26)H_AH_B), 1.22 (3H, d, $J = 6.9$ Hz, C(27)CH₃), 0.89 (9H, s, Si(CH₃)₃), 0.05 (6H, s, Si(CH₃)₂);

¹³C NMR (101 MHz, CDCl₃) δ_C 175.0 (C28), 80.0 (C22), 79.3 (C25), 75.2 (C25-CH₂O), 65.2 (C21), 40.1 (C26), 35.6 (C23), 32.3 (C27), 26.7 (C24), 25.9 (Si(CH₃)₃), 18.4 (Si(CH₃)₃), 16.0 (C27-CH₃), –5.3 (SiCH₃), –5.5 (SiCH₃);

The spectral data were consistent with those previously reported.⁵²

(R)-3-((2R,5R)-5-(((tert-Butyldimethylsilyl)oxy)methyl)-2-(hydroxymethyl)tetrahydrofuran-2-yl)-N-methoxy-N,2-dimethylpropanamide (249)



AlMe₃ (2.0 M in heptane, 6.34 mL, 12.7 mmol) was added to a solution of *N,O*-dimethylhydroxylamine hydrochloride (1.24 g, 12.7 mmol) dissolved in THF (13 mL) at 0 °C. The mixture was stirred for 10 min, before a solution of lactone **250** (797 mg, 2.53 mmol) in

THF (13 mL) was added dropwise. The reaction mixture was stirred for 5 h at 0 °C and then quenched with EtOAc (40 mL) and a solution of Rochelle's salt (sat., 40 mL). The layers were separated and the aqueous layer was extracted with EtOAc (3 × 25 mL). The combined organic layers were washed with Rochelle's salt solution (sat., 25 mL), dried (MgSO₄), filtered, and concentrated *in vacuo*. Purification by flash column chromatography (SiO₂, 75:25 Pentane:EtOAc) afforded Weinreb amide **249** (873 mg, 92%) as a colourless oil.

$R_f = 0.4$ (50:50 Et₂O:Pentane);

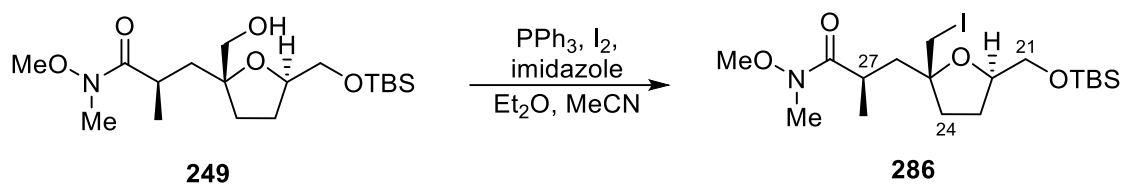
$[\alpha]_D^{25} -40.2$ ($c = 1.18$, CH₂Cl₂);

¹H NMR (400 MHz, CDCl₃) δ_H 4.07–4.00 (1H, m, C(22)H), 3.70 (3H, s, OCH₃), 3.70 (1H, dd, $J = 10.6, 3.6$, C(21)H_AH_B), 3.52 (1H, dd, $J = 10.7, 3.3$ Hz, C(21)H_AH_B), 3.36–3.29 (1H, m, C(25)CH_AH_BOH), 3.29–3.18 (2H, m, C(25)CH_AH_BOH, OH), 3.17 (3H, s, NCH₃), 3.14–3.06 (1H, m, C(27)H), 2.23 (1H, dd, $J = 14.4, 10.2$ Hz, C(26)H_AH_B), 2.05 (1H, ddd, $J = 12.1, 8.2, 3.8$ Hz, C(23)H_AH_B), 1.98–1.88 (2H, m, C(24)H₂), 1.65 (1H, dt, $J = 12.1, 9.4$ Hz, THF-CH_AH_BCH), 1.38 (1H, dd, $J = 14.4, 2.8$ Hz, CH(CH₃)CH_AH_B), 1.12 (3H, d, $J = 7.0$ Hz, C(27)CH₃), 0.89–0.84 (9H, m, Si(CH₃)₃), 0.06–0.00 (6H, m, Si(CH₃) × 2);

¹³C NMR (101 MHz, CDCl₃) δ_C 178.6 (C28), 85.3 (C25), 79.5 (C22), 67.1 (C25-CH₂OH), 65.3 (C21), 61.4 (OCH₃), d₃ (C26), 34.4 (C23), 32.4 (NCH₃), 30.9 (C27), 27.4 (C24), 25.9 (Si(CH₃)₃), 19.8 (C27-CH₃), 18.4 (Si(CH₃)₃), –5.5 (SiCH₃), –5.5 (SiCH₃);

The spectral data were consistent with those previously reported.⁵²

(R)-3-((2R,5R)-5-(((tert-Butyldimethylsilyl)oxy)methyl)-2-(iodomethyl)tetrahydrofuran-2-yl)-N-methoxy-N,2-dimethylpropanamide (286)



Weinreb amide **249** (1.50 g, 4.15 mmol) was dissolved in toluene (41 mL) and stirred. Triphenylphosphine (2.176 g, 8.30 mmol), imidazole (367 mg, 5.39 mmol), and iodine (1.79 g, 7.05 mmol) were added sequentially, which was heated to 80 °C and stirred for 3 h. The mixture was cooled to room temperature, diluted with EtOAc (260 mL), washed with a solution of Na₂S₂O₃ (0.1 M, 130 mL), and then brine (260 mL). The crude product was dried (MgSO₄), filtered, and then concentrated *in vacuo*. Purification by flash column chromatography (SiO₂, 90:10 Pentane:CH₂Cl₂, then 50:50 EtOAc:Pentane) afforded iodide **286** (1.52 g, 78%) as a colourless oil.

R_f = 0.4 (80:20 Pentane:EtOAc);

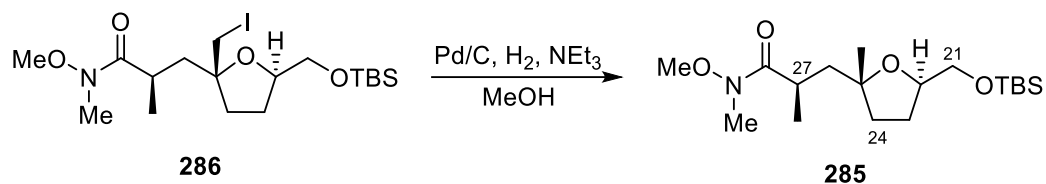
[α]_D²⁵ –8.7 (c = 0.78, CH₂Cl₂);

¹H NMR (400 MHz, CDCl₃) δ_H 4.16–4.01 (1H, m, C(22)H), 3.72 (3H, s, OCH₃), 3.60 (2H, d, J = 4.5 Hz, C(21)H₂), 3.31 (1H, d, J = 10.3 Hz, C(25)CH_AH_B), 3.22 (1H, d, J = 10.2 Hz, C(25)CH_AH_B), 3.18 (3H, s, NCH₃), 3.06 (1H, br. s., C(27)H), 2.27 (1H, dd, J = 14.4, 8.6 Hz, C(26)H_AH_B), 2.09–1.74 (5H, m, C(23)H₂, C(24)H₂, C(26)H_AH_B), 1.18 (3H, d, J = 7.0 Hz, C(27)CH₃), 0.89 (9H, s, SiC(CH₃)₃), 0.05 (6H, s, Si(CH₃)₂);

¹³C NMR (101 MHz, CDCl₃) δ_C 178.2 (C28), 83.4 (C25), 80.6 (C22), 65.6 (C21), 61.6 (OCH₃), 41.7 (C26), 35.5 (C23), 32.6 (NCH₃), 30.8 (C27), 27.8 (C24), 25.9 (SiC(CH₃)₃), 19.5 (C27-CH₃), 18.3 (SiC(CH₃)₃), 15.8 (C25-CH₂I), –5.3 (SiCH₃), –5.4 (SiCH₃);

The spectral data were consistent with those previously reported.⁵²

(R)-3-((2R,5R)-5-(((tert-Butyldimethylsilyl)oxy)methyl)-2-methyltetrahydrofuran-2-yl)-N-methoxy-N,2-dimethylpropanamide (285)



To an RBF charged with iodide **286** (1.63 g, 3.45 mmol) was added, MeOH (52 mL), palladium on carbon (10 wt%, 371 mg, 3.48 mmol), and NEt₃ (0.46 mL, 3.3 mmol). The resulting solution was purged with argon three times and then with H₂ gas five times, before being stirred under an atmosphere of hydrogen for 24 h. The mixture was filtered through Celite® and then concentrated *in vacuo*. Purification by flash column chromatography (SiO₂, 95:5 to 88:12 Pentane:EtOAc) afforded **285** (1.19 g, 100%) as a colourless oil.

R_f = 0.4 (20:80 EtOAc:Pentane);

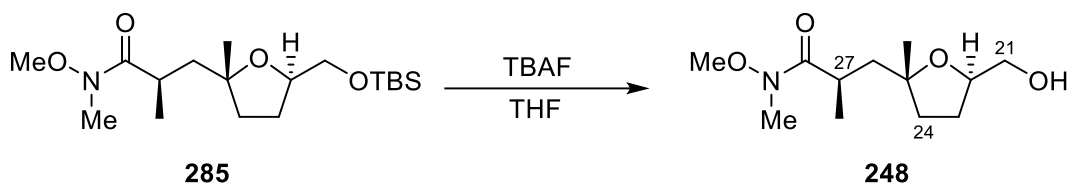
[α]_D²⁵ –13.8 (c = 1.1, CH₂Cl₂);

¹H NMR (400 MHz, CDCl₃) δ_H 4.01–3.93 (1H, m, C(22)H), 3.72 (3H, s, OCH₃), 3.61 (1H, dd, J = 10.4, 4.6 Hz, C(21)H_AH_B), 3.51 (1H, dd, J = 10.4, 5.6 Hz, C(21)H_AH_B), 3.18 (3H, s, NCH₃), 3.15–3.07 (1H, m, C(27)HCH₃), 2.09 (1H, dd, J = 14.1, 8.5 Hz, C(26)H_AH_B), 2.01–1.88 (1H, m, C(23)H_AH_B), 1.82–1.59 (3H, m, C(23)H_AH_B, C(24)H₂), 1.51 (1H, dd, J = 14.1, 3.8 Hz, C(26)H_AH_B), 1.18–1.12 (6H, m, C(27)CH₃, C(25)CH₃), 0.88 (9H, s, SiC(CH₃)₃), 0.04 (6H, s, Si(CH₃)₂);

¹³C NMR (101 MHz, CDCl₃) δ_C 178.7 (C28), 82.8 (C25), 79.2 (C22), 66.3 (C21), 61.4 (OCH₃), 44.0 (C26), 37.7 (C23), 32.7 (NCH₃), 31.2 (C25-CH₃), 28.2 (C24), 26.4 (C27), 25.9 (SiC(CH₃)₃), 19.8 (C27-CH₃), 18.4 (SiC(CH₃)₃), –5.3 (SiCH₃), –5.3 (SiCH₃);

The spectral data were consistent with those previously reported.⁵²

(R)-3-((2R,5R)-5-((S)-1-Hydroxyprop-2-yn-1-yl)-2-methyltetrahydrofuran-2-yl)-N-methoxy-N,2-dimethylpropanamide (248)



TBS ether **285** (666 mg, 2.85 mmol) was dissolved in anhydrous THF (9.0 mL) and stirred. TBAF (1 M in THF, 6.02 mL, 6.02 mmol) was added to the solution, which was stirred at room temperature for 3 h and then quenched with a solution of NH₄Cl (sat., 45 mL). The layers were allowed to separate and the aqueous layer was extracted with EtOAc (4 × 45 mL). The organic layers were combined, dried (MgSO₄), filtered, and concentrated *in vacuo*. Purification by flash column chromatography (SiO₂, 98:2 to 90:10 CH₂Cl₂:MeOH) afforded alcohol **248** (449 mg, 99%) as a colourless oil.

R_f = 0.3 (90:10 CH₂Cl₂:MeOH);

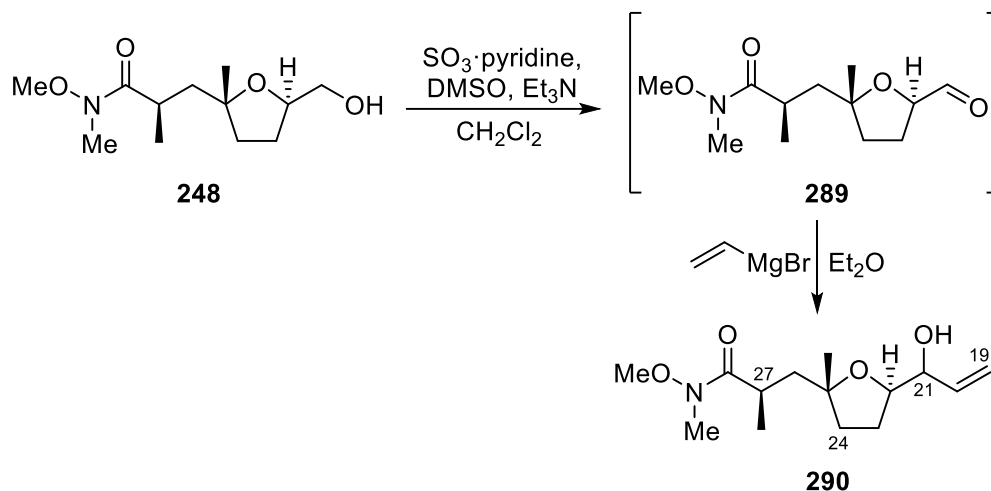
[α]_D²⁵ −7.6 (c = 0.2, CHCl₃);

¹H NMR (400 MHz, CDCl₃) δ_H 4.00 (1H, dd, *J* = 6.0, 3.3 Hz, C(22)H), 3.67 (3H, s, CH₃O), 3.58 (1H, dd, *J* = 11.4, 3.5 Hz, C(21)H_AH_B), 3.45 (1H, dd, *J* = 11.4, 5.5 Hz, C(21)H_AH_B), 3.13 (3H, s, NCH₃), 3.09 (1H, br. s., C(27)H), 2.39 (1H, br. s., OH), 2.10 (1H, dd, *J* = 14.2, 9.1 Hz, C(26)H_AH_B), 1.93–1.82 (2H, m, C(23)H_AH_B), 1.79–1.68 (2H, m, C(24)H₂), 1.61–1.58 (1H, m, OH), 1.47 (1H, dd, *J* = 14.2, 3.5 Hz, C(26)H_AH_B), 1.14–1.07 (6H, m, C(27)CH₃, C(25)CH₃);

¹³C NMR (101 MHz, CDCl₃) δ_C 178.7 (C28), 82.9 (C25), 79.1 (C22), 65.2 (C21), 61.4 (OCH₃), 43.9 (C26), 37.5 (C23), 32.5 (NCH₃), 30.8 (C25-CH₃), 27.2 (C24), 26.7 (C27), 19.6 (C27-CH₃);

The spectral data were consistent with those previously reported.⁵²

(2R)-3-((2R,5R)-5-(1-Hydroxyallyl)-2-methyltetrahydrofuran-2-yl)-N-methoxy-N,2-dimethylpropanamide (290)



To a solution of alcohol **248** (2.05 g, 8.36 mmol) and Et_3N (11.3 mL, 81.1 mmol) in CH_2Cl_2 (41 mL) at 0 °C was added $\text{SO}_3 \cdot \text{py}$ (5.19 g, 32.6 mmol) in DMSO (34.7 mL, 488.0 mmol). The reaction was warmed to room temperature and stirred for 2.5 h, and then diluted with EtOAc (200 mL). The solution was washed with brine (200 mL). The aqueous layer was extracted with EtOAc (4 × 200 mL). The combined organic layers were partially concentrated *in vacuo* to ca. 100 mL. The organic layer was then washed with brine (200 mL) and the aqueous layer was re-extracted with EtOAc (3 × 200 mL). The combined organic layers were dried (MgSO_4), filtered and concentrated *in vacuo*.

The crude aldehyde (assumed quant., 8.36 mmol) was directly carried to the next step without purification, and transferred to a flask containing Et_2O (82 mL) and cooled to -78 °C. Vinyl magnesium bromide (1 M in THF, 13.4 mL, 13.4 mmol) was added at -78 °C and was stirred for 1 hour. The reaction was quenched with NH_4Cl (sat. 100 mL) and the layers were separated. The aqueous layer was extracted with EtOAc (4 × 150 mL). The organic layers were combined, dried (MgSO_4), filtered, and concentrated *in vacuo*. Purification by flash column

chromatography (SiO₂, 50:50 pentane:Et₂O) afforded allylic alcohol **290** (1.35 g, 60%) as a colourless oil. The diastereomeric ratio could not be determined at C-21.

R_f = 0.5 (50:50 Pentane:Acetone);

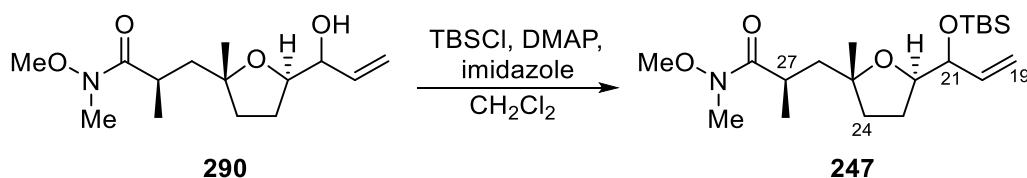
[α]_D²⁵ -9.8 (c = 1.0, CHCl₃);

¹H NMR (400 MHz, CDCl₃) δ_H 5.74 (1H, ddd, J = 17.4, 10.6, 5.6 Hz, C(20)H), 5.26 (1H, dt, J = 17.3, 1.7 Hz, C(19)H_AH_B), 5.12 (1H, dt, J = 10.6, 1.6 Hz, C(19)H_AH_B), 4.17 (1H, dtd, J = 5.4, 3.6, 1.7 Hz, C(21)H), 3.95–3.86 (1H, m, C(22)H), 3.67 (3H, s, OCH₃), 3.12 (3H, s, NCH₃), 3.08 (1H, s, C(27)H), 2.37 (1H, s, OH), 2.13–2.05 (1H, m, C(26)H_AH_B), 1.88–1.77 (1H, m, C(23)H_AH_B), 1.76–1.65 (2H, m, C(24)H_AH_B, C(23)H_AH_B), 1.64–1.53 (1H, m, C(24)H_AH_B), 1.46 (1H, dd, J = 14.2, 3.6 Hz, C(26)H_AH_B), 1.12 (3H, s, C(23)CH₃), 1.10 (3H, d, J = 7.0 Hz, C(27)CH₃);

¹³C NMR (101 MHz, CDCl₃) δ_C 178.6 (C28), 136.3 (C20), 115.9 (C19), 82.9 (C25), 81.3 (C22), 72.7 (C21), 61.3 (OCH₃), 43.8 (C26), 37.6 (C24), 32.5 (NCH₃), 30.9 (C27), 26.2 (C25-CH₃), 24.8 (C23), 19.6 (C27-CH₃).

The spectral data were consistent with those previously reported.³⁶

(2R)-3-((2R,5R)-5-(1-((tert-Butyldimethylsilyl)oxy)allyl)-2-methyltetrahydrofuran-2-yl)-N-methoxy-N,2-dimethylpropanamide (247)



Alcohol **290** (1.38 g, 5.09 mmol) was dissolved in CH₂Cl₂ (42 mL) and cooled to 0 °C. TBSCl (2.30 g, 15.3 mmol) and imidazole (2.30 g, 33.8 mmol) were added to the solution with vigorous stirring. The solution was then warmed to room temperature and was stirred for 15 h. The reaction mixture was quenched with water (100 mL). The layers were allowed to separate and

the aqueous layer was extracted with CH_2Cl_2 (4×100 mL). The organic layers were combined, dried (MgSO_4), filtered, and then concentrated *in vacuo*. Purification by flash column chromatography (SiO_2 , 100:0 to 85:15 Pentane:EtOAc) afforded silyl ether **247** (1.52 g, 77%) as a colourless oil.

$R_f = 0.7$ (60:40 Pentane:EtOAc);

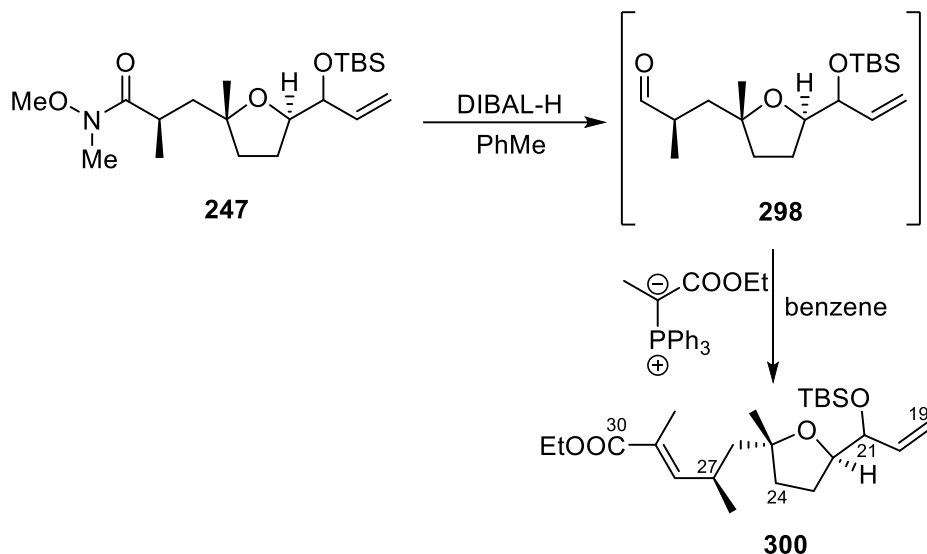
$[\alpha]_D^{25} -22.2$ ($c = 1.0$, CHCl_3);

$^1\text{H NMR}$ (400 MHz, CDCl_3) δ_{H} 5.77 (1H, ddd, $J = 17.3, 10.5, 5.6$ Hz, C(20)H), 5.18 (1H, dt, $J = 17.2, 1.8$ Hz, C(19) H_AH_B), 5.03 (1H, dt, $J = 10.5, 1.6$ Hz, C(19) H_AH_B), 4.11–4.03 (1H, m, C(21)H), 3.75 (1H, ddd, $J = 7.8, 6.7, 4.4$ Hz, C(22)H), 3.68 (3H, s, OCH_3), 3.13 (3H, s, NCH_3), 3.10–3.05 (1H, s, C(27)H), 2.07 (1H, dd, $J = 14.1, 8.6$ Hz, C(26) H_AH_B), 1.92–1.71 (2H, m, C(23) H_2), 1.68–1.51 (2H, m, C(23) H_2), 1.45 (1H, dd, $J = 14.1, 3.8$ Hz, C(26) H_AH_B), 1.12–1.07 (6H, m, C(25) CH_3 , C(27) CH_3), 0.86 (9H, s, $\text{Si}(\text{CH}_3)_2\text{C}(\text{CH}_3)_3$), 0.01 (3H, s, $\text{Si}(\text{CH}_3)(\text{CH}_3)\text{C}(\text{CH}_3)_3$), -0.02 (3H, s, $\text{Si}(\text{CH}_3)(\text{CH}_3)\text{C}(\text{CH}_3)_3$);

$^{13}\text{C NMR}$ (101 MHz, CDCl_3) δ_{C} 178.7 (C28), 139.2 (C20), 114.7 (C19), 82.7 (C25), 81.9 (C22), 75.1 (C21), 61.3 (OCH_3), 43.8 (C26), 37.8 (C24), 32.4 (NCH_3), 31.2 (C27), 26.0 (C25- CH_3), 26.0 (C23), 26.0 ($\text{SiC}(\text{CH}_3)_3$), 19.6 (C27- CH_3), 18.1 ($\text{SiC}(\text{CH}_3)_3$), -4.5 (SiCH_3), -4.7 (SiCH_3);

The spectral data were consistent with those previously reported.³⁶

Ethyl (4*R*,*E*)-5-((2*R*,5*R*)-5-(1-((*tert*-butyldimethylsilyl)oxy)allyl)-2-methyltetrahydrofuran-2-yl)-2,4-dimethylpent-2-enoate (300)



To a solution of Weinreb amide **247** (1.38 g, 3.57 mmol) in THF (65 mL) at -78°C was added DIBAL-H (1 M in THF, 14.3 mL, 14.3 mmol) dropwise. The reaction was stirred for 1 hour 20 min at -78°C . The reaction was then quenched with EtOAc (7 mL) and then warmed to room temperature before Rochelle's salt solution (sat. 7 mL) was added. The layers were allowed to separate and the aqueous layer was extracted with EtOAc (4 \times 40 mL). The combined organic layers were concentrated *in vacuo* and then diluted with Et₂O (75 mL) and distilled water (100 mL). The layers were allowed to separate, and the aqueous layer was re-extracted with Et₂O (4 \times 75 mL). The combined organic layers were dried (MgSO₄), filtered, and the concentrated *in vacuo*.

The crude aldehyde (assumed quant., 3.57 mmol) was dried azeotropically in benzene (3 \times 5 mL). To an RBF equipped with a condenser was added (carboxyethylidene)triphenylphosphorane (4.53 g, 12.5 mmol) and benzene (81 mL). The crude aldehyde was then added as a solution in THF (12.2 mL) to the RBF, and the reaction was heated to reflux and stirred for 17 h. The reaction was cooled to room temperature before it was quenched with NH₄Cl (sat. 10 mL). The mixture was diluted with EtOAc (15 mL) and the

layers were separated. The aqueous layer was extracted with EtOAc (3 × 15 mL). The combined organic layers were dried (MgSO₄), filtered, and the concentrated *in vacuo*. Purification by column chromatography (SiO₂, 100:0 to 97:3 to 95:5 Pentane:Et₂O) afforded ester **300** (980 mg, 67% over two steps) as a colourless oil.

R_f = 0.40 (85:15 Pentane:Et₂O);

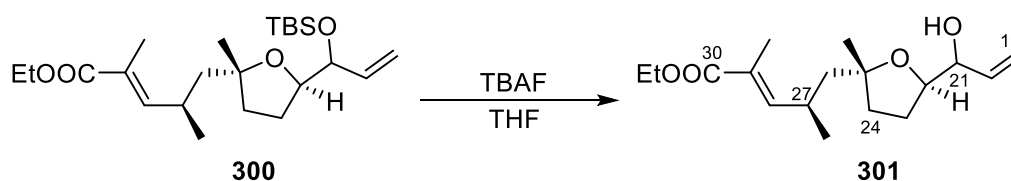
[α]_D²⁵ −10.8 (c = 1.0, CHCl₃);

¹H NMR (400 MHz, CDCl₃) δ_H 6.63–6.58 (1H, m, C(28)H), 5.78 (1H, ddd, J = 17.2, 10.5, 5.7 Hz, C(20)H), 5.20 (1H, dq, J = 17.2, 1.8 Hz, C(19)H_AH_B), 5.09–5.03 (1H, m, C(19)H_AH_B), 4.16 (2H, q, J = 7.1 Hz, OCH₂CH₃), 4.10–4.04 (1H, m, C(21)H), 3.76–3.69 (1H, m, C(22)H), 2.74–2.61 (1H, m, C(27)H), 1.92–1.83 (1H, m, C(23)H_AH_B), 1.84–1.81 (3H, m, C(29)CH₃), 1.81–1.72 (1H, m, C(23)H_AH_B), 1.70–1.48 (4H, m, C(26)H₂, C(24)H₂), 1.29–1.26 (3H, m, OCH₂CH₃), 1.14 (3H, s, C(25)CH₃), 1.00 (3H, d, J = 6.7 Hz, C(27)CH₃), 0.88 (9H, s, SiC(CH₃)₃), 0.04 (3H, s, SiCH₃), 0.00 (3H, s, SiCH₃);

¹³C NMR (101 MHz, CDCl₃) δ_C 168.4 (C30), 149.0 (C28), 139.2 (C20), 124.8 (C29), 114.9 (C19), 83.0 (C25), 82.0 (C22), 75.2 (C21), 60.3 (OCH₂CH₃), 47.8 (C26), 37.6 (C24), 30.1 (C27), 26.7 (C25-CH₃), 26.3 (C23), 25.9 (SiC(CH₃)₃), 21.4 (C27-CH₃), 18.2 (SiC(CH₃)), 14.3 (OCH₂CH₃), 12.2 (C29-CH₃), −4.5 (SiCH₃), −4.6 (SiCH₃).

The spectral data were consistent with those previously reported.³⁶

Ethyl (4*R*,*E*)-5-((2*R*,5*R*)-5-(1-hydroxyallyl)-2-methyltetrahydrofuran-2-yl)-2,4-dimethylpent-2-enoate (301)



Silyl ether **300** (980 mg, 2.39 mmol) was dissolved in THF (95 mL) and stirred. TBAF (1 M in THF, 7.76 mL, 7.76 mmol) was added to the solution, which was stirred at room temperature for 8 h and then quenched with a solution of NH₄Cl (sat., 100 mL). The organic and aqueous layers were allowed to separate, and the aqueous layer was extracted with EtOAc (4 × 100 mL). The organic layers were combined, dried (MgSO₄), filtered, and concentrated *in vacuo*. Purification by flash column chromatography (SiO₂, 100:0 to 85:15 EtOAc:Pentane) afforded alcohol **301** (481 mg, 68%) as a colourless oil.

$R_f = 0.2$ (90:10 Pentane:EtOAc);

$[\alpha]_D^{25} -12.0$ ($c = 0.5$, CHCl₃);

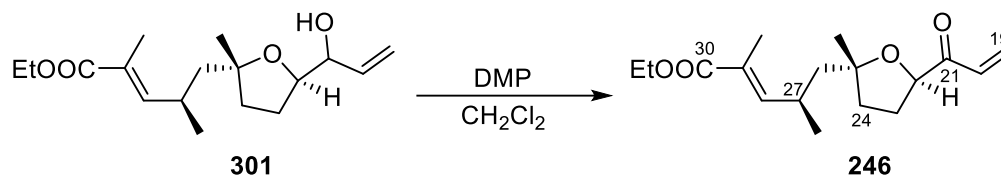
¹H NMR (400 MHz, CDCl₃) δ_H 6.62 (1H, dd, $J = 10.1, 1.5$ Hz, C(28)H), 5.77 (1H, ddd, $J = 17.3, 10.6, 5.8$ Hz, C(20)H), 5.30 (1H, dt, $J = 17.4, 1.6$ Hz, C(19)H_AH_B), 5.16 (1H, dt, $J = 10.6, 1.6$ Hz, C(19)H_AH_B), 4.21–4.18 (1H, m, C(21)H), 4.16 (2H, qd, $J = 7.1, 1.1$ Hz, OCH₂CH₃), 3.86 (1H, ddd, $J = 9.5, 5.8, 3.6$ Hz, C(22)H), 2.74–2.63 (1H, m, C(27)H), 2.25 (1H, d, $J = 2.7$ Hz, OH), 1.93–1.85 (1H, m, C(23)H_AH_B), 1.84 (3H, d, $J = 1.5$ Hz, C(29)CH₃), 1.81–1.53 (5H, m, C(26)H₂, C(24)H₂, C(23)H_AH_B), 1.27 (3H, t, $J = 7.1$ Hz, OCH₂CH₃), 1.17 (3H, s, C(25)CH₃), 1.01 (3H, d, $J = 6.8$ Hz, C(27)CH₃);

¹³C NMR (126 MHz, CDCl₃) δ_C 168.4 (C30), 148.7 (C28), 136.3 (C20), 124.9 (C29), 116.2 (C19), 83.3 (C25), 81.3 (C22), 72.7 (C21), 60.4 (OCH₂CH₃), 47.8 (C26), 37.6 (C24), 30.0 (C27), 26.7 (C25-CH₃), 25.0 (C23), 21.3 (C27-CH₃), 14.3 (OCH₂CH₃), 12.3 (C29-CH₃).

The spectral data were consistent with those previously reported.³⁶

Ethyl (*R,E*)-5-((2*R*,5*R*)-5-acryloyl-2-methyltetrahydrofuran-2-yl)-2,4-dimethylpent-2-enoate

(246)



To a solution of allylic alcohol **301** (48.0 mg, 162 μmol) in CH_2Cl_2 (2.5 mL) was added NaHCO_3 (68.0 mg, 0.810 mmol) and DMP (192 mg, 0.453 mmol) and the reaction was stirred at room temperature for 2 h. The reaction was quenched with NaHCO_3 (sat., 4 mL) and $\text{Na}_2\text{S}_2\text{O}_3$ (sat., 4 mL), and the layers were separated. The aqueous layer was extracted with EtOAc (3 \times 10 mL). The combined organic layers were dried (MgSO_4), filtered, and concentrated *in vacuo*. Purification by flash column chromatography (SiO_2 , 95:5 to 80:20 Pentane:EtOAc) afforded enone **246** (47.7 mg, 100%) as a colourless oil.

$R_f = 0.3$ (85:15 Pentane:EtOAc);

$[\alpha]_D^{25} -5.6$ ($c = 1.0$, CHCl_3);

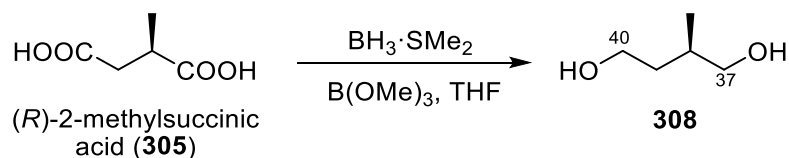
$^1\text{H NMR}$ (400 MHz, CDCl_3) δ_{H} 6.72 (1H, dd, $J = 17.5, 10.6$ Hz, C(20)*H*), 6.62 (1H, dq, $J = 10.1, 1.5$ Hz, C(28)*H*), 6.34 (1H, dd, $J = 17.5, 1.5$ Hz, C(19)*H*_A*H*_B), 5.76 (1H, dd, $J = 10.6, 1.7$ Hz, C(19)*H*_A*H*_B), 4.44 (1H, t, $J = 7.8$ Hz, C(22)*H*), 4.16 (2H, qd, $J = 7.1, 1.4$ Hz, OCH_2CH_3), 2.78–2.65 (1H, m, C(27)*H*), 2.24–2.12 (1H, m, C(23)*H*_A*H*_B), 2.09–1.96 (1H, m, C(23)*H*_A*H*_B), 1.84 (3H, d, $J = 1.4$ Hz, C(29) CH_3), 1.80–1.58 (4H, m, C(26) H_2 , C(24) H_2), 1.26 (3H, t, $J = 7.1$ Hz, OCH_2CH_3), 1.20 (3H, s, C(25) CH_3), 1.03 (3H, d, $J = 6.8$ Hz, C(27) CH_3);

$^{13}\text{C NMR}$ (101 MHz, CDCl_3) δ_{C} 200.4 (C21), 168.4 (C30), 148.4 (C28), 131.8 (C20), 129.3 (C19), 125.1 (C29), 85.1 (C25), 82.1 (C22), 60.4 (OCH_2CH_3), 47.8 (C26), 37.2 (C24), 30.0 (C27), 29.1 (C23), 26.3 (C25- CH_3), 21.3 (C27- CH_3), 14.2 (OCH_2CH_3), 12.3 (C29- CH_3).

The spectral data were consistent with those previously reported.³⁶

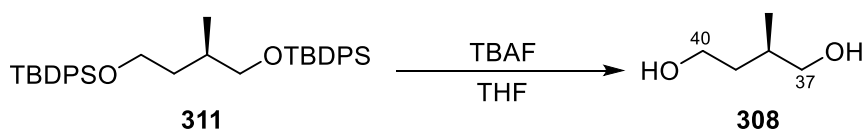
(R)-2-Methylbutane-1,4-diol (**308**)

Procedure A:



Borane dimethyl sulphide (28.7 mL, 303 mmol) and trimethyl borate (32.5 mL, 291 mmol) were dissolved in THF (100 mL) and then cooled to 0 °C. (R)-2-Methylsuccinic acid (10.0 g, 75.7 mmol) dissolved in THF (50 mL) was added dropwise to the solution. The solution was then warmed to room temperature and stirred for 16 h. The reaction was quenched by dropwise addition of MeOH (150 mL). The solvent was removed *in vacuo* and subsequent purification by flash column chromatography (SiO₂, 50:50 to 75:25 EtOAc:Pentane) afforded diol **308** (7.16 g, 93%) as a colourless oil.

Procedure B:



TBAF (1.0 M in THF, 15.1 mL, 15.1 mmol) was added to a solution of **311** (2.20 g, 3.78 mmol) in THF (15 mL) at room temperature. The reaction mixture was heated to 50 °C and stirred for 7 h. The reaction mixture was then cooled to room temperature and quenched with a solution of NH₄Cl (sat., 29 mL). The layers were allowed to separate and the aqueous layer was extracted with EtOAc (3 × 70 mL). The organic layers were combined, dried (MgSO₄), filtered, and then concentrated *in vacuo*. Purification by flash chromatography (SiO₂, 90:10 Pentane:EtOAc, then pure acetone) afforded diol **308** (377 mg, 96%) as a colourless oil.

R_f = 0.2 (90:10 CH₂Cl₂:MeOH);

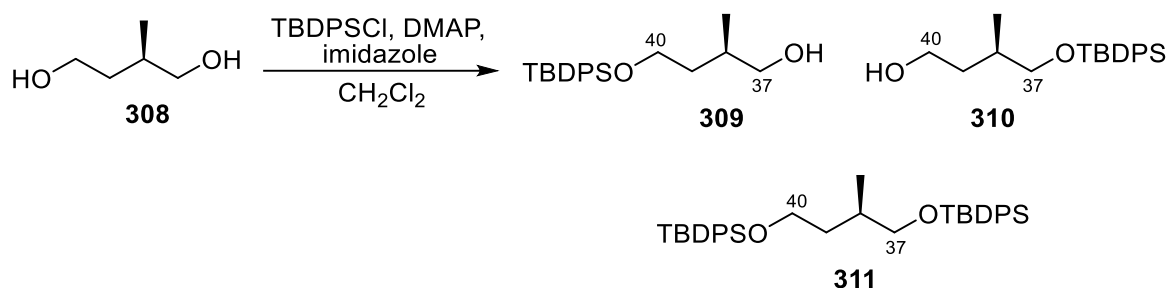
$[\alpha]_D^{25} +14.9$ ($c = 0.75$, CH_2Cl_2);

$^1\text{H NMR}$ (400 MHz, CDCl_3) δ_{H} 3.75 (1H, dt, $J = 10.9, 5.3$ Hz, C(40) $H_{\text{A}}H_{\text{B}}$), 3.68–3.59 (1H, m, C(40) $H_{\text{A}}H_{\text{B}}$), 3.54 (1H, dd, $J = 10.7, 4.4$ Hz, C(37) $H_{\text{A}}H_{\text{B}}$), 3.51–3.31 (3H, m, C(37) $H_{\text{A}}H_{\text{B}}$, OH x 2), 1.86–1.71 (1H, m, C(38) H), 1.67–1.48 (2H, m, C(39) H_2), 0.91 (3H, d, $J = 6.9$ Hz, C(38) CH_3);

$^{13}\text{C NMR}$ (101 MHz, CDCl_3) δ_{C} 68.1 (C37), 60.9 (C40), 37.5 (C39), 34.1 (C38), 17.3 (C38- CH_3);

The spectral data were consistent with those previously reported.⁷³

(*R*)-4-((*tert*-Butyldiphenylsilyl)oxy)-2-methylbutan-1-ol (**309**)



Diol **308** (7.15 g, 68.7 mmol), imidazole (5.14 g, 75.5 mmol), and DMAP (839 mg, 6.87 mmol) were dissolved in CH_2Cl_2 (685 mL). *tert*-Butyl(chloro)diphenylsilane (19.7 mL, 76.6 mmol) was added dropwise to the solution, which was stirred at room temperature for 16 h. The reaction was quenched with a solution of NH_4Cl (sat., 420 mL). The layers were allowed to separate and the aqueous layer was extracted with EtOAc (3 × 420 mL). The organic layers were combined, dried (MgSO_4), filtered, and then concentrated *in vacuo*. Purification by flash chromatography (SiO_2 , 97:3 to 90:10 Pentane:EtOAc, then pure acetone) afforded an inseparable mixture of **309** and **310** (16.3 g, 69%) as a colourless oil. Di-substituted side-product **311** (8.39 g, 21%) was also isolated as a colourless oil.

Compound 309:

$R_f = 0.5$ (80:20 Pentane:EtOAc);

$[\alpha]_D^{25} +5.3$ ($c = 0.96$, CHCl_3 ; lit. $+6.6$, $c = 1.9$, CHCl_3);

$^1\text{H NMR}$ (400 MHz, CDCl_3) δ_{H} 7.77–7.65 (4H, m, PhH), 7.49–7.36 (6H, m, PhH), 3.81–3.63 (2H, m, C(40) H_2), 3.58–3.44 (2H, m, C(37) H_2), 1.93–1.77 (1H, m, C(38)H) 1.76–1.43 (2H, m, C(39) H_2), 1.07 (9H, m, $\text{SiC}(\text{CH}_3)_3$), 0.91 (3H, m, CH CH_3);

$^{13}\text{C NMR}$ (101 MHz, CDCl_3) δ_{C} 135.5 (quat. Ph- C_{Ar}), 133.4 (quat. Ph- C_{Ar}), 129.7 (Ph- C_{Ar}), 127.7 (Ph- C_{Ar}), 68.2 (C37), 62.5 (C40), 36.7 (C39), 33.9 (C38), 26.8 ($\text{SiC}(\text{CH}_3)_3$), 19.1 ($\text{SiC}(\text{CH}_3)_3$), 17.1 (C38- CH_3);

The spectral data were consistent with those previously reported.⁷³

Compound 310:

$R_f = 0.9$ (80:20 Pentane:EtOAc);

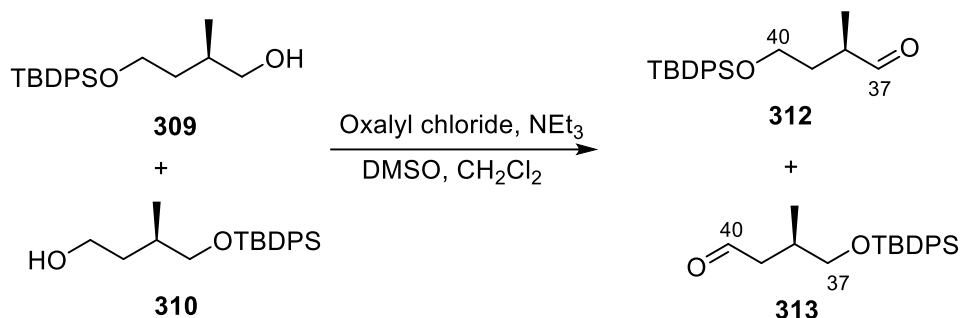
$[\alpha]_D^{25} +2.3$ ($c = 0.78$, CH_2Cl_2);

$^1\text{H NMR}$ (400 MHz, CDCl_3) δ_{H} 7.52 (8H, dd, $J = 5.7, 1.8$ Hz, PhH), 7.30–7.18 (12H, m, PhH), 3.56 (2H, t, $J = 6.6$ Hz, C(37) H_2), 3.40–3.28 (2H, m, C(40) H_2), 1.80–1.70 (1H, m, C(39) $H_{\text{A}}H_{\text{B}}$), 1.70–1.61 (1H, m, C(39) $H_{\text{A}}H_{\text{B}}$), 1.27–1.16 (1H, m, C(38)H), 0.91 (18H, d, $J = 2.8$ Hz, $\text{SiC}(\text{CH}_3)_3 \times 2$), 0.75 (3H, d, $J = 6.6$ Hz, C38- CH_3);

$^{13}\text{C NMR}$ (101 MHz, CDCl_3) δ_{C} 135.6 (Ph- $C_{\text{Ar}} \times 4$), 134.1 (quat. Ph- $C_{\text{Ar}} \times 4$), 129.5 (Ph- $C_{\text{Ar}} \times 4$), 127.6 (Ph- $C_{\text{Ar}} \times 4$), 68.9 (C37), 62.1 (C40), 36.1 (C39), 32.5 (C38), 26.9 ($\text{SiC}(\text{CH}_3)_3$), 26.9 ($\text{SiC}(\text{CH}_3)_3$), 19.3 ($\text{SiC}(\text{CH}_3)_3$), 19.2 ($\text{SiC}(\text{CH}_3)_3$), 16.8 (CH(CH_3));

The spectral data were consistent with those previously reported.⁷³

(R)-4-((tert-Butyldiphenylsilyl)oxy)-2-methylbutanal (312)



DMSO (2.49 mL, 35.0 mmol) was added to a solution of oxalyl chloride (1.51 mL, 4.32 mmol) dissolved in CH₂Cl₂ (240 mL) at -78 °C and the mixture was stirred for 30 min. After which, a solution of alcohol **309** and **310** (4.00 g, 11.7 mmol) dissolved in CH₂Cl₂ (80 mL) was added dropwise to the mixture, which was stirred for 30 min. NEt₃ (8.14 mL, 58.4 mmol) was then added dropwise and the mixture was stirred for an additional 30 min, before being warmed to 0 °C and then quenched with a solution of NH₄Cl (sat., 80 mL). The layers were allowed to separate and the aqueous layer was extracted with CH₂Cl₂ (3 × 80 mL). The organic layers were combined, dried (MgSO₄), filtered, and then concentrated *in vacuo*. The crude product was carried directly to the next step.

Compound 312:

R_f = 0.8 (90:10 Pentane:EtOAc);

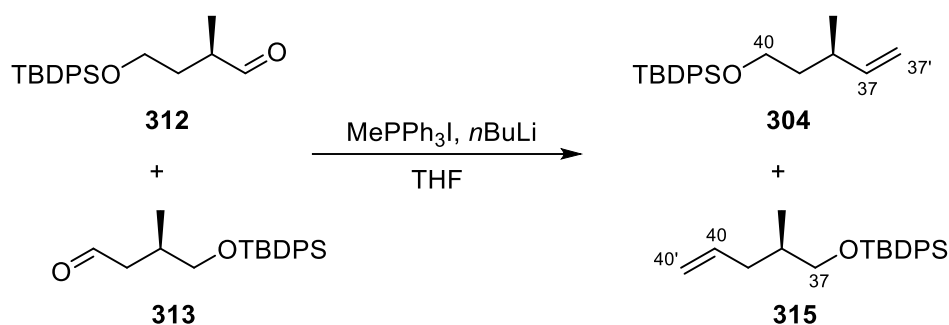
[α]_D²⁵ +35.6 (c = 1.0, CH₂Cl₂);

¹H NMR (400 MHz, CDCl₃) δ_H 9.60 (1H, d, J = 1.6 Hz, C(37)H), 7.60–7.55 (4H, m, PhH), 7.40–7.27 (6H, m, PhH), 3.72–3.56 (2H, m, C(40)H₂), 2.57–2.46 (1H, m, C(38)H), 1.98–1.88 (1H, m, C(39)H_AH_B), 1.59–1.50 (1H, m, C(39)H_AH_B), 1.01 (3H, d, J = 7.1 Hz, C(38)CH₃), 0.97 (9H, s, SiC(CH₃)₃).

^{13}C NMR (101 MHz, CDCl_3) δ_{c} 204.9 (C37), 135.5 (Ph- C_{Ar}), 133.5 (quat. Ph- C_{Ar}), 129.7 (Ph- C_{Ar}), 127.7 (Ph- C_{Ar}), 61.1 (C40), 43.5 (C38), 33.4 (C39), 26.8 ($\text{SiC}(\text{CH}_3)_3$), 19.1 ($\text{SiC}(\text{CH}_3)_3$), 13.1 (C38- CH_3);

The spectral data were consistent with those previously reported.⁷³

(*R*)-tert-Butyl((3-methylpent-4-en-1-yl)oxy)diphenylsilane, 536 and (*R*)-tert-Butyl((2-methylpent-4-en-1-yl)oxy)diphenylsilane (304)



$n\text{BuLi}$ (2.5 M in hexanes, 9.82 mL, 24.5 mmol) was added dropwise to a suspension of methyltriphenylphosphonium iodide (10.4 g, 25.7 mmol) in freshly distilled THF (84 mL) at 0 °C. The resulting mixture was stirred for 15 min. A solution of aldehydes **312** and **313** (3.98 g, 11.7 mmol, azeotropically distilled three times in benzene) dissolved in THF (28 mL) was then added dropwise to the mixture, which was subsequently warmed to room temperature and stirred for 12 h. After which, the reaction was quenched with a solution of NH_4Cl (sat., 60 mL). The layers were allowed to separate and the aqueous layer was extracted with Et_2O (3 \times 60 mL). The organic layers were combined, dried (MgSO_4), filtered, and then concentrated *in vacuo*. Purification by flash column chromatography (SiO_2 , 99:1 to 98:2 Pentane: CH_2Cl_2) afforded alkene **304** (2.44 g, 62% over two steps) and alkene **315** (795 mg, 20% over two steps) as colourless oils.

Compound 304:

$R_f = 0.4$ (90:10 Pentane:CH₂Cl₂);

$[\alpha]_D^{25} +55.5$ (c 1.0, CH₂Cl₂);

¹H NMR (400 MHz, CDCl₃) δ_H 7.72–7.64 (4H, m, PhH), 7.47–7.34 (6H, m, PhH), 5.74–5.61 (1H, m, C(37)H), 5.01–4.86 (2H, m, C(37')H₂), 3.69 (2H, t, $J = 6.6$ Hz, C(40)H₂), 2.44–2.31 (1H, m, C(38)H), 1.62–1.52 (2H, m, C(39)H₂) 1.06 (9H, s, SiC(CH₃)₃), 0.98 (3H, d, $J = 6.8$ Hz, C(38)-CH₃).

¹³C NMR (101 MHz, CDCl₃) δ_C 144.3 (C37), 135.6 (Ph-C_{Ar}), 134.1 (quat. Ph-C_{Ar}), 129.5 (Ph-C_{Ar}), 127.6 (Ph-C_{Ar}), 112.6 (C37'), 61.9 (C40), 39.2 (C39), 34.2 (C38), 26.9 (SiC(CH₃)₃), 20.1 (C38-CH₃), 19.2 (SiC(CH₃)₃).

The spectral data were consistent with those previously reported.⁷³

Compound 315:

$R_f = 0.5$ (90:10 Pentane:CH₂Cl₂);

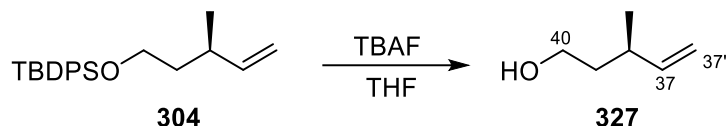
$[\alpha]_D^{25} +70.6$ (c = 1.0, CH₂Cl₂);

¹H NMR (400 MHz, CDCl₃) δ_H 7.73–7.66 (4H, m, PhH), 7.48–7.35 (6H, m, PhH), 5.78 (1H, ddt, $J = 17.1, 10.3, 7.2$ Hz, C(40)H), 5.07–4.95 (2H, m, C(40')H₂), 3.57–3.47 (2H, m, C(37)H₂), 2.33–2.23 (1H, m, C(38)H), 1.99–1.87 (1H, m, C(39)H_AH_B), 1.84–1.72 (1H, m, C(39)H_AH_B), 1.08 (9H, s, SiC(CH₃)₃), 0.93 (3H, d, $J = 6.7$ Hz, C(38)-CH₃);

¹³C NMR (101 MHz, CDCl₃) δ_C 137.3 (Ph-C_{Ar}), 135.6 (C40), 134.0 (quat. Ph-C_{Ar}), 129.5 (Ph-C_{Ar}), 127.6 (Ph-C_{Ar}), 115.7 (C40'), 68.3 (C37), 37.6 (C39), 35.7 (C38), 26.9 (SiC(CH₃)₃), 19.3 (SiC(CH₃)₃), 16.4 (C38-CH₃);

The spectral data were consistent with those previously reported.⁷³

(R)-3-Methylpent-4-en-1-ol 5 (327)



Tetrabutylammonium fluoride (1 M in THF, 12.9 mL, 12.9 mmol) was added to a stirring solution of alkene **304** (2.18 g, 6.44 mmol) in THF (13 mL). The reaction mixture was warmed to 50 °C and stirred for 3 h. The reaction was then quenched with a solution of NH₄Cl (sat., 25 mL). The layers were allowed to separate and the aqueous layer was extracted with Et₂O (3 × 100 mL). The organic layers were combined, dried (MgSO₄), filtered, and then concentrated *in vacuo*. Purification by flash column chromatography (SiO₂, 95:5 to 75:25 Pentane:Et₂O) afforded alcohol **327** (511 mg, 79%) as a colourless oil.

R_f = 0.4 (50:50 Pentane:Et₂O);

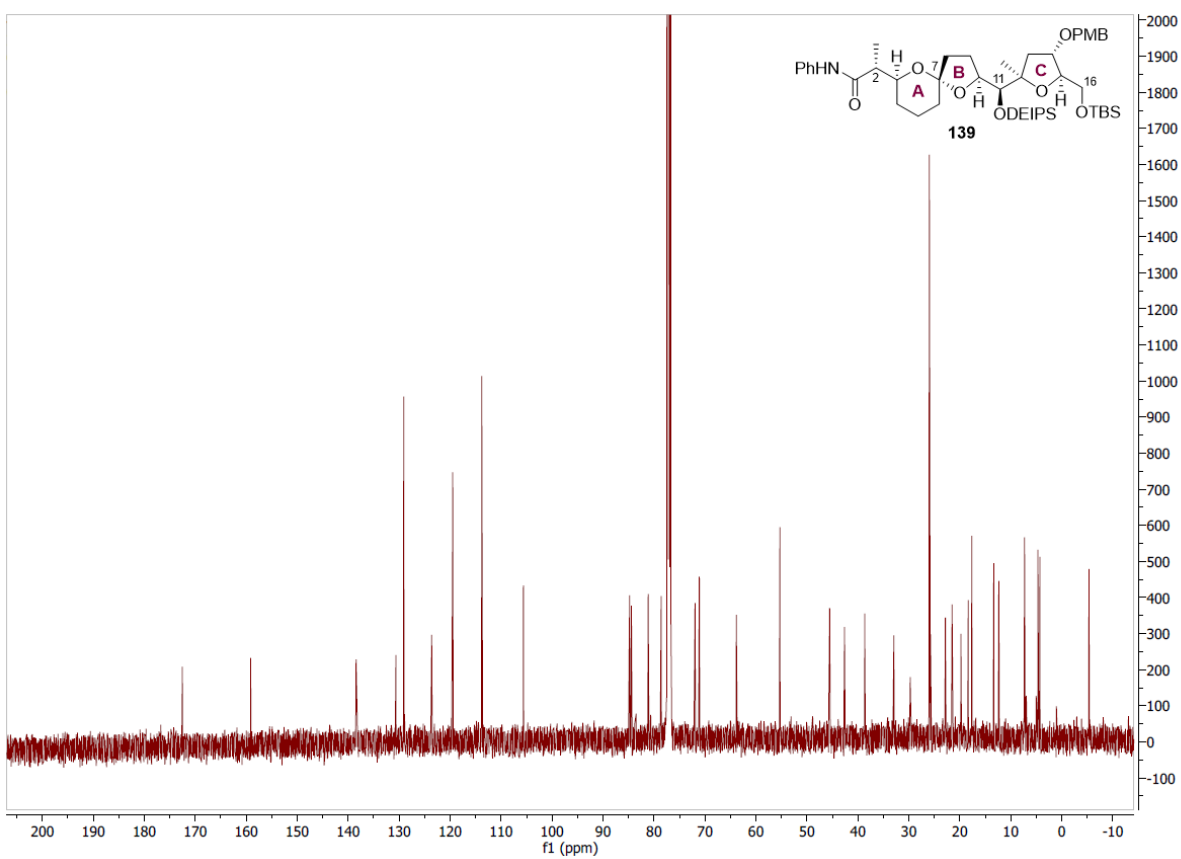
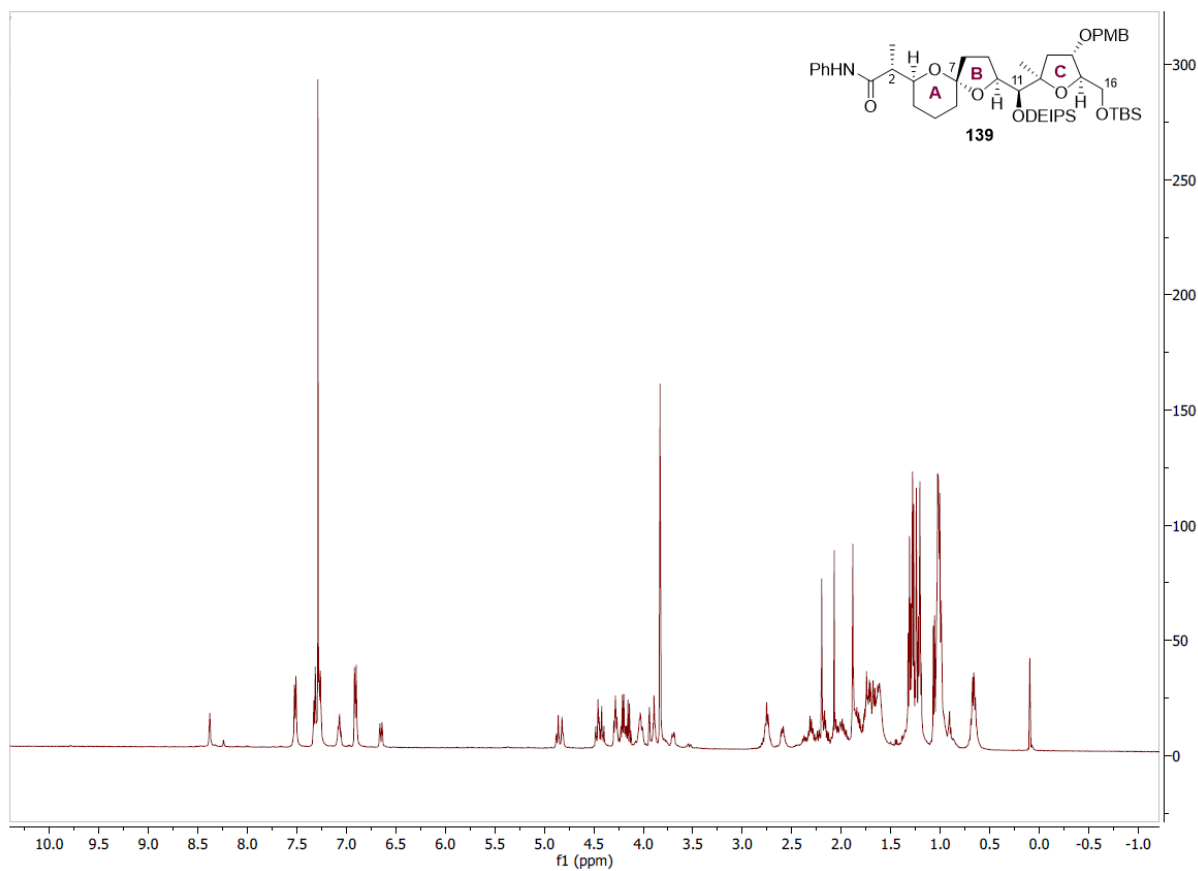
¹H NMR (400 MHz, CDCl₃) δ_H 5.72 (1H, ddd, *J* = 17.6, 10.1, 7.8 Hz, C(37)*H*), 5.09–4.91 (2H, m, C(37')*H*₂), 3.67 (2H, t, *J* = 6.9 Hz, (40)*H*₂), 2.30 (1H, dt, *J* = 7.1, 7.1 Hz, C(38)*H*), 1.61–1.52 (2H, m, C(39)*H*₂), 1.02 (3H, d, *J* = 6.8 Hz, C(38)-CH₃);

¹³C NMR (101 MHz, CDCl₃) δ_C 144.2 (C37), 113.1 (C37'), 61.2 (C40), 39.3 (C39), 34.9 (C38), 20.4 (C38-CH₃).

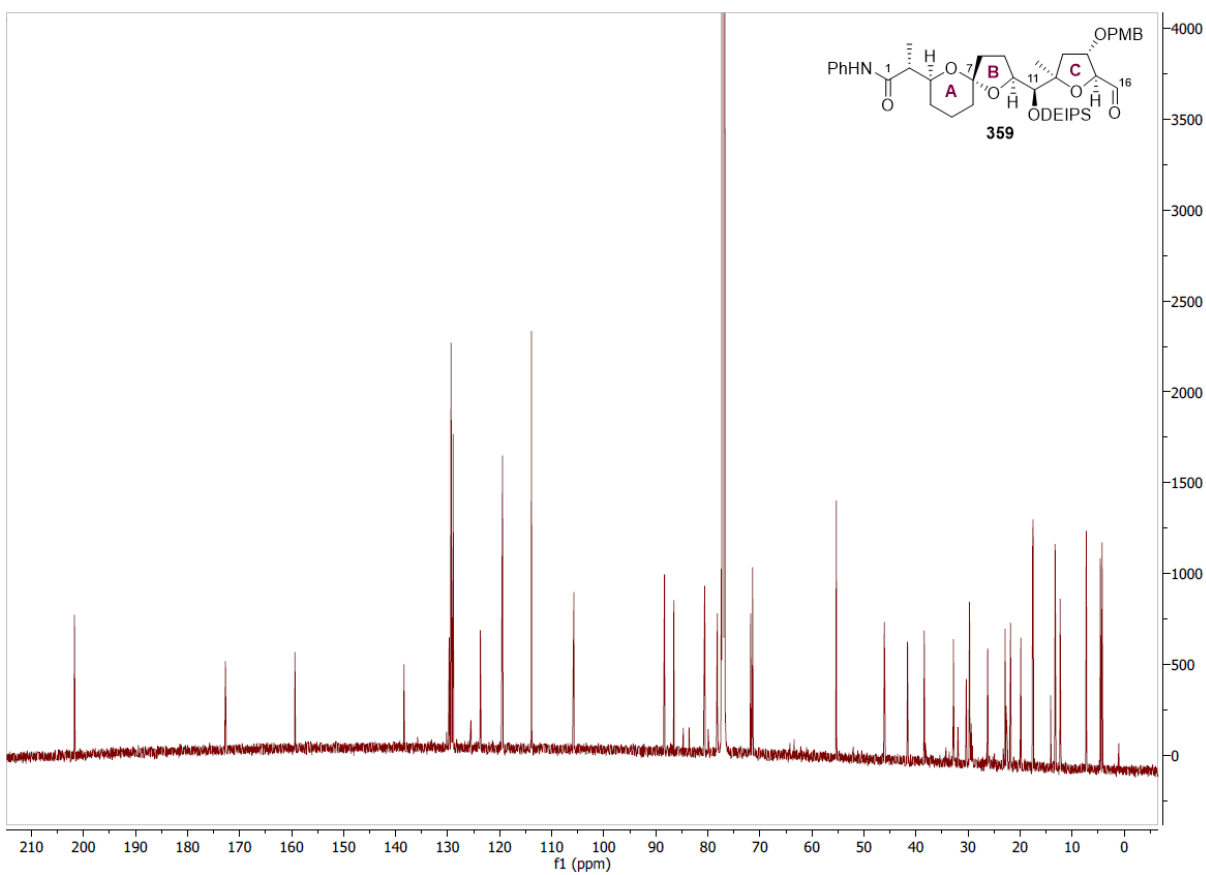
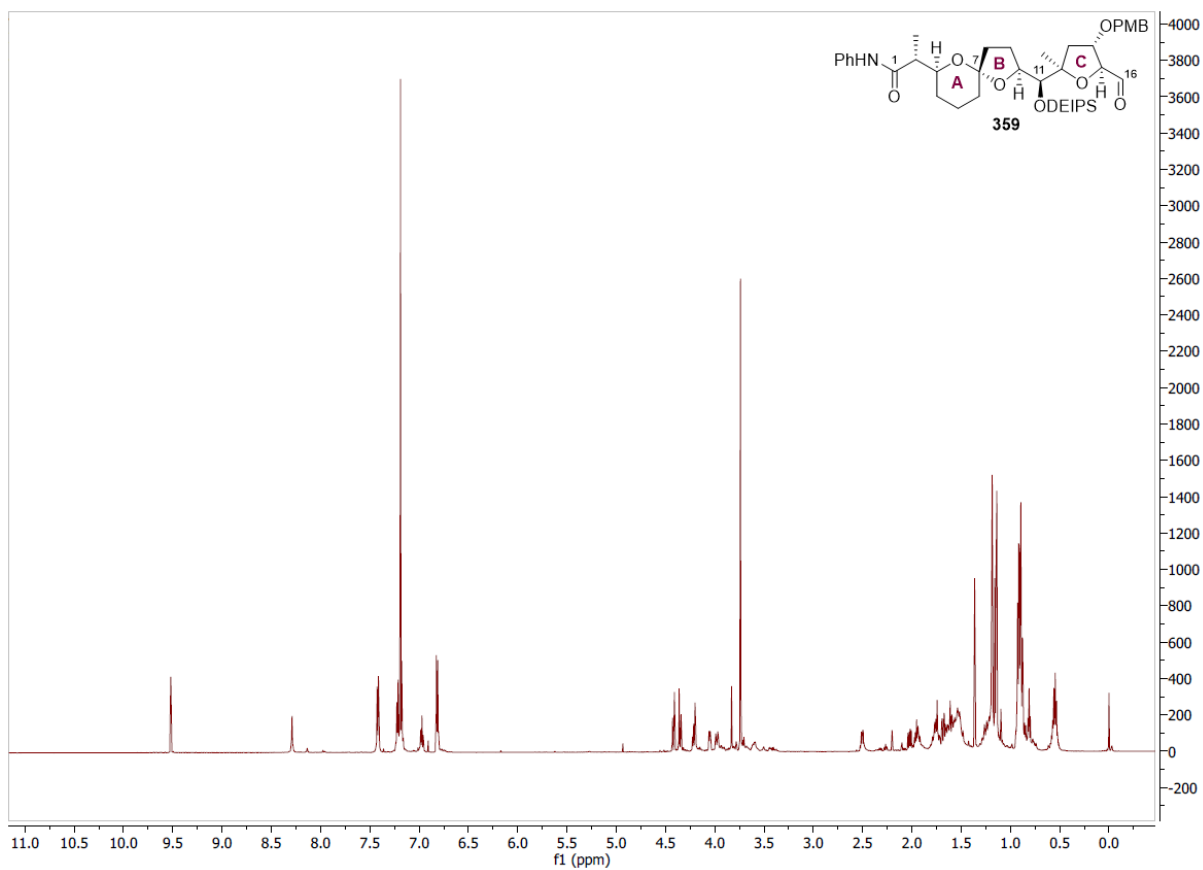
The spectral data were consistent with those previously reported.⁷³

5.2 Selected NMR spectra

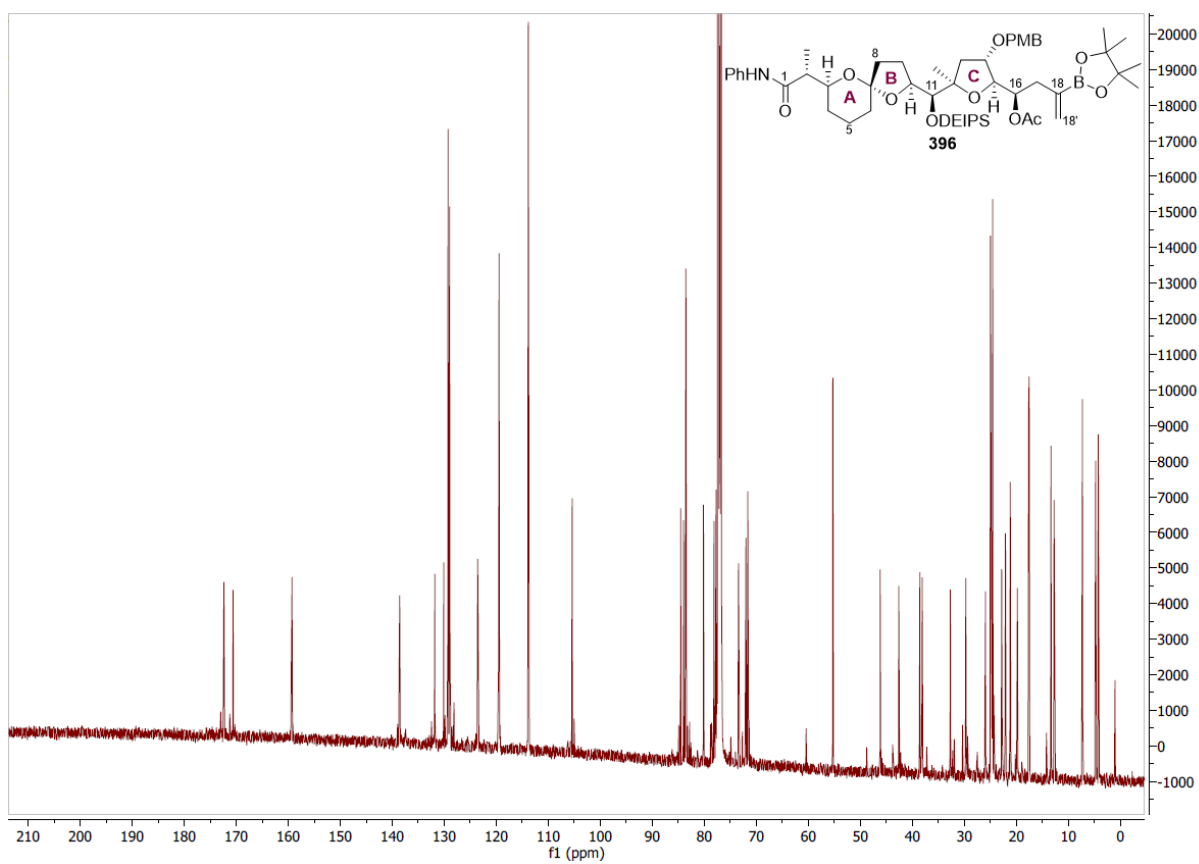
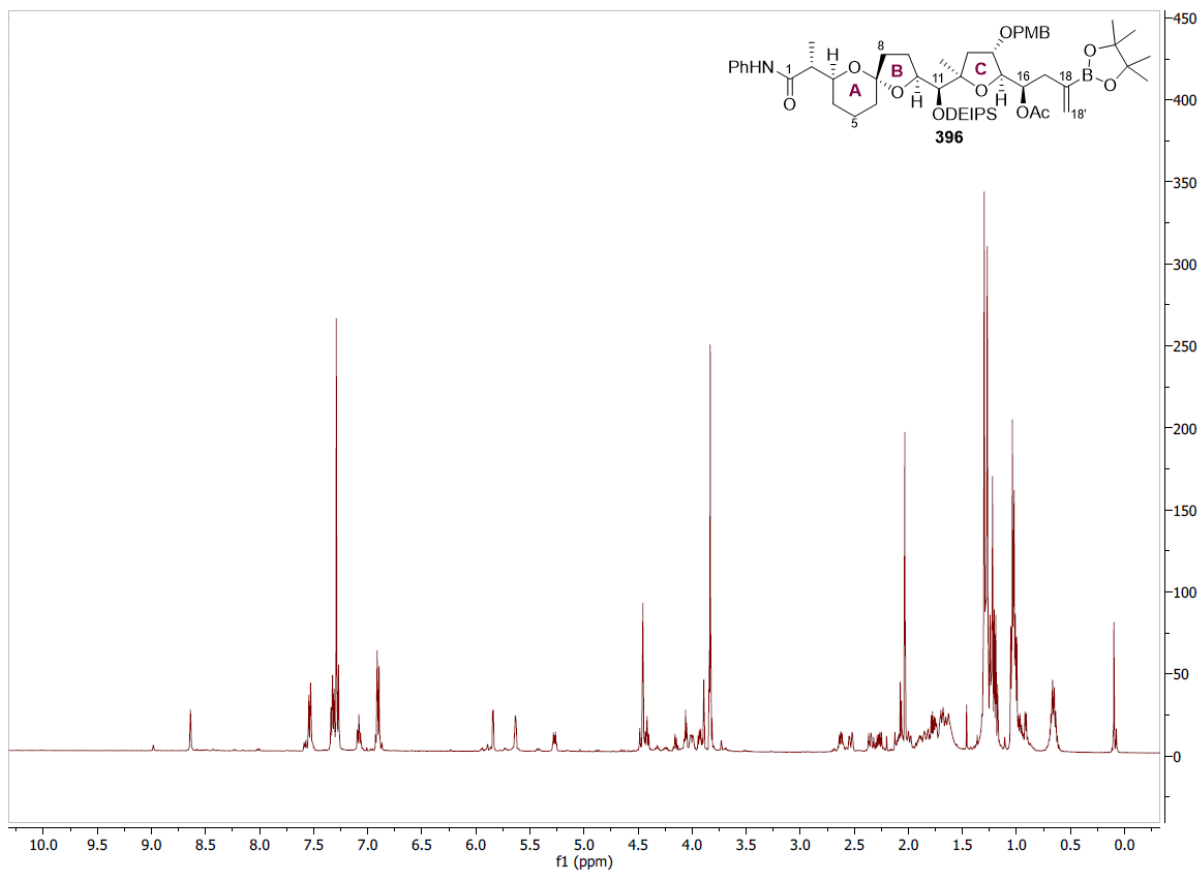
ABC spiroketal 139



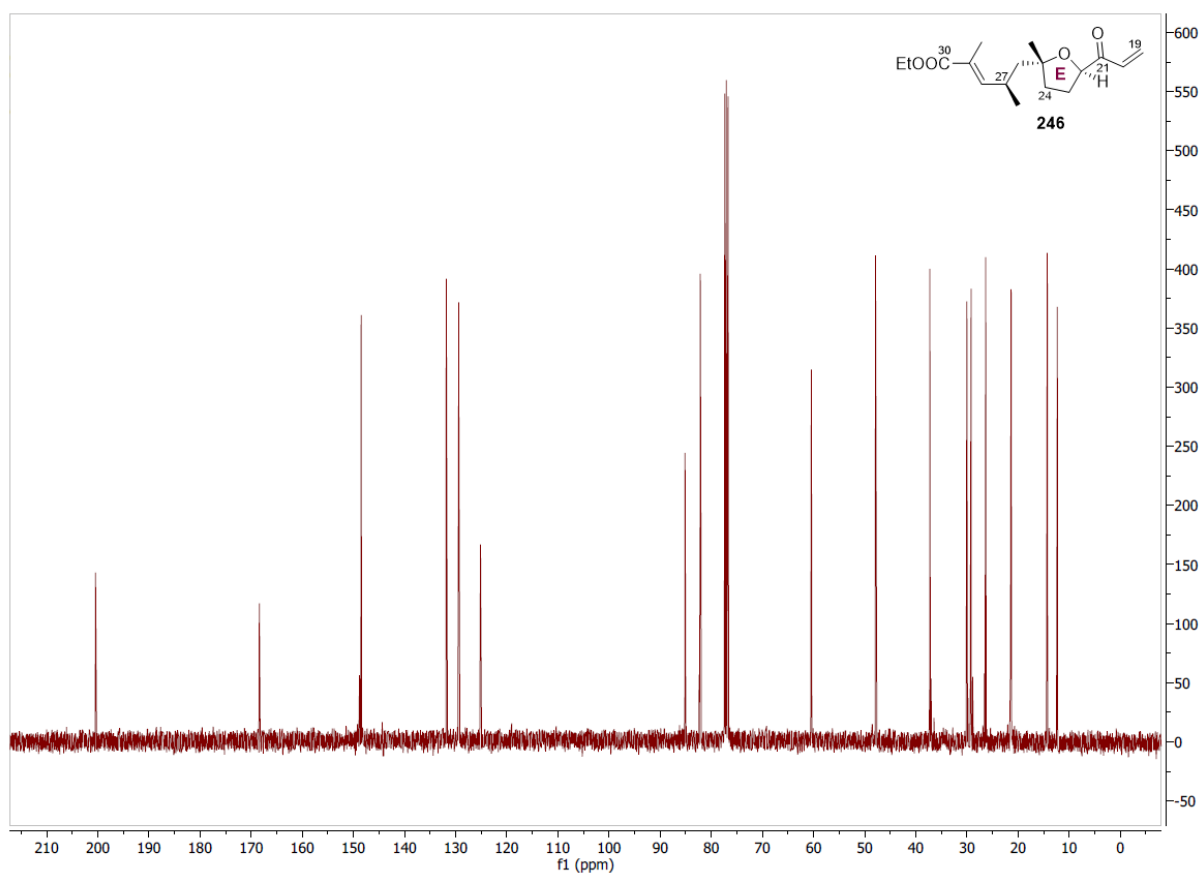
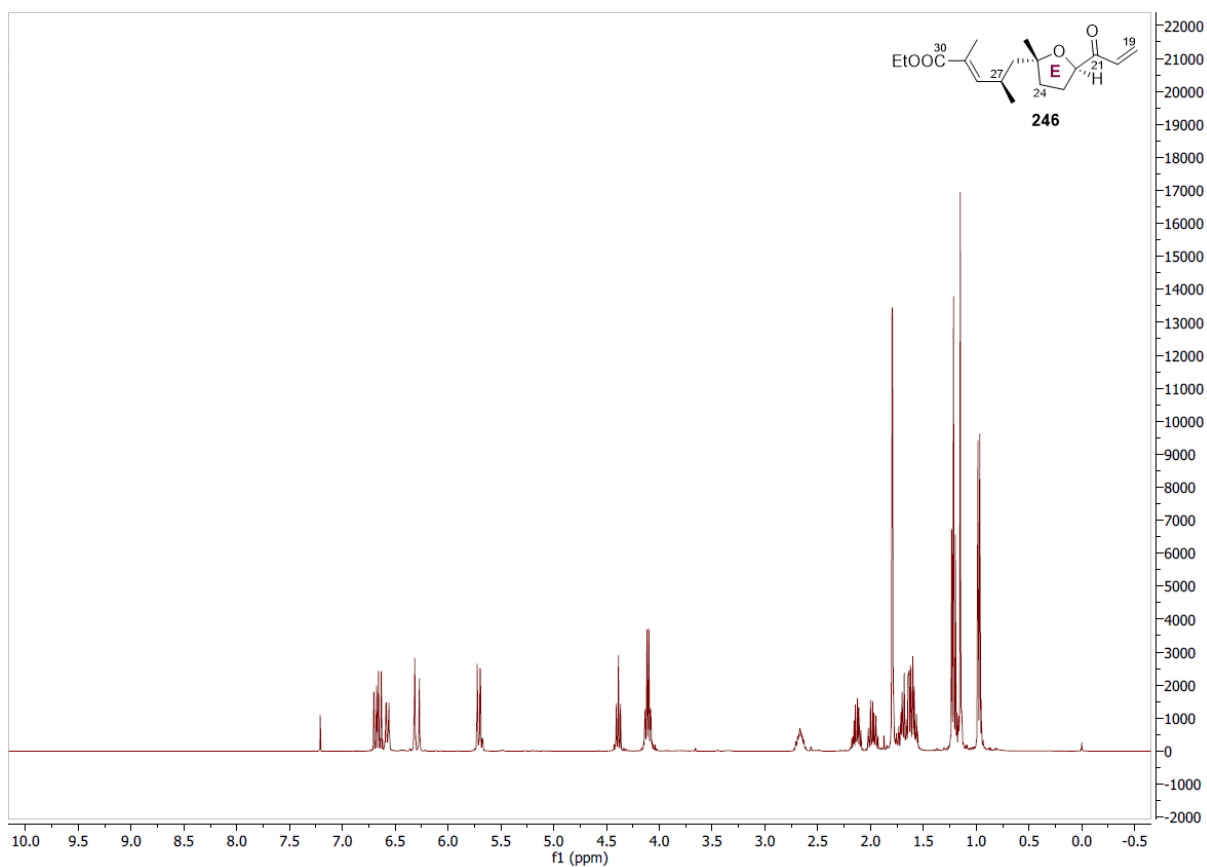
ABC aldehyde 359



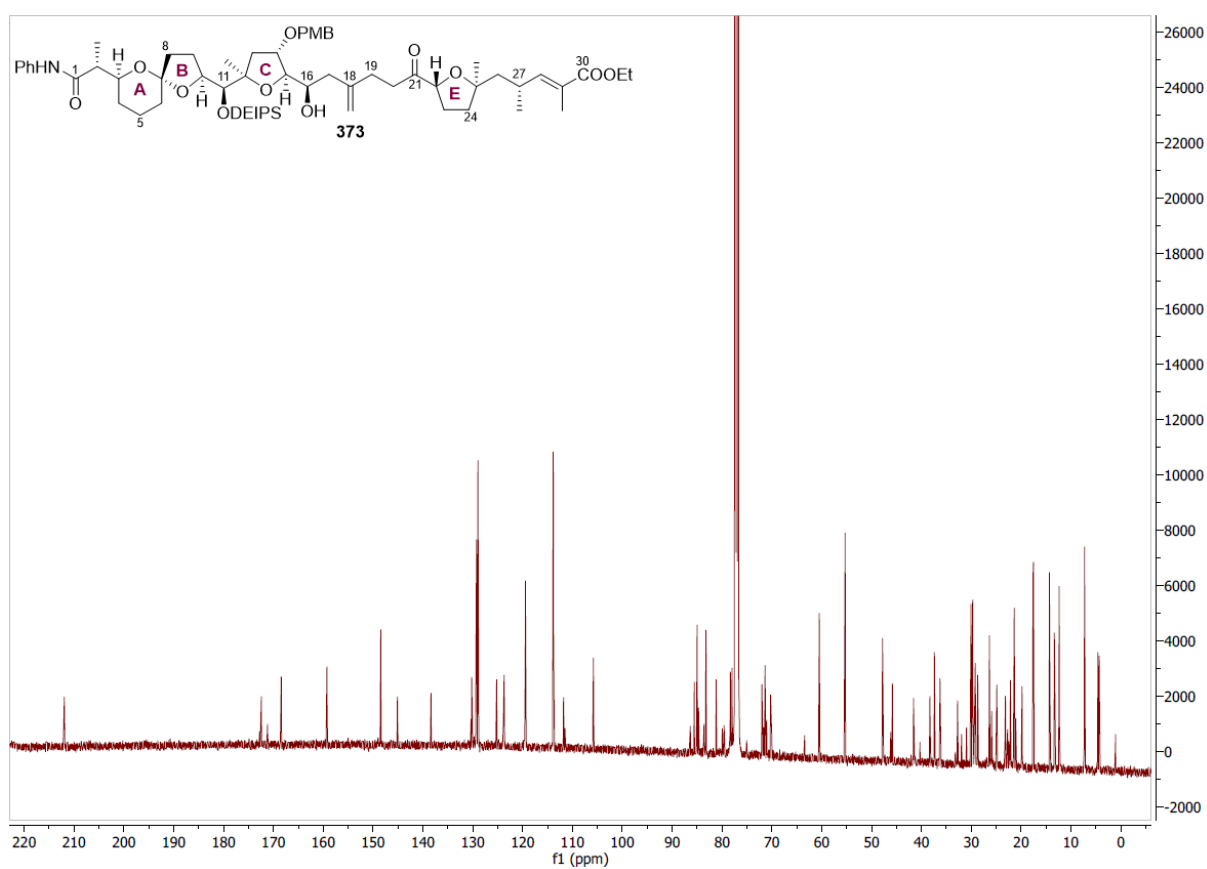
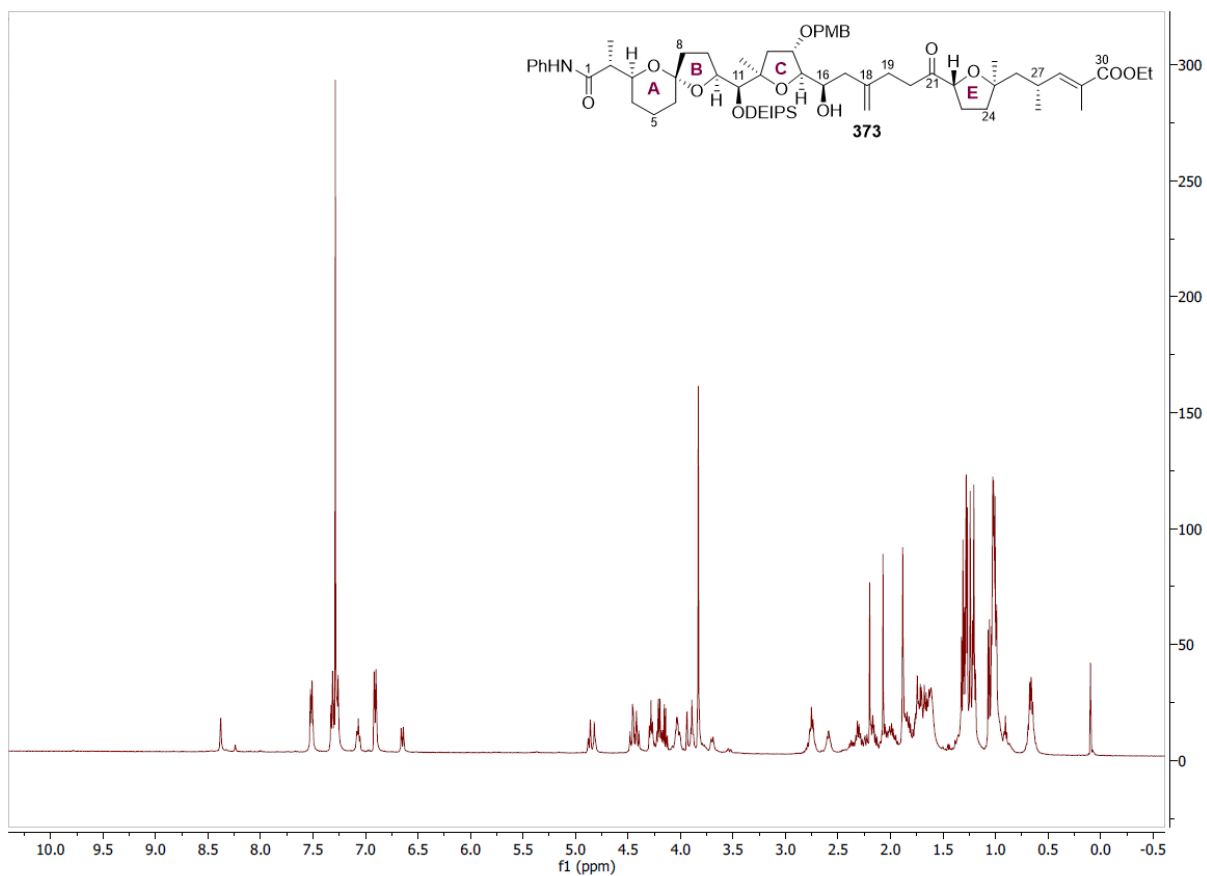
Acetate 396



E fragment 246



ABCE fragment 373



REFERENCES

- (1) Haefner, B. Drugs from the Deep: Marine Natural Products as Drug Candidates. *Drug Discov. Today*, **2003**, *8* (12), 536–544.
- (2) Jimeno, J.; Faircloth, G.; Sousa-Faro, J.; Scheuer, P.; Rinehart, K. New Marine Derived Anticancer Therapeutics – A Journey from the Sea to Clinical Trials. *Mar. Drugs*, **2004**, *2* (1), 14–29.
- (3) Yasumoto, T.; Murata, M.; Oshima, Y.; Sano, M. Diarrhetic Shellfish Toxins. *Tetrahedron*, **1985**, *41* (6), 1019–1025.
- (4) Jung, J. H.; Sim, C. J.; Lee, C.-O. Cytotoxic Compounds from a Two-Sponge Association. *J. Nat. Prod.*, **1995**, *58* (11), 1722–1726.
- (5) Sasaki, K.; Satake, M.; Yasumoto, T. Identification of the Absolute Configuration of Pectenotoxin-6, a Polyether Macrolide Compound, by NMR Spectroscopic Method Using a Chiral Anisotropic Reagent, Phenylglycine Methyl Ester. *Biosci. Biotechnol. Biochem.*, **1997**, *61* (10), 1783–1785.
- (6) Sasaki, K.; Wright, J. L. C.; Yasumoto, T. Identification and Characterization of Pectenotoxin (PTX) 4 and PTX7 as Spiroketal Stereoisomers of Two Previously Reported Pectenotoxins. *J. Org. Chem.*, **1998**, *63* (8), 2475–2480.
- (7) Halim, R.; Brimble, M. A. Synthetic Studies towards the Pectenotoxins : A Review. *Org. Biomol. Chem*, **2006**, *4*, 4048–4058.
- (8) Evans, D.; Rajapakse, H.; Chiu, A.; Stenkamp, D. Asymmetric Syntheses of Pectenotoxins-4 and - C40 Subunits and Fragment Assembly **. *Angew. Chem. Int. Ed.*, **2002**, *41*, 4573–4576.
- (9) James, K. J.; Carmody, E. P.; Gillman, M.; Kelly, S. S.; Draisci, R.; Lucentini, L.; Giannetti, L. Identification of a New Diarrhoetic Toxin in Shellfish Using Liquid Chromatography

- with Fluorimetric and Mass Spectrometric Detection. *Toxicon*, **1997**, *35* (6), 973–978.
- (10) Sandvik, M.; Miles, C. O.; Wilkins, A. L.; Fæste, C. In Vitro Hepatic Biotransformation of the Algal Toxin Pectenotoxin-2. *Toxicon X*, **2020**, *6* (October 2019), 100031.
- (11) Miles, C. O.; Wilkins, A. L.; Munday, J. S.; Munday, R.; Hawkes, A. D.; Jensen, D. J.; Cooney, J. M.; Beuzenberg, V. Production of 7-Epi-Pectenotoxin-2 Seco Acid and Assessment of Its Acute Toxicity to Mice. *J. Agric. Food Chem.*, **2006**, *54* (4), 1530–1534.
- (12) Suzuki, T.; Mackenzie, L.; Stirling, D.; Adamson, J. Pectenotoxin-2 Seco Acid: A Toxin Converted from Pectenotoxin-2 by the New Zealand Greenshell Mussel, *Perna Canaliculus*. *Toxicon*, **2001**, *39* (4), 507–514.
- (13) Yasumoto, T. PTX-2SA and Other Open Chain PTXs. *Chemistry Letters*. 1998.
- (14) Burgess, V.; Shaw, G. Pectenotoxins - An Issue for Public Health a Review of Their Comparative Toxicology and Metabolism. *Environ. Int.*, **2001**, *27* (4), 275–283.
- (15) Ishige, M.; Satoh, N.; Yasumoto, T. Pathological Studies on Mice Administered with the Causative Agent of Diarrhetic Shellfish Poisoning (Okadaic Acid and Pectenotoxin-2). *Hokkaidoritsu Eisei Kenkyushoho*, **1988**, *38*, 15–18.
- (16) Miles, C. O.; Wilkins, A. L.; Munday, R.; Dines, M. H.; Hawkes, A. D.; Briggs, L. R.; Sandvik, M.; Jensen, D. J.; Cooney, J. M.; Holland, P. T.; Quilliam, M. A.; MacKenzie, A. L.; Beuzenberg, V.; Towers, N. R. Isolation of Pectenotoxin-2 from *Dinophysis Acuta* and Its Conversion to Pectenotoxin-2 Seco Acid, and Preliminary Assessment of Their Acute Toxicities. *Toxicon*, **2004**, *43* (1), 1–9.
- (17) Fladmark, K. E.; Serres, M. H.; Larsen, N. L.; Yasumoto, T.; Aune, T.; DØskeland, S. O. Sensitive Detection of Apoptogenic Toxins in Suspension Cultures of Rat and Salmon Hepatocytes. *Toxicon*, **1998**, *36* (8), 1101–1114.
- (18) Jordan, M. A.; Wilson, L. Microtubules and Actin Filaments: Dynamic Targets for Cancer Chemotherapy. *Curr. Opin. Cell Biol.*, **1998**, *10* (1), 123–130.

- (19) Allingham, J. S.; Miles, C. O.; Rayment, I. A Structural Basis for Regulation of Actin Polymerization by Pectenotoxins. *J. Mol. Biol.*, **2007**, *371* (4), 959–970.
- (20) Hori, M.; Matsuura, Y.; Yoshimoto, R.; Ozaki, H.; Yasumoto, T.; Karaki, H.; فرهاد, خ. Actin Depolymerizing Action by Marine Toxin, Pectenotoxin-2. *Nippon Yakurigaku Zasshi*, **1999**, *114*, 225–229.
- (21) Evans, D. A.; Rajapakse, H. A.; Chiu, A.; Stenkamp, D. Asymmetric Syntheses of Pectenotoxins-4 and -8, Part II: Synthesis of the C20-C30 and C31-C40 Subunits and Fragment Assembly. *Angew. Chem. Int. Ed.*, **2002**, *41* (23), 4573–4576.
- (22) Evans, D. A.; Rajapakse, H. A.; Stenkamp, D. Asymmetric Syntheses of Pectenotoxins-4 and -8, Part I: Synthesis of the C1-C19 Subunit. *Angew. Chem. Int. Ed.*, **2002**, *41* (23), 4569–4573.
- (23) Fujiwara, K.; Aki, Y. ichi; Yamamoto, F.; Kawamura, M.; Kobayashi, M.; Okano, A.; Awakura, D.; Shiga, S.; Murai, A.; Kawai, H.; Suzuki, T. Synthesis of the C8-C20 and C21-C30 Segments of Pectenotoxin 2. *Tetrahedron Lett.*, **2007**, *48* (26), 4523–4527.
- (24) Fujiwara, K.; Suzuki, Y.; Koseki, N.; Murata, S. I.; Murai, A.; Kawai, H.; Suzuki, T. Improved Synthesis of C8-C20 Segment of Pectenotoxin-2. *Tetrahedron Lett.*, **2011**, *52* (43), 5589–5592.
- (25) Fujiwara, K.; Suzuki, Y.; Koseki, N.; Aki, Y. I.; Kikuchi, Y.; Murata, S. I.; Yamamoto, F.; Kawamura, M.; Norikura, T.; Matsue, H.; Murai, A.; Katoono, R.; Kawai, H.; Suzuki, T. Total Synthesis of Pectenotoxin-2. *Angew. Chem. Int. Ed.*, **2014**, *53* (3), 780–784.
- (26) Seiji, A.; Kenshu, F.; Akio, M. The Synthesis of the Common C31-C40 Fragment of Pectenotoxins. *Synlett*, **1997**, *11*, 1300–1302.
- (27) Samadi, M.; Munoz-Letelier, C.; Poigny, S.; Guyot, M. Synthetic Studies on Spongistatins: Synthesis of the C29-C44 Fragment. *Tetrahedron Lett.*, **2000**, *41* (18), 3349–3353.

- (28) Fujiwara, K.; Kobayashi, M.; Yamamoto, F.; Aki, Y. I.; Kawamura, M.; Awakura, D.; Amano, S.; Okano, A.; Murai, A.; Kawai, H.; Suzuki, T. Synthesis of the Common Left-Half Part of Pectenotoxins. *Tetrahedron Lett.*, **2005**, *46* (30), 5067–5069.
- (29) Richardson, M. S. W.; Tame, C. J.; Poole, D. L.; Donohoe, T. J. Rhodium-Catalysed Vinyl 1,4-Conjugate Addition Coupled with Sharpless Asymmetric Dihydroxylation in the Synthesis of the CDE Ring Fragment of Pectenotoxin-4. *Chem. Sci.*, **2019**, *10* (25), 6336–6340.
- (30) Donohoe, T. J.; Lipiński, R. M. Interplay of Cascade Oxidative Cyclization and Hydride Shifts in the Synthesis of the ABC Spiroketal Ring System of Pectenotoxin-4. *Angew. Chem. Int. Ed.*, **2013**, *52* (9), 2491–2494.
- (31) Roushanbakhti, A.; Liu, Y.; Winship, P. C. M.; Tucker, M. J.; Akhtar, W. M.; Walter, D. S.; Wrigley, G.; Donohoe, T. J. Cobalt versus Osmium: Control of Both Trans and Cis Selectivity in Construction of the EFG Rings of Pectenotoxin 4. *Angew. Chem. Int. Ed.*, **2017**, *56* (47), 14883–14887.
- (32) Evans, D. A.; MacMillan, D. W. C.; Campos, K. R. C₂-Symmetric Tin(II) Complexes as Chiral Lewis Acids, Catalytic Enantioselective Anti Aldol Additions of Enolsilanes to Glyoxylate and Pyruvate Esters. *J. Am. Chem. Soc.*, **1997**, *119* (44), 10859–10860.
- (33) Rajapakse, H. A. Asymmetric Syntheses of Pectenotoxins-4 and -8, PhD Thesis, Harvard University, Cambridge, Massachusetts, 2002.
- (34) Reetz, M. T.; Kessler, K. Chelation- and Non-Chelation-Controlled Additions to 2-O-Benzyl-3-O-(tert-butyltrimethylsilyl)-glyceraldehyde. *J. Org. Chem.*, **1985**, *50* (25), 5434–5436.
- (35) Scheidt, K. A.; Chen, H.; Follows, B. C.; Chemler, S. R.; Coffey, D. S.; Roush, W. R. Tris(dimethylamino)sulfonium difluorotrimethylsilicate, a mild reagent for the removal of silicon protecting groups. *J. Org. Chem.*, **1998**, *63* (19), 6436–6437.

- (36) Richardson, M. S. W. Towards the Total Synthesis of Pectenotoxin-4: Synthesis of the CDE and F Rings, DPhil Thesis, University of Oxford, 2018.
- (37) Lipiński, R. M. Synthesis of the ABC Fragment of Pectenotoxin-4, DPhil Thesis, University of Oxford, 2012.
- (38) Yang, X. Towards the Total Synthesis of the ABC Fragment of Pectenotoxin-4, DPhil Thesis, University of Oxford, 2016.
- (39) Chattopadhyay, A. (R)-2,3-O-Cyclohexylidene-glyceraldehyde, a Versatile Intermediate for Asymmetric Synthesis of Homoallyl and Homopropargyl Alcohols in Aqueous Medium. *J. Org. Chem.*, **1996**, *61* (18), 6104–6107.
- (40) Chattopadhyay, A.; Mamdapur, V. R. (R)-2,3-O-Cyclohexylidene-glyceraldehyde, a Versatile Intermediate for Asymmetric Synthesis of Chiral Alcohol. *J. Org. Chem.*, **1995**, *60* (3), 585–587.
- (41) Frantz, D. E.; Fässler, R.; Carreira, E. M. Facile Enantioselective Synthesis of Propargylic Alcohols by Direct Addition of Terminal Alkynes to Aldehydes [3]. *J. Am. Chem. Soc.*, **2000**, *122* (8), 1806–1807.
- (42) El-Sayed, E.; Anand, N. K.; Carreira, E. M. Asymmetric Synthesis of γ -Hydroxy α,β -Unsaturated Aldehydes via Enantioselective Direct Addition of Propargyl Acetate to Aldehydes. *Org. Lett.*, **2001**, *3* (19), 3017–3019.
- (43) Boyall, D.; Frantz, D. E.; Carreira, E. M. Efficient Enantioselective Additions of Terminal Alkynes and Aldehydes under Operationally Convenient Conditions. *Org. Lett.*, **2002**, *4* (15), 2605–2606.
- (44) Lipiński, R. M. Synthesis of the ABC Fragment of Pectenotoxin-4.
- (45) Zhang, D.; Ready, J. M. Iron-Catalyzed Carbometalation of Propargylic and Homopropargylic Alcohols. *J. Am. Chem. Soc.*, **2006**, *128* (47), 15050–15051.
- (46) Pilgrim, B. S.; Donohoe, T. J. Osmium-Catalyzed Oxidative Cyclization of Dienes and

- Their Derivatives. *J. Org. Chem.*, **2013**, *78* (6), 2149–2167.
- (47) Stiles, M.; Winkler, R. R.; Chang, Y. L.; Traynor, L. Stereochemical Assignments for β -Ketols Formed by Aldol Addition of Three Simple Ketones to p-Nitrobenzaldehyde. *J. Am. Chem. Soc.*, **1964**, *86* (16), 3337–3342.
- (48) House, H. O.; Crumrine, D. S.; Teranishi, A. Y.; Olmstead, H. D. Chemistry of Carbanions. XXIII. Use of Metal Complexes to Control the Aldol Condensation. *J. Am. Chem. Soc.*, **1973**, *95* (10), 3310–3324.
- (49) Ager, D. J.; Prakash, I.; Schaad, D. R. 1,2-Amino Alcohols and Their Heterocyclic Derivatives as Chiral Auxiliaries in Asymmetric Synthesis. *Chem. Rev.*, **1996**, *96* (2), 835–875.
- (50) Ley, S. V.; Smith, S. C.; Woodward, P. R. Further Reactions of T-Butyl 3-Oxobutanthioate and t-Butyl 4-Diethyl-Phosphono-3-Oxobutanthioate : Carbonyl Coupling Reactions, Amination, Use in the Preparation of 3-Acyltetramic Acids and Application to the Total Synthesis of Fuligorubin A. *Tetrahedron*, **1992**, *48* (6), 1145–1174.
- (51) Winship, P. C. M. The Development and Applications of the Lewis Acid-Mediated Osmium-Catalysed Oxidative Cyclisation, DPhil Thesis, 2011.
- (52) Liu, Y. Synthesis of the CDE & EFG Ring Systems of Pectenotoxin-4, DPhil Thesis, University of Oxford, 2016.
- (53) Gao, F.; Hoveyda, A. H. α -Selective Ni-Catalyzed Hydroalumination of Aryl- and Alkyl-Substituted Terminal Alkynes: Practical Syntheses of Internal Vinyl Aluminums, Halides, or Boronates. *J. Am. Chem. Soc.*, **2010**, *132* (32), 10961–10963.
- (54) Archer, R. M.; Royer, S. F.; Mahy, W.; Winn, C. L.; Danson, M. J.; Bull, S. D. Syntheses of 2-Keto-3-Deoxy-D-Xylonate and 2-Keto-3-Deoxy-L-Arabinonate as Stereochemical Probes for Demonstrating the Metabolic Promiscuity of *Sulfolobus Solfataricus* towards D-Xylose and L-Arabinose. *Chem. - A Eur. J.*, **2013**, *19* (8), 2895–2902.

- (55) Comins, D. L.; Dehghani, A. Pyridine-Derived Triflating Reagents: An Improved Preparation of Vinyl Triflates from Metallo Enolates. *Tetrahedron Lett.*, **1992**, *33* (42), 6299–6302.
- (56) Hofstra, J. L.; Poremba, K. E.; Shimozone, A. M.; Reisman, S. E. Nickel-Catalyzed Conversion of Enol Triflates into Alkenyl Halides. *Angew. Chem. Int. Ed.*, **2019**, *58* (42), 14901–14905.
- (57) Tojo, G.; Marcos, F. *Oxidation of Alcohols to Aldehydes and Ketones*; Springer, 2006.
- (58) Meyer, S. D.; Schreiber, S. L. Acceleration of the Dess-Martin Oxidation by Water. *J. Org. Chem.*, **1994**, *59* (24), 7549–7552.
- (59) Kocienski, P. J. *Protecting Groups*, 3rd ed.; Thieme, 2005.
- (60) He, H. M.; Fanwick, P. E.; Wood, K.; Cushman, M. A Novel 1,3 O → C Silyl Shift and Deacylation Reaction Mediated by Tetra-n-Butylammonium Fluoride in an Aromatic System. *J. Org. Chem.*, **1995**, *60* (18), 5905–5909.
- (61) Brummel, B. R.; Lee, K. G.; McMillen, C. D.; Kolis, J. W.; Whitehead, D. C. One-Pot Absolute Stereochemical Identification of Alcohols via Guanidinium Sulfate Crystallization. *Org. Lett.*, **2019**, *21* (23), 9622–9627.
- (62) De Mico, A.; Margarita, R.; Parlanti, L.; Vescovi, A.; Piancatelli, G. A Versatile and Highly Selective Hypervalent Iodine (III)/ 2,2,6,6-Tetranylethyl-1-Piperidinyloxy-Mediated Oxidation of Alcohols to Carbonyl Compounds. *J. Org. Chem.*, **1997**, *62* (20), 6974–6977.
- (63) Takemoto, Y.; Yoshida, H.; Takaki, K. Facile Access to Vic -Borylstannylalkanes via Copper-Catalyzed Three-Component Borylstannylation of Alkenes. *Synth.*, **2014**, *46* (22), 3024–3032.
- (64) Le, H.; Kyne, R. E.; Brozek, L. A.; Morken, J. P. Catalytic Enantioselective Allyl-Allyl Cross-Coupling with a Borylated Allylboronate. *Org. Lett.*, **2013**, *15* (7), 1432–1435.
- (65) Hesse, M. J.; Essafi, S.; Watson, C. G.; Harvey, J. N.; Hirst, D.; Willis, C. L.; Aggarwal, V. K.

- Highly Selective Allylboration of Aldehydes Using α,α -Disubstituted Allylic Pinacol Boronic Esters. *Angew. Chem. Int. Ed.*, **2014**, *53* (24), 6145–6149.
- (66) Miura, T.; Nakahashi, J.; Sasatsu, T.; Murakami, M. Synthesis of γ -Boryl-Substituted Homoallylic Alcohols with Anti Stereochemistry Based on a Double-Bond Transposition. *Angew. Chem. Int. Ed.*, **2019**, *58* (4), 1138–1142.
- (67) Burns, A. R.; Lam, H. W.; Roy, I. D. Enantioselective, Rhodium-Catalyzed 1,4-Addition of Organoboron Reagents to Electron-Deficient Alkenes. *Org. React.*, **2017**, *93*, 1.
- (68) Kina, A.; Iwamura, H.; Hayashi, T. A Kinetic Study on Rh/Binap-Catalyzed 1,4-Addition of Phenylboronic Acid to Enones: Negative Nonlinear Effect Caused by Predominant Homochiral Dimer Contribution. *J. Am. Chem. Soc.*, **2006**, *128* (12), 3904–3905.
- (69) Hayashi, T.; Takahashi, M.; Takaya, Y.; Ogasawara, M. Catalytic Cycle of Rhodium-Catalyzed Asymmetric 1,4-Addition of Organoboronic Acids. Arylrhodium, Oxa- π -Allylrhodium, and Hydroxorhodium Intermediates. *J. Am. Chem. Soc.*, **2002**, *124* (18), 5052–5058.
- (70) Gottlieb, H. E.; Kotlyar, V.; Nudelman, A. NMR Chemical Shifts of Common Laboratory Solvents as Trace Impurities. *J. Org. Chem.*, **1997**, *62* (21), 7512–7515.
- (71) Fulmer, G. R.; Miller, A. J. M.; Sherden, N. H.; Gottlieb, H. E.; Nudelman, A.; Stoltz, B. M.; Bercaw, J. E.; Goldberg, K. I. NMR Chemical Shifts of Trace Impurities: Common Laboratory Solvents, Organics, and Gases in Deuterated Solvents Relevant to the Organometallic Chemist. *Organometallics*, **2010**, *29* (9), 2176–2179.
- (72) Frigerio, M.; Santagostino, M.; Sputore, S. A User-Friendly Entry to 2-Iodoxybenzoic Acid (IBX). *J. Org. Chem.*, **1999**, *64* (12), 4537–4538.
- (73) Tucker, M. J. Novel Synthetic Routes Towards Trans-THFs and Application Towards the FG Fragment of Pectenotoxin-4, DPhil Thesis, University of Oxford, 2013.